



HAL
open science

Description and functional analysis of the t-SNARE SNAP33 in *Arabidopsis thaliana*

Houda Henchiri

► **To cite this version:**

Houda Henchiri. Description and functional analysis of the t-SNARE SNAP33 in *Arabidopsis thaliana*.
Vegetal Biology. Université Paris-Saclay, 2021. English. NNT : 2021UPASL098 . tel-03620519

HAL Id: tel-03620519

<https://theses.hal.science/tel-03620519>

Submitted on 26 Mar 2022

HAL is a multi-disciplinary open access archive for the deposit and dissemination of scientific research documents, whether they are published or not. The documents may come from teaching and research institutions in France or abroad, or from public or private research centers.

L'archive ouverte pluridisciplinaire **HAL**, est destinée au dépôt et à la diffusion de documents scientifiques de niveau recherche, publiés ou non, émanant des établissements d'enseignement et de recherche français ou étrangers, des laboratoires publics ou privés.

Description et caractérisation fonctionnelle
du t-SNARE SNAP33 chez *Arabidopsis*
thaliana

Description and functional analysis of the
t-SNARE SNAP33 in *Arabidopsis thaliana*

Thèse de doctorat de l'université Paris-Saclay

École doctorale n° 577 : Structure et Dynamique des Systèmes Vivants (SDSV)
Spécialité de doctorat : Sciences de la vie et de la santé
Unité de recherche : Université Paris-Saclay, CNRS, INRAE, Univ Evry, Institute of Plant
Sciences Paris-Saclay (IPS2), 91405, Orsay, France.
Réfèrent : Université d'Évry Val d'Essonne

**Thèse présentée et soutenue à Paris-Saclay,
Le 08/12/2021, par
Houda HENCHIRI**

Composition du Jury

Marianne Delarue Pr, UPSaclay, IPS2, Paris-Saclay	Présidente
Laurent Deslandes DR, CNRS, LIPM, Castanet Tolosan	Rapporteur
Sylvie German Retana DR, INRAE, Biologie du Fruit et Pathologie, Villenave d'Ornon	Rapportrice
Nicolas Frei dit Frey MCF, UPS Toulouse, LRSV, Toulouse	Examineur

Direction de la thèse

Bénédicte Sturbois Pr, UEVE, IPS2, Paris-Saclay	Directrice de thèse
Jean Bigeard IGR, UEVE, IPS2, Paris-Saclay	Co-Encadrant

Acknowledgments

To begin, I would like to express my gratitude to my supervisors, Jean Bigeard and Bénédicte Sturbois, for warmly welcoming me to the "stress signaling" team, for the time you devoted to my project, your availability, your patience, motivation, and knowledge. I am grateful to you for guiding me during my research, the teachings, and the writing of this thesis, I have learned a great deal.

I would like to express my gratitude to our team leader, "Jeannot" for his advice at team meetings, his sense of humor, and all the interesting talks we had.

Thank you to Marie Boudsocq for your interest in my project and the several times you showed me how to conduct experiments; whenever I come to you for assistance, you pull out all your old protocols and notebooks and show me how to do it from A to Z!

I would like to express my gratitude to Julien Lang for his guidance on some experiments, his comments during our team meetings, as well as for his support at the end of my Master 2.

Thanks to Sarah Regnard, my cheerful office colleague, for her good humor and for watering my plants on multiple occasions. Thanks to Erwan Le Deunff for his curiosity regarding my project and for watering my plants too.

Thanks to Heribert Hirt for his advice and comments during our team meetings.

In general, I would like to express my gratitude to everyone in the team (current and past).

Thanks to Tiffany Delormel with whom we laughed a lot, for our discussions, for the Biotechno experience, for the advice as a "Senior" PhD student, and for your continued support even after leaving the lab. By the way, Thanks to the Sushi team, Tiffany, Bastien Malbert, and Kevin Baudry!

Many thanks to Baptiste Genot, who provided invaluable assistance throughout my Master 2 internship. Thanks to Daria Zhydovych (our previous intern), Nolwenn Bonade Bottino, Cécile Sozen, Eleonora rolli and Liliana Avila Ospina.

I'd like to thank Emilie Seguinot, Pauline Duminil, Mael Jeuffrard, Axellou, Vladimir Daric, Claire Benezech, and Marine Guilcher for the laughs and the precious moments we shared together in and out of the lab.

Additionally, I would like to thank everyone I was able to interact with at IPS2 Richard Rigo, Corentin Moreau, Pierre Gautrat, Dario Monachello, Livia Merendino, Sophie Blanchet, Valérie Geffroy, Gilles Chatel-Innocenti (notably for the *npr1* seeds), Nathalie Glab, Halima Morin (for immunolocalization experiments), Cécile Raynaud (for the *P35S::NahG* lines), and the administrative, greenhouse, logistics, and informatics team.

I would like to thank Emmanuelle Issakidis for her assistance in protein cloning and purification, and to Gwilherm Brisou for showing me how to perform Ethylene quantifications.

I would like to express my gratitude to my thesis committee members for their advice, Alia Dellagi (who has been my mentor since my first year of Master's), Axellou (De Julien De Zelicourt), and Hakim Mireau.

Additionally, I would like to express my gratitude to the project's collaborators: Farid El Kasmi from the University of Tübingen for the stimulating discussions we had. to the transcriptomic platform: José Cañas, Etienne Delannoy and Marie-Laure Martin Magniette, to Sylvie Citerne and Grégory Mouille from the Chemistry-Metabolism platform of the IJPB.

I would like to thank my precious Sebastien, my friends, especially Ambre Guillory (my best buddy since I've been in France), with whom I've spent a lot of time discussing science (among many other things), Hayat Sehki, and Mathilde Gregoire (for the R scripts).

Finally, I would like to express my gratitude to my family: **MY PARENTS**, without whom I wouldn't be able to continue my studies in France and who have always supported me, my twin sister (my cheerleader), and my two brothers.

Table of contents

CHAPTER I – INTRODUCTION	1
1. Plant immunity: how plants detect the presence of pathogenic microbes and generate the immune response	4
1.1. PATTERN-TRIGGERED IMMUNITY (PTI)	6
1.1.1. PRRs: the main players of PTI	6
1.1.2. Signaling downstream of PRRs	6
1.2. EFFECTOR-TRIGGERED IMMUNITY (ETI)	12
1.2.1. ETI, the second layer of defense against more adapted pathogens	12
1.2.2. Resistance proteins: the main players of ETI	12
1.2.3. The guard and decoy model of effector perception by NLRs	13
1.2.4. Regulations of R proteins	15
1.2.5. Regulation of NLRs downstream signaling.....	16
1.2.6. ETI outputs: a continuity of PTI responses?	17
2. Mitogen-activated Protein Kinases (MAPKs): hubs with an essential role in immune signaling	19
2.1. MAPKs in Arabidopsis	19
2.1.1. MAPKKKs	20
2.1.2. MAPKKs	21
2.1.3. MAPKs	21
2.2. Mechanisms regulating MAPK modules specificity, substrate specificity, and signaling	22
2.2.1. Mechanisms regulating MAPK module specificity.....	22
2.2.2. Mechanisms regulating MAPK substrate specificity	22
2.2.3. Mechanisms regulating MAPK signaling.....	23
2.3. The role of MPK3, MPK4, and MPK6 in immunity	23
2.3.1. MAPKKK3/MAPKKK5-MKK4/MKK5-MPK6/MPK3 pathway	24
2.3.2. MEKK1-MKK1/MKK2-MPK4 pathway	26
2.3.3. MAPKs are targets of pathogenic effectors.....	28
2.3.4. MAPKs in ETI.....	28
3. The role of hormones in immunity.....	29
3.1. SA pathway	29
3.1.1. SA biosynthesis	29
3.1.2. SA metabolism	31
3.1.3. Regulation of SA biosynthesis	32
3.1.4. Signaling downstream of SA	33
3.1.5. SAR	34

3.2.	JA pathway.....	36
3.2.1.	JA biosynthesis	36
3.2.2.	JA perception and downstream signaling	37
3.2.3.	Regulation of the JA pathway	38
3.3.	Ethylene pathway.....	39
3.3.1.	ET biosynthesis.....	39
3.3.2.	ET perception and signaling	39
3.3.3.	ET pathway regulation.....	40
3.4.	Crosstalk between defense hormones	40
3.4.1.	JA-ET.....	41
3.4.2.	JA-SA	41
3.4.3.	SA-ET.....	42
4.	The importance of membrane trafficking in plant immunity	43
4.1.	Overview of the trafficking pathways in plants	44
4.1.1.	The secretory and vacuolar pathway	44
4.1.2.	The endocytic pathway	45
4.2.	The involvement of membrane trafficking in plant immunity.....	47
4.2.1.	The importance of the secretory machinery in plant immunity.....	47
4.2.2.	Unconventional secretory pathways in plant immunity	49
4.2.3.	The role of the endocytic pathway in plant immunity.....	51
4.3.	SNAREs: Very conserved proteins and the main executors of membrane fusion processes in the endomembrane system of plants	52
4.3.1.	Nomenclature and classification.....	52
4.3.2.	SNAREs are involved in plant immunity: the case of SYP121 and its interacting SNARE partners.....	53
4.3.3.	SNAP33 is a SNAP25-like gene with an intriguing trait	55
5.	Objectives of my Ph.D.	57
CHAPTER II – RESULTS.....		58
1.	Characterization of the lesion-mimic phenotype of <i>snap33</i> mutants.....	59
1.1.	Isolation of novel <i>snap33</i> mutants	59
1.2.	<i>snap33</i> knock-out mutants display constitutive cell death and H ₂ O ₂ accumulation 60	
1.3.	MPK3, MPK4, and MPK6 activation upon flg22 treatment is more intense in the <i>snap33</i> mutants.....	60
1.4.	High temperatures partially suppress the dwarf phenotype of <i>snap33</i>	61
1.5.	Transcriptomic analyses of the <i>snap33-1</i> mutant confirm that <i>SNAP33</i> mutation results in constitutive expression of defense-related genes.....	62
1.5.1.	Experimental design	62

1.5.2.	Analyses of the differentially expressed genes.....	63
1.6.	<i>snap33</i> 's phenotype is related to constitutive defense signaling	67
1.6.1.	The SA, JA, and ET marker genes are up-regulated in the <i>snap33</i> mutants ..	67
1.6.2.	SA, JA, and ET levels are higher in the <i>snap33-1</i> mutant.....	67
1.6.3.	<i>snap33-1</i> 's phenotype is partially reverted by mutations in the JA and SA pathways.....	68
1.6.4.	R protein signaling is constitutively induced in the <i>snap33-1</i> mutant.....	72
1.6.5.	<i>snap33-1</i> 's phenotype is partially dependent on CPK5 and TN2.....	73
1.7.	Discussion.....	74
1.7.1.	The phenotype of <i>snap33</i> resembles that of several lesion-mimic mutants ...	75
1.7.2.	The SA sector is dominant in the <i>snap33</i> mutant	76
1.7.3.	<i>snap33</i> mutants mimic ETI responses	77
1.7.4.	Is the <i>snap33</i> phenotype only related to auto-immunity?.....	81
1.8.	Conclusion and perspectives.....	84
2.	Studying the relationship between SNAP33 and the MEKK1-MKK2-MPK4 MAPK module.....	85
2.1.	SNAP33 PTMs and interactions	86
2.1.1.	SNAP33 PTMs	86
2.1.2.	SNAP33 interactions	87
2.2.	Is SNAP33 an interacting partner of MEKK1-MKK2-MPK4 MAPK module?... 88	
2.2.1.	SNAP33 interacts with MEKK1, MKK2, and MPK4 in vivo by BiFC.....	88
2.2.2.	SNAP33 does not interact with MEKK1, MKK2, and MPK4 by Y2H.....	88
2.2.3.	SNAP33 does not interact with MKK2 and MPK4 by in vitro pull-down assays	89
2.2.4.	SNAP33 does not interact with MKK2 and MPK4 by co-immunoprecipitation assays in vivo	89
2.3.	Is SNAP33 a substrate of the MEKK1-MKK2-MPK4 MAPK module?	90
2.3.1.	Kinase assays using the in vitro produced recombinant proteins.....	91
2.3.2.	Kinase assay using the in vivo purified MPK4 and MKK2	91
2.4.	Is there a genetic relationship between SNAP33 and the MAPK module?.....	92
2.4.1.	<i>snap33-1</i> phenotype is not suppressed by the <i>summ2-8</i> mutation	92
2.4.2.	<i>snap33-1</i> phenotype is not suppressed by the <i>smn1</i> mutation.....	93
2.5.	Discussion.....	93
2.5.1.	Is SNAP33 an interacting partner of the MAPK module?	95
2.5.2.	Is SNAP33 a substrate of MPK3, MPK4, and MPK6?	96
2.5.3.	SNAP33 is not involved in the same pathway as that of the MEKK1-MKK2-MPK4 MAPK module.....	97
	CHAPTER III - GENERAL CONCLUSIONS AND PERSPECTIVES.....	99

1. Summary of my results	100
2. Perspectives	101
CHAPTER IV - MATERIALS AND METHODS	102
1. Materials.....	103
1.1. Plant material	103
1.2. AGI number of the main genes	103
1.3. Bacterial strains.....	103
1.4. Yeast strains	104
1.5. Growth media.....	104
1.5.1. Plant growth media.....	104
1.5.2. Bacteria and yeast growth media.....	104
1.6. Vectors	104
1.7. Primers	106
1.7.1. Cloning primers	106
1.7.2. Genotyping primers	106
1.7.3. Quantitative PCR primers.....	106
1.7.4. RT PCR primers	106
1.8. Antibiotics.....	106
1.9. Antibodies	107
1.9.1. Primary antibodies	107
1.9.2. Secondary antibodies	107
2. Methods.....	107
2.1. Plant methods.....	107
2.1.1. Plant growth.....	107
2.1.2. Hormone quantification.....	108
2.1.3. BiFC experiments	109
2.1.4. Stainings	109
2.2. Protoplast methods.....	110
2.2.1. Protoplast's isolation	110
2.2.2. Protoplast's transformation.....	110
2.3. Bacteria methods.....	111
2.3.1. Bacterial transformation	111
2.3.2. Agrobacterium transformation	111
2.4. Yeast methods.....	111
2.4.1. Yeast transformation.....	111
2.4.2. Yeast two-hybrid (Y2H) analysis for protein-protein interaction	112
2.5. DNA methods	112

2.5.1.	Plasmid DNA isolation.....	112
2.5.2.	Plant DNA extraction for genotyping.....	112
2.5.3.	PCRs	113
2.5.4.	dCAPS genotyping	113
2.5.5.	Cloning PCRs	113
2.5.6.	DNA migration	113
2.5.7.	DNA digestion.....	113
2.5.8.	DNA sequencing.....	114
2.5.9.	Cloning	114
2.6.	RNA methods.....	114
2.6.1.	RNA isolation	114
2.6.2.	cDNA synthesis	115
2.6.3.	Quantitative PCRs	115
2.6.4.	Transcriptomic analyses	115
2.7.	Protein methods	116
2.7.1.	Native protein extraction	116
2.7.2.	Bradford protein dosage	117
2.7.3.	Recombinant protein expression and purification	117
2.7.4.	Co-immunoprecipitation assays for protein-protein interactions	119
2.7.5.	Pull-down assays	119
2.7.6.	Kinase assays	120
2.7.7.	SDS- PAGE and immunoblotting.....	121
2.8.	Plotting, data interpretation and statistical analyses	121
	REFERENCES.....	123
	SUPPLEMENTARY DATA	162

List of figures and tables

Figure 1.1.	Schematic view summarizing the cellular and physiological events occurring during PTI in response to PAMP elicitation using the flg22-FLS2 PAMP/RLK model	p7
Figure 1.2.	Schematic view of effector-triggered immunity (ETI) in plants	p13
Figure 1.3.	Schematic view of MAPK module activation in plants	p21
Figure 1.4.	Schematic view of MEKK1-MKK1/2-MPK4 and MAPKKK3/5-MKK4/5-MPK3/6 modules downstream of PRR activation	p25
Figure 1.5.	Schematic view summarizing SA biosynthesis and metabolism in Arabidopsis	p30
Figure 1.6.	Schematic view summarizing the SA signaling pathway downstream PAMP and effector perception	p33
Figure 1.7.	Schematic view summarizing metabolite and protein-mediated signaling during systemic acquired resistance	p35
Figure 1.8.	Schematic view summarizing the JA biosynthesis and signaling pathway	p36
Figure 1.9.	Schematic view summarizing the ET biosynthesis and signaling pathway	p39
Figure 1.10.	Schematic view summarizing the crosstalks between SA, JA, and ET pathways	p41
Figure 1.11.	Schematic view summarizing the trafficking pathways in plants under resting conditions	p46
Figure 1.12.	Schematic view summarizing the unconventional trafficking pathway in plants during immune responses	p50
Figure 1.13.	Schematic view of vesicle fusion by the SNARE complex	p52
Figure 1.14.	Schematic view of an unrooted phylogenetic tree of the SNARE family in Arabidopsis	p53
Figure 1.15.	Schematic view of a phylogenetic tree of SNAP25 proteins in plants	p55
Figure 2.1.	Characterization of <i>snap33</i> T-DNA insertion mutants	p59
Figure 2.2.	The <i>snap33</i> knock-out mutants display constitutive cell death and H ₂ O ₂ accumulation	p60
Figure 2.3.	Activation of MPK3, MPK4, and MPK6 is more intense in the <i>snap33</i> mutants compared to WT-1 upon flg22 treatment	p61
Figure 2.4.	High temperatures partially suppress the dwarf phenotype of the <i>snap33-1</i> mutant	p61
Figure 2.5.	The experimental design of <i>snap33-1</i> vs WT-1 RNA-sequencing (RNA-seq) analysis and preliminary results	p62
Figure 2.6.	Analyses of the differentially-expressed genes (DEGs) between <i>snap33-1</i> and WT-1 at 5 and 12 days	p63
Figure 2.7.	GO enrichment analyses of the <i>snap33-1</i> up-regulated genes at 5 and 12 days	p64
Figure 2.8.	Overlap between the "plant-type hypersensitive response" GO category and genes up-regulated in <i>snap33-1</i> at 12 days	p65
Figure 2.9.	Bar graphs showing the expression of selected genes from the 12 days RNA-seq data and involved in the SA pathway and R protein signaling	p66
Figure 2.10.	Bar graphs showing the expression of selected genes from the RNA-seq data of 12 days <i>snap33-1</i> and WT-1 involved in early PTI signaling and in JA and ET hormonal pathways	p67
Figure 2.11.	GO enrichment analyses of the <i>snap33-1</i> down-regulated genes at 5 and 12 days	p68
Figure 2.12.	The <i>snap33-1</i> transcriptome displays similarity to stress-treated plants	p69
Figure 2.13.	SA and JA-ET marker genes are up-regulated in the <i>snap33</i> mutants compared to WT-1	p70

Figure 2.14.	SA JA and ET levels are higher in the <i>snap33</i> mutant compared to WT-1	p71
Figure 2.15.	Morphological phenotypes of WT-1, <i>snap33-1</i> , <i>snap33-1 sid2-2</i> , <i>snap33-1 coi1-34</i> , <i>snap33-1 ein2-1</i> , <i>sid2-2</i> , <i>coi1-34</i> and <i>ein2-1</i>	p72
Figure 2.16.	Phenotypic and molecular analyses of <i>snap33-1 sid2-2</i> plants	p73
Figure 2.17.	Morphological phenotypes of WT-1, <i>snap33-1</i> , <i>snap33-1 sid2-2 coi1-34</i> , <i>snap33-1 sid2-2 ein2-1</i> , <i>snap33-1 coi1-34 ein2-1</i> , <i>sid2-2 coi1-34</i> , <i>sid2-2 ein2-1</i> , and <i>coi1-34 ein2-1</i>	p74
Figure 2.18.	Morphological phenotypes of WT-1, <i>snap33-1</i> , <i>snap33-1 P35::NahG</i> and <i>P35::NahG</i>	p75
Figure 2.19.	Morphological phenotypes of WT-1, <i>snap33-1</i> , <i>snap33-1 npr1-1</i> and <i>npr1-1</i>	p76
Figure 2.20.	Morphological phenotypes of WT-1, <i>snap33-1</i> , <i>snap33-1 fmo1-1</i> , and <i>fmo1-1</i>	p76
Figure 2.21.	Morphological phenotypes of WT-1, <i>snap33-1</i> , <i>snap33-1 ndr1-1</i> , <i>snap33-1 eds1-2</i> , <i>snap33-1 ndr1-1 eds1-2</i> , and <i>ndr1-1 eds1-2</i>	p77
Figure 2.22.	Morphological phenotypes of WT-1, <i>snap33-1</i> , <i>snap33-1 amsh3-4</i> and <i>amsh3-4</i>	p78
Figure 2.23.	Morphological phenotypes of WT-1, <i>snap33-1</i> , <i>snap33-1 tn2-1</i> , <i>tn2-1</i> , <i>snap33-1 cpk5-1</i> and <i>cpk5-1</i>	p79
Figure 2.24.	<i>snap33-1</i> 's transcriptome displays similarity to other lesion-mimic mutants	p81
Figure 2.25.	<i>snap33-1</i> 's transcriptome displays similarity to an ETI-response transcriptome	p82
Figure 2.26.	Working model for events occurring in the <i>snap33-1</i> mutant	p83
Figure 3.1.	MEKK1, MKK2, MPK4, and SNAP33 expression in different perturbation studies	p85
Figure 3.2.	MEKK1, MKK2, MPK4, and SNAP33 expression at different plant developmental stages and in different plant tissues or organs	p86
Figure 3.3.	The protein sequence and domain organization of SNAP33 and the post-translational modifications (PTMs) identified on SNAP33	p87
Figure 3.4.	Interactions of SNAP33	p88
Figure 3.5.	SNAP33 interacts with MEKK1, MKK2, and MPK4 in BiFC assay	p89
Figure 3.6.	SNAP33 does not interact with MEKK1, MKK2, nor MPK4 in yeast two-hybrid assay	p90
Figure 3.7.	<i>In vitro</i> pull-down assay does not allow concluding on the interaction between SNAP33 and MPK4	p90
Figure 3.8.	SNAP33 does not interact with MPK4 and MKK2 by <i>in vivo</i> co-IP assays	p91
Figure 3.9.	GST-SNAP33 is not phosphorylated by MPK3, MPK4, and MPK6 <i>in vitro</i>	p92
Figure 3.10.	SNAP33-STREP is not phosphorylated by MPK3, MPK4, and MPK6 <i>in vitro</i>	p93
Figure 3.11.	GST-SNAP33 and SNAP33-STREP are not phosphorylated by MPK4, and MKK2 proteins purified from protoplasts	p93
Figure 3.12.	<i>sum2-8</i> mutation does not revert the phenotype of <i>snap33-1</i>	p94
Figure 3.13.	<i>smn1</i> mutation does not revert the phenotype of <i>snap33-1</i>	p95
Table 1.	Summary of the genotypes generated with <i>snap33-1</i> , with a brief description of their phenotype	p80
Table 2.	Mutant lines used in this study	p103
Table 3.	Cloning primers	p103
Table 4.	Genotyping primers	p105
Table 5.	RT-qPCR primers	p107
Table 6.	RT-PCR primers	p107
Table 7.	protoplasts' isolation and transformation solutions	p108

Table 8.	PCR mix	p109
Table 9.	Enzymes used for dCAPS analyses	p110

Abbreviations

μL	micro-Liter
μM	micro-molar
ACC	1-aminocyclopropane-1-carboxylic acid
ACS	1-aminocyclopropane-1-carboxylic acid (ACC) synthase
ADP	Adenosine diphosphate
ADR1	accelerated disease resistance 1
ALD1	AGD2-like defense response protein 1
AMSH3	associated molecule with the SH3 domain of STAM 3
ANAC	Arabidopsis NAC domain-containing transcription factor
ATP	Adenosine triphosphate
avr	avirulence
Aza	azelaic acid
BAK1	brassinosteroid insensitive 1 (BRI1)-associated kinase 1
BiFC	Bimolecular fluorescence complementation
BIK1	botrytis-induced kinase 1
CBP60g	CaM-binding protein 60-like g
CCV	clathrin-coated vesicles
CDPK	calcium-dependent protein kinase
CERK1	chitin-elicitor receptor kinase 1
CNL	coiled coil-NLR
COI-1	coronatine insensitive 1
Col-0	Columbia-0
CPK	calmodulin-domain protein kinase CDPK isoform
CTR1	constitutive triple response 1
DAB	3,3'-Diaminobenzidine
DAMP	damage-associated molecular pattern
DGDG	digalactosyl-diacylglycerol
DTT	dithiothreitol
EDS	enhanced disease susceptibility
EE	early endosome
EIL1	EIN3-like1
EIN	ethylene insensitive
EPS1	enhanced <i>Pseudomonas susceptibility</i> 1
ER	endoplasmic reticulum
ERF	ethylene response factor
ET	ethylene
ETI	effector-triggered Immunity
EXO	exocyst
Flg22	flagellin 22

FLS2	flagellin-sensing 2
FMO1	flavin monooxygenase 1
FW	Fresh weight
g	gram
h	hour
His	histidine
HR	Hypersensitive response
Hz	hertz
<i>i.e</i>	in other words
ICS	isochorismate synthase
ILV	intraluminal vesicles
IP	immuno-precipitation
JA	jasmonic acid
JAR1	jasmonate resistant 1
JAZ	jasmonate zim domain
kV	kilo Volt
l	liter
Ler	Landsberg erecta
LMM	lesion-mimic mutant
LOX	lipoxygenase
LV	lytic vacuole
M	molar
MAPK	mitogen-activated Protein Kinase
MAPKK	mitogen-activated Protein Kinase Kinase
MAPKKK	mitogen-activated Protein Kinase Kinase Kinase
MBP	myelin basic protein
mg	milligram
min	minute
ml	milli-liter
mM	milli-molar
MVB	multivesicular bodies
NADPH	nicotinamide adenine dinucleotide phosphate
NahG	salicylate hydroxylase
NDR1	non-specific disease resistance 1
NHP	N-hydroxypipicolinic acid
NLR	nucleotide-binding Leucine-rich repeat receptor
nM	nanomolar
NPR1	non-expresser of pathogenesis-related (PR) genes 1
NRG1	N-required gene 1
ORA59	octadecanoid-responsive Arabidopsis AP2/ERF59
P	proline
PAD	phytoalexin deficient

PAL	phenylalanine ammonia lyase
PAMP	pathogen-associated Molecular Pattern
PBS1	avirulence protein <i>Pseudomonas phaseolicola B</i> (AvrPphB)-susceptible 1
PBS3	aminotransferase avrPphB Susceptible 3
PCD	programmed cell death
PDF1.2	plant defensin 1.2
Pip	pipecolic acid
PM	plasma membrane
PMSF	phenylmethanesulfonyl fluoride
PRR	Pattern-recognition receptors
<i>Pst</i>	<i>Pseudomonas syringae</i>
<i>Pst</i> DC3000	<i>Pseudomonas syringae</i> pv. <i>tomato</i> (<i>Pst</i>) DC3000
<i>Pst</i> DC3000 <i>hrcC</i>	<i>Pseudomonas syringae</i> pv. <i>tomato</i> (<i>Pst</i>) DC3000 mutant defective in type III secretion of effectors
PTI	pattern-triggered Immunity
PTM	post-translational modification
PVC	prevacuolar compartment
R protein	resistance protein
RBOHD	respiratory burst oxidase protein D
RIN4	RPM1-interacting protein 4
RLCK	receptor like cytoplasmic kinase
RLK	receptor-like kinase
RLP	receptor-like protein
ROS	reactive oxygen species
rpm	revolutions per minute of rotor
RPM1	resistance to <i>Pseudomonas syringae</i> pv. <i>Maculicola</i>
RPP	resistance to <i>Peronospora parasitica</i>
RPP4	recognition of <i>Peronospora Parasitica</i> 4
RPS	resistance to <i>Pseudomonas syringae</i>
RRS1	resistance to <i>Ralstonia solanacearum</i> 1
RT	room temperature
s	second
S	serine
SA	salicylic acid
SAG101	senescence-associated gene 101
SAR	systemic acquired resistance
SARD	SAR deficient
SDS PAGE	sodium dodecyl sulfate polyacrylamide gel electrophoresis
SERK	somatic embryogenesis receptor kinases
SID	salicylic acid induction deficient
SNAP	soluble N-ethylmaleimide-sensitive factor (NSF) adaptor proteins
SNARE	soluble N-ethyl-maleimide sensitive factor attachment protein receptor

SNC1	suppressor of <i>npr1-1</i> , constitutive 1
SUMM2	suppressor of <i>mkk1 mkk2 2</i>
T	threonine
TF	transcription factor
TGN	trans-Golgi network
TNL	toll-interleukin-NLR
v	volume
VSP	vegetative storage proteins
Ws	Wassilewskija
WT	wild type
xg	Relative Centrifuge Force
Y2H	yeast-two-hybrid
ZAR1	HopZ-Activated resistance 1
α	anti

CHAPTER I – INTRODUCTION

About 12,000 years ago, humans created agriculture for sustainable food production. Since then, agricultural areas have expanded to reach about 38% of land surface to ensure a sustainable food supply for a rapidly growing population (Land Use in Agriculture by the Numbers, 2020).

Since the green revolution, plants have been selected for practical farming purposes and high yield; however, this has resulted in a decline in genetic diversity. Moreover, the majority of agro-ecosystems are planted in intensive monocultures. Together with a notable increase in the international trade of agricultural products, such practices have fueled the emergence of infectious plant diseases (Anderson et al., 2004). Plant diseases can have dire consequences on economic, social, and ecological scales. For example, the potato late blight, a disease caused by the oomycete *Phytophthora infestans*, was responsible for the potato famine in Europe in the 19th century and led to a large number of deaths and migrations in Ireland. Plant diseases cause approximately 20% to 40% yield loss in major crops (Savary et al., 2012). Several strategies have been adopted to tackle this issue, including the expansion of cultivated areas and elite variety breeding. Additionally, the green revolution generated an entire industry of chemical products used to control invading plants and pathogens. However, most of these approaches have proven to be effective only in the short term, as pathogens often quickly develop resistance under the powerful evolutionary constraint exerted by pesticides. Additionally, pesticides are damaging to the environment, and agricultural growth frequently occurs at the expense of forests, which significantly contribute to global warming (Martin, 2008).

Therefore, a better understanding of plants' interaction with microorganisms and their environment is a crucial step toward improving our agriculture to overcome future challenges that include managing the associated global food security and restraining the hazardous impact of agriculture on the environment.

***Arabidopsis thaliana*: a model species to understand the biology of angiosperms**

Since the 2000s, *Arabidopsis thaliana*, a member of the *Brassicaceae* family, has become a model for plant genetics and molecular biology research. *Arabidopsis*' relatively small genome (125 Mbp), small size, short life cycle (about eight weeks from germination to mature seed), and its ability to produce a large number of seeds by self-pollination make it a practical tool for genetic studies. It is easily transformable using the bacteria *Agrobacterium tumefaciens*,

initially identified as the causal agent of crown gall disease in plants. *Agrobacterium tumefaciens* possesses the unique ability to transfer a defined tumor-inducing DNA to eukaryotes and integrate it into the genome (Bourras et al., 2015). Replacing the tumor-inducing genes with exogenous DNA allows the introduction of any desired gene into the plant. Furthermore, Arabidopsis' genome has been sequenced (The Arabidopsis genome initiative, 2000) and extensive collections of mutants and public databases including genomic, proteomic, and functional data from previous analyses (e.g., TAIR and NASC) are available for the scientific community. Finally, its relative phylogenetic proximity with various widely cultivated species (rape, mustard, radish, turnip, cabbage, etc.) makes knowledge transfer from *A. thaliana* convenient for agronomical uses.

Context of my Ph.D. project

I have realized my Ph.D. at IPS2 (The Institute of Plant Sciences, Paris-Saclay, Orsay, France), in the Stress Signaling group (supervised by Jean Colcombet), a part of the Physiology and Signaling department. Our team's research is primarily focused on developing novel ways for better understanding the signaling processes of mitogen-activated protein kinase (MAPK) and calcium-dependent protein kinase (CDPK) modules in the context of stress responses. One of our chief goals is to unravel the roles of MAPKs and CDPKs during biotic and abiotic stresses and other processes, including seed germination.

Overview of the dissertation contents

In the Introduction (Chapter I), I provide an overview of the immune system of plants as it has been described throughout the pertinent literature concerning plant-pathogen interactions with a focus on results obtained for *A. thaliana*-*Pseudomonas syringae* plant-pathogen system. The respective roles of MAPKs and phytohormonal pathways in immunity are then explored in more depth. Finally, the role of membrane trafficking in immunity, with a particular focus on the soluble N-ethylmaleimide-sensitive-factor attachment protein receptor (SNARE) SNAP33, is reported. In the Results section (Chapter II.1), I present our findings on the characterization of the *snap33* mutant, with the main conclusion being that *snap33* has an auto-immune phenotype that mimics the phenotype of plants constitutively exposed to pathogens. In the second section of the Results (Chapter II.2), I explore a potential relationship between SNAP33 and two MAPK modules involved in immunity. We found that SNAP33 does not interact with the proteins of the MAPK module MEKK1-MKK2-MPK4 and is not a substrate of MPK3, MPK4,

and MPK6. Additionally, the phenotype of *snap33* was not reverted by any of the known suppressors of *mekk1*, *mkk1 mkk2*, and *mpk4* phenotypes. Therefore, our data suggest that SNAP33 and the MAPK module MEKK1-MKK2-MPK4 function independently, even though both are involved in immune responses.

1. Plant immunity: how plants detect the presence of pathogenic microbes and generate the immune response

As a source of nutrients to most species, plants are exposed to many pathogenic microorganisms ranging from bacteria, viruses, fungi, and oomycetes. Depending on how they extract nutrients from plants, pathogenic microorganisms are divided into three categories, namely biotrophs, hemibiotrophs, and necrotrophs. While biotrophs thrive on living tissues by blocking host defenses and sustaining feeding processes, necrotrophs degrade the plant cell-walls using hydrolytic enzymes and feed on dead tissues. Hemibiotrophs exhibit an in-between pattern where they start as biotrophs and then end up killing the plant cells (Glazebrook, 2005). Plants have developed several complex mechanisms to fight off pathogenic microbes. These mechanisms include constitutive defenses mediated by preformed physical barriers and phytoanticipins, which prevent pathogen entry, and inducible defenses, which are activated by sensing the presence of the pathogen by specialized receptors.

Constitutive defenses

Epidermal cells, which make the outermost cell layer of plants, are overlaid with a waxy cuticle. Then, all plant cells are interlocked in a complex cell wall matrix, which pathogens must navigate through to access the host cells' plasma membrane (PM) (Ziv et al., 2018). The apoplast, the space between cell walls and the PM, is physiologically inhospitable for microbial pathogens. Indeed, plants constitutively synthesize precursors of phytoanticipins, such as glucosinolates and saponins in the apoplast (Piasecka et al., 2015). Upon detection of pathogens, phytoanticipins are converted to antimicrobial compounds to ward off pathogens (Piasecka et al., 2015). These barriers drastically decrease the number of possible entry points for pathogens. However, some pathogens developed several strategies to overcome the physical barriers of plants. For instance, fungal pathogens employ specialized infection structures, called appressoria, to generate a focused turgor pressure and penetrate the cell wall (Ryder & Talbot, 2015). Bacteria use natural openings such as stomata and hydathodes to

penetrate the intercellular space of plants (Huang, 2003). Necrotrophic pathogens, on the other hand, degrade host cell walls by producing a cocktail of cell wall-degrading enzymes (Rodriguez-Moreno et al., 2018; Wilson, 2008), and viruses enter plant cells through wounds (Gergerich & Dolja, 2006).

Inducible defenses

A pathogen that successfully breaches the physical barriers encounters a whole other complex immune system including receptors, signaling components, hormones, and resistance proteins, all contributing to the thickening of cell walls by the secretion of callose/papillae, to the secretion of antimicrobial compounds, and eventually to localized programmed cell death (PCD) aimed at limiting the pathogen to the infected area. All these processes require a coordinated response of the plant and fine-tuned regulations to induce an adequate response.

The inducible immune system of plants has been described as two-layered (Jones & Dangl, 2006). The first layer relies on PM-resident receptor-like kinases (RLKs) and receptor-like proteins (RLPs), which enable the detection of surrounding extracellular pathogens. Pattern-recognition receptors (PRRs), RLKs and RLPs, recognize pathogen-associated molecular patterns (PAMPs), which represent a molecular signature among a class of microbes, including specific proteins, lipopolysaccharides, and pathogen-associated cell wall components commonly found in microbes (Zhang et al., 2010). Upon detecting PAMPs, RLKs and RLPs trigger a pattern-triggered immune response, termed pattern-triggered immunity (PTI) (Jones & Dangl, 2006).

In the second layer, the recognition of microbes occurs in the intracellular space by specific receptors, commonly known as resistance (R) proteins, and was developed against more adapted pathogens that can secrete virulence factors, also known as effectors inside the host's cells. Although effectors are initially intended to suppress PTI (Toruño et al., 2016), plants can sense their presence, through R proteins, and induce an immune response. This second effector-mediated immune response, termed effector-triggered immunity (ETI), was developed by repeated exposure to the above-described virulent pathogens (Jones & Dangl, 2006). ETI and PTI share several signaling components and responses; however, the former is more intense and long-lasting (Tsuda & Katagiri, 2010).

Although previously described as independent, PTI and ETI share several responses and signaling pathways (Tsuda & Katagiri, 2010). In addition, recent studies indicate that the

components of the two layers of immunity cooperate to initiate an efficient immune response (more detail will be provided in section 1.2.6) (Yuan et al., 2021).

1.1. PATTERN-TRIGGERED IMMUNITY (PTI)

1.1.1. *PRRs: the main players of PTI*

As stated above, PRRs recognize PAMPs, which represent a molecular signature among a class of microbes (Yu et al., 2017). PRRs can be RLKs or RLPs depending on the nature of their intracellular domain, which mediates downstream signal transduction (Macho & Zipfel, 2014; Zipfel, 2008). Additionally, each PRR contains a specific ligand-binding extracellular domain (Wan et al., 2019). Based on the structure of the extracellular domain, RLPs and RLKs have been further classified into several types, including leucine-rich repeat (LRR) receptors, lysine motifs (LysM) receptors, lectin-domain receptors, and others (Wan et al., 2019). Examples of LRR receptors include the RLK flagellin-sensing 2 (FLS2), which binds an N-terminal 22-amino acid epitope of bacterial flagellin (flg22) (Chinchilla et al., 2006), and the RLP, RLP23, which recognizes the Necrosis and ethylene-inducing peptide 1-like protein (NLP) 20 (nlp20), NLPs are found in a wide range of bacteria, fungi, and oomycetes (Albert et al., 2015). Examples of LysM extracellular domain receptors include the chitin sensors chitin-elicitor receptor kinase 1 (CERK1) and the lysin motif receptor kinase 5 (LYK5) (Cao et al., 2014; Liu et al., 2012). Upon detecting the related PAMPs, PRRs transduce the signal from the cell surface to the intracellular compartments to generate a PTI. PTI can also be induced and amplified by damage-associated molecular patterns (DAMPs) produced by the plant as a result of pathogen-induced cell wall breakdown. DAMPs are detected by certain PRRs, which trigger additional downstream responses (Hou et al., 2019). For example, pectin fragments or oligogalacturonides (OGs) derived from the degradation of cell walls are recognized by the PRR wall-associated kinase 1 (WAK1), which subsequently activates a PTI (Brutus et al., 2010). The DAMP Plant elicitor peptide 1 (Pep1), a 23-amino acid peptide generated from the precursor protein PROPEP1, is recognized by the (LRR) RLK perception of the Arabidopsis danger signal peptide 1 (PEPR1), which subsequently induces defense responses (Huffaker et al., 2006; Krol et al., 2010).

1.1.2. *Signaling downstream of PRRs*

Upon PAMP binding, RLKs and RLPs dimerize or associate with other receptors such as somatic embryogenesis receptor kinases (SERKs) and activate downstream receptor-like cytoplasmic

kinases (RLCKs) to trigger downstream responses (Macho & Zipfel, 2014). For example, the chitin receptor CERK1 forms a complex with ligand-binding receptor LYK5 and activates RLCK VII proteins to activate downstream signaling (Rao et al., 2018).

A well-documented PRR example is the perception of bacterial flagellin by the receptor FLS2 (Chinchilla et al., 2006). The flg22–FLS2 ligand-receptor interaction has been used as a model to decipher early signaling events occurring downstream of PAMP perception.

In the absence of flg22, FLS2 is associated with the receptor-like cytoplasmic kinase (RLCK) botrytis-induced kinase 1 (BIK1) (Lu et al., 2010). Immediately upon flg22 perception, FLS2 forms a PRR complex with brassinosteroid insensitive 1 (BRI1)-associated kinase 1 (BAK1/SERK3) (Chinchilla et al., 2007). Following that, BAK1 phosphorylates BIK1, which in turn phosphorylates FLS2 and BAK1 (Lu et al., 2010). This results in the dissociation of BIK1 from the FLS2-BAK1 PRR complex and enables BIK1 to trigger the generation of reactive oxygen species (ROS) via phosphorylation of the PM nicotinamide adenine dinucleotide phosphate (NADPH) oxidase known as respiratory burst oxidase homolog D (RBOHD) (figure 1.1) (Kadota et al., 2014; Li et al., 2014).

Signaling downstream of PRRs involves several intermediates, the earliest being Ca^{2+} and ROS (Couto & Zipfel, 2016). Following that, MAPKs and CDPKs transduce the signal to multiple intracellular defense responses, including a transcriptional reprogramming which is crucial for launching a robust and effective defense response (Tena et al., 2011) (figure 1.1). Several other components are involved in signaling during PTI and are discussed in detail by Bigeard et al. (2015) The recognition of PAMPs or DAMPs by their cognate PRRs results in transcriptional reprogramming of a set of common genes with distinct temporal dynamics. In fact, numerous genes are commonly increased by treatment with flg22 or fungal chitin or with OGs (Denoux et al., 2008). Thus, it is likely that various MAMPs/DAMPs trigger similar signaling pathways that result in similar transcriptional modifications with different dynamics and amplitude (Cole & Tringe, 2021).

Calcium Ca^{2+}

Almost immediately after flg22 perception, a Ca^{2+} influx occurs in the cytosol (Yuan et al., 2017). BIK1 operates as an effector kinase in several PRR complexes and is necessary for flg22-induced cytosolic Ca^{2+} increase and stomatal closure (Couto & Zipfel, 2016; Li et al., 2014). Recent investigations have demonstrated that BIK1 directly activates Ca^{2+} channels during PTI. Upon

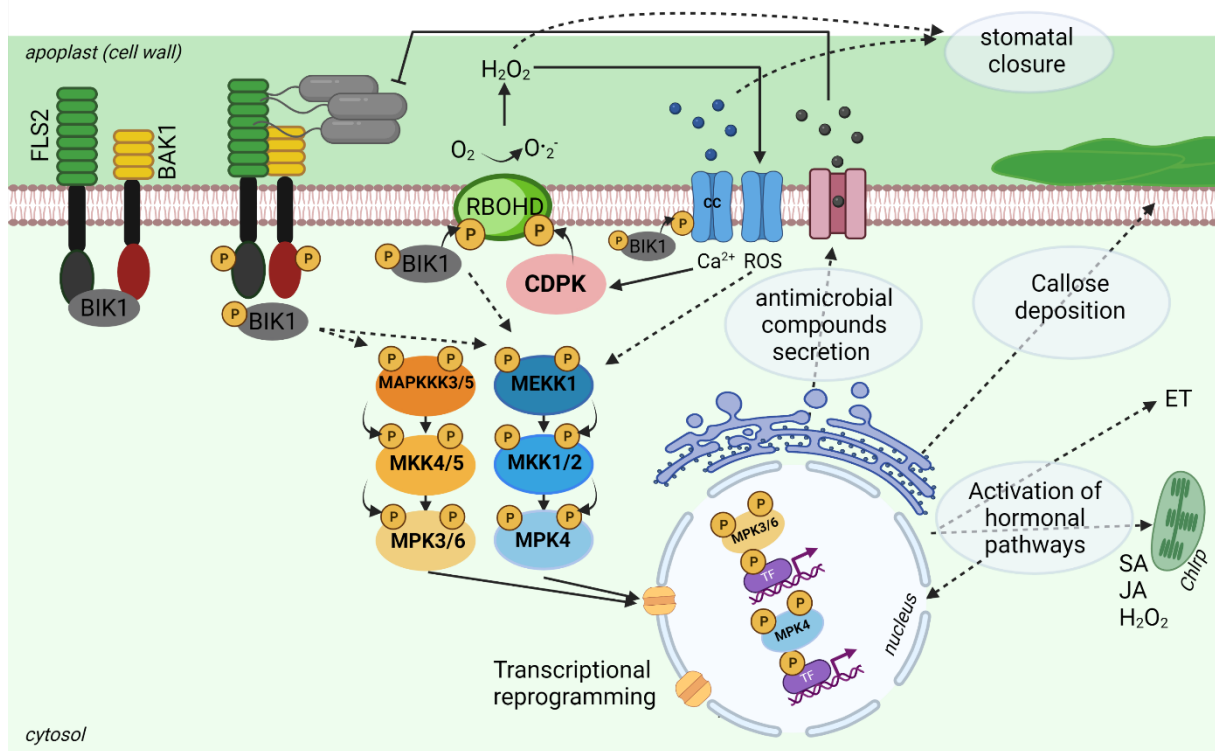


Figure 1.1. Schematic view summarizing the cellular and physiological events occurring during PTI in response to PAMP elicitation using the flg22-FLS2 PAMP/RLK model. At resting conditions, FLS2 is associated with the RLCK BIK1. Immediately upon flg22 detection, FLS2 associates with BAK1, and the complex is phosphorylated by BIK1. BIK1 then dissociates from the PRR complex and subsequently phosphorylates downstream components to trigger ROS burst, Ca^{2+} influx, and MAPK activation. Ca^{2+} influx activates CDPKs and induces a conformational change of RBOHD. CDPKs phosphorylate RBOHD and other downstream targets such as transcription factors (TFs) and contribute to the transcriptional reprogramming occurring in PTI. Two MAPK modules are activated in response to flg22: MAPKKK3/5-MKK4/5-MPK3/6 and MEKK1-MKK1/2-MPK4, MPK3, MPK4, and MPK6 phosphorylate downstream TFs and other substrates to activate transcriptional reprogramming and hormonal pathways of mainly SA, JA, and ET. Ultimately, these regulations lead to the production and secretion of antimicrobial metabolites and proteins, callose deposition to reinforce cell walls, and stomatal closure to limit pathogen entry. CC: calcium channels; Chltp: Chloroplast; TF: transcription factor; SA: salicylic acid; JA: jasmonic acid; and ET: ethylene. Solid arrows indicate direct effects, while dashed arrows indicate indirect effects.

flg22 treatment, BIK1 phosphorylates the cyclic nucleotide-gated channel (CNGC) CNGC4 to activate the calcium channel formed by CNGC4 and CNGC2 (Tian et al., 2019). The calcium-permeable-channel OSCA1.3 is also activated by BIK1 in a kinase activity-dependent way to initiate a Ca^{2+} influx (Thor et al., 2020). Additionally, it was demonstrated that OSCA1.3 and its phosphorylation by BIK1 are critical for flg22-induced stomatal closure (Thor et al., 2020). As a result of these findings, BIK1 appears to be the link between pathogen sensing by PRRs and calcium signaling. The increase in cytosolic Ca^{2+} concentration is associated with PM depolarization and extracellular alkalization by an influx of H^+ and efflux of Cl^- , NO_3^- , and K^+ (Jeworutzki et al., 2010). Calcium influx activates many calcium sensors, including CDPKs, calmodulins (CaMs), calcineurin B-like (CBs), and calcium- and calmodulin-dependent protein kinases (CCaMKs) (Boudsocq & Sheen, 2013). These sensors trigger various reactions, including gene expression and enzyme activity (Boudsocq & Sheen, 2013). CDPKs promote defenses in response to a range of PAMPs and DAMPs, including flg22 and OGs, mainly through phosphorylation of substrates such as transcription factors (TFs) and proteins involved in hormone processes (Yip Delormel & Boudsocq, 2019). Notably, CPK4, CPK5, CPK6, and CPK11 phosphorylate RBOHD to induce ROS accumulation in response to flg22 recognition (Boudsocq et al., 2010; Dubiella et al., 2013; Gao et al., 2013; Kadota et al., 2014). The *cpk5 cpk6* double mutant and the *cpk5 cpk6 cpk11* triple mutant show a compromised immune response to *Pseudomonas syringae* pv. *tomato* (*Pst*) DC3000 (Boudsocq et al., 2010). Conversely, transgenic lines overexpressing *CPK5* (*P35::CPK5*) showed enhanced resistance to *Pst* DC3000 (Dubiella et al., 2013). Interestingly, a recent study discovered that the phosphorylation of the chitin-binding PRRs LYK5 and LYK6 by CPK5 and CPK6 is required to activate immune responses downstream chitin perception (Huang et al., 2020). This work demonstrates that CPK5 and CPK6 are engaged in early signaling, at the PRR level, during PTI.

ROS

ROS regulate various physiological responses in plants (Manna et al., 2019). Although ROS are produced in several subcellular organelles, including chloroplasts, mitochondria, and peroxisomes, most of the research on PTI-induced ROS was focused on ROS produced by the plasma membrane RBOHs (Janků et al., 2019). Besides being phosphorylated by BIK1 and CDPKs, RBOHD undergoes direct regulations by Ca^{2+} . Indeed, Ca^{2+} ions bind to the N-terminal region of RBOHD and induce a conformational change on its EF-hand motifs (Ogasawara et al.,

2008). Phosphorylation by BIK1 and CDPKs and Ca^{2+} regulations on RBOHD are required for its activity (Ogasawara et al., 2008).

Few minutes after PAMP perception, a ROS burst mediated by RBOHD is detected after approximately 2 minutes (min) and reaches a peak after about 10 min (Nühse et al., 2007). RBOHD produces membrane-impermeable superoxide $\text{O}_2^{\cdot-}$ ions in the apoplast. $\text{O}_2^{\cdot-}$ is then dismutated into membrane-permeable hydrogen peroxide, H_2O_2 , which can be relocated to the cytosol and organelles to trigger cellular responses (Suzuki et al., 2011) (figure 1.1). ROS accumulation in the cytosol leads to an altered cell's redox state, which is believed to trigger the oxidation of components of hormonal signaling pathways, thus modifying their activity (Noctor et al., 2018). As an example, the modified redox state of the cell during pathogen infection contributes to the activation of non-expressor of pathogenesis-related (PR) genes 1 (NPR1), a key protein in salicylic acid (SA) signaling (Mou et al., 2003). In response to PAMPs, RBOHD-dependent ROS generation induces callose deposition to reinforce cell walls and stomatal closure to prevent further pathogen entrance (Kadota et al., 2014; Liu & He, 2016).

MAPKs

MAPK modules are generally cascades of at least three proteins: a mitogen-activated protein kinase kinase kinase (MAPKKK), a mitogen-activated protein kinase kinase (MAPKK), and a MAPK, which are hierarchically activated via a cascade of phosphorylation (Widmann et al., 1999) (see CHAPTER 1.2 for more details). Two MAPK modules were characterized as instrumental in response to flg22: the module involving MAPKKK3/5-MKK4/5-MPK3/6 and the module involving MEKK1-MKK1/2-MPK4 (Gao et al., 2008; Sun et al., 2018). The events which occur between PRR activation and MAPK modules activation remained obscure until the recent identification of a family of RLCKs termed RLCK VII, which directly activate MAPK modules by phosphorylation. In fact, Bi and his colleagues showed that members of RLCK VII phosphorylate MEKK1 and MAPKKK5 on Ser603 and Ser599, respectively, and these phosphorylations are required for the activation of MPK4 and MPK3/6, respectively (Bi et al., 2018).

In response to PAMPs, MPK3, MPK4, and MPK6's activation is fast and transient, with a peak at 15 min after elicitation (Nühse et al., 2000). Numerous studies have been conducted on MPK3, MPK4, and MPK6 and their respective modules to understand the role of MAPKs in immunity. MAPK activation triggers reprogramming of gene expression and enzymatic regulations chiefly by phosphorylation of downstream substrates (Frei dit Frey et al., 2014; Lee et al., 2015;

Rayapuram et al., 2018; Tena et al., 2011). In fact, up to 36% of the flg22-upregulated genes and 68% of the flg22-downregulated genes were affected in at least one of the MAPK mutants *mpk3*, *mpk4*, and *mpk6* (Frei dit Frey et al., 2014).

An example that illustrates the role of MAPKs in PTI responses is the regulation of the WRKY33 transcription factor involved in camalexin production. WRKY33 forms a nuclear complex with MPK4 and the MAP kinase substrate 1 (MKS1) in resting conditions. After PAMP perception, MPK4 phosphorylates MKS1 and triggers the release of WRKY33 from the complex, which will subsequently activate the transcription of defense-related genes (Andreasson et al., 2005; Qiu et al., 2008). WRKY33 is also dually regulated by the CDPKs CPK5 and CPK6, and the MAPKs MPK3 and MPK6 to increase its DNA binding and transactivation activity, respectively, in response to *Botrytis cinerea* infection (Mao et al., 2011; Zhou et al., 2020). Active WRKY33 is recruited on a conserved W-box sequence in the promoters of numerous genes, including the phytoalexin-dependent 3 (PAD3) encoding for the cytochrome P450 monooxygenase 71B15 (CYP71B15) required for the final step of the biosynthesis of the antimicrobial compound camalexin (Mao et al., 2011; Qiu et al., 2008; Zhou et al., 2020). The WRKY33 example demonstrates that MAPKs and CDPKs share common substrates, which is consistent with previous transcriptomic studies that found a shared list of MAPKs and CDPKs-regulated genes (Boudsocq et al., 2010).

Hormones

Extensive studies on *Arabidopsis* and *Nicotiana tabacum* have shown that SA, jasmonic acid (JA), and ethylene (ET) are the main hormones that regulate immunity (Bürger & Chory, 2019; Pieterse et al., 2012). SA is generally assumed to trigger local and systemic responses to ward off biotrophic pathogens, while JA and ET pathways are rather employed against necrotrophic pathogens (Glazebrook, 2005; Thomma et al., 2001) More details on hormonal pathways are provided in Chapter I.3.

SA is produced in response to elicitation by flg22 and is associated with the accumulation of the antimicrobial PR proteins. Disruption of SA signaling impacts the expression of a subset of PAMP-induced genes (Tsuda et al., 2009). SA, in conjunction with N-hydroxy pipecolic acid (NHP), contribute to the establishment of systemic acquired resistance (SAR) to protect distant uninfected tissues (Gao et al., 2015). Indeed, PAMP treatment was shown to induce SAR (Mishina & Zeier, 2007). Interestingly, CPK5 was reported to be involved in the induction of

SAR upstream of SA and NHP (Guerra et al., 2020). In fact, the expression of several SAR-markers was altered in the *cpk5* mutant, and NHP levels are increased in transgenic lines overexpressing *CPK5* (Guerra et al., 2020).

ET biosynthesis is also induced in response to PAMPs and pathogens (Guan et al., 2015a). ET biosynthetic enzymes 1-aminocyclopropane-1-carboxylic acid (ACC) synthase 2 (ACS2) and 6 (ACS6) are stabilized by the phosphorylation by MPK6 in response to flg22 (Liu & Zhang, 2004). Later it was shown that the MAPKs, MPK3, and MPK6 activate the expression of *ACS2* and *ACS6* genes via WRKY33 TF and promote the stability of *ACS2* and *ACS6* by phosphorylation as well (Li et al., 2012). *ACS2*, *ACS6*, and ET levels are lower in the *cpk5 cpk6* double mutant in response to PAMPs and *Botrytis cinerea* infection indicating that CDPKs also play an essential role in ET biosynthesis (Gravino et al., 2015). The role of ET in PTI was also demonstrated by the observation that the ethylene-insensitive 2 (*ein2*) mutant exhibits a reduced ROS burst and callose deposition in response to flg22 compared to wild-type (WT) plants (Tintor et al., 2013). Although Nomura and colleagues reported no significant change in JA levels in response to flg22 (Nomura et al., 2012) and despite the fact that JA and SA are thought to act antagonistically against biotrophic and necrotrophic pathogens in plants, subsequent work using combinatorial mutants of the SA, JA, and ET hormonal sectors demonstrated that the JA pathway is required for a robust response to flg22 (Kim et al., 2014; Tsuda et al., 2009). Additionally, the SA, JA, and ET sectors, and a defense sector depending on phytoalexin-deficient 4 (*PAD4*), which is engaged in SA signaling and has an immune role independent of SA, account for approximately 80% of flg22-induced responses (Glazebrook et al., 2003; Kim et al., 2014). In the *dde2 ein2 pad4 sid2* quadruple mutant in which the four signaling sectors SA, JA, ET, and *PAD4* are all disrupted, MAPK activation was not significantly changed in response to flg22, showing that the signaling network defined by SA, JA, ET, and *PAD4* sectors mainly control late PTI responses (Tsuda et al., 2009); *DDE2* and *SID2* are essential for JA and SA biosynthesis in response to pathogen attack, respectively (Park et al., 2002.; Wildermuth et al., 2001).

1.2. EFFECTOR-TRIGGERED IMMUNITY (ETI)

1.2.1. *ETI, the second layer of defense against more adapted pathogens*

PTI is a critical and effective layer of defense, which has prompted numerous pathogens to develop strategies to circumvent it (Asai & Shirasu, 2015; Hogenhout et al., 2009). Adapted bacteria use the type III protein secretion system to release virulence proteins called effectors that suppress or alter plant defensive responses by disrupting components of PTI and successfully invade the host (Asai & Shirasu, 2015; Galán et al., 2014). Filamentous pathogens release effectors via feeding structures called haustoria, which are extensions of their hyphae inserted into host cells to form a biotrophic interface termed the extrahaustorial matrix (Giraldo & Valent, 2013).

When a pathogen successfully suppresses the host's defenses, the outcome of the plant-pathogen interaction is referred to as effector-triggered susceptibility (ETS), and the effector is referred to as a virulence factor (Jones & Dangl, 2006). It has been postulated that through repeated exposure to the pathogen, plants evolved and developed the ability to detect the presence of effectors via intracellular receptors, which activate an immune response termed effector-triggered immunity (ETI) (Han, 2019; Jones & Dangl, 2006). The effectors herein are referred to as avirulence (Avr) factors because they promote resistance in the host (Flor, 1971). Pathogens, on the other hand, are continually evolving too in order to prevent the recognition of their effectors by the host. This evolutionary arms race between plants and pathogens was described by Jones & Dangl as the Zig-Zag model describing the co-evolutionary interactions between the pathogen and the host leading to the dominance of one of the two organisms over the other (Jones & Dangl, 2006). ETI triggers similar responses as those observed during PTI (Peng et al., 2018). However, they are more intense and last longer than PTI (Tsuda & Katagiri, 2010). In addition, ETI is usually accompanied by a programmed cell death (PCD) surrounding the infection site, also termed hypersensitive response (HR). The PCD aims to restrict the pathogen to infected cells to prevent further invasion (Wu et al., 2014).

1.2.2. *Resistance proteins: the main players of ETI*

ETI relies on cytoplasmic receptors referred to as R proteins which recognize effector proteins and activate the second layer of plant immune responses (Wu et al., 2014). Resistance genes

generally encode for nucleotide-binding leucine-rich repeat (NLR) proteins, comprising a central nucleotide-binding (NB) domain and a C-terminal leucine-rich repeats (LRRs) domain. NLR genes belong to a large, conserved, and rapidly evolving family of genes. For instance, a range of 167 to 251 NLR genes per accession were annotated in *Arabidopsis*, and 571 in *Medicago truncatula* (Shao et al., 2016; Van de Weyer et al., 2019). NLR genes fall into two major classes of proteins, the TIR-NLR (TNLs) class, and the CC-NLR (CNLs) class. The two classes are differentiated by their N-terminal domain, either containing a Toll-interleukin-1 receptor (TIR) or a coiled-coil (CC) domain. Intriguingly, the TNL class of NLRs lacks in monocotyledonous plants (Shao et al., 2016). Recent studies revealed a small, distinct, very conserved class of NLRs with resistance to powdery mildew 8 (RPW8) and CC containing N-terminal domain (Shao et al., 2016). Two other classes of NLR proteins with extra domains or truncated structures lacking the LRR or NB domain were also discovered (Cesari, 2018).

Based on the earliest studies, it was considered that each R gene confers resistance to a specific pathogen by directly interacting with an effector in a ligand-receptor pattern, a phenomenon referred to as gene-for-gene interaction (Biezen & Jones, 1998; Flor, 1971). While this is true in many cases, there are more examples of NLRs indirectly recognizing effectors than direct recognition. Moreover, recent findings report that one NLR engages other related and unrelated NLRs for downstream signaling (Nguyen et al., 2021).

1.2.3. *The guard and decoy model of effector perception by NLRs*

The guard model of effector perception

Indirect recognition of effectors by NLRs involves other proteins, usually involved in immunity and manipulated by the pathogen to increase disease. In this case, the R proteins/NLR monitor the integrity of the targeted protein and initiate an ETI upon modification of the target (figure 1.2). This recognition mechanism is commonly referred to as the guard model, in which an R protein guards the effector-targeted component (van der Hoorn & Kamoun, 2008). A well-known example of such a mechanism is the one involving resistance to *Pseudomonas syringae* pv. *Maculicola* (RPM1)-interacting protein 4 (RIN4). RIN4 is a negative regulator of plant immunity and is manipulated by *Pseudomonas syringae* effectors AvrB, AvrRpm1, and AvrRpt2 to alter the plant's immune response (Mackey et al., 2002). Two CNLs, namely RPM1 and resistant to *Pseudomonas syringae* 2 (RPS2), monitor RIN4 and activate defenses in

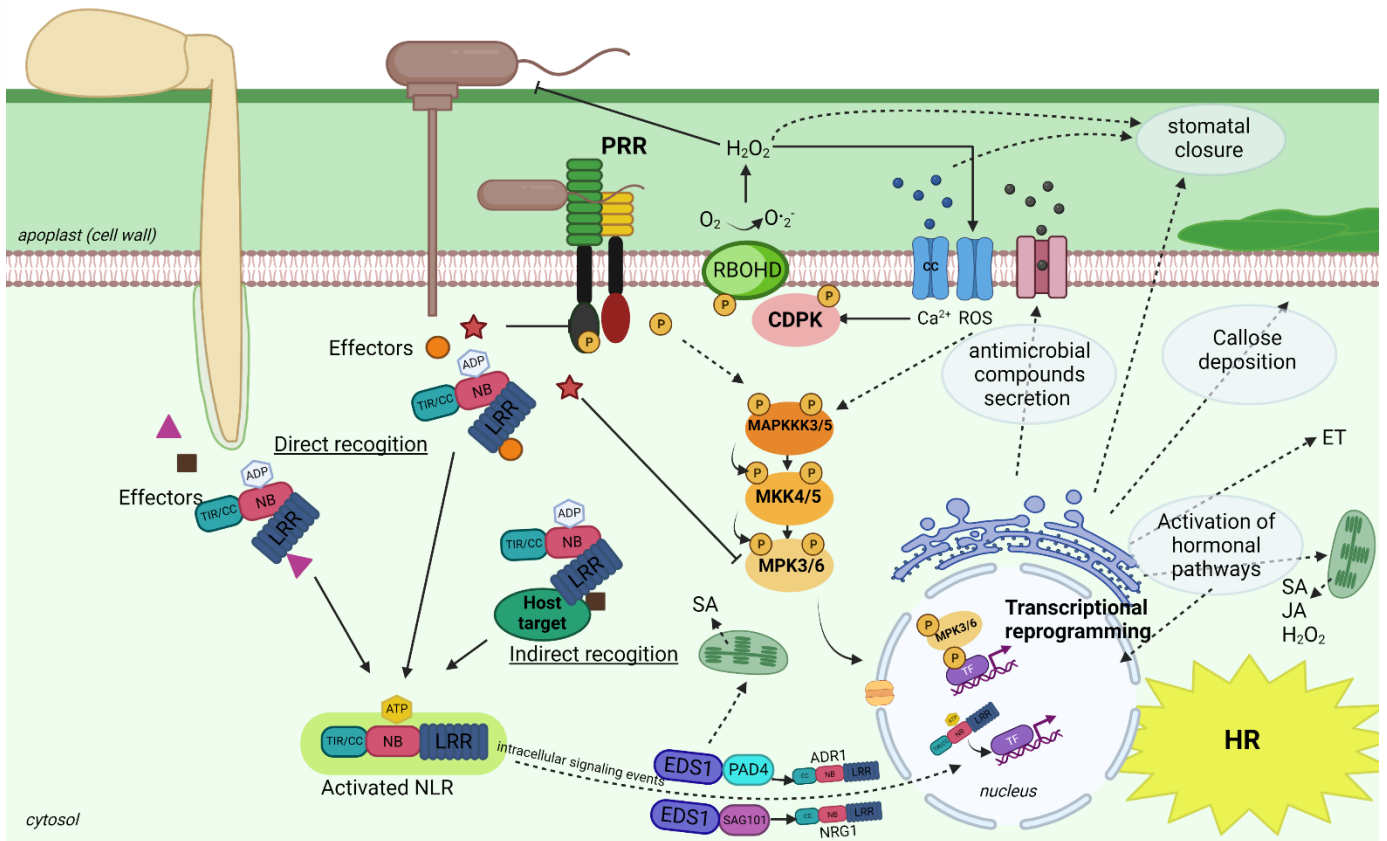


Figure 1.2. Schematic view of effector-triggered immunity (ETI) in plants. Several PTI signaling events occur upon PAMP recognition, such as activation of MAPK modules, Ca^{2+} influx into the cytosol, and production of ROS. Such events lead to transcriptional reprogramming, activation of hormonal pathways, antimicrobial compounds production, stomatal closure, and callose deposition. To suppress the PTI, pathogens secrete effectors inside the host cells, which inhibit PTI by targeting some of its components, such as MAPKs. When these effectors are recognized by nucleotide-binding (NB) and leucine-rich-repeat (LRR)- receptors (NLRs), the second immune layer, ETI, takes place. NLRs directly or indirectly perceive pathogenic effectors, leading to a conformational change and several intracellular signaling events involving EDS1, PAD4, SAG101, and the two helpers CC_R -NLRs NRG1 and ADR1, which trigger the hypersensitive response (HR) and other defense responses. CC: calcium channels; TF: transcription factors. Solid arrows indicate direct effects, and dashed arrows indicate indirect effects.

response to its altered state (Marathe & Dinesh-Kumar, 2003). AvrB and AvrRpm1 hyperphosphorylate RIN4 likely to suppress host defenses. The phosphorylated state of RIN4 is sensed by RPM1, which consequently triggers an ETI (Mackey et al., 2002). AvrRpt2, on the other hand, cleaves RIN4 which results in the activation of an RPS2-dependent immunity (Mackey et al., 2003). Mutation of *RIN4* causes lethality due to a constitutive induction of immunity by RPS2, and *rin4's* phenotype is rescued by *RPS2* knock-out mutations (Mackey et al., 2002, 2003).

The decoy model of effector perception

Decoy proteins are structurally similar to guarded proteins but seem to have no role in immunity other than being "baits" for pathogenic effectors to induce immunity. The decoy system is thought to widen the plant's spectrum of pathogen detection, resulting in a better defense against pathogens (Cesari, 2018; van der Hoorn & Kamoun, 2008). One example of such a mechanism is the one involving the decoy protein avirulence protein *Pseudomonas phaseolicola B* (AvrPphB)-susceptible 1 (PBS1). PBS1 is structurally similar to BIK1. BIK1 can be targeted and cleaved by the *Pseudomonas phaseolicola* effector AvrPphB to compromise resistance. PBS1 is also targeted by AvrPphB and triggers RPS5-mediated cell death (Shao et al., 2003). In this case, PBS1 is an RPS5-guarded decoy protein that enhances AvrPphB sensing and intensifies the plants' defense responses. Several other examples of guard and decoy examples are reviewed by Cesari, (2018) and Van Der Hoorn & Kamoun, (2008).

Another decoy strategy of effector recognition, termed the integrated decoy model, was reported. In this case, an NLR has an integrated decoy domain in its structure which was likely acquired throughout evolution (Cesari, 2018). The resulting protein is therefore self-monitored. One such example is the R protein resistance to *Ralstonia solanacearum* 1 (RRS1). RRS1 possesses a WRKY C-terminal domain which is acetylated by the *Ralstonia solanacearum* acetyltransferase effector PopP2. The acetylation of RRS1 impairs its DNA-binding ability and promotes RRS1 binding to another R protein, RPS4, which subsequently activates immune responses (Le Roux et al., 2015; Sohn et al., 2014).

1.2.4. Regulations of R proteins

Activation mechanism of NLRs

Effector recognition is hypothesized to induce a conformational change in NB-LRRs, blocking inhibition and releasing the NLR to activate downstream signaling (Collier & Moffett, 2009). The LRR domain is believed to be the interface by which the NLR senses changes in its direct environment and exerts an inhibitory activity in the absence of pathogenic effectors. The lack of inhibition by the LRR domain switches the NB domain from an inactive ADP-bound state to an active ATP-bound state (Collier & Moffett, 2009; Takken & Govere, 2012). The ATP-bound state opens the molecule to expose its N-terminal domains for interaction with downstream signaling components (Takken & Govere, 2012).

Oligomerization of NLRs

Some cases of NLRs homo- and hetero-oligomerization were reported to be required for activation of downstream signaling (reviewed by Chiang & Coaker, (2015) and Kapos et al., 2019)). The resulting complex is referred to as the "resistosome" (in reference to the formation of the inflammasome in the animal counterpart). One example of the heterodimerization of NLRs involves the CNL HopZ-Activated resistance 1 (ZAR1) (Wang et al., 2019). At resting conditions, ZAR1 interacts with the pseudo-kinase resistance-related kinase 1 (RKS1) via its LRR domain. ZAR1-RKS1 senses the uridylation of PBS1-like protein 2 (PBL2) by the effector AvrAC from the microbial pathogen *Xanthomonas campestris* pv. *campestris* (Xcc) (Wang et al., 2015). Upon uridylation, PBL2 interacts with ZAR1-RKS1 and induces a conformational change in ZAR1, leading to the release of ADP and the development of a ZAR1-RKS1-PBL2 complex (Wang et al., 2019). ATP binding causes a further conformational change within the NB domain of ZAR1, promoting the complex oligomerization required for disease resistance (Wang et al., 2019). Cryogenic electron microscopy analyses of the "resistosome" ZAR1-RKS1-PBL2 structure showed that the complex forms a funnel-like structure in the PM which was proposed to function as a calcium channel to initiate immune responses (Wang et al., 2019). Another example is the heterodimerization of the two TNLs, RPS4 and RRS1, via their TIR domains which is also required for effector recognition and signaling (Williams et al., 2014). In this case, RRS1 mediates the recognition of the effector, and RPS4 activates disease resistance (Sohn et al., 2014).

Regulation of NLRs' subcellular localization

While some NLRs, such as the rice NLRs RGA4 and RGA5, which mediate disease resistance against the fungal pathogen *Magnaporthe oryzae*, remain cytosolic in the presence of their cognate effector (Césari et al., 2014), other studies have shown that nuclear accumulation of NLRs is required for the induction of defense responses (Burch-Smith et al., 2007; Shen et al., 2007; Wirthmueller et al., 2007), which is mediated by the nucleocytoplasmic trafficking machinery (Cheng et al., 2009; Palma et al., 2005; Zhang & Li, 2005).

As an example, mutations of the nucleoporin modifier of c (SNC1) 7 (MOS7) strongly compromised the resistance mediated by the CNLs RPM1, and RPS5 and the TNLs SNC1 and recognition of *Peronospora Parasitica* 4 (RPP4) (Cheng et al., 2009). In the nucleus, SNC1 interacts with the transcriptional repressor topless-related protein 1 (TPR1). SNC1-TPR1 complex represses the negative regulators of immunity during ETI (Zhu et al., 2010).

Transcriptional regulation of NLRs

NLRs are also regulated at the transcriptional level (Kapos et al., 2019). Indeed, the binding sites of certain transcription factors involved in immunity, such as WRKYs, are enriched among NLR promoters (Mohr et al., 2010). For instance, the NLR RPS4 showed an increased expression in the presence of the effector AvrRps4 (Zhang & Gassmann, 2007) and several NLRs showed an induced expression upon exogenous SA application (Shirano et al., 2002). Furthermore, several studies have indicated that DNA methylation and histone modifications modulate the expression level of NLR-encoding genes. For instance, mutation of *MOS1* resulted in altered methylation in the promoter region of *SNC1* and suppression of the auto-immune phenotype of *snc1*, which otherwise constitutively expresses *SNC1* and displays an auto-immune phenotype (Li et al., 2015).

Some cases of post-transcriptional regulations are also required to induce immunity by some R proteins (Li et al., 2015). For example, in the case of RPS4, splicing mechanisms generate an active form of the R protein, which subsequently activates immune responses (Zhang & Gassmann, 2007).

1.2.5. Regulation of NLRs downstream signaling

Except for some examples of interactions between NLRs and transcription factors, the immediate downstream targets of activated R proteins remain largely unknown. Previous

studies have shown that, generally, nucleocytoplasmic, lipase-like related proteins enhanced disease susceptibility 1 (EDS1), PAD4, and senescence-associated gene 101 (SAG101) are genetically required for signaling downstream TNL-type of R proteins. Conversely, the integrin-like non-specific disease resistance 1 (NDR1) is genetically required for signaling downstream of CNLs (Aarts et al., 1998). While valid for some cases, recent studies reported that EDS1 is required for signaling downstream some CNLs, too (Bhandari et al., 2019). Moreover, recent studies placed EDS1-PAD4-SAG101 as a major NLR immunity signaling node (Lapin et al., 2019). Indeed, EDS1 hetero-dimerizes with PAD4 and SAG101 to form two distinct nodes which cooperate with two RNLs, respectively, accelerated disease resistance 1 (ADR1) and N-required gene 1 (NRG1) families. Indeed, two functionally redundant NRG1 paralogues (NRG1.1 and NRG1.2) and three redundant ADR1 paralogs (ADR1, ADR1-L1, and ADR1-L2) were shown to be engaged for signaling and for the induction of cell-death downstream several TNLs and CNLs, including RPS2, RPP1, RPP4, SNC1, RPM1 and RRS1/RPS4 (Bonardi et al., 2011; Castel et al., 2019; Jubic et al., 2019; Saile Id et al., 2020). These RNLs were therefore termed “helper NLRs” (figure 1.2). The *adr1 adr1-l1 adr1-l2* triple mutant was shown to suppress the auto-immune phenotype of *snc1*, and the auto-immune phenotype of the double mutant *bak1 bkk1* (BAK1-like 1 (BKK1) is the closest paralog of BAK1) (Dong et al., 2016; Wu et al., 2020). EDS1-SAG101 heterodimer forms a complex with NRG1-type helper RNLs to promote immunity downstream TNLs, whereas EDS1-PAD4 forms a complex with ADR1 helpers to promote CNL and TNL-triggered immunity (Dongus & Parker, 2021; Sun et al., 2020). Moreover, the EDS1-PAD4-ADR1 node transcriptionally activates an SA sector, which mediates local and systemic defenses in PTI (Dongus & Parker, 2021) (figure 1.2).

Another interesting finding in the realm of NLRs was recently described by Wan et al. and Horsefield et al., who demonstrated that TNLs display nicotinamide adenine dinucleotide (NAD) hydrolase activity, as similarly reported for their animal counterpart. This activity is required to induce cell death downstream effector recognition (Horsefield et al., 2019; Wan et al., 2019).

1.2.6. ETI outputs: a continuity of PTI responses?

As mentioned earlier, ETI displays similar responses as those observed during PTI. However, they are more intense and last longer compared to PTI (Jones & Dangl, 2006; Tsuda & Katagiri, 2010). For instance, MAPKs and CDPKs are activated transiently during PTI, but exhibit

sustained activity during ETI (Gao et al., 2013; Tsuda et al., 2013). ROS production also shows a different pattern during ETI. While fast and transient during PTI, ROS burst is biphasic, with a much stronger and more sustained second peak during ETI (Levine et al., 1994; Yuan et al., 2021). During infection, ROS accumulation triggers cell death by promoting cell wall structural proteins cross-linking and peroxidation of membrane lipids to disrupt the integrity of the membrane (O'Brien et al., 2012), and cell death is reduced in *Pst* DC3000-infected *rbohD* mutants compared to WT plants (Liu & He, 2016).

Much like in PTI, the hormones SA, JA, and ET play an essential role in ETI. In fact, using a combinatorial mutation approach, Tsuda et al. reported an additive effect of SA, JA, and ET in response to the effector AvrRpt2 and in response to flg22 (Tsuda et al., 2009). SA specifically promotes cell death during ETI (Dalio et al., 2021; Radojičić et al., 2018). It has been proposed that ROS activate SA signaling. SA, in turn, causes more ROS production by two mechanisms, inhibition of the respiratory chain in the mitochondria resulting in an electron flow imbalance and decreasing the amounts of antioxidant enzymes. These pathways result in a constant amplification cycle of SA-ROS, which causes cell death (Herrera-Vásquez et al., 2015).

Gene expression during PTI and ETI shows a substantial overlap, as demonstrated by the study of Navarro and coworkers, who showed that a large common set of genes are up-regulated in response to flg22 and in response to *Pseudomonas syringae* effectors AvrB and AvrRpt2 (Navarro et al., 2004). Although similar responses with different intensities were observed in both PTI and ETI, the mechanisms activating these responses during ETI were poorly understood. In a recent study, Ngou et al. showed that induction of ETI using the effector only does not activate ROS accumulation (Ngou et al., 2021). In this study, the authors used transgenic lines expressing the AvrRps4 effector, which is recognized by intracellular TNLs RRS1 and RPS4, under the control of an estradiol-inducible promoter. The application of estradiol alone did not lead to ROS accumulation in this line. However, when the same estradiol-inducible lines were treated with both estradiol and flg22, it led to an elevated ROS accumulation. Therefore, this study shows that ETI requires a potentiation by PTI to effectively activate immune responses (Ngou et al., 2021). Indeed, in the natural environment, plants are rarely exposed to an effector without also being exposed to the PAMP of the pathogen delivering the effector. In another recent study, Yuan et al. showed that surface-localized PRRs are necessary for the efficient activation of ETI (Yuan et al., 2021). By showing that PRR and co-

receptor mutants fail to mount an effective ETI in response to infection by ETI-eliciting *Pseudomonas* strain, thus the authors further validated the necessity of potentiation of ETI by PTI components. Overall, these studies show that ETI is more likely a continuity and an amplification of PTI against avirulent pathogens.

2. Mitogen-activated Protein Kinases (MAPKs): hubs with an essential role in immune signaling

Post-translational modifications (PTMs) are crucial mechanisms used by living cells to diversify the function of their proteome and coordinate their signaling networks (Barber & Rinehart, 2018). Phosphorylation is ubiquitous in eukaryotic cells and is believed to be one of the most common PTMs among eukaryotes (Olsen & Mann, 2013). One of the remarkable characteristics of phosphorylation is the ability to modify the chemical properties of phosphorylated amino acids, thus increasing chemical diversity on the surface of proteins (Johnson & Lewis, 2001). Consequently, phosphorylation mediates signaling by modifying proteins' structural conformation, enzymatic activity, stability, binding partners, and subcellular localization (Johnson & Lewis, 2001). In eukaryotic cells, protein kinases catalyze the transfer of the terminal phosphate group from ATP or GTP to the hydroxyl group of serine (S), threonine (T), or tyrosine (Y) residues (Fischer and Krebs, 1992). In Arabidopsis, 4% of the genome code for protein kinases (Arabidopsis Genome Initiative, 2000), and about 10% of those belong to the superfamily of MAPKs (Colcombet & Hirt, 2008). In eukaryotes, MAPKs form a highly conserved family of enzymes, and in plants, MAPKs are involved in biotic and abiotic stress signaling, development, and hormonal processes (Colcombet & Hirt, 2008). In the following sections, MAPK families present in Arabidopsis will be presented. Then, the regulatory mechanisms governing the activation and signaling of MAPK modules will be reported. In Section 3.3, I will first briefly address the techniques used to identify and study MAPK substrates, then the involvement of MPK3, MPK4, and MPK6 in plant immunity will be explored.

2.1. MAPKs in Arabidopsis

A conventional MAPK cascade involves three kinases: a MAPKKK (or MAP3K) which phosphorylates and activates a MAPKK (or MAP2K). An activated MAP2K activates a MAPK by phosphorylation as well (Widmann et al., 1999). Each MAPK phosphorylates its substrates on a unique conserved pattern of residues (figure 1.3).

Sequencing and annotation of the Arabidopsis genome allowed the identification of 20 genes coding for putative MAPKs, ten genes for putative MAP2Ks, and approximately 60 for putative MAP3Ks (Ichimura et al., 2002).

2.1.1. MAPKKKs

In Arabidopsis, the MAPKKK family is the biggest group of MAPKs, with a more extensive range of domain composition. The MAPKKK family is divided into three major classes. The first class of MAPKKKs is MEKK-like MAPKKKs, which contain similar kinases as those found in mammalian MEKKs and yeast MAPKKKs, such as AtMEKK1 (Ichimura et al., 2002; Jonak et al., 2002). The two other classes code for Raf-like kinases and ZIK-like kinases, which do not appear to be engaged in MAPK modules (Colcombet & Hirt, 2008). One of the best-studied Raf-like kinases is CTR1 (Constitutive Triple Response 1), involved in ethylene-mediated signaling and defense responses (Kieber et al., 1993).

In mammals, MAPKKKs are activated by autophosphorylation or phosphorylation of one or more serine or threonine residues, which can be mediated by MAPKKKK (MAP4K) (Widmann et al., 1999). Other mechanisms include interaction with small GTP-binding protein of the Ras or Rho family, oligomerization, and subcellular relocalization (Widmann et al., 1999). In plants, however, few studies have described mechanisms of MAP3K activation, and none of the 10 Arabidopsis MAP4Ks have been confirmed to control a MAPK pathway (Jonak et al., 2002).

Several studies, however, reported promising candidates upstream MAP3Ks. For instance, MEKK1-MKK2-MPK4/MPK6 MAPK module is regulated by the Calcium/calmodulin-regulated receptor-like kinase CRLK1 in response to cold stress (Yang et al., 2010). CRLK1 interacts with MEKK1 and is required to activate the MAPK module in response to cold (Yang et al., 2010). Moreover, CRLK1 phosphorylates MEKK1 *in vitro*, making it a good candidate for direct upstream activation of MEKK1 (Furuya et al., 2013). A family of RLCKs has recently emerged as direct upstream activators of MAPK modules in response to biotic stress. Genetic studies revealed that members of RLCK VII are required for activation of MAPK modules MAPKKK3/5-MKK4/5-MPK6/3 and MEKK1-MKK1/2-MPK4 in response to chitin, and PBL19, a RLCK VII-4 member, was shown to directly phosphorylate MAPKKK5 and MEKK1 in response to several PAMPs, including flg22 and chitin (Cui et al., 2018; Bi et al., 2018).

2.1.2. MAPKKs

MAP3Ks generally phosphorylate MAP2Ks on two amino acids on an S/T-X₅-S/T conserved motif in the activation loop (Ichimura et al., 2002) (figure 1.3). In Arabidopsis, only ten putative MAP2Ks have been identified compared to 60 and 20 MAP3K and MAPKs, respectively, suggesting that a single MAP2K can be involved in several MAPK modules (Andreasson & Ellis, 2010). Phylogenetic analysis of MAP2Ks shows four distinct groups. MKK1, MKK2, and MKK6 are members of Group A, of which MKK1 and MKK2 are functionally related to MPK4 and MEKK1 (Gao et al., 2008; Ichimura et al., 1998; Teige et al., 2004). Group C encompasses MKK4 and MKK5, which are functionally related to MPK3, MPK6, MAPKKK3, and MAPKKK5. MKK3 is the only member of group B, which is structurally distinct from all the other MAP2Ks, and group D, MKK7 to MKK10 are involved in several processes, including growth and stress response (Dóczi et al., 2019; Xin et al., 2018; Xu et al., 2008).

2.1.3. MAPKs

MAP2Ks phosphorylate MAPKs on threonine and tyrosine in a I-X-Y motif in their activation loop (Ichimura et al., 2002), and an active MAPK phosphorylates its substrates on an S/T-P motif (Ichimura et al., 2002) (figure 1.3). Phylogenetic studies and sequence comparisons classified plant MAPKs into four groups, A to D. A, B and C groups encompassing MPK3, MPK6, MPK10 (group A), MPK4, MPK5, MPK11, MPK12, MPK13 (group B), MPK1, MPK2, MPK7 and MPK14 (group C) are phosphorylated on a I-E-Y motif, whereas group D containing MPK8, MPK9, and MPK15 to MPK20 are phosphorylated on a I-D-Y motif. A, B, and C MAPKs have a common docking (CD) site which mediates the interaction with MAPKKs, substrates, and MAPK phosphatases and corresponds to the amino-acid sequence [LH][LHY]Dxx[DE]xx[DE]EPxC on their C-terminal region (Tanoue et al., 2000). On the other hand, most MAPKKs, MAPK phosphatases, and substrates bind MAPKs through a docking site (D-site) containing [K/R][K/R][K/R]x(1-5)[L/I]x[L/I] sequence that contributes to the specificity of the interaction (Bardwell et al., 2001). Additional docking domains in MAPK substrates have been found, including the DEF (docking site for ERK, EXFP) FxFP and the LxxRR amino-acid sequence (Biondi & Nebreda, 2003).

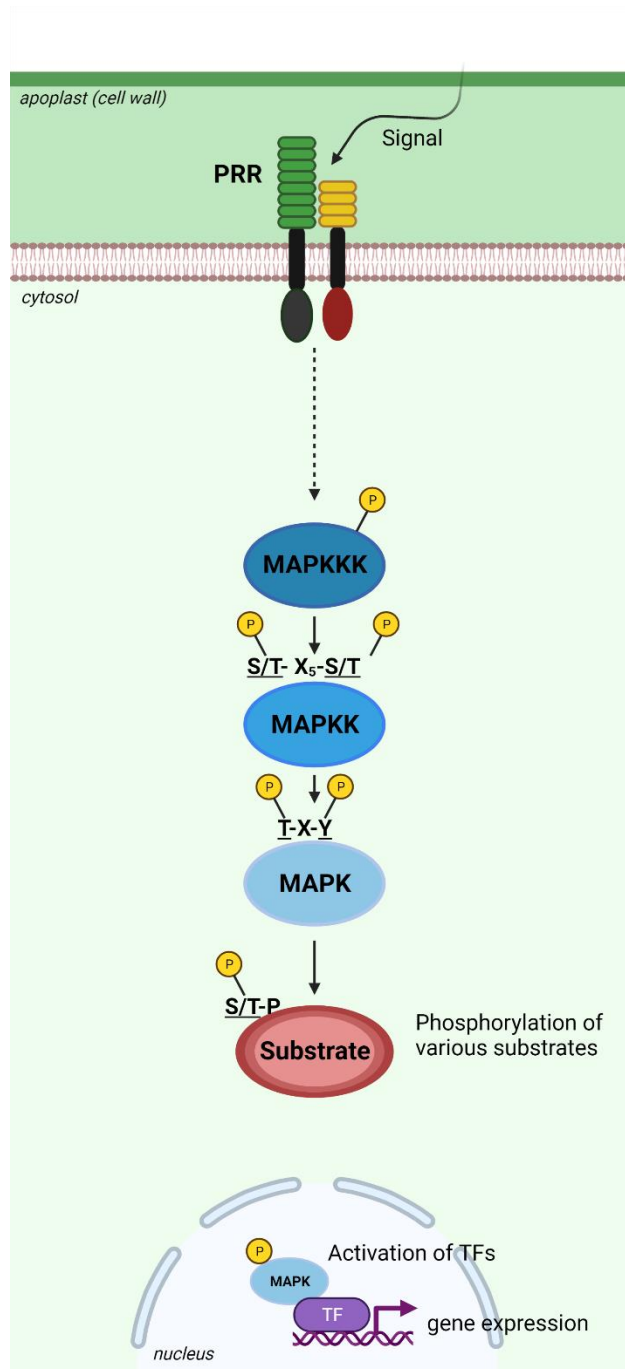


Figure 1.3. Schematic view of MAPK module activation in plants. The MAPKKK is first phosphorylated and activated by upstream activators (refer to text for more details). The activated MAPKKK phosphorylates and thereby activates a MAPKK on a conserved S/T-X₅-S/T motif. Next, the MAPKK phosphorylates the downstream MAPK on a T-X-Y motif. Finally, the MAPK phosphorylates its substrates, such as TF, on S/T-P motif. TF: Transcription factor. Solid arrows indicate direct effects, while dashed arrows indicate indirect effects.

2.2. Mechanisms regulating MAPK modules specificity, substrate specificity, and signaling

2.2.1. *Mechanisms regulating MAPK module specificity*

The specificity of a MAPK module is mediated by the coordinated expression of its components and the interaction with other proteins (Bigeard & Hirt, 2018). In yeasts and mammals, scaffold proteins contribute to the specificity of a MAPK module by connecting the MAPK cascade components through a single adaptor that enables the interaction with upstream activating factors (Dard & Peter, 2006; Yoshioka, 2004). In plants, however, few examples of scaffolds have been reported to date. In Arabidopsis, the receptor for activated c kinase 1 (RACK1) is the unique clear example of a scaffold so far. RACK1 scaffolds the MAPK module MEKK1-MKK4/5-MPK3/6 and connects it to the β -subunit of a heterotrimeric G-protein at the PM (Cheng et al., 2015; Su et al., 2015). G β is involved in a complex that detects bacterial proteases. Upon perceiving bacterial proteases, the MAPK module separates from the RACK1-G β complex and initiates downstream signaling (Cheng et al., 2015; Su et al., 2015). In plants, MAP3Ks have been proposed to act as scaffolds based on the discovery that MEKK1 directly interacts with both MKK1/MKK2 and MPK4 via its kinase domain and amino-terminal tail, respectively, which also indicate that MEKK1 may control the module's specificity (Ichimura et al., 1998).

2.2.2. *Mechanisms regulating MAPK substrate specificity*

MAPKs interact with and phosphorylate a diverse range of substrates in a spatially and temporally specific manner to transduce signals. As briefly mentioned earlier, an active MAPK phosphorylates its substrate on a minimal S/T-P motif of residues, implying that proline at position +1 of the phosphorylated site is the minimal motif required for phosphorylation by a MAPK (Berriri et al., 2012). Berriri et al. also reported that MPK6 displays increased phosphorylation on peptides with a basic amino acid at position +2 surrounding the phosphorylation site (Berriri et al., 2012). Other factors that influence the specificity of a MAPK substrate include the presence of docking sites on the substrate (section 2.1.3) and co-expression and co-localization of MAPKs and their substrates in the same subcellular compartment (Bigeard & Hirt, 2018).

2.2.3. Mechanisms regulating MAPK signaling

Phosphatases were discovered to regulate the duration and amplitude of MAPK activity via targeted S/T dephosphorylation, which deactivates and shuts down the MAPKs following activation (Luan, 2003). Phosphatases from three distinct families interact with MAPKs in Arabidopsis: dual-specificity phosphatases (DSPs), phosphotyrosine-specific protein phosphatases (PTPs), and protein phosphatases 2C (PP2Cs). In the Arabidopsis genome, there is a single PTP gene (PTP1), approximately 23 DSPs, and 76 PP2Cs (Kerk et al., 2002). The AP2C phosphatase belonging to the PP2C family interacts with and regulates the activity of MPK4 and MPK6 in response to wounding, and the *ap2c* mutant showed increased activation of MPK4 and MPK6, as well as elevated JA-ET hormone levels compared to WT (Schweighofer et al., 2007). Map kinase phosphatase 1 (MKP1) from the DSP family interacted with MPK3, MPK4, and MPK6 *in vitro* and *in vivo* and was shown to dephosphorylate MPK6 in protoplasts (Bartels et al., 2009; Ulm et al., 2002). PTP1 and MKP2 interact with MPK3 and MPK6, and MKP2 was shown to dephosphorylate MPK3 and MPK6 *in vitro* (Bartels et al., 2009; Lee & Ellis, 2007). Consistent with its role in MAPKs dephosphorylation, *mkp1* mutant displayed an increased and prolonged MPK3 and MPK6 activity in response to *Pst* DC3000 and increased resistance to *Pst* DC3000 (Anderson et al., 2011). The *mkp1 ptp1* double mutant displayed a severely dwarf phenotype with a constitutive accumulation of free and total SA and camalexin, and mutations of MPK3 and MPK6 distinctly suppressed the phenotype of *mkp1 ptp1* (Bartels et al., 2009). These studies show that MAPK phosphatases have an essential function in regulating MAPK activity to maintain homeostasis.

2.3. The role of MPK3, MPK4, and MPK6 in immunity

During the last decade, significant research efforts have been carried out to identify substrates of MAPKs mainly by high throughput experiments such as yeast two-hybrid (Y2H) screens, protein microarrays, and *MAPKs* loss-of-function mutations coupled with phosphoproteomic approaches as reviewed by Zhang et al. (2016). The identification of mutations that make MAPKs constitutively active (gain of function) or constitutively inactive (loss of function) enabled the use of the strategies mentioned above to further identify specific MAPK substrates and to better understand the role of MAPKs in plants (Berriri et al., 2012; Genot et al., 2017; Ren et al., 2002). Additionally, the generation of phospho-mimic substrates (by substituting the phosphorylated residue, on the S/T-P motif, for an aspartate/glutamate) and phospho-dead

substrates (by substituting the phosphorylated residue for an alanine) has been used to investigate the effect of phosphorylation on the substrate protein's function (Zhang et al., 2016). The three Arabidopsis MAPKs MPK3, MPK4, and MPK6 and their orthologs in other species were identified decades ago as strongly activated by various stresses and have been extensively characterized since then. As stated earlier, MPK3, MPK4, and MPK6 are involved in the two MAPK modules MEKK1-MKK1/MKK2-MPK4 and MAPKKK3/MAPKKK5-MKK4/MKK5-MPK3/MPK6 and are activated downstream several receptor kinases in response to biotic stress (Gao et al., 2008; Sun et al., 2018). In response to flg22, MPK3, MPK4, and MPK6 are rapidly activated, their activation level reaches a peak at 15 minutes and lasts about 30 minutes, whereas, in response to the effector AvrRpt2, MAPKs activation starts 3 hours after treatment and lasts about 4 hours in an RPS2 dependent way (Gao et al., 2008; Tsuda et al., 2013).

2.3.1. MAPKKK3/MAPKKK5-MKK4/MKK5-MPK6/MPK3 pathway

Identification of the MAPKKK3/MAPKKK5-MKK4/MKK5-MPK6/MPK3 MAPK module

The interaction between MKK4/MKK5 and MPK3/MPK6 was demonstrated using Y2H assays and transient expression of constitutively active MKK4 or MKK5 in protoplasts, and the latter showed that expression of either of the two MAP2Ks activates MPK3 and MPK6 (Asai et al., 2002; Jin et al., 2008). These studies showed that MKK4 and MKK5 function redundantly upstream of MPK3 and MPK6 during immunity.

The MAP3Ks MAPKKK3 and MAPKKK5, functioning upstream MKK4/MKK5-MPK6/MPK3 during immunity, have only been discovered recently by Sun et al., by showing that MAPKKK3 and MAPKKK5 interact with and phosphorylate MKK4 and MKK5 (Sun et al., 2018). Moreover, the activation of MPK3 and MPK6 in response to flg22 is abolished in the *mapkkk3 mapkkk5* double mutant (Sun et al., 2018). As a result, *mapkkk3 mapkkk5* showed an enhanced susceptibility when challenged by *Pst* DC3000 *hrcC*, a *Pseudomonas* strain deficient in the delivery of type III effectors further indicating an essential role of the module in PTI (Sun et al., 2018). MPK3 and MPK6 are thought to have redundant functions in plant growth and defense signaling, as both single mutants display a WT-like macroscopic phenotype, and the double mutant *mpk3 mpk6* is lethal (Guan et al., 2014). However, previous transcriptomic and phosphoproteomic studies on *mpk3* and *mpk6* single mutants revealed specificities of each MAPK, highlighting the only partial redundancy between the two MAPKs (Frei dit Frey et al., 2014; Rayapuram et al., 2018, 2021). For instance, *mpk3* shows a reduced callose accumulation in response to flg22, while

mpk6 shows a similar callose accumulation as the WT (Frei dit Frey et al., 2014).

Contribution of MPK3 and MPK6 to immunity

As briefly stated earlier in the introduction, MPK3 and MPK6 are involved in camalexin and ET biosynthesis in response to flg22. Other studies also revealed a prominent role of both MAPKs in response to the necrotrophic fungus *Botrytis cinerea* (Ren et al., 2008). Indeed, *mpk3* and *mpk6* mutants show a decreased camalexin level and an enhanced susceptibility to infection by *Botrytis cinerea* compared to WT (Ren et al., 2008). Additionally, MPK3 and MPK6 promote ET biosynthesis in response to *Botrytis cinerea* by increasing the expression and stability of two rate-limiting enzymes involved in ET biosynthesis, ACS2 and ACS6 (Han et al., 2010; Ren et al., 2008) (figure 1.4). Further, MPK3 and MPK6 are involved in the production of 4-methoxyindole-3-yl-methylglucosinolate (4MI3G), an indole-glucosinolate (IGS) with antimicrobial activity against pathogens and herbivore insects (Xu et al., 2016). In this case, MPK3 and MPK6 phosphorylate ethylene-responsive factor 6 (ERF6), a TF that activates genes involved in indole-3-yl-methylglucosinolate (I3GS) biosynthesis and genes involved in the conversion of I3GS to 4MI3G (Xu et al., 2016) (figure 1.4). Interestingly the expression of a phospho-mimic version of ERF6 was shown to constitutively activate defense genes related to fungal resistance, including plant defensins *PDF1.1* and *PDF1.2*, and confers enhanced resistance to *Botrytis cinerea* (Meng et al., 2013). Another reported substrate of MPK3 is the bZIP transcription factor VirE2-interacting protein1 (VIP1). VIP1's phosphorylation by MPK3 triggers its relocalization to the nucleus, where it induces the expression of the *PR1* gene, showing that MPK3 activates SA-responsive genes (Djamei et al., 2007).

In another study, Su et al. showed that MPK3 and MPK6 are both involved in stomatal immunity (Su et al., 2017). The authors used a line that expresses an MPK6 mutant-variant, termed $MPK6^{YG}$, sensitized to a chemical that renders it inactive (Xu et al., 2014). The *mpk3 mpk6 P_{MPK6}::MPK6^{YG}* line was developed to overcome the seedling lethality of the *mpk3 mpk6* double mutant and allowed further analyses of the role of MPK3 and MPK6 in plants. Upon inactivation of MPK6 in the *mpk3 mpk6 P_{MPK6}::MPK6^{YG}* background, the MPK3 and MPK6 null activity mutant resulted in a reduced stomatal closure in response to flg22 and *Pst* DC3000 (Su et al., 2017). Altogether, these findings demonstrate that MPK3 and MPK6 are required for the initiation of defenses against variety of pathogens.

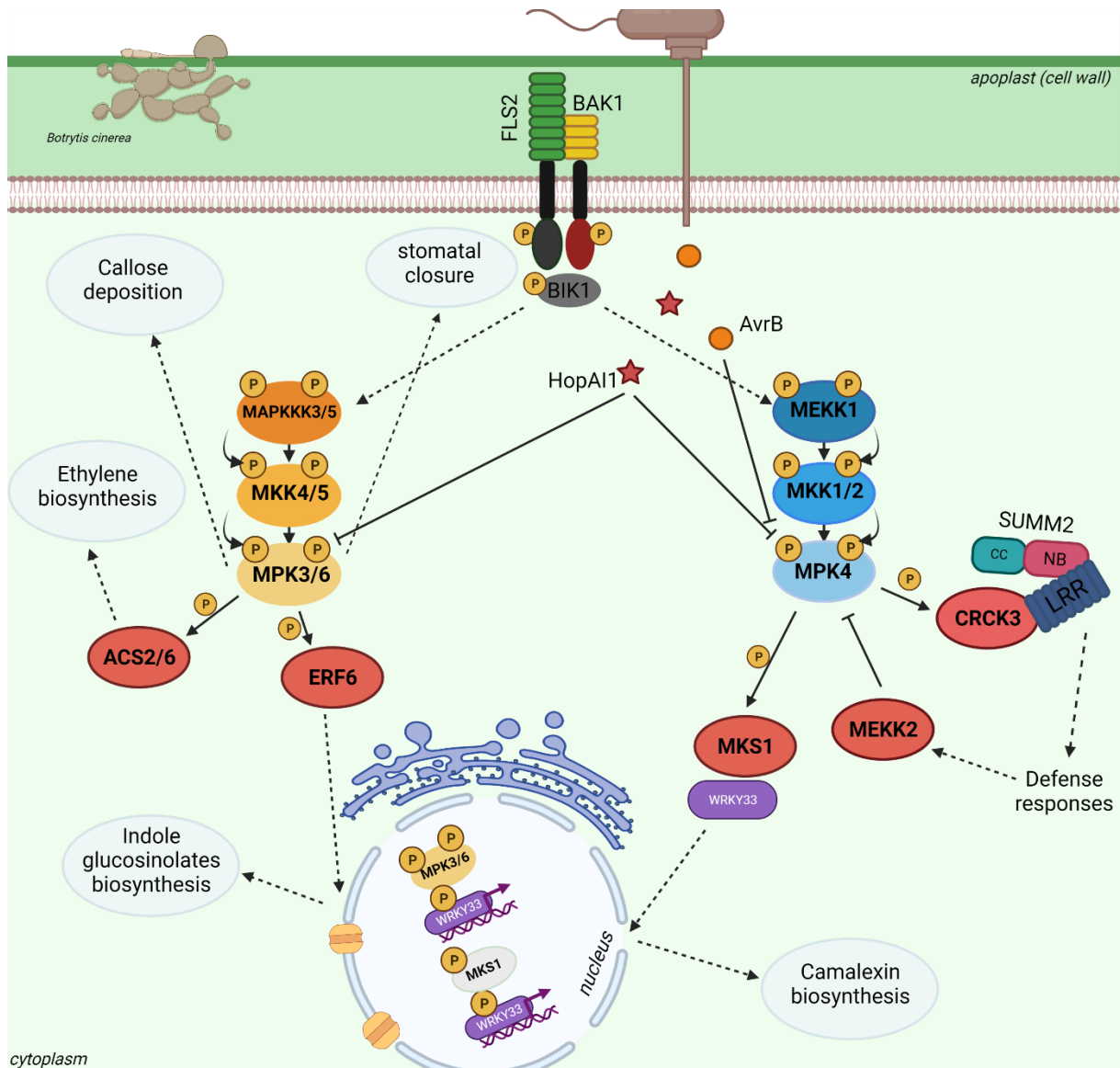


Figure 1.4. Schematic view of MEKK1-MKK1/2-MPK4 and MAPKKK3/5-MKK4/5-MPK3/6 modules downstream of PRR activation. Perception of PAMPs (such as flg22) by their cognate receptors activates downstream MAPK modules. MEKK1-MKK1/2-MPK4 and MAPKKK3/5-MKK4/5-MPK3/6 modules activate transcription factors like WRKY33 to activate the expression of defense genes. WRKY33 increases camalexin production through its TF activity, which is activated by MPK3/MPK6. At resting conditions, WRKY33 is bound to MKS1 and MPK4 in an inactive complex. MPK4 phosphorylates MKS1 in response to PAMPs, causing the complex to dissociate and WRKY33 to translocate to the nucleus, where it activates transcription of target genes. MPK3 and MPK6 activate ethylene and indole glucosinolates biosynthesis through phosphorylation of ACS2/6 and ERF6, respectively. Pathogens decrease MAPK-mediated immune responses by secreting effectors into the intracellular space: AvrB induces the phosphorylation of MPK4, and HopAI1 dephosphorylates MPK3, MPK4, and MPK6. HopAI1 activity on MPK4 leads to activation of SUMM2-dependent immunity, sensed by reduced phosphorylation on CRCK3. MEK2 inhibits MPK4 phosphorylation to amplify SUMM2-dependent responses. Solid arrows indicate direct effects, and dashed arrows indicate indirect effects. Adapted from (Thulasi Devendrakumar et al., 2018).

2.3.2. MEKK1-MKK1/MKK2-MPK4 pathway

Identification of the MEKK1-MKK1/MKK2-MPK4 module

MEKK1-MKK1/MKK2-MPK4 cascade was the first complete MAPK module identified in plants. The module's interactions were initially identified using Y2H (Ichimura et al., 1998) and were subsequently validated *in planta* using bimolecular fluorescence complementation (BiFC) (Gao et al., 2008). The latter showed that the interactions between MEKK1 and MKK1/MKK2 occur at the plasma membrane, whereas MKK1 and MKK2 interact with MPK4 at the plasma membrane and in the nucleus (Gao et al., 2008). Besides its function in immunity, MPK4 is involved in response to cold and salt stress (Meng & Zhang, 2013). Moreover, MPK4 is involved in cytokinesis in another MAPK module, including the MAP2K MKK6 (Kosetsu et al., 2010), showing a diversified role of this protein and its implication in different complexes.

MEKK1-MKK1/MKK2-MPK4: a MAPK module with a contrasting role in immunity

The earliest studies of the MEKK1-MKK1/MKK2-MPK4 module suggested that the module negatively regulates immunity (Petersen et al., 2000). In fact, *mekk1* and *mpk4* single mutants and the double mutant *mkk1 mkk2* displayed an autoimmune phenotype with constitutive expression of SA marker genes, constitutive accumulation of ROS, increased resistance to pathogens, extensive cell death, and a severe dwarf morphology (Petersen et al., 2000; Zhang et al., 2012). Transcriptomic analyses of the *mpk4* mutant revealed that 969 genes are constitutively up-regulated in *mpk4* compared to WT (Frei dit Frey et al., 2014). Gene ontology analysis of the *mpk4* up-regulated genes showed an enrichment of the biological processes "immune responses," "cell death," "SA," and "JA" (Frei dit Frey et al., 2014). Complementation of *mpk4* with a constitutively active version of MPK4 (CA-MPK4) resulted in a phenotype similar to that of WT, which fails to accumulate SA in response to *Pseudomonas syringae* infection (Berriri et al., 2012), indicating that MPK4 might function as a negative regulator of the SA pathway. To understand the molecular mechanisms behind the autoimmunity of *mekk1*, *mkk1 mkk2*, and *mpk4*, a screen for suppressors of the phenotype of *mkk1 mkk2* was carried out and allowed the identification of the *summ2* mutant (for suppressor of *mkk1 mkk2 2*), which completely suppress the dwarf phenotype of the *mkk1 mkk2* double mutant (Zhang et al., 2012). *mkk1 mkk2 summ2* and *mekk1 summ2* and *mpk4 summ2* displayed a WT-like morphology. Mapping of the *summ2* mutation revealed that the mutated gene encodes a CC-type NLR (Zhang et al., 2012), suggesting that the MEKK1-MKK1/2-MPK4 module is guarded

by the SUMM2 CNL, which senses perturbations on the module and subsequently activates an ETI-like SUMM2-mediated response (Zhang et al., 2012).

Although MPK4 does not interact with SUMM2, the same group later discovered that MPK4 interacts with and phosphorylates calmodulin-binding receptor-like kinase 3 (CRCK3/SUMM3), which was also identified in the *mkk1 mkk2* suppressor-screen (Zhang et al., 2017). CRCK3 interacts with SUMM2 and is required for the phenotype of *mpk4*. Furthermore, CRCK3 displays a decreased phosphorylation in *mpk4* than WT (Zhang et al., 2017). As a result, it was proposed that SUMM2 senses the disruption of the MAPK module by monitoring the phosphorylation state of its substrate CRCK3 (Zhang et al., 2017) (figure 1.4). MEKK2/SUMM2 is an additional suppressor of *mkk1 mkk2* (Kong et al., 2012), MEKK2 interacts with MPK4 but not with SUMM2, and the expression level of *MEKK2* is elevated in *mpk4* compared to WT (Kong et al., 2012). Overexpression of MEKK2 leads to CRCK3- and SUMM2-dependent defense responses, leading to the conclusion that MEKK2 functions upstream of SUMM2 and CRCK3 (Kong et al., 2012). A subsequent study demonstrated that SUMM2-mediated immunity activates MEKK2, which inhibits MPK4 activity to amplify the immune response induced by SUMM2 (Nitta et al., 2020) (figure 1.4).

Another protein related to the same pathway is the mRNA decay factor PAT1. PAT1 is also a substrate of MPK4 and interacts with MPK4 upon flg22 perception (Roux et al., 2015). Further evidence linking PAT1 to MPK4 is that *pat1* mutant shows constitutive defense phenotype, similar to *mpk4*, which is SUMM2-dependent (Roux et al., 2015). Altogether, these results indicate that SUMM2 guards the entire MEKK1-MKK1/2-MPK4 pathway by monitoring the state of its substrates.

MEKK1-MKK1/2-MPK4 is essential for basal immunity in addition to being protected by a resistance protein. Indeed, the identification of *summ2* enabled the investigation of MEKK1 and MKK1/2's contribution to basal immunity, which was previously impossible due to *mekk1*, *mkk1 mkk2*, and *mpk4*'s autoimmune phenotype (Zhang et al., 2012). When infected with virulent pathogens, *mekk1 summ2* and *summ2 mkk1 mkk2* plants displayed increased susceptibility than *summ2* and WT plants, indicating that MAPK module is a positive regulators of immune responses (Zhang et al., 2012). These findings indicate that the MEKK1-MKK1/2-MPK4 cascade might contribute to plant defense against pathogens via SUMM2 and via alternative substrates in a SUMM2-MKK2-CRCK3 independent pathway. As stated earlier, MPK4 phosphorylates

other substrates with positive roles in immunity. For instance, MPK4 phosphorylates MKS1 to trigger the release of WRKY33 from the MPK4-MKS1-WRKY33 complex, which promotes camalexin biosynthesis (Qiu et al., 2008) and MKS1 was shown to play a positive role in immunity as its overexpression in WT plants activates an SA-dependent defense pathway (Andreasson et al., 2005).

2.3.3. MAPKs are targets of pathogenic effectors

In agreement with the proposed model in which resistance proteins guard MEKK1-MKK1/2-MPK4, MPK4, and MPK3 and MPK6, were reported to be targeted by pathogenic effectors. For instance, AvrB, a *Pseudomonas syringae* effector, targets MPK4. AvrB interacts with MPK4 to trigger the JA pathway and promote plant susceptibility in an MPK4-dependent way (Cui et al., 2010). In the same study that identified the suppressors of *mkk1 mkk2*, Zhang et al. showed that HopAI1, a *Pseudomonas syringae* effector, interacts with MPK4 and decreases its activity leading to reduced phosphorylation of CRCK3 and activation of SUMM2-mediated defense responses (Zhang et al., 2012). In fact, the transgenic lines ectopically expressing HopAI1 showed constitutive activation of immune responses and cell death in a SUMM2-dependent way (Zhang et al., 2012). HopAI1 has also been shown to target MPK3 and MPK6 for dephosphorylation via its phospholyase activity, leading to reduced callose deposition and increased susceptibility to *Pseudomonas syringae* (Zhang et al., 2007).

2.3.4. MAPKs in ETI

In response to AvrRpt2, Tsuda et al. reported a later and more sustained activation of MPK3 and MPK6 compared to the transient activation reported in response to PAMPs. In the same study, the authors showed that the sustained activation of MPK3 and MPK6, induced by expression of a constitutively active (CA) version of MKK4, contributes to the robustness of the immune system by inducing SA-responsive genes in the salicylic acid-deficient mutant *sid2* (Tsuda et al., 2013), altered in SA biosynthesis. In line with this, analyses of the up-regulated genes in the gain of function lines CA-MPK3 and CA-MKK4, which express a constitutively active version of MPK3 and MKK4, respectively, showed a considerable overlap with the SA-responsive genes observed in AvrRpt2-induced ETI (Genot et al., 2017; Tsuda et al., 2013). However, the sustained activation of MPK3 and MPK6 was abolished in *rps2* plants lacking the NLR that recognizes AvrRpt2, showing that MAPKs activation in ETI occurs downstream of NLR

activation (Tsuda et al., 2013). In line with this, a recent study under review by Lang et al. reported that in response to AvrRpt2, MPK3 and MPK6 display an EDS1- and NDR1-dependent sustained activity, further showing that MPK3 and MPK6's sustained activity depends on NLR downstream signaling components (Lang et al., 2021). Furthermore, the same authors identified two R genes whose expression is specifically induced by MPK3 and MPK6 in response to AvrRpt2 in an EDS1- and NDR1-dependent way, indicating that MPK3/6 are not only activated during ETI but also amplify the ETI response by activating NLR genes (Lang et al., 2021). In another study, Su et al. reported that the sustained activity of MPK3 and MPK6 during ETI is required for ROS accumulation and photosynthetic genes inhibition, two critical mechanisms required for an effective ETI response (Su et al., 2018). Altogether, these studies reveal a key role of MPK3, MPK4, and MPK6 during the two layers of plant immunity.

3. The role of hormones in immunity

Phytohormones are signal molecules with an essential role in all aspects of plant life, including growth, development, reproduction, and interaction with the surrounding environment. Plants regulate different processes of their biology by producing a diverse set of phytohormones that act by modulating gene expression (Checker et al., 2018). As mentioned earlier in the introduction, SA, JA, and ET are the main hormones of plant immunity. SA signaling is commonly known to activate defenses against biotrophic pathogens, while JA-ET signaling activates defenses against necrotrophic pathogens (Glazebrook, 2005; Li et al., 2019).

Other hormones, such as abscisic acid (ABA), gibberellic acid, cytokinins, and brassinosteroids, were instead considered as modulators of SA and JA-ET pathways during immunity (Bürger & Chory, 2019; Li et al., 2019).

This section explores the biosynthesis and signaling pathways of SA, JA, and ET, as well as the crosstalk between the three hormonal pathways.

3.1. SA pathway

3.1.1. SA biosynthesis

In Arabidopsis, SA is produced via two distinct pathways, both originating from the shikimate pathway's end product, chorismate: the isochorismate (IC) pathway and the phenylalanine ammonia-lyase (PAL) pathway (Dempsey et al., 2011; Ding & Ding, 2020).

The IC pathway

The IC pathway is the main pathway for basal and pathogen-induced SA synthesis in Arabidopsis, accounting for 90% of SA production compared to 10% for the PAL pathway (Dempsey et al., 2011; Ding & Ding, 2020). In an SA-induction defective screen, isochorismate synthase 1 (ICS1) and its close homolog ICS2 were discovered to mediate the first committed step of SA biosynthesis in chloroplasts (figure 1.5). In response to virulent or avirulent pathogens, SA production in the *ics1/sid2-2* mutant is 10 to 20 times lower than in WT (Nawrath & Métraux, 1999). ICS2, on the other hand, accounts for a small part in SA biosynthesis, as evidenced by a similar degree of SA accumulation in *ics2* compared to WT following UV exposure, a condition which increases SA accumulation, indicating an uneven redundancy between ICS1 and ICS2 (Garcion et al., 2008). These findings imply that ICS2 may be required for SA biosynthesis in different biological processes or contexts.

ICS1 and ICS2 convert the precursor chorismate to isochorismate (IC) in response to stress via their isochorismate synthase activity. The IC is subsequently transferred to the cytosol through EDS5 (Nawrath et al., 2002) (figure 1.5). EDS5 is a MATE-transporter protein (multidrug and toxin extrusion transporter) that is quickly up-regulated in response to *Pseudomonas syringae* infection (Nawrath et al., 2002), and the *eds5/sid1* mutant does not accumulate SA in response to pathogens (Nawrath & Métraux, 1999). Once in the cytosol, IC is transformed to IC-9-Glu by the aminotransferase avrPphB Susceptible 3 (PBS3), which uses its amino-acid transferase activity to bind IC to glutamate (Torrens-Spence et al., 2019). Finally, enhanced *Pseudomonas susceptibility* 1 (EPS1) converts IC-9-Glu to SA (Torrens-Spence et al., 2019) (figure 1.5). Similar to ICS1 and EDS5, EPS1 and PBS3 were discovered in a forward genetic screen seeking mutants with increased sensitivity to *Pseudomonas syringae* (Warren et al., 1999; Zheng et al., 2009).

The PAL pathway

The PAL pathway is an intermediate for tryptophan (Trp), phenylalanine (Phe), and tyrosine (Tyr) biosynthesis (Ding & Ding, 2020). In the PAL pathway, SA biosynthesis begins by the conversion of chorismate to Phe, which is subsequently transferred to the cytosol, where phenylalanine ammonia lyases (PALs) metabolize it to trans-cinnamic acid (t-CA). t-CA is transformed to SA via ortho-coumaric acid or via benzaldehyde, followed by hydroxylation of benzoic acid (BA) to SA (Ding & Ding, 2020) (figure 1.5).

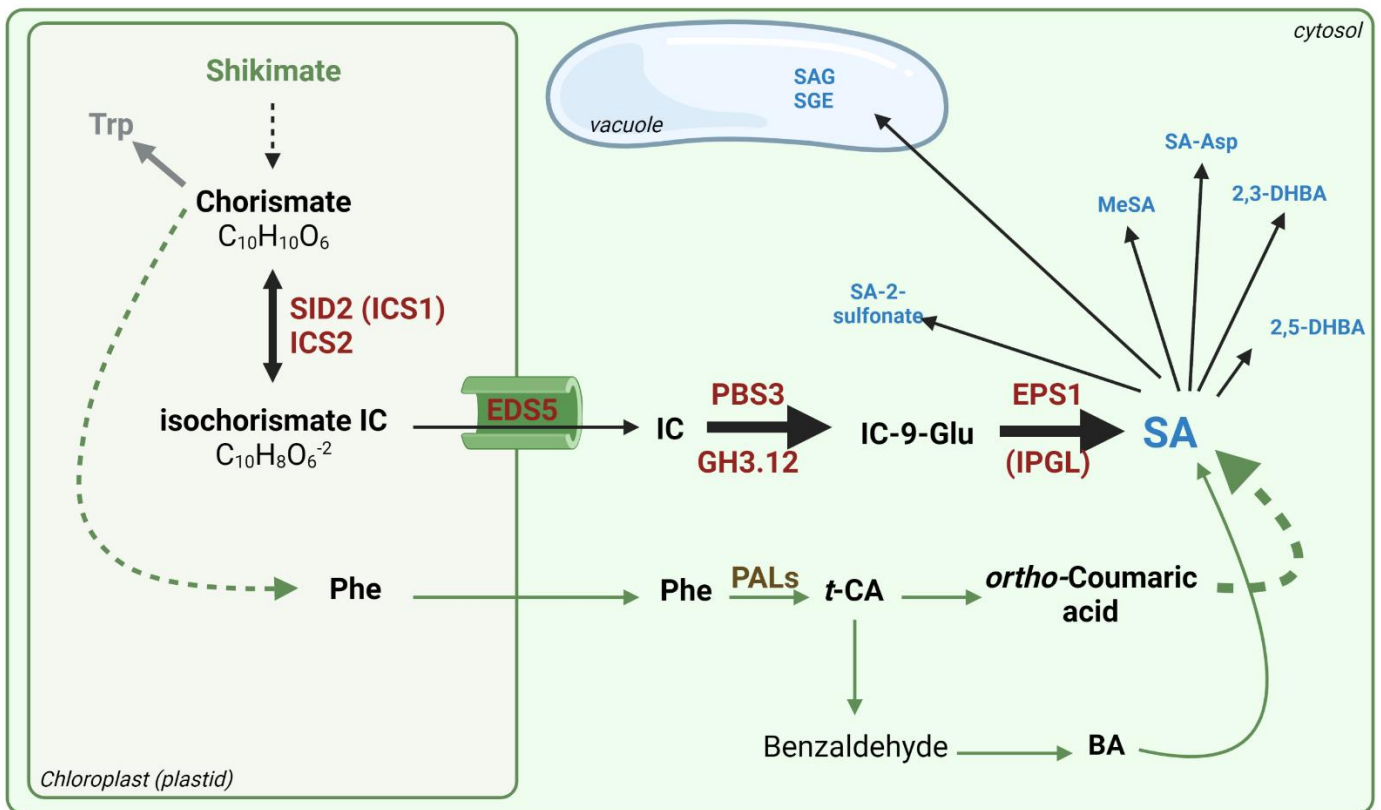


Figure 1.5. Schematic view summarizing SA biosynthesis and metabolism in Arabidopsis. In plants, SA is synthesized by two pathways: the isochorismate (IC) pathway and the phenylalanine ammonia-lyase (PAL) pathway. Both routes begin in chloroplasts using chorismate as a substrate. SID2/ICS1 and ICS2 convert chorismate to IC in response to stress. EDS5 then transports IC to the cytosol. PBS3 (GH3.12) converts IC to isochorismoyl-9-glutamate (IC-9-Glu), and finally, IC-9-Glu is converted to SA by EPS1 (IPGL). In the PAL pathway, chorismate is converted into phenylalanine (Phe). PALs then convert Phe to trans-cinnamic acid (t-CA). t-CA may be transformed into ortho-coumaric acid, which can subsequently be turned to SA. Alternatively, t-CA is converted into benzaldehyde and then to benzoic acid (BA), which is, in turn, hydroxylated to SA. SA can be metabolized into several derivatives: SAG, SGE, MeSA, SA-Asp, 2,5 and 2,3 DHBA, and SA-2-sulfonate. SAG and SGE are the most abundant derivatives and are stored in vacuoles. Solid arrows indicate direct effects, while dashed arrows indicate indirect effects.

Even though it is regarded as a modest contributor to SA biosynthesis in response to infections, mutating the four Arabidopsis PAL genes decreases SA levels to 50% compared to WT and leads to enhanced bacterial growth of *Pst* DC3000 (Huang et al., 2020). These data suggest that the IC pathway may require the PAL pathway for optimal efficiency.

3.1.2. SA metabolism

SA can be transformed into several derivatives by glycosylation, methylation, amino acid conjugation, sulfonation, or hydroxylation. Some derivatives are active, while others have been reported to be inactive and may function as storage forms (Ding & Ding, 2020) (figure 1.5).

SA glycosylation

SA beta glucoside (SAG) and the glucose ester of SA (SGE) are among the most abundant derivatives of SA. The uridine diphosphate (UDP)-glucosyltransferase (UGT) UGT74F2, also known as salicylic acid glucosyltransferase 1 (SGT1), generates SAG and SGE (Song, 2006). SAG can also be formed by UGT74F1 (Dean & Delaney, 2008). SAG and SGE are inactive derivatives of SA, and *SGT1* levels drop in response to SA or *Pseudomonas syringae* (Song, 2006). In line with this, overexpression of SGT1 resulted in increased sensitivity to *Pseudomonas syringae* due to a decrease in free SA levels (Song et al., 2008). SAG is stored in vacuoles, allowing it to operate as a long-term storage form of SA that is readily hydrolyzed into active SA after being remobilized to other cellular sites (Vaca et al., 2017).

SA methylation

In plants, SA can be methylated to MeSA by S-adenosyl-L-methionine (SAM)-dependent methyltransferases (MTs) (Shine et al., 2019). In Arabidopsis, the methylation of SA is catalyzed by the SAM-MT carboxyl methyltransferase 1 (BSMT1) (Chen et al., 2003). MeSA is a volatile inactive derivative that can be converted back to SA via the esterase activity of methyl esterases (MES), the orthologs of the tobacco SA-binding protein 2 (*NtSABP2*) (Kumar & Klessig, 2003; Vlot et al., 2008). MeSA is believed to function as an airborne signal that contributes to SA delivery to distal tissues during infection (Shulaev et al., 1997). Section 3.1.5 below contains additional information about MeSA's role in the SAR.

Other SA modifications

SA can be conjugated to produce a number of different compounds that are considered to be inactive in plants. Although some are accumulated in response to pathogens, their functions

in plant immunity remain to be determined. Several of these compounds include the hydroxylated forms of SA such as dihydroxybenzoic acids 2,3DHBA and 2,5DHBA, sulfonated SA-2-sulfonate, and amino acid conjugated SA, reviewed by Dempsey et al. (2011) and Ding & Ding (2020).

3.1.3. Regulation of SA biosynthesis

Activation of SA biosynthesis during PTI

Extensive research, including mutant screens, has revealed several necessary proteins for the induction of SA biosynthesis and signaling during pathogen infection. SARD1 and its homolog CBP60g, two transcription factors whose expression is substantially elevated in response to *Pseudomonas syringae* infection, are considered as master regulators of SA biosynthesis during PTI, ETI, and SAR (Zhang et al., 2010). CaM-binding protein 60-like g (CBP60g) and SAR deficient 1 (SARD1) act directly on *ICS1* and *EDS5*'s expression in response to pathogens to promote SA biosynthesis (Zhang et al., 2010). Increased intracellular Ca²⁺ levels, in response to pathogen perception, lead to CaM binding and activation of CBP60g, which in turn increases the transcription of *ICS1* (Wang et al., 2009). No CaM binding is necessary for SARD1 activation (Wang et al., 2009). Additional analysis found some overlap between CBP60g and SARD1 function, with CBP60g required for SA production early during infection whereas SARD1 is required later (Wang et al., 2011). The RLCKs PTI-compromised receptor-like cytoplasmic kinase 1 (PCRK1) and PCRK2 are essential regulators of SA biosynthesis in PTI and SAR and upstream of SARD1 and CBP60g. PCRK1 and PCRK2 interact with FLS2 and are phosphorylated in response to flg22 elicitation (Kong et al., 2016). The *pcrk1 pcrk2* double mutant shows reduced *ICS1*, *SARD1*, and *CBP60g* expressions and SA levels in response to flg22 compared to WT. Additionally, SAR is compromised in *pcrk1 pcrk2* double mutant (Kong et al., 2016). Several other TFs were reported to regulate *ICS1*'s expression directly or indirectly by modulating *SARD1* and *CBP60g* expression and are reviewed by Huang et al. (2019) and Zhang & Li (2019).

Activation of SA biosynthesis during ETI

Previous genetic investigations showed that *EDS1* and *PAD4* are required for SA synthesis downstream NLRs activation (Cui et al., 2017). Indeed, *eds1* and *pad4* mutants do not generate SA in response to *Pst* DC3000 infection (Cui et al., 2017). Consistently, overexpression of both *PAD4* and *EDS1* results in constitutive SA production and expression of SA markers such as *CBP60g*, *SARD1*, and *PBS3* (Cui et al., 2017). As a result of these findings, EDS1 and PAD4 are

considered to be upstream of transcription factors in the SA pathway in an ETI context (figure 1.6). As briefly mentioned earlier in the introduction, recent studies reported the importance of EDS1, PAD4, and ADR1 in SA signaling, not only for R proteins signaling but also for PTI and basal resistance (Tian et al., 2020). In fact, Tian *et al.* showed that in the *eds1*, *pad4*, and *adr1* mutants, flg22-induced immune responses are impaired, demonstrated by reduced SA levels in the three mutants and an increased susceptibility to *Pto* DC3000 *hrcC* compared to WT (Tian et al., 2020). These results show that R-protein-mediated signaling is also activated and required for PTI. In addition to CBP60g and SARD1, WRKY TFs have been demonstrated to influence the expression of SA biosynthesis-associated genes during ETI. For instance, WRKY8 and WRKY48 were shown to control *ICS1* expression in response to pathogen elicitation (Gao et al., 2013; van Verk et al., 2011), and expression of *ICS1* is decreased in the *wrky8* and *wrky48* mutants in response to *Pseudomonas syringae* effectors AvrRpm1, AvrRpt2, and AvrB compared to WT (Gao et al., 2013). Besides, Van Verk et al. showed that WRKY28 and WRKY46 directly promote the expression of *ICS1* and *PBS3*, respectively, during infection (van Verk et al., 2011).

3.1.4. Signaling downstream of SA

Accumulation of SA in infected cells leads to an altered redox state. The modified redox state triggers the shift of NPR1, a key protein of SA signaling, from an inactive oligomeric state to an active monomeric state (Mou et al., 2003). Thioredoxins TRX-h3 and TRX-h5 catalyze NPR1 monomerization through cysteine residue reduction (Cys156) (Mou et al., 2003). NPR1 has a Broad-Complex, Tramtrack, and Bric a Brac (BTB) domain at the N-terminus, central ankyrin-repeats, and a transcriptional activation motif at the C-terminus (Rochon et al., 2006). SA binding and transcriptional activation are both promoted by the C-terminal domain. Mutations in this region prevent SA-binding and disrupt NPR1's role in promoting SA-induced defense gene expression (Rochon et al., 2006).

Monomeric, SA-bonded NPR1 translocates from the cytosol to the nucleus, where it interacts with members of the TGA family of bZIP transcription factors TGA2, TGA5, and TGA6 (Fan & Dong, 2002; Zhang & Li, 2019). NPR1-associated TGAs will subsequently activate the transcription of several genes, including *PR* genes (Després et al., 2000; Ding et al., 2018) (figure 1.6). Among PRs, *PR1*, which encodes for a secreted protein, is the best characterized and is often used as a robust marker of an activated SA response.

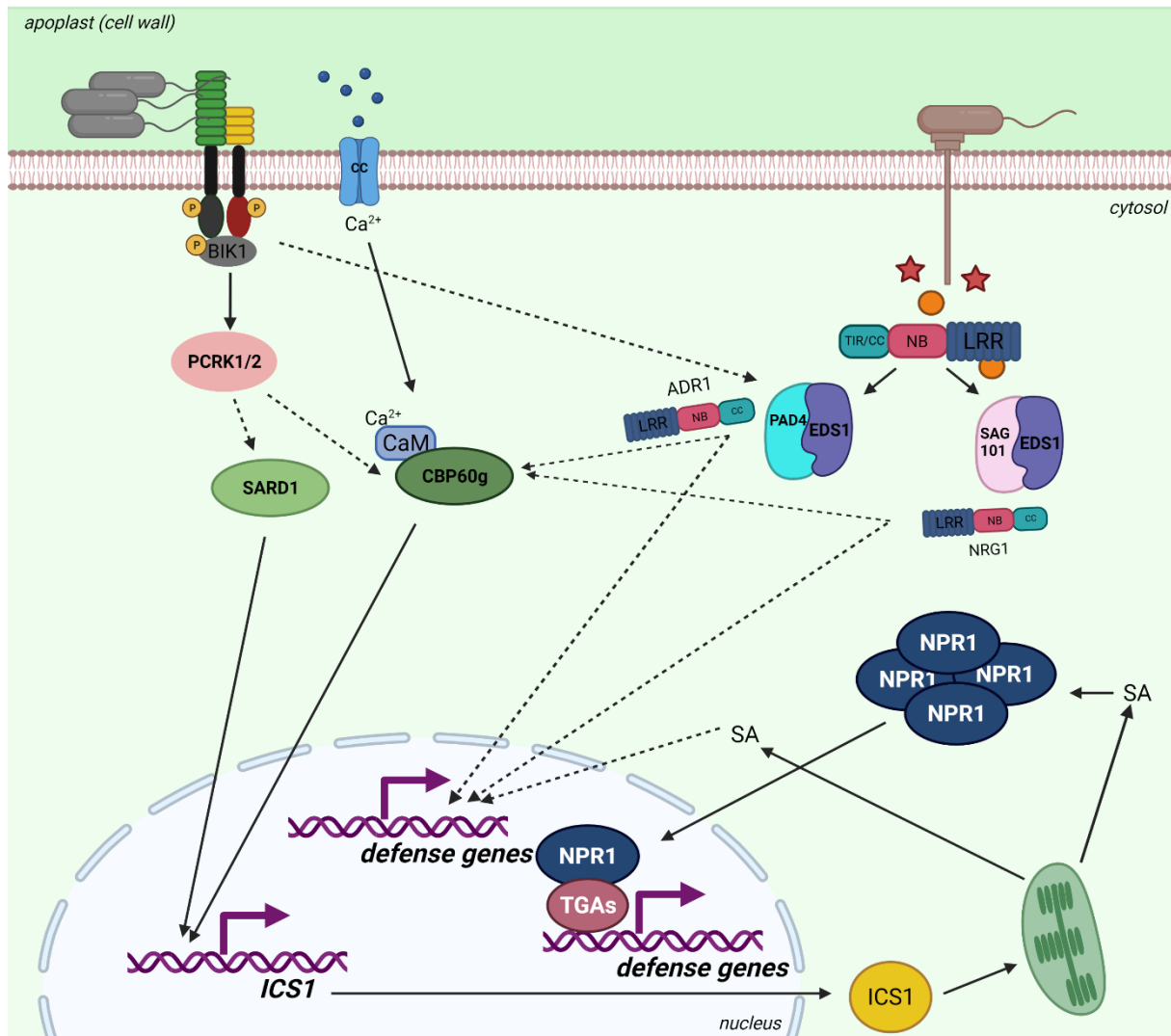


Figure 1.6. Schematic view summarizing the SA signaling pathway downstream PAMP and effector perception. When PAMPs are detected, BIK1 activates PCRK1 and PCRK2, which then activate SARD1 and CBP60g, two key transcription factors in the SA pathway. CaM binding activates CBP60g in response to increased levels of Ca²⁺. As a result, CBP60g and SARD1 activate the transcription of *ICS1*. *ICS1* will, in turn, activate SA biosynthesis in chloroplasts. Increased levels of SA promote the monomerization of NPR1, which subsequently translocates to the nucleus to activate SA-responsive genes by binding to TGAs transcription factors. In an ETI context, the perception of effectors by R proteins leads to activation of EDS1, which interacts with PAD4 or SAG101 depending on the R protein (CNL or TNL). Similarly, EDS1 signaling will induce the activation of SARD1 and CBP60g, which in turn activate SA biosynthesis and signaling through *ICS1* and NPR1, respectively. Recent studies showed that EDS1-PAD4 signaling is also activated during PTI downstream PRR activation and contributes to PTI responses. Solid arrows indicate direct effects, while dashed arrows indicate indirect effects.

NPR3 and NPR4, which have a similar structure to NPR1, have also been reported to respond to SA. NPR3 and NPR4 function as repressors that negatively regulate SA-responsive genes when SA levels are low (Ding et al., 2018), whereas, under high SA levels, NPR3 and NPR4 are suppressed to enable the activation of SA-responsive genes (Ding et al., 2018).

3.1.5. SAR

SAR is an induced defense response that leads to broad-spectrum, long-lasting systemic resistance following infection (Cameron et al., 1999; Shine et al., 2019). SAR induction requires a mobile signal to travel across cells and establish a priming environment in distal, non-infected tissues. When inoculated with a pathogen, the distal tissues activate defenses in a faster way (Conrath, 2006). Numerous parameters are necessary for an efficient perception of the mobile signal during SAR, including the following: 1) an intact cuticle 2) an intact digalactosyl-diacylglycerol (DGDG), the primary plant galactolipid that serves as a precursor for the synthesis of azelaic acid (Aza), a critical component of SAR signaling (Shine et al., 2019). Additionally, DGDG is required for the accumulation of SA and nitric oxide (NO) in chloroplasts. 3) the presence of two plasmodesmata (PD) localizing proteins, PDL1 and PDL5, that are involved in the symplastic transport of signaling molecules (Lim et al., 2016) (figure 1.7). Plants deficient in these components can produce the SAR signal but cannot sense it (Shine et al., 2019). Extensive genetic screens searching for mutants impaired in SAR allowed the identification of numerous components that have been proposed as SAR mobile signals.

SA and MeSA

Despite the central role of SA in SAR, as demonstrated by the loss of SAR in transgenic plants over-expressing the bacterial enzyme NahG which degrades SA to catechol (Delaney et al., 1994), the hypothesis that SA is the mobile signal that induces SAR has been disputed by early data from grafting experiments in tobacco (Vernooij et al., 1994). In this study, Vernooij et al. showed that rootstocks of transgenic NahG plants infected with the Tobacco Mosaic Virus (TMV) could induce SAR in grafted WT tissues (Vernooij et al., 1994).

However, more recent studies showed that SA is transported from infected tissues to systemic parts via the apoplastic pathway, demonstrated by a high content of SA in the apoplastic fluids (Lim et al., 2016). Moreover, labeling studies performed by Shulaev et al. demonstrated that 70% of the SA contained in systemic tissues come from infected tissues (Shulaev et al., 1995).

Taken together, these findings establish that SA is the mobile signal which activates SAR and is transported to distal tissues by phloem loading through the apoplast (Lim et al., 2016) (figure 1.7). MeSA requirement for SAR signaling has also been a matter of debate across the literature. Indeed, some research reported its significance for SAR by demonstrating that infected tissues produce more MeSA, and that SABP2, the enzyme that converts MeSA to SA, is required for SAR, and that MeSA treatment enhances *PR* gene expression in plants (Kumar & Klessig, 2003; Park et al., 2007; Shulaev et al., 1997). Other studies, however, reported that overexpression of BSMT1 in rice, the enzyme responsible for the conversion of SA to MeSA, results in an impaired SAR (Koo et al., 2014). (Koo et al., 2007). Consistently, *bsmt1* mutants had an elevated level of systemic SA and could induce an efficient SAR (Attaran et al., 2009). However, another study later demonstrated that the importance of MeSA is dependent on the amount of light received by plants following infection, with MeSA being essential for plants that received very little light after infection and prior to dark time (Liu et al., 2011).

N-hydroxypipicolinic acid (NHP)

NHP was recently identified as a critical mobile signal for SAR in plants (Tian & Zhang, 2019). NHP biosynthesis starts in the chloroplasts by deamination of lysine (Lys) by AGD2-like defense response protein 1 (ALD1) to form Δ^1 -piperidine-2-carboxylic acid (P2C) (Cecchini et al., 2015; Song et al., 2004). P2C is then converted to pipicolinic acid (Pip) by Arabidopsis SAR-deficient 4 (SARD4) (Ding et al., 2016). Finally, FMO1 catalyzes the N-hydroxylation of Pip, yielding NHP (Chen et al., 2018). *fmo1* mutants highly accumulate Pip but are unable to produce NHP (Chen et al., 2018). The importance of NHP as a mobile signal for SAR induction was evidenced by a compromised SAR in *ald1*, *sard4*, and *fmo1* mutants (Chen et al., 2018; Jing et al., 2011; Mishina & Zeier, 2006).

Interestingly, several components of the SA pathway have been reported to be essential for NHP biosynthesis in Arabidopsis. For instance, SARD1 and CBP60g regulate the expression of *ALD1*, *SARD4*, and *FMO1* in response to pathogens (Sun et al., 2018). Moreover, overexpression of *SARD1* leads to increased *ALD1* and *SARD4* expression (Sun et al., 2018). EDS5, on the other hand, is required for the transport of Pip from chloroplasts to the cytosol (Rekhter et al., 2019) (figure 1.7).

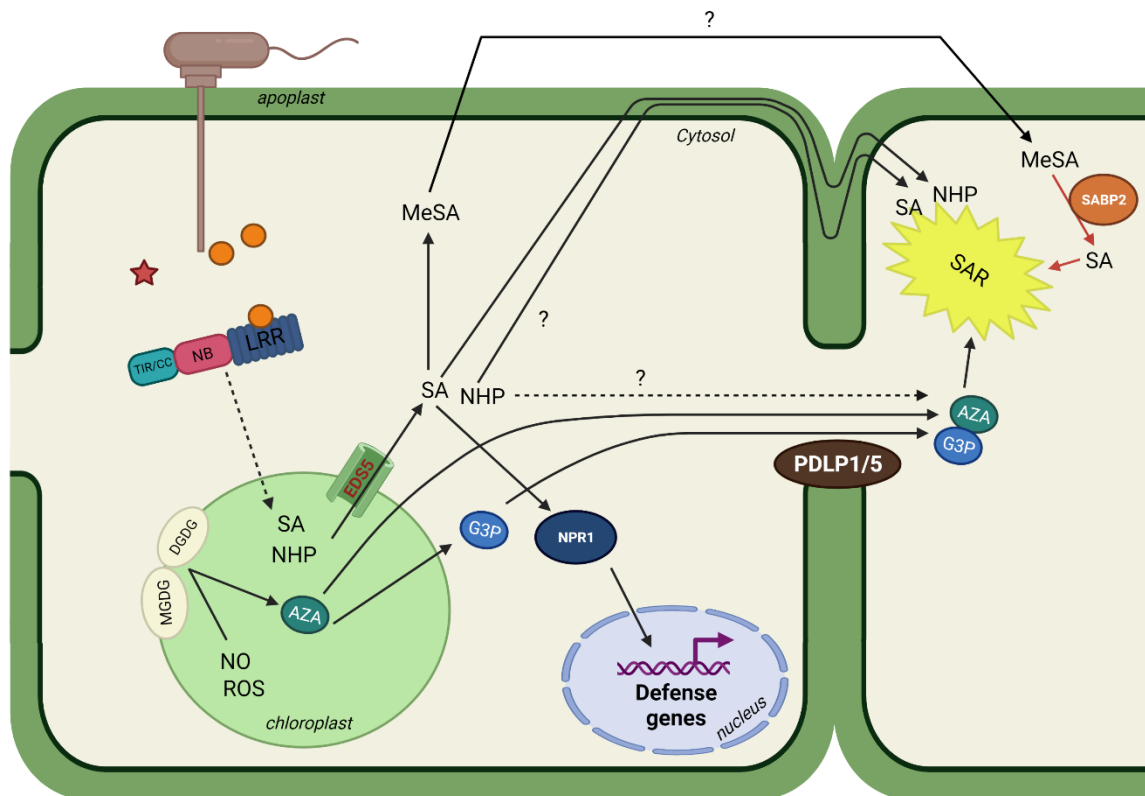


Figure 1.7. Schematic view summarizing metabolite and protein-mediated signaling during systemic acquired resistance. During infection by avirulent pathogens, the recognition of effectors by R proteins activates SAR. In local tissues, pathogen perception induces the accumulation of SA, NHP, NO, and ROS. NO, and ROS catalyze the generation of AZA from MGDG and DGDG. AZA induces the expression of glycerol-3-phosphate (G3P) biosynthetic genes to generate G3P. AZA and G3P are transported to systemic tissues by the symplastic route mediated by PDLP1 and PDLP5. SA transport occurs through the apoplast and possibly via the gaseous methylated derivative MeSA, which is converted back to SA by SABP2. NHP is a mobile signal that may move to distant tissues via the phloem. AZA, G3P, SA, and NHP activate NPR1-dependent SAR in distal tissues. Solid arrows indicate direct effects, and dashed arrows indicate indirect effects. NO: nitric oxide; NHP: N-hydroxy-pipecolic acid; AZA: azelaic-acid. Adapted from (Shine et al., 2019).

Other molecules

Other compounds were reported to be involved in SAR (Gao et al., 2015; Shine et al., 2019). For instance, NO and ROS enhance the synthesis of Aza from the oleic (18:1), linoleic (18:2), and linolenic (18:3) fatty acids produced after pathogen infection, via the hydrolysis of plant chloroplastic DGDG and monogalactosyl-diacylglycerol (MGDG) (Wang et al., 2014; Yu et al., 2013). Aza then promotes the synthesis of glycerol-3-phosphate (G3P) (Wang et al., 2014). Subsequently, Aza and G3P cross the symplastic route and trigger SAR in distal tissues (Lim et al., 2016) (figure 1.7).

3.2. JA pathway

Jasmonic acid (JA) and its metabolites, including methyl jasmonate, MeJA, and isoleucine-conjugated jasmonate, JA-Ile, are commonly designated as jasmonates (JAs), a subgroup of oxylipins derived from 12-oxo-phytodienoic acid (OPDA). In plant immunity, the JA pathway is involved in protecting plants from necrotrophic pathogens and injuries.

3.2.1. JA biosynthesis

Mechanical or insect-induced wounding releases DAMPs and elicits local and systemic plant defenses. In tomato (*Lycopersicon esculentum*), systemin, an 18 amino-acid peptide, is released in the apoplast after wounding or insect attack (Jacinto et al., 1997). Sensing of systemin leads to the biosynthesis of JA.

JA biosynthesis starts from fatty acids released from the chloroplast's membrane galactolipids upon wounding or pathogen infection. In Arabidopsis, there are three pathways for the synthesis of JAs, including the octadecane pathway starting from α -linolenic acid (18:3). α -linolenic acid is oxygenated by JA-synthetase enzymes 13-lipoxygenases (LOX) proteins and converted to oxo-phytodienoic acid (12-OPDA) through several steps (Gupta et al., 2020; Turner et al., 2002). 12-OPDA is then transported to the peroxisome for subsequent reduction and β -oxidation steps that give rise to JA (Guan et al., 2019; Theodoulou et al., 2005). JA is transformed into various derivatives in the cytosol, of which is isoleucine-jasmonate, the active compound that initiates downstream signaling (Staswick & Tiryaki, 2004). JA is also methylated to MeJA, which has been reported to play a role in disease resistance as well (Seo et al., 2001) (figure 1.8).

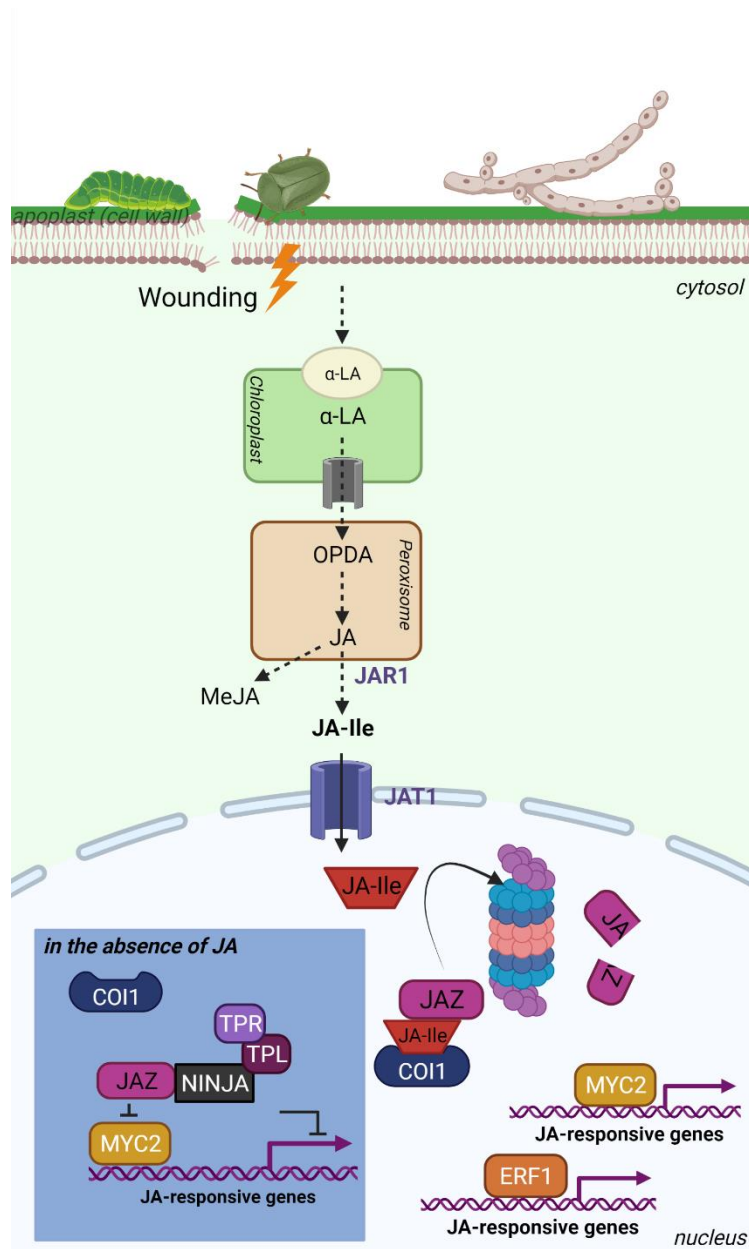


Figure 1.8. Schematic view summarizing the JA biosynthesis and signaling pathway. A variety of environmental disturbances, such as injury by chewing insects or infection by a necrotrophic disease, trigger JA biosynthesis. Fatty acids like linolenic acid are used to initiate JA production in the chloroplasts. α -LA is transformed to OPDA via several steps. OPDA is subsequently carried to peroxisomes, where it undergoes several enzymatic steps which give rise to JA. In the cytosol, JA is transformed to a variety of derivatives, among which JA-Ile is an active compound and initiates downstream signaling. JA-Ile is formed by conjugation of JA to isoleucine by JAR1. JA-Ile is transported to the nucleus via JAT1, where it interacts with the COI1 receptor to promote the degradation of JAZ repressors. JAZ degradation allows the activation of JA-responsive genes by MYC2 and ERF1. In the absence of JA, however, JAZ proteins repress the expression of JA-responsive genes by interacting with NINJA, which recruits the repressors TPL and TPL-related (TPR) proteins to repress JA-responsive genes. Solid arrows indicate direct effects, while dashed arrows indicate indirect effects.

3.2.2. JA perception and downstream signaling

Jasmonate resistant 1 (JAR1) mediates the conjugation of JA to isoleucine to form JA-Ile in response to stress (Staswick & Tiryaki, 2004). JA-Ile is then transported to the nucleus by the ABC transporter JAT1/ABCG16, where it is perceived by its receptor coronatine insensitive 1 (COI1) (Yan et al., 2009). COI1 is a nuclear F-box involved in an S PHASE KINASE-ASSOCIATED PROTEIN 1 (SKP1)-CULLIN-F-BOX (SCF)-type E3 ubiquitin ligase complex. Earlier studies showed that *coi1* mutant is entirely defective in JA responses (Feys et al., 1994; Xie et al., 1998). JA-Ile promotes the association of COI1 to the transcriptional repressors JASMONATE ZIM-DOMAIN PROTEINs (JAZs) (Thines et al., 2007). COI1-associated JAZs are targeted by the E3 ubiquitin ligase complex SCF^{COI1} for 26S proteasome-mediated degradation (Thines et al., 2007). Consequently, the absence of repression by JAZ proteins leads to the expression of JA-Ile-responsive genes. However, at resting conditions and low levels of JA-Ile, JAZ proteins bind to and inhibit the activity of JA-positive transcriptional regulators (Chini et al., 2007) (figure 1.8). Some corepressors are recruited to work in concert with JAZ proteins to inhibit JA-positive transcriptional regulators, Topless (TPL) and Topless-related (TPR) corepressors are recruited through the novel JAZ interactor (NINJA), which has an ethylene response factor (ERF)-associated amphiphilic repression (EAR) motif (Pauwels et al., 2010). This JAZ-NINJA-TPL-TPR repressor complex strongly associates with transcription factors and prevents them from activating downstream JA-responsive genes (Pauwels et al., 2010; Wasternack & Strnad, 2018) (figure 1.8). Upon JA-Ile production, two main branches of JA-responsive genes are activated depending on the stimuli and the presence of other hormones. The first branch depends on the basic helix-loop-helix leucine zipper (bHLH-zip) transcription factor MYC2 (originally called JIN1, for jasmonate insensitive 1) and activates JA-mediated response to wounding (Boter et al., 2004; Dombrecht et al., 2007; Lorenzo et al., 2004). MYC2 up-regulates JA marker genes *vegetative storage proteins (VSPs)* and *lipoxygenase 2 (LOX2)*, with the concomitant action of ABA (Bell et al., 1995; Berger et al., 1996; Lorenzo et al., 2004; Vos et al., 2013). The second branch is activated in response to necrotrophic pathogens, depends on the TF Ethylene-Responsive Factor1 (ERF1), and leads to the up-regulation of the marker gene *PDF1.2* with the concomitant action of ET (Lorenzo et al., 2003; Zarei et al., 2011). Interestingly, the MYC2 and ERF branches are antagonistic. MYC2 acts as a negative regulator of the ERF branch via the Arabidopsis NAC domain-containing transcription factors *ANAC109* and *ANAC055*, which have been shown to positively regulate *VSP* genes but negatively regulate *PDF1.2* (Bu et al., 2008).

3.2.3. Regulation of the JA pathway

JA signaling is regulated to maintain homeostasis and avoid the detrimental growth effects caused by excessive JA (Zhang & Turner, 2008). JA-associated responses are regulated by two different mechanisms, either by controlling the JA-Ile concentration or by regulations of JA-associated genes.

JA-Ile catabolism

JA-Ile is deactivated by ω -oxidation by the action of cytochrome P450 oxygenase and yields 12-hydroxy-jasmonic acid isoleucine, a low activity derivative, or by double oxygenation, which yields an inactive form (Koo et al., 2014; Heitz et al., 2012). JA-Ile is also hydrolyzed by amino-hydrolases that cleave JA-Ile to JA and Ile (Woldemariam et al., 2012).

Regulations of JA-associated genes

As part of a negative feedback loop, it has been shown that elevated levels of JA-Ile induce the transcription of JAZ repressors (Chung et al., 2008). Additionally, some JAZs are resistant to SCF^{COI1}-mediated degradation (Shyu et al., 2012). In fact, JAZs contain a degradation signal (degron) that COI1 recognizes for subsequent degradation (Shyu et al., 2012). The sequence of the degron motif differs amongst JAZs, resulting in variable affinity for COI1 between JAZs. This variability allows a fine-tuned transcriptional regulation in response to different concentrations of JA (Shyu et al., 2012)(Shyu et al., 2012). Additionally, post-transcriptional regulations have been shown to control JA responses (Chung et al., 2010). *JAZ10* is an example of how splicing variants of JAZs with or without the degron may be generated (Moreno et al., 2013). Alternative splicing of *JAZ10* results in a splicing variant missing the intron-containing the degron sequence, allowing the matching protein to function as a transcriptional repressor and avoid COI1 targeting (Moreno et al., 2013). Another family of JA-sensitive proteins implicated in the negative regulation of the JA response is the Jasmonate-associated MYC2-like (JAM) clade of bHLH-type proteins (Sasaki-Sekimoto et al., 2013). JAMs compete with MYC2 for JA-responsive gene promoters, but they lack MYC2's conserved activation domain, resulting in negative regulation of MYC2-targeted genes (Sasaki-Sekimoto et al., 2013).

Numerous other processes, including MYC2 ubiquitination and degradation, contribute to the negative control of JA signaling and are discussed in detail by Gupta et al. (2020).

3.3. Ethylene pathway

ET is a gaseous hormone that plays an essential role in plant immunity. Besides ET's prominent role in fruit ripening, ET regulates numerous processes in growth and development (Dubois et al., 2018).

3.3.1. *ET biosynthesis*

ET is produced from the precursor amino-acid methionine. Methionine is converted to S-adenosyl methionine (SAM) by SAM synthase (SAMS). SAM is then converted to the intermediate compound 1-aminocyclopropane-1-carboxylic acid (ACC) by the rate-limiting ACC synthases (ACSs) (Adams & Yang, 1979; Sato & Theologis, 1989). ACC is finally converted to ET by the ACC-oxidase (ACO) (Wang et al., 2002; Schaller & Kieber, 2002) (figure 1.9.a). ACO has been previously reported to function in the cytosol of tomato (*lycopersicon esculentum*) and apple fruit (*Malus domestica*), suggesting that ET biosynthesis occurs in the cytosol (Chung et al., 2002; Reinhardt et al., 1994).

3.3.2. *ET perception and signaling*

ET sensing occurs via a set of transmembrane kinases known as ET receptors in the ER membrane (Chen et al., 2002; Grefen et al., 2008). These include the proteins ethylene-response 1 (ETR1) and ETR2, as well as the ethylene response sensor 1 (ERS1) and ERS2, and the ethylene insensitive 4 (EIN4) (Grefen et al., 2008). ET receptors form homodimers, with each dimer covalently binding a Cu^{2+} cofactor to enable ET binding. Cu^{2+} is supplied via the copper transporter responsive to antagonist 1 (RAN1) (Hoppen et al., 2019) and can also be directly absorbed from chaperones (Hoppen & Groth, 2020).

ET receptors are involved in ET-signaling via the Raf-like kinase constitutive triple response 1 (CTR1) (Kieber et al., 1993a). In the absence of ET, ET receptors activate CTR1, which then phosphorylates EIN2 (Huang et al., 2003; Ju et al., 2012) (figure 1.9.b). EIN2 is the primary executor of ET signaling. It has an N-terminal transmembrane domain and a cytosolic C-terminal domain called CEND (Alonso et al., 1999). In the absence of ET, CEND is phosphorylated by CTR1 to promote EIN2 degradation via the 26S proteasome, mediated by two F-box proteins, EIN2-targeting protein 1 (ETP1) and ETP2, thus inhibiting ET responses (Ju et al., 2012; Qiao et al., 2009) (figure 1.9.b). The presence of ET is believed to induce a conformational shift in the ET receptors, rendering them unable to activate CTR1 (Wang et al.,

2006). As a result, EIN2 is stabilized and cleaved to release its C-terminal CEND domain (Wen et al., 2012). Subsequently, the CEND domain inhibits the translation of two F-box proteins, EIN3-binding F-box protein 1 (EBF1) and EBF2, by sequestering their mRNAs in processing bodies (P-bodies) (Li et al., 2015; Merchante et al., 2015). The negative control imposed on EBF1 and EBF2 prevents them from negatively regulating the TF EIN3 and EIN3-like1 (EIL1), which would be otherwise constitutively degraded by the proteasome (An et al., 2010; Guo & Ecker, 2003) (figure 1.9.b). Additionally, CEND translocates to the nucleus to recruit EIN2-nuclear-associated protein 1 (ENAP1), which promotes histone acetylation on EIN3 DNA targets, thus allowing EIN3 to initiate transcriptional activation (Wen et al., 2012; Zhang et al., 2016, 2017) (figure 1.9.b). EIN3 promotes the expression of transcription factors such as ERF1 and octadecanoid-responsive Arabidopsis AP2/ERF59 (ORA59), which contribute to the expression of ET-responsive genes and the activation of the ET responses.

3.3.3. *ET pathway regulation*

Negative regulation of ET is mainly mediated by CTR1. Indeed, the *ctr1* mutant exhibits a constitutive ethylene response (Kieber et al., 1993). CTR1 phosphorylates the CEND domain of EIN2 to promote its degradation to negatively regulate ET signaling. The importance of CTR1's regulations on EIN2 was demonstrated by showing that the expression of a phospho-dead version of *EIN2* in the *ein2* mutant leads to a *ctr1*-like phenotype (Ju et al., 2012).

3.4. Crosstalk between defense hormones

Extensive studies on hormonal pathways interactions were conducted using various methods, including mutant screens and exogenous hormone applications (Aerts et al., 2021). These investigations uncovered a complex network of hormonal pathways with synergistic, antagonistic, and additive interactions, which are commonly referred to as hormonal crosstalk. Hormonal crosstalk allows the plant to develop a robust immune system and select one pathway over the others depending on the colonization strategy of the pathogen (Spoel et al., 2007; Spoel & Dong, 2008). Additionally, hormone crosstalks are required to maintain the balance between growth and defense to minimize the fitness cost of defense responses (Denancé et al., 2013). In this section, the crosstalks between SA, JA, and ET are explored.

3.4.1. JA-ET

Generally, ET is considered to function together with JA in plant defenses against necrotrophic pathogens by activating the ERF-branch of JA (Li et al., 2019.; Penninckx et al., 1998). The ERF branch of the JA pathway is activated by EIN3 and EIL1 upstream the TFs ORA59 and ERF1, which directly activate the expression of ERF-branch marker genes such as *PDF1.2* (Lorenzo et al., 2003; Zarei et al., 2011; Zhu et al., 2011) (figure 1.10). The ERF branch is, however, suppressed by the MYC2 branch of JA. In fact, Song et al. reported that MYC2 represses the activity of EIN3 either directly, by binding to EIN3 to prevent it from activating its target genes, and indirectly by up-regulating the expression of *EBF1*, which promotes the degradation of EIN3 (Song et al., 2014). In the same way, EIN3 binds to MYC2 to inhibit its transactivation activity (Song et al., 2014; Zhang et al., 2014). Zhu et al. reported that JAZ proteins are also involved in inhibiting the ERF branch of JA/ET by directly interacting with EIN3 and recruiting the histone deacetylase HDA6 as a corepressor of the EIN3-induced *ORA59* and *ERF1* gene expression (Zhu et al., 2011) (figure 1.10).

3.4.2. JA-SA

The first evidence of an SA-JA crosstalk was initially demonstrated in tomato, where the exogenous application of SA and its acetylated version aspirin hindered the JA-dependent wound response (Pena-Cortés et al., 1993). The JA-SA antagonistic relationship was also evidenced by discovering the phytotoxin coronatine generated by *Pseudomonas syringae* (Brooks et al., 2005). Coronatine mimics the function of JA-Ile and induces the MYC2 branch of the JA-signaling pathway, which stimulates the expression of three NAC-domain TFs, *ANAC019*, *ANAC055*, and *ANAC072* (Zheng et al., 2012). The NAC TFs inhibit the expression of the SA biosynthesis gene *ICS1* and activate the SA methyltransferase gene *BSMT1* (figure 1.10), thereby increasing MeSA levels and decreasing free SA levels (Zheng et al., 2012). As a result, resistance to *Pst* DC3000 is lowered. These findings were corroborated by discovering that *myc2* mutant plants exhibit increased SA levels, higher *PR1* expression, and enhanced resistance to *Pst* DC3000 compared to WT plants (Laurie-Berry et al., 2007). Similarly, mutations of the JA receptor coding gene *COI1* result in increased endogenous SA levels and higher resistance to *Pseudomonas syringae* (Kloek et al., 2001). SA, on the other hand, antagonizes the JA pathway via WRKY TFs. In fact, the W-box motif, bound by WRKYs, is overrepresented in the promoters of JA-responsive genes that are repressed by SA (Van der Does et al., 2013). Studies

on the *ssi2* mutant, identified in a suppressor screen of the *npr1* mutant, which displayed high SA levels and repressed JA-inducible genes (Kachroo et al., 2001), revealed that two WRKY TFs are involved in the repression of JA responses in this mutant, namely WRKY50 and WRKY51. In fact, the W-box containing JA-inducible genes, such as *PDF1.2* and *VSP2*, that are repressed in the *ssi2* mutant, were no longer repressed in the *ssi2 wrky50* or *ssi2 wrky51* double mutants (Gao et al., 2011). Overexpression of WRKY70 increases SA-responsive PR genes' expression while suppressing JA-responsive marker gene *PDF1.2* in an NPR1-dependent way (Li et al., 2004, 2006). Several other WRKYs were reported to be involved in the SA-JA crosstalk and were reviewed by Caarls et al. (2015); Pieterse et al. (2012), and Yang et al. (2015). NPR1 has also been reported to play a significant role in the SA-JA antagonism. Indeed, Spoel et al. showed that JA-responsive genes which are repressed by exogenous SA treatment were no longer repressed in the *npr1-1* mutant (Spoel et al., 2003).

Synergistic interactions between SA and JA have also been reported (Liu et al., 2016). In plants infected by *Pseudomonas syringae* pv. *maculicola* strain ES4326 expressing the effector AvrRpt2, NPR3, and NPR4 interact with JAZs repressors in an SA-dependent way (Liu et al., 2016). NPR3 and NPR4 target JAZs for degradation by recruiting the Cullin3 (Cul3) ubiquitin E3 ligase (figure 1.10). The degradation of JAZs leads to an increased JA signaling required for an efficient HR against *Pseudomonas syringae* pv. *maculicola* ES4326 (Liu et al., 2016). In contrast, a recent study by Cui et al. showed that EDS1 antagonizes the JA pathway by interacting with MYC2 to prevent binding to its target promoters in an AvrRps4-induced ETI context (Cui et al., 2018) (figure 1.10). This antagonistic interaction results in a lower MYC2-induced *BSMT1* expression and MYC2 repression of *ICS1* expression, leading to higher free SA levels in response to AvrRps4 and efficient response to the hemibiotrophic *Pst* DC3000 (Cui et al., 2018). However, it is important to note that the results reported by Liu et al. (2016) were observed only four hours after inoculation by *Pseudomonas syringae* pv. *maculicola* ES4326. Therefore, Cui et al. concluded that synergistic crosstalk might occur early during ETI, but SA and JA remain mainly antagonistic, and that their results emphasize the importance of prioritizing SA over JA pathways in TNL-mediated immune response (Cui et al., 2018).

3.4.3. SA-ET

As was demonstrated above for JA, SA also inhibits the ET pathway. Previous studies have shown that TGA2, TGA5, and TGA6, the positive regulators of the NPR1-dependent SA-

signaling pathway, are required to induce the expression of *PDF1.2* in response to the ET precursor ACC and in the absence of SA (Zander et al., 2010). Microarray analyses comparing WT and *tga2 tga5 tga6* mutant plants revealed that 374 genes were activated in WT plants following treatment with ACC, of which 136 were depending on TGA2, TGA5, and TGA6. Half of these ACC-inducible TGA-dependent genes were suppressed by SA in WT plants following combined treatment with ACC and SA. This result implies a function for TGAs in both the activation and repression of some ethylene-responsive genes in response to ACC and SA, respectively (Zander et al., 2014). The authors also found that TGAs bind to the promoter region of the *ORA59* TF and promote repression in response to SA (figure 1.10). The authors hence concluded that SA suppresses ET signaling by inhibiting the expression of the TF *ORA59* through TGA2, TGA5, and TGA6 (Zander et al., 2014).

ET has also been shown to antagonize the SA pathway (Chen et al., 2009). Indeed, the *ein3 eil1* double mutant showed a higher expression of *ICS1* compared to WT, and Chromatin Immunoprecipitation (ChIP) and electrophoretic mobility shift assay (EMSA) tests revealed that EIN3 binds to the promoter region of *ICS1* (Chen et al., 2009). Additionally, SA levels are increased in the *ein3 eil1* double mutant compared to WT (Chen et al., 2009).

4. The importance of membrane trafficking in plant immunity

The endomembrane system of eukaryotic organisms comprises several organelles, each with its own set of membrane lipids and cargo proteins. Membrane trafficking is a crucial cellular activity in eukaryotic cells that allows cargoes to be transported to the appropriate compartment via small membrane-enclosed transport vesicles to maintain cellular homeostasis. Studies on mammals, yeast, and plants showed that highly conserved components coordinate membrane trafficking among eukaryotic species (More et al., 2020). This section will cover a brief overview of protein trafficking routes identified in plants, followed by an examination of the secretory and endocytic systems' roles in plant immunity. Following that, SNARE's function and involvement in immunity will be explored, and finally, the research performed on the SNARE protein SNAP33 will be covered.

In eukaryotes, three major trafficking pathways have been identified: (i) the secretory pathway, which transports newly synthesized proteins from the endoplasmic reticulum (ER) through the Golgi apparatus and the Trans-Golgi network (TGN), and then to the plasma membrane or

extracellular space; (ii) the vacuolar route, which transports newly synthesized proteins from ER to TGN and the vacuole; and (iii) the endocytic pathway, which enables external cargoes to be internalized and recycles plasma membrane-localized proteins to early endosomes, and eventually to the late endosomes or vacuole for degradation (Bassham et al., 2008; Jürgens, 2004). Each trafficking route begins with vesicle budding from the donor membrane, transport to the target compartment, tethering, and finally, vesicle fusion (Jürgens, 2004).

Vesicle budding involves small GTPases belonging to the ADP ribosylation factor (ARF) and the secretion-associated RAS superfamily 1 (SAR1) proteins (Cevher-Keskin, 2013). Depending on the compartment, a specific ARF/SAR1 GTPase is activated by a transmembrane guanine nucleotide exchange factor (GEF) protein and mediates the recruitment of coat proteins (Cevher-Keskin, 2013). Rat brain (Rab) type GTPases, on the other hand, direct the vesicles to the target compartment and define the specificity of the destination. Tethering of a vesicle to the target membrane is mediated by the interaction of the Rab GTPase with a specific set of tethering factors depending on the destination (Stenmark, 2009; Whyte & Munro, 2002). Each tethering step is controlled by a unique tethering complex, such as conserved oligomeric golgi (COG), which functions in retrograde trafficking inside the Golgi, HOPS-CORVET (homotypic fusion and vacuole protein sorting-class C core vacuole/endosome tethering vacuole protein sorting), which tethers vesicles to the lysosome/vacuole, and exocyst involved in the last step of the secretory pathway (Whyte & Munro, 2002). Finally, vesicle fusion to the PM is achieved by the assembly of a ternary SNARE complex at the target membrane (Jahn et al., 2003).

4.1. Overview of the trafficking pathways in plants

4.1.1. *The secretory and vacuolar pathway*

The secretory route in plants is engaged in the delivery of cell wall components to mediate growth and expansion, as well as the transport of PM-residing proteins to the PM, and is also involved in abiotic and biotic stress responses (Kim & Brandizzi., 2016; Kwon et al., 2008; Wang & Dong., 2011; Wang et al., 2020).

The secretory pathway starts in the endoplasmic reticulum (ER) (figure 1.11). The proteins targeted to the secretory pathway carry a signal peptide that drives their entry to the ER (Vitale & Denecke, 1999). In the ER, the signal peptide is cleaved to enable a correct folding of the protein, and the folding is further checked through the ER quality control (Brandizzi et al., 2003).

Correctly folded proteins are then packaged into membrane-enclosed vesicles by COPII proteins to enable their anterograde transport to the Golgi apparatus (Alberts et al., 2002). The Golgi apparatus consists of several stacks of cisternae. The proteins pass through the Golgi either by vesicle movement or by cisternal maturation to reach the trans-Golgi network (TGN), the secretory pathway's sorting station, which determines the final destination of each protein (Viotti et al., 2012). From the TGN, proteins with vacuolar sorting signals are recognized by vacuolar sorting receptors (VSRs), and are then transported to the late endosome/prevacuolar compartment (PVC), also known as multivesicular bodies (MVB), which contain numerous intraluminal vesicles (ILVs), and eventually the lytic vacuole (LV) or the protein storage vacuole (PSV) (Tse et al., 2004) (figure 1.11). Proteins without vacuolar sorting signals are targeted to the PM or the extracellular space (figure 1.11). In this secretory pathway, the exocyst complex of tethering factors mediates the early steps of exocytosis (Jürgens, 2004). There are eight exocyst members in plants: Sec3, Sec5, Sec6, Sec8, Sec10, Sec15, Exo70, and Exo84 (Žárský et al., 2013). The exocyst is a multiprotein complex required for the interaction of vesicles with the plasma membrane before SNARE-mediated fusion and contributes to the specificity of the target membrane (Žárský et al., 2013).

4.1.2. *The endocytic pathway*

Endocytosis provides a major entry route for membrane proteins, lipids, and extracellular molecules into the cell (Šamaj et al., 2005). Multiple cellular processes require endocytosis, such as nutrient uptake, signal transduction, and plant-microbe interactions (Irani & Russinova, 2009; Leborgne-Castel et al., 2010).

The endocytic pathway begins by invagination of the PM. Internalized cargoes first arrive at the early endosomes (EE)/TGN, the sorting station of the newly internalized cargoes. From the TGN/EE, the internalized cargoes are either recycled back to the PM or transported to the late endosomes (LE) or MVBs, where they are destined to the lysosome/vacuole for degradation (Fan et al., 2015; Floyd, 2015).

Cargoes internalization

Internalization of cargoes via endocytosis is mediated by clathrin-coated vesicles (CCV) (Chen et al., 2011). CCV formation at the PM starts by the association of adaptor proteins (AP) complex with the PM component phosphatidylinositol 4,5-bisphosphate (PIP₂), a phospholipid present

in the internal leaflet of the PM (Floyd, 2015). The AP-PIP2-cargo complex induces the recruitment of clathrin around the newly formed membrane invagination (Floyd, 2015). When the CCV matures, a dynamin-related protein (DRP) type GTPase is recruited to dissociate the newly formed CCV from the PM (Chen et al., 2011). Once the CCV is pinched off the membrane, the clathrin coatomers are dissociated, and the vesicle is targeted to the TGN/EE (Viotti et al., 2012). From the TGN/EE, the cargoes are either recycled back to the PM or directed to the LE/MVB and the vacuole for degradation (Viotti et al., 2012) (figure 1.11).

The TGN is a station for receiving and sorting endocytosed cargoes and cargoes arriving from the ER following the secretory and vacuolar pathway, as mentioned earlier in the secretory pathway section (Viotti et al., 2012). The TGN contains different classes of cargoes suggesting that the TGN might have separate compartments, each with a specific set of cargoes (Reyes et al., 2011). The budding of vesicles, containing cargoes destined for recycling to the PM, from TGN/EE, is mediated by ARF GEFs belonging to the GNOM and BIG families (Viotti et al., 2012).

Degraded cargoes

Post-translational modifications of PM proteins, such as ubiquitination and phosphorylation, are major signals for triggering their internalization by endocytosis (Chen et al., 2011; Reyes et al., 2011). Ubiquitinated cargoes, such as PRRs, are sequestered in LEs and are later transported to the vacuole for degradation. LE is also called MVB because it contains small vesicles bound by an outer limiting membrane. The formation of ILVs and sequestration of cargoes are mediated by a series of protein complexes called endosomal sorting complexes required for transport (ESCRTs) (Floyd, 2015).

ESCRT-0 binds to the endosomal membrane after recognizing ubiquitinated membrane protein cargoes on their way to degradation. It also attaches to ESCRT-I in the cytoplasm and recruits it to the endosomal membrane. The ESCRT-I and ESCRT-II complexes are thought to cause membrane distortion, which leads to cargo-containing vesicles' internalization into the MVB. ESCRT-II recruits ESCRT-III to the membrane, which is required to tighten the inward budding membrane neck and scission to release the ILV inside the MVB. SKD1 is required to dismantle the ESCRT complex and restore it for future budding rounds (Reyes et al., 2011). It is important to note that despite the high conservation of the endocytic machinery in eukaryotes, ESCRT-0 is lacking in plant species, and other proteins have been found to carry out the ESCRT-0 function in plants (Floyd, 2015).

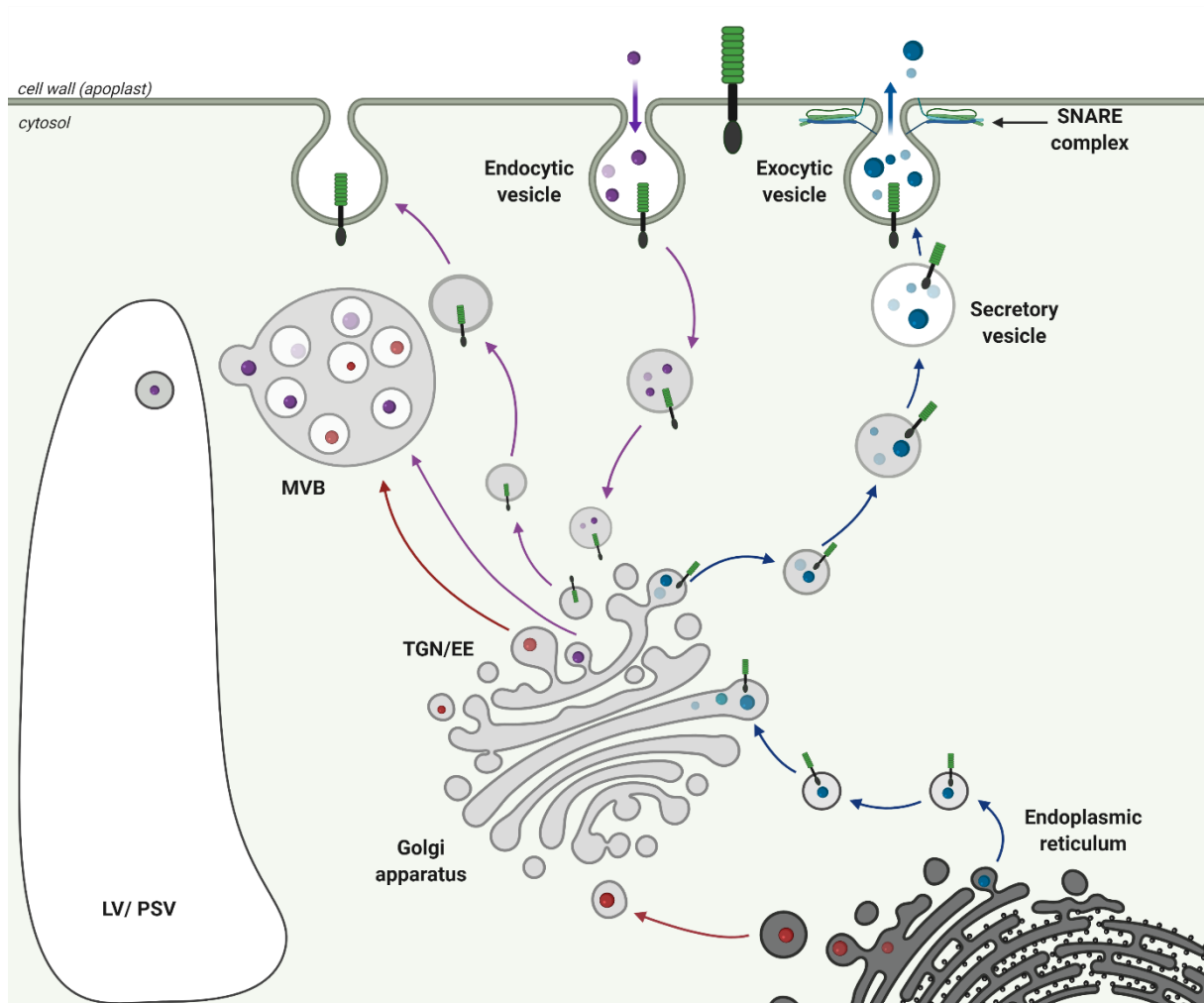


Figure 1.11. Schematic view summarizing the trafficking pathways in plants under resting conditions. Secreted molecules and PM receptors are targeted to the extracellular space (apoplast) and to the PM, respectively, through the default secretory pathway (blue arrows). The secreted cargoes enter the ER via their signal peptide where they are translated and packaged into vesicles. The vesicles then travel through the Golgi cisternae to reach the TGN/EE, the sorting station of different cargoes. From the TGN/EE the proteins which are targeted to the LV/PSV are transported through MVBs (red arrows). Secreted proteins are delivered from the TGN/EE to the plasma membrane (blue arrows) and fused to the target membrane by SNARE complexes. PM receptors, such as FLS2, undergo constitutive endocytosis, which induces the internalization of FLS2 to the TGN/EE. From the TGN/EE, internalized FLS2 is recycled back to the PM (purple arrows). TGN: trans-Golgi network; EE: early endosome; PSV: protein storage vacuole; LV: lytic vacuole; MVB: multivesicular bodies.

Not all proteins reaching the LE are destined for degradation. In yeast and mammals, it was reported that some deubiquitinases promote the recycling of PM resident proteins from MVB via deubiquitination (Piper et al., 2014). Such deubiquitinating proteins have been identified in humans as AMSH (associated molecule with the SH3 domain of STAM) and USP8 (ubiquitin-specific protease 8) and have been shown to associate directly with the ESCRT-0 complex, as well as with some ESCRT-III components (Valencia et al., 2016). In Arabidopsis, three AMSH proteins, AMSH1, AMSH2, and AMSH3, have significant sequence similarities to human AMSH (Isono et al., 2010). AMSH3 can hydrolyze Lys48-linked and Lys63-linked ubiquitin chains, *in vitro* and *in vivo*. Although the specific role of AMSH3 in endosomal trafficking is unclear, it is required for proper MVB formation and appropriate trafficking between the TGN and the vacuole (Isono et al., 2010).

There is also evidence of an internalization process that is CCV independent. It starts from the membrane microdomains and is induced by the clustering of transmembrane proteins (Fan et al., 2015; Šamaj et al., 2005).

4.2. The involvement of membrane trafficking in plant immunity

In plants, pathways of membrane trafficking are critical for disease resistance. Their involvement was demonstrated by discovering that mutations in genes involved in the membrane trafficking system affect the plant's immune responses (Gu et al., 2017; Inada & Ueda, 2014). In addition, the development of very advanced microscopic technologies, combined with labeling experiments, enabled the visualization of different cellular compartments and organelles and their dynamics during plant-microbe interactions.

4.2.1. *The importance of the secretory machinery in plant immunity*

As mentioned earlier, in the conventional secretory pathway, the cargoes follow the ER to TGN/EE pathway and are subsequently directed to the PM for exocytosis. In this route, the tethering proteins belonging to the exocyst family mediate the docking of vesicles to the PM by interacting with small GTPases and membrane lipids. Several members of the EXO70 family were reported to be important in plant defense response. For instance, disruption of genes encoding two members of the EXO70 family, *EXO70B2* and *EXO70H1*, leads to an increased susceptibility to infection by *Pseudomonas syringae* (Pečenková et al., 2011). In addition,

EXO70H1 and *EXO70B2* expression levels are increased in response to several PAMPs, including flg22 (Pečenková et al., 2011; Zipfel et al., 2004). Papillae formation around powdery mildew *Blumeria graminis* penetration sites were altered in *exo70h1* and *exo70b2* mutants (Pečenková et al., 2011). The interaction between *EXO70B2* and *EXO70H1* and the phenotypes of *exo70b2* and *exo70h1* mutants suggest that they are part of a tethering complex involved in the secretion of anti-microbial compounds. In another study, Stegmann et al. showed that *exo70b2* mutant is impaired in PAMP-triggered responses, such as ROS burst and MPK3 activation, indicating that *EXO70B2* is also associated with signal transduction in immunity (Stegmann et al., 2012). Another *EXO70* subunit with a reported role in immunity is *EXO70B1*. *EXO70B1* is the closest homolog of *EXO70B2* (Stegmann et al., 2012). Knocking out *EXO70B1* leads to a reduced defense response to the avirulent *Pst* DC3000 in young seedlings due to altered PTI responses (Stegmann et al., 2013). However, at later growth stages, *exo70b1* displayed an increased resistance due to constitutive activation of CPK5 and an atypical intracellular R protein lacking the LRR domain, namely TIR-NBS2 (TN2) (Liu et al., 2017; Zhao et al., 2015). Later, it was discovered that the *Pseudomonas syringae* effector AvrPtoB targets *EXO70B1* (Wang et al., 2019). AvrPtoB triggers the degradation of *EXO70B1* via ubiquitination, likely to alter the *EXO70B1*-mediated secretion of defense-related molecules, which in turn lead to activation of TN2, which is otherwise maintained in an inactive state by *EXO70B1* (Wang et al., 2019). This work reveals that pathogen effectors target components of the trafficking machinery. More recently, Wang and colleagues showed that the abundance of FLS2 at the PM depends on the exocyst subunits *EXO70B1* and *EXO70B2*. Indeed, the abundance of FLS2 at the PM is significantly decreased in *exo70b1* and *exo70b2* mutants (Wang et al., 2020). Overall, these findings indicate that the *EXO70* vesicle tethering family plays various roles in plant immunity, including anti-microbial compound secretion, signaling, and PRR delivery.

Another interesting example showing the importance of the secretory pathway in plant defense is the regulation of RBOHD localization upon oomycete *Phytophthora cryptogea* (*P. cryptogea*) treatment in tobacco Bright Yellow-2 (BY-2) cells (Noirot et al., 2014). In this study, the authors showed that GFP-fused RBOHD localizes to the Golgi cisternae and another unidentified compartment in untreated cells. However, when treated with the cryptogein effector purified from *P. cryptogea*, the Golgi-associated pool of RBOHD is relocated to the PM to increase ROS production in the apoplast (Noirot et al., 2014). Thus, this study reveals that plants enhance

their secretory activity in response to pathogens to relocate important defense components to their function compartment to trigger defense responses.

Further evidence demonstrating the involvement of the secretory pathway in the delivery of anti-microbial compounds was shown by identifying *SNARE* mutants with impaired delivery of anti-microbial compounds and decreased resistance to pathogens and will be detailed later in the manuscript (see section 4.4). Several other studies reported the importance of the secretory machinery in plant defense response by analyzing mutants of Rab GTPases and other tethering factors and are reviewed by Gu et al. (2017); Inada & Ueda (2014); Ruano & Scheuring (2020).

4.2.2. *Unconventional secretory pathways in plant immunity*

Previous proteomic investigations revealed that approximately 50% of secreted proteins lack a signal that directs them to the secretory route, commonly known as leaderless proteins. This finding shows that some released proteins may not take the regular secretory routes (Drakakaki & Dandekar, 2013; Nickel & Rabouille, 2009). Furthermore, microscopic investigations revealed the presence of unique structures that function as secretory vesicles, such as ER bodies and exocyst-positive organelle (EXPO) in infected plants (Gu et al., 2017; Ruano & Scheuring, 2020). Moreover, vesicular structures that ordinarily serve as vacuolar compartments function as secretory vesicles during a pathogen attack (Drakakaki & Dandekar, 2013; Ruano & Scheuring, 2020). However, these unconventional transport mechanisms lack healthy plants, and most of them are not well known. Therefore, they were designated unconventional secretory pathways (figure 1.12) (Drakakaki & Dandekar, 2013; Ruano & Scheuring, 2020).

ER bodies

The ER is made up of tubules and cisternae that form a highly ordered structure. In the *Brassicales* order, including *Arabidopsis thaliana*, ER-derived rod-shaped structures with luminal continuity to the ER were identified and termed ER bodies (Nakano et al., 2014). ER bodies are present in cotyledons, hypocotyls and roots under normal conditions and accumulate high amounts of β -glucosidase (Matsushima et al., 2003).

The earliest studies found that ER bodies are missing in mature plant rosette leaves under normal conditions, but they increase in number after wounding or JA treatment, suggesting that the β -glucosidase-containing ER bodies produce defense compounds when plants are damaged by insects or by wounding (Matsushima et al., 2002).

The following study by Watanabe et al. described a new immune response known as enhanced secretion of proteins localized in ER bodies (ESPER) (Watanabe et al., 2013). They found that the two anti-microbial proteins PDF1.2 and PR1, accumulate in ER bodies at resting conditions and are released in the apoplast in response to the non-adapted pathogenic fungus *Colletotrichum gloeosporioides* by a mechanism that seems to bypass the default TGN route (Ruano & Scheuring, 2020; Watanabe et al., 2013) (figure 1.12).

MVBs

Although MVBs are considered as late endosomes involved in cargoes transport from TGN/EE to the vacuole as well as in cargo recycling during endocytosis (Contento & Bassham, 2012; Hu et al., 2020), MVBs were also found to mediate secretion during defense responses as part of an unconventional secretory pathway (figure 1.12) (Ruano & Scheuring, 2020).

It has been shown that the ILVs of the MVBs can fuse with the PM to release their contents into the extracellular space as exosomes (Hu et al., 2020; Li et al., 2018). An and colleagues used transmission electron microscopy, cytochemistry, and immunocytochemistry to demonstrate this process (An et al., 2006). The authors showed that MVBs accumulate around cell wall appositions or papillae and carry H₂O₂ or other autofluorescent phenolic compounds in plants infected with powdery mildew fungus (An et al., 2006). Another study further reported the accumulation of such unconventional secretory vesicles by showing that infection with *Pst* DC3000 promotes the biogenesis of MVBs (Wang et al., 2014). Wang et al. showed that MVB biogenesis requires LYST-Interacting Protein 5 (LIP5) in response to *Pst* DC3000. MPK3 and MPK6 phosphorylate LIP5, and its phosphorylation is crucial for its MVB biogenesis activity and resistance to *Pst* DC3000 (Wang et al., 2014).

In another study, Pečenková and colleagues showed that PR1 colocalizes prominently with the MVBs, indicating that PR1 can also be secreted via the MVBs in addition to the conventional ER-TGN/EE secretory pathway (Pečenková et al., 2017).

Exocyst positive organelle

The exocyst positive organelle (EXPO) is another vesicular structure engaged in unconventional secretion (Gu et al., 2017). The double membrane structure of EXPO distinguishes it from MVBs and TGN/EE, as well as the fact that it is uniquely labeled by exocyst complex proteins such as EXO70A1, EXO70B1, and EXO70E2 (Wang et al., 2010) (figure 1.12). Moreover, EXPOs are not labeled by any standard endomembrane markers used to identify the Golgi apparatus, the

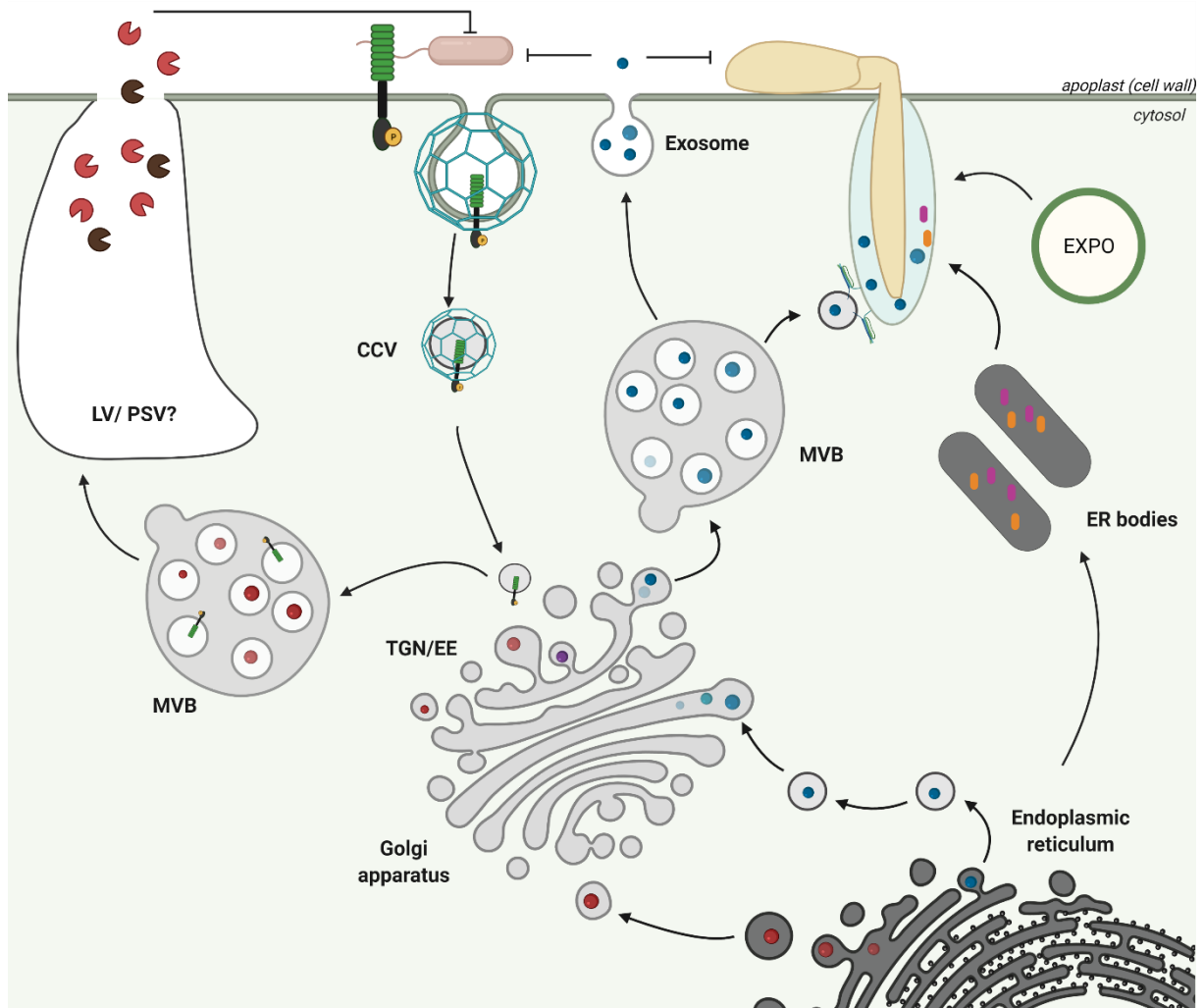


Figure 1.12. Schematic view summarizing the unconventional trafficking pathway in plants during immune responses. When attacked by pathogens, plants use unconventional secretory pathways to secrete antimicrobial compounds. These unconventional secretory pathways include secretion through MVBs, which release their content as exosomes in pathogen penetration sites (fungal pathogens) or the extracellular apoplastic space (bacterial pathogens). ER bodies are rod-shaped ER-derived structures that contain antimicrobial proteins and that were also observed during infection. However, the processes behind the release of ER-bodies containing antimicrobial proteins remain unknown. It might be via fusion to the PM. Another unusual secretory vesicle that was observed during pathogen infection is the exocyst-positive organelles (EXPO) which transport cargoes of unknown nature. During the bacterial invasion, vacuoles (LV/PSV) were found to merge with PM and discharge their contents (refer to text for details). Besides these unconventional secretory pathways, some PRRs, such as FLS2, were shown to undergo clathrin-mediated endocytosis upon bacterial recognition, and this internalization is critical for signal transmission and quenching. CCV: clathrin-coated vesicle; TGN: trans-Golgi network; EE: early endosome; PSV: protein storage vacuole; LV: lytic vacuole; MVB: multivesicular bodies. Adapted from (Gu et al., 2017).

TGN, or MVB (Wang et al., 2010). The identity of EXPO-transported cargoes remains, however, unknown.

Vacuole

The vacuole is the largest plant organelle, and it can take up to 90% of the cellular volume and performs a variety of activities. Vacuoles store phytoanticipins as inactive precursors. Such phytoanticipins include cyanogenic glycosides and glucosinolates, which are rapidly transformed into physiologically active antibiotics by plant enzymes in response to pathogen infection or herbivore damage (Floyd, 2015). Moreover, vacuoles contain several enzymes and anti-microbial proteins (Floyd, 2015). Two pathways for vacuole-mediated defenses have been reported. First, vacuoles can collapse and leak their contents into the cell as part of a cell suicide strategy to promote virus resistance by restricting it to infected cells (Hatsugai et al., 2006). Vacuoles can also fuse to the PM and discharge their contents into the extracellular space when plants are challenged with *Pst* DC3000 (Hatsugai et al., 2009) (figure 1.12).

4.2.3. *The role of the endocytic pathway in plant immunity*

The importance of the endocytic pathway in plant immunity was evidenced by its role in regulating the levels of PM-located receptors such as PRRs (Mbengue et al., 2016). Studies on FLS2 trafficking showed that it undergoes constitutive recycling through the endosomal pathway under normal unstressed conditions and a flg22-induced internalization which seems to be required for downstream signaling (Beck et al., 2012; Robatzek et al., 2006). Indeed, Beck et al. reported that FLS2 recycles through the endocytic pathway as part of a process that regulates its steady-state levels at the PM (Beck et al., 2012). Other studies showed that flg22 treatment induces a clathrin-mediated internalization of FLS2, which depends on its phosphorylation state (Mbengue et al., 2016; Robatzek et al., 2006) (figure 1.12). Indeed, substitutions in the FLS2 phosphorylation site yielding a phospho-dead version of FLS2 abolished its flg22-induced internalization and flg22-induced responses such as ROS accumulation (Robatzek et al., 2006). flg22-induced internalization of FLS2 leads to its degradation, which is probably required for signaling and signal quenching to avoid excessive induction of FLS2-induced responses (Robatzek et al., 2006). Later, another study reported that mutations in the ESCRT components of the endocytic machinery compromised FLS2 internalization as well as flg22-induced stomatal closure, showing that the endocytosis of FLS2 upon flg22 binding is essential for downstream signaling and indicating that FLS2 signals from

both the PM and the endocytic compartments (Bourdais et al., 2019; Spallek et al., 2013). Mutation of the Dynamin- Related Protein 2B (DRP2B), involved in the internalization of FLS2, resulted in an altered PTI response to *Pst* DC3000 *hrcC* infection, shown by enhanced early PTI responses, including increased cytosolic Ca^{2+} concentration and ROS production, but compromised late PTI outcomes, including *PR1* expression (Smith et al., 2014). Overall these studies show that the endocytic pathway plays an important role in plant immunity by signal transduction and by maintaining homeostasis.

4.3. SNAREs: Very conserved proteins and the main executors of membrane fusion processes in the endomembrane system of plants

SNAREs are very conserved proteins among the eukaryotic clade and are the central players in vesicle fusion processes in the endomembrane system (Khurana et al., 2018). SNARE proteins were initially discovered as components of the synaptic secretory vesicles responsible for neurotransmitter release at neural synapses (Clary & Rothman, 1990). The nomenclature SNARE stands for SNAP Receptor and is based on their ability to interact with the soluble N-ethyl-maleimide-sensitive factor attachment protein (SNAP) (Clary & Rothman, 1990).

The mechanism of vesicle-to-membrane fusion via SNAREs was later described by Nobel laureates James E. Rothman, Randy W. Schekman, and Thomas C. Südhof, who proposed the SNARE hypothesis to explain the fusion process (Rothman, 2013; Söllner et al., 1993). According to this hypothesis, a SNARE associated with a vesicle (v-SNARE) and SNAREs on the target membrane (t-SNAREs) form a complex which pulls the lipid bilayers together and initiates a membrane merge (Söllner et al., 1993). During the fusion process, the SNARE complex acts as a receptor for SNAP, which recruits the ATPase protein N-ethyl-maleimide-sensitive fusion protein (NSF). The energy generated by ATP hydrolysis by NSF is subsequently used to induce vesicle fusion (Rothman, 2013; Söllner et al., 1993) (figure 1.13).

4.3.1. Nomenclature and classification

SNAREs were formerly classified as t-SNAREs and v-SNAREs based on their localization during the fusion process. Later, additional SNARE proteins were discovered and could not be easily assigned to these two groups. Therefore, a classification based on amino-acid sequence has emerged (Weimbs et al., 1997). Indeed, SNAREs share a common 60 to 70 amino acid sequence

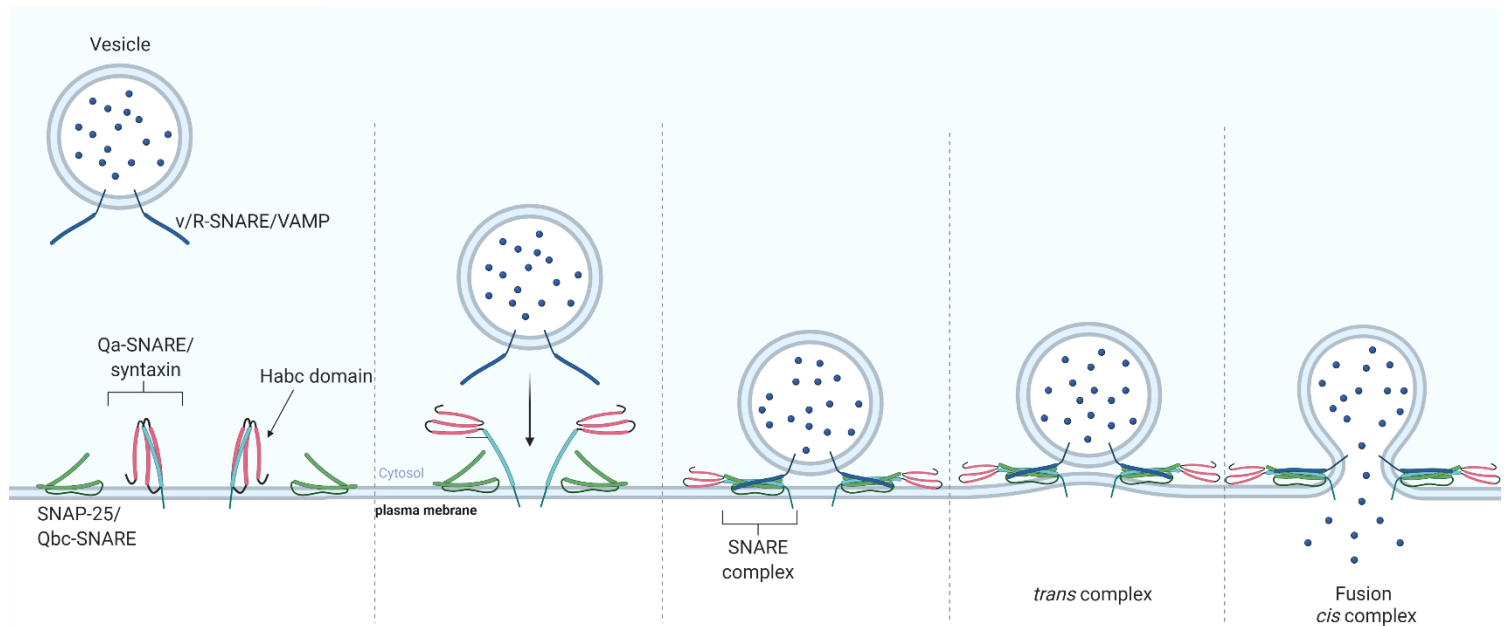


Figure 1.13. Schematic view of vesicle fusion by the SNARE complex. At resting conditions and in the absence of vesicles, the Qa-SNARE/syntaxin is maintained in a closed “conformation” by the Habc domain, which interacts with the SNARE domain to prevent constitutive interaction between the Qa-SNARE/syntaxin and its other SNARE partners. Vesicle fusion is initiated by opening (activating) a closed Qa-SNARE/syntaxin on the target membrane, which is mediated by proteins from the Sec1/Munc18 family, which unfold the closed conformation of the Qa-SNARE/syntaxin. The resulting “open” conformation allows the association of Qa-SNARE/syntaxin helices with helices provided by the membrane-associated Qbc- and by the vesicle-associated R-SNARE. Association of the Qa, Qb Qc, and R helices in a *trans* complex is accompanied by an increase in the core α -helical structure density that promotes the transition to the *cis* complex, membrane fusion, and the release of vesicle cargo into the acceptor compartment. Adapted from Lipka et al., (2007).

in their N-terminal part, termed SNARE motif (Weimbs et al., 1997). The central residue in the SNARE motif is either arginine (R) or glutamine (Q), with t-SNAREs being Q-SNAREs and most of the v-SNAREs being R-SNAREs (Fasshauer et al., 1998). R-SNAREs are often referred to as vesicle-associated membrane proteins (VAMPs) due to their presence on vesicles. Q-SNAREs are further subdivided into four subgroups: Qa-SNAREs, also referred to as syntaxins, Qb-SNAREs, Qc-SNAREs, and Qbc-SNAREs, also called SNAP25-like proteins containing two SNARE domains. A functional SNARE complex assembles into a four-helix bundle in which each α -helix is represented by a different SNARE motif, with a Qbc-SNARE/SNAP25-like protein contributing two α -helices or Qb- and Qc-SNAREs contributing one α -helix each; a Qa-SNARE which contributes with one α -helix, and the R-SNARE contributing with one α -helix (Lipka et al., 2007). The terminology Qa-SNAREs, Qb-SNAREs, Qc-SNAREs, and Qbc-SNAREs was established based on the position of the SNARE motif in the four-helix bundle (Lipka et al., 2007; Zwilling et al., 2007). Qa-SNAREs/syntaxins contain an auto-inhibitory motif termed Habc (figure 1.13), which interacts with the SNARE motif on the same polypeptide to generate an inactive "closed conformation" that is unable to interact with the other SNAREs (Misura et al., 2001; Munson et al., 2000). Proteins from the Sec1/Munc18 (SM) family of small GTP-binding Rab proteins can unfold the closed Qa-SNAREs, switching them to the active form (also known as the "open" conformation) to enable the formation of the SNARE complex (Burgoyne & Morgan, 2007; Waters & Hughson, 2000). The interaction of the helices of the cognate SNAREs forms a complex referred to as the trans complex, which evolves into a denser helical complex referred to as the cis-complex and mediates membrane fusion (figure 1.13) (Lipka et al., 2007). Fifty-four SNARE genes have been identified in Arabidopsis (Sanderfoot et al., 2000), with 18 Qa-SNAREs/Syntaxins, 11 Qb-SNAREs, 8 Qc-SNAREs, 14 R-SNAREs/VAMPs, and 3 Qbc-SNAREs/SNAP25-like proteins (figure 1.14) (Uemura et al., 2004). SNARE proteins show multiple localization patterns, including the ER, the Golgi apparatus, the TGN, endosomes, plasma membrane, PVC, and vacuoles, indicating their involvement in all stages of vesicular trafficking in Arabidopsis (Uemura et al., 2004).

4.3.2. SNAREs are involved in plant immunity: the case of SYP121 and its interacting SNARE partners

The first identified SNARE protein with a role in plant defenses was the Qa-SNARE SYP121. SYP121 was identified in a screen for mutants with a decreased penetration resistance to the

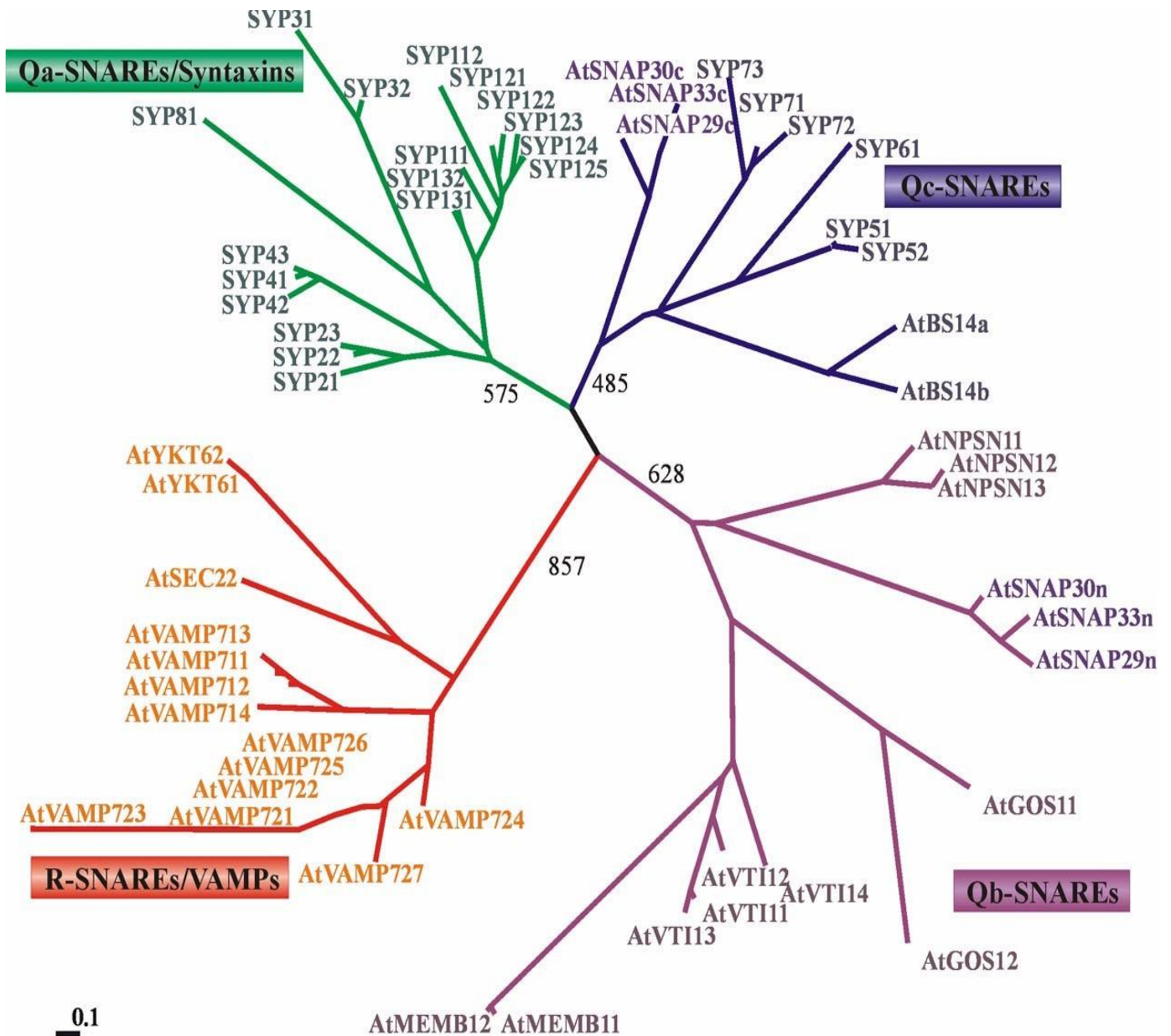


Figure 1.14. Schematic view of an unrooted phylogenetic tree of the SNARE family in Arabidopsis.

The phylogenetic tree was generated using the SNARE motifs, which included 67 amino acid residues. The scale bar represents the Dayhoff distance between the SNARE molecules. The SNARE proteins were divided into four distinct groups based on the similarity of their SNARE domains (green, Qa-SNARE/Syntaxin; purple, Qb-SNARE; blue, Qc-SNARE; and red, R-SNARE/VAMP).

Uemura et al. (2004)

barley powdery mildew fungus *Blumeria graminis f. sp. hordei* (*Bgh*) using Arabidopsis. The goal was to uncover genes involved in non-host resistance to fungal diseases (Collins et al., 2003). Three mutants with an impaired penetration resistance were recovered from this screen, namely *pen1*, *pen2*, and *pen3* (Collins et al., 2003). *pen1*, *pen2*, and *pen3* mutants displayed significantly increased entry rates of the non-adapted *Bgh*. *PEN2* and *PEN3* encode a mitochondria/peroxisome-localized myrosinase and a PM-residing ABC transporter, respectively (Fuchs et al., 2016; Lipka et al., 2005; Stein et al., 2006). *PEN1*, on the other hand, encodes the PM Qa-SNARE/syntaxin SYP121 (Collins et al., 2003). Further biochemical and genetic studies revealed that *PEN2* and *PEN3* function together in a secretory pathway in which *PEN2* cleaves the precursor glucosinolates into active compounds, which are then transported via *PEN3* to the apoplastic space to promote resistance against fungal pathogens, whereas *PEN1/SYP121* functions independently in a SNARE complex which mediates the secretion of anti-microbial compounds during infection (Kwon et al., 2008; Stein et al., 2006). Both secretory mechanisms are required for pre-invasive resistance, while the post-invasive resistance was shown to be mediated by the SA pathway via the regulatory proteins *EDS1*, *PAD4*, and *SAG101* (Collins et al., 2003; Lipka et al., 2005). Indeed, in *pen* mutants, the infection by *Bgh* showed an increased cell death rate which was *EDS1*, *PAD4*, and *SAG101* dependent (Collins et al., 2003; Lipka et al., 2005).

Later work based on co-expression data identified the R-SNAREs *VAMP721* and *VAMP722* and the Qbc-SNARE/SNAP25-like *SNAP33* as the SNARE partners of *PEN1/SYP121* (Kwon et al., 2008). Indeed, *PEN1/SYP121* forms an SDS-resistant complex with *VAMP721/722* and *SNAP33* (Kwon et al., 2008). Because the *vamp721* and *vamp722* single mutants showed an intact penetration resistance to *Bgh*, whereas silencing both *VAMP721* and *VAMP722* genes showed a decreased penetration resistance at similar levels as those observed in *pen1*, it was concluded that *VAMP721* and *VAMP722* function redundantly during the fusion process mediated by the SNARE complex (Kwon et al., 2008). The function of the complex during *Bgh* infection was validated by microscopic analyses of the localization of *PEN1*, *SNAP33*, and *VAMP722*, which showed that these proteins become focally localized to *Bgh* entry sites during infection (Assaad et al., 2004; Kwon et al., 2008). Later, another study showed that the atypical R protein resistance to powdery mildew 8.2 (RPW8.2) is transiently located to *VAMP721* and *VAMP722* vesicles and is transported to the extrahaustorial membrane (EHM), which envelops the haustorial complex of the *Golovinomyces orontii* fungus during infection. This finding showed

that VAMP721 and VAMP722, and probably their SNARE partners PEN1/SYP121 and SNAP33, are also involved in post-invasive resistance to fungal diseases (Kim et al., 2014).

Additional investigations showed that the *pen1/syp121* mutant displayed minor cell wall defects and delayed production of cell wall appositions when infected with *Bgh* (Assaad et al., 2004). The same study revealed another Qa-SNARE, *SYP122*, which co-expressed with *PEN1/SYP121* and exhibited an even higher up-regulation following pathogen infection than *PEN1/SYP121* (Assaad et al., 2004). *SYP122* is the closest homolog of *PEN1/SYP121* and displays a similar location as *PEN1/SYP121*. Moreover, the *syp122* mutant displayed stronger cell wall defects than *pen1/syp121* (Assaad et al., 2004).

Analyses of the *pen1 syp122* double mutant showed that it exhibits a dwarf morphology which indicates a significant level of redundancy between both genes (Assaad et al., 2004). Following studies revealed that the *pen1 syp122* double mutant displays a lesion-mimic mutant (LMM) and exhibits a constitutive expression of defense genes in an *EDS1*, *PAD4*, *NDR1*, *SID2*, *EDS5*, *FMO1*, *ALD1*, and *NPR1*-dependent way (Zhang et al., 2008). The *pen1 syp122* double mutant can be almost completely rescued by combining mutations in two of these genes, indicating that the LMM phenotype is caused by autoimmunity rather than developmental abnormalities (Zhang et al., 2008). A recent study aiming at uncovering the molecular mechanisms behind *pen1 syp122* auto-immunity revealed that knocking out the ESCRT-III-associated deubiquitinase *AMSH3* completely restores the *pen1 syp122* phenotype (Torsten Schultz-Larsen et al., 2018). The same study showed that *AMSH3* is required for the stability of the RPM1 and RPS2 CNLs as demonstrated by an abolished AvrRpm1 and AvrRpt2-induced cell death in *amsh3* mutant. This finding suggests that the phenotype of the *pen1 syp122* double mutant is caused by constitutive NLR signaling stabilized by *AMSH3* (Torsten Schultz-Larsen et al., 2018).

Several other SNAREs were reported to be involved in immune responses and were reviewed by Kwon et al. (2020).

4.3.3. *SNAP33 is a SNAP25-like gene with an intriguing trait*

Genes of the SNAP25 subfamily are very conserved among eukaryotes and plant species (figure 1.15) (Won & Kim, 2020). Unlike other SNAREs, SNAP25 proteins have two SNARE domains (Qb and Qc) separated by a linker region (Won & Kim, 2020). In mammals, SNAP25 proteins have

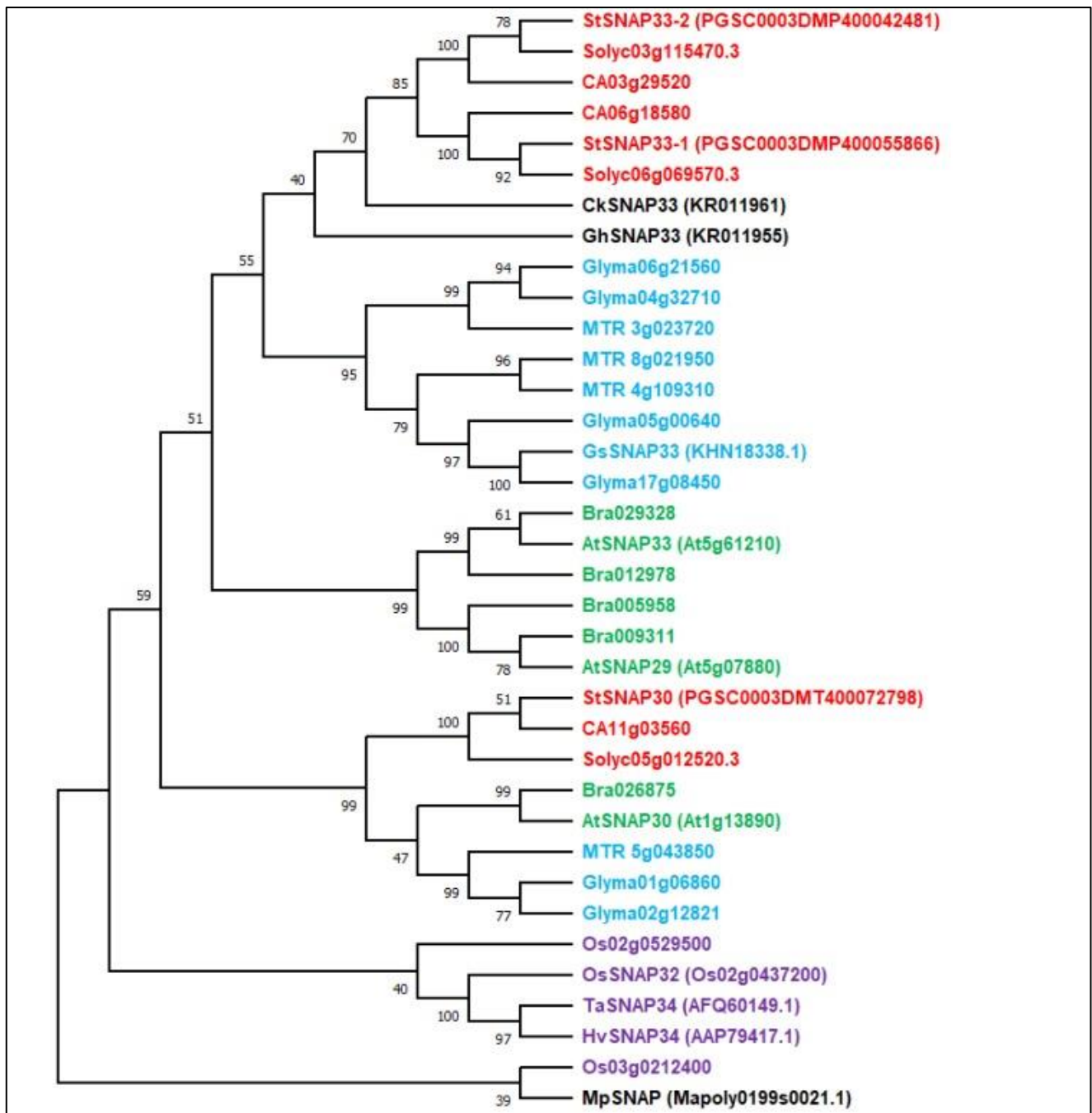


Figure 1.15. Schematic view of a phylogenetic tree of SNAP25 proteins in plants. Phylogenetic tree from the study Won et al., (2020). Phylogenetic analysis was performed using MEGAX software with full amino acid sequences of the retrieved SNAP25 proteins from public databases; UniProt, GenBank, Sol Genomics, and Phytozome, and additionally only functionally studied SNAP25 proteins from *Glycine soja*, *Hordeum vulgare*, *Triticum aestivum*, *Gossypium hirsutum*, and *Cynanchum komarovii*. The bootstrap values from 1000 replicates are depicted at the nodes. Different colors indicate the following: green, Brassicaceae; red, Solanaceae; blue, Fabaceae; violet, Poaceae; black, other functionally reported SNAP25 proteins.

Won et al. (2020)

a specific membrane-binding domain which enables their PM anchoring (Gonzalo et al., 1999). However, plant SNAP25 proteins lack this region; therefore, it is unclear how SNAP25 homologs localize to cellular membranes (Won & Kim, 2020). One possibility is that plant SNAP25 proteins may connect with membranes through lipid modifications (Won & Kim, 2020).

In Arabidopsis, three genes encode SNAP25 proteins, namely *SNAP29*, *SNAP30*, and *SNAP33* (Uemura et al., 2004; Won & Kim, 2020). *SNAP29*, *SNAP30*, and *SNAP33* display different expression patterns, with *SNAP29* being exclusively expressed in stamen and roots, *SNAP30* expressed in pollen, and *SNAP33* is expressed ubiquitously in plants and shows no tissue or developmental stage-specific expression but shows the highest expression-level in leaves (Heese et al., 2001; Lipka et al., 2007).

SNAP33 is involved in cytokinesis

As mentioned earlier, SNAP33 is a PM-localized SNAP25-like/Qbc-SNARE which forms a complex with PEN1/SYP121 and VAMP721/722 and is involved in the secretion of anti-microbial compounds during fungal infection (Kwon et al., 2008). The earliest studies identified SNAP33 as an interacting partner of the cytokinesis-specific Qa-SNARE/syntaxin KNOLLE (meaning tuber-shaped in German) (Kasmi et al., 2013; Lauber et al., 1997; Lukowitz et al., 1996). SNAP33 formed a SNARE complex with KNOLLE and VAMP721/722 and was localized to the cell plate of dividing cells (Heese et al., 2001; Kasmi et al., 2013), showing that SNAP33 mediates vesicle fusion in several processes with different SNARE partners and in diverse biological processes in plants. Interestingly, heterologous overexpression of *CkSNAP33* from *Cynanchum komarovii* in Arabidopsis WT plants led to increased root length and leaf area, evidenced by increased cell number, showing a conserved function of SNAP33 in cytokinesis among plant species (Wang et al., 2017). However, *snap33* single knockout mutant has mild cytokinetic abnormalities, indicating that other SNAREs have overlapping functions during cytokinesis (Heese et al., 2001; Kasmi et al., 2013).

SNAP33 is involved in stress responses, and the *snap33* mutant displays a dwarf senescent morphology

Further evidence showing that SNAP33 is an important component of plant immunity was earlier reported by Wick et al., (2003). In their study, the authors showed that *SNAP33* is up-regulated in response to inoculations with the fungus *Plectosporium tabacinum*, with virulent and avirulent forms of the oomycete *Hyaloperonospora parasitica*, with *Pst* bacteria carrying or

not the AvrRpt2 effector, as well as in response to SA treatment (Wick et al., 2003). Moreover, *SNAP33*'s expression correlated with *PR1*, suggesting that *SNAP33* and its SNARE partners might be involved in *PR1* secretion during infection by diverse pathogens (Wick et al., 2003). In the same paper, the authors reported an induced expression of *SNAP33* in response to wounding, suggesting that *SNAP33* is also involved in abiotic stress and/or in response to herbivory insects (Wick et al., 2003). Moreover, overexpression of *GhSNAP33* and *CkSNAP33* from cotton *Gossypium hirsutum* and *Cynanchum komarovii*, respectively, led to increased resistance to the fungus *Verticillium dahliae* in *Arabidopsis* (Wang et al., 2017, 2018).

The *snap33* knockout mutant develops large necrotic lesions on the cotyledons and rosette leaves and eventually dies before flowering (Heese et al., 2001). Interestingly, a similar phenotype was observed in potato *Solanum tuberosum* (Eschen-Lippold et al., 2012). Indeed, downregulation of *StSNAP33* led to the development of necrotic regions on leaves accompanied by an increased SA concentration in non-infected leaves (Eschen-Lippold et al., 2012). *SNAP33* interacts with EXO70B1 and EXO70B2, two tethering proteins with a role in protein secretion during immunity (described above), indicating that *SNAP33* connects tethering factors to the plasma membrane to direct secretion during infection (Pečenková et al., 2011; Zhao et al., 2015).

5. Objectives of my Ph.D.

As previously stated, membrane trafficking is critical for plant immunity, as evidenced by the numerous studies indicating that pathogens target membrane trafficking components to promote disease (Ruano & Scheuring, 2020). The research on *SNAP33* reported above demonstrates that it is a crucial component of the plant immune system and has a conserved role across plant species. *snap33*'s macroscopic phenotype is comparable to that of other lesion-mimic mutants' (LMM) phenotypes with constitutively active immune responses. However, the molecular processes underlying this trait are still unknown. Therefore, the first objective of my Ph.D. work was to better characterize the phenotype of *snap33* at the macroscopic and molecular levels and identify the genetic pathways responsible for this trait (CHAPTER II.1). My second Ph.D. objective (CHAPTER II.2) was to assess a potential connection between *SNAP33* and the MAPK module MEKK1-MKK2-MPK4. Indeed, both parts are involved in immunity and share several characteristics (more detail in CHAPTER II.2).

CHAPTER II – RESULTS

1. Characterization of the lesion-mimic phenotype of *snap33* mutants

Given that a large number of lesion-mimic mutants reported in the literature demonstrate constitutive activation of defenses (Bruggeman et al., 2015), we examined whether this holds true for the *snap33* mutant. In this section, I present the results obtained notably from transcriptomic and genetic analyses of the *snap33* mutant to elucidate the molecular processes behind the formation of lesions and the ensuing dwarf morphology of the *snap33* mutant.

1.1. Isolation of novel *snap33* mutants

Heese et al. previously identified the *snap33* mutant in the Wassilewskija (*Ws*) ecotype, which will be referred to as *snap33^{Ws}* hereafter (Heese et al., 2001). Due to the availability of most mutants in the Col-0 ecotype and to generate combinatorial mutants with the same genetic background, we chose to characterize *snap33* mutants in the Col-0 ecotype. Five T-DNA insertion lines, namely SALK_075519 (*snap33-1*), SALK_063806 (*snap33-2*), GABI_094E01 (*snap33-3*), SALK_119791 (*snap33-4*) and SALK_034227 (*snap33-5*), were identified from the Arabidopsis Biological Resource Center (ABRC) T-DNA collection in the locus of *SNAP33* (AT5G61210) (figure 2.1). The *snap33* homozygous mutant plants were isolated from the T-DNA insertion lines by PCR. A recessive phenotype co-segregated with the T-DNA insertion in the *snap33-1*, *snap33-2*, and *snap33-3* lines, but not in the *snap33-4* and *snap33-5* lines (figure 2.1.b). *snap33-1* carries a T-DNA insertion in the first exon of the *SNAP33* locus, *snap33-2* in the 3rd intron, and *snap33-3* in the 4th exon (figure 2.1.a). *snap33-4* carries a T-DNA insertion 738 bp upstream of the start codon, in the 5'UTR, and *snap33-5* carries a T-DNA insertion 953 bp upstream of the start codon, in the promoter region (figure 2.1.a). The WT plants used hereafter are out-segregated from *snap33-1^{+/-}* and termed wild type-1 (WT-1). RT-PCR analysis of *SNAP33*'s expression in WT-1 plants and *snap33* homozygous mutant plants showed that the *snap33-4* and *snap33-5* lines, with a WT-like phenotype, express *SNAP33* at similar levels as WT-1 (figure 2.1.c). The *snap33-1*, *snap33-2*, and *snap33-3* lines do not express *SNAP33* relative to the WT and display the same dwarf lesioned phenotype previously reported for the *snap33^{Ws}* knockout line in the *Ws* ecotype (figure 2.1.b) (Heese et al., 2001). These results further show that the lesion-mimic phenotype is related to the loss of function of *SNAP33*. *snap33-1*, *snap33-2*, and *snap33-3* homozygous mutant plants do not survive until

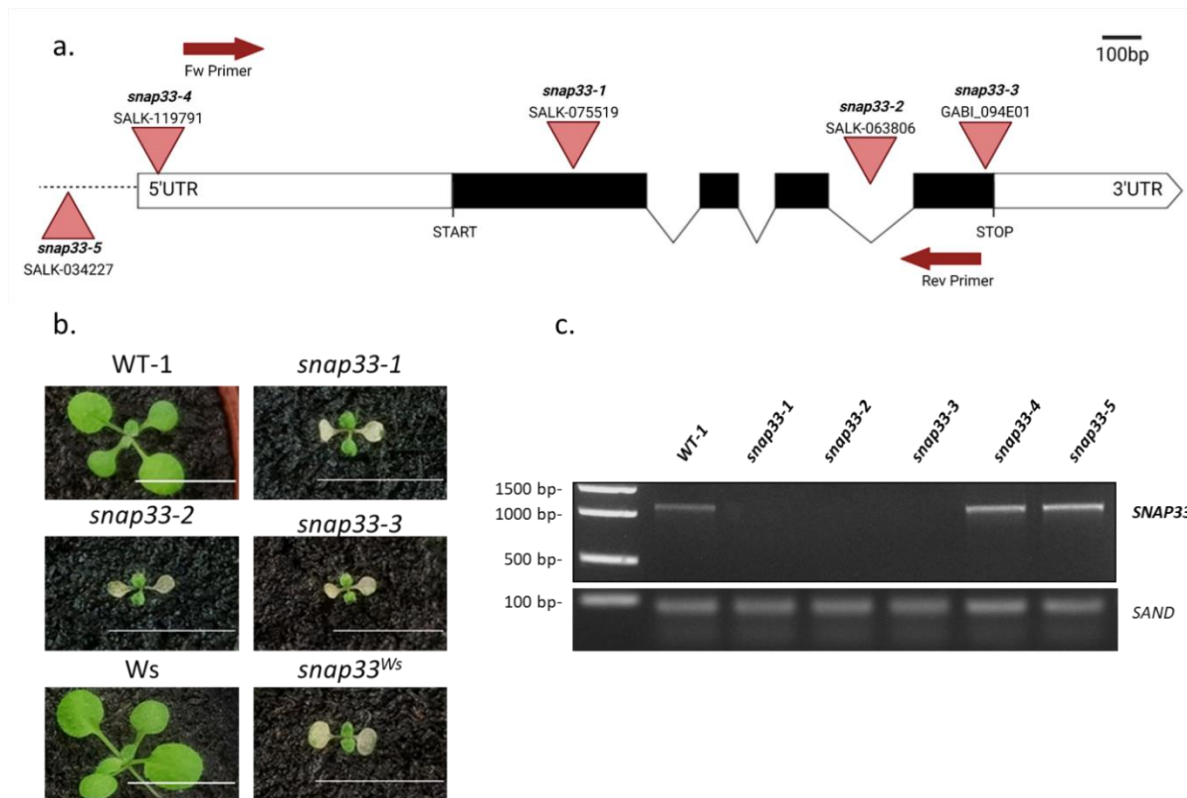


Figure 2.1. Characterization of *snap33* T-DNA insertion mutants. **a.** Schematic diagram of *SNAP33* genomic region (2585 bp) and the location of the T-DNA insertion in the *snap33-1*, *snap33-2*, *snap33-3*, *snap33-4*, and *snap33-5* mutants. The four exons of *SNAP33* are represented as black boxes, and the ATG START and the STOP codons are indicated. The introns are represented as black lines. White boxes represent the untranslated (UTR) regions, 5'UTR and 3'UTR. Triangles indicate the sites of T-DNA (not drawn to scale) insertions. *snap33-1* has a T-DNA insertion in the first exon, at 297 bp from the START codon, *snap33-2* has a T-DNA insertion at 1029 bp from the START codon, and *snap33-3* has a T-DNA insertion at 1332 bp from the START codon. *snap33-4* and *snap33-5*, in which the T-DNAs are inserted at 738 bp (5'UTR) and 953 bp (promoter region) upstream of the START codon, respectively, did not display the early-lesioned phenotype of *snap33-1*, *snap33-2*, and *snap33-3* (not shown); Fw primer and Rev Primer indicate the forward and reverse primers used to analyze the expression of *SNAP33* by RT-PCR. **b.** Morphology of 13-day-old seedlings of *snap33-1*, *snap33-2*, *snap33-3*, and *snap33^{Ws}* mutants compared to the out-segregated line (WT-1) and *Ws*. Note the yellowish cotyledons of *snap33-1*, *snap33-2*, *snap33-3*, and *snap33^{Ws}*; **c.** The upper panel depicts the analyses of *SNAP33*'s expression in the WT-1, *snap33-1*, *snap33-2*, *snap33-3*, *snap33-4*, and *snap33-5* by RT-PCR using the Fw and Rev primers (red arrows on the panel a) designated to amplify 1135 bp of the 1523 bp mRNA sequence of *SNAP33*. *SAND* was used as the endogenous reference gene.

the reproductive stage and eventually die after about five weeks of growth. Therefore, to characterize the phenotype of *snap33*, we used *snap33-1*, *snap33-2*, and *snap33-3* segregating populations and selected the *snap33* homozygous plants by PCR and based on their morphological phenotype.

1.2. *snap33* knock-out mutants display constitutive cell death and H₂O₂ accumulation

To investigate whether the lesions observed in the *snap33-1*, *snap33-2*, and *snap33-3* homozygous mutants are attributed to dead cells and/or ROS accumulation, we performed trypan-blue and 3,3'-diaminobenzidine (DAB) stainings on 20-day-old seedlings grown in long-day conditions without stress (figure 2.2). Trypan-blue dye passes through damaged-cell membranes and stains vasculature tissues but is not absorbed by viable impermeable cells (Wees, 2008). The results in figure 2.2 show that the three *snap33* mutants exhibit multiple dead cells on cotyledons and rosette leaves, whereas no dead cells were observed on the WT-1. DAB is oxidized in the presence of H₂O₂ and of specific haem-containing proteins, such as peroxidases, forming a dark brown precipitate (Daudi & O'Brien, 2012). DAB staining experiments show that H₂O₂ is constitutively accumulating in the *snap33-1*, *snap33-2*, and *snap33-3* mutants, as evidenced by the presence of brown patches on rosette leaves and cotyledons. No dark-brown patches were observed in the WT-1. These results show that in the *snap33* mutants, there is spontaneous cell death and H₂O₂ accumulation in the *snap33* mutants, which indicates that there might be a constitutive activation of defense responses at resting conditions.

1.3. MPK3, MPK4, and MPK6 activation upon flg22 treatment is more intense in the *snap33* mutants

To analyze early defense response induction in the *snap33* mutants, we measured the activation of MPK3, MPK4, and MPK6 proteins in *snap33-1*, *snap33-2*, and *snap33-3* mutants after flg22 treatment compared to WT-1. To do that, we performed immunoblotting experiments using an anti-pTpY antibody that detects phosphorylated MPK3, MPK4, and MPK6. As stated earlier in the introduction, MPK3, MPK4, and MPK6 are activated in response to flg22. Their activation levels reach a peak at 15 minutes (min) and last about 30 min (Nühse et al., 2000; Zipfel et al., 2006). Therefore an activation kinetics analysis was carried out at 0, 15, and 30 min after flg22

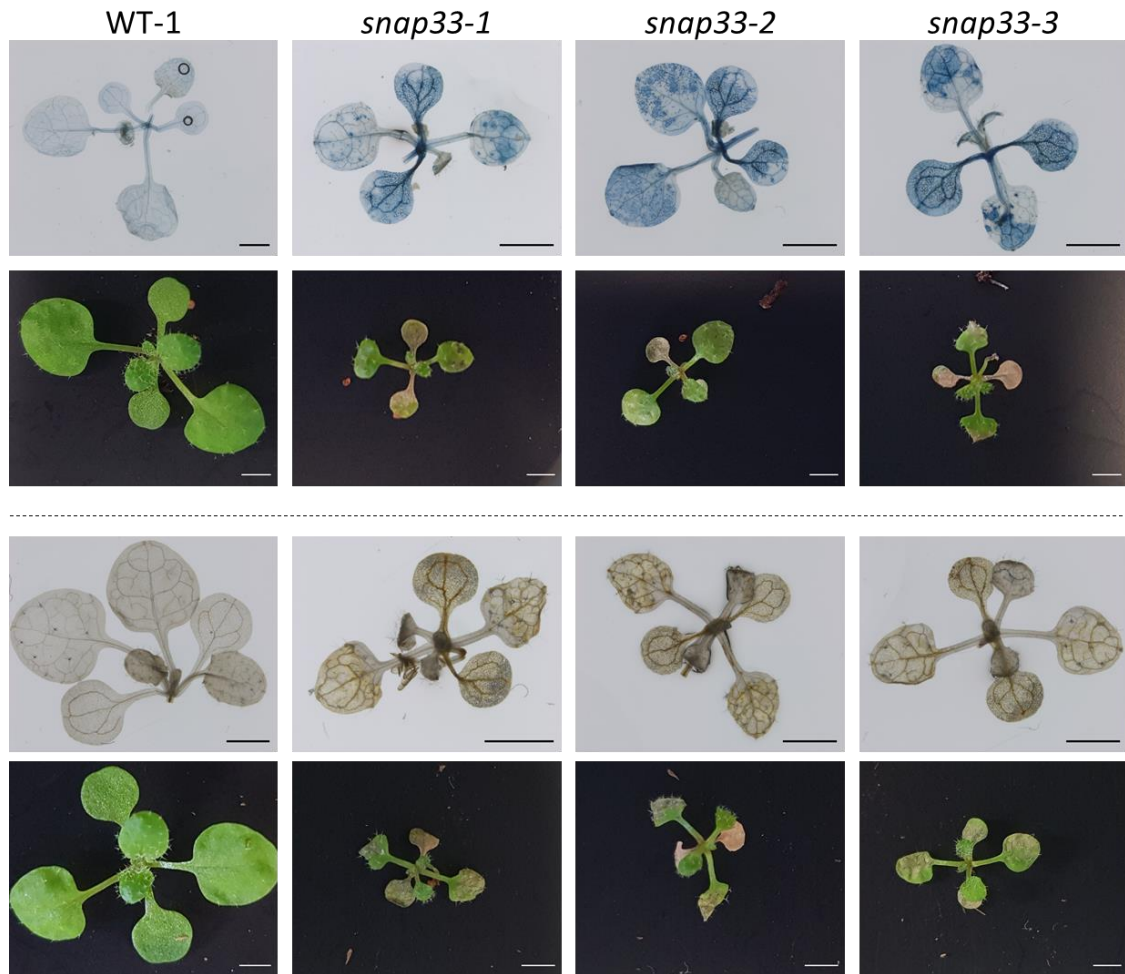


Figure 2.2. The *snap33* knock-out mutants display constitutive cell death and H₂O₂ accumulation. Representative pictures of 20-day-old seedlings stained with trypan blue (top panel) and DAB (lower panel). Cell death appears as dark blue patches (top panel), and ROS accumulation appears as brown patches (lower panel) on the *snap33* mutants. The photographs show the morphological phenotype of WT-1, *snap33-1*, *snap33-2*, and *snap33-3* seedlings before staining. Scale bars represent 2 mm. These experiments were carried out 3 times (3 biological replicates) with similar results. In each replicate, 3 plants of each genotype were stained.

application in the *snap33* mutants and WT-1. As shown in figure 2.3, MPK3, MPK4, and MPK6 activation appear stronger at 15 and 30 min in the *snap33* mutants compared to WT-1, indicating a more intense induction of PTI responses in the *snap33* mutants. MPK3, MPK4, and MPK6 do not seem to be activated at resting condition (0 min time point (figure 2.3)), which indicates that the mutation of *SNAP33* does not trigger a constitutive MAPK signaling. To investigate whether the over-activation of MPK3, MPK4, and MPK6 observed at 15 and 30 min of flg22 treatment is related to a higher protein level of the MAPKs, we performed immunoblotting analyses using anti-MPK3, anti-MPK4, and anti-MPK6 antibodies. The results in figure 2.3 show that the *snap33* mutants accumulate higher amounts of MPK3 and MPK4 proteins at resting conditions and after flg22 treatment. However, there is no obvious over-accumulation of MPK6 protein in the *snap33* mutants. These results suggest that the increased level of MAPK activation upon flg22 treatment is probably partly related to increased protein levels. These results also indicate that *MPK3* and *MPK4* might be transcriptionally up-regulated, or their corresponding proteins might be stabilized in the *snap33* mutants compared to WT-1. Although not reported throughout literature as a common trait of auto-immune phenotypes, the over-accumulation of MPK3 and MPK4 might reflect a state of priming in the *snap33* mutants, probably leading to a stronger immune response upon pathogen perception.

1.4. High temperatures partially suppress the dwarf phenotype of *snap33*

Several studies demonstrated that high temperatures partially or entirely revert dwarfism in auto-immune mutants. For instance, the dwarfism of *mekk1* and *mpk4* mutants observed at 22°C was partially rescued at 30°C (Su et al., 2007). High temperatures affect many biological processes in plants, especially hormonal pathways that have a tight relationship with temperature and environmental conditions, as reviewed by Castroverde & Dina, (2021). Huot and colleagues have shown that *Pst* DC3000-induced SA biosynthesis is suppressed at 28~30°C, leading to decreased resistance to *Pst* DC3000 (Huot et al., 2017). The authors also showed that high temperatures (28~30°C) inhibit *ICS1* expression leading to a reduced SA accumulation (Huot et al., 2017). To test whether elevated temperatures may also revert the *snap33* mutant's phenotype, the *snap33-1* mutant was grown at 30°C under long-day conditions. As illustrated in figure 2.4, *snap33-1*'s dwarf phenotype was partially suppressed by high temperatures (30°C) (figure 2.4.a) compared to *snap33-1* plants grown at 22°C (figure

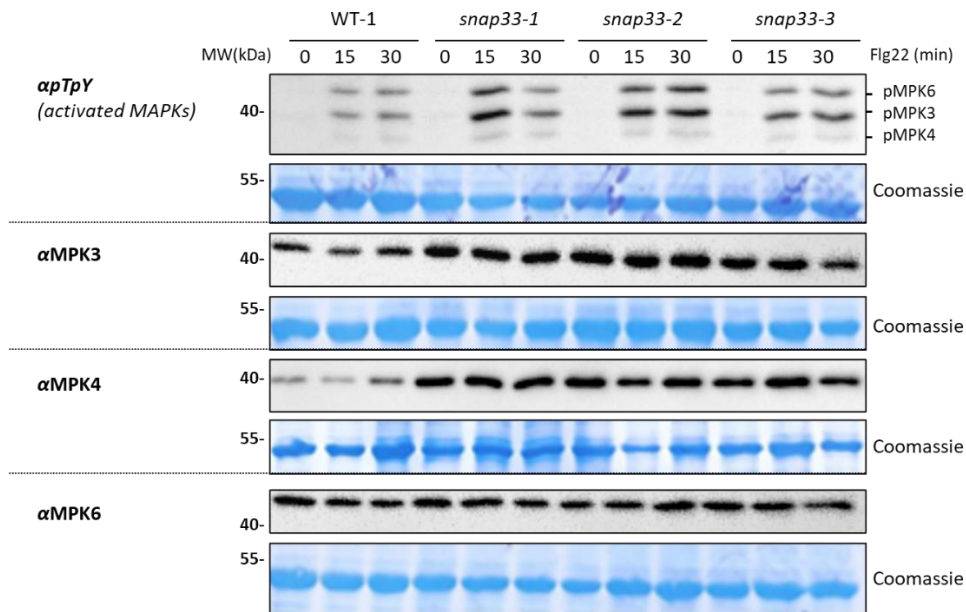


Figure 2.3. Activation of MPK3, MPK4, and MPK6 is more intense in the *snap33* mutants compared to WT-1 upon flg22 treatment. WT-1, *snap33-1*, *snap33-2*, and *snap33-3* plants were grown *in vitro* for 13 days, treated with 100 nM flg22, and harvested after 0, 15, and 30 min after flg22 treatment. The activation of MPK3, MPK4, and MPK6 was detected by immunoblotting analysis using an anti-pTpY antibody (α -pTpY). The accumulation of MPK3, MPK4, and MPK6 was assessed by immunoblotting analysis using antibodies specific to the corresponding proteins (α -MPK3, α -MPK4, and α -MPK6). Coomassie blue staining was performed after blotting to assess total protein loading in each well; the ~55 kDa protein band corresponds to the RuBisCO large subunit. This experiment was performed twice with similar results.

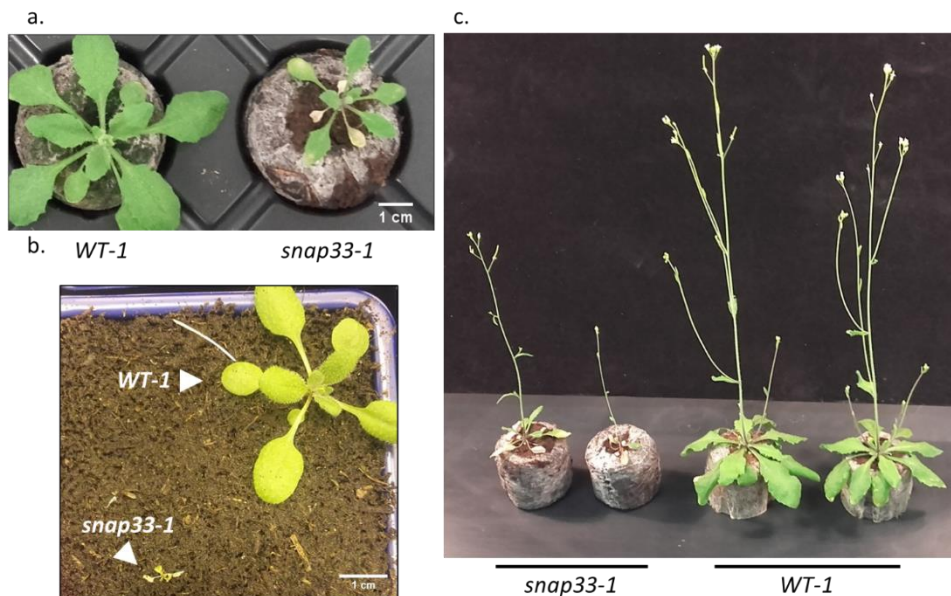


Figure 2.4. High temperatures partially suppress the dwarf phenotype of the *snap33-1* mutant. **a.** Photograph of *snap33-1* and WT-1 grown at 30°C for 4 weeks. **b.** Photograph of *snap33-1* and WT-1 grown for 4 weeks at 22°C. Notice the difference between *snap33-1* grown at 30°C (a) and 22°C (b). **c.** Later growth-stages (45 days) at 30°C, showing that under elevated temperatures, *snap33-1* mutants are able to flower and produce few siliques.

2.4.b). Moreover, the mutant reached the reproductive stage and produced few flowers and siliques when grown at 30°C (figure 2.4.c). These findings indicate that the *snap33* mutant's phenotype might be partially related to an over-accumulation of SA. However, the necrotic lesions persist at 30°C (figure 2.4.a), indicating that if the phenotype of *snap33* completely depends on SA, the remaining SA at 30°C still leads to strong immune responses. This result also suggests that temperature-insensitive pathways, besides SA, might be involved in the development of lesions and the dwarfism of the *snap33* mutant.

1.5. Transcriptomic analyses of the *snap33-1* mutant confirm that *SNAP33* mutation results in constitutive expression of defense-related genes

1.5.1. Experimental design

To further characterize the *snap33* mutant and identify the molecular mechanisms behind the *snap33*'s dwarf and lesioned phenotype, we performed transcriptomic analyses via RNA-sequencing (RNA-seq) of the *snap33-1* mutant compared to WT-1. We took advantage of the partial reversion of *snap33*'s phenotype by high temperatures to generate *snap33-1* homozygous seeds to analyze the mutant at 5 days of growth, *i.e.*, at an early stage before the development of lesions. To avoid any experimental bias, we also used these homozygous *snap33-1* seeds to analyze the mutant at 12 days of growth, *i.e.*, after the onset of lesions (figure 2.5.a). Gene expression was thus assayed in three biological replicates of 5-day-old and 12-day-old WT-1 and *snap33-1* plants. The three biological replicates of each genotype were separated by 24 h each and grown in the same chamber to reduce the environmental impacts on transcriptomic analyses, as indicated in the RNA-seq experimental design in figure 2.5.a. *snap33-1* plants from each biological replicate were analyzed by RT-PCR, confirming that all pooled plants do not express *SNAP33* (figure 2.5.b). Two-dimensional principal component analysis (PCA) of normalized counts revealed differences between samples collected at 5 days and 12 days (figure 2.5.c). The *snap33-1* and WT-1 samples showed the most remarkable difference at 12 days, while this difference was much lower at 5 days (figure 2.5.c). Biological replicates of each genotype and time point combination were all highly grouped, indicating a high level of reproducibility among biological replicates (figure 2.5.c).

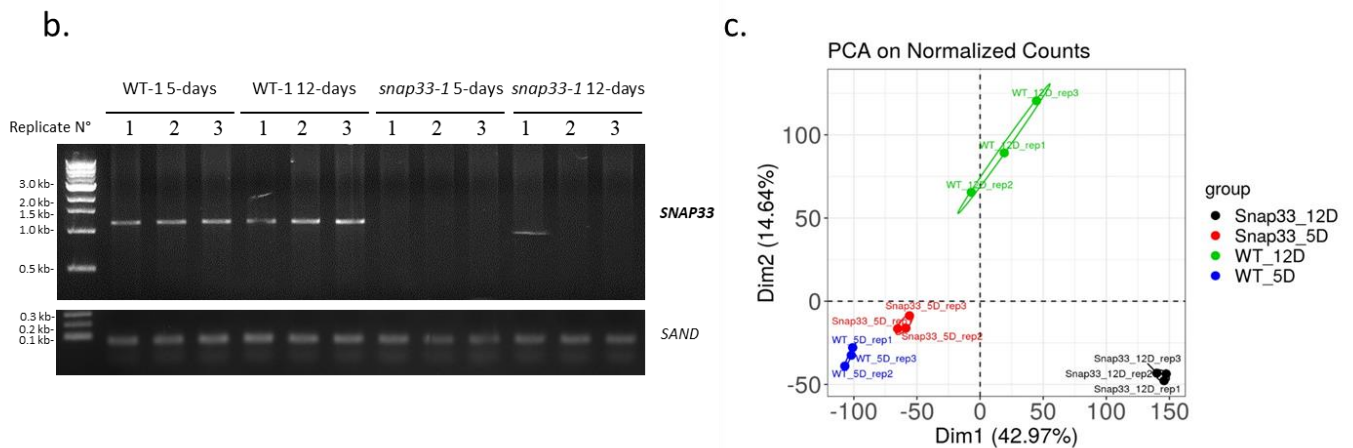
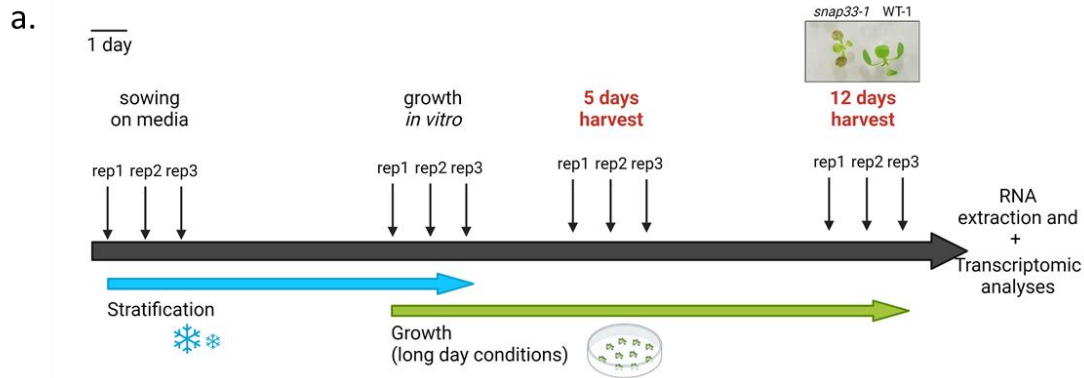


Figure 2.5. The experimental design of *snap33-1* vs WT-1 RNA-sequencing (RNA-seq) analysis and preliminary results. **a.** Timeline of *snap33-1* and WT-1 growth and harvest for RNA-seq analyses: *snap33-1* and WT-1 were sown on ½ MS and 0.5% agar media and stratified for 7 days before growth. The three biological of 5 and 12 days replicates analyzed by RNA-sequencing were grown with 24 h difference. The plants analyzed at 5 and 12 days were grown at the same time, in the same chamber, and harvested accordingly. **b.** *SNAP33* expression analyses in the WT-1 and *snap33-1* plants used for the transcriptomic analyses: the upper panel shows the RT-PCR analyses performed using primers that amplify 1135 bp of *SNAP33* mRNA (see primers in figure 2.1.a), showing that all *snap33-1* samples used for the transcriptomic study do not express *SNAP33* compared to WT-1 samples. *SAND* (lower panel) was used as the endogenous reference gene. **c.** Two-dimensional PCA analyses on normalized counts of the WT-1 and *snap33-1* samples. Each point represents an RNA-seq sample. Sample groups are indicated using different colors as indicated in the legend.

1.5.2. Analyses of the differentially expressed genes

Transcriptomic data indicated that 20,938 genes were expressed, of which 2591 were differentially expressed in 5-day-old seedlings between *snap33-1* and WT-1, and 7998 genes were differentially expressed in 12-day-old seedlings (p -value ≤ 0.05) (figure 2.6.a). Analyses of the differentially expressed genes (DEGs) revealed that 1662 and 4173 genes were up-regulated (p -value ≤ 0.05) in the *snap33-1* mutant relative to WT-1 at 5 and 12 days, respectively (figure 2.6.a), with 672 and 2015 genes showing a two-fold or more up-regulation ($\log_2FC \geq 1$) at 5 and 12 days, respectively, compared to WT-1 (figure 2.6.b). 929 and 3825 genes were down-regulated (p -value ≤ 0.05) in the *snap33-1* mutant relative to WT-1 at 5 and 12 days, respectively (figure 2.6.a), with 175 and 954 showing a two-fold or more down-regulation ($\log_2FC \leq -1$) at 5 and 12 days compared to WT-1, respectively (figure 2.6.b).

snap33-1's DEGs are involved in development and stress response

To obtain an overview of the cellular responses associated with the DEGs, we performed MapMan analyses on the 2591 and 7998 DEGs obtained at 5 and 12 days, respectively (p -value ≤ 0.05) (figure 2.6.c). The results show that at 5 days, several genes associated with biotic stress are up-regulated and increase in number at 12 days. The other biological process which shows the most altered expression pattern is "development". These results indicate that the phenotype of *snap33* might be associated with the up-regulation of defense responses which starts at early developmental stages.

snap33-1's RNA-seq data show an increased expression of defense-related genes

Comparison of the up-regulated genes with \log_2 -fold change (\log_2FC) ≥ 1 at 5 and 12 days shows an overlap of 288 genes between the two conditions (figure 2.7). The GO analysis of these 288 common genes reveals enrichment of biological processes associated with stress response, such as "response to hypoxia", "response to wounding", "response to jasmonic acid", "response to salicylic acid", and "response to chitin" (figure 2.7). These analyses reveal that the *snap33-1* mutant displays an increased expression of stress-related genes already at 5 days of growth. GO processes associated with SA and JA hormonal pathways are significantly enriched in the 288 common genes at 5 and 12 days (figure 2.7). Moreover, MapMan analyses of "Biotic Stress" related pathways revealed that ABA and ET-related genes are also up-regulated in the *snap33-1* mutant (Supplementary figure 1), showing that in the *snap33-1* mutant, there is an increased expression of ABA, SA, JA, and ET-related genes starting at early growth stages.

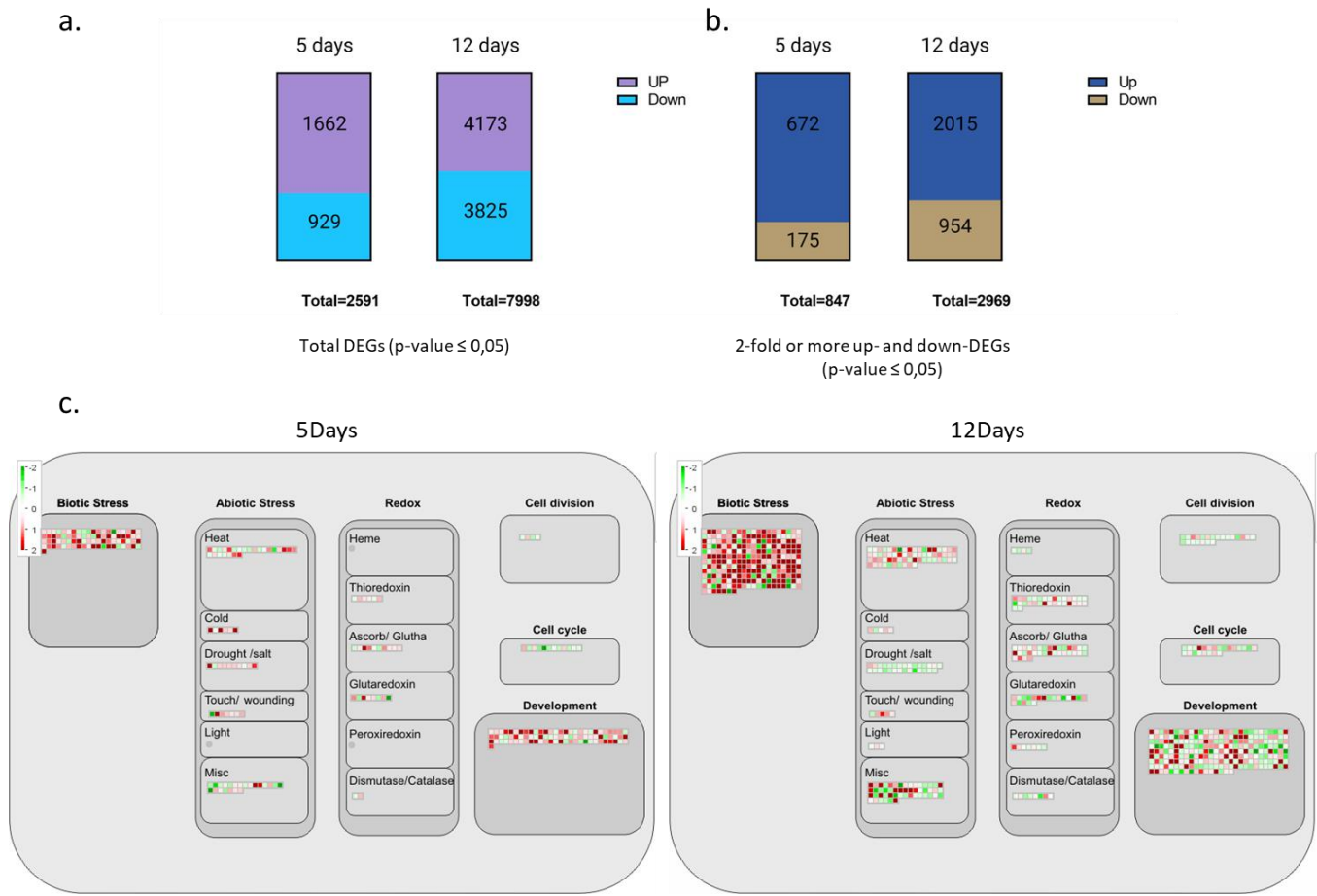


Figure 2.6. Analyses of the differentially-expressed genes (DEGs) between *snap33-1* and WT-1 at 5, and 12 days. **a.** Schematic view of the up-regulated and down-regulated DEGs detected at 5 and 12 days with p-values ≤ 0.05 . **b.** Schematic view of the up-regulated and down-regulated DEGs detected at 5 and 12 days with a Log2 fold-change (Log2FC) ≥ 1 or ≤ -1 and p-values ≤ 0.05 . **c.** MapMan analyses of the DEGs in *snap33-1* at 5 and 12 days showing an overview of the altered cellular responses in the *snap33-1* mutant: all DEGs at 5 and 12 days with p-values ≤ 0.05 were used to perform a MapMan analysis. Red squares indicate up-regulated genes, and green squares represent down-regulated genes found in *snap33-1* compared to WT-1. Each square represents a gene.

GO analysis of the 384 and 1727 genes that were specifically up-regulated at 5 and 12 days, respectively, revealed enrichment of biological processes involved in stress-responses, too (figure 2.7). In addition, at 5 days, other biological functions related to abiotic stress responses and metabolism, such as “response to water deprivation”, “response to absence of light”, “cold acclimation”, “response to salt stress”, “response to fructose”, “response to glucose”, “sterol biosynthetic process”, and carbohydrate process” are enriched which indicate that mutation of the *SNAP33* gene affects several metabolic and stress-related processes in plants (figure 2.7). Interestingly, at 12 days, there is a significant enrichment of the GO term “plant-type hypersensitive response” which is often associated with R-protein signaling and ETI responses (figure 2.7). Analyses of the genes associated with the GO term “plant-type hypersensitive response” (GO:0009626) revealed that 27 genes out of the 76 genes belonging to this GO category are up-regulated in *snap33-1* at 12 days. As represented in figure 2.8, these 27 genes are indeed associated with SA and SAR, and R-protein signaling, such as *SARD1*, *CBP60g*, *PBS3*, *NPR1*, *FMO1*, *EDS1*, *PAD4*, *NDR1*, *ADR1*, and *RPS2* (figure 2.8). *MPK3* and *MKK4*, which also belong to the GO “plant-type hypersensitive response”, are both up-regulated in the *snap33-1* mutant, which is in line with the previous results obtained in section II1.3 (figure 2.4), which showed an over-accumulation of MPK3 protein in unstressed *snap33* mutants compared to WT-1. This result suggests that MPK3 protein over-accumulation in *snap33* is related to increased transcription of the corresponding gene.

12-days *snap33-1* up-regulated genes are involved in plant defense responses

Because we found that stress-related gene expression is increased in the *snap33-1* mutant compared to WT-1 at both 5 and 12 days, and to have a broader picture of altered biotic-stress related pathways in the *snap33* mutant, we chose to undertake further analyses of the up-regulated genes using the 12 days time point, which showed the highest number of up-regulated genes. To do that, we performed a GO analysis of Molecular Functions (MFs) enriched among the 12-days up-regulated genes using the g: profiler tool (Supplementary Table 1). We found that MF associated with signal transduction, such as “protein serine kinase activity”, “protein threonine kinase activity”, “protein serine/threonine kinase activity”, and “protein kinase activity” are significantly enriched in the *snap33-1*'s transcriptome, which suggests the involvement of numerous signaling pathways in the *snap33-1* mutant (Supplementary Table 1). Analyses of the 163 genes found in these categories show that many genes coding for

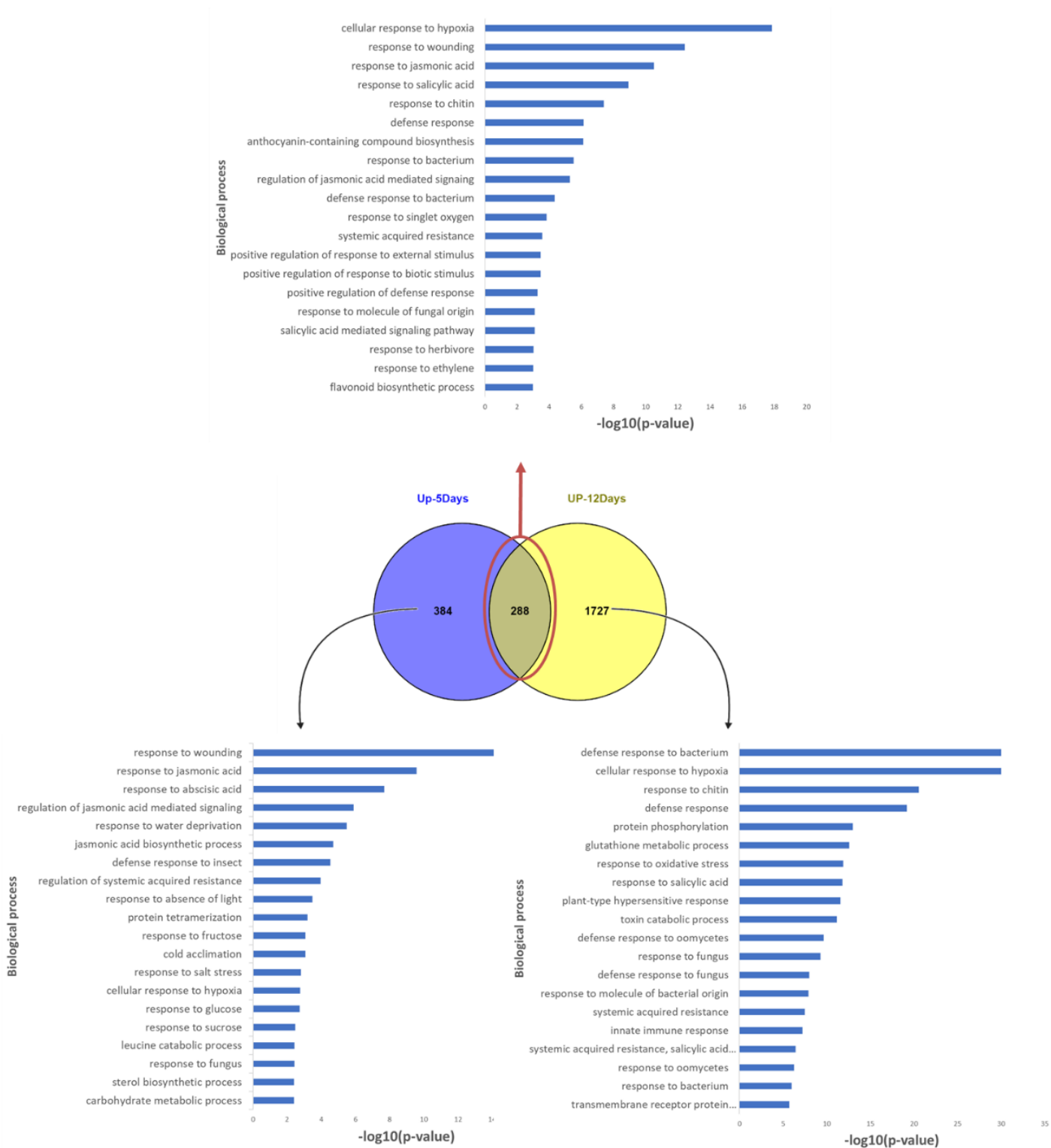
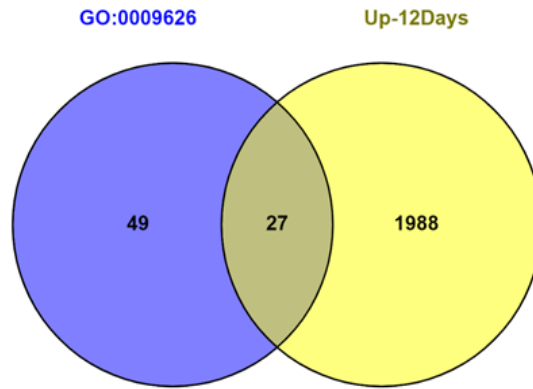


Figure 2.7. GO enrichment analyses of the *snap33-1* up-regulated genes at 5 and 12 days. GO enrichment of biological processes of the 288 common up-regulated genes at 5 and 12 days (upper graph), the 384 genes specifically up-regulated at 5 days (lower left graph), and 1727 genes specifically up-regulated at 12 days in *snap33-1* (lower right graph). The top 20 significant categories are represented on the vertical axis, and the horizontal axis represents the $-\log_{10}(p\text{-value})$ of the significant pathways. Greater $-\log_{10}(p\text{-value})$ scores correlate with increased statistical significance. The GO analyses were performed using the TopGo “elim” method (Alexa et al., 2006).

CDPKs, MAPKs, RLKs, and RLCKs, involved in biotic-stress signal transduction, are up-regulated in *snap33-1* (Supplementary Table 2). We also found an enrichment of MF associated with "NAD⁺ nucleotidase, cyclic ADP-ribose generating", "NAD⁺ nucleosidase activity", "NAD(P)⁺ nucleosidase activity" and "ADP-binding", all of which are associated with the activity of NLR genes (Supplementary Table 1). Analysis of the genes belonging to these categories revealed an abundance of NLR genes (Supplementary Table 3), suggesting that several R proteins accumulate in the *snap33-1* mutant. To gain further insights into the altered pathways in the *snap33-1* mutant, we performed a KEGG pathway analysis; interestingly, we found that the KEGG term "plant-pathogen interaction" is the most significantly enriched pathway, followed by "phenylpropanoid biosynthesis" and "MAPK signaling pathway", all of which are associated with plant defense responses (Supplementary Table 4).

In light of the results obtained by GO, MapMan, and KEGG analyses, which indicate a high enrichment of the defense-related pathways, we searched for SA, JA, and ET-related genes in the list of DEGs at 12 days. As shown in figure 2.9.a, many genes involved in the SA pathway are strongly up-regulated in the *snap33-1* mutant compared to WT-1. These SA up-regulated genes include genes involved in SA biosynthesis, such as *CBP60g*, *SARD1*, *ICS1*, *EDS5*, and *PBS3*, genes involved in SA signaling, such as *NPR1*, and the SA-marker genes *PR1* and *PR2* (figure 2.9.a). SAR-associated genes *FMO1* and *ALD1*, involved in NHP biosynthesis, were also found up-regulated in our analyses, suggesting that there is a constitutive SAR in *snap33-1* (figure 2.9.a). In addition, we found *EDS1*, *NDR1*, *SAG101*, and *PAD4*, involved in R-protein signaling upstream of SA, and helper NLRs *ADR1* and *NRG1.1*, as up-regulated in *snap33-1* (figure 2.9.b). We also found some JA-ET-related genes as up-regulated in *snap33-1*, including *VSP1*, *ACS6*, *ORA59*, *ERF1* and *PDF1.2* (figure 2.10.a). As we found an over-accumulation of MPK3 and MPK4 in the *snap33-1* compared to WT-1, we searched for genes involved in early PTI signaling. We found that besides *MPK3* and *MPK4* up-regulation in *snap33-1*, *MKK4* and *MAPKKK5* are up-regulated too, showing that genes coding for members of the MAPK module MAPKKK3/5-MKK4/5-MPK3/6 are up-regulated in the *snap33-1* mutant (figure 2.10.b). Other genes involved in PTI responses, such as *RBOHD*, *PAD3*, and *WRKY33*, are also up-regulated in the *snap33-1* (figure 2.10b).



AGI number	name	description
AT4G12720	AtNUDT7	MutT/nudix family protein [Source:UniProtKB/TrEMBL
AT1G73805	SARD1	Protein SAR DEFICIENT 1 [Source:UniProtKB/Swiss-Prot
AT1G19250	FMO1	Probable flavin-containing monooxygenase 1 [Source:UniProtKB/Swiss-Prot
AT3G50930	HSR4	Protein HYPER-SENSITIVITY-RELATED 4 [Source:UniProtKB/Swiss-Prot
AT1G64280	NPR1	Regulatory protein NPR1 [Source:UniProtKB/Swiss-Prot
AT3G50470	HR3	MLA10 [Source:UniProtKB/TrEMBL
AT3G20600	NDR1	Protein NDR1 [Source:UniProtKB/Swiss-Prot
AT2G47130	SDR3A	Short-chain dehydrogenase reductase 3a [Source:UniProtKB/Swiss-Prot
AT3G48090	EDS1	Protein EDS1 [Source:UniProtKB/Swiss-Prot
AT1G51660	MKK4	MKK4 [Source:UniProtKB/TrEMBL
AT4G23210	CRK13	Cysteine-rich receptor-like protein kinase 13 [Source:UniProtKB/Swiss-Prot
AT5G20480	EFR	LRR receptor-like serine/threonine-protein kinase EFR [Source:UniProtKB/Swiss-Prot
AT5G13320	PBS3	Auxin-responsive GH3 family protein [Source:TAIR
AT3G45640	MPK3	MPK3 [Source:UniProtKB/TrEMBL
AT3G01420	DOX1	Alpha-dioxygenase 1 [Source:UniProtKB/Swiss-Prot
AT4G12010	DSC1	Disease resistance-like protein DSC1 [Source:UniProtKB/Swiss-Prot
AT1G08450	CRT3	Calreticulin-3 [Source:UniProtKB/Swiss-Prot
AT2G26560	PLP2	Patatin-like protein 2 [Source:UniProtKB/Swiss-Prot
AT1G59870	ABCG36	ABC transporter G family member 36 [Source:UniProtKB/Swiss-Prot
AT2G01180	ATPAP1	phosphatidic acid phosphatase 1 [Source:TAIR
AT1G33560	ADR1	Disease resistance protein ADR1 [Source:UniProtKB/Swiss-Prot
AT4G26090	RPS2	Disease resistance protein RPS2 [Source:UniProtKB/Swiss-Prot
AT3G52430	PAD4	Lipase-like PAD4 [Source:UniProtKB/Swiss-Prot
AT4G36280	MORC2	Protein MICRORCHIDIA 2 [Source:UniProtKB/Swiss-Prot
AT3G50480	HR4	RPW8-like protein 4 [Source:UniProtKB/Swiss-Prot
AT5G26920	CBP60G	Calmodulin-binding protein 60 G [Source:UniProtKB/Swiss-Prot
AT3G26470	AT3G26470	Powdery mildew resistance protein, RPW8 domain-containing protein [Source:UniProtKB/TrEMBL

Figure 2.8. Overlap between the “plant-type hypersensitive response” GO category and genes up-regulated in *snap33-1* at 12 days. 27 genes out of the 76 genes belonging to the “plant-type hypersensitive response” GO category (GO:0009626) were found as constitutively up-regulated at 12 days in *snap33-1* compared to WT-1. Analyses of the 27 common genes (Table) revealed an enrichment of genes involved in the SA pathway and defense responses.

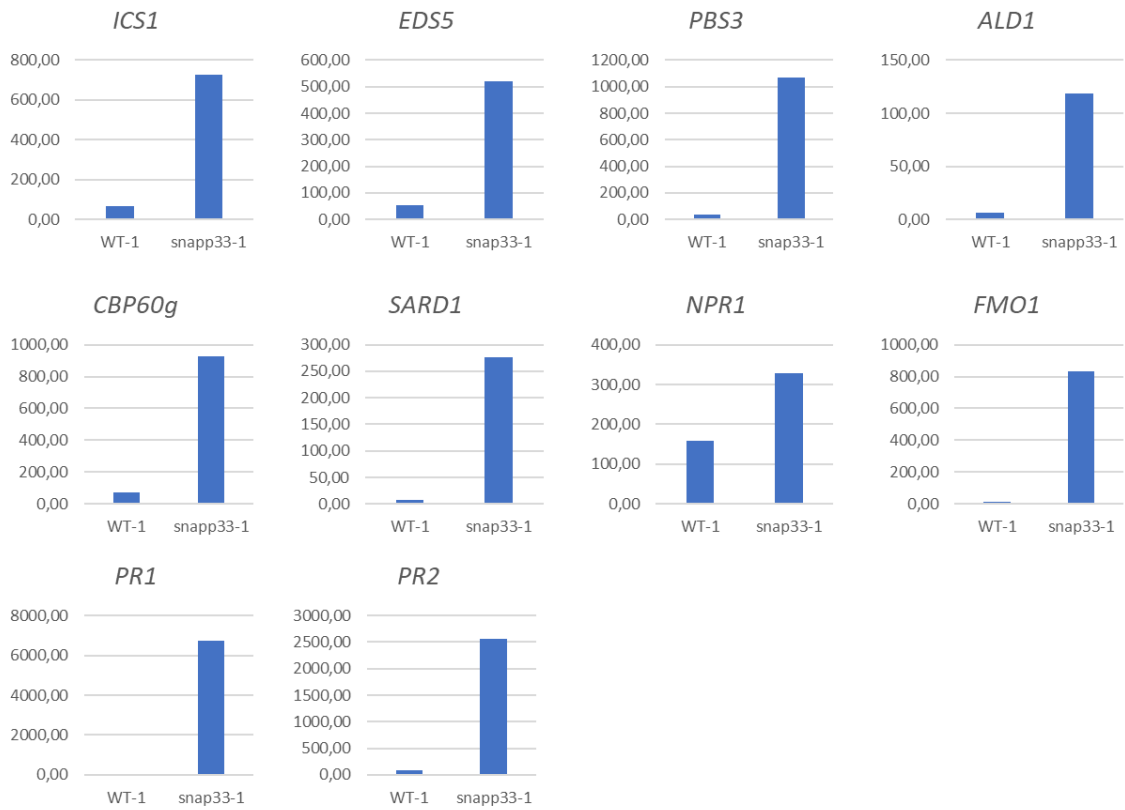
snap33-1's down-regulated genes are involved in growth and cell wall organization

Comparison of the down-regulated genes with $\log_2FC \leq -1$ ($p\text{-value} \leq 0.05$) at 5 and 12 days shows an overlap of 44 genes between the two conditions (figure 2.11). The GO analysis of these 44 common genes reveals enrichment of biological processes related to cell wall organization and biogenesis, such as "plant-type cell-wall organization" and "wax biosynthetic process", and also biological processes related to the abscisic acid hormone and others (figure 2.11). GO analyses of genes exclusively down-regulated at 5 or 12 days show significant enrichment of biological processes related to the cell wall as well, indicating that mutation of *SNAP33* affects the expression of cell wall-related genes and is reminiscent of the phenotype of the SNARE mutants *syp121* and *syp122*, which showed an altered cell wall organization (Assaad et al., 2004). At 5 days, there is also a decreased expression of genes involved in growth (brassinosteroid pathway) consistent with the observed dwarf phenotype of *snap33-1* (figure 2.11). Overall, the analyses of up-regulated and down-regulated genes show that mutation of *SNAP33* leads to the downregulation of genes associated with growth and development and up-regulation of genes involved in plant-defense responses.

snap33-1 resembles pathogen-treated plants at the transcriptomic level

The Genevestigator Signature tool compares an experiment's transcript expression levels to a selection of other transcriptomic data and highlights experiments with similar gene expression. The 200 most highly up-regulated genes and 200 most highly down-regulated genes with $p\text{-value} \leq 0.001$ in the transcriptome of *snap33-1* at 5 or 12 days were used as a *snap33-1* signature to search for experiments with similar transcriptomic changes. For each comparison, a relative similarity factor is calculated (figure 2.12.a). Signature analyses of 5 and 12 days DEGs revealed considerable similarity to several transcriptomic studies, including pathogen-treated plants and mutants of genes involved in plant immunity, such as *bak1* and *mkk1 mkk2* (figure 2.12.a). Interestingly, the transcriptomic study that showed the most similarity to the *snap33-1*'s 12-days transcriptome is that of transgenic plants overexpressing *RPS4 (35S::RPS4-HS)* which encodes the TNL that recognizes the AvrRps4 effector of *Pst* DC3000 and induces an ETI response (Heidrich et al., 2013; Wirthmueller et al., 2007). Analysis of the complete overlap between *snap33-1*'s 12-days transcriptome and the transcriptomic data of *35S::RPS4-HS* study shows an overlap of 1083 up-regulated genes and an overlap of 304 down-regulated genes (figure 2.12). To gain further insights into the biological processes associated with the

a.



b.

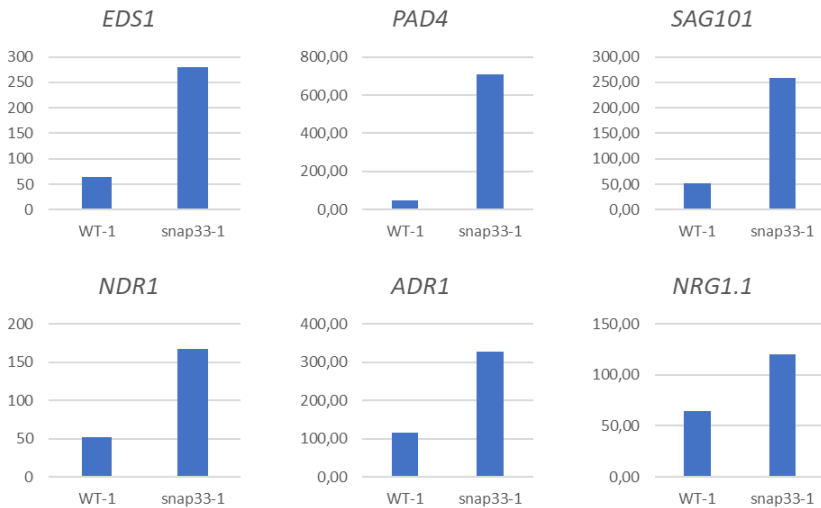


Figure 2.9. Bar graphs showing the expression of selected genes from the 12 days RNA-seq data and involved in the SA pathway and R protein signaling. a. Expression of genes involved in the SA pathway and found in the RNA-seq data as up-regulated two-fold or more ($\text{Log}_2\text{FC} \geq 1$) in *snap33-1* compared to WT-1. **b.** Expression of genes involved in R-protein/NLR signaling and found in the RNA-seq data as up-regulated two-fold or more in *snap33-1* compared to WT-1 ($p\text{-value} \leq 0.05$). The data represented here are the normalized mean counts of each gene for each genotype obtained by the RNA-seq analyses.

commonly up-regulated genes, we performed a GO analysis of MF. We found similar GO terms as those previously obtained on *snap33-1* up-regulated genes at 12 days, such as "protein kinase activity", "protein threonine kinase activity", "NAD+ nucleotidase, cyclic ADP-ribose generating", "NAD+ nucleosidase activity", "NAD(P)+ nucleosidase activity" and "ADP-binding" (Supplementary Table 5). Analyses of genes belonging to the "NAD+ nucleotidase, cyclic ADP-ribose generating", "NAD+ nucleosidase activity", "NAD(P)+ nucleosidase activity" and "ADP binding" GO categories show that *snap33-1*'s transcriptome and *P35S::RPS4-HS*'s transcriptome share several R genes, indicating that the phenotype of *snap33-1* might be related to constitutive R protein signaling (Supplementary Table 6).

1.6. *snap33* 's phenotype is related to constitutive defense signaling

Because the transcriptomic analyses showed that in the *snap33-1* mutant, there is a significant enrichment of genes involved in defense responses, we chose to analyze the contribution of defense hormone pathways to the *snap33-1* mutant's phenotype. Therefore, in this section, I will present the results obtained from these analyses.

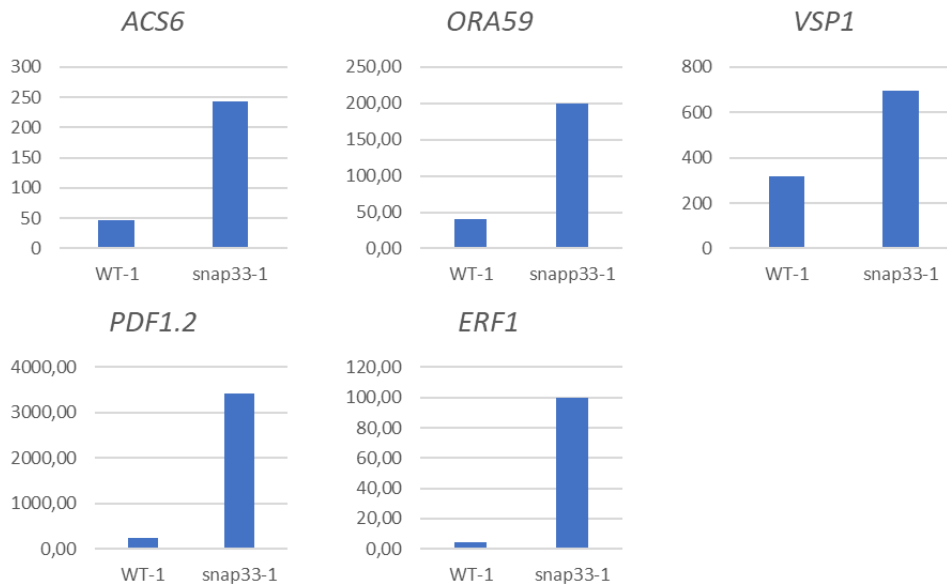
1.6.1. *The SA, JA, and ET marker genes are up-regulated in the snap33 mutants*

The transcriptomic data show that in *snap33-1*, there is constitutive up-regulation of defense-related genes, especially those involving the hormonal pathways SA, JA, and ET. To validate the RNA-seq results, we analyzed some SA and JA-ET marker genes' expression by RT-quantitative PCR (RT-qPCR) in 12-day-old WT-1, *snap33-1*, *snap33-2*, and *snap33-3* plants. The tested SA marker genes were *PR1* and *PR2*, and the tested JA-ET marker genes were *PR4*, *ERF1*, and *PDF1.2*. RT-qPCR results show that all tested marker genes are up-regulated in *snap33-1*, *snap33-2*, and *snap33-3* compared to WT-1 (figure 2.13). Although not statistically significant because of variability among *snap33* replicates, these results align with those obtained by the transcriptomic analyses and must be repeated.

1.6.2. *SA, JA, and ET levels are higher in the snap33-1 mutant*

Given the increased SA and JA-ET marker genes expression in the *snap33* mutants, we examined whether hormone levels are similarly elevated. SA, JA, and ET levels were measured in 13-day-old *snap33* and WT-1 seedlings. *snap33-1* plants produce higher SA, JA, and ET levels than WT-1 plants, with roughly nine-fold more SA and 34-fold more JA (figure 2.14). ET levels

a.



b.

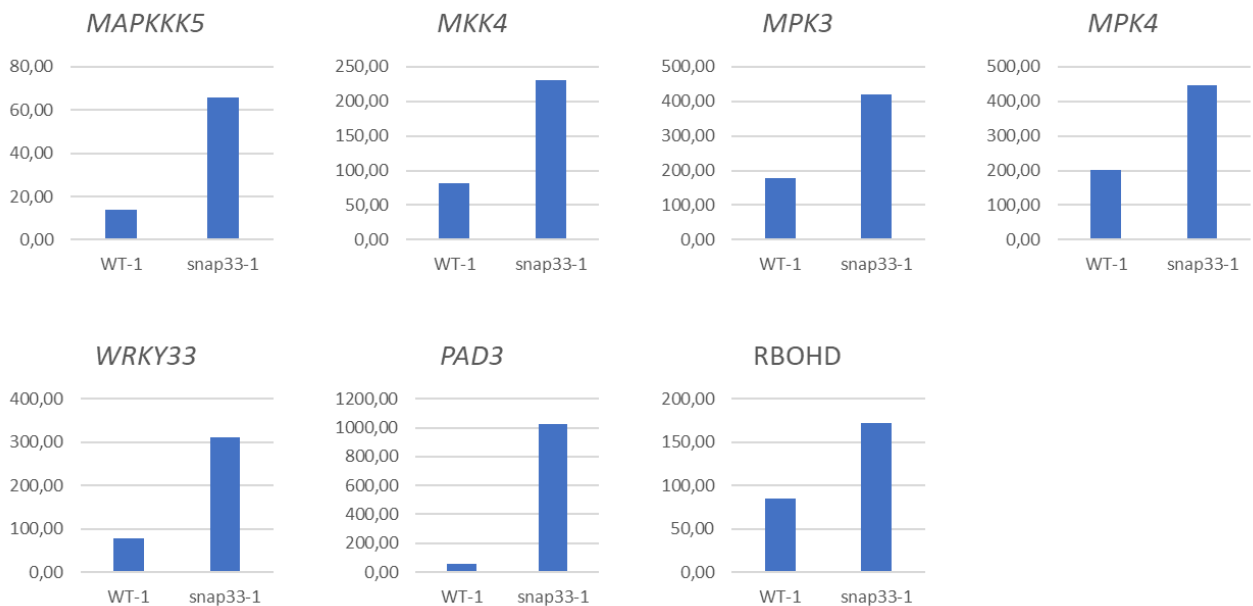


Figure 2.10. Bar graphs showing the expression of selected genes from the RNA-seq data of 12 days *snap33-1* and WT-1 involved in early PTI signaling and in JA and ET hormonal pathways. **a.** Expression of genes involved in JA and ET pathways and found in the RNA-seq data as up-regulated two-fold or more ($\text{Log}_2\text{FC} \geq 1$) in *snap33-1* compared to WT-1. **b.** Expression of genes involved in PTI and found in the RNA-seq data as up-regulated two-fold or more in *snap33-1* compared to WT-1. The data represented here are the normalized mean counts of each gene for each genotype and obtained by the RNA-seq analyses.

are around five-fold those of WT-1 in the *snap33-1*, *snap33-2*, and *snap33-3* mutants (figure 2.14). Moreover, we found increased glycosylated SA (SAG) levels in the *snap33-1* mutant, indicating an increase of both free and stored SA levels in the *snap33-1* mutant (figure 2.14). These findings corroborate the previous results obtained by transcriptomic data, which indicate a constitutive activation of the SA and JA/ET pathways in the *snap33* mutant.

1.6.3. *snap33-1's* phenotype is partially reverted by mutations in the JA and SA pathways

Disruptions of SA and JA pathways partially revert the phenotype of *snap33-1*

As the *snap33-1* mutant showed increased SA, JA, and ET levels, as well as increased expression levels of the corresponding marker genes, we investigated whether mutations in genes involved in SA biosynthesis and JA and ET signaling could rescue *snap33-1's* phenotype. To do this, we crossed the *snap33-1* mutant with *sid2-2*, *coi1-34*, and *ein2-1* mutants to examine the dependence of the *snap33-1's* phenotype on the SA, JA, and ET pathways, respectively. As stated earlier, COI1 and EIN2 are the key signaling components of the JA and ET pathways, respectively, and SID2 is involved in pathogen-induced SA biosynthesis. The double mutants were obtained by crossing *snap33-1^{+/-}* heterozygous plants with the homozygous *sid2-2*, *coi1-34*, and *ein2-1*. As shown in figure 2.15.a, the homozygous *sid2-2*, *coi1-34*, and *ein2-1* mutants display a WT-1-like macroscopic phenotype. The double mutants were isolated by PCR and grown simultaneously on Jiffy pots in the same growth chamber for accurate phenotypic comparison and evaluation of rosette weight. As shown in figure 2.15, the *snap33-1 ein2-1* double mutant displays a similar phenotype as the *snap33-1* single mutant with an average fresh weight (FW) of 0.43 mg compared to 0.42 mg, respectively, indicating that *snap33-1's* phenotype is not dependent on the ET signaling pathway. The *snap33-1 coi1-34* double mutant showed a slightly improved morphology with an average FW of 1 mg, more than twice that of the *snap33-1* mutant, indicating that the JA pathway affects the phenotype of *snap33-1* (figure 2.15). On the other hand, the *snap33-1 sid2-2* mutant displays a more obvious larger rosette size compared to the *snap33-1* mutant (figure 2.15.a), with an average FW of 4.1 mg, about ten-fold that of the *snap33-1* mutant, showing that the phenotype of the *snap33-1* mutant is partially dependent on the SA pathway (figure 2.15). Analyses of cell death and H₂O₂ accumulation in 20-day-old seedlings of the *snap33-1 sid2-2* double mutant showed that the *SID2* mutation largely suppressed the cell death and H₂O₂ over-accumulation phenotypes of

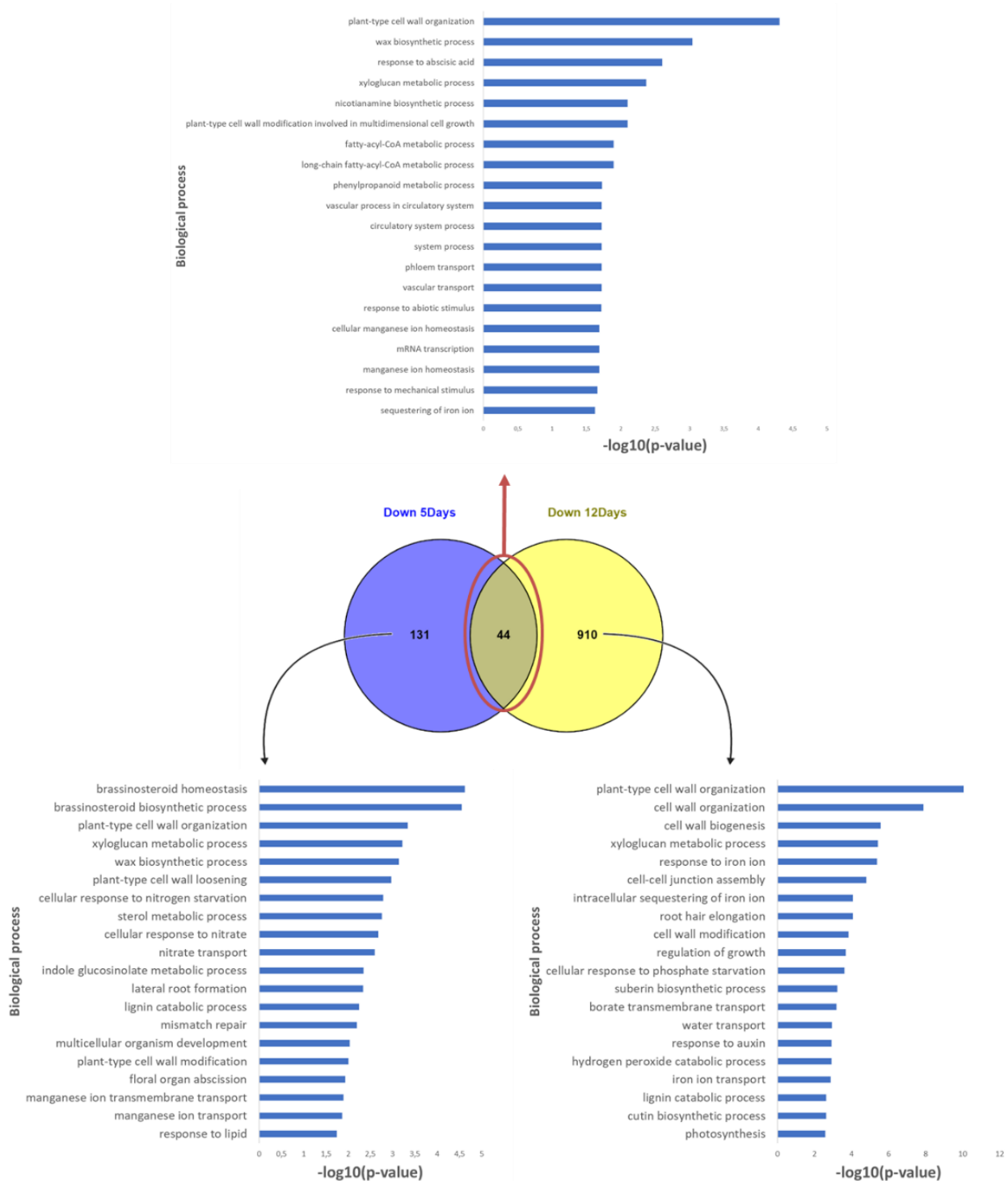


Figure 2.11. GO enrichment analyses of the *snap33-1* down-regulated genes at 5 and 12 days. Bar charts showing the top 20 enriched GO terms of biological processes obtained by analyzing the 44 common down-regulated genes between 5 and 12 days (upper graph), the 131 down-regulated genes at 5 days (lower left graph), and the 910 genes down-regulated at 12 days in *snap33-1* (lower right). The top 20 significant categories are represented on the vertical axis, and the horizontal axis represents the $-\text{Log}_{10}(p\text{-value})$ of the significant pathways. Greater $-\text{Log}_{10}(p\text{-value})$ scores correlate with increased statistical significance. The GO analyses were performed using the TopGo “elim” method (Alexa et al., 2006).

the *snap33-1* mutant (figure 2.16.a). However, at later stages and as depicted in figure 2.15.a, the 35-day-old *snap33-1 sid2-2* presents several lesions on leaves and cotyledons, showing that *SID2* mutation only delays the appearance of lesions in *snap33-1*. This result is similar to that obtained by growing *snap33-1* at high temperatures and correlates with the fact that at 30°C, *SID2/ICS1* expression is decreased, as reported by Huot et al. (2017). We also analyzed the activation of MPK3, MPK4, and MPK6 in response to flg22 treatment and MPK4 and MPK6 protein levels in the *snap33-1 sid2-2* double mutant. As shown in figure 2.16.b, *SID2* mutation restored the MAPK activation to WT-1 levels, and the protein levels of MPK4 and MPK6 were also largely reduced in the *snap33-1 sid2-2* double mutant, indicating that MAPKs' over-activation and increased protein levels are mainly depending on SA. It is important to note that unlike the results observed in section 1.3 we noticed that MPK6 protein levels are higher in the *snap33-1* mutant compared to WT-1, therefore to conclude on MPK6's overaccumulation in *snap33*, these experiments must be repeated. We also observed a reduced accumulation of MPK3 in the *snap33-1 sid2-2* mutant in another experiment (Data not shown). RT-qPCR analyses showed that *PR1*'s transcripts are no longer up-regulated in the *snap33-1 sid2-2* double mutant compared to *snap33-1* single mutant (figure 2.16.c). This result was expected as it is known that *PR1* is no longer induced in the *sid2* background upon pathogen infection (Wildermuth et al., 2001). However, *PDF1.2* expression was higher in *snap33-1 sid2-2* compared to *snap33-1* (figure 2.16.c), showing that in the *snap33-1 sid2-2* double mutant, there might be a suppression of the antagonistic effect of SA on JA/ET leading to enhanced expression of JA/ET marker genes. The ensuing enhanced JA/ET signaling in *snap33-1 sid2-2* might explain the only partial reversion of *snap33-1* by *sid2-2*.

Combinatorial mutations of the JA and SA pathways tend to further revert *snap33-1*'s phenotype

As the SA and JA-ET pathways are antagonistic, and given the results obtained by the RT-qPCR experiments on *snap33-1 sid2-2*, which showed an even higher expression of *PDF1.2* in the *snap33-1 sid2-2* double mutant compared to *snap33-1* (figure 2.16.c), we hypothesized that in the *snap33-1 ein2-1* and *snap33-1 coi1-34* double mutants, the SA pathway might be enhanced due to a suppression of the antagonistic effects of the JA or ET pathways on the SA pathway. Therefore, combinatorial mutations of the SA and JA/ET pathways might lead to even greater suppression of the auto-immune dwarf phenotype of *snap33-1*. To test this hypothesis, we generated the *snap33-1 sid2-2 coi1-34*, *snap33-1 sid2-2 ein2-1* and *snap33-1 ein2-1 coi1-34*

a.

Top 10 most similar perturbations at 12 days	Experiment Title	Relative similarity
shift 28°C to 19°C study 2 (35S::RPS4-HS) / 28°C (35S::RPS4-HS)	GSE50019: Study of expression changes during RPS4-mediated resistance in Arabidopsis using a temperature-inducible system	1,358
<i>P. parasitica</i> (30h) / non-infected root samples (Col-0)	GSE20226: Arabidopsis thaliana/Phytophthora parasitica compatible interaction transcriptome	1,346
CMP (24h) / solvent treated root culture samples (24h)	GSE28431: Skipsey: Fenclorim safening of Arabidopsis	1,333
<i>P. syringae</i> pv. <i>maculicola</i> (Col-0) / mock treated leaf samples (Col-0)	GSE18978: Arabidopsis thaliana mutant leaves treated with <i>Pseudomonas syringae</i> ES4326	1,331
shift 28°C to 19°C study 3 (35S::RPS4-HS rrs1-11) / 28°C (35S::RPS4-HS rrs1-11)	GSE50019: Study of expression changes during RPS4-mediated resistance in Arabidopsis using a temperature-inducible system	1,324
Pep2 study 2 (bak1-3) / mock treated seedling samples (bak1-3)	GSE40354: Expression analysis of Arabidopsis ein2 and bak1 mutants treated with the elicitors elf18 and Pep2	1,321
<i>S. sclerotiorum</i> study 2 (coi1-2) / mock inoculated rosette leaf samples (coi1-2)	E-MEXP-3122: Transcription profiling by array of Arabidopsis mutant for coi1 after infection with <i>Sclerotinia sclerotiorum</i>	1,304
mkk1 mkk2 / Col-0	GSE10646: BTH treated mkk1, mkk2 and mkk1/2 knockout mutant	1,296
<i>P. parasitica</i> (10.5h) / non-infected root samples (Col-0)	GSE20226: Arabidopsis thaliana/Phytophthora parasitica compatible interaction transcriptome	1,29
<i>P. parasitica</i> (6h) / non-infected root samples (Col-0)	GSE20226: Arabidopsis thaliana/Phytophthora parasitica compatible interaction transcriptome	1,281

Top 10 most similar perturbations at 5 days	Experiment Title	relative similarity
<i>L. huidobrensis</i> (Col-0) / untreated rosette leaf samples (Col-0)	GSE33505: Expression data from volatile treated and insect damaged Arabidopsis thaliana	1,401
OPDA study 2 (tga2-5-6) / solvent treated (tga2-5-6) seedlings	GSE10749: Response of Arabidopsis cell culture to cyclopentenone oxylipins	1,319
<i>P. syringae</i> pv. <i>tomato</i> study 8 (DC3000) / mock inoculated leaf samples	GSE5520: Genome-wide transcriptional analysis of the compatible <i>A. thaliana</i> - <i>P. syringae</i> pv. <i>tomato</i> DC3000 interaction	1,307
ozone / air treated seedlings	E-GEOD-5722: Functional Genomics of Ozone Stress in Arabidopsis	1,302
OPDA study 2 (Col-0) / solvent treated (Col-0) seedlings	GSE10749: Response of Arabidopsis cell culture to cyclopentenone oxylipins	1,301
flu1-1 / Col-0 [shift low light to dark to high light (flu1-1) / shift low light to dark to high light (Col-0)]	GSE49596: A New Mediator of Singlet Oxygen Responses in <i>Chlamydomonas</i> and Arabidopsis	1,268
osmotic study 4 (shoot) / mock treated Col-0 shoot samples	GSE36789: Transcriptome Profiling of Roots and leaves Under High Osmotic Stress in Arabidopsis	1,263
MeJA study 4 (Col-0) / mock treated plant samples (Col-0)	E-MEXP-883: Comparison of mock-treated vs. methyl jasmonate-treated wild type (Col-0) vs. <i>myc2</i> (<i>jln1-9</i>) mutant Arabidopsis lines	1,245
low R/FR + MeJA (2h) / low R/FR (2h)	GSE35700: Expression data from low R:FR - JA crosstalk in Arabidopsis	1,244
MeJA study 2 (3h) / mock treated seedlings (3h)	AtGenExpress: response of wild-type seedlings to seven phytohormones (IAA, zeatin, GA3, ABA, MJ, ACC, BL)	1,235

b.

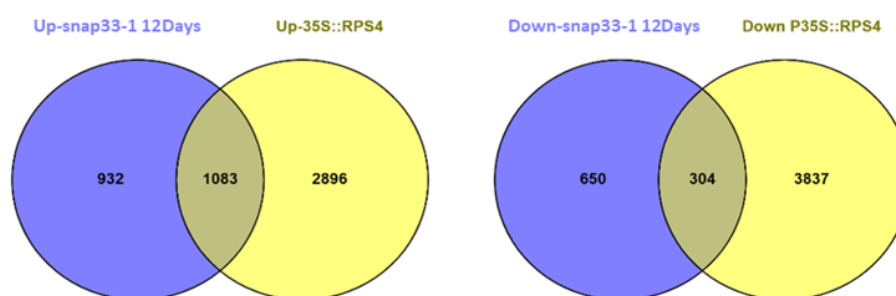


Figure 2.12. The *snap33-1* transcriptome displays similarity to stress-treated plants. a. Experiments that showed the most important similarity to *snap33-1* deregulations at 5 and 12 days. The 200 genes with the highest $\log_2(\text{FC})$ and the 200 genes with the most negative $\log_2(\text{FC})$ (p -value ≤ 0.05) from the RNA-seq data of *snap33-1* at 5 or 12 days were used with their corresponding $\log_2(\text{FC})$ values to screen for transcriptomic data with the most similarities. **b.** Venn diagrams showing the overlap between the *snap33-1* DEGs at 12 days and the *P35S::RPS4-HS* transcriptome (Heidrich et al., 2013).

triple mutants. As depicted in figure 2.17, the *snap33-1 sid2-2 coi1-34* triple mutant shows a significantly improved morphology compared to *snap33-1 coi1-34* with an average weight of 9 mg compared to 1 mg and 0.4 mg for the double mutant *snap33-1 coi1-34* and the *snap33-1* mutants, respectively. Although the *snap33-1 sid2-2 coi1-34* triple mutant is not statistically different from the *snap33-1 sid2-2* double mutant, the larger rosette morphology displayed by individuals of this genotype, as well as its mean FW values, indicate that mutations of both SA and JA pathways tend to suppress the *snap33-1* mutant phenotype in an even stronger way compared to mutation of the SA pathway only (figure 2.17.a). The *snap33-1 sid2-2 ein2-1* triple mutant did not show an improved phenotype than *snap33-1 sid2-2*, showing that the *snap33-1* phenotype might not depend on the ET pathway. The *snap33-1 coi1-34 ein2-1* triple mutant was statistically and morphologically similar to the *snap33-1* mutant, possibly because the SA pathway might be further induced in this genotype and takes over the suppressive effects that might be provided by the JA and ET pathway mutations. Altogether, these results indicate that the *snap33-1* mutant's phenotype might depend more on the SA pathway than the JA and ET pathways, although all three pathways are induced in this mutant. Generation of the *snap33-1 sid2-2 coi1-34 ein2-1* quadruple mutant would help conclude on the contribution of the three pathways to the phenotype of *snap33-1*.

P35S::NahG, but not *npr1-1*, strongly reverts the phenotype of *snap33-1*

As the introduction of the *sid2-2* mutation partially reverted the phenotype of *snap33-1* (figures 2.15 and 2.16), we further analyzed the dependence of *snap33-1*'s phenotype on the SA pathway. As mentioned in the introduction, the biosynthesis of SA occurs via two pathways, namely the ICS1-ICS2-dependent IC pathway and the PAL pathway. We hypothesized that in the *snap33-1* mutant SA might be biosynthesized not only via *ICS1* but also via *ICS2* and/or the PAL pathway. To test our hypothesis, we crossed *snap33-1* with a transgenic line ectopically expressing the bacterial enzyme *NahG* (*P35S::NahG*), an enzyme which converts SA to catechol, to abolish SA accumulation in the *snap33-1* mutant (Delaney et al., 1994; Gaffney et al., 1993). Plants expressing *P35S::NahG* lose resistance to biotrophic pathogens and are unable to establish the SAR when infected by pathogens (Gaffney et al., 1993).

Moreover, Heck et al. reported a decreased ET production upon pathogen infection in the *P35S::NahG* transgenic plants (Heck et al., 2003). As shown in figure 2.18, the ectopic expression of *NahG* in *snap33-1* plants leads to a very strong reversion of its phenotype. Indeed, *snap33-*

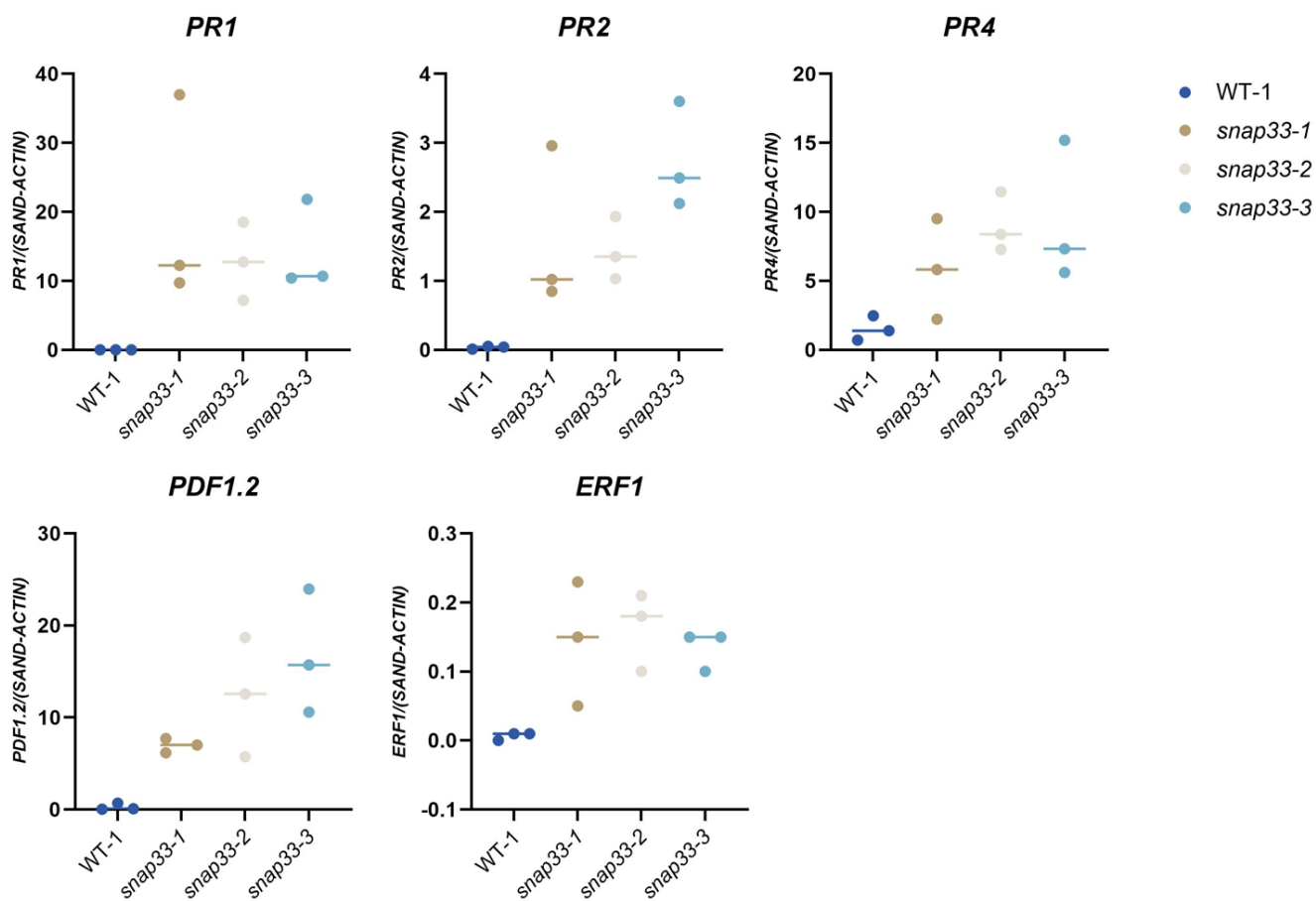


Figure 2.13. SA and JA-ET marker genes are up-regulated in the *snap33* mutants compared to WT-1. Total RNAs were extracted from 12-day-old seedlings of WT-1, *snap33-1*, *snap33-2*, and *snap33-3* plants and used for RT-qPCR analyses to measure the expression of *PR1*, *PR2*, *PR4*, *ERF1*, and *PDF1.2*. The plotted values were obtained from three biological replicates and represent the fold-change compared to the reference genes *SAND* and *ACTIN*. Bars represent the median value.

1 *P35S::NahG* plants' rosette size is similar to that of *P35S::NahG* line, with an average rosette weight of 70 mg and 170 mg, respectively (figure 2.18.b). Although the rosette weight is lower when compared to WT-1 plants, *snap33-1 P35S::NahG* displayed a much healthier phenotype with no apparent lesions on rosette leaves (figure 2.18.a). These results show that the phenotype of *snap33-1* largely depends on the SA pathway and indicate that the SA accumulation in *snap33-1* does not depend on ICS1 only and probably involves ICS2 and the PAL pathway. Further analyses of the *snap33-1 P35S::NahG* plants will provide further insights into the involvement of SA in the phenotype of *snap33-1*.

Because *NPR1* is up-regulated in the *snap33-1* mutant (figure 2.9) and to test whether the phenotype of *snap33-1* might be reverted by suppression of SA signaling, *snap33-1* was crossed with the *npr1-1* mutant. As shown in figure 2.19.a, the *snap33-1 npr1-1* double mutant was slightly bigger than *snap33-1*, with five times the average rosette weight of *snap33-1*, 4.8 mg compared to 0.8 mg, respectively (figure 2.19.b). This result shows that the introduction of *npr1-1* mutation in the *snap33-1* leads to seemingly a weaker reversion compared to *NahG* ectopic expression, suggesting that the phenotype of *snap33-1* is related to SA over-accumulation, which impacts not only the *NPR1*-dependent pathway but also *NPR1*-independent pathways.

Since several SAR marker genes, including *ALD1* and *FMO1*, are up-regulated in the *snap33-1* mutant (figure 2.9) and to test whether other SAR mutants might suppress the phenotype of *snap33-1*, we crossed *snap33-1* with the *fmo1-1* mutant. *FMO1* is involved in the last step of NHP biosynthesis, and *fmo1* mutants are unable to accumulate SA in distant tissues. As a result, they are unable to establish a SAR upon infection with biotrophic pathogens (Chen et al., 2018; Jing et al., 2011; Mishina & Zeier, 2006). As depicted in figure 2.20, the *snap33-1 fmo1-1* double mutant shows a larger morphology than *snap33-1*, and the lesions are less apparent in this double mutant than *snap33-1*, indicating that NHP accumulation contributes to the phenotype of *snap33-1*. Analyses of rosette weight, cell death, and ROS accumulation will provide further insights into the NHP pathway's role in the *snap33-1*'s phenotype.

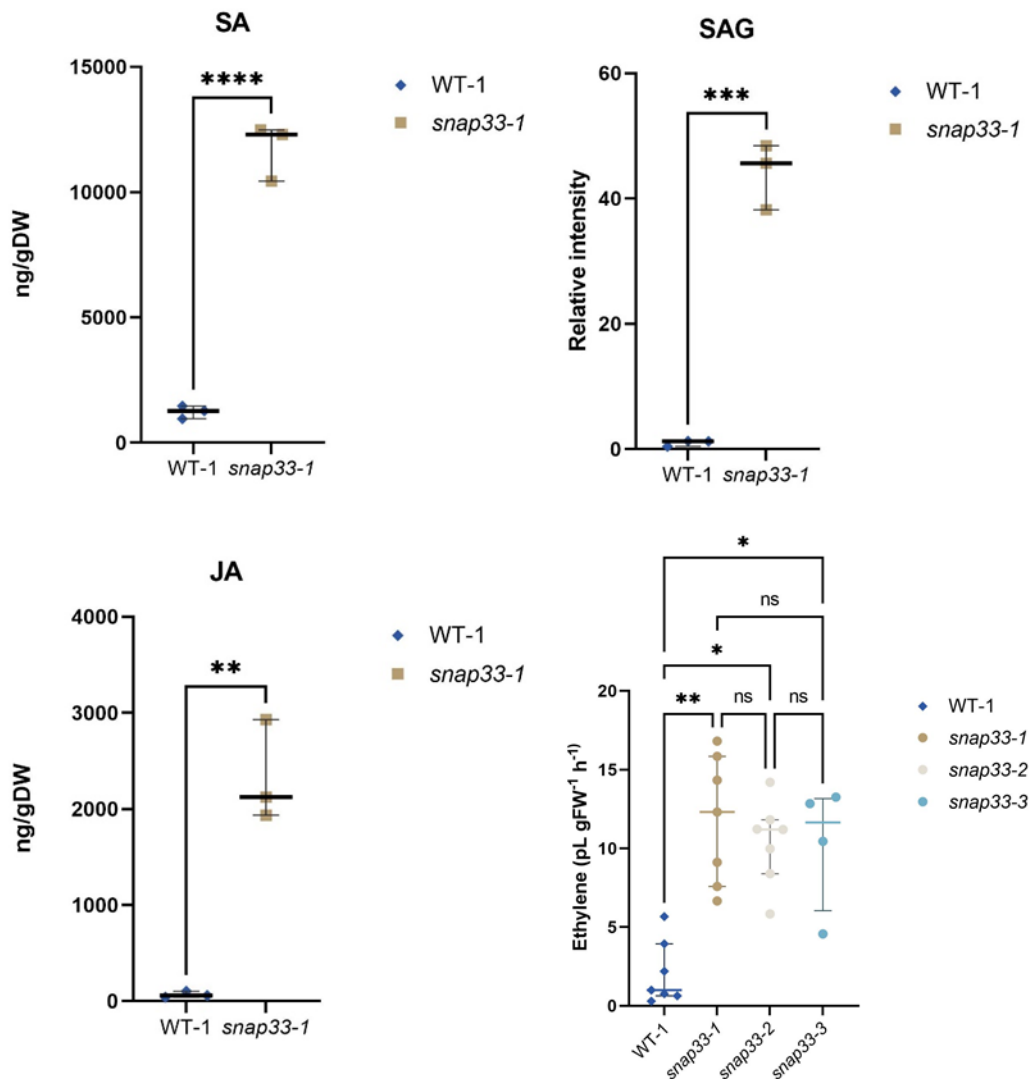


Figure 2.14. SA JA and ET levels are higher in the *snap33* mutant compared to WT-1. Free and glycosylated SA levels in 13-day-old WT-1 and *snap33-1* seedlings (upper panel). The lower left panel shows the JA levels in 13-day-old WT-1 and *snap33-1* seedlings. The SA, SAG, and JA plotted values were obtained from three biological replicates; asterisks denote statistically significant differences in unpaired t-tests with two asterisks [**] indicate p-value < 0.01, and four asterisks [****] indicate p-value < 0.0001. The lower right panel shows the ET emission levels in 13-day-old WT-1, *snap33-1*, *snap33-2*, and *snap33-3* seedlings. Seedlings were grown on ½ MS media and transferred into capped bottles to allow ET accumulation during 24 hours. The plotted values were obtained from three biological replicate with at least one measure in each replicate for each genotype; asterisks denote statistically significant differences in the Kruskal Wallis (Benjamini Hochberg false discovery rate (FDR)) test, with one asterisk [*] indicates a p-value<0.05 and two asterisks [**] indicate a p-value<0.01. Bars indicate the median values and interquartile range; DW: dry weight, FW: fresh weight, h: hour.

1.6.4. R protein signaling is constitutively induced in the *snap33-1* mutant

Introduction of the *ndr1-1* and *eds1-2* mutations in the *snap33-1* background partially reverts its phenotype

Given that we found an abundance of up-regulated R genes in the transcriptome of *snap33-1* (Supplementary Table 3), and because R proteins are known to induce SA biosynthesis and SA signaling upon sensing perturbations by effectors, we investigated whether the phenotype of *snap33-1* is related to constitutive R protein signaling. To do this, we crossed *snap33-1* with the *eds1-2* and *ndr1-1* mutants. As mentioned earlier in the introduction, EDS1 is required for signaling downstream TNLs as well as several CNLs, and NDR1 was reported to be required for signaling downstream some CNLs. As shown in figure 2.21.a, the two double mutants *snap33-1 eds1-2* and *snap33-1 ndr1-1* displayed a slightly larger rosette size compared to the *snap33-1* single mutant, with an average rosette weight of 1.7 mg and 1.5 mg, respectively, compared to 1 mg for *snap33-1* (figure 2.21.b). These results suggest that the *SNAP33* mutation might induce the activation of both TIR- and CC-type NLRs. To test this hypothesis, we generated the *snap33-1 eds1-2 ndr1-1* triple mutant. As depicted in figure 2.21.c, the triple mutant *snap33-1 eds1-2 ndr1-1* displays seemingly a larger rosette size compared to *snap33-1* (figure 2.21.b). Although this result requires further analysis by rosette weight measurements on a larger number of plants and comparison with the two double mutants *snap33-1 ndr1-1* and *snap33-1 eds1-2*, it strongly suggests that the phenotype of *snap33-1* partially depends on constitutive activation of a CC-type NLR or at least one CNL and one TNL, since *EDS1* and *NDR1* are both genetically required for signaling downstream some CNLs, and *EDS1* is genetically required for signaling downstream TNLs (see CHAPTER I 1.2.5). However, the only partial reversion of *snap33-1* by *eds1-2 ndr1-1* suggests that if *snap33-1*'s phenotype is completely related to constitutive R protein signaling, these activated R proteins signal via EDS1 and NDR1 and via a pathway that bypasses EDS1 and NDR1.

The phenotype of *snap33-1* is partially dependent on CNL proteins signaling

As previously stated, *AMSH3* codes for a deubiquitinating (DUB) protein required for signaling downstream CNLs, including *RPM1* and *RPS2*, by stabilizing their corresponding proteins (Torsten Schultz-Larsen et al., 2018). Introduction of the *amsh3-4* mutation, in which the DUB activity of *AMSH3* is abolished, in the *syp121 syp122* double mutant completely suppresses its auto-immune phenotype (Torsten Schultz-Larsen et al., 2018). *SNAP33* interacts with both

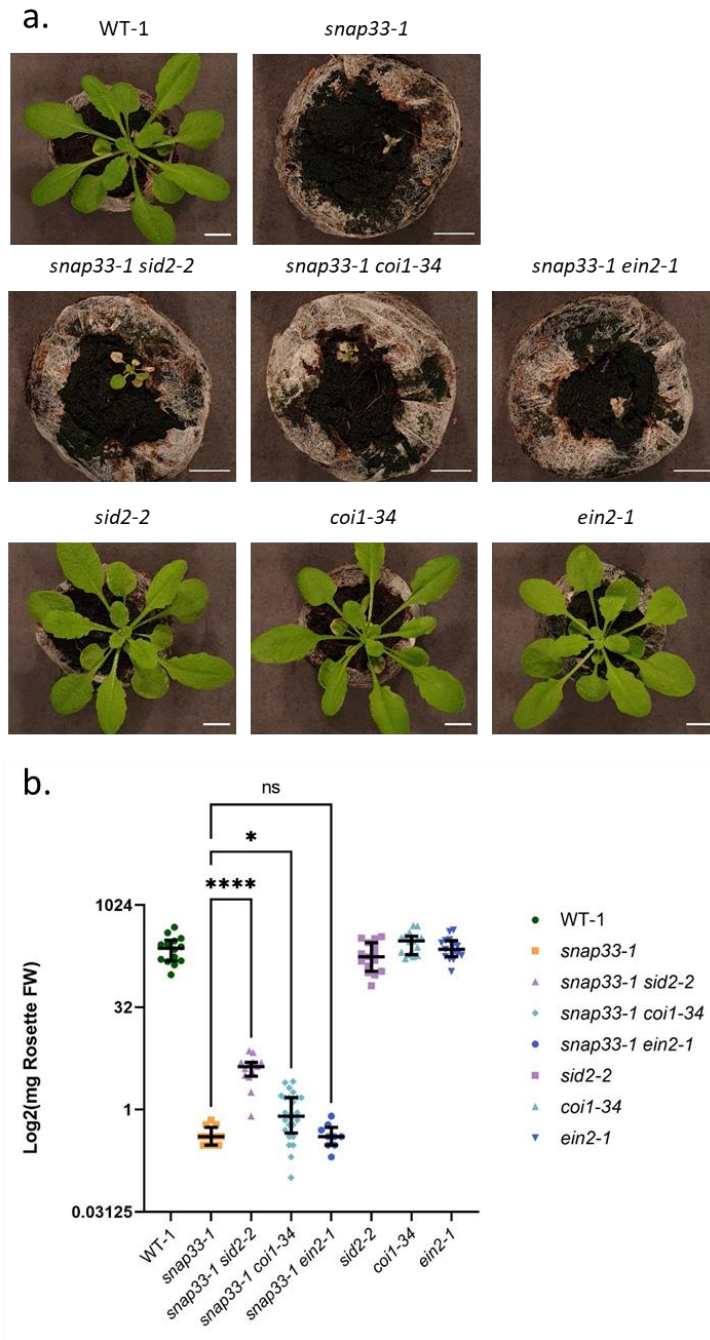


Figure 2.15. Morphological phenotypes of WT-1, *snap33-1*, *snap33-1 sid2-2*, *snap33-1 coi1-34*, *snap33-1 ein2-1*, *sid2-2*, *coi1-34* and *ein2-1*. **a.** Representative pictures of 35-day-old soil-grown plants. Scale bars represent 1 cm. **b.** Biomass of aerial parts of the analyzed genotypes. Plotted values are the Log2 of rosette fresh weight (FW) (see Supplementary data 1 for linear values) with WT-1, *snap33-1*, *snap33-1 sid2-2*, *snap33-1 coi1-34*, *snap33-1 ein2-1*, *sid2-2*, *coi1-34* and *ein2-1* average fresh weight, respectively, of 243.4 mg (n=14), 0.4 mg (n=12), 4.1 mg (n=13), 1 mg (n=25), 0.4 mg (n=9), 212.3 mg (n=15), 320.4 mg (n=15) and 258 mg (n=15). Bars indicate the median value and interquartile range. Asterisks denote statistically significant differences in the Kruskal Wallis test (Benjamini Hocheberg FDR), with one asterisk [*] indicates p-value<0.05 and four asterisks [****] p-value<0.0001; ns stands for not significant. The data presented here are the results of one biological replicate. Descriptive statistics and linear values are provided in Supplementary data 1.

SYP121/PEN1 and SYP122 and forms a SNARE complex with SYP121/PEN1 involved in the secretion of antimicrobial compounds (Kwon et al., 2008). We thus generated the *snap33-1 amsh3-4* double mutant to see if *snap33-1*'s phenotype can be similarly suppressed by *amsh3-4*. As shown in figure 2.22.a, *snap33-1 amsh3-4* displays a larger rosette size compared to *snap33-1*, with an average rosette weight of 14.5 mg compared to 1.9 mg, respectively, approximately 7 times bigger than *snap33-1* (figure 2.22.b). This finding shows that the *snap33-1* phenotype partially depends on *AMSH3*, and thus possibly partially on RPM1 and RPS2 NLRs. These results further support the involvement of R proteins in the *snap33-1* phenotype. However, the distinct level of suppression of *snap33-1* and *syp121 syp122* by *amsh3-4* suggests that SNAP33, SYP121, and SYP122 carry out distinct functions in plants.

1.6.5. *snap33-1*'s phenotype is partially dependent on CPK5 and TN2

SNAP33 interacts with EXO70B1, a tethering factor involved in the delivery of FLS2 to the PM together with EXO70B2 (Pečenková et al., 2011; Wang et al., 2020; Zhao et al., 2015). As mentioned earlier in the introduction, *exo70b1* mutant exhibits an auto-immune phenotype due to constitutive activation of CPK5 and the atypical TIR-NBS R protein TN2 (Liu et al., 2017). Indeed, both *CPK5* and *TN2* were recovered from a screen of suppressors of *exo70b1*'s phenotype, and Liu et al. reported that TN2 activates CPK5 in the *exo70b1* background (Liu et al., 2017). Later the same group showed that EXO70B1 is targeted by the *Pto* DC3000 effector AvrPtoB which induces TN2-mediated immune responses, and they concluded that TN2 guards EXO70B1 (Wang et al., 2019). *snap33-1*'s transcriptomic analysis show that *TN2* and *CPK5*, as well as other *CDPKs* and *TN* genes, are constitutively up-regulated in the *snap33-1* mutant (Supplementary Tables 2 and 3). Because SNAP33 interacts with EXO70B1, we tested whether the phenotype of *snap33-1* is also dependent on TN2. Therefore, we crossed the *snap33-1* mutant with the *tn2-1* mutant. As depicted in figure 2.23.a, the phenotype of *snap33-1 tn2-1*, observed on a few individuals, does not show a clear difference with *snap33-1*. The analysis of a larger number of plants is required to conclude on the eventual *TN2* dependency of *snap33-1*'s phenotype.

As CPK5 was activated by TN2 in the *exo70b1* mutant, Liu et al. proposed that CPK5 might have a unique role downstream NLRs by initiating NLRs-downstream signaling (Liu et al., 2017). Moreover, CPK5 was shown to play an important role in SAR (introduction section 1.1.2).

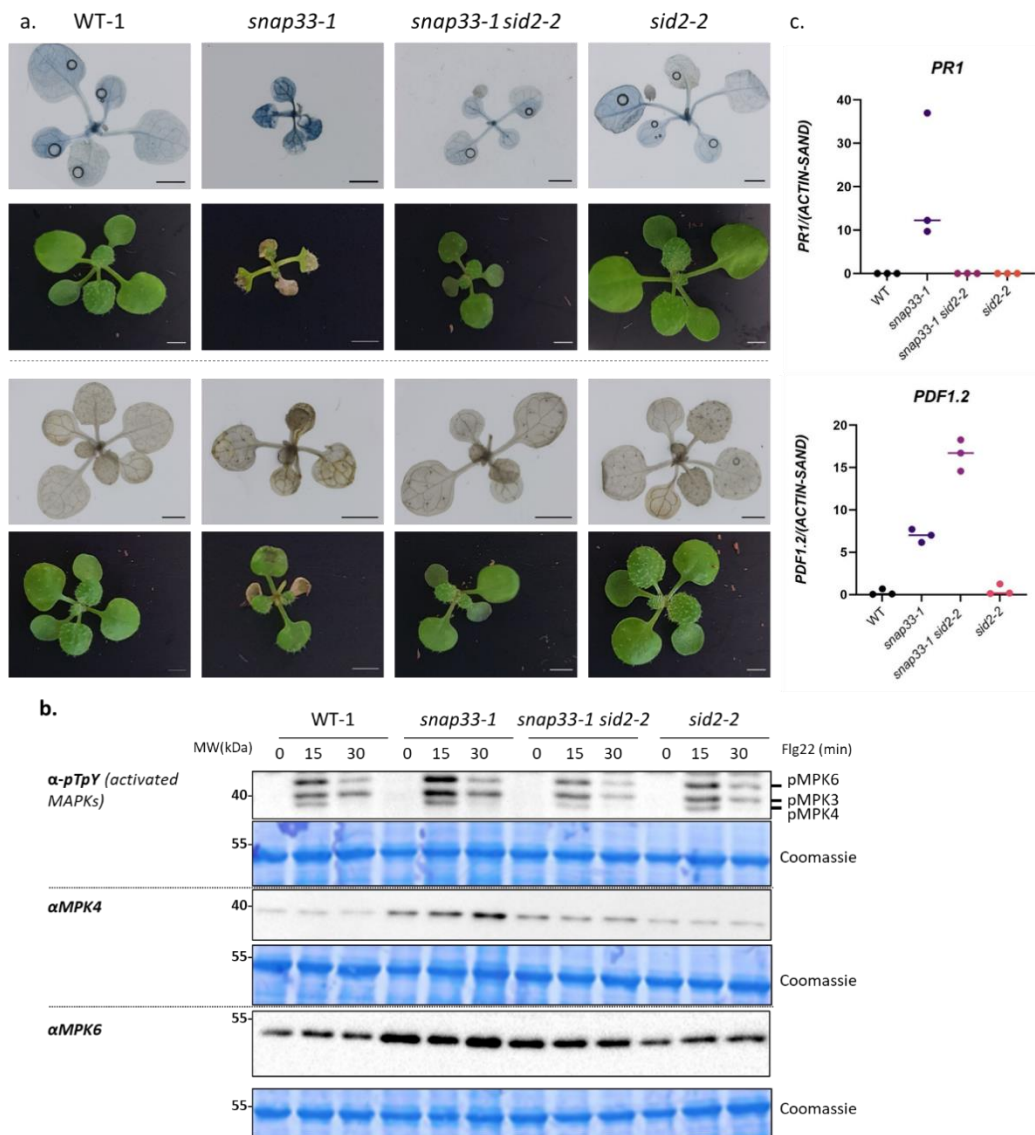


Figure 2.16. Phenotypic and molecular analyses of *snap33-1 sid2-2* plants. **a.** Representative pictures of 20-day-old seedlings stained with trypan blue (top panel) and DAB (lower panel). Cell death appears as dark blue patches (top panel), and ROS accumulation appears as brown patches (lower panel). The photographs show the morphological phenotype of 20-day-old seedlings of WT-1, *snap33-1*, *snap33-1 sid2-2*, and *sid2-2* plants before staining (It is important to note that these experiments were performed at the same time as those observed in figure 2.2.) Scale bars represent 2 mm. **b.** WT-1, *snap33-1*, *snap33-1 sid2-2*, and *sid2-2* plants were grown *in vitro* for 13 days, treated with 100 nM flg22, and harvested after 0, 15, and 30 min flg22 treatment. The activation of MPK3, MPK4, and MPK6 was detected by immunoblotting analysis using an anti-pTpY antibody (α -pTpY). The accumulation of MPK3, MPK4, and MPK6 was assessed by immunoblotting analysis using antibodies specific to the corresponding proteins (α -MPK3, α -MPK4, and α -MPK6). Coomassie blue staining was performed after blotting to assess protein loading in each well; the ~55 kDa protein band corresponds to the RuBisCO large subunit. This experiment was performed twice with similar results. **c.** Quantitative RT-PCR (RT-qPCR) analysis of *PR1* and *PDF1.2* in *snap33-1*, *snap33-1 sid2-2*, *sid2-2* and WT-1. Total RNA extracted from rosette leaves of 12-day-old Arabidopsis *snap33-1*, *snap33-1 sid2-2*, *sid2-2* mutant plants, and WT-1 plants were used for RT-qPCR analysis to measure the expression of *PR1* and *PDF1.2*. The plotted values were obtained from three biological replicates and represent the fold-change compared to the reference genes *SAND* and *ACTIN*. Bars represent the median value.

Therefore, we tested whether CPK5 is involved in the phenotype of *snap33-1*. As shown in figure 2.23.b, *snap33-1 cpk5-1* displayed a slightly increased rosette size compared to the *snap33-1* mutant (figure 2.23.b) with an average rosette weight of 1.7 mg compared to 0.9 mg, respectively, almost twice the weight of *snap33-1* (figure 2.23.c). These results suggest that *snap33-1*'s auto-immune phenotype is partly linked to CPK5's activity.

1.7. Discussion

SNAP33 is a SNAP25-like/Qbc-SNARE involved in the last step of vesicle fusion during secretion in the default secretory pathway. Previous studies showed that SNAP33 forms a SNARE complex with the syntaxin/Qa-SNARE SYP121/PEN1 and the R-SNAREs VAMP721/722 involved in secretion of anti-microbial compounds during infection by *Bgh* (Kwon et al., 2008). SNAP33 is also involved in cytokinesis with the syntaxin/Qa-SNARE KNOLLE (Heese et al., 2001; Kasmi et al., 2013). *SNAP33* is up-regulated in response to a variety of stresses, including pathogen infection, wounding, and SA application (Wick et al., 2003). Mutation in the *SNAP33* gene of the Arabidopsis *Ws* ecotype, *snap33^{Ws}*, leads to a dwarf phenotype with the formation of spontaneous lesions as early as the seedling stage (Heese et al., 2001).

Despite the early identification of the *snap33^{Ws}* mutant almost two decades ago, no more investigations have been done to elucidate the molecular mechanisms behind this mutant's lesion-mimic phenotype, which is probably due to its lethality and inability to generate seeds.

In this first section of Chapter II, I reported the experiments we conducted to determine the processes underlying *snap33*'s phenotype. We first identified five new allelic *snap33* mutants in the Col-0 ecotype, each with a different T-DNA insertion in the *SNAP33* locus. Among them, *snap33-1*, *snap33-2*, and *snap33-3* do not express *SNAP33* and display the lesion-mimic phenotype previously reported in the *Ws* ecotype (Heese et al., 2001), which further validates the tight association of the lesion-mimic phenotype with the *SNAP33* locus. Surprisingly, the *snap33-4* and *snap33-5* lines, in which the T-DNAs are inserted in the 5'UTR and promoter region, respectively, express *SNAP33*. These findings suggest that modifying the 5'UTR region and the proximal promoter of *SNAP33* has no detrimental effects on its expression. It has been previously noted that insertions into the promoter region can result in overexpression of the downstream gene. It would therefore be interesting to conduct additional analysis on these lines to determine whether they express *SNAP33* differently than WT-1, as these lines could be

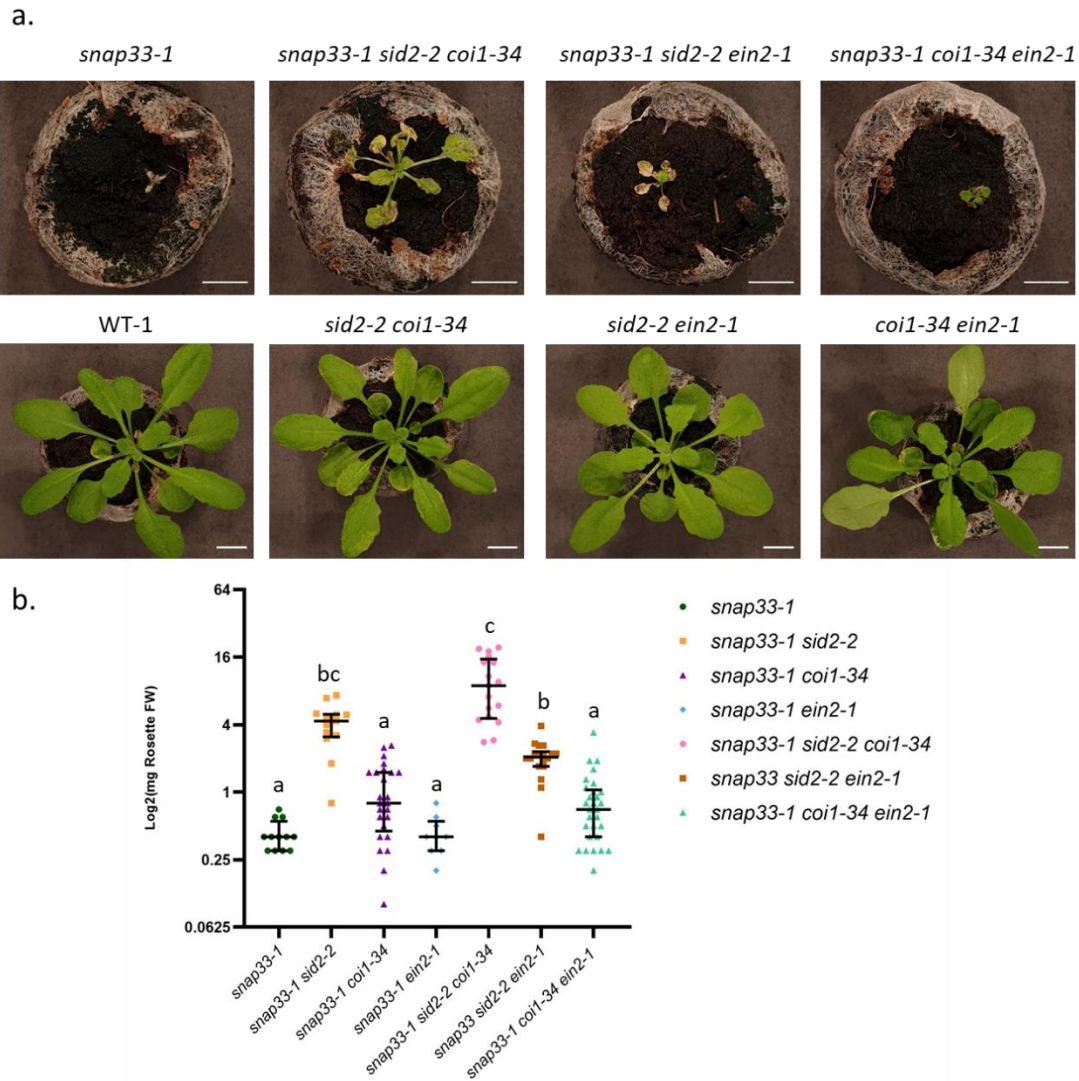


Figure 2.17. Morphological phenotypes of WT-1, *snap33-1*, *snap33-1 sid2-2 coi1-34*, *snap33-1 sid2-2 ein2-1*, *snap33-1 coi1-34 ein2-1*, *sid2-2 coi1-34*, *sid2-2 ein2-1*, and *coi1-34 ein2-1*. **a.** Representative pictures of 35-day-old soil-grown plants. Scale bars represent 1 cm. **b.** Biomass of aerial parts of the analyzed genotypes. Plotted values are the Log₂ of rosette fresh weight (FW) with WT-1, *snap33-1*, *snap33-1 sid2-2 coi1-34*, *snap33-1 sid2-2 ein2-1*, *snap33-1 coi1-34 ein2-1*, *sid2-2 coi1-34*, *sid2-2 ein2-1*, and *coi1-34 ein2-1* average weight are 243.5 mg (n=14), 0.4 mg (n=12), 9.9 mg (n=17), 2 mg (n=18), and 0.8 mg (n=29), respectively. Bars indicate the median with interquartile range. Lowercase letters indicate statistical differences among groups ($P \leq 0.05$; Kruskal Wallis test, Benjamini Hochberg FDR). This figure is an extension of figure 2.15, the genotypes were generated and weighed at the same time. The data presented here are the results of one biological replicate and were generated from the same experiment presented in figure 2.15. Descriptive statistics and linear values of the represented genotypes, as well as the control genotypes *sid2-2 coi1-34*, *sid2-2 ein2-1*, and *coi1-34 ein2-1*, are provided in Supplementary data 1.

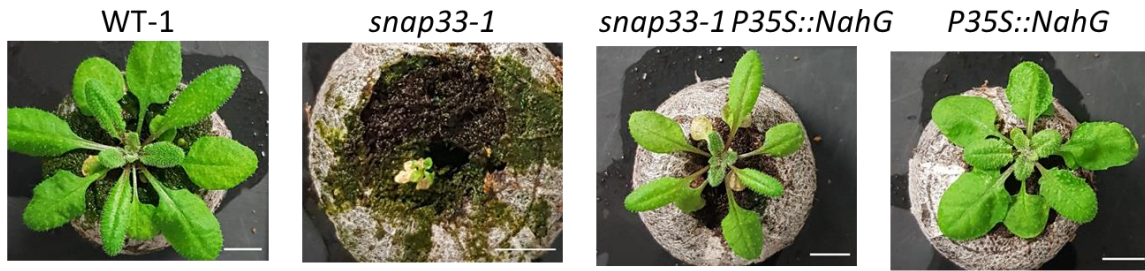
used for a variety of other purposes, including the analysis of the plant's resistance or susceptibility to multiple pathogens as a result of increased or decreased *SNAP33* expression.

1.7.1. *The phenotype of snap33 resembles that of several lesion-mimic mutants*

The characterization of *snap33-1*, *snap33-2*, and *snap33-3* phenotypes reveals that mutation of *SNAP33* leads to the development of spontaneous necrotic lesions, which coincide with dead cells and cells that accumulate H₂O₂ (figure 2.2). Additionally, transcriptomic analyses of *snap33-1* revealed an up-regulation of a substantial number of genes involved in stress responses at both 5 and 12 days of growth (figure 2.6.b). Several LMMs reported throughout the literature have also been shown to display spontaneous lesions (Bruggeman et al., 2015). Lesions vary among LMMs according to the mutated gene. Numerous mutants involved in photosynthetic processes have a lesion formation pattern dependent on light intensity or duration. For instance, mutations in the photorespiratory gene *catalase 2* (*CAT2*), which encodes a dismutase important in ROS homeostasis, resulted in an elevated cell death rate dependent on the photoperiod (Queval et al., 2007).

Mutations in genes involved in plant immunity resulted in a pattern of lesion appearance that varied according to the plant's developmental stage, which may indicate the gene's involvement in several functions at different developmental stages. For example, the *exo70b1* mutant develops spontaneous lesions after five weeks of growth (Zhao et al., 2015). The double mutant *syp121 syp122* develops severe necrotic lesions after 2-3 weeks of normal growth (Zhang et al., 2008), at a later stage compared to the *snap33* mutant, which develops lesions as early as 8-10 days of growth. Analyses of the 358 genes reported to be up-regulated by Zhang et al. in the two-week-old *syp121 syp122* double mutant (Zhang et al., 2008) revealed that 87% of these genes are also up-regulated in *snap33-1* (figure 2.24.a), which is unsurprising given *SYP121* and *SYP122*'s involvement in common processes with *SNAP33*, and given the fact that several mutants involved in the SA pathway and which partially revert the phenotype of *syp121 syp122*, such as *sid2* and *npr1*, also partially revert *snap33-1*'s phenotype. The presence of more up-regulated genes in the *snap33-1* mutant compared to the *syp121 syp122* mutant suggests that *SNAP33* performs more diverse functions in the plant. Yet, we cannot rule out other explanations inherent to the two studies, such as the growing conditions. Importantly, *SNAP33* is the sole *SNAP25/Qbc*-SNARE expressed in *Arabidopsis* leaves (Lipka et

a.



b.

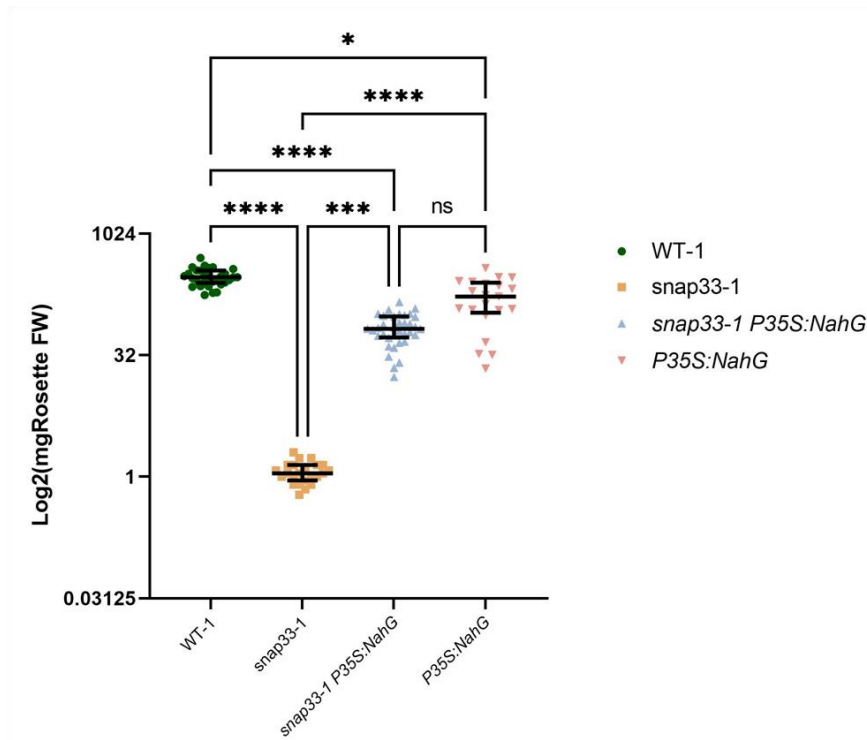


Figure 2.18. Morphological phenotypes of WT-1, *snap33-1*, *snap33-1 P35::NahG* and *P35::NahG*.

a. Representative pictures of 35-day-old soil-grown plants. Scale bars represent 1 cm. **b.** Biomass of aerial parts of the analyzed genotypes. Plotted values are the Log₂ of rosette fresh weight (FW) with WT-1, *snap33-1*, *snap33-1 P35::NahG* and *P35::NahG* average weight 300.7 mg (n=30), 1.152 mg (n=23), 70.71 mg (n=36), 170 mg (n=21), respectively. Bars indicate the median with interquartile range. Asterisks denote statistically significant differences in the Kruskal Wallis test (Benjamini Hochberg FDR), with one asterisk [*] indicates p-value<0.05, three asterisks [***] indicate p-value<0.001, and four asterisks [****] p-value<0.0001. Descriptive statistics and linear values are provided in Supplementary data 2.

al., 2007), suggesting that no other SNAP25/Qbc SNARE can compensate for its absence and explaining why its mutation is detrimental to the plant.

mpk4 is another LMM that exhibits constitutive cell death and ROS accumulation (Gao et al., 2008). The transcriptome of *mpk4* mutant reveals a substantial overlap with that of *snap33-1*, with 46% of genes up-regulated in the 13-day-old *mpk4* also up-regulated in the 12-day-old *snap33-1* (figure 2.24.b). The overlap between *snap33-1* and *mpk4* indicates that *snap33-1* mutation induces similar processes as those induced in the *mpk4* mutant. Additionally, Genevestigator analysis revealed that the *mkk1 mkk2* double mutant transcriptome displays similarity to that of 12-day-old *snap33-1* (figure 2.12.a), suggesting a possible functional link between the MEKK1-MKK1/MKK2-MPK4 module and SNAP33.

1.7.2. The SA sector is dominant in the *snap33* mutant

RNA-seq analyses of *snap33-1* mutant revealed that several genes involved in the SA and JA/ET pathways are significantly up-regulated in the *snap33-1* mutant as early as 5 days of growth (figure 2.7). Furthermore, SA, JA, and ET levels are higher in the *snap33-1* mutant compared to WT-1 at resting conditions, indicating that *snap33-1* constitutively accumulates these hormones (figure 2.14).

In light of these findings, we employed a targeted genetic approach by crossing *snap33-1* with known mutants affecting the SA, JA, and ET hormone pathways to determine whether these pathways are involved in *snap33-1*'s phenotype (Table 1). Our results indicate that the *snap33-1* phenotype mainly depends on the SA sector, as the *sid2-2* mutation partially reverted the phenotype of *snap33-1*, whereas *coi1-34* only slightly improved the phenotype of *snap33-1*, and no differences were found between the *snap33-1 ein2-1* double mutant and *snap33-1* (figure 2.15). Due to the antagonistic interaction between the SA and JA/ET pathways, it is expected that mutation of one hormonal pathway in *snap33-1* would result in enhanced signaling of the other. The detection of a higher level of *PDF1.2* expression in *snap33-1 sid2-2* compared to *snap33-1* (figure 2.16.c), which is probably related to a lower antagonistic effect of SA on the JA/ET branch, supports such hypothesis. As a result of the JA/ET pathways' antagonistic effects on SA being reduced in the *snap33-1 coi1-34* and *snap33-1 ein2-1* double mutants, it would be expected that the SA pathway would become more activated and might take over the suppressive effects that might be provided by the *coi1-34* and *ein2-1* mutations in *snap33-1* (preliminary RT-qPCR results on *snap33-1 coi1-34* and *snap33-1 ein2-1* indeed

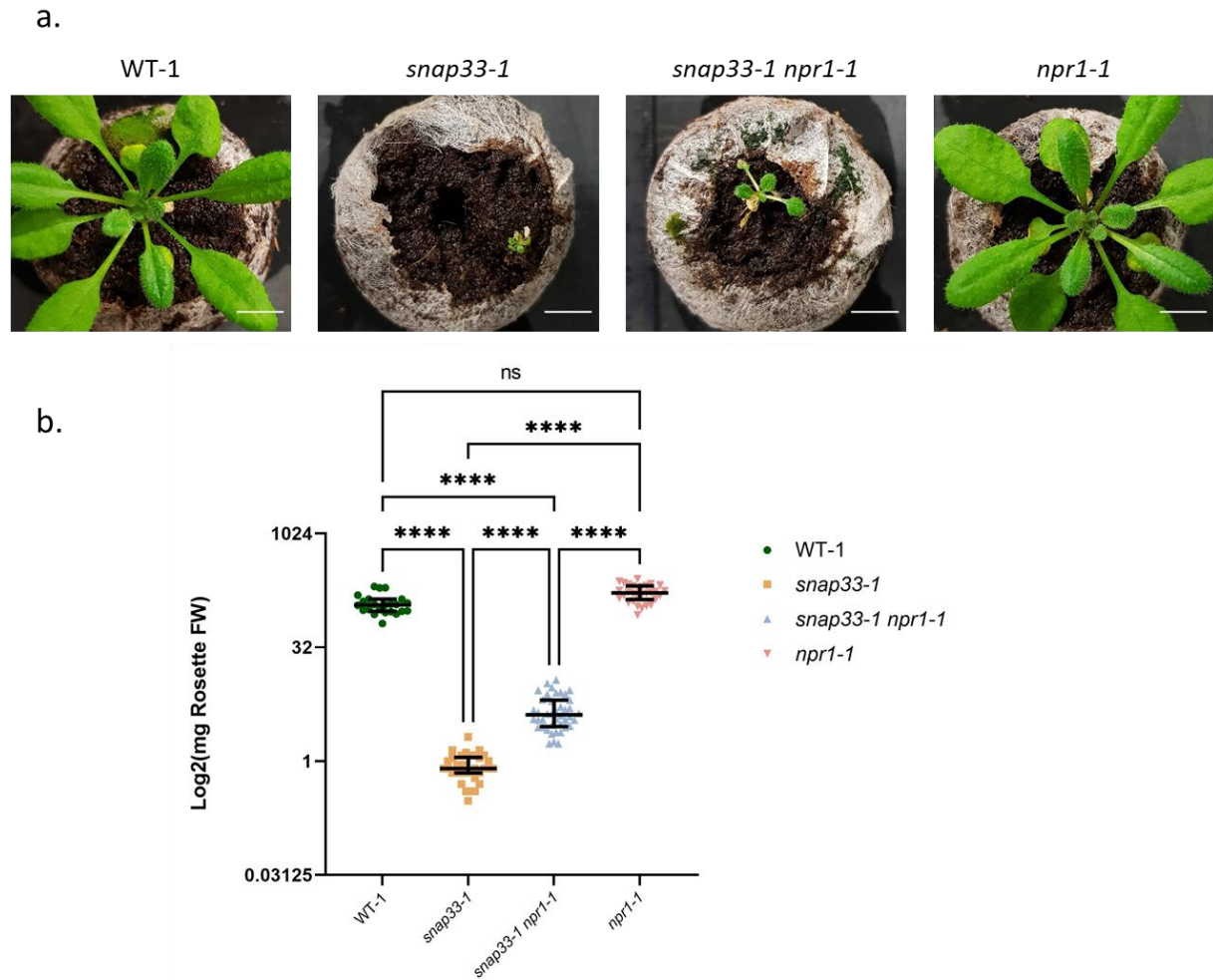


Figure 2.19. Morphological phenotypes of WT-1, *snap33-1*, *snap33-1 npr1-1* and *npr1-1*.

a. Representative pictures of 35-day-old soil-grown plants. Scale bars represent 1 cm. **b.** Biomass of aerial parts of the analyzed genotypes. Plotted values are the Log₂ of rosette fresh weight (FW) with WT-1, *snap33-1*, *snap33-1 npr1-1* and *npr1-1* average weight of 121,5 mg (n=23), 0,88 mg (n=34), 4,81 mg (n=42), and 169,7 mg (n=30), respectively. Bars indicate the median with interquartile range. Asterisks denote statistically significant differences in the Kruskal Wallis test (Benjamini Hochberg FDR), with four asterisks [****] P < 0.0001. Descriptive statistics and linear values are provided in Supplementary data 3.



Figure 2.20. Morphological phenotypes of WT-1, *snap33-1*, *snap33-1 fmo1-1*, and *fmo1-1*. Representative pictures of 21-day-old soil-grown plants. Scale bars represent 1 cm.

support this expectation). Indeed, we discovered that the *snap33-1 coi1-34 ein2-1* triple mutant does not vary morphologically from *snap33-1*, which supports such a hypothesis (figure 2.17). These results indicate that the SA dominates in *snap33-1*; in other words, the SA pathway might play a more important role in the phenotype of *snap33-1* than JA and ET, and JA/ET might contribute differently to the phenotype of *snap33*.

Furthermore, we discovered that *snap33-1* plants ectopically expressing *NahG* have a far healthier phenotype, with an almost WT-like morphology (figure 2.18). This finding demonstrates that SA accumulation is not solely dependent on ICS1/SID2 in the *snap33-1* mutant and suggests that in the triple mutants *snap33-1 sid2-2 coi1-34* and *snap33-1 sid2-2 ein2-1*, the remaining *SID2*-independent SA continues to have a significant effect on the plant that exceeds the suppression that might be provided by the simultaneous mutations of *SID2* and *COI1* or *SID2* and *EIN2*. Previous studies reported that the *P35S::NahG* line is unable to accumulate ET in response to pathogens (Heck et al., 2003). Therefore, it would be interesting to validate such observations in the *snap33-1 P35S::NahG* line as this implies that *P35S::NahG* suppresses not only the SA accumulation in *snap33-1* but also ET. Crossing *snap33-1 P35S::NahG* with *coi1-34* will help determine whether the JA pathway contributes to the phenotype of *snap33-1* and reverts *snap33-1 P35S::NahG*'s phenotype to WT-like levels.

1.7.3. *snap33* mutants mimic ETI responses

The *snap33-1* mutant displays several traits of ETI

RNA-seq analysis revealed that mutation of *SNAP33* induces the expression of a high number of genes involved in defense responses (figures 2.6, 2.8 to 2.10). The results of GO analysis revealed an enrichment of GO categories associated with the biotic stress response (figure 2.7). Additionally, we found an up-regulation of R protein signaling components in *snap33-1* and an abundance of up-regulated NLR genes at 12 days of growth (Supplementary Table 3). Constitutive SA accumulation, H₂O₂ accumulation, and cell death are all markers of an ETI response. We also found an over-accumulation of MPK3, MPK4, and MPK6 in the *snap33-1* mutant, which might also be associated with an ETI-like response (figure 2.3). Indeed, in the recent studies of Ngou et al. and Yuan et al. (also mentioned in the introduction section 1.2.6), the authors showed that inducing an ETI alone, without activating a PTI, by expressing Avr proteins under an inducible promoter in WT plants, leads to up-regulation of PTI components including *MPK3*, *MPK6*, and *RBOHD* as well as an accumulation of their corresponding proteins

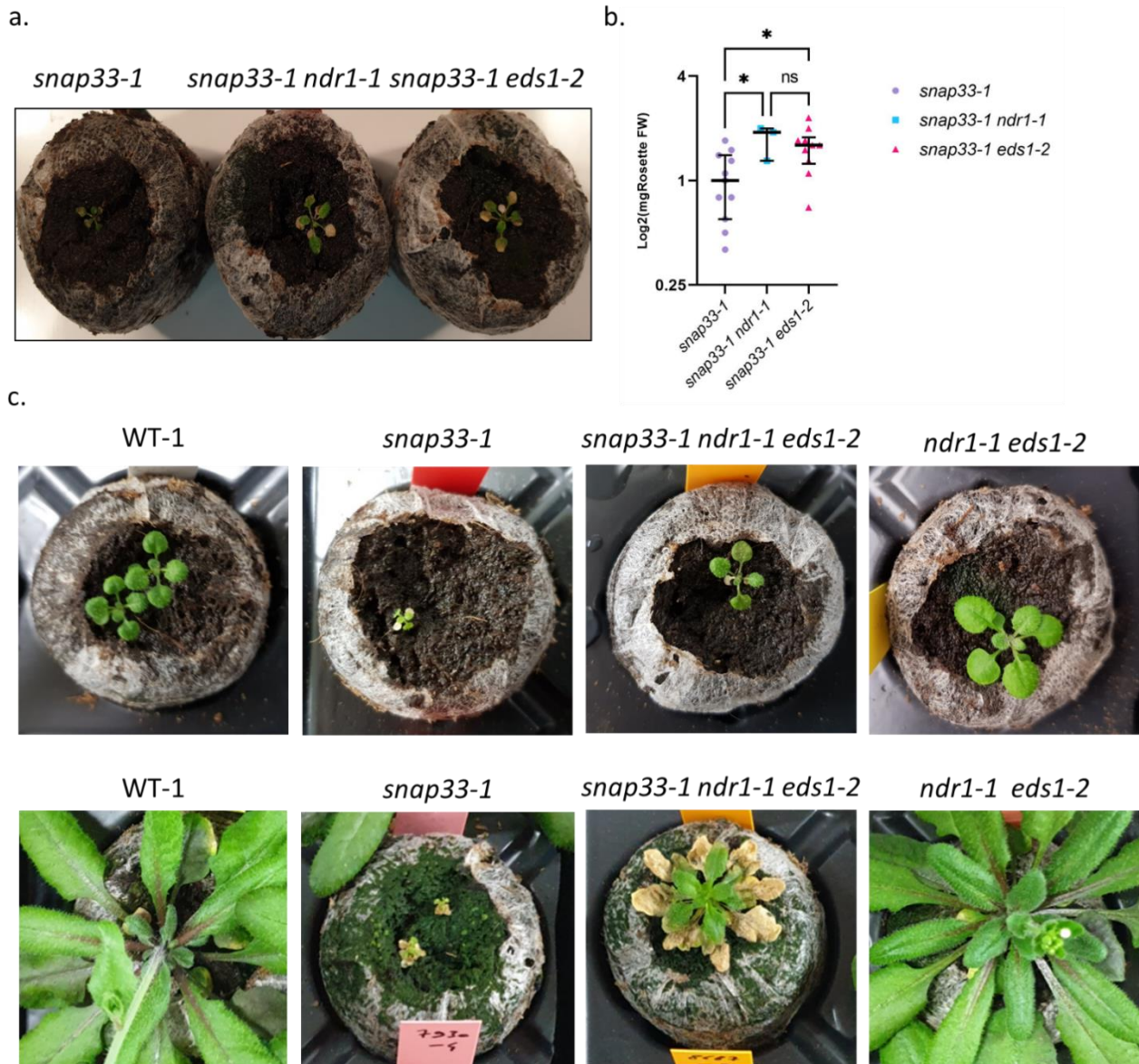


Figure 2.21. Morphological phenotypes of WT-1, *snap33-1*, *snap33-1 ndr1-1*, *snap33-1 eds1-2*, *snap33-1 ndr1-1 eds1-2*, and *ndr1-1 eds1-2*. **a.** Representative pictures of 24-day-old soil-grown *snap33-1*, *snap33-1 ndr1-1* and *snap33-1 eds1-2* plants. **b.** Biomass of aerial parts of *snap33-1*, *snap33-1 ndr1-1* and *snap33-1 eds1-2* plants. Plotted values are the Log₂ of rosette fresh weight (FW), with *snap33-1*, *snap33-1 ndr1-1* and *snap33-1 eds1-2* average weight, respectively, of 1 mg (n=11), 1.7 mg (n=3), 1.55 mg (n=10). Bars indicate the median with interquartile range. Asterisks denote statistically significant differences in the Kruskal Wallis test (Benjamini Hochberg FDR), with one asterisk [*] indicates p-value<0.05. **c.** Representative pictures of 20-day-old (upper panel) and 46-day-old (lower panel) soil-grown WT-1, *snap33-1*, *snap33-1 ndr1-1 eds1-2*, and *ndr1-1 eds1-2* plants. Descriptive statistics and linear values are provided in Supplementary data 4.

(Ngou et al., 2021; Yuan et al., 2021). The authors concluded that during infection with avirulent pathogens, effector recognition increases the abundance of PTI components to compensate for pathogen manipulation/perturbations and to promote the PTI response, and generate an efficient ETI (Ngou et al., 2021). Therefore, the accumulation of MAPKs, as well as several other defense genes, both at the transcript and protein levels, indicates that there is a state of ETI priming in *snap33-1* which resembles that of the induction of ETI alone described by Ngou et al. (2021). Moreover, a comparison of genes up-regulated in *snap33-1* at 12 days and the 2197 AvrRps4 effector-induced genes reported in the study of Ngou et al., (2021), showed an overlap of 948 genes (figure 2.25), and we found that *snap33-1*'s transcriptome resembles that of plant overexpressing the NLR RPS4 (figure 2.12) (Heidrich et al., 2013), overall indicating that *SNAP33* mutation induces similar processes as those induced during ETI.

As previously reported, JA is highly accumulating in the *snap33-1* mutant. JA is generally antagonistic to SA but was also found to positively contribute to a robust ETI (Tsuda et al., 2009). Spoel and colleagues showed that infections with *Pseudomonas syringae* DC3000 carrying the avirulence protein AvrRpt2, which induces a hypersensitive response, induced a 4-fold increase in JA levels (Spoel et al., 2003). Moreover, synergistic interactions have been found between the two pathways during ETI where the SA-responsive genes NPR3 and NPR4 activate the JA signaling pathway by promoting the degradation of JAZ proteins (Liu et al., 2017). It was proposed that plants employ such synergistic interaction to avoid inducing susceptibility to necrotrophs around cells undergoing an HR/PCD during ETI (Liu et al., 2017).

Interestingly, in a more recent study, Betsuyaku and colleagues showed that SA and JA do not signal in the same cells during ETI. Using a live-imaging strategy, they showed that the PR1 SA-marker protein accumulates in *Pseudomonas syringae* DC3000 AvrRpt2-infected cells undergoing a HR, whereas the VSP1 JA marker accumulates in areas surrounding the dead cells (Betsuyaku et al., 2018). The authors concluded that the induction of JA signaling around HR-undergoing cells is employed as a strategy to protect the living cells from secondary infections by necrotrophic pathogens (which thrive on dead tissues). Based on these findings, such processes might explain what happens in the *snap33-1* mutant, where SA generation is triggered by the absence of *SNAP33* and crosses a threshold at some point during growth, causing HR-like cell death in many cells. The SA overabundance and ensuing cell death events may cause JA accumulation and signaling in surrounding cells in order to save the remaining

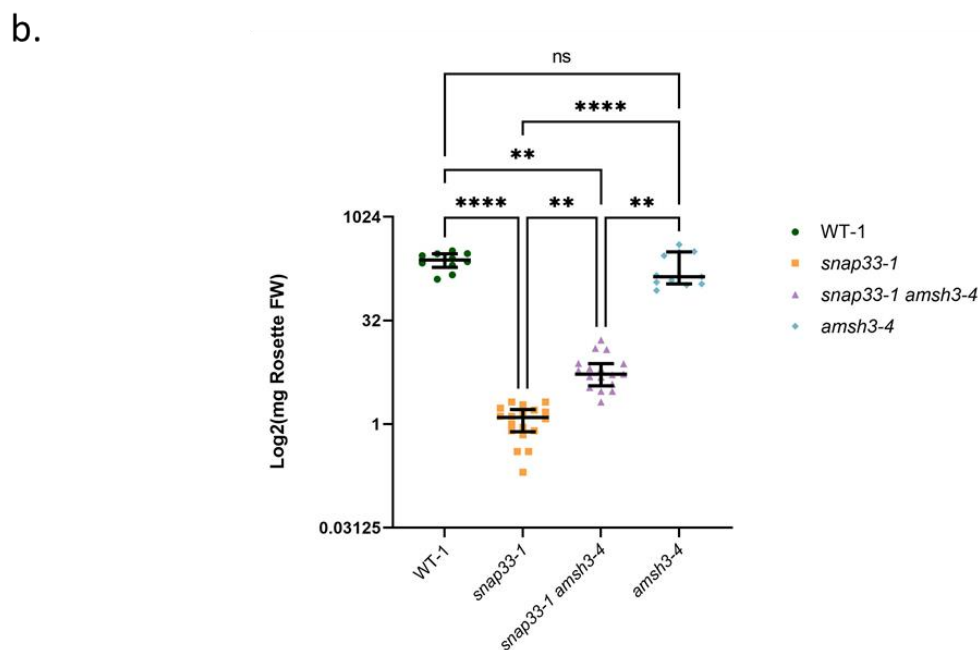


Figure 2.22. Morphological phenotypes of WT-1, *snap33-1*, *snap33-1 amsh3-4* and *amsh3-4*.

a. Representative pictures of 34-day-old soil-grown WT-1, *snap33-1*, *snap33-1 amsh3-4* and *amsh3-4* plants. Scale bars represent 1 cm. **b.** Biomass of aerial parts of WT-1, *snap33-1*, *snap33-1 amsh3-4* and *amsh3-4* plants. Plotted values are the Log₂ of rosette fresh weight (FW) with WT-1, *snap33-1*, *snap33-1 amsh3-4* and *amsh3-4* average weight, respectively, of 238.7 mg (n=10), 1.1 mg (n=18), 6.5 mg (n=17), and 194.8 mg (n=11). Bars indicate the median with interquartile range. Asterisks denote statistically significant differences in the Kruskal Wallis test (Benjamini Hochberg FDR), with two asterisks [**] indicate p-value<0.01, three asterisks [***] indicate p-value<0.001, and four asterisks [****] p-value<0.0001. Descriptive statistics and linear values are provided in Supplementary data 5.

surviving cells. Because SNAP33 is missing in all cells and SA production spreads to distant cells via SAR mobile signals, such as NHP and MeSA, SA accumulates in all cells, and an HR-like response spreads to the whole plant, causing it to collapse.

Is SNAP33 a guarded protein?

Further evidence hinting to an ETI-like response in the *snap33-1* mutant is the partial suppression by *amsh3-4* and *ndr1-1 eds1-2*, which also indicates that several NLRs might contribute to the phenotype of *snap33-1*, some of which might not use the canonical EDS1- and NDR1-signaling pathways. It has previously been reported that NLRs are transcriptionally up-regulated upon sensing effector perturbations, which leads to the up-regulation of additional NLRs via SA-responsive WRKYs in a positive feedback loop aiming at amplifying the defense response (Lai & Eulgem, 2018; Mohr et al., 2010; Zhang & Gassmann, 2007). We found that many *snap33-1*-induced NLRs were similarly induced in a transcriptomic analysis of SA-treated WT plants ((Liu et al., 2019); GSE34047), suggesting that in the *snap33-1* mutant, NLR-induced SA up-regulates several other NLRs to amplify immune responses (Supplementary Table 7). Among the up-regulated NLR genes in the transcriptome of *snap33-1* at 12 days, we found *ADR1* and *NRG1* helper NLRs members (Supplementary Table 3). Helper NLRs have been reported to induce SA accumulation (Roberts et al., 2013). Although helper NLRs were shown to be necessary for signaling downstream numerous NLRs, the mechanisms by which they are activated are unclear, and it has been proposed that helpers may be activated by detecting changes in other NLRs (Baggs et al., 2017). These findings imply that SNAP33 is a guarded protein and that sensor NLRs directly guarding SNAP33 activate helper *ADR1* and *NRG1* and other NLRs through SA to generate an ETI response. A similar process was described for the *bak1 bkk1* double mutant, which demonstrated an up-regulation of numerous NLRs, including the *ADR1* family members, mutations of which completely suppressed the *bak1 bkk1* LMM phenotype (Wu et al., 2020).

Are MAPKs active in *snap33-1*?

Recently, a study by our lab, currently under revision, showed that two TNL genes (AT4G11170 and AT3G04220) are specifically up-regulated by transient and sustained MPK3 activation, during PTI and ETI, respectively, in an *NDR1*- and *EDS1*-dependent manner (Lang et al., 2021). These genes were also found as significantly up-regulated in the transcriptome of *snap33-1* compared to WT-1 at 12 days (Supplementary Table 3). This finding suggests that in *snap33-*

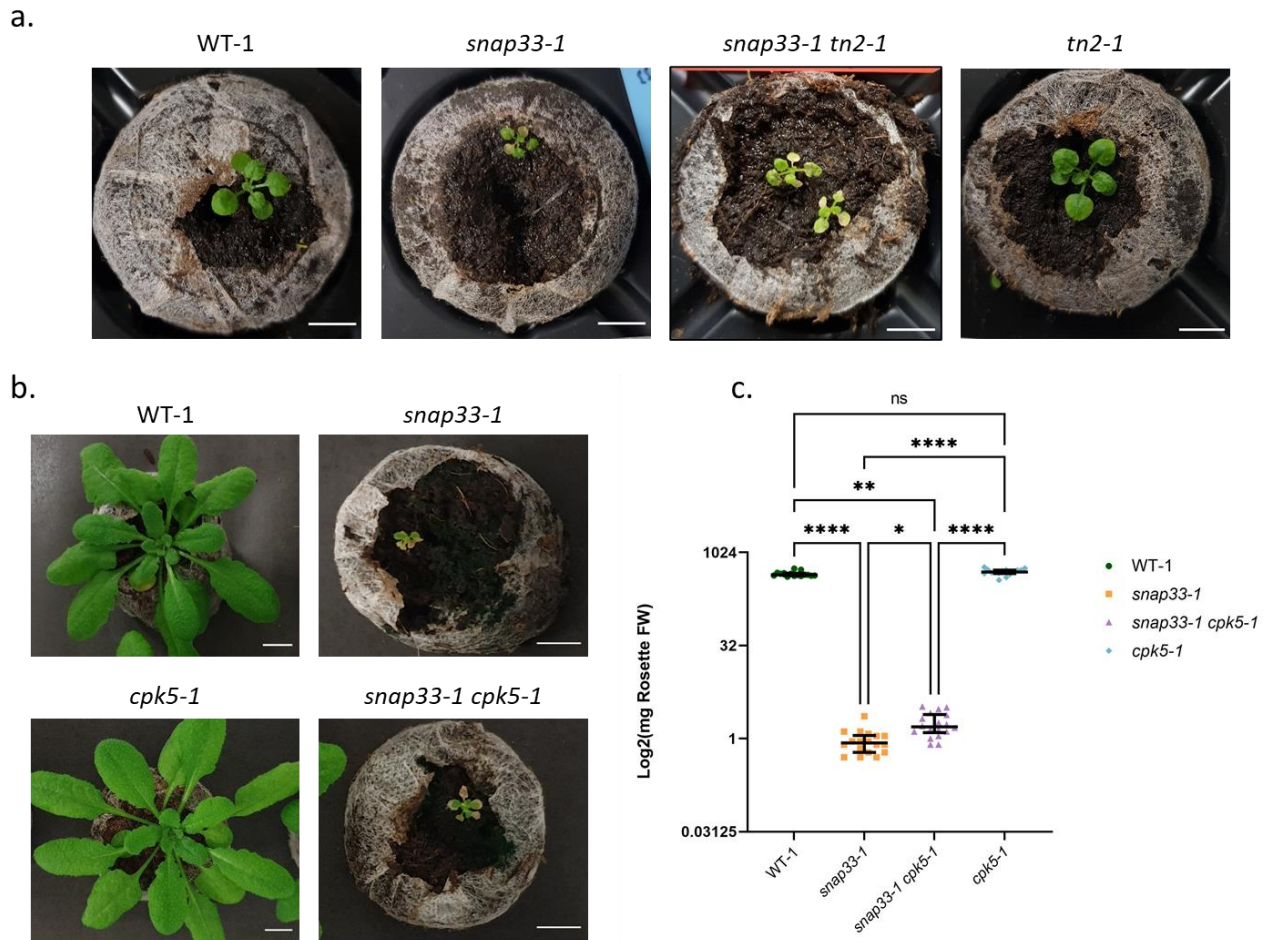


Figure 2.23. Morphological phenotypes of WT-1, *snap33-1*, *snap33-1 tn2-1*, *tn2-1*, *snap33-1 cpk5-1* and *cpk5-1*. **a.** Representative pictures of 20-day-old soil-grown WT-1, *snap33-1*, *snap33-1 tn2-1* and *tn2-1* plants. Scale bars represent 1 cm. **b.** Representative pictures of 35-day-old soil-grown WT-1, *snap33-1*, *snap33-1 cpk5-1* and *cpk5-1* plants. Scale bars represent 1 cm. **c.** Biomass of aerial parts of WT-1, *snap33-1*, *snap33-1 cpk5-1* and *cpk5-1* plants. Plotted values are the Log₂ of rosette fresh weight (FW) with WT-1, *snap33-1*, *snap33-1 cpk5-1* and *cpk5-1* average weight, respectively, of 458.6 mg (n=15), 0.9 mg (n=18), 1.7 mg (n=18), and 495.7 mg (n=15). Bars indicate the median with interquartile range. Asterisks denote statistically significant differences in the Kruskal Wallis test (Benjamini Hochberg FDR), with one asterisk [*] indicate p-value<0.05, two asterisks [**] indicate p-value<0.01, and four asterisks [****] P-value<0.0001. Descriptive statistics and linear values are provided in Supplementary data 6.

1, the two R genes AT4G11170 and AT3G04220 are up-regulated in response to an SA-dependent MPK3 activation. However, our results (Results section 1.3) show that at resting conditions, the MAPKs MPK3, MPK4, and MPK6 are not constitutively active in *snap33-1* yet constitutively over-accumulating. These findings suggest that, in the *snap33* mutants, there might be a basal activity of MPK3, and possibly MPK4 and MPK6 too, which leads to the up-regulation of the TNLs AT4G11170 and AT3G04220, as well as eventually to ET biosynthesis by phosphorylation of ACS2 and ACS6 proteins, as previously reported by Han et al., (2010) and Ren et al., (2008). Indeed, Guan et al. showed that ET biosynthesis is potentiated by an SA treatment in a MAPK-dependent way during ETI (Guan et al., 2015b). Therefore, we hypothesize that MPK3, MPK4, and MPK6 might be active in some cells, probably those undergoing SA accumulation and cell death, and thus could not be detected by the anti-pTpY immunoblotting on whole plants. It would thus be interesting to investigate in more depth the activity of these MAPKs in *snap33-1* using a more sensitive approach, such as a radioactive kinase assay, by purification of MPK3, MPK4, and MPK6 from *snap33-1* at later stages when the HR spreads to the whole plant. It would also be interesting to cross *snap33-1* with the *mpk3 mpk6 proMPK6::MPK6^{YG}* line (Su et al., 2017) (described in the introduction section 2.1) to investigate whether the expression of the R genes AT4G11170 and AT3G04220 is still occurring in the absence of MPK3 and MPK6, and to more globally assess the dependence of *snap33-1*'s phenotype on MPK3 and MPK6. Additionally, it would be interesting to confirm the MAPK over-accumulation's dependency on SA. This may be accomplished by analyzing the protein levels of MPK3, MPK4, and MPK6 in the *snap33-1 P35S::NahG* line, in which the SA is completely eliminated.

Working model for the mechanisms occurring in the *snap33-1* mutant

Based on my main results and the hypotheses stated above, a working model is presented in figure 2.26 in which we hypothesize that SNAP33 or its function is guarded by at least two sensor NLR proteins that use the canonical and the non-canonical NDR1-EDS1 signaling route. The sensor NLRs induce the activation of EDS1 and NDR1, as well as ADR1 and NRG1 helper NLRs. EDS1 and NDR1, and helper NLRs induce an SA accumulation and signaling via SID2 and other pathways (ICS2/PAL). The helper proteins have also been shown to oligomerize and form PM channels that induce a calcium influx required for cell death induction (Jacob et al., 2021). Since there is an up-regulation of helper NLRs in *snap33-1* (Supplementary Table 3), we

Table 1. Summary of the genotypes generated with *snap33-1*, with a brief description of their phenotype.

Genotype	Function#	Rosette weight ratio*	Lesion suppression
<i>snap33-1</i>	-	-	-
<i>snap33-1 sid2-2</i>	SA biosynthesis	~10	delayed
<i>snap33-1 coi1-34</i>	JA signaling	~2.5	no
<i>snap33-1 ein2-1</i>	ET signaling	~1	no
<i>snap33-1 sid2-2 coi1-34</i>	SA, JA	~23	no
<i>snap33-1 sid2-2 ein2-1</i>	SA, ET	~5	no
<i>snap33-1 coi1-34 ein2-1</i>	JA, ET	~2	no
<i>snap33-1 P35S::NahG</i>	SA accumulation	~62	delayed ¹
<i>snap33-1 npr1-1</i>	SA signaling	~5.5	no
<i>snap33-1 ndr1-1</i>	CNLs signaling	~2	no
<i>snap33-1 eds1-2</i>	TNLs signaling	~2	no
<i>snap33-1 ndr1-1 eds1-2</i>	NLRs signaling	n.d	delayed
<i>snap33-1 amsh3-4</i>	NLRs stability Deubiquitinase: reverts <i>syp121 syp122</i>	~5.5	delayed
<i>snap33-1 tn2-1</i>	TIR-NBS2 reverts <i>exo70b1</i>	n.d	delayed
<i>snap33-1 cpk5-1</i>	Calcium signaling, partially reverts <i>exo70b1</i>	~2	no

n.d: Not done

#: Brief description of the function of the corresponding proteins, except for SNAP33, which is not indicated

*: Mean of rosette weight of the genotype/mean of rosette weight of *snap33-1* (see detailed culture conditions in the manuscript)

¹: Rosette lesions are macroscopically suppressed in *snap33-1 P35S::NahG*, but cotyledons are still showing lesions

hypothesize that they might initiate a calcium influx in *snap33-1*. The calcium influx activates several proteins in *snap33-1*, including CDPKs, which will promote ROS accumulation by activating the RBOHD protein. CDPKs might promote the up-regulation of other NLRs by targeting WRKY TFs. Indeed, NLR promoters were found to be enriched in WRKY binding motifs (Mohr et al., 2010). Therefore, it is conceivable that CDPKs cause the up-regulation of NLRs in *snap33-1* via WRKY TFs, particularly considering our finding that *CPK5* mutation partially reverts the *snap33-1* phenotype (figure 2.23). CaMs are also activated by Ca^{2+} and might initiate an SA accumulation by binding to CBP60g, one of the key TFs which induces the expression of *SID2/ICS1*. CBP60g has also been reported to activate NHP accumulation. Therefore, SA and NHP might travel to distant cells to initiate a SAR and SA accumulation in distal tissues (figure 2.26).

SA accumulation further amplifies the immune responses by activating the expression of other NLRs, possibly via TFs too. SA also activates SA-responsive genes such as NPR1, NPR3, and NPR4, among which NPR3 and NPR4 activate JA signaling by promoting the degradation of JAZ proteins. SA also leads to the accumulation of MAPKs, which might become active at some point and trigger the biosynthesis of ET by stabilizing the ACS ET biosynthetic enzymes. All these mechanisms occur in *snap33-1* in many cells and, at some point, all leave areas end up dead due to an over-induction of immune responses. As mentioned earlier, a JA accumulation might be induced in cells surrounding the HR, possibly via SAR signals (like MeSA or NHP), but the SA effect ends up dominating and leads to the spread of HR in the whole plant.

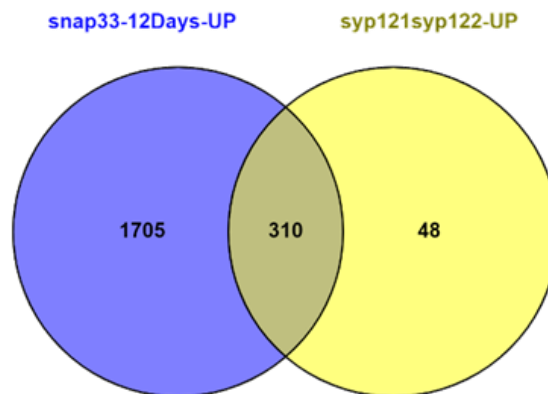
1.7.4. *Is the snap33 phenotype only related to auto-immunity?*

Is the phenotype of *snap33-1* associated with developmental defects?

Because SNAP33 is involved in other processes besides immunity, such as cytokinesis (Heese et al., 2001; Kasmi et al., 2013), and because it belongs to the SNARE protein family, which has a wide range of functions in plants, including cell expansion and growth (Campanoni & Blatt, 2007), one might hypothesize that the phenotype of *snap33-1* is also related to developmental defects.

In fact, mutation of *SYP121/PEN1*, the SNARE partner of SNAP33, leads to abnormal cell wall structures (Assaad et al., 2004), and Waghmare and colleagues showed that *PEN1/SYP121* is involved in the secretion of proteins involved in cell wall modification (Waghmare et al., 2018). *SYP121/PEN1*, *SNAP33*, and *VAMP721/722* are also involved in K^+ channel delivery to the PM

a.



b.

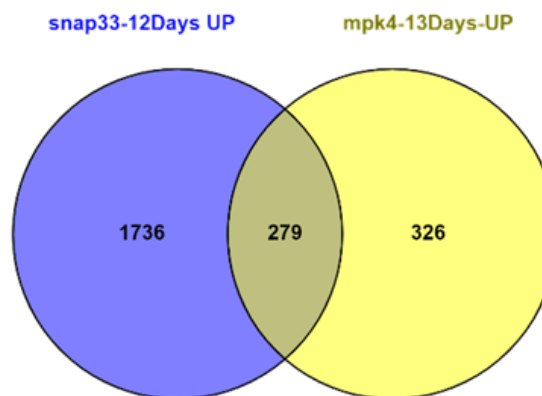


Figure 2.24. *snap33-1*'s transcriptome displays similarity to other lesion-mimic mutants.

a. Venn diagram showing the overlap between up-regulated genes in 12-day-old *snap33-1* vs. WT-1, and up-regulated genes in the *syp121 syp122* double mutant (Zhang et al., 2008) **b.** Venn diagram showing the overlap between up-regulated genes in 12-day-old *snap33-1* vs. WT-1, and up-regulated genes in *mpk4* mutant (Frei dit Frey et al., 2014).

and gating to regulate cell expansion (Lefoulon et al., 2018; Waghmare et al., 2019). VAMP721 and VAMP722 have also been reported to be important in maintaining growth during immunity (Yun et al., 2013). A recent study by Zhang and colleagues showed that VAMP721 and VAMP722 are required for appropriate post-Golgi trafficking of auxin transporters (Zhang et al., 2021). In fact, the *vamp721 vamp722* double mutant exhibits multiple growth defects and shows an altered distribution of auxin transporters (Zhang et al., 2021).

These findings, together with the fact that some down-regulated genes found in *snap33-1* transcriptome are involved in cell wall biogenesis and brassinosteroid homeostasis coupled with the observation of abnormal root phenotype of *snap33-1* (preliminary results in Supplementary figure 2), suggest that *snap33-1*'s phenotype might also be related to developmental defects, especially since SNAP33 is involved in cytokinesis in root tips (Heese et al., 2001). Therefore, it would be interesting to see whether *snap33-1 P35::NahG* displays developmental defects, especially in the roots, to conclude whether SNAP33 is essential for plant growth.

Is the phenotype of *snap33-1* associated with altered oxygen uptake?

Because the GO term "response to hypoxia" was considerably enriched in the analyses of *snap33-1*'s transcriptome (figure 2.7), we wondered whether, in the *snap33-1* mutant, there might be an altered oxygen uptake. Hypoxia in plants is caused by a decrease in oxygen availability as a result of severe environmental conditions, such as flooding events that result in waterlogging or a state of submergence, or due to a transitory increase in oxygen consumption in plant tissues (Loreti & Perata, 2020). Analyses of the enriched genes in the GO term "response to hypoxia" (Supplementary Table 8) show that some genes up-regulated in *snap33-1* are clearly related to response to hypoxia, such as *ERF71* (AT2G47520), *HUP54* (AT4G27450), *HUP26* (AT3G10020) and *NAC102* (AT5G63790) (Supplementary Table 8). However, many genes enriched in the GO hypoxia are also more generally related to biotic stress, such as *RBOHD*, *CBP60g*, *PBS3*, and *FMO1*. Interestingly, GO analyses (with the same tool used for *snap33-1*) of the up-regulated genes reported by Ngou et al. on plants expressing *AvrRps4* (Ngou et al., 2021) shows that "cellular response to hypoxia" is also significantly enriched (figure 2.25.b). Therefore, hypoxia in *snap33-1* might be a general response induced by defense gene induction, maybe related to ROS over-accumulation, which decreases the amount of oxygen necessary to the other oxygen-dependent functions of the plant.

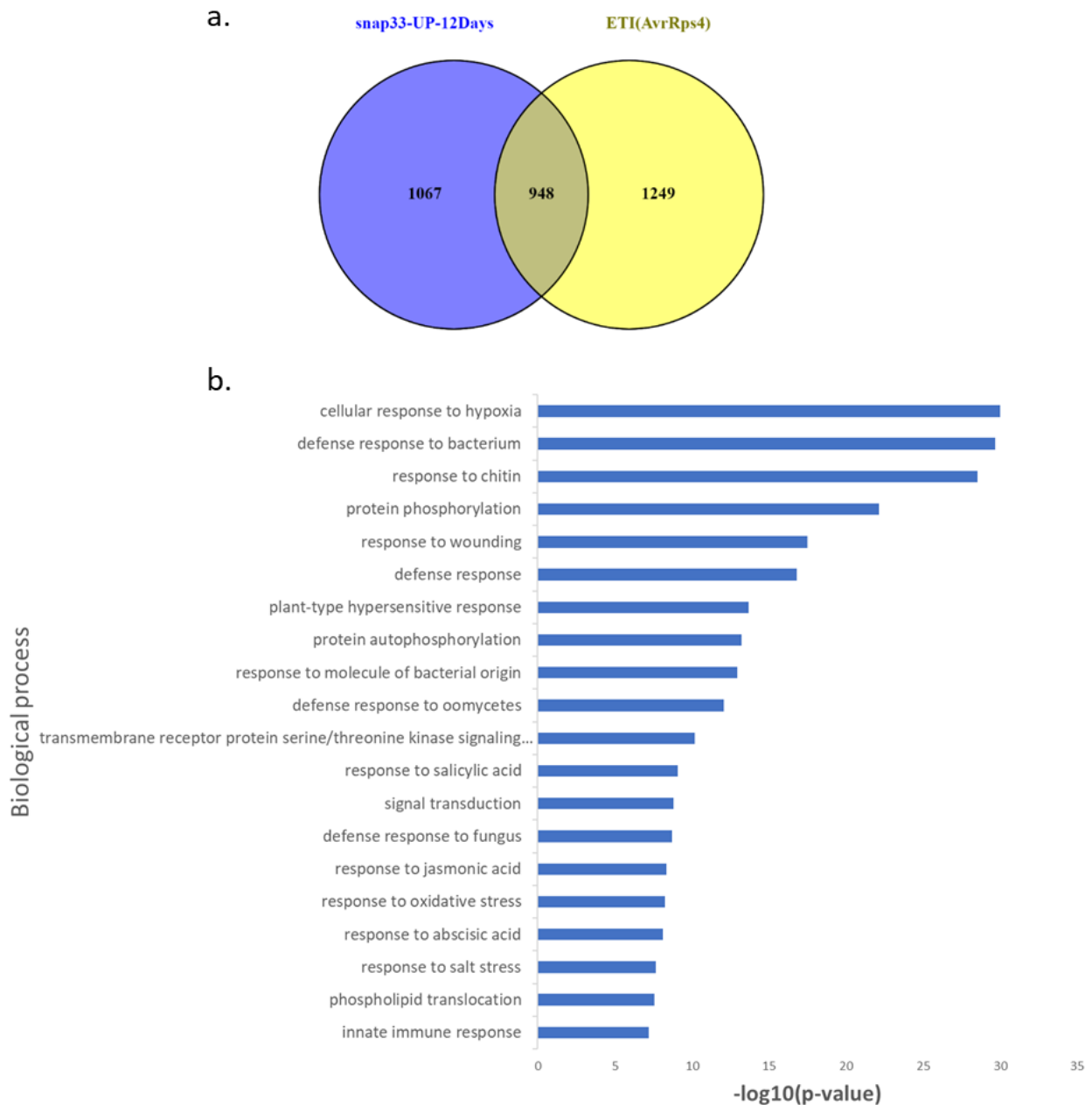


Figure 2.25. a. *snap33-1*'s transcriptome displays similarity to an ETI-response transcriptome. Venn diagram showing the overlap between up-regulated genes in 12-day-old *snap33-1* vs. WT-1, and up-regulated genes in the transgenic lines expressing AvrRps4 under the control of an inducible promoter, described in Ngou et al. (2021). **b.** Diagram showing the results obtained from the GO enrichment analyses of AvrRps4 expressing lines reported by Ngou et al., (2021). The top 20 significant categories are represented on the vertical axis, and the horizontal axis represents the $-\log_{10}(\text{p-value})$ of the significant pathways. Greater $-\log_{10}(\text{p-value})$ scores correlate with increased statistical significance. The GO analyses were performed using the TopGo "elim" method (Alexa $\ddot{\text{A}}$ et al., 2006).

Is SNAP33 involved in chloroplast integrity and/or lipid transport?

Two independent studies by Kleffman et al. and Peltier et al., aiming at identifying chloroplast-associated proteins by cell fractionation analyses, found SNAP33 as associated with the plastid's envelope and in total chloroplast fractions, respectively (Kleffmann et al., 2004; Peltier et al., 2004). Despite the fact that no plastid/chloroplastic localization of SNAP33 has been documented using labeling experiments to date, these findings suggest that SNAP33 may play a role in chloroplasts. SNAP33 could thus be involved in delivering proteins and/or lipids to the chloroplast, and a lack of SNAP33 could result in a loss of homeostasis of the chloroplast. In fact, several LMMs reported in the literature were associated with altered chloroplast integrity or lipid metabolism (Bruggeman et al., 2015). For example, disruption of the FZO-like (FZL) protein, a membrane remodeling dynamin GTPase, with a crucial role in thylakoid and chloroplast morphology, induces alteration in chloroplast number, size, and shape (Landoni et al., 2013). As a result, the *fzl* mutant displays spontaneous cell death, and ROS and SA over-accumulation, showing that damages to the chloroplast membranes lead to a lesion-mimic phenotype (Landoni et al., 2013). A recent study also reported that altering the ratio of galactolipid MGDG :DGDG by mutation of *DGDG synthase 1 (DGD1)* leads to JA overproduction and changes in chloroplast shape (Yu et al., 2020). However, unlike the *snap33* mutant, LMMs with altered chloroplast metabolism usually exhibit a light-dependent phenotype that is aggravated by prolonged light exposure (*i.e.*, long day conditions). We found no phenotypic difference between *snap33* plants produced in short-day and *snap33* plants grown in long-day conditions (preliminary data not shown). Therefore, if the LMM phenotype of *snap33-1* is dependent on chloroplastic deregulation, it is more likely to be linked to chloroplast structural deregulations rather than light-dependent photosynthetic metabolism. Besides, because SNAP33 is involved in vesicular fusion, it is also plausible that it might play a role in lipid transport. Indeed, several LMMs have been associated with an altered sphingolipids' transport or metabolism. For instance, *accelerated cell-death 11 (acd11)*, mutated in a sphingosine transfer protein, shows a phenotype similar to the one described here for *snap33-1*. Indeed, *acd11* shows constitutive SA accumulation, up-regulation of SA- and SAR-markers *PR1*, *PR2*, *FMO1*, *EDS1*, and *PAD4*, and spontaneous cell death and ROS accumulation (Brodersen et al., 2002). Moreover, as reported for the *snap33-1* mutant, expression of *P35::NahG* in the *acd11* background led to a strong reversion of *acd11* phenotype, but no reversion was found by crossing *acd11* with *ein2-1* (Brodersen et al., 2002).

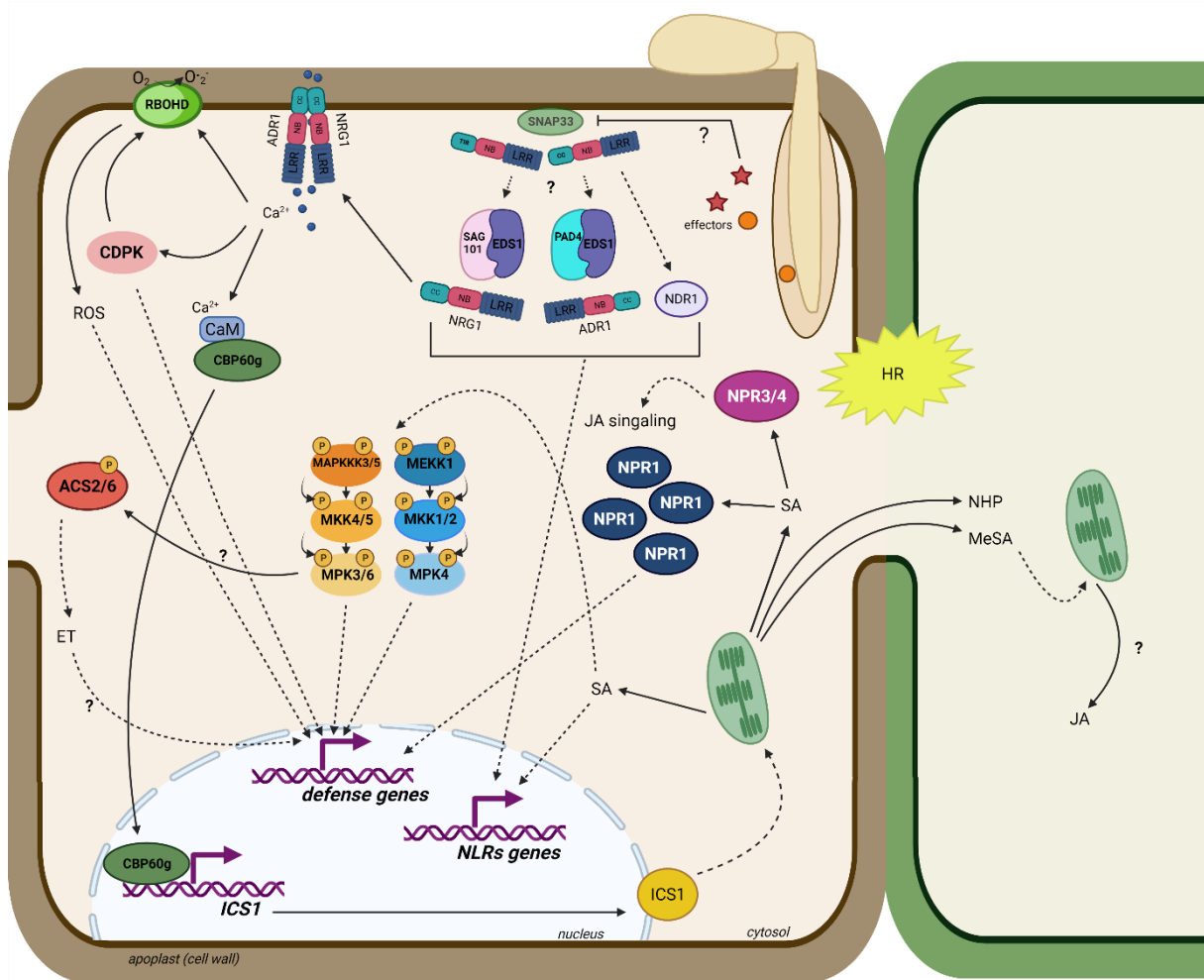


Figure 2.26. Working model for events occurring in the *snap33-1* mutant. SNAP33 is most likely a guarded protein, alteration of which results in the activation of defense responses initiated by guard NLR proteins. SA biosynthesis and signaling are activated by guard NLRs via EDS1 and NDR1, PAD4, SAG101, and helper NLRs (NRG1 and ADR1 proteins). ADR1 and NRG1 may also initiate a Ca^{2+} influx by forming calcium channels in the plasma membrane. Ca^{2+} will then drive ROS generation by modifying RBOHD and activating CDPKs, which contribute to ROS production via RBOHD phosphorylation. CDPKs may also be involved in the transcriptional misregulation of the *snap33-1* mutant and in the up-regulation of additional NLRs to amplify the defense responses. Calcium will also indirectly activate CaMs, which promote SA production by binding to CBP60g, the key TF involved in SA biosynthesis. SA overabundance promotes the upregulation of defense genes as well as their protein accumulation, among which the MAPKs MPK3, MPK4, and MPK6 were found to be overabundant in an SA-dependent manner. The overabundance of MAPKs may result in enhanced basal activity of these proteins, which might contribute to the upregulation of defense genes and ET production via ACS proteins. SA-responsive NPR1 proteins will also contribute to defense genes upregulation, and NPR3/4 may trigger JA signaling by inducing JAZ protein degradation. a SAR, SAR mobile signals, such as (continued)

Although investigating a possible role of SNAP33 in chloroplast or lipid metabolism may be difficult, a metabolomic study of the *snap33* mutant to determine whether PCD-inducing metabolites such as ceramides are over-accumulating in the *snap33-1* mutant, a closer look at the localization of SNAP33 in chloroplasts during resting and stressed conditions, and visualizing the structure of chloroplasts in the *snap33-1* mutant, might help to understand whether SNAP33 might have a function in chloroplasts or lipid metabolism.

1.8. Conclusion and perspectives

A working model based on our key findings is shown in figure 2.26. In this study, we found that the *snap33-1* mutant is a lesion-mimic mutant whose phenotype is mostly dependent on SA accumulation and several results strongly suggest that SNAP33 is a guarded protein, mutation of which induces an ETI-like response. Literature data show that SNAP33 is a PM localized protein involved in the delivery of proteins and probably cell wall components to the PM/ extracellular space/ apoplast (Waghmare et al., 2018; Wick et al., 2003). A major question remains regarding whether the *snap33-1* phenotype results from an imbalanced PM membrane homeostasis, which indirectly leads to the activation of immune responses, or whether SNAP33 is a target of pathogenic effectors and is a guarded protein whose disruption results in an ETI-like auto-immune phenotype. Said differently, is it SNAP33 itself which is guarded (whatever the mechanism) and whose absence leads to immunity, or is it its function whose disruption leads to immunity? To answer this question, a strategy could be to transform the *snap33* mutant with *SNAP33* mutant variants in which the SNARE function of SNAP33 would be impaired. Such mutations leading to the abrogation of the SNARE function were previously reported (Lagow et al., 2007; Ossig et al., 2000; Scales et al., 2001).

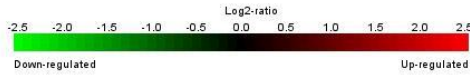
Another key approach, which has been applied for several LMMs, which might help understand further the molecular mechanisms underlying *snap33* phenotype, would be to screen without a priori for suppressors of the *snap33-1* phenotype. This strategy could yield novel suppressors that are directly involved in the development of immune responses downstream of SNAP33. This approach could be made via EMS mutagenesis of homozygous *snap33-1* seeds (produced at high temperatures as previously mentioned). This method, however, may be complicated by *snap33*'s severe phenotype and knowing that even the *sid2-2* mutation only results in a very partial phenotype reversion of *snap33-1*.

Figure 2.26. Working model for events occurring in the *snap33-1* mutant. Because SA accumulation causes NHP, will travel to distant cells to promote SA accumulation and signaling in distant tissues SA accumulation leads to a positive feedback loop of defense responses activation and to an HR that spreads to all cells, and the plant dies. As mentioned in the text, JA biosynthesis might occur in areas surrounding the cells undergoing an HR in order to protect these cells by antagonizing SA, but the dominant effect of SA leads to the spread of HR in all cells. Solid arrows indicate direct effects, while dashed arrows indicate indirect effects.

2. Studying the relationship between SNAP33 and the MEKK1-MKK2-MPK4 MAPK module

In the previous section, I reported the experiments we conducted to characterize the *snap33* mutant. *snap33* shares several characteristics with previously described lesion-mimic mutants, these characteristics include constitutive expression of a high number of defense-related genes. Our data suggest that SNAP33 is a guarded protein whose mutation causes constitutive activation of immune responses. I have reported that *snap33-1*'s 12-days transcriptome exhibits substantial overlap with that of the *mpk4* mutant (figure 2.24). Genevestigator analyses also indicated similar expression patterns with the transcriptome of the double mutant *mkk1 mkk2* (figure 2.12). Both SNAP33 and the MEKK1-MKK2-MPK4 MAPK module are involved in immunity, and analyses of their previously reported expression (Genevestigator) show that these proteins exhibit similar expression patterns in response to a variety of perturbations, including PAMPs, pathogen treatments, and mutations or overexpression of immune-related genes, as well as similar expression patterns during development (figure 3.1). *SNAP33*, *MEKK1*, *MKK2*, and *MPK4* also show a similar expression pattern during growth and in the different plant tissues or organs (figure 3.2). A previous study aiming at identifying proteins enriched in the plasma membrane in response to AvrRpt2 induced-expression (*i.e.*, during ETI) reported enrichment of both MPK4 and SNAP33 at the plasma membrane, suggesting that SNAP33 and MPK4 might function together during immunity (Elmore et al., 2012). Additionally, SNAP33 and MPK4 are both involved in cytokinesis as shown by similar localization of both proteins at the cell plate of dividing cells by the two independent studies of Heese et al. (2001) and Kosetsu et al. (2010), respectively, suggesting that SNAP33 and MPK4 might function together during cytokinesis. In an exploratory/preliminary high-throughput experiment by our group aiming at identifying proteins that interact with the MEKK1-MKK2-MPK4 MAPK module, at resting and stress conditions, SNAP33 was potentially found to bind to the three MAPKs (more details in section 2.1.2). In light of the literature data and our findings, we decided to report known SNAP33 interactions and post-translational modifications (PTMs) to investigate a putative relationship/link between SNAP33 and the MAPK module. Therefore, in the following sections, I will first report previous data from the literature on SNAP33's interactions and post-translational modifications, and preliminary results obtained in our laboratory. In the second

Dataset: 3240 perturbations from data selection: AT_AFFY_ATH1-6
 Showing 4 measure(s) of 4 gene(s) on selection: AT-13



80 of 3240 perturbations fulfilled the filter criteria

Filter values for selected measure(s)

Arabidopsis thaliana (80)	MEKK1	MKK2	MPK4	SNAP33	Piscore	Log2-ratio	Fold-Change	p-value
AT-00113 (6) cycloheximide / mock treated seedlings	Red	Red	Red	Red	5.94	2.72	6.66	0.007
AT-00211 (3) P. syringae pv. tomato study 6 (Ws-0) / mock-inoculated leaf samples (...)	Red	Red	Red	Red	4.91	2.15	4.43	0.005
AT-00684 (3) ozone study 4 (abi1td) / untreated rosette leaf samples (abi1td)	Red	Red	Red	Red	7.97	1.99	3.97	<0.001
AT-00202 (8) P. syringae pv. tomato study 9 (DC3118 Cor-) / mock inoculated leaf sa...	Red	Red	Red	Red	3.00	1.87	3.83	0.025
AT-00665 (7) shift 28°C to 19°C study 3 (35S:RPS4-HS) / 28°C (35S:RPS4-HS)	Red	Red	Red	Red	6.14	1.81	3.53	<0.001
AT-00665 (6) shift 28°C to 19°C study 2 (35S:RPS4-HS rrs1-11) / 28°C (35S:RPS4-H...	Red	Red	Red	Red	5.88	1.80	3.47	<0.001
AT-00665 (4) shift 28°C to 19°C study 2 (35S:RPS4-HS) / 28°C (35S:RPS4-HS)	Red	Red	Red	Red	7.09	1.79	3.47	<0.001
AT-00211 (1) P. syringae pv. tomato study 6 (eds1-1) / mock-inoculated leaf samples...	Red	Red	Red	Red	2.78	1.78	3.44	0.027
AT-00391 (3) flg22 + GA (1h) / untreated leaf disc samples (Ler)	Red	Red	Red	Red	3.38	1.78	3.15	0.012
AT-00665 (9) shift 28°C to 19°C study 3 (35S:RPS4-HS rrs1-11) / 28°C (35S:RPS4-H...	Red	Red	Red	Red	5.11	1.75	3.38	0.001
AT-00602 (3) cycloheximide study 4 (pBeaconRFP_GR-ABI3) / mock treated root prot...	Red	Red	Red	Red	4.18	1.75	3.24	0.004
AT-00211 (2) P. syringae pv. tomato study 6 (pad4-5) / mock-inoculated leaf samples...	Red	Red	Red	Red	3.09	1.73	3.30	0.016
AT-00391 (6) flg22 study 6 (Ler) / flg22 study 8 (1h)	Red	Red	Red	Red	4.28	1.72	3.26	0.003
AT-00258 (1) syringolin study 2 / solvent treated leaf samples (syl_404_bc2)	Red	Red	Red	Red	5.55	1.63	3.09	<0.001
AT-00391 (7) flg22 study 6 (Ler) / untreated leaf disc samples (Ler)	Red	Red	Red	Red	2.55	1.57	2.77	0.024
AT-00128 (4) EF-Tu (elf26) (60min) / untreated whole plant samples (Ler-0)	Red	Red	Red	Red	4.68	1.57	2.96	0.001
AT-00345 (1) high light study 4 (distal) / low light grown leaf samples	Red	Red	Red	Red	3.59	1.54	2.92	0.005
AT-00561 (2) antimycin A (rao1-1) / mock treated shoot samples (rao1-1)	Red	Red	Red	Red	5.84	1.46	2.75	<0.001
AT-00309 (1) B. graminis (ataf1-1) / non-infected rosette leaf samples	Red	Red	Red	Red	4.08	1.45	2.77	0.002
AT-00602 (2) cycloheximide / dexamethasone study 2 (pBeaconRFP_GR-ABI3) / mo...	Red	Red	Red	Red	3.07	1.45	2.63	0.008
AT-00319 (1) light/drought (aox1a(sall)) / untreated leaf samples (aox1a(sall))	Red	Red	Red	Red	3.02	1.45	2.71	0.008
AT-00120 (26) salt study 2 (late) / untreated root samples (late)	Red	Red	Red	Red	5.33	1.44	2.90	<0.001
AT-00681 (4) S. sclerotiorum study 2 (Col-0) / mock inoculated rosette leaf samples ...	Red	Red	Red	Red	3.96	1.41	2.65	0.002
AT-00391 (8) flg22 study 6 (penta) / untreated leaf disc samples (penta)	Red	Red	Red	Red	4.41	1.40	2.66	<0.001
AT-00392 (4) flg22 study 4 (35S:miR393) / untreated leaf disc samples (35S:miR393)	Red	Red	Red	Red	3.35	1.40	2.62	0.004
AT-00393 (4) P. syringae pv. tomato study 12 (sid2) / untreated leaf tissue samples (...)	Red	Red	Red	Red	2.84	1.39	2.61	0.009
AT-00681 (3) S. sclerotiorum study 2 (col1-2) / mock inoculated rosette leaf samples...	Red	Red	Red	Red	5.49	1.37	2.59	<0.001
AT-00202 (11) P. syringae pv. tomato study 10 (DC3000) / mock inoculated leaf sam...	Red	Red	Red	Red	2.83	1.37	2.62	0.008
AT-00561 (3) antimycin A (rao1-2) / mock treated shoot samples (rao1-2)	Red	Red	Red	Red	4.97	1.37	2.58	<0.001
AT-00392 (1) NAA + flg22 (1h) / untreated leaf disc samples (Col-0)	Red	Red	Red	Red	3.32	1.34	2.56	0.003
AT-00275 (3) hypoxia study 2 (late+recovery) / untreated seedlings (late)	Red	Red	Red	Red	4.26	1.33	2.52	<0.001
AT-00392 (5) flg22 study 4 (Col-0) / untreated leaf disc samples (Col-0)	Red	Red	Red	Red	2.91	1.32	2.52	0.006
AT-00406 (1) P. syringae pv. maculicola (Col-0) / mock treated leaf samples (Col-0)	Red	Red	Red	Red	4.90	1.31	2.47	<0.001
AT-00679 (1) RALF (30min) / mock treated seedling samples (30min)	Red	Red	Red	Red	5.21	1.30	2.46	<0.001
AT-00561 (1) antimycin A (AOX1a:LUC) / mock treated shoot samples (AOX1a:LUC)	Red	Red	Red	Red	4.73	1.30	2.46	<0.001
AT-00419 (2) drought study 6 (srk2cf) / untreated plant samples (srk2cf)	Red	Red	Red	Red	5.14	1.29	2.44	<0.001
AT-00403 (5) M6PR OX / Col-0 Hoagland solution watered M6PR OX leaf samples / ...	Red	Red	Red	Red	2.89	1.29	2.44	0.008
AT-00169 (1) chitin / mock treated seedlings	Red	Red	Red	Red	3.96	1.28	2.46	<0.001
AT-00419 (1) drought study 6 (Col-0) / untreated plant samples (Col-0)	Red	Red	Red	Red	4.98	1.24	2.37	<0.001
AT-00215 (6) 35S::amiR-white-2(MIR172a) / Col-0	Red	Red	Red	Red	2.85	1.24	2.36	0.005
AT-00309 (2) B. graminis (Col-0) / non-infected rosette leaf samples	Red	Red	Red	Red	3.63	1.21	2.31	0.001
AT-00398 (2) circadian clock (Ca2+)cyt / nicotinamide (53h) / circadian clock (Ca2+)c...	Red	Red	Red	Red	1.89	1.20	2.31	0.026
AT-00682 (1) low light + DBMIB (0.5h) / low light study 4 (6h)	Red	Red	Red	Red	4.72	1.18	2.27	<0.001
AT-00106 (17) P. syringae pv. tomato study 3 (DC3000) / mock inoculated leaf sampl...	Red	Red	Red	Red	1.91	1.15	2.17	0.021
AT-00392 (8) flg22 study 5 (Col-0) / untreated leaf disc samples (Col-0)	Red	Red	Red	Red	3.92	1.14	2.20	<0.001
AT-00391 (10) flg22 study 7 (Ler) / flg22 study 8 (2h)	Red	Red	Red	Red	1.51	1.14	2.32	0.047
AT-00532 (2) primisulfuron-methyl (24h) / mock treated leaf samples (24h)	Red	Red	Red	Red	1.76	1.13	2.12	0.028
AT-00392 (3) flg22 study 4 (35S:AFB1) / untreated leaf disc samples (35S:AFB1)	Red	Red	Red	Red	2.36	1.13	2.21	0.008
AT-00618 (4) high light study 7 (AtWRKY63 OE1) / untreated leaf samples (AtWRKY6...	Red	Red	Red	Red	4.28	1.13	2.18	<0.001
AT-00682 (2) low light + DBMIB (2h) / low light study 4 (6h)	Red	Red	Red	Red	4.51	1.13	2.18	<0.001
AT-00286 (7) iron deficiency study 2 (late) / mock treated root samples	Red	Red	Red	Red	1.93	1.12	2.19	0.019
AT-00345 (2) high light study 4 (exposed) / low light grown leaf samples	Red	Red	Red	Red	2.78	1.12	2.18	0.003
AT-00253 (2) flg22 study 2 (3h) / H2O treated Col-0 seedlings (3h)	Red	Red	Red	Red	1.58	1.11	2.29	0.038
AT-00398 (4) circadian clock (Ca2+)cyt / nicotinamide (61h) / circadian clock (Ca2+)c...	Red	Red	Red	Red	1.52	1.10	2.16	0.042
AT-00325 (2) syringolin study 3 (late) / solvent treated leaf samples (Col-0; late)	Red	Red	Red	Red	3.33	1.10	2.12	<0.001
AT-00215 (5) 35S::amiR-white-1(MIR172a) / Col-0	Red	Red	Red	Red	2.80	1.06	2.09	0.002
AT-00107 (8) HrpZ (4h) / H2O treated leaf samples (4h)	Red	Red	Red	Red	2.87	1.02	2.04	0.002
AT-00398 (3) circadian clock (Ca2+)cyt / nicotinamide (57h) / circadian clock (Ca2+)c...	Red	Red	Red	Red	1.66	1.01	2.03	0.023
AT-00664 (1) antimycin A study 2 (anac017-1) / mock treated shoot samples (anac0...	Red	Red	Red	Red	2.91	1.00	2.01	0.001
AT-00656 (16) salt / FACS study 3 (3h) / root endodermis and quiescent center proto...	Red	Red	Red	Red	3.10	1.00	2.01	<0.001
AT-00406 (20) pad4-1 / ein2 / P. syringae pv. maculicola (pad4) / P. syringae pv. mac...	Red	Red	Red	Red	1.94	-0.99	-2.01	0.011
AT-00515 (3) callus formation (48h) / untreated root samples	Red	Red	Red	Red	2.18	-1.02	-2.05	0.007
AT-00670 (2) cold study 22 (Col) / untreated rosette leaf samples (Col)	Red	Red	Red	Red	1.91	-1.04	-2.05	0.015
AT-00406 (18) pad4-1 / Col-0 / P. syringae pv. maculicola (pad4) / P. syringae pv. mac...	Red	Red	Red	Red	3.15	-1.07	-2.09	0.001
AT-00406 (19) pad4-1 / col1 / P. syringae pv. maculicola (pad4) / P. syringae pv. macu...	Red	Red	Red	Red	3.23	-1.09	-2.11	0.001
AT-00694 (9) two-cycle RNA labeling (root tip) / one-cycle RNA labeling (root tip)	Red	Red	Red	Red	3.03	-1.09	-2.13	0.002
AT-00490 (8) germination (24h) / stratification (48h)	Red	Red	Red	Red	3.77	-1.10	-2.15	<0.001
AT-00490 (3) germination (6h) / seed desiccation	Red	Red	Red	Red	2.75	-1.13	-2.20	0.004
AT-00694 (7) two-cycle RNA labeling (root elongation zone) / one-cycle RNA labeling ...	Red	Red	Red	Red	3.41	-1.18	-2.29	0.001
AT-00490 (5) germination (12h) / seed desiccation	Red	Red	Red	Red	3.33	-1.24	-2.38	0.002
AT-00081 (2) fls2-17 / Ler-0	Red	Red	Red	Red	2.34	-1.32	-2.49	0.017
AT-00202 (10) P. syringae pv. tomato study 9 (DC3118 Cor-hrpS) / P. syringae pv. to...	Red	Red	Red	Red	2.22	-1.36	-2.67	0.024
AT-00490 (10) germination (48h) / stratification (48h)	Red	Red	Red	Red	4.89	-1.43	-2.89	<0.001
AT-00286 (4) iron deficiency / protoplasting / iron deficiency study 8 (24h)	Red	Red	Red	Red	3.33	-1.51	-2.83	0.006
AT-00264 (2) rga-Δ17 / Ler-EV	Red	Red	Red	Red	4.19	-1.55	-2.92	0.002
AT-00665 (13) 35S:RPS4-HS eds1-2 / 35S:RPS4-HS [shift 28°C to 19°C study 3 (35...	Red	Red	Red	Red	4.42	-1.58	-2.99	0.002
AT-00490 (7) germination (24h) / seed desiccation	Red	Red	Red	Red	5.07	-1.58	-3.02	<0.001
AT-00211 (5) P. syringae pv. tomato study 7 (eds1-1) / P. syringae pv. tomato study 6 ...	Red	Red	Red	Red	2.40	-1.60	-3.05	0.032
AT-00665 (12) 35S:RPS4-HS eds1-2 / 35S:RPS4-HS [shift 28°C to 19°C study 2 (35...	Red	Red	Red	Red	7.03	-1.76	-3.39	<0.001
AT-00490 (9) germination (48h) / seed desiccation	Red	Red	Red	Red	6.34	-1.90	-3.77	<0.001

created with GENEVESTIGATOR

Figure 3.1. MEKK1, MKK2, MPK4, and SNAP33 expression in different perturbation studies (Genevestigator data).

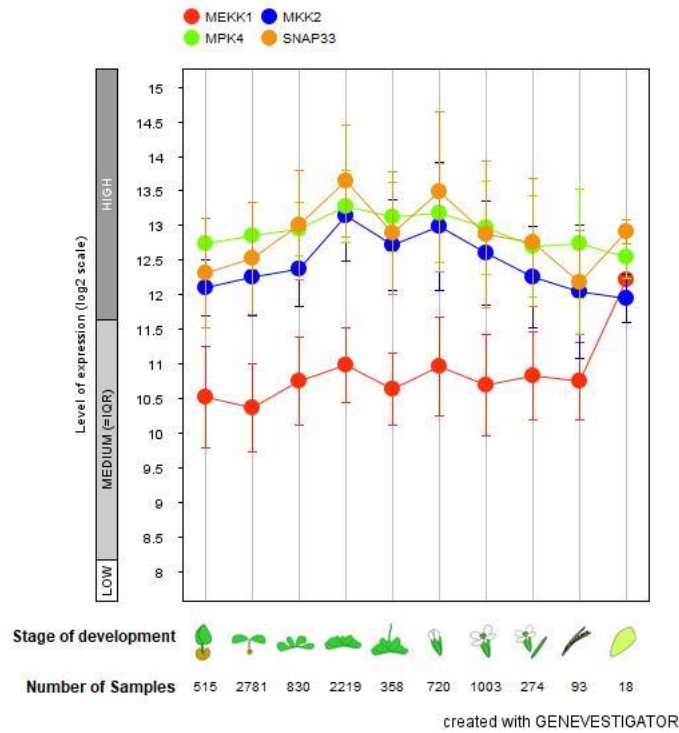
part, I will present the results we obtained from analyzing a putative relationship between SNAP33 and the MEKK1-MKK2-MPK4 MAPK module.

2.1. SNAP33 PTMs and interactions

2.1.1. *SNAP33 PTMs*

As depicted in figure 3.3.a, several phosphosites and two ubiquitination sites were identified on the SNAP33 protein, suggesting that PTMs regulate the activity, stability, localization, and/or interactions of SNAP33. S29 and S47 phosphorylation sites were very often identified in phosphoproteomic studies, including some aiming at identifying stress-induced phosphorylations (figure 3.3.b). For instance, S29 has been identified as a significantly phosphorylated residue in response to flg22 elicitation by the study of Benschop et al. (2007). In addition, the syntaxin partner of SNAP33, SYP121/PEN1, has also been reported to be phosphorylated in response to ABA in a lectin receptor-like kinase VI.4 (LECRK-VI.4-1) dependent way, showing that it is a putative substrate of LECRK-VI.4-1 (Zhang et al., 2019). Besides, SYP121/PEN1 was reported as a putative substrate of MPK3 and MPK6 by the phosphoproteomic study of Lassowskat et al. (2014). These data suggest that phosphorylation events regulate SNAREs and that MAPKs possibly contribute to this regulation. For instance, it is conceivable that the assembly of a SNARE complex and the specificity of the members involved are regulated by phosphorylation. In the SNAP33 protein's sequence, two phosphosites, namely S7 and S194, are compatible with the S/T-P MAPK phosphorylation motif (minimal MAPK motif). Interestingly, Wang and colleagues reported that S194 is phosphorylated in response to flg22 (Wang et al., 2020). S194 was also identified in the study of Umezawa et al. as showing an increased phosphorylation pattern in response to drought in one biological replicate but not in the other two replicates of the same study (Umezawa et al., 2013). Phosphorylation on S7 was identified in a study aimed at identifying targets of Clade E Growth-Regulating (EGR) Type 2C phosphatases during growth and in response to drought stress, but the phosphorylation of the S7 residue does not seem to depend on EGR activity or drought stress.

Dataset: 10 developmental stages from data selection: AT_AFFY_ATH1-6
 Showing 4 measure(s) of 4 gene(s) on selection: AT-13



Dataset: 127 anatomical parts from data selection: AT_AFFY_ATH1-6
 Showing 4 measure(s) of 4 gene(s) on selection: AT-13

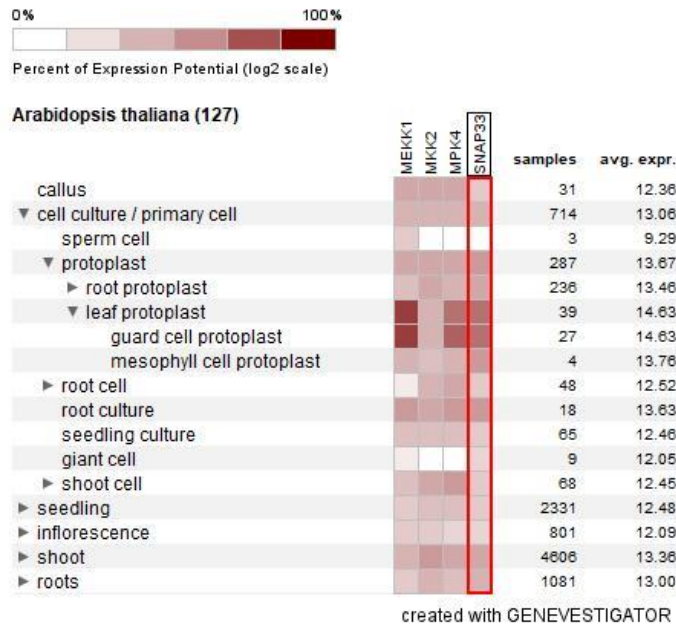


Figure 3.2. *MEKK1*, *MKK2*, *MPK4*, and *SNAP33* expression at different plant developmental stages and in different plant tissues or organs (Genevestigator data).

2.1.2. SNAP33 interactions

Analyses of SNAP33's interactions show that it mainly interacts with other SNAREs and exocyst proteins and indicate that little is known about the proteins that regulate SNAP33 at the protein level (figure 3.4).

A previous study by our team, aiming at identifying MEKK1, MKK2, and MPK4's *in vivo* interacting partners, identified SNAP33 as a potential interactor of the MAPK module (unpublished data). In this study, each MAPK (MEKK1, MKK2, MPK4) was expressed *in planta* under the control of its endogenous promoter and fused to 3 tags (9xMYC, 8xHis, Step-tag II) for tandem affinity purification (TAP), which included two steps affinity purification to lower the amount of non-specific interactions. After the two purification steps, the interacting partners were identified by mass spectrometry (MS) (Bigéard et al., 2014). The TAP-MS approach was performed twice, first as an approach to identify the interacting partners of the MEKK1-MKK2-MPK4 MAPK in flg22-stressed (15 min after flg22 application) and unstressed samples, and included a control GFP list from *P35S::GFP-9xMYC,8xHis,Step-tagII* expressing plants. The second TAP-MS approach aimed at identifying PTMs of the MAPK module in a context of flg22 stress kinetics (0, 15, and 30 min). The same lines were employed for this second strategy, and the experiment similarly generated the MAPK module's interaction partners. Among the candidates, SNAP33 was identified as a putative interactor of MEKK1, MKK2, and MPK4.

Considering the multiple literature data which suggest that SNAP33 and the MEKK1-MKK2-MPK4 MAPK module may function together in immunity, and the results obtained by our lab from the TAP-MS experiments, we hypothesized that SNAP33 stability or interactions could be regulated by the MAPK module as a putative MPK4 substrate during immunity or/and cytokinesis. SNAP33 could also be involved in the transport of the MAPKs to the plasma membrane. As mentioned earlier, MPK4 and SNAP33 were both localized at the plasma membrane during ETI, and MEKK1 and MKK2 were also shown to localize at the plasma membrane (Gao et al., 2008).

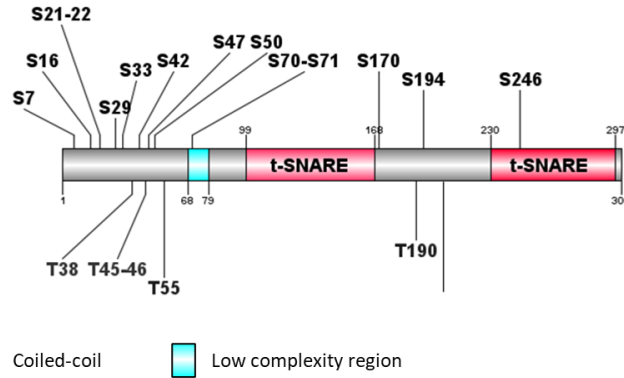
Therefore, we first assessed the interaction between SNAP33 and the MEKK1-MKK2-MPK4 module. Then, we tested whether SNAP33 is a substrate of MPK4 and other immune MAPKs. Finally, we analyzed a potential genetic relationship between SNAP33 and the MAPK module.

a. **AT5G61210: SOLUBLE N-ETHYLMALDEIMIDE-SENSITIVE FACTOR ADAPTOR PROTEIN 33**
Uniprot ID: Q9S7P9

```

10      20      30      40      50
MFGLRKSPAN LPKHNSVDLK SSKPNPFDSD DESDNKHTLN PSKRTTSEPS
60      70      80      90     100
LADMTNPFGG ERVQKGDSSS SKQSLFNSK YQYKNNFRDS GGIENQSVQE
110     120     130     140     150
LEGYAVYKAE ETKSVQGCL KVAEDIRSDA TRTLVMLHDQ GEQITRTHHK
160     170     180     190     200
AVEIDHDLSR GEKLLGSLGG MFSKTWKPKK TRPINGPVVT RDDSPTRRVN
210     220     230     240     250
HLEKREKLGL NSAPRGQSRT REPLPESADA YQRVEMEKAK QDDGLSDLSD
260     270     280     290     300
ILGELKNMAV DMGSEIEKQN KGLDHLHDDV DELNFRVQQS NQRGRLLGK

```



b.

Site	Count	Modification	Sequence
S7	4	Phosphorylation	MFGLRK(S)PANLPKHNSV
S16	4	Phosphorylation	KSPANLPKHN(S)VDLKSSKPNP
S29	51	Phosphorylation	LKSSKPNPFD(S)DDESDNKHTL
S33	5	Phosphorylation	KPNPFDSDDE(S)DNKHTLNPSK
T38	2	Phosphorylation	DSDES D NKH(T)LNPSKRTSE
T45	8	Phosphorylation	NKHTLNPSKR(T)TSEPSLADMT
T46	10	Phosphorylation	KHTLNPSKR(T)SEPSLADMTN
S47	38	Phosphorylation	HTLNPSKR(T)E P SLADMTNP
S50	3	Phosphorylation	NPSKR(T)SEPS(S)LADMTNPF G G
S173	1	Phosphorylation	KLLGSLGGMF(S)KTWKPKKTRP
S194	3	Phosphorylation	INGPVVTRDD(S)PTRRVNHLEK
T190	2	Phosphorylation	KTRPINGPVV(T)RDDSPTRRVN
K204	1	Ubiquitination	SPTRRVNHLE(K)REKLG L NSAP
K207	1	Ubiquitination	RRVNHLEKRE(K)LGLNSAPRGQ

Figure 3.3. The protein sequence and domain organization of SNAP33 and the post-translational modifications (PTMs) identified on SNAP33. a. The upper panel shows the protein sequence of SNAP33, the phosphorylated residues are highlighted in red and the ubiquitinated residues are highlighted in purple. The lower panel shows a schematic figure depicting the domains of SNAP33 protein and the position of the modified residues on the protein, S for Serine, T for Threonine and K for Lysine. b. Table listing SNAP33's PTMs and the number of times each modification was identified. Data were retrieved from the PhosPhAt4.0 database. Displayed are the phosphosites which were identified in at least two phosphoproteomic studies.

2.2. Is SNAP33 an interacting partner of MEKK1-MKK2-MPK4 MAPK module?

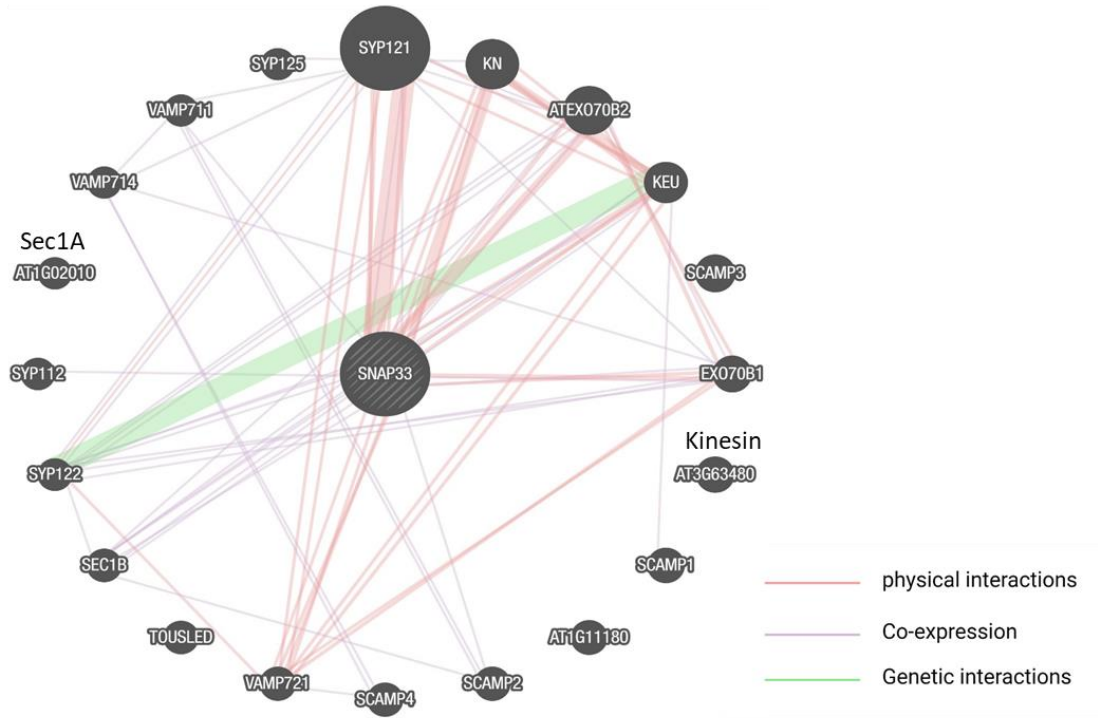
2.2.1. *SNAP33 interacts with MEKK1, MKK2, and MPK4 in vivo by BiFC*

To assess a putative interaction between SNAP33 and members of the MEKK1-MKK2-MPK4 MAPK module, we first used the bimolecular fluorescence complementation (BiFC) approach by transient expression in *Nicotiana benthamiana* leaves. The previously described interaction between Globosa and Deficiens occurring in the nucleus and at the plasma membrane (Marion et al., 2008) was used as a positive control in our experiments. SNAP33 and the three members of the MAPK module were fused to the N-terminal and C-terminal fragments of YFP, respectively. Three to four-week-old *N. benthamiana* leaves were co-transformed with YFP^N-SNAP33 and either YFP^C-MPK4 / YFP^C-MKK2 / YFP^C-MEKK1. We observed YFP fluorescence at the cytosol/ plasma membrane in either of the combinations used above, showing that SNAP33 interacts with MEKK1, MKK2, and MPK4 *in vivo* (figure 3.5). We did not detect YFP fluorescence in all of the negative controls (YFP^N-SNAP33 + YFP^C-Deficiens, YFP^C-MPK4 + YFP^N-Globosa, YFP^C-MKK2 + YFP^N-Globosa, and YFP^C-MEKK1 + YFP^N-Globosa), showing that the interactions between SNAP33 and the MEKK1-MKK2-MPK4 MAPK module are specific. Additionally, the presence of the YFP signal at the plasma membrane/cytosol is consistent with the previously reported subcellular localizations of SNAP33, MEKK1, MKK2, and MPK4.

2.2.2. *SNAP33 does not interact with MEKK1, MKK2, and MPK4 by Y2H*

To validate the interactions between SNAP33 and MEKK1, MKK2, and MPK4 reported by BiFC using a different technique, we performed a yeast two-hybrid (Y2H) assay. The reporter yeast strains MaV103 and MaV203 were transformed with MEKK1, MKK2, MPK4, and SNAP33 fused to the GAL4 activation domain (GAL4-AD) or to the GAL4 binding domain (GAL4-BD) (figure 3.6). After mating, the generated diploids were grown on selective media. Yeasts transformed with MEKK1 fused to GAL4-BD were unable to grow and therefore could not be used in this assay. The resulting chimeric protein is probably lethal to the yeast cells. As depicted in figure 3.6, we observed the previously reported interactions between MEKK1 and MKK2, between MKK2 and MPK4 (Gao et al., 2008), and between MEKK1 and MPK4 (Ichimura et al., 1998) (figure

a.



b.

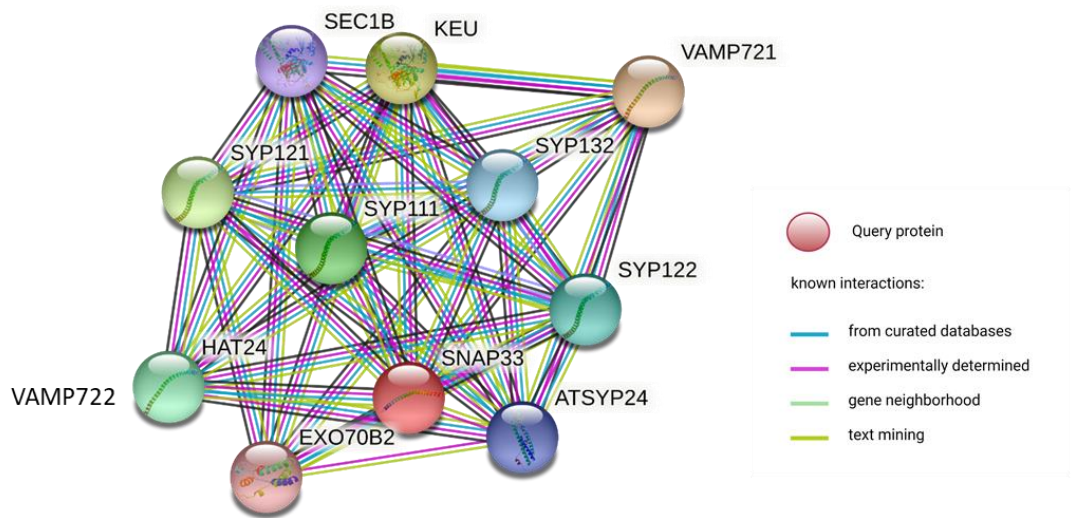


Figure 3.4. Interactions of SNAP33. Schematic figures showing notably SNAP33's protein interactions reported by GeneMania (a.) and STRING (b.) databases.

3.6). However, we did not observe any interaction between SNAP33 and the members of the MAPK module using this method and a variety of 3AT concentrations.

2.2.3. *SNAP33 does not interact with MKK2 and MPK4 by in vitro pull-down assays*

In parallel to the Y2H experiments, we examined the interactions between SNAP33 and MKK2 and MPK4 by *in vitro* pull-down assays using the recombinant proteins His-MKK2, His-MPK4 and GST-SNAP33. To test whether MPK4 interacts with SNAP33 in its activated conformation, we included the constitutively active version of MPK4, which harbors two substitutions, namely D198G and E202A, termed MPK4^{D198G/E202A} (or CA-MPK4), and which was previously identified and described by our team (Berriri *et al.*, 2012). *In vitro*-purified GST-SNAP33 and GST alone were incubated with His-tagged MPK4 (MPK4^{WT}) or constitutively active His-tagged MPK4 (MPK4^{D198G/E202A}). GST-SNAP33 and GST were then precipitated with glutathione beads. Immunoblotting analyses showed that MPK4^{WT} and MPK4^{D198G/E202A} co-precipitated *in vitro* with GST-SNAP33, but even more strongly with GST alone (figure 3.7). These results prevent drawing conclusions on the interaction between SNAP33 and MPK4 and suggest that MPK4 can interact with GST. No exploitable results were obtained using His-MKK2 (data not shown) and thus will not be described here.

2.2.4. *SNAP33 does not interact with MKK2 and MPK4 by co-immunoprecipitation assays in vivo*

Because we found that SNAP33 interacts with MEKK1, MKK2, and MPK4 *in vivo* using BiFC, but not by Y2H or *in vitro* pull-down assay, we hypothesized that the interactions might occur only *in vivo* because they depend, for instance, on PTMs or other proteins, or because the proteins are correctly folded *in planta* which might not be the case in yeast or *in vitro*.

We thus sought to evaluate the interaction between SNAP33 and MEKK1, MKK2, and MPK4 *in vivo* through co-immunoprecipitation (co-IP) following transient expression in *N. benthamiana* leaves using flg22 kinetics to determine whether the interactions might be affected in response to biotic stress. To do that, we used cloning vectors that yield a SNAP33 protein N-terminally fused to GFP, and MEKK1, MKK2, and MPK4 proteins C-terminally fused to a myc-tag. *Agrobacterium* cells transformed with MEKK1 fused to the myc-tag were unable to grow and thus could not be used in this assay. The resulting chimeric protein is probably lethal to the *Agrobacterium* cells. *N. benthamiana* leaves were co-infiltrated with the adequate

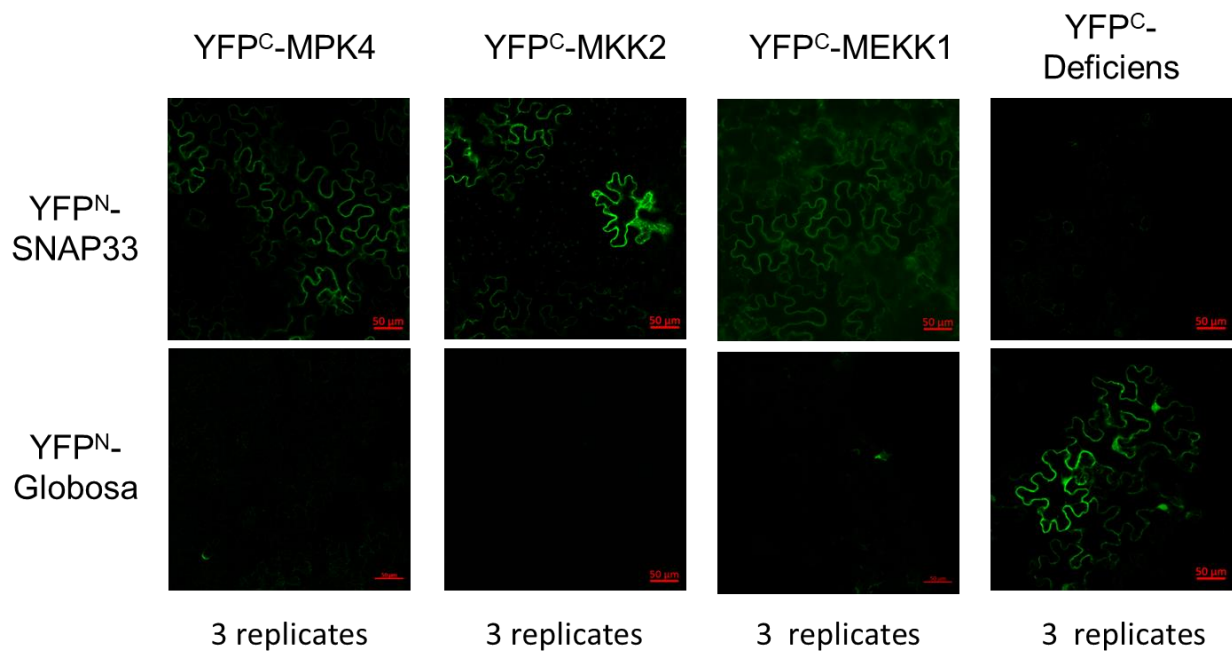


Figure 3.5. SNAP33 interacts with MEKK1, MKK2, and MPK4 in BiFC assay. SNAP33 was fused to the N-terminal fragment of YFP (YFP^N), MEKK1, MKK2, and MPK4 were fused to the C-terminal fragment of YFP (YFP^C). All constructs were expressed under the control of the cauliflower mosaic virus 35S promoter in 3-4 week old *N.benthamiana* leaves. Microscopic observations were performed 4 days after infiltration. YFP fluorescence was observed only with the transiently expressed YFP^N-SNAP33 and YFP^C-MPK4/MKK2/MEKK1, but not in YFP^N-SNAP33 and YFP^C-Deficiens or YFP^C-MPK4/MKK2/MEKK1 and YFP^N Globosa combinations. The combination YFP^N-Globosa and YFP^C-Deficiens was used as a positive control. Scale Bar represents 50 μ m. These experiments were performed at least three times with similar results.

Agrobacterium strains, and after 24 h, the leaves were treated with flg22 and harvested for co-IP analyses. As depicted in figure 3.8.a, MKK2 and MPK4 co-precipitated with GFP-SNAP33 but also co-precipitated in samples lacking the GFP-SNAP33 protein, showing that the interactions with SNAP33 might not be specific. These findings preclude any conclusion regarding the interaction between SNAP33 and MPK4 or MKK2.

To further analyze the interaction between SNAP33 and MPK4, we took advantage of the *snap33 Prom^{SNAP33}::myc-SNAP33* stable line expressing a functional chimeric myc-SNAP33 protein, which rescued the phenotype of *snap33* in the *Ws* ecotype. This line was generated and described previously by Heese et al. (2001). We also performed a PAMP kinetics to determine whether the interactions might be affected by biotic stress. As the *Ws* ecotype is insensitive to flg22 (Bauer et al., 2001), we used the PAMP elf18 derived from the *Pseudomonas syringae* Elongation factor Tu (EF-Tu) and recognized by the LRR-RLK EF-Tu receptor (EFR) (Zipfel et al., 2006) to induce a PTI in the *snap33 Prom^{SNAP33}::myc-SNAP33* line. The myc-SNAP33 protein was immuno-precipitated from 13-day-old seedlings of *snap33 Prom^{SNAP33}::myc-SNAP33* line. The presence of MPK4 in the eluates was assessed by immunoblotting using an antibody directed against MPK4. The same experiment was performed on the WT *Ws* ecotype as a negative control to assess MPK4's nonspecific binding. As shown in figure 3.8.b, MPK4 was not co-immunoprecipitated with SNAP33 protein in Arabidopsis extracts, neither in untreated samples (Point 0) nor in elf18-treated samples.

2.3. Is SNAP33 a substrate of the MEKK1-MKK2-MPK4 MAPK module?

Because numerous phosphorylation sites were identified on SNAP33's sequence, of which S7 and S194 are compatible with MAPK phosphorylation motif (figure 3.3), we investigated whether SNAP33 is a substrate of the MEKK1-MKK2-MPK4 MAPK module. As MPK3 and MPK6 are also involved in immunity and previous studies have reported that MPK3, MPK4, and MPK6 share common substrates (Rayapuram et al., 2018), we also included MPK3 and MPK6 in our experiments to test whether they phosphorylate SNAP33. To do that, we performed *in vitro* kinase assays using recombinant MAPK proteins produced in *E. coli* and using the MPK4 protein produced *in vivo* in protoplasts.

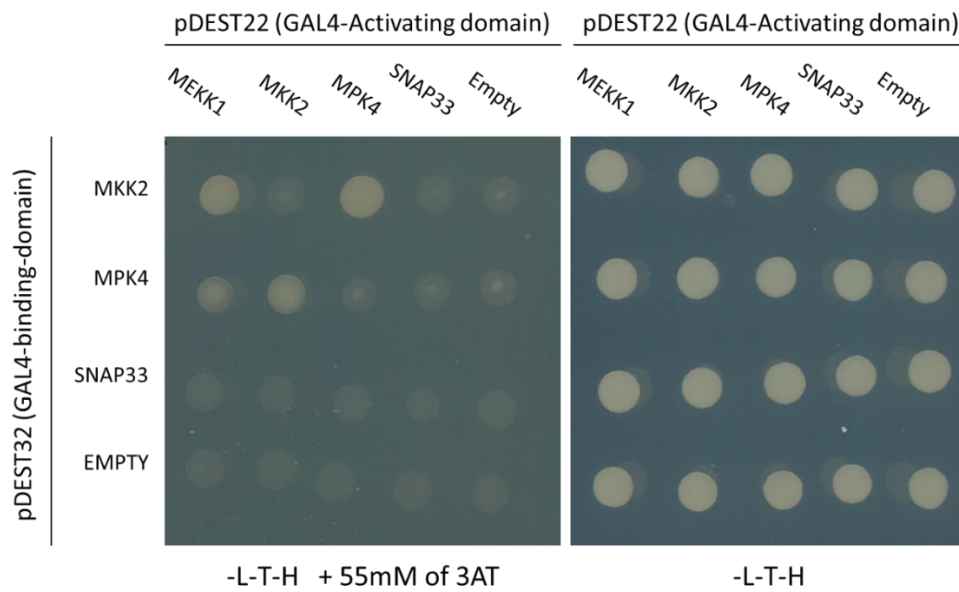


Figure 3.6. SNAP33 does not interact with MEKK1, MKK2, nor MPK4 in yeast two-hybrid assay. Diploid yeasts obtained after mating were spotted on YNB selective growth media -L-T-H supplemented with 55 mM of 3-amino-1H-1,2,4-triazole (3AT). Growth plates were scanned after 24 h of growth. Empty refers to yeasts transformed with pDEST22 or pDEST32 without fused protein. This experiment was repeated at least three times with similar results.

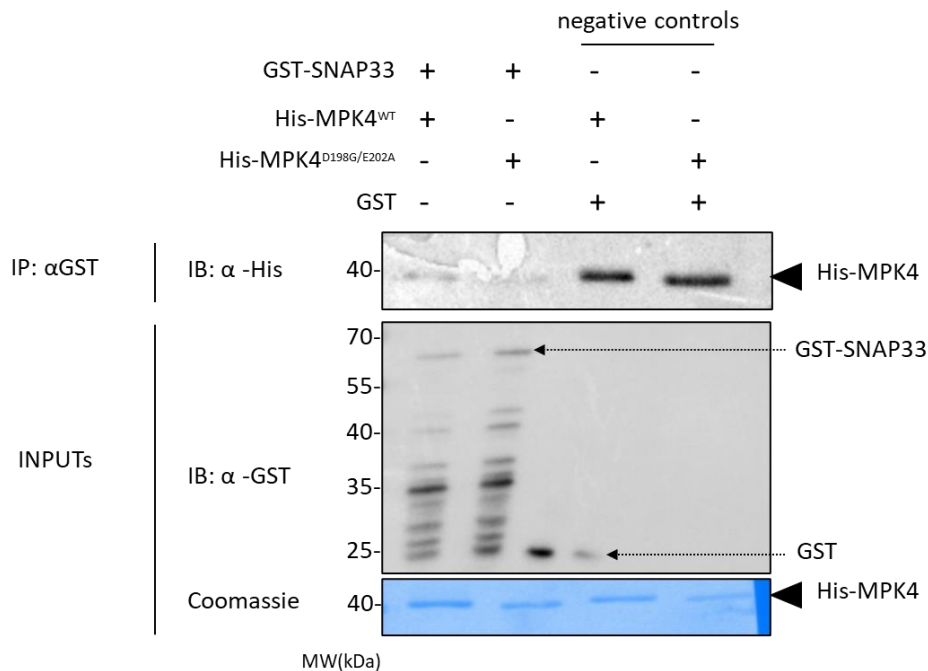


Figure 3.7. *In vitro* pull-down assay does not allow concluding on the interaction between SNAP33 and MPK4. The pull-down assay was conducted with GST-binding resin after purified GST-SNAP33 and GST were incubated with His-MPK4^{WT} or constitutively active MPK4 (His-MPK4^{D198G/E202A}). The GST-SNAP33 and GST inputs were subjected to immunoblotting with anti-GST antibodies as controls (middle panel). The His-MPK4 inputs were analyzed by Coomassie staining of the gel. IP: immunoprecipitation; IB: immunoblotting. This experiment was conducted only once.

2.3.1. Kinase assays using the *in vitro* produced recombinant proteins

To test whether SNAP33 might be a substrate of MPK3, MPK4, and MPK6, we performed *in vitro* kinase assays using the constitutively activated recombinant proteins His-MBP-MPK3^{T119C}, His-MPK4^{D198G/E202A}, and His-MPK6^{D218G/E222A}, previously identified and described by our team (Berriri et al., 2012), and the recombinant protein GST-SNAP33 (figure 3.9.b). GST-SNAP33 was incubated with each MAPK and radioactive [γ -³³P] ATP. In parallel, a kinase assay on myelin-basic protein (MBP) using the MAPK recombinant proteins was performed as a control to determine the activity of the tagged MAPKs. As depicted in figure 3.9, no obvious phosphorylation was observed on SNAP33 by either of the tested MAPKs. A very faint band that coincides with the size of GST-SNAP33 when incubated with MPK3^{T119C} was observed, indicating that SNAP33 might be a substrate of MPK3 (indicated by an arrow in the phospho-image, figure 3.9.a). However, the very low intensity of the band questions the relevance of this result. Proteins considered as *in vitro* MAPK substrates usually display more intense signals. Given the low intensity of the observed band (figure 3.9.a) and the fact that the S7 site is on the very N-terminal part of the SNAP33 protein, we hypothesized that the GST tag on the N-terminal part of SNAP33 might somehow prevent or lower the phosphorylation of SNAP33 by MPK3, MPK4, and MPK6. Therefore, we produced a C-terminally tagged version of SNAP33 by introducing a STREP tag to the C-terminal part of SNAP33. The expected size of SNAP33-STREP protein is 40 kDa (figure 3.10.b). Besides testing MPK3, MPK4 and MPK6, we also added MKK2 to test whether MKK2 might phosphorylate SNAP33 (figure 3.10.a). For this, we used a constitutively activated version of MKK2 (MKK2-EE) harboring two substitutions, on T220 and T226, to glutamate residues (Teige et al., 2004). As depicted in figure 3.10.a, no phosphorylation was observed by MPK3 or any of the other tested MAPKs. We observed an intense band when SNAP33-STREP was incubated with MKK2-EE and His-MPK4, which coincides with MPK4's phosphorylation by MKK2.

2.3.2. Kinase assay using the *in vivo* purified MPK4 and MKK2

To investigate whether MPK4 or MKK2 phosphorylates SNAP33 under more physiological conditions, we purified, from protoplasts, an HA-tagged version of MPK4 (MPK4-HA) co-expressed with a constitutively activated myc-tagged MKK2-EE, and also a purified WT, as well as constitutively activate (MKK2-EE) version of MKK2 alone. The purified/immunoprecipitated

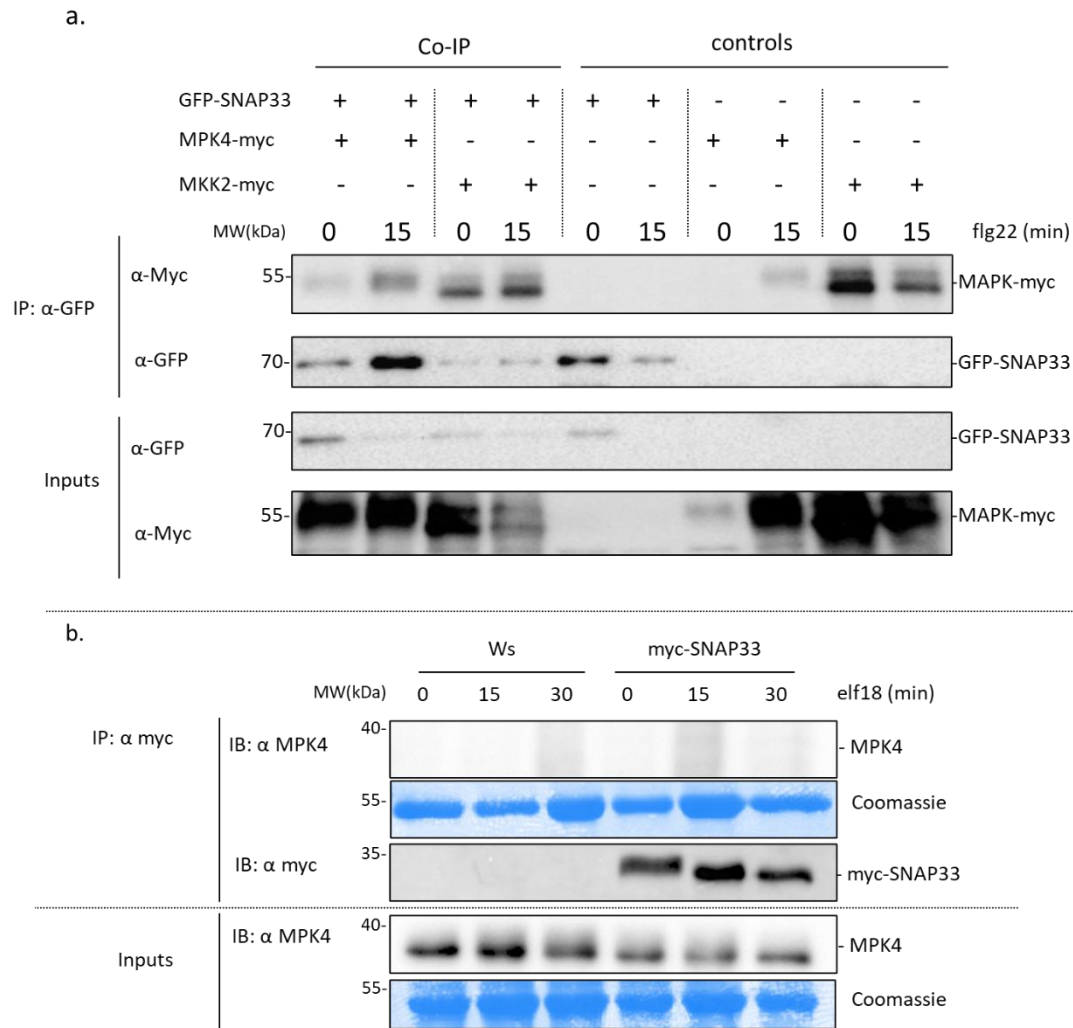


Figure 3.8. SNAP33 does not interact with MPK4 and MKK2 by *in vivo* co-IP assays. **a.** Co-immunoprecipitation (co-IP) assay to investigate the interaction between SNAP33 and MKK2/MPK4 after co-expression in *N. benthamiana* leaves. The leaves were treated 24 h after co-infiltration with 100 nM of flg22 and harvested after 0 (untreated) and 15 min of flg22 application. The expression of SNAP33 was assessed by anti-GFP immunoblotting after immunoprecipitation (2nd panel from the top). The inputs panel shows the expression of all the proteins before immunoprecipitation. This experiment was repeated 3 times with similar results **b.** *In vivo* co-immunoprecipitation (co-IP) to test the interaction between SNAP33 and MPK4 in the *snap33 Prom^{SNAP33}::myc-SNAP33* line. myc-SNAP33 proteins were immunoprecipitated from the *snap33 Prom^{SNAP33}::myc-SNAP33* plants treated with 100 nM of elf18 and harvested at 0 (untreated), 15 and 30 min after elf18 application. In parallel, the same experiment was performed on the WT Ws as a negative control lacking myc-SNAP33. MPK4 expression was verified in inputs by immunoblotting with anti-MPK4 antibody before IP (3rd panel from the top), and the presence of myc-SNAP33 in the eluates was verified by immunoblotting after IP with an anti-myc antibody (3rd panel from the top). IP: immunoprecipitation; IB: immunoblotting. This experiment was repeated 3 times with similar results.

MPK4-HA and MKK2-myc were then used for an *in vitro* kinase assay on the recombinant protein GST-SNAP33. As a control, the experiment included two samples in which neither of the MAPKs was expressed. As depicted in figure 3.11.a, very faint bands which coincide with GST-SNAP33 were observed in all samples, including the control, showing that GST-SNAP33 is not phosphorylated by MPK4 and MKK2 using this approach and suggesting that SNAP33 might not be a substrate of these MAPKs. We performed a similar approach on SNAP33-STREP using MPK4-HA expressed in flg22-treated protoplasts. As depicted in figure 3.11.b, no obvious phosphorylation of SNAP33-STREP was detected using this approach either.

2.4. Is there a genetic relationship between SNAP33 and the MAPK module?

The data presented in the preceding sections demonstrate that SNAP33 is probably not a substrate of the MAPK module MEKK1-MKK2-MPK4. Additionally, we were unable to validate the interactions between SNAP33 and the MEKK1-MKK2-MPK4 MAPK module observed by BiFC using the additional above-mentioned techniques (Y2H, pull-down, and co-IP). We thus tested a putative genetic relationship between *SNAP33* and *MEKK1*, *MKK2*, and *MPK4*. To do that, we crossed *snap33* with known suppressors of the *mekk1*, *mkk1 mkk2*, and *mpk4* mutant phenotype.

2.4.1. *snap33-1* phenotype is not suppressed by the *summ2-8* mutation

As mentioned earlier in the introduction (section 2.3.2), a screen for suppressors of the *mkk1 mkk2* phenotype identified the *summ2* mutation (for SUPpressor of *mkk1 mkk2*) (Zhang et al., 2012). The *summ2* mutation rescues the dwarf phenotype of not only *mkk1 mkk2* but also that of *mekk1* and *mpk4* (Zhang et al., 2012). Mapping the mutation revealed that *SUMM2* encodes a CNL (Zhang et al., 2012). The authors concluded that *SUMM2* guards the MAPK module and activates immune responses upon sensing its disruption. As *snap33* also displayed an auto-immune phenotype which is probably related to constitutive NLR signaling, we investigated whether the constitutive induction of defense responses also depends on *SUMM2* in the *snap33-1* mutant. To do that, we crossed *snap33-1*^{+/-} with *summ2-8* knockout mutant. As depicted in figure 3.12., *snap33-1 summ2-8* did not show a difference with *snap33-1*, with an average weight of 0.9 and 0.93 mg, respectively. Therefore *snap33-1*'s phenotype does not

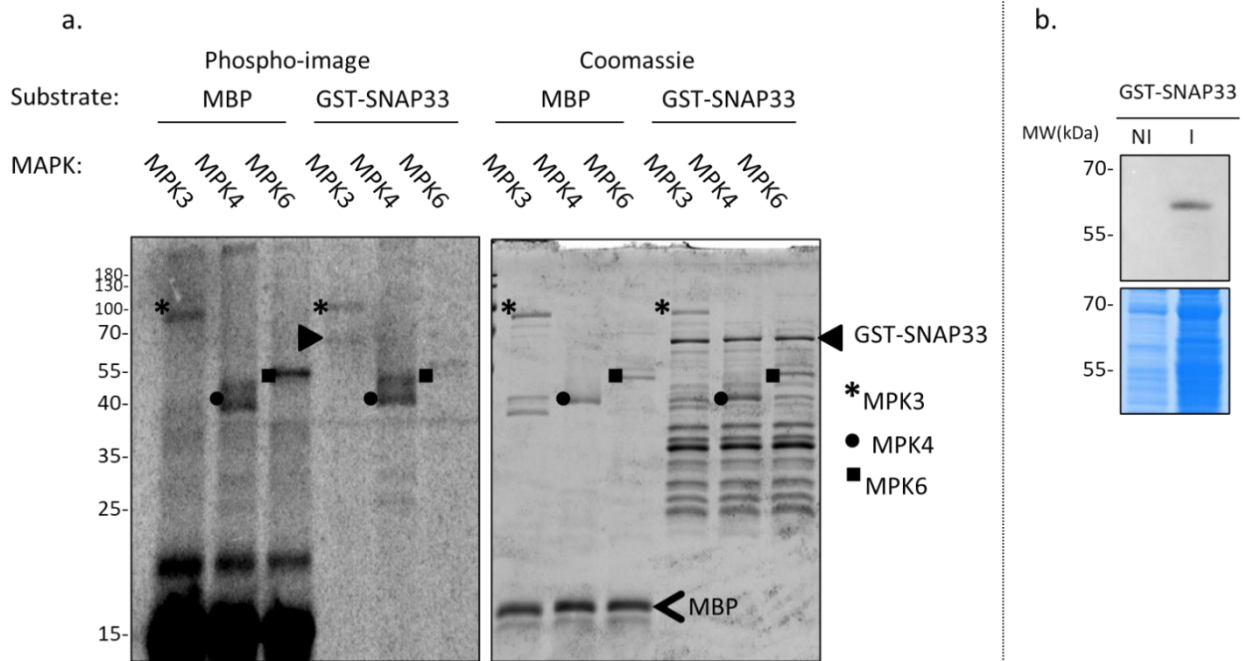


Figure 3.9. GST-SNAP33 is not phosphorylated by MPK3, MPK4, and MPK6 *in vitro*. **a.** *In vitro* phosphorylation of GST-SNAP33 and MBP by the constitutively active MAPKs His-MBP-MPK3^{T119C}(MPK3), His-MPK4^{D198G/E202A} (MPK4), and His-MPK6^{D218G/E222A}(MPK3). Left image: phospho-image of the kinase assay performed on GST-SNAP33 and MBP by MPK3, MPK4, and MPK6; right image: Coomassie staining of all loaded proteins. *, • and ▪ indicate the autophosphorylation of MPK3, MPK4, and MPK6, respectively, on the phospho-image panel and the loaded MPK3, MPK4 and MPK6 on the Coomassie panel; GST-SNAP33 and MBP are indicated with a full and a thin arrowhead, respectively. Note: the faint band indicated by an arrowhead in the phospho-image coincides with the expected molecular weight of GST-SNAP33 in the MPK3 well. **b.** The Immunoblot shows the migration of the produced GST-SNAP33 recombinant protein. NI (not-induced): refers to extracts from bacteria before induction of GST-SNAP33 production; I (induced): extracts from bacteria after induction of GST-SNAP33 production.

depend on *SUMM2*, suggesting that SNAP33 is not involved in the same pathway as the MEKK1-MKK2-MPK4-SUMM2 module.

2.4.2. *snap33-1* phenotype is not suppressed by the *smn1* mutation

In an independent suppressor screen conducted on a dwarf auto-immune line overexpressing the N-terminal regulatory domain of MEKK1 (which phenocopies the phenotype of *mekk1*), the *smn1* (suppressor of MEKK1-N overexpression-induced dwarf 1) mutation was identified (Takagi et al., 2019). The *SMN1* gene encodes a TNL, also known as *RPS6*, involved in resistance to *Pseudomonas syringae* (Kim et al., 2009). As reported for *summ2*, *smn1* reverts the phenotype of *mekk1*, *mkk1 mkk2*, and *mpk4*, and it was hence suggested that SMN1 guards a target downstream of the MEKK1-MKK2-MPK4 MAPK pathway, acting in a *SUMM2*-independent signaling pathway (Takagi et al., 2019). Because the *smn1* mutant reported by Takagi et al., (2019) was identified in the Landsberg erecta (Ler) accession and *snap33-1* is in Col-0 background, we identified other *smn1* mutants in the Col-0 ecotype. Three T-DNA insertion lines, namely SALK_029541C (*smn1-1*), SALK_029328 (*smn1-2*), and SALK_204713C (*smn1-3*), were identified from the Arabidopsis Biological Resource Center (ABRC) T-DNA collection in the locus of *SMN1* (AT5G46470) (figure 3.13.a). The *smn1* homozygous mutant plants were isolated from the T-DNA insertion lines by PCR, and the expression of *SMN1* was assessed by RT-PCR. None of the identified *smn1* mutants expressed *SMN1* (figure 3.13.b). We did not test whether the *smn1* mutant of the Col-0 background suppresses the phenotype of *mekk1*, *mkk1 mkk2*, and *mpk4* in the Col-0 ecotype. To test whether *smn1* mutation reverts the phenotype of *snap33-1* and whether *SNAP33* could be involved in this alternative, *SUMM2*-independent branch of the MEKK1-MKK2-MPK4 MAPK pathway, we crossed *snap33-1*^{+/-} with *smn1-1*. As depicted in figure 3.13.c, our results show no obvious difference between *snap33-1* and *snap33-1 smn1-1*. Although further validation by rosette weight analyses is required, these results suggest that *SMN1* is not involved in the phenotype of *snap33-1* and thus suggest that *SNAP33* is not involved in the alternative MEKK1-MKK2-MPK4-SMN1 pathway.

2.5. Discussion

In this second section of the results, I reported the experiments we conducted to investigate a putative relationship between *SNAP33* and the MEKK1-MKK2-MPK4 MAPK module. Because

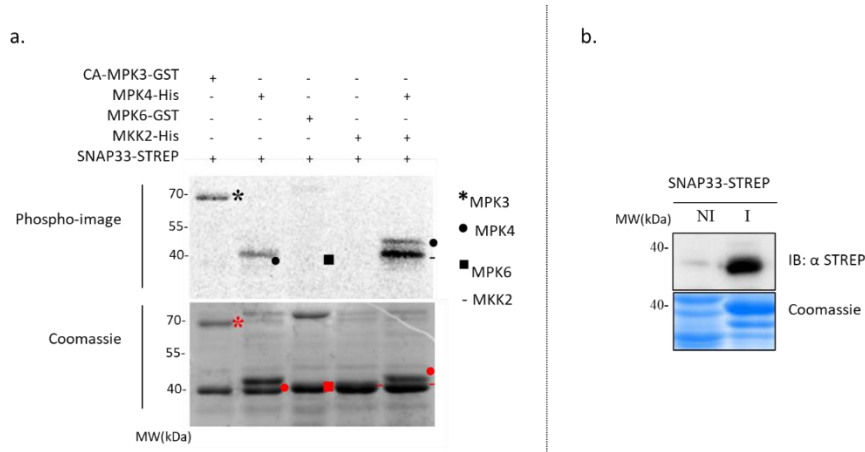


Figure 3.10. SNAP33-STREP is not phosphorylated by MPK3, MPK4, and MPK6 *in vitro*. **a.** *In vitro* phosphorylation of SNAP33-STREP by the constitutively active MAPKs His-MBP-MPK3^{T119C}(MPK3), His-MPK4^{D198G/E202A} (MPK4), His-MPK6^{D218G/E222A}(MPK3), and MKK2-DD (MKK2). Upper panel: phospho-image of the kinase assay performed on SNAP33-STREP by MPK3, MPK4, MPK6, and MKK2; lower image: Coomassie staining of all loaded proteins. *, •, ▪, and - indicate the position of MPK3, MPK4, MPK6, and MKK2, respectively, on the phospho-image panel and the loaded MPK3, MPK4, MPK6 and MKK2 on the Coomassie panel. **b.** Immunoblot showing the migration of the produced SNAP33-STREP recombinant protein. NI (not-induced): refers to extracts from bacteria before induction of SNAP33-STREP production; I (induced): extracts from bacteria after induction of SNAP33-STREP production.

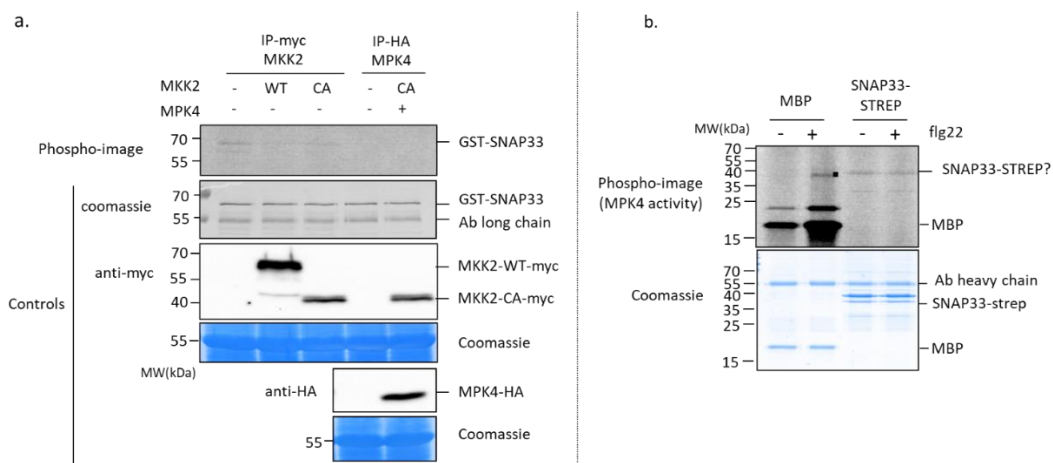


Figure 3.11. GST-SNAP33 and SNAP33-STREP are not phosphorylated by MPK4, and MKK2 proteins purified from protoplasts. **a.** *In vitro* phosphorylation of GST-SNAP33 using MPK4 and MKK2 produced and purified after expression in protoplasts. Negative controls in which neither MPK4 nor MKK2 were expressed are included. The phospho-image shows the kinase assays. The expression of MKK2 and MPK4 in protoplasts was assessed by immunoblotting with anti-myc and anti-HA antibodies, respectively (controls). Coomassie shows total protein loading. **b.** *In vitro* phosphorylation of SNAP33-STREP using MPK4 produced and purified after expression in protoplasts. MPK4 was purified from flg22-stressed or unstressed protoplasts. The phospho-image shows the kinase assays with MPK4 on SNAP33-STREP. MBP was used as a control for MPK4 activity. Coomassie shows total protein loading. ▪ indicates the position of the auto-phosphorylated form of MPK4 when incubated with MBP.

both SNAP33 and the MEKK1-MKK2-MPK4 MAPK module are involved in immunity, exhibit similar expression patterns in response to biotic stress and during development, and similar subcellular localizations (figure 3.2), we speculated that both components might function together during immunity or other processes in Arabidopsis. Moreover, the phenotype of the *snap33* mutant is similar to that of the *mekk1*, *mkk1 mkk2*, and *mpk4* mutants, and the transcriptome of *snap33-1* shows a substantial overlap and similarity with that of *mpk4* and *mkk1 mkk2*, respectively (figures 2.12. and 2.24.b). SNAP33 and MPK4 are both involved in cytokinesis and localize to the cell plate of dividing cells (Heese et al., 2001; Kosetsu et al., 2010). Additionally, SNAP33 was identified by our team as a candidate interacting partner of the MEKK1-MKK2-MPK4 module in TAP-MS experiments aiming at identifying MEKK1, MKK2, and MPK4 interacting partners (unpublished data). All these data, together with the fact that SNAP33 is a phosphorylated protein, prompted us to investigate whether there might be a relationship between SNAP33 and the MEKK1-MKK2-MPK4 MAPK module. Besides, some proteins involved in endomembrane trafficking were found to be phosphorylated by MAPKs in response to stress. For instance, EXO70B2 (described in the introduction section 4.2.1), a member of the exocyst family involved in vesicles tethering to the plasma membrane prior to SNARE-mediated fusion, is phosphorylated by MPK3 (Brillada et al., 2020). The phosphorylation of EXO70B2 by MPK3 regulates its localization to active secretion sites. The same team previously demonstrated, via phosphoproteomic analyses, that PEN1/SYP121, the Qa-SNARE/Syntaxin partner of SNAP33, is a putative substrate of MPK3 and MPK6 in response to flg22, due to its significantly increased phosphorylation state in plants expressing a constitutively active version of MKK5 (Lassowskat et al., 2014). Therefore, we hypothesized that SNAP33 could be a substrate of MPK4, which might regulate its activity, stability, localization, and/or interactions. In fact, two phosphosites previously identified on SNAP33 are compatible with the S/T-P MAPK phosphorylation motif (S7 and S194) (figure 3.3). Additionally, we speculated that SNAP33 might regulate the MAPK module's localization, possibly by trafficking to distinct cellular compartments. Another hypothesis, based on the possibility that SNAP33 interacts with the three MAPK module components, is that it might operate as a scaffold of the MAPK module.

Therefore, to investigate the potential relationship between SNAP33 and the MEKK1-MKK2-MPK4 MAPK module, we first looked at their interactions, then at putative phosphorylation of

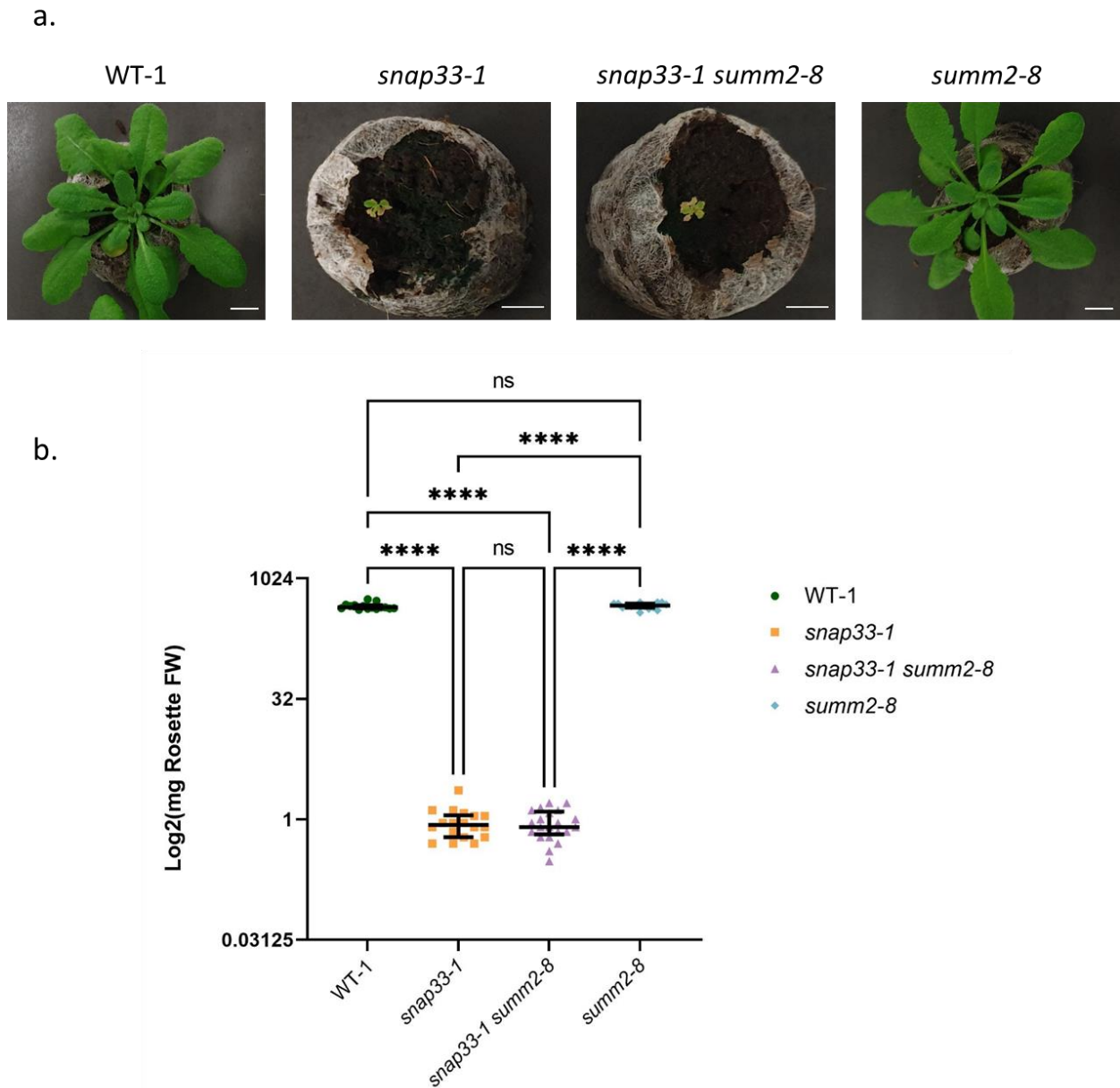


Figure 3.12. *summ2-8* mutation does not revert the phenotype of *snap33-1*. **a.** Representative pictures of 35-day-old soil-grown WT-1, *snap33-1*, *snap33-1 summ2-8* and *summ2-8* plants. Scale bars represent 1 cm. **b.** Biomass of aerial parts of the analyzed genotypes. Plotted values are the Log₂ of rosette fresh weight (FW) (see Supplementary data 7 for linear values and descriptive statistics) with WT-1, *snap33-1*, *snap33-1 summ2-8* and *summ2-8* average fresh weight of 458.6 mg (n=15), 0.93 mg (n=18), 0.9 mg (n=21), and 465.4 mg (n=15), respectively (it is important to note that these experiments were performed at the same time as those observed in figure 2.23.b/c). Bars indicate the median value and interquartile range. Asterisks denote statistically significant differences in the Kruskal Wallis test (Benjamini Hocheberg FDR), with four asterisks [****] P < 0.0001; ns stands for not significant. The data presented here are the results of one biological replicate.

SNAP33 by MPK4 (and other immune MAPKs), finally at a putative genetic relationship between the two components.

2.5.1. *Is SNAP33 an interacting partner of the MAPK module?*

We found that SNAP33 and the proteins of the MEKK1-MKK2-MPK4 MAPK module interact by BiFC in *N. benthamiana* leaves (figure 3.5). The YFP signals indicate that the interactions occur at the plasma membrane/cytosol, which is consistent with the previously reported subcellular localization of both SNAP33 and MEKK1, MKK2, and MPK4. However, we could not validate these interactions by Y2H and by *in vitro* pull-down assays (figures 3.6 and 3.7). Given the results obtained by Y2H and pull-down assays, we speculated that the interactions might occur only *in vivo* because they might depend on PTMs or other proteins or because the proteins are correctly folded *in planta*, which might not be the case in yeast or in bacteria. Therefore, to validate the results obtained by BiFC through *in vivo* approaches, we tested the interactions between SNAP33 and MPK4 and MKK2 *in planta* either by transitory expression in *N. benthamiana* leaves or using the stable line *snap33 Prom^{SNAP33}::myc-SNAP33*. We also included PAMP treatments to test whether biotic stress affects the interactions (increased or decreased). However, we did not observe any interactions between SNAP33 and MKK2/MPK4 by any of the approaches mentioned above (figure 3.8). It is thus possible that these interactions are too transient to be detected by Co-IP but can be detected by BiFC as it is known that BiFC tends to stabilize the interactions through the reconstitution of YFP. Another technique that might be used to investigate the possibility of a transient interaction between SNAP33 and MEKK1, MKK2, and MPK4 is the TurboID-based proximity labeling for *in vivo* identification of protein-protein interactions (Mair et al., 2019; Zhang et al., 2019). This technique employs proximity labeling, in which the protein of interest is fused to an enzyme that catalyzes the formation of labile biotinyl-AMP. Biotinyl-AMP in its free form diffuses around the target protein and biotinylates proximal proteins within 10 nm. Thus, biotin has the ability to mark even transiently interacting partners. Mass spectrometry analyses can subsequently be used to identify the biotinylated proteins. This technique could not only validate whether SNAP33 and MEKK1, MKK2, and MPK4 interact, but it could also identify other putative interactors of SNAP33.

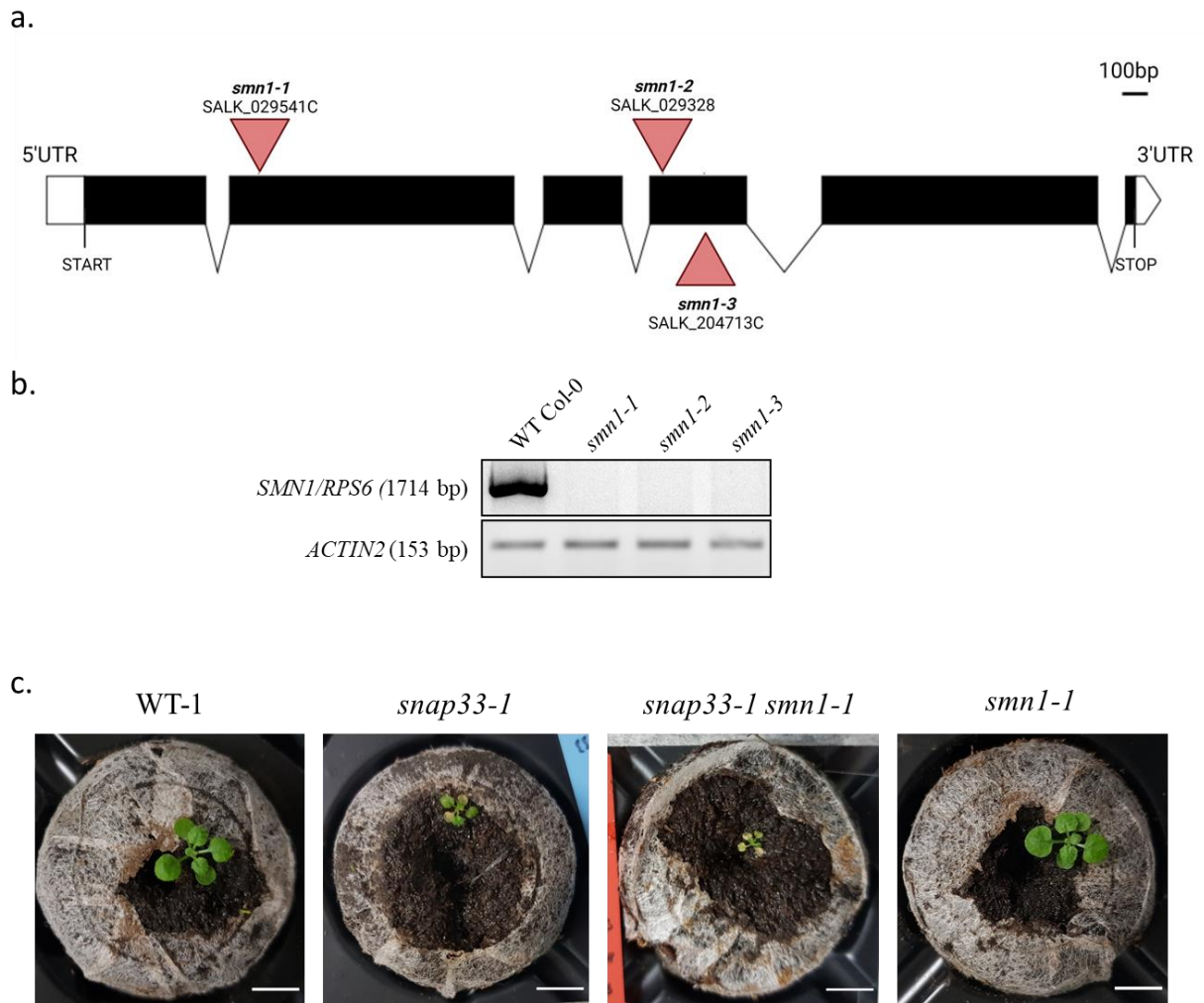


Figure 3.13. *smn1* mutation does not revert the phenotype of *snap33-1*. **a.** Schematic diagram of *SMN1/RPS6* genomic region (4399 bp) and the location of the T-DNA insertion in the *smn1-1*, *smn1-2*, and *smn1-3* mutants. The six exons of *SMN1/RPS6* are represented as black boxes, and the ATG START and the STOP codons are indicated. The introns are represented as black lines. White boxes represent the untranslated (UTR) regions, 5'UTR and 3'UTR. Triangles indicate the sites of T-DNA insertions (not drawn to scale). *smn1-1* has a T-DNA insertion in the second exon, at 681 bp from the START codon, *smn1-2* has a T-DNA insertion at 2260 bp from the START codon, and *smn1-3* has a T-DNA insertion at 2422 bp from the START codon. **b.** The upper panel depicts the analyses of *SMN1/RPS6* expression in the WT Col-0, *smn1-1*, *smn1-2*, and *smn1-3* plants by RT-PCR designated to amplify 1714 bp of the 4997 bp mRNA sequence of *SMN1*. *ACTIN2* was used as the endogenous reference gene. **c.** Representative pictures of 21-day-old soil-grown WT-1, *snap33-1*, *snap33-1 smn1-1* and *smn1-1* plants. Scale bars represent 1 cm.

2.5.2. *Is SNAP33 a substrate of MPK3, MPK4, and MPK6?*

Because several phosphoproteomic investigations indicated that SNAP33 is phosphorylated on multiple residues, and two of those are compatible with S/T-P MAPK phosphorylation sites (S7 and S194) (figure 3.3), we tested *in vitro* whether SNAP33 is phosphorylated by MPK3, MPK4, and MPK6. Our results did not show an obvious phosphorylation of SNAP33 by any of the tested MAPKs (figures 3.9, 3.10, and 3.11), suggesting that it is not a substrate of any of these proteins. We can not exclude a technical bias, for instance, a tagged version of SNAP33 might yield a misfolded SNAP33, which prevents its phosphorylation by MAPKs. However, since we produced SNAP33 with an N-terminal and a C-terminal tag, this bias seems unlikely. Ultimately, one could express SNAP33 *in vivo* in protoplasts or tobacco leaves and purify the SNAP33 protein using an antibody directed against SNAP33. The purified untagged version of SNAP33 could subsequently be used for an *in vitro* kinase assay using the constitutively active versions of MAPKs. Antibodies directed against SNAP33 were previously described and used in the studies of Heese et al., (2001) and Wick et al., (2003). Another approach is to express SNAP33 and MAPKs in protoplasts and then compare the phosphorylation state of SNAP33 in samples containing SNAP33 alone or in combination with MAPKs using mass spectrometry.

SNAP33 might also be an indirect target of MAPKs. Indeed, Rayapuram et al. identified SNAP33 as a putative indirect target of MPK6 by showing that its phosphorylation on S47 (which is not compatible with a MAPK phosphorylation motif) is significantly decreased in the *mpk6* mutant (Rayapuram et al., 2018), suggesting, for instance, that MPK6 might phosphorylate a protein kinase which subsequently phosphorylates SNAP33. Such kinase could be identified by the TurboID-based proximity labeling approach described in the previous section. This approach could also identify other kinases which directly interact with SNAP33 and could be performed upon different stress conditions to identify the putative SNAP33 regulators in different contexts.

Analysis of the sequence of SNAP33 shows that it might also be a CDPK substrate. Indeed, the S47 and S50 residues are part of an SxxS motif that fits with a CDPK phosphorylation motif (figure 3.3.a). Therefore, it would be interesting to test whether CDPKs can phosphorylate SNAP33, especially CPK5 and CPK6, which play an important role in plant immunity.

More generally, and to conclude on this section, it would be interesting to investigate the role of SNAP33's phosphosites, especially S29 and S47 phosphorylation events, which were often

identified in phosphoproteomic studies. This could be performed by mutating these sites to yield phospho-mimic and phospho-dead versions of SNAP33. Transformation of the *snap33* mutant with these mutated versions could potentially reveal some regulatory mechanisms. The phospho-variant versions of SNAP33 could, for instance, modify its interactions with its other SNARE partner. Finally, it would be interesting to investigate whether the SNAP33's SNARE partner SYP121/PEN1 is a genuine substrate of MPK3 and MPK6, as suggested by the study of Lassowskat et al. (2014). These investigations would also help to identify the regulations of the SNARE complex SYP121-SNAP33-VAMP721/722, which plays a key role in Arabidopsis immunity.

2.5.3. *SNAP33 is not involved in the same pathway as that of the MEKK1-MKK2-MPK4 MAPK module*

Given that *snap33*, *mekk1*, *mkk1 mkk2*, and *mpk4* mutants display similar phenotypes and that the transcriptome of *snap33-1* shows substantial overlap with that of *mpk4* and *mkk1 mkk2*, we tested whether the known suppressors of *mekk1*, *mkk1 mkk2*, and *mpk4*, namely *summ2-8* and *smn1*, might suppress the phenotype of *snap33-1*. Our results show that *summ2-8* and *smn1* do not revert the phenotype of *snap33-1* (figures 3.12 and 3.13), indicating that SNAP33 is not involved in the same pathways as those of the MEKK1-MKK2-MPK4 MAPK module. Given the results obtained by the generation of the *snap33-1 ndr1-1 eds1-2* triple mutant described in 1.6.4, which suggest that *snap33-1*'s phenotype is probably depending on several NLRs, it is not overall surprising to find that the single *smn1* and *summ2-8* mutations are not reverting the phenotype of *snap33-1*. However, the total absence of any suppression of *snap33-1* by *summ2-8* shows that SUMM2 is not involved at all in the *snap33-1*'s phenotype, neither directly (in the guard hypothesis) nor indirectly (by being one of the NLRs that might be activated by the SA overaccumulation in *snap33-1*), otherwise one could expect that the double mutant displays a slight reversion when compared to the *snap33-1* mutant. Such conclusions cannot be drawn yet on the *snap33-1 smn1* double mutant, as the results obtained on this double mutant need further analyses on a larger number of *snap33-1 smn1-1* plants.

Another hypothesis that fits the indirect regulation of SNAP33 by MAPKs and a potential genetic relationship between both components is that *SNAP33*'s expression might be regulated indirectly by MAPKs through transcription factors during immunity. Such a hypothesis can be investigated by analyzing the expression of *SNAP33* in the *mpk3*, and *mpk6* mutants and the

mpk4 summ2-8 double mutant, compared to that of the WT plants in response to biotic stress (flg22, for example). Such comparisons can also be performed in the *mpk3 mpk6 proMPK6::MPK6^{YG}* line to test whether *SNAP33*'s expression depends on the MAPKKK3/5-MKK4/5-MPK3/6 MAPK module in biotic stress context.

CHAPTER III - GENERAL CONCLUSIONS AND PERSPECTIVES

1. Summary of my results

The endomembrane system of plants plays a critical role in several aspects of plants' life, including growth and interaction with other organisms. However, our understanding of how it functions in plants remains limited. SNAREs, which mediate vesicle fusion to membranes, are presumably involved in all vesicle tethering events in plants and hence play a key role in plants. Mutation of *SNAP33*, a Qbc/SNAP25-like SNARE, induces severe lesions which spread into the whole plant, leading to its death and inability to reproduce. To better understand why, we first characterized the molecular phenotype of *snap33* mutants using staining experiments on three *snap33* allelic mutants, which revealed that the *snap33* mutants exhibit spontaneous cell death and H₂O₂ accumulation. We also found that MAPKs are over accumulating in the *snap33-1* mutant, which leads to a stronger activation pattern upon PAMP treatment. Transcriptomic analyses of the *snap33-1* mutant at 5 and 12 days of growth showed that it displays a spontaneous expression of defense genes as early as after 5 days of growth, and at 12 days, the mutant showed the over-expression of numerous NLR genes. We also analyzed the pathways responsible for the development of the *snap33-1*'s phenotype by crossing the *snap33-1* mutant with mutants impaired in hormone signaling and immune pathways. We found that it mainly depends on the SA pathway and NLR signaling by showing that the phenotype of *snap33-1* is almost completely reverted and partially reverted by mutations of these two pathways, respectively. Our results thus strongly suggest that SNAP33 is a guarded protein whose mutation leads to an ETI-like response.

Second, in an attempt to understand how SNAP33 is regulated during immunity, we investigated a potential relationship between SNAP33 and the MEKK1-MKK2-MPK4 module. Indeed, literature data and preliminary results obtained in our team suggested that SNAP33 and the MEKK1-MKK2-MPK4 MAPK module might interact and function together during immunity. However, we could not find an obvious relationship between SNAP33 and this MAPK module. In fact, we found that SNAP33 interacts with MEKK1, MKK2, and MPK4 only via BiFC experiments and not by Y2H, pull-down, and co-IP assays. Additionally, SNAP33 was not phosphorylated *in vitro* neither by MPK4 nor by MPK3 or MPK6, indicating that it is not a substrate of any of these proteins. Moreover, the crosses between *snap33-1* and known suppressors of mutants of the MAPK module did not revert the phenotype of *snap33-1*, showing that there is no genetic relationship between SNAP33 and the MEKK1-MKK2-MPK4

MAPK module. Therefore, our results suggest that SNAP33 and the MEKK1-MKK2-MPK4 MAPK module might not function together even though both are involved in immunity.

2. Perspectives

As our results strongly suggest that SNAP33 is a guarded protein, it would be interesting to identify the guarding NLR(s) and the putative effectors that target SNAP33. It could be performed, for instance, via the TurboID approach that I mentioned previously and by performing a Y2H screen using SNAP33 as bait against a library of effectors. In addition, identifying the interacting partners of SNAP33, in plants, in both resting and diverse stress conditions might lead to the identification of context-specific regulators of SNAP33, such as proteins kinases that might phosphorylate SNAP33. Indeed, several phosphorylation sites were identified on the SNAP33 protein.

It would also be interesting to identify the cargoes which are secreted by SNAP33. Such investigations can be performed by comparing the secreted cargoes in WT plants and those in the *snap33* mutant, by growing the two genotypes in liquid media and analyzing the proteins released in the media as previously performed on *syp121* and *syp122* (Waghmare et al., 2018). Ideally this experiment would be performed by comparing the secreted cargoes in the *snap33-1* mutant to those of a WT, the *syp121* mutant, and another auto-immune phenotype, such as *mpk4*, to identify the cargoes which are secreted specifically by SNAP33 (and not those secreted as a result of the auto-immune phenotype of *snap33*).

Finally, it was reported that overexpression of *GhSNAP33* or *CkSNAP33* in Arabidopsis increases resistance to the filamentous pathogen *Verticillium dahliae* (Wang et al., 2017, 2018). Additionally, Arabidopsis lines overexpressing *GhSNAP33* exhibited better tolerance to drought stress, and Arabidopsis lines overexpressing *CkSNAP33* displayed increased rosette size, indicating that *CkSNAP33* promotes growth in Arabidopsis. It would be interesting to validate these findings with AtSNAP33 and apply them to major crops, as this could have significant agricultural implications.

CHAPTER IV - MATERIALS AND METHODS

1. Materials

1.1. Plant material

The WT-1 line out-segregated from *snap33-1+/-* was used as a control for most of the experiments performed in this work. The Wassilewskija (Ws) WT ecotype was used as a control for some experiments, as indicated in CHAPTER II.2. The mutant lines used in this study are listed in Table 2

1.2. AGI number of the main genes

The AGI identifiers of the main genes used in this study are: *SNAP33* (AT5G61210), *SID2/ICS1* (AT1G74710), *COI1* (AT2G39940), *EIN2* (AT5G03280), *NPR1* (AT1G64280), *EDS1* (AT3G48090), *NDR1* (AT3G20600), *FMO1* (AT1G19250), *TN2* (AT1G17615), *AMSH3* (AT4G16144), *CPK5* (AT4G35310), *SUMM2* (AT1G12280), *SMN1/RPS6* (AT5G46470), *MEKK1* (AT4G08500), *MKK2* (AT4G29810), *MPK4* (AT4G01370), *MPK3* (AT3G45640), *MPK6* (AT2G43790), *SAND* (AT3G28390), *ACTIN2* (AT3G18780), *EDS5* (AT4G39030), *PBS3* (AT5G13320), *ALD1* (AT2G13810), *CBP60g* (AT5G26920), *SARD1* (AT1G73805), *PR1* (AT2G14610), *PR2* (AT3G57260), *PR4* (AT3G04720), *PAD4* (AT3G52430), *SAG101* (AT5G14930), *ADR1* (AT1G33560), *NRG1.1* (AT5G66900), *ACS6* (AT4G11280), *ORA59* (AT1G06160), *VSP1* (AT5G24780), *PDF1.2* (AT5G44420), *ERF1* (AT3G23240), *MAPKKK5* (AT5G66850), *MKK4* (AT1G51660), *WRKY33* (AT2G38470), *PAD3* (AT3G26830), *RBOHD* (AT5G47910), *RPS4* (AT5G45250), *BAK1* (AT4G33430), *BKK1* (AT2G13790), *SYP121* (AT3G11820), *SYP122* (AT3G52400), *VAMP721* (AT1G04750), *VAMP722* (AT2G33120).

1.3. Bacterial strains

Non recombined Gateway vectors were propagated in *Escherichia coli* (*E. coli*) DB3.1 strain (Invitrogen). Recombined Donor and Destination Gateway vectors, as well as regular cloning vectors, were transformed into DH5 α (Invitrogen). For protein purification, *E. coli* strains BL21 or Rosetta were used. For BiFC and co-immunoprecipitation (co-IP) experiments performed in *Nicotiana benthamiana* leaves, the strain GV3101 of *Agrobacterium tumefaciens* (*A. tumefaciens*) was used.

Table 2. Mutant lines used in this study

Mutant	Ecotype	Line or NASC stock	Reference
<i>snap33-1</i>	Col-0	SALK_075519	This work
<i>snap33-2</i>	Col-0	SALK_063806	This work
<i>snap33-3</i>	Col-0	GABI_094E01	This work
<i>snap33-4</i>	Col-0	SALK_119791	This work
<i>snap33-5</i>	Col-0	SALK_034227	This work
<i>snap33^{WS}</i>	Ws	EFS396	(Heese et al., 2001)
<i>sid2-2</i>	Col-0	Deletion	(Wildermuth et al., 2001)
<i>coi1-34</i>	Col-0	Substitution	(Acosta et al., 2013)
<i>ein2-1</i>	Col-0	Substitution	(Guzmán & Ecker, 1990)
<i>P35S:: NahG</i>	Col-0		(Lawton et al., 1995)
<i>npr1-1</i>	Col-0	Substitution	(Cao et al., 1994, 1997)
<i>eds1-2</i>	Col-0	Transposon insertion	(Bartsch et al., 2006)
<i>ndr1-1</i>	Col-0	Deletion	(Century et al., 1995)
<i>fmo1-1</i>	Col-0	SALK_026163C	(Bartsch et al., 2006)
<i>tn2-1</i>	Col-0	Substitution	(Zhao et al., 2015b)
<i>amsh3-4</i>	Col-0	Substitution	(Torsten Schultz-Larsen et al., 2018)
<i>cpk5-1</i>	Col-0	SAIL_657C06	(Boudsocq et al., 2010)
<i>snap33 Prom^{SNAP33}::myc-SNAP33</i>	WS		(Heese et al., 2001)
<i>summ2-8</i>	Col-0	SAIL_1152_A06	(Zhang et al., 2012)
<i>smn1-1</i>	Col-0	SALK_029541C	This work
<i>smn1-2</i>	Col-0	SALK_029328	This work
<i>smn1-3</i>	Col-0	SALK_204713C	This work

Table 3. Cloning primers

Gene	Experiment	Forward primer	Reverse primer
<i>SNAP33</i> AT5G6121 0	Cloning <i>SNAP33</i> 's coding sequence in pGENI vector	CATGCCATGGGATTTGGTTTA AGG	CCGCTCGAGCTTTCCAAGCA AACG
<i>SNAP33</i> AT5G6121 0	Cloning <i>SNAP33</i> 's coding sequence in pDONR207 vector	GGAGATAGAACCATGTTTGG TTTAAGGAAATCACCG	TCCACCTCCGGATCMCTTTC CAAGCAAACGGCGAC

1.4. Yeast strains

The yeast *Saccharomyces cerevisiae* (*S. cerevisiae*) was used for yeast two-hybrid experiments. Two strains, namely MaV103 strain (MAT α) and MaV203 strain (MAT α), were used for mating after being transformed with the adequate vectors (pDEST22 or pDEST32). MaV103 strain is leu2-3,112; trp1-901; his3 Δ 200; ade2-101; cyh2R; can1R; gal4 Δ ; gal80 Δ ; GAL1::lacZ; HIS3UASGAL1::HIS3@LYS2; SPAL10::URA3. MaV203 strain is leu2-3,112; trp1-901; his3 Δ 200; ade2-101; cyh2R; can1R; gal4 Δ ; gal80 Δ ; GAL1::lacZ; HIS3UASGAL1::HIS3@LYS2; SPAL10::URA3.

1.5. Growth media

1.5.1. Plant growth media

For *in vitro* growth, 1/2 MS solid or liquid media was prepared with Murashige Skoog Basal Salts (Sigma M6899), and 0.05% MES hydrate (Sigma M8250), pH was adjusted with KOH to 5.7 and 0.5% of agar (type E agar Sigma A4675) was added before autoclaving. For rosette weight analyses, the plants were grown on jiffy pots (Syngenta).

1.5.2. Bacteria and yeast growth media

For *E. coli* and *A. tumefaciens* growth, Luria Bertani (LB) medium containing 1% Bacto-tryptone, 0.5% NaCl, 0.5% Bacto-yeast extract and 1% NaCl was used. For solid medium 1% Bacto-agar was added before autoclaving. The adequate antibiotics were added after autoclaving and before bacteria plating. Yeasts were grown and mated on YPD media containing 1% yeast extract, 2% peptone, and 2% dextrose. Diploid yeasts were grown on YNB media containing yeast nitrogen base without amino acids 0.17% (SIGMA Y1251), 2% dextrose (SIGMA D9434), 0.5% (NH₄)₂SO₄ (SIGMA A4915), 0.2% of Drop out powder medium (US Biological, D9537), pH was adjusted to 5.6 with NaOH 5M. For solid media, 2% of bacto-agar (Fisher scientific, BD 214010) was added before autoclaving.

1.6. Vectors

The following vectors were used in this study:

pDONR207 Gateway® Donor vector (Invitrogen) used to clone genes into Gateway® Entry vectors. Gentamycin resistance.

pDEST22 Gateway® Destination vector (Invitrogen) for constitutive expression of chimeric proteins of interest in yeast. The sequence of interest is fused to the sequence of the Gal4 activation domain on its N-terminal part. Ampicillin resistance.

pDEST32 Gateway® Destination vector (Invitrogen) used for yeast two-hybrid assay. The plasmid allows the overexpression of chimeric proteins of interest in yeast. The sequence of interest is fused to the sequence of Gal4 DNA binding domain on their N-terminal part. This vector was modified to provide kanamycin resistance.

pDEST15 Gateway® Destination vector (Invitrogen) for production of recombinant proteins harboring an N-terminal GST-tag in *E. coli*. Ampicillin resistance.

pDEST17 Gateway® Destination vector (Invitrogen) for production of recombinant proteins harboring an N-terminal His-tag in *E. coli*. Ampicillin resistance.

pGENI a modified pET16b vector which carries an N-terminal poly-his TAG. pET16b was modified in a way that allows the production of either N-terminally his-tagged proteins or C-terminally STREP-tagged proteins, and was used to produce SNAP33-STREP recombinant protein (This vector was kindly provided by Dr. Emmanuelle Issakidis). Ampicillin resistance.

pGEX-6P-1 GST-Expression vector used for production of C-terminally GST-tagged proteins in *E. coli*. Ampicillin resistance.

pGWB6 Gateway compatible plasmid driving the expression of N-terminally GFP-tagged proteins under the control of the 35S promoter. Used for transient protein overexpression in *Nicotiana benthamiana* leaves in co-IP assays. Kanamycin resistance.

pGWB20 Gateway compatible plasmid driving the expression of a C-terminally MYC-tagged protein under the control of the 35S promoter. Used for transient protein overexpression in *Nicotiana benthamiana* leaves in co-IP assays. Kanamycin resistance.

pBIFC1 Gateway compatible split-YFP destination vector driving the expression of a protein N-terminally fused to the N-terminal moiety of YFP (YFP_n) under the control of the 35S promoter. Used for transient protein overexpression in *Nicotiana benthamiana* leaves in BiFC assays. Spectinomycin resistance.

pBIFC2 Gateway compatible split-YFP destination vector driving the expression of a protein C-terminally fused to the N-terminal moiety of YFP (YFP_n) under the control of the 35S promoter.

Table 4. Genotyping primers

Gene	Mutation/ insertion	Target	Forward primer (5' to 3')	Reverse primer (5' to 3')	Product size
<i>SNAP33</i>		WT allele	TGTTTTGGTTTCTGCAGGA AG	GATAAGCATCAGCTGATT CGG	1015 bp
<i>SNAP33</i>	<i>SALK_0755</i> 19 (<i>snap33-1</i>)	T-DNA insertion	ATTTTGCCGATTTTCGGAA C (LBb1.3-SALK)	GATAAGCATCAGCTGATT CGG	502 bp
<i>SNAP33</i>		WT allele	TCCTATAAATGGTCCCCT CG	CCCTTGATTGTAGCTGA GG	1089 bp
<i>SNAP33</i>	<i>SALK_0638</i> 06 (<i>snap33-2</i>)	T-DNA insertion	TCCTATAAATGGTCCCCT CG	ATTTTGCCGATTTTCGGAA C	1000 bp
<i>SNAP33</i>		WT allele	GACTGAACTCAGCACCCA GAG	ATTGATTGTCGAGTTTGTG GC	1107 bp
<i>SNAP33</i>	<i>GABI_094E</i> 01 (<i>snap33-3</i>)	T-DNA insertion	ATATTGACCATCATACTC ATTGC	ATTGATTGTCGAGTTTGTG GC	700 bp
<i>SNAP33</i>		WT allele	TTGGACTGCTGATGATGT CTG	TATCACATCGAAAAGATG CCG	1194 bp
<i>SNAP33</i>	<i>SALK_1197</i> 91 (<i>snap33-4</i>)	T-DNA insertion	ATTTTGCCGATTTTCGGAA C (LBb1.3-SALK)	TATCACATCGAAAAGATG CCG	511-811 bp
<i>SNAP33</i>		WT allele	AACAACAGTAACCCCCAA AGC	TCAAACATCGATTCAAA GGC	1147 bp
<i>SNAP33</i>	<i>SALK_0342</i> 27 (<i>snap33-5</i>)	T-DNA insertion	ATTTTGCCGATTTTCGGAA C (LBb1.3-SALK)	TCAAACATCGATTCAAA GGC	589-889 bp
<i>SID2</i>		WT allele	CAACCACCTGGTGCACCA GC	AAGCAAAATGTTTGAGTC AGCA	879 bp
<i>SID2</i>	<i>sid2-2</i> deletion mutation	Mutated allele	TTCTTCATGCAGGGGAGG AG	AAGCAAAATGTTTGAGTC AGCA	510 bp
<i>EDS1</i>		WT allele	TCAGGTATCTGTTATTTAT CATC	CCCTTTCTAGTTTCCTTGA GCTAAG	300 bp
<i>EDS1</i>	<i>eds1-2</i> Transposon insertion	mutated allele	TCAGGTATCTGTTATTTAT CATC	CCCTTTCTAGTTTCCTTGA GCTAAG	no amplification
<i>NDR1</i>		WT allele	GTGTGCCTACTGAGTCG	AGGTGAGACCAGCTGTG A	1300 bp
<i>NDR1</i>	<i>ndr1-1</i>	Deletion mutation	GTGTGCCTACTGAGTCG	AGGTGAGACCAGCTGTG A	400 bp
<i>EIN2</i>	<i>ein2-1</i>	substituti on	AGAGAGTTGGATGTAAA GTACTCTACGTCT	TCAAGGATCGCAGATAAG TGCTCC	470 bp sequenced or digested for dCAPS genotyping
<i>COI1</i>	<i>coi1-34</i>	substituti on	GATCTCTTTTGATTGGATG CAAGAACTCAGACGATA T	TCATATTGGCTCCTTCAG GACTCTAACAGTTG	494 bp sequenced or digested for dCAPS genotyping

Used for transient protein overexpression in *Nicotiana benthamiana* leaves in BiFC assays. Spectinomycin resistance.

pBIFC3 Gateway compatible split-YFP destination vector driving the expression of a protein N-terminally fused to the C-terminal moiety of YFP (YFPn) under the control of the 35S promoter. Used for transient protein overexpression in *Nicotiana benthamiana* leaves in BiFC assays. Spectinomycin resistance.

pBIFC4: Gateway compatible split-YFP destination vector driving the expression of a protein C-terminally fused to the C-terminal moiety of YFP (YFPn) under the control of the 35S promoter. Used for transient protein overexpression in *Nicotiana benthamiana* leaves in BiFC assays. Spectinomycin resistance.

1.7. Primers

1.7.1. Cloning primers

The primers used for SNAP33 cloning are listed in Table 3.

The primers used to clone MKK2, MPK3, MPK4, and MPK6 and the primers used to generate constitutively active versions of these proteins are described in Berriri et al., (2012) and Teige et al., (2004).

1.7.2. Genotyping primers

The primers used for plant genotyping are listed in Table 4.

1.7.3. Quantitative PCR primers

The primers used for RT-qPCR analyses are listed in Table 5.

1.7.4. RT PCR primers

The primers used for RT-PCR analyses are listed in Table 6.

1.8. Antibiotics

Antibiotics for bacteria/plasmid selection were used at the following concentrations in both liquid and solid media: kanamycin 50 µg/mL, gentamycin 10 µg/mL, ampicillin 50 µg/mL, spectinomycin 100 µg/mL.

<i>FMO1</i>		WT allele	CTTTTCGGTTGGACTTGG AAC	CTGCTTTGGACGTATCCT ACG	1039 bp
<i>FMO1</i>	<i>SALK_0261 63C (fmo1- 1)</i>	Mutated allele	ATTTTGCCGATTTCGGAA C (LBb1.3-SALK)	CTGCTTTGGACGTATCCT ACG	485-785 bp
<i>AMSH3</i>	<i>amsh3-4</i>	substituti on	ATTGTCCCAGATAATGCT ACCGGAGGCGGTGGCAA TCGTAATGGTA	ATCTGGCTTTGTGAAATG GTGC	470 bp sequenced or digested for dCAPS genotyping
<i>CPK5</i>		WT allele	TCGTCCAAATTGACCTT GAC	GAGGAAACAGCGGAGAG AGAC	986 bp
<i>CPK5</i>	<i>SAIL_657C0 6 (cpk5-1)</i>	Mutated allele	TTCATAACCAATCTCGAT ACAC	GAGGAAACAGCGGAGAG AGAC	500 bp
<i>TN2</i>	<i>tn2-1</i>	substituti on	AGGACCTTCATTAGCTTT CTTTACAAAGAACTCATT GAAATGGGAATT	CCAAATTGGTCAGAGCTT GTC	367 bp sequenced or digested for dCAPS genotyping
<i>SUMM2</i>		WT allele	AAGGTTTATGCATCAACG TGG	GAAACATGGTTTCACCTG CTC	1175 bp
<i>SUMM2</i>	<i>SAIL_1152_ A06 (summ2-8)</i>	Mutated allele	AAGGTTTATGCATCAACG TGG	TAGCATCTGAATTCATA ACCAATCTCGATACAC	598 bp
<i>NPR1</i>	<i>npr1-1</i>	substituti on	CTCGAATGTACATAAGGC	CGGTTCTACCTTCAAAG	293 bp sequenced or digested for dCAPS genotyping
<i>NahG</i>		Trangen ic lines overexpr essing NahG	ACTGGAActCTGCCGCTA	TGAGTTACTAGGGCGTGC	293 bp
<i>SMN1</i>		WT allele	TTCTTCCTCCTCCTTCT CG	CAAAACATCTCAAGAGCC AGC	1168 bp
<i>SMN1</i>	<i>SALK_0295 41C (smn1- 1)</i>		ATTTTGCCGATTTCGGAA C (LBb1.3-SALK)	CAAAACATCTCAAGAGCC AGC	553-853 bp
<i>SMN1</i>		WT allele	ATGGTCATGAGAGGTGTA CGC	AGAGCTCCTCAAAGGAA TGC	1047 bp
<i>SMN1</i>	<i>SALK_0293 28 (smn1- 2)</i>		ATTTTGCCGATTTCGGAA C (LBb1.3-SALK)	AGAGCTCCTCAAAGGAA TGC	505-805 bp
<i>SMN1</i>		WT allele	TGCAGAATTGTAACGAAT TGG	ATGGTCATGAGAGGTGTA CGC	1163 bp
<i>SMN1</i>	<i>SALK_2047 13C (smn1- 3)</i>		ATTTTGCCGATTTCGGAA C (LBb1.3-SALK)	ATGGTCATGAGAGGTGTA CGC	563-863 bp

1.9. Antibodies

1.9.1. Primary antibodies

Anti-pTpY Rabbit monoclonal antibody (Phospho-p44/42 MAPK (Erk1/2) (Thr202/Tyr204)), Cell Signaling (ref. 4370S)

Anti-myc Rabbit polyclonal antibody SIGMA (ref. C3956)

Anti-myc Mouse polyclonal antibody SIGMA (ref. M5546)

Anti-His Mouse monoclonal antibody SIGMA/Roche (ref. 11922416001)

Anti-GFP Mouse monoclonal antibody Roche (ref 11814460001)

Anti-MPK3 Rabbit polyclonal antibody SIGMA (ref. M8318)

Anti-MPK4 Rabbit polyclonal antibody (Davids Biotechnologie, Regensburg, Germany.)

Anti-MPK6 Rabbit polyclonal antibody SIGMA (ref. A7104)

Anti-GST Rabbit polyclonal antibody SIGMA (G7781)

Anti-HA Mouse monoclonal antibody SIGMA (A2095)

1.9.2. Secondary antibodies

Anti-rabbit Goat polyclonal antibody conjugated to peroxidase SIGMA (ref. A6154)

Anti-mouse Goat polyclonal antibody conjugated to peroxidase SIGMA (ref. A5906)

2. Methods

2.1. Plant methods

2.1.1. Plant growth

Plants used for protein or RNA analyses were grown *in vitro* on ½ MS solid media in growth rooms on long day conditions: 16 hours light, 8 hours dark, 60% humidity, 23°C. The plants were transferred to ½ MS liquid media one day prior to harvesting in case of stress treatment. The flg22 and elf18 treatments were performed at a final concentration of 100 nM diluted in liquid ½ MS media.

Multiplication and plant crossings were grown in the greenhouse under long-day conditions (16h light, 8h darkness, 22-24°C).

Table 5. RT-qPCR primers

Gene	AGI number	Forward primer (5' to 3')	Reverse Primer (5' to 3')
<i>SAND</i>	AT2G28390	AACTCTATGCAGCATTTGATCCACT	TGATTGCATATCTTTATCGCCATC
<i>ACTIN2</i>	AT3G18780	CGTTTCTATGATGCACTTGTGTG	GGGAACAAAAGGAATAAAGAGG
<i>PR1</i>	AT2G14610	GATCCTCGTGGGAATTATGTG	TTCTCGTAATCTCAGCTCTTATTG
<i>PR2</i>	AT3G57260	ATCGTTGGAAATCGTGGTGT	CCTTCTCGGTGATCCATTCT
<i>PR4</i>	AT3G04720	CGTGAGTGCTTATTGCTCCA	ATACTTGCTCCGCCATGC
<i>ERF1</i>	AT3G23240	GATGGTTGTTCTCCGTTGT	ACCCAAAAGCTCCTCAAGGT
<i>PDF1.2</i>	AT5G44420	TTTGCTGCTTTCGACGCAC	TAACATGGGACGTAACAGATA

Table 6. RT-PCR primers

Gene	ATG number	Forward primer (5' to 3')	Reverse Primer (5' to 3')
<i>SNAP33</i>	AT5G61210	CTTGGGTCGTTCTGAGTCGTC	CCACGTTGGTTTGATTGTTGC
<i>SMN1</i>	AT5G46470	AGAGCTCCTTCAAAGGAATGC	AGTAGTCTCATCCTCATCATCC
<i>ACTIN2</i>	AT3G18780	CGTTTCTATGATGCACTTGTGTG	GGGAACAAAAGGAATAAAGAGG
<i>SAND</i>	AT2G28390	AACTCTATGCAGCATTTGATCCACT	TGATTGCATATCTTTATCGCCATC

To take representative pictures of all the generated genotypes and for staining assays, plants were grown on Trigard (Syngenta) treated soil (Jiffy) in Percival plant growth chambers (PlantClimatics) on long-day conditions, 16h light, 8h dark, 60% humidity, 20°C. Double and triple mutants were generated by crossing and were genotyped with the appropriate oligonucleotides listed in Table 4

2.1.2. *Hormone quantification*

JA, SA and SAG quantification

For each sample, 1.5 mg of dry powder were extracted with 0.8 ml of acetone/water/acetic acid (80/19/1 v:v:v). SA and JA stable labeled isotopes used as internal standards were prepared as described in le Roux et al. (2014). 1 ng of each standard was added to the sample. The extract was vigorously shaken for 1min, sonicated for 1 min at 25 Hz, shaken for 10 min at 10°C in a Thermomixer (Eppendorf®), and then centrifuged (8000xg, 10 °C, 10 min). The supernatants were collected, and the pellets were re-extracted twice with 0.4 ml of the same extraction solution, then vigorously shaken (1 min) and sonicated (1 min, 25 Hz). After the centrifugations, the three supernatants were pooled and dried (Final Volume 1.6 ml). Each dry extract was dissolved in 100 µl of acetonitrile/water (50/50 v/v), filtered, and analyzed using a Waters Acquity ultra-performance liquid chromatograph coupled to a Waters Xevo Triple quadrupole mass spectrometer TQS (UPLC-ESI-MS/MS). The compounds were separated on a reverse-phase column (Uptisphere C18 UP3HDO, 100*2.1 mm*3 µm particle size; Interchim, France) using a flow rate of 0.4 ml min⁻¹ and a binary gradient: (A) acetic acid 0.1 % in water (v/v) and (B) acetonitrile with 0.1 % acetic acid, the column temperature was 40 °C, the following binary gradient was used (time, % A): (0 min, 98 %), (3 min, 70 %), (7.5 min, 50 %), (8.5 min, 5 %), (9.6 min, 0%), (13.2 min, 98 %), (15.7 min, 98 %). Mass spectrometry was conducted in electrospray and Multiple Reaction Monitoring scanning mode (MRM mode), negative ion mode. Relevant instrumental parameters were set as follows: capillary 1.5 kV (negative mode), source block, and desolvation gas temperatures 130 °C and 500 °C, respectively. Nitrogen was used to assist the cone and desolvation (150 l h⁻¹ and 800 l h⁻¹, respectively), argon was used as the collision gas at a flow of 0.18 ml min⁻¹.

ET quantification

Ethylene measurements were performed as described by Thain et al. (2004) with the following adjustments. Seeds from each genotype were sterilized and sown in vitro for 12 days. From

Table 7. protoplasts' isolation and transformation solutions

Enzymatic solution		
	Stocks concentration	Final concentration
H ₂ O (qsp)		
MES pH 5.7	200mM	20mM
KCL	2M	20mM
Mannitol	0.8M	400mM
heated for few minutes at 70°C		
Cellulase (w/v, Yakult)		1.5%
Macerozyme (w/v, Yakult)		0.4%
Heated for 5 minutes at 55°C		
Cooled at room temperature		
BSA	10%	0.1%
CaCl ₂	1M	10mM
filtered with a 0.45 µm filter		

MMG solution		
	Stocks concentration	Final concentration
H ₂ O (qsp)		
MES pH 5.7	200mM	4mM
Mannitol	0.8M	400mM
MgCl ₂	2M	15mM
filtered with a 0.45 µm filter		

W5 solution		
	Stocks concentration	Final concentration
H ₂ O (qsp)		
MES pH 5.7	200mM	20mM
NaCl	5M	154mM
CaCl ₂	1M	152mM
KCL	2M	5mM
filtered with a 0.45 µm filter		

WI solution		
	Stocks concentration	Final concentration
H ₂ O (qsp)		
MES pH 5.7	200mM	4mM
Mannitol	0.8M	500mM
KCl	2M	20mM
filtered with a 0.45 µm filter		

PEG solution		
	Stocks concentration	Final concentration
H ₂ O (qsp)		
PEG (sigma 81240)		40% (w/v)
Mannitol	0.8M	0.2M
CaCl ₂	1M	50mM

each genotype, four 12-day-old plants were incubated in impermeable airtight vials for 24 hours in darkness and at 23°C to allow ethylene accumulation. The vials were then flushed with hydrocarbon free air (Air liquid) at a flow rate of 3 L.h⁻¹, and ethylene emission was measured with a photo-acoustic detector ETD-300 in combination with a gas handling system. The ETD-300 is a state-of-the-art ethylene detector based on laser photoacoustic spectroscopy.

2.1.3. BiFC experiments

BiFC experiments were performed as described by Sparkes et al., (2006). Transformed *Agrobacterium* cells were incubated overnight at 28°C in LB liquid media with antibiotics (spectinomycin pBiFC). The cells were then pelleted (1000 g, 10 min) and resuspended in infiltration media containing 5 mg/ml of D-glucose, 50 mM MES, 2 mM Na₃PO₄·12H₂O, and 0.5 mM Acetosyringone. After resuspension, the cells were washed again with the infiltration media to remove residual antibiotics via centrifugation at 1000 g for 10 min at room temperature. Bacterial suspensions at OD₆₀₀ of 0.2 were used for split-YFP experiments. The bacterial suspensions were inoculated using a 1 ml syringe without a needle by gentle pressure on the lower epidermal surface. Agro-infiltrated plants were incubated under normal growth conditions for 2-5 days at 22–24 °C. Microscopic observations were made using a Carl Zeiss LSM880 laser scanning confocal microscope using a 40x lens.

2.1.4. Stainings

Trypan blue staining

For trypan blue staining, 20-day-old seedlings were immersed in a trypan blue solution containing 0.02% trypan blue powder (SIGMA ALDRICH T6146), 33.3% lactic acid, 33.3% phenol, and 33.3% glycerol, all diluted in ethanol 100%. For staining, the samples were boiled at 95°C for 3 min, then washed with a 2.5 g/ml solution of chloral hydrate with gentle agitation for 4 to 6 hours to remove the dye. Afterward, the samples were stored in 50% glycerol and analyzed using LEICA MZ16F binocular.

DAB staining

DAB staining was performed as described in Daudi & O'Brien, (2012) to detect hydrogen peroxide. Seedlings were immersed in DAB solution containing 0.1% of DAB powder (Ref. D8001), 0.05% tween, and 10 mM Na₂HPO₄. Vacuum infiltration was applied for 5 min for efficient staining. The samples were then incubated at dark on shaking for 4 to 5 hours.

Table 8. PCR mix

Reagent	Volume (μl) for 1 reaction in a total 15 μl volume	Final concentration
Taq buffer (10x)	1.5	1X
dNTP mix (4x 25 mM)	0.07	4x 0.117 mM
Forward (10 μ M)	0.3	0.2 μ M
Reverse (10 μ M)	0.3	0.2 μ M
Taq DNA Polymerase	1	0.2 units/ μ L
MilliQ water	10.83	
DNA	2	

Following incubation, the samples were boiled with ethanol: acetic acid: glycerol 3:1:1 solution for bleaching. The samples were then stored in 50% glycerol before imaging. The samples were analyzed using LEICA MZ16F binocular.

2.2. Protoplast methods

2.2.1. *Protoplast's isolation*

To isolate protoplasts, rosette leaves were cut into thin strips using a scalpel. The strips were then immersed in an enzymatic solution (Table 7) for half an hour under vacuum to promote tissue infiltration by the enzymes and 2.5 hours without vacuuming and on dark conditions during the whole time.

To recover the protoplasts, a volume of W5 (Table 7) solution was added to the enzymatic-protoplasts solution. After gentle homogenization, the solution was filtered through a filtering cloth (35-75 μm). The protoplasts were then centrifuged for 2 minutes at 100xg at room temperature with a deceleration of 1. The supernatant was gently withdrawn to avoid aspirating or disturbing the protoplasts. The protoplasts were resuspended in 4 ml of W5 solution, and their concentration was measured using a hemacytometer. While waiting to be transformed, the protoplasts were incubated on ice to sediment. The protoplast pellet was then resuspended in the solution of MMG to get a final concentration of $2\text{-}4 \cdot 10^5$ protoplasts /ml.

2.2.2. *Protoplast's transformation*

The transformation of protoplasts was carried out by successively adding to a tube of 2ml 20 μg of DNA, $2\text{-}4 \cdot 10^5$ protoplasts (carefully collected with a cut cone), and 220 μl of PEG solution (Table 7). To homogenize the mix, the tubes were gently tapped at the bottom. After 5 minutes of incubation, 880 μl of W5 solution was added and gently mixed to trigger the transformation. The tubes were centrifuged for 2 minutes at 100xg at room temperature with a deceleration of 1. The supernatant was removed, and the protoplast pellet was resuspended in the W1 solution (Table 7). Transformed protoplasts were incubated in a growth chamber overnight to allow gene expression. The protoplasts were then collected by 20 s 10000xg centrifugation, the supernatant was removed using a syringe, and the pellets were stored at -80°C .

Table 9. Enzymes used for dCAPS analyses

Mutant	Restriction enzyme	Point mutation	Result
<i>coi1-34</i>	NsiI	G1324 => A (CDS)	494 bp amplicon- the WT allele amplicon is digested into 41 + 453 bp fragments
<i>ein2-1</i>	BsmAI	C1666 => T (CDS)	401 bp amplicon- the WT allele amplicon is digested into 369 + 32 bp fragments
<i>npr1-1</i>	NlaIII	C3865 => T (FLG)	293 bp amplicon- the WT allele amplicon is digested into a 199 + 94 bp fragments
<i>amsh3-4</i>	KpnI	C3529 => T (FLG)	470 bp amplicon- the WT allele amplicon is digested into a 47 + 423 bp fragments
<i>tn2-1</i>	EcoRI	C182 => T (FLG)	367 bp amplicon- the WT allele amplicon is digested into 44 bp + 323 bp fragments

CDS = coding sequence

FLG = full-length genomic sequence

2.3. Bacteria methods

2.3.1. Bacterial transformation

a volume of 100 µl of thermo-competent cells was mixed with 100 ng of plasmid DNA and incubated on ice for ten minutes. Bacteria were then heat shocked for 90 seconds at 42°C on a water bath and immediately moved on ice for an additional ten minutes. 900 µl of LB was added, and the mix was incubated for 1 hour at 37°C with gentle shaking. The mix was then centrifuged at 4000 g to pellet the cells. The cells were resuspended in 30~40 µl of liquid LB and plated on LB solid media supplemented with the appropriate antibiotics and incubated overnight at 37°C.

2.3.2. *Agrobacterium* transformation

40 µl of thermo-competent *Agrobacterium tumefaciens* cells were mixed with 100 ng of plasmid DNA and incubated on ice for ten minutes. The cells were incubated for 5 minutes on liquid nitrogen, 3 min at 37°C, followed by 2 more minutes on liquid nitrogen, 3 minutes at 37°C, and then were immediately transferred on ice for 5 minutes. 900 µl of LB was added, and the mix was incubated for 4 hours at 28 °C under shaking. Next, the mix was centrifuged at 4000 g to pellet the cells, and the cells were resuspended in 30~40 µl liquid LB and plated on LB solid media supplemented with the appropriate antibiotics and incubated overnight at 28°C.

2.4. Yeast methods

2.4.1. Yeast transformation

Overnight MaV203 and MaV103 yeast cultures from single colonies were diluted to get an $OD_{600} = 0.3$ in 50 ml final volume of liquid YPD media and incubated for an additional 3 hours at 30°C. Next, the cells were pelleted and washed with 25 ml of sterilized deionized water and resuspended in 2 ml of a solution containing 1x LiAc 1x TE (10x LiAc is 1 M of LiAc; 10x TE buffer containing 100 mM of Tris pH 7.5 and 10 mM of EDTA). The cells were incubated at RT for 10 min. For yeast transformation, 100 µl of previously prepared cells were mixed with 1 µg of plasmid DNA (pDEST22 for GAL4-AD fusion or pDEST32 for GAL4-BD fusion), 10 µl of salmon sperm (10 mg/ml) and 700 µl of a mix containing 1x LiAc 1x TE 40% PEG. The mixture was incubated at 30°C for 30 minutes, 85 µl of DMSO was added before proceeding to heat shock at 42°C for 7 minutes. Afterward, the cells were washed with 1 ml of TE 1x and resuspended in

0.5 ml of TE 1x. Finally, the cells were spread on solid YNB medium lacking tryptophan (for MaV203) or leucine (for MaV103 cells). All washing steps were performed by centrifugation at 2500 rpm to pellet the cells.

2.4.2. Yeast two-hybrid (Y2H) analysis for protein-protein interaction

Colonies from transformed MaV103 and MaV203 were mixed with 200 ml of YPD and incubated overnight at 30°C to allow mating. Diploids cells were diluted 200 times in water, and 5 µL droplets were spotted on agar plates containing selective medium lacking leucine, tryptophane, and histidine and supplemented with 20, 30, or 40 mM of 3-AT (3-Amino-1,2,4-triazole). Growth was monitored during one week at 30°C.

2.5. DNA methods

2.5.1. Plasmid DNA isolation

NucleoSpin Plasmid Mini kit for plasmid DNA extraction (MARCHERY NAGEL) was used to isolate plasmid DNA from bacteria. Extraction yields were quantified using a NanoDrop spectrophotometer (Thermo Scientific).

2.5.2. Plant DNA extraction for genotyping

The method for extracting plant DNA is adapted from Edwards et al., (1991). To begin, 96-well plates were prepared by placing an iron bead into each well. Each plant was picked for approximately half a leaf. The plate was then immersed in liquid nitrogen to freeze the leaves. Next, the frozen tissues were ground for one minute at 20 Hz with a tissue lyser (Tissue-lyser II, Qiagen). The plate was centrifuged for one minute at 2500 rpm to pellet the leaf powder. 300 µl of DNA extraction buffer containing 200 mM Tris-HCl pH 7.5, 250 mM NaCl, 25 mM EDTA, and 0.5% SDS was added. After homogenization by shaking with the tissue lyser (15Hz) for 4 minutes, the plate was centrifuged for 5 minutes at 4000rpm to pellet plant debris. To precipitate DNA, 75 µl of each supernatant was transferred to a 96-well PCR plate containing 75 µl of isopropanol. The plate was incubated at room temperature for 5 min and then centrifuged at 4000rpm for 1 hour to pellet the DNA. After removing the isopropanol, the plate was dried for 40 minutes at 37°C. Finally, the DNA was resuspended in 100 µl of sterile deionized water by 30 minutes incubation at 37°C.

2.5.3. *PCRs*

Genotyping PCRs were carried out using either a house-produced Taq DNA polymerase or the Terra Taq (TAKARA, Cat #639270). PCR mix for plant genotyping using house-produced Taq DNA polymerase is shown in Table 8.

Taq buffer 10x contains 100 mM Tris-HCl pH 7.9, 25 mM MgCl₂, 500 mM KCl and 0.5% NP-40. The PCR program starts with a five-minute denaturation step at 94°C, then 35 to 40 cycles of denaturation at 94°C during 30 sec; 30 sec of annealing at 55°C (± 5°C); elongation at 72°C (1 min/kb for House Taq)). Finally, a 7 minutes extension step at 72°C.

2.5.4. *dCAPS genotyping*

For point mutations, the mutated allele was genotyped via derived cleaved amplified polymorphic sequence analysis (dCAPS) after amplification with genotyping primers listed in Table 4. The restriction enzymes used for mutants genotyped by dCAPS are listed in Table 9.

2.5.5. *Cloning PCRs*

High-fidelity DNA polymerase (Bio-Rad, ref. 172-5331) was used for PCRs intended to clone genes of interest. gDNA and cDNAs produced from the Col-0 Arabidopsis ecotype were used, respectively, as a template for locus cloning or coding sequences. The PCRs were performed according to the supplier's instructions, and the oligonucleotides are described in Table 3.

2.5.6. *DNA migration*

For electrophoresis, 1 to 2.5% agarose (SeaKem LE Agarose, Lonza) was dissolved in 0.5x TAE buffer (AccuGENE; 50x TAE contains 2 M of Tris-acetate and 0.05 M EDTA, Lonza). Then 0.5 µg/ml of ethidium bromide (Mobio) was added to the mix. PCR products were diluted with 4x DNA loading dye (30% (v/v) glycerol. 0.25% (w/v) bromophenol blue) before loading. DNA ladders from New England Biolabs were used as DNA size standards. Running was carried out at 100-150 V constant. DNA migration was visualized under UV light (AlphaMager, ProteinSimple).

2.5.7. *DNA digestion*

Restriction enzymes were purchased from New England Biolabs. DNA digestion was used on backbones to verify cloning and for the detection of plants carrying Single Nucleotide

Polymorphisms using dCAPS (2.4.4) for genotyping. DNA digestions were performed according to the supplier's instructions.

2.5.8. DNA sequencing

DNA sequencing was performed by the Sequencing Service of Eurofins.

2.5.9. Cloning

Gateway® cloning – BP reaction

Gateway® BP recombination reactions were performed with enzymes from Invitrogen (ref. 11789-100) according to the supplier's instructions to clone genes in Gateway® pDONR207.

Gateway® cloning – LR reaction

Gateway® LR recombination reactions were performed with enzymes from Invitrogen (ref. 11791-100) according to the supplier's instructions to clone genes in Gateway® pDEST22, pDEST32, pDEST15, pDEST17, pBIFC1, 2, 3, 4, and pGWB6 and 20 vectors. Reactions were performed overnight at 25°C in 5 µL final volume.

Creation of pGENI vector for SNAP33-STREP recombinant protein production

I first amplified the SNAP33 coding sequence using the primers listed in Table 3. The forward and reverse primer added an NcoI restriction site to the N-terminal sequence of SNAP33, and an XhoI restriction site to the C-terminal end of the same sequence, respectively. Next, the amplified sequence of SNAP33 and the pGENI vector were both digested with NcoI and XhoI according to the manufacturer's instructions. The two generated DNA fragments were extracted from agarose gels after running using Qiaquick Gel Extraction kit (Qiagen, Ref.28707) and ligated using T4 DNA ligase (Sigma-Aldrich, Ref. [D2886](#)) according to the manufacturer's instructions.

2.6. RNA methods

2.6.1. RNA isolation

RNA extraction was performed on ground plant material using NucleoSpin RNA Plus, Mini kit for RNA purification with DNA removal column (MARCHERY NAGEL, Ref. 740984.50) according to the manufacturer's instructions. The extracted RNA's concentration was measured by NanoDrop spectrophotometer (Thermo Scientific).

2.6.2. *cDNA synthesis*

For reverse transcription, 500 ng to 3 µg of RNA were mixed with 1 µl of Oligo-(dT) (500µg/ml) primers and 1 µl of 10 mM dNTP mix. The mix was incubated for 5 minutes at 65°C for primers annealing and chilled quickly on ice. Next, 4 µl of 5x First-Strand Buffer, 2 µl of DTT 0.1 M and 1 µl of RNaseOUT (40 UNITS; ThermoFisher 10777-019) were added and incubated at 42°C for 2 minutes. 1 µl of SUPERSCRIPT II RT (200 UNITS; ThermoFisher 18064-022) was added, and water was added to a final volume of 20 µl. The mixture was incubated for 50 minutes at 42°C to allow cDNA synthesis, and then the reaction was inactivated by heating at 70°C.

2.6.3. *Quantitative PCRs*

RT-qPCR analyses were performed with TB Green Premix Ex Taq II (TAKARA, Cat. #RR820A). 10 ng of cDNA were mixed with 4 µL of TB Green Premix Ex Taq II 2x solution and with 2 µL of Forward and Reverse primers mix (400 nM final concentration for each primer) in an 8 µl final volume. Each sample was run in triplicate. The following PCR program was used: 95°C for 30 sec; 40 × [95°C for 5 sec and 60°C for 20 sec]. qPCR reactions were carried out in CFX384 Touch Real-Time PCR (Biorad) and analyzed with CFX Manager Software (Biorad).

2.6.4. *Transcriptomic analyses*

RNA-sequencing experiments were performed on 5-day-old and 12-day-old *snap33-1* and WT-1 plants grown on ½ MS solid media prepared with Murashige Skoog Basal Salts (Sigma M6899) and 0.05% MES hydrate (Sigma M8250), pH adjusted with KOH to 5.7, and 0.5% of agar (type E agar Sigma A4675) added before. Plants were grown at 23 °C, 60% humidity, and in long-day photoperiod conditions (18 hours light and 6 hours dark).

Each sample is composed of at least 35 seedlings. Total RNA was extracted using NucleoSpin® RNA Plus, RNA isolation kit (Marchery Nagel) according to the supplier's instructions and was further purified using the RNA Clean & Concentrator Kits (Zymo Research®, California, U.S.A.). RNA-seq libraries were constructed by the POPS platform (IPS2) using the QuantSeq 3' mRNA-Seq library prep kit (LeXogen®, for illumina) with UMI (T. Smith et al., 2017) according to the supplier's instructions. The libraries were sequenced in single-end (SE) mode with 150 bases for each read on a NextSeq500 to generate between 10.9 and 14.4 million reads per sample. UMIs were removed and appended to the read identifier with the extract command of UMI-tools (v1.0.1,(T. Smith et al., 2017)). Reads, where any UMI base quality score falls below 10,

were removed. To remove adapter sequences, poly(A), poly(G) sequences, and low quality nucleotides reads were trimmed with BBduk from the BBmap suite (v38.84, (Bushnell, 2014)) with the options `k=13 ktrim=r useshortkmers=t mink=5 qtrim=r trimq=10 minlength=30`. Trimmed reads were then mapped and counted using STAR (v2.7.3a, Dobin et al. 2013), with the following parameters `--alignIntronMin 5 --alignIntronMax 60000 --alignMatesGapMax 6000 --alignEndsType Local--outFilterMultimapNmax 20 --outFilterMultimapScoreRange 0 --outSAMprimaryFlag AllBestScore --mismatchNoverLmax 0.6` on the *Arabidopsis thaliana* genome reference (TAIR10+ARAPORT11+MtCol0). Reads with identical mapping coordinates and UMI sequences were collapsed to remove PCR duplicates using the `dedup` command of UMI-tools with the default directional method parameter. RSeQC (v2.6.6; (Wang et al., 2012)) was used to evaluate deduplicated mapped reads distribution. Deduplicated reads were counted using HTSeq version (v0.12.4.; (Anders et al., 2015)) (HTseq-count mode intersection-nonempty) based on the *A. thaliana* TAIR10-ARAPORT11 annotation. Between 88,4 and 90.7% of the reads were associated with annotated genes. Differential expression analysis was performed using the Bioconductor packages edgeR (v 3.26.8; (Robinson et al., 2010)). We excluded genes with low expression levels and examined those with at least 0.6 counts per million in at least 3 samples. Counts were normalized using the TMM method (edgeR). The differential analysis was based on a negative binomial generalized log-linear model (GLM), where the log of the gene expression was modeled by the 2 biological factors describing the experiment and the technical replicate factor. An interaction term between the biological factors genotype and collection date was included in the model. The distribution of the resulting p-values followed the quality criterion described by Rigai et al., (2018). Genes with an adjusted p-value (FDR, Benjamini-Hochberg adjustment (Benjamini & Hochberg, 1995)) below 0.05 were considered as differentially expressed.

2.7. Protein methods

Protein extraction methods were performed on frozen crushed samples stored at -80°C.

2.7.1. Native protein extraction

About 150 mg of frozen plant powder were resuspended in 200 µL of native protein extraction buffer containing 50 mM Tris-HCl pH 7.5, 150 mM NaCl, 0.1% NP40, 5 mM EGTA, 0.1 mM DTT, protease inhibitors (Complete cocktail (Roche), and phosphatase inhibitors: 1 mM NaF, 0.5 mM

Na₃VO₄, 15 mM B-glycerophosphate, and 15 mM 4-nitrophenyl phosphate. After gently homogenizing the mixture with a pipet, it was centrifuged at 20000 g for 15 minutes at 4°C, and the supernatant (150 L) was collected and maintained on ice. After quantification (2.6.2), the concentrations were adjusted to 1 µg/µl and mixed with 1x Laemmli for denaturation at 95°C for 10 min before sodium dodecyl sulfate-polyacrylamide gel electrophoresis (SDS-PAGE). The Laemmli buffer contains 80 mM Tris pH 6.8, 0.1 M DTT, 10% Glycerol, and 0.004% bromophenol blue.

2.7.2. *Bradford protein dosage*

For Bradford protein quantification, a BSA standard range was prepared from 0.5 to 2.5 µg / 10 µl (Thermo Scientific). Protein quantification was performed in a 96-well Elisa plate, 10 µl of each diluted sample (diluted 20 times) and of the BSA standard were loaded to the wells and mixed with 250 µl of Bradford reagent (Sigma Aldrich). Measurements were taken using TECAN reader, and the samples were normalized (diluted with appropriate extraction buffer) to 1 µg/µL. Normalized protein extracts were then mixed with Laemmli buffer (1X final concentration) and incubated at 95°C for 10 minutes before SDS-PAGE.

2.7.3. *Recombinant protein expression and purification*

For recombinant protein expression, the appropriate plasmid was multiplied in *E. coli* cells. The bacteria carrying the plasmids were first multiplied by incubation on LB media containing the appropriate antibiotics at 37°C until the preparation reached an OD₆₀₀ of 0.6 to 0.7. Next, protein production was induced by adding 0.2 mM of IPTG, and the culture was incubated at 20°C for 20 hours for maximum yield. Prior to the purification of the generated proteins, the cells were pelleted at 4°C, 5000 g (20 min) to remove any remaining LB and kept at -20°C.

His and GST-tagged protein purification

Pellets from 200 ml of bacterial culture were mixed with 18 ml of 1x PBS buffer containing 140 mM NaCl, 2.7 mM KCl, 10 mM Na₂HPO₄, and 1.8 mM KH₂PO₄, at pH 7.3 adjusted with HCl, supplemented with 1% triton and 1x anti-protease Cocktail (Roche). After homogenization, the mixture was incubated on ice for 20 minutes with 1 ml of lysozyme (10 mg/ml) to disrupt bacterial membranes. Then 124 µl of DTT 400 mM and 1% of N-Lauroylsarcosine were added. Next, the mixture was subjected to 4 sonication steps (ice power 5, frequency duty 50%) of 1 min each to disrupt bacterial cell membranes further. Afterward, the mixture was centrifuged

at 8000 g for 10 minutes at 4°C to pellet bacterial debris, and the cleared lysate was collected for protein purification. Ni-Resin (Thermo Scientific) beads were used for His-tagged proteins, and Glutathione Sepharose beads (Macherey-Nagel) were used for GST-tagged proteins. Washed beads (with PBS 1x) were added to the mixture and incubated for 1 hour at 4°C for binding by gentle shaking on a rotating wheel.

For His-tagged proteins, the cleared lysate was loaded on the Ni-Resin column to bind proteins, and then the column was washed 4 times with 2 ml of wash buffer containing PBS 1x and 10 mM of imidazole. Next, bound proteins were eluted with a buffer containing PBS 1x, 200 mM of imidazole, and 10% glycerol.

For GST-tagged proteins, 500 µl of beads were added to the cleared lysate, and the mixture was incubated at 4°C on gentle shaking for 1 hour. After that, the beads were washed 4 times, dried and incubated for 10 min at 4°C with 200 µl of reduced Glutathione 20 mM pH 8 (in 1 M Tris pH 10 buffer) to elute bound proteins. After centrifuging, the supernatant containing the eluted proteins was kept. The elution was repeated twice for maximum yield.

STREP-tagged protein purification

For Strep-tagged proteins, the pellets of 100 ml of bacterial culture were resuspended in 1 ml of a wash buffer containing 100 mM Tris/HCl pH 8, 150 mM NaCl, and 1 mM EDTA. The cells were sonicated about 4 times at power 5 and centrifuged at 13000rpm for 15 minutes at 4°C. Meanwhile, 200 µl Strep-Tactin® (IBA-life sciences) columns were prepared by two washing steps using 200 µl of wash buffer. Next, the previously prepared lysate was loaded to the column for protein binding, and the column was washed 5 times (wash buffer). Protein elution was carried out 5 times by adding an elution buffer containing 100 mM Tris/HCl pH 8, 150 mM NaCl and 1 mM EDTA, and 2.5 mM desthiobiotin to the column.

For each purification (STREP, GST, and His-tagged proteins), small aliquots (10~20 µl) were retrieved from each elution and washing steps to ensure that the purification proceeded as planned and to estimate the concentration of the eluted proteins with BSA standards on Coomassie blue-stained (0.75% Coomassie R250, 20% EtOH, 10% acetic acid) SDS-PAGE gels. Immunoblotting was also performed to ensure that the protein was purified.

Protein dialysis

After purification of proteins of interest using the methods presented above, the eluted proteins were subjected to dialysis to remove unwanted molecules and replace them with 30

mM Tris HCl and 20% glycerol buffer. To do that, Slide-A-Lyzer G2 Dialysis Cassettes from ThermoScientific (Ref. 87718) were used according to the manufacturer's instructions.

2.7.4. Co-immunoprecipitation assays for protein-protein interactions

For co-immunoprecipitation analyses conducted on *snap33 Prom^{SNAP33::myc-SNAP33}* lines, about 150 mg of frozen-crushed plant powder were resuspended in 200 μ L of native protein extraction buffer containing 50 mM Tris-HCl pH 7.5, 150 mM NaCl, 0.1% NP40, 10% glycerol, protease inhibitors (complete EDTA-free cocktail (Roche), 1 mM PMSF, and phosphatase inhibitors (1 mM NaF, 0.5 mM Na₃VO₄, 15 mM B-glycerophosphate and 15 mM 4-nitrophenyl phosphate). The suspension was centrifuged at 16000 g for 15 min at 4 °C, and the supernatant (150 μ L) was collected and kept on ice while determining protein concentration by Bradford protein dosage assay. 60 μ g of total proteins was denatured with 12 μ L of 6X Laemmli buffer and kept for input controls. 400 μ g of total proteins were used for immunoprecipitations. Immunoprecipitations were carried out by adding 2 μ L of the anti-myc antibodies to the extract. The mixture was then incubated for one hour at 4°C on gentle shaking on a rotating wheel to allow antibodies binding (10 rpm). For purification, 20 μ L of A-protein Sepharose beads were added to the sample and incubated for an hour at 4°C on gentle shaking on a rotating wheel (10 rpm). Next, the beads were pelleted by centrifugation at 1000xg 4°C for 1 minute and washed 3 times using 400 μ L of the extraction buffer. After washings, 25 μ L of 2x laemmli buffer was added, and the samples were boiled for 10 minutes at 95°C for protein elution. The samples were centrifuged at 16000 g for 2 minutes to pellet the beads, and the supernatants were used for immunoblotting.

For co-immunoprecipitation assays performed in *N. benthamiana*, the leaves were infiltrated as described in 2.1.3 of this chapter, and the proteins were purified and analyzed similarly as in co-IP assays described in this section but using G-protein Sepharose beads to bind anti-GFP antibodies.

2.7.5. Pull-down assays

The *in vitro* pull-down assays were performed with recombinant proteins. 1 to 2 μ g of GST-tagged bait proteins and GST were incubated for one hour at 4°C on a rotating wheel with 50 μ L of Glutathione sepharose 4B and 400 μ L of binding buffer containing 25 mM Tris pH 7.4, 75

mM NaCl, 0.5 mM EDTA, 0.5 mM DTT, 0.01% Triton X-100, and 1% protease inhibitor cocktail (Roche). The washed beads were incubated with 1 to 2 µg of prey protein for 4 hours at 4°C on a rotating wheel. Next, the beads were washed 4 times with binding buffer, and bound proteins were eluted with Laemmli 1X at 95°C for 15 minutes. The binding was then analyzed with an SDS-PAGE followed by immunoblotting using the appropriate antibodies.

2.7.6. Kinase assays

Kinase assay using recombinant protein

For phosphorylation assays with purified recombinant proteins, 1 µg of each MAPK and 1 µg of the putative substrate were mixed in a total volume of 26 µl containing 7 µl of kinase buffer. The kinase buffer contained 120 mM Tris-HCl pH 7.5, 60 mM MgCl₂, 20 mM EGTA, 4 mM DTT, 0.1 mM ATP and 1 µCi of [γ -³³P] ATP. The reaction was incubated for 30min at room temperature and quenched with Laemmli 1x and 15 minutes heating at 95°C. The samples were migrated on an SDS-PAGE gel. The gel was then dried and exposed to a storage phosphor screen after about 5 days of signal accumulation. A Typhoon 9410 imager was used to analyze the kinase assay on the phosphor screen (GE Healthcare). To control the inputs, the dried gel was then immersed in water and stained with Coomassie blue.

Kinase assay with proteins produced and purified from protoplasts

Protein Extraction from protoplasts was carried out as described in 2.6.1. The HA and myc-tagged proteins were purified from protein extracts by adding 1 µl of anti-Ha and anti-myc antibodies. The samples were incubated for 3 hours on a rotating wheel (10 rpm) at 4°C to allow antibodies binding. After that, 20 µl of 50% diluted A-protein Glutathione Sepharose beads (Roche) were added, and the mix was incubated for an additional hour for binding. The beads were then pelleted and washed 3 times with 1 ml of protein extraction buffer and washed two times with the Kinase buffer described in the previous section. The beads were then pelleted and dried by removing the Kinase buffer using sharp cone. The beads-bound proteins were used for the *in vitro* kinase assay. The immunoprecipitated myc-tagged proteins were subjected to the same process, but with G-protein Sepharose beads.

The kinase assay was then conducted as described in the previous section.

2.7.7. SDS- PAGE and immunoblotting

Proteins were separated on sodium dodecyl sulfate-polyacrylamide gel electrophoresis (SDS-PAGE) under a constant amperage of 15 mA per gel in the running buffer. After migrating, the proteins were transferred onto an ethanol-activated PVDF membrane (GE Healthcare) for 1 h at a constant voltage of 100 V in the transfer buffer. Blots were blocked with 5% BSA (SIGMA, ref. A9647) before α pTpY antibody probing or with 5% non-fat dry milk before other antibodies probing in 1x TBS-T (1xTBS + 0.1% Tween20) overnight at 4°C on very gentle shaking. The membrane was then washed 3 times with a TBS-T solution (15 minutes each wash) to remove non-bound antibodies. Then the membrane was incubated for an additional hour at RT with a peroxidase-coupled secondary antibody. Next, the membrane was washed 3x15min with TBS-T solution. The antigen-antibody interaction was detected with enhanced chemiluminescence reagent (ECL Prime, GE Healthcare ref. RPN303F) using a ChemiDoc imaging system (Biorad) and analyzed with Image Lab Software (Biorad). Coomassie blue staining of membranes was also carried out for protein loading control.

SDS-PAGE gel.

- Stacking gel was prepared in 2.0 ml final volume with 4.67% Bis Acrylamide, 125 mM Tris HCl pH 6.8, 0.1% SDS, 22 mM TEMED, and 0.05% APS (NH₄ persulfate)
- Resolving gel was prepared in 4 ml volume containing 10% Bis-Acrylamide, 375 mM TrisHCl pH 8.8, 5% SDS, 5.5 mM TEMED, 0.03% APS (NH₄ persulfate)

Buffers.

- 10 x running buffer is 30.3 g/L Tris base, 72.1 g/L glycine, 144 g/L, 10 g SDS
- 10x transfer Buffer (TB) is 30.3 g/L Tris base, 144 g/L glycine (for transfer: 10 % 10x TB, 20 % ethanol 96%)
- 10x TBS is 87.66 g/L NaCl₂, 121.1 g/L Tris base, pH 7.5 (TBS-T is prepared with 1xTBS + 0.1% Tween20)

2.8. Plotting, data interpretation and statistical analyses

RT-qPCR data and the data collected from rosette weight measurements were analyzed (statistically) and plotted using Graphpad (Prism) software (<https://www.graphpad.com/>) and using R commander.

MapMan software (<https://mapman.gabipd.org/home>) was used to analyze the altered cellular processes and biotic stress pathways in *snap33* R commander for GO enrichment analyses (Alexa & et al., 2006) and g:Profiler database (<https://biit.cs.ut.ee/gprofiler/gost>).

The Signature tool from Genevestigator was used to identify similar transcriptomes from other previous studies. Gene expression in different tissues, different plant developmental stages, and in perturbation studies was retrieved from Genevestigator (Anatomy, Perturbations, and Development tools). For transcriptomic data comparison, the data from each transcriptomic study was retrieved from NCBI's Gene Expression Omnibus (GEO) database (<https://www.ncbi.nlm.nih.gov/geo/>) using the GSE identifier (as in figure 2.12.a). The Venn diagrams were drawn using Venny online tool (<https://bioinfogp.cnb.csic.es/tools/venny/>). The manuscript's figures were drawn using Biorender (<https://biorender.com/>), and SNAP33 protein domains and PTM sites were drawn using Dog2.0 (<http://dog.biocuckoo.org/>). SNAP33's PTMs were retrieved from PhosPhAt4.0 database (<http://phosphat.uni-hohenheim.de/phosphat.html>) and SNAP33's interactions were retrieved from GeneMANIA (<https://genemania.org/>) and STRING (<https://string-db.org/>) databases.

REFERENCES

- Aarts, N., Metz, M., Holub, E., Staskawicz, B. J., Daniels, M. J., & Parker, J. E. (1998). Different requirements for EDS1 and NDR1 by disease resistance genes define at least two R gene-mediated signaling pathways in Arabidopsis. *Proceedings of the National Academy of Sciences of the United States of America*, *95*(17), 10306–10311. <https://doi.org/10.1073/pnas.95.17.10306>
- Adams, D. O., & Yang, S. F. (1979). Ethylene biosynthesis: Identification of 1-aminocyclopropane-1-carboxylic acid as an intermediate in the conversion of methionine to ethylene. *Proceedings of the National Academy of Sciences of the United States of America*, *76*(1), 170. <https://doi.org/10.1073/PNAS.76.1.170>
- Aerts, N., Mendes, M. P., & Wees, S. C. M. van. (2021). Multiple levels of crosstalk in hormone networks regulating plant defense. *The Plant Journal*, *105*(2), 489–504. <https://doi.org/10.1111/TPJ.15124>
- Albert, I., Böhm, H., Albert, M., Feiler, C. E., Imkampe, J., Wallmeroth, N., Brancato, C., Raaymakers, T. M., Oome, S., Zhang, H., Krol, E., Grefen, C., Gust, A. A., Chai, J., Hedrich, R., van den Ackerveken, G., & Nürnberger, T. (2015). An RLP23–SOBIR1–BAK1 complex mediates NLP-triggered immunity. *Nature Plants* *2015 1:10*, *1*(10), 1–9. <https://doi.org/10.1038/nplants.2015.140>
- Alberts, B., Johnson, A., Lewis, J., Raff, M., Roberts, K., & Walter, P. (2002). *Transport from the ER through the Golgi Apparatus*. <https://www.ncbi.nlm.nih.gov/books/NBK26941/>
- Alexa A, A., rg Rahnenfü hrer, J., & Lengauer, T. (2006). Improved scoring of functional groups from gene expression data by decorrelating GO graph structure. *22*(13), 1600–1607. <https://doi.org/10.1093/bioinformatics/btl140>
- Alonso, J. M., Hirayama, T., Roman, G., Nourizadeh, S., & Ecker, J. R. (1999). EIN2, a bifunctional transducer of ethylene and stress responses in Arabidopsis. *Science*, *284*(5423), 2148–2152. <https://doi.org/10.1126/SCIENCE.284.5423.2148>
- An, F., Zhao, Q., Ji, Y., Li, W., Jiang, Z., Yu, X., Zhang, C., Han, Y., He, W., Liu, Y., Zhang, S., Ecker, J. R., & Guo, H. (2010). Ethylene-Induced Stabilization of ETHYLENE INSENSITIVE3 and EIN3-LIKE1 Is Mediated by Proteasomal Degradation of EIN3 Binding F-Box 1 and 2 That Requires EIN2 in Arabidopsis. *The Plant Cell*, *22*(7), 2384. <https://doi.org/10.1105/TPC.110.076588>
- An, Q., Hüchelhoven, R., Kogel, K.-H., & Bel, A. J. E. van. (2006). Multivesicular bodies participate in a cell wall-associated defence response in barley leaves attacked by the pathogenic powdery mildew fungus. *Cellular Microbiology*, *8*(6), 1009–1019. <https://doi.org/10.1111/J.1462-5822.2006.00683.X>
- Analysis of the genome sequence of the flowering plant Arabidopsis thaliana. (2000). *Nature*, *408*(6814), 796–815. <https://doi.org/10.1038/35048692>
- Anders, S., Pyl, P. T., & Huber, W. (2015). HTSeq—a Python framework to work with high-throughput sequencing data. *Bioinformatics*, *31*(2), 166. <https://doi.org/10.1093/BIOINFORMATICS/BTU638>
- Anderson, J. C., Bartels, S., Besteiro, M. A. G., Shahollari, B., Ulm, R., & Peck, S. C. (2011). Arabidopsis MAP Kinase Phosphatase 1 (AtMKP1) negatively regulates MPK6-mediated PAMP responses and resistance against bacteria. *The Plant Journal*, *67*(2), 258–268. <https://doi.org/10.1111/J.1365-313X.2011.04588.X>
- Anderson, P. K., Cunningham, A. A., Patel, N. G., Morales, F. J., Epstein, P. R., & Daszak, P. (2004). Emerging infectious diseases of plants: Pathogen pollution, climate change and agrotechnology drivers. *Trends in Ecology and Evolution*,

- 19(10), 535–544. <https://doi.org/10.1016/j.tree.2004.07.021>
- Andreasson, E., & Ellis, B. (2010). Convergence and specificity in the Arabidopsis MAPK nexus. *Trends in Plant Science*, 15(2), 106–113. <https://doi.org/10.1016/J.TPLANTS.2009.12.001>
- Andreasson, E., Jenkins, T., Brodersen, P., Thorgrimsen, S., Petersen, N. H. T., Zhu, S., Qiu, J.-L., Micheelsen, P., Rocher, A., Petersen, M., Newman, M.-A., Bjørn Nielsen, H., Hirt, H., Somssich, I., Mattsson, O., & Mundy, J. (2005). The MAP kinase substrate MKS1 is a regulator of plant defense responses. *The EMBO Journal*, 24(14), 2579–2589. <https://doi.org/10.1038/sj.emboj.7600737>
- Asai, S., & Shirasu, K. (2015). Plant cells under siege: plant immune system versus pathogen effectors. *Current Opinion in Plant Biology*, 28, 1–8. <https://doi.org/10.1016/J.PBI.2015.08.008>
- Asai, T., Tena, G., Plotnikova, J., Willmann, M. R., Chiu, W. L., Gomez-Gomez, L., Boller, T., Ausubel, F. M., & Sheen, J. (2002). Map kinase signalling cascade in Arabidopsis innate immunity. *Nature*, 415(6875), 977–983. <https://doi.org/10.1038/415977a>
- Assaad, F. F., Qiu, J.-L., Youngs, H., Ehrhardt, D., Zimmerli, L., Kalde, M., Wanner, G., Peck, S. C., Edwards, H., Ramonell, K., Somerville, C. R., & Thordal-Christensen, H. (2004). The PEN1 Syntaxin Defines a Novel Cellular Compartment upon Fungal Attack and Is Required for the Timely Assembly of Papillae. *Molecular Biology of the Cell*, 15(11), 5118. <https://doi.org/10.1091/MBC.E04-02-0140>
- Attaran, E., Zeier, T. E., Griebel, T., & Zeier, J. (2009). Methyl salicylate production and jasmonate signaling are not essential for systemic acquired resistance in Arabidopsis. *Plant Cell*, 21(3), 954–971. <https://doi.org/10.1105/tpc.108.063164>
- Baggs, E., Dagdas, G., & Krasileva, K. v. (2017). NLR diversity, helpers and integrated domains: making sense of the NLR IDentity. *Current Opinion in Plant Biology*, 38, 59–67. <https://doi.org/10.1016/J.PBI.2017.04.012>
- Barber, K. W., & Rinehart, J. (2018). The ABCs of PTMs. *Nature Chemical Biology*, 14(3), 188. <https://doi.org/10.1038/NCHEMBIO.2572>
- Bardwell, A. J., Flatauer, L. J., Matsukuma, K., Thorner, J., & Bardwell, L. (2001). A Conserved Docking Site in MEKs Mediates High-affinity Binding to MAP Kinases and Cooperates with a Scaffold Protein to Enhance Signal Transmission. *The Journal of Biological Chemistry*, 276(13), 10374. <https://doi.org/10.1074/JBC.M010271200>
- Bartels, S., Anderson, J. C., González Besteiro, M. A., Carreri, A., Hirt, H., Buchala, A., Métraux, J.-P., Peck, S. C., & Ulm, R. (2009). MAP KINASE PHOSPHATASE1 and PROTEIN TYROSINE PHOSPHATASE1 Are Repressors of Salicylic Acid Synthesis and SNC1-Mediated Responses in Arabidopsis. *The Plant Cell*, 21(9), 2884–2897. <https://doi.org/10.1105/TPC.109.067678>
- Bassham, D. C., Brandizzi, F., Otegui, M. S., & Sanderfoot, A. A. (2008). The Secretory System of Arabidopsis. *The Arabidopsis Book / American Society of Plant Biologists*, 6, e0116. <https://doi.org/10.1199/TAB.0116>
- Bauer, Z., Gó Mez-Gó Mez, L., Boller, T., & Felix, G. (2001). Sensitivity of Different Ecotypes and Mutants of Arabidopsis thaliana toward the Bacterial Elicitor Flagellin Correlates with the Presence of Receptor-binding Sites*. <https://doi.org/10.1074/jbc.M102390200>
- Beck, M., Zhou, J., Faulkner, C., MacLean, D., & Robatzek, S. (2012). Spatio-Temporal Cellular Dynamics of the Arabidopsis Flagellin Receptor Reveal Activation Status-Dependent Endosomal Sorting. *The Plant Cell*, 24(10), 4205–4219. <https://doi.org/10.1105/TPC.112.100263>

- Bell, E., Creelman, R. A., & Mullet, J. E. (1995). A chloroplast lipoxygenase is required for wound-induced jasmonic acid accumulation in Arabidopsis. *Proceedings of the National Academy of Sciences of the United States of America*, 92(19), 8675–8679. <https://doi.org/10.1073/pnas.92.19.8675>
- Benjamini, Y., & Hochberg, Y. (1995). Controlling the False Discovery Rate: A Practical and Powerful Approach to Multiple Testing. *Journal of the Royal Statistical Society: Series B (Methodological)*, 57(1), 289–300. <https://doi.org/10.1111/J.2517-6161.1995.TB02031.X>
- Benschop, J. J., Mohammed, S., O’Flaherty, M., Heck, A. J. R., Slijper, M., & Menke, F. L. H. (2007). Quantitative phosphoproteomics of early elicitor signaling in Arabidopsis. *Molecular and Cellular Proteomics*, 6(7), 1198–1214. <https://doi.org/10.1074/mcp.M600429-MCP200>
- Berger, S., Bell, E., & Mullet, J. E. (1996). Two methyl jasmonate-insensitive mutants show altered expression of AtVsp in response to methyl jasmonate and wounding. *Plant Physiology*, 111(2), 525–531. <https://doi.org/10.1104/pp.111.2.525>
- Berriri, S., Garcia, A. V., dit Frey, N. F., Rozhon, W., Pateyron, S., Leonhardt, N., Montillet, J. L., Leung, J., Hirt, H., & Colcombet, J. (2012). Constitutively active mitogen-activated protein kinase versions reveal functions of Arabidopsis MPK4 in pathogen defense signaling. *Plant Cell*, 24(10), 4281–4293. <https://doi.org/10.1105/tpc.112.101253>
- Betsuyaku, S., Katou, S., Takebayashi, Y., Sakakibara, H., Nomura, N., & Fukuda, H. (2018). Salicylic Acid and Jasmonic Acid Pathways are Activated in Spatially Different Domains Around the Infection Site During Effector-Triggered Immunity in Arabidopsis thaliana. *Plant and Cell Physiology*, 59(1), 8. <https://doi.org/10.1093/PCP/PCX181>
- Bhandari, D. D., Lapin, D., Kracher, B., von Born, P., Bautor, J., Niefind, K., & Parker, J. E. (2019). An EDS1 heterodimer signalling surface enforces timely reprogramming of immunity genes in Arabidopsis. *Nature Communications*, 10(1), 1–13. <https://doi.org/10.1038/s41467-019-08783-0>
- Bi, G., Zhou, Z., Wang, W., Li, L., Rao, S., Wu, Y., Zhang, X., Menke, F. L. H., Chen, S., & Zhou, J. M. (2018). Receptor-like cytoplasmic kinases directly link diverse pattern recognition receptors to the activation of mitogen-activated protein kinase cascades in Arabidopsis. *Plant Cell*, 30(7), 1543–1561. <https://doi.org/10.1105/tpc.17.00981>
- Biezen, E. A. van der, & Jones, J. D. G. (1998). Plant disease-resistance proteins and the gene-for-gene concept. *Trends in Biochemical Sciences*, 23(12), 454–456. [https://doi.org/10.1016/S0968-0004\(98\)01311-5](https://doi.org/10.1016/S0968-0004(98)01311-5)
- Bigeard, J., Colcombet, J., & Hirt, H. (2015). Signaling mechanisms in pattern-triggered immunity (PTI). In *Molecular Plant* (Vol. 8, Issue 4, pp. 521–539). Cell Press. <https://doi.org/10.1016/j.molp.2014.12.022>
- Bigeard, J., & Hirt, H. (2018). Nuclear signaling of plant MAPKs. *Frontiers in Plant Science*, 9(April), 1–18. <https://doi.org/10.3389/fpls.2018.00469>
- Bigeard, J., Pflieger, D., Colcombet, J., Gérard, L., Mireau, H., & Hirt, H. (2014). Protein complexes characterization in Arabidopsis thaliana by tandem affinity purification coupled to mass spectrometry analysis. *Methods in Molecular Biology (Clifton, N.J.)*, 1171, 237–250. https://doi.org/10.1007/978-1-4939-0922-3_18
- BIONDI, R. M., & NEBREDA, A. R. (2003). Signalling specificity of Ser/Thr protein kinases through docking-site-mediated interactions. *Biochemical Journal*, 372(1), 1–13. <https://doi.org/10.1042/BJ20021641>

- Bonardi, V., Tang, S., Stallmann, A., Roberts, M., Cherkis, K., & Dangl, J. L. (2011). Expanded functions for a family of plant intracellular immune receptors beyond specific recognition of pathogen effectors. *Proceedings of the National Academy of Sciences of the United States of America*, *108*(39), 16463–16468. <https://doi.org/10.1073/pnas.1113726108>
- Boter, M., Ruíz-Rivero, O., Abdeen, A., & Prat, S. (2004). Conserved MYC transcription factors play a key role in jasmonate signaling both in tomato and Arabidopsis. *Genes and Development*, *18*(13), 1577–1591. <https://doi.org/10.1101/gad.297704>
- Boudsocq, M., & Sheen, J. (2013). CDPKs in immune and stress signaling. *Trends in Plant Science*, *18*(1), 30–40. <https://doi.org/10.1016/j.tplants.2012.08.008>
- Boudsocq, M., Willmann, M. R., McCormack, M., Lee, H., Shan, L., He, P., Bush, J., Cheng, S. H., & Sheen, J. (2010). Differential innate immune signalling via Ca²⁺ sensor protein kinases. *Nature*. <https://doi.org/10.1038/nature08794>
- Bourdais, G., McLachlan, D. H., Rickett, L. M., Zhou, J., Siwoszek, A., Häweker, H., Hartley, M., Kuhn, H., Morris, R. J., MacLean, D., & Robatzek, S. (2019). The use of quantitative imaging to investigate regulators of membrane trafficking in Arabidopsis stomatal closure. *Traffic*, *20*(2), 168–180. <https://doi.org/10.1111/TRA.12625>
- Bourras, S., Rouxel, T., & Meyer, M. (2015). Agrobacterium tumefaciens Gene Transfer: How a Plant Pathogen Hacks the Nuclei of Plant and Nonplant Organisms. <http://Dx.Doi.Org/10.1094/PHYTO-12-14-0380-RVW>, *105*(10), 1288–1301. <https://doi.org/10.1094/PHYTO-12-14-0380-RVW>
- Brandizzi, F., Hanton, S., DaSilva, L. L. P., Boevink, P., Evans, D., Oparka, K., Denecke, J., & Hawes, C. (2003). ER quality control can lead to retrograde transport from the ER lumen to the cytosol and the nucleoplasm in plants. *The Plant Journal*, *34*(3), 269–281. <https://doi.org/10.1046/J.1365-313X.2003.01728.X>
- Brillada, C., Teh, O.-K., Ditengou, F. A., Lee, C.-W., Klecker, T., Saeed, B., Furlan, G., Zietz, M., Hause, G., Eschen-Lippold, L., Hoehenwarter, W., Lee, J., Ott, T., & Trujillo, M. (2020). Exocyst subunit Exo70B2 is linked to immune signaling and autophagy. *The Plant Cell*. <https://doi.org/10.1093/plcell/koaa022>
- Brodersen, P., Petersen, M., Pike, H. M., Olszak, B., Skov, S., Ødum, N., Jørgensen, L. B., Brown, R. E., & Mundy, J. (2002). Knockout of Arabidopsis ACCELERATED-CELL-DEATH1 encoding a sphingosine transfer protein causes activation of programmed cell death and defense. *Genes & Development*, *16*(4), 490. <https://doi.org/10.1101/GAD.218202>
- BROOKS, D. M., BENDER, C. L., & KUNKEL, B. N. (2005). The Pseudomonas syringae phytotoxin coronatine promotes virulence by overcoming salicylic acid-dependent defences in Arabidopsis thaliana. *Molecular Plant Pathology*, *6*(6), 629–639. <https://doi.org/10.1111/J.1364-3703.2005.00311.X>
- Bruggeman, Q., Raynaud, C., Benhamed, M., & Delarue, M. (2015). To die or not to die? Lessons from lesion mimic mutants. *Frontiers in Plant Science*, *6*(JAN), 1–22. <https://doi.org/10.3389/FPLS.2015.00024>
- Brutus, A., Sicilia, F., Macone, A., Cervone, F., & Lorenzo, G. de. (2010). A domain swap approach reveals a role of the plant wall-associated kinase 1 (WAK1) as a receptor of oligogalacturonides. *Proceedings of the National Academy of Sciences of the United States of America*, *107*(20), 9452. <https://doi.org/10.1073/PNAS.1000675107>
- Bu, Q., Jiang, H., Li, C. B., Zhai, Q., Zhang, J., Wu, X., Sun, J., Xie, Q., & Li, C. (2008). Role of the Arabidopsis thaliana NAC transcription factors ANAC019 and

- ANAC055 in regulating jasmonic acid-signaled defense responses. *Cell Research*, 18(7), 756–767. <https://doi.org/10.1038/cr.2008.53>
- Burch-Smith, T. M., Schiff, M., Caplan, J. L., Tsao, J., Czymmek, K., & Dinesh-Kumar, S. P. (2007). A novel role for the TIR domain in association with pathogen-derived elicitors. *PLoS Biology*. <https://doi.org/10.1371/journal.pbio.0050068>
- Bürger, M., & Chory, J. (2019). Stressed Out About Hormones: How Plants Orchestrate Immunity. *Cell Host and Microbe*, 26(2), 163–172. <https://doi.org/10.1016/j.chom.2019.07.006>
- Burgoyne, R. D., & Morgan, A. (2007). Membrane Trafficking: Three Steps to Fusion. *Current Biology*, 17(7), R255–R258. <https://doi.org/10.1016/J.CUB.2007.02.006>
- Bushnell, B. (2014). *BBMap: A Fast, Accurate, Splice-Aware Aligner*. 3–5.
- Caarls, L., Pieterse, C. M. J., & van Wees, S. C. M. (2015). How salicylic acid takes transcriptional control over jasmonic acid signaling. *Frontiers in Plant Science*, 0(MAR), 170. <https://doi.org/10.3389/FPLS.2015.00170>
- Cameron, R. K., Paiva, N. L., Lamb, C. J., & Dixon, R. A. (1999). Accumulation of salicylic acid and PR-1 gene transcripts in relation to the systemic acquired resistance (SAR) response induced by *Pseudomonas syringae* pv. tomato in *Arabidopsis*. *Physiological and Molecular Plant Pathology*, 55(2), 121–130. <https://doi.org/10.1006/pmpp.1999.0214>
- Campanoni, P., & Blatt, M. R. (2007). Membrane trafficking and polar growth in root hairs and pollen tubes. *Journal of Experimental Botany*, 58(1), 65–74. <https://doi.org/10.1093/JXB/ERL059>
- Cao, Y., Liang, Y., Tanaka, K., Nguyen, C. T., Jedrzejczak, R. P., Joachimiak, A., & Stacey, G. (2014). The kinase LYK5 is a major chitin receptor in *Arabidopsis* and forms a chitin-induced complex with related kinase CERK1. *ELife*, 3. <https://doi.org/10.7554/ELIFE.03766>
- Castel, B., Ngou, P.-M., Cevik, V., Redkar, A., Kim, D.-S., Yang, Y., Ding, P., & Jones, J. D. G. (2019). Diverse NLR immune receptors activate defence via the RPW8-NLR NRG1. *New Phytologist*, 222(2), 966–980. <https://doi.org/10.1111/NPH.15659>
- Castroverde, C. D. M., & Dina, D. (2021). Temperature regulation of plant hormone signaling during stress and development. *Journal of Experimental Botany*. <https://doi.org/10.1093/JXB/ERAB257>
- Cecchini, N. M., Jung, H. W., Engle, N. L., Tschaplinski, T. J., & Greenberg, J. T. (2015). ALD1 regulates basal immune components and early inducible defense responses in *Arabidopsis*. *Molecular Plant-Microbe Interactions*, 28(4), 455–466. <https://doi.org/10.1094/MPMI-06-14-0187-R>
- Cesari, S. (2018). Multiple strategies for pathogen perception by plant immune receptors. *New Phytologist*, 219(1), 17–24. <https://doi.org/10.1111/nph.14877>
- Césari, S., Kanzaki, H., Fujiwara, T., Bernoux, M., Chalvon, V., Kawano, Y., Shimamoto, K., Dodds, P., Terauchi, R., & Kroj, T. (2014). The NB-LRR proteins RGA4 and RGA5 interact functionally and physically to confer disease resistance. *The EMBO Journal*, 33(17), 1941. <https://doi.org/10.15252/EMBJ.201487923>
- Cevher-Keskin, B. (2013). ARF1 and SAR1 GTPases in Endomembrane Trafficking in Plants. *International Journal of Molecular Sciences*, 14(9), 18181. <https://doi.org/10.3390/IJMS140918181>
- Checker, V. G., Kushwaha, H. R., Kumari, P., & Yadav, S. (2018). Role of Phytohormones in Plant Defense: Signaling and Cross Talk. *Molecular Aspects of Plant-Pathogen Interaction*, 159–184. https://doi.org/10.1007/978-981-10-7371-7_7

- Chen, F., D'Auria, J. C., Tholl, D., Ross, J. R., Gershenzon, J., Noel, J. P., & Pichersky, E. (2003). An *Arabidopsis thaliana* gene for methylsalicylate biosynthesis, identified by a biochemical genomics approach, has a role in defense. *Plant Journal*, *36*(5), 577–588. <https://doi.org/10.1046/j.1365-313X.2003.01902.x>
- Chen, H., Xue, L., Chintamanani, S., Germain, H., Lin, H., Cui, H., Cai, R., Zuo, J., Tang, X., Li, X., Guo, H., & Zhou, J.-M. (2009). ETHYLENE INSENSITIVE3 and ETHYLENE INSENSITIVE3-LIKE1 Repress SALICYLIC ACID INDUCTION DEFICIENT2 Expression to Negatively Regulate Plant Innate Immunity in *Arabidopsis*. *The Plant Cell*, *21*(8), 2527–2540. <https://doi.org/10.1105/TPC.108.065193>
- Chen, X., Irani, N. G., & Friml, J. (2011). Clathrin-mediated endocytosis: the gateway into plant cells. *Current Opinion in Plant Biology*, *14*(6), 674–682. <https://doi.org/10.1016/J.PBI.2011.08.006>
- Chen, Y. C., Holmes, E. C., Rajniak, J., Kim, J. G., Tang, S., Fischer, C. R., Mudgett, M. B., & Sattely, E. S. (2018). N-hydroxy-pipecolic acid is a mobile metabolite that induces systemic disease resistance in *Arabidopsis*. *Proceedings of the National Academy of Sciences of the United States of America*, *115*(21), E4920–E4929. <https://doi.org/10.1073/pnas.1805291115>
- Chen, Y.-F., Randlett, M. D., Findell, J. L., & Schaller, G. E. (2002). Localization of the Ethylene Receptor ETR1 to the Endoplasmic Reticulum of *Arabidopsis**. *Journal of Biological Chemistry*, *277*(22), 19861–19866. <https://doi.org/10.1074/JBC.M201286200>
- Cheng, Y. T., Germain, H., Wiermer, M., Bi, D., Xu, F., Garcia, A. V., Wirthmueller, L., Després, C., Parker, J. E., Zhang, Y., & Li, X. (2009). Nuclear pore complex component MOS7/Nup88 is required for innate immunity and nuclear accumulation of defense regulators in *Arabidopsis*. *Plant Cell*, *21*(8), 2503–2516. <https://doi.org/10.1105/tpc.108.064519>
- Cheng, Z., Li, J.-F., Niu, Y., Zhang, X.-C., Woody, O. Z., Xiong, Y., Djonović, S., Millet, Y., Bush, J., McConkey, B. J., Sheen, J., & Ausubel, F. M. (2015). Pathogen-Secreted Proteases Activate a Novel Plant Immune Pathway. *Nature*, *521*(7551), 213. <https://doi.org/10.1038/NATURE14243>
- Chiang, Y.-H., & Coaker, G. (2015). Effector Triggered Immunity: NLR Immune Perception and Downstream Defense Responses. *The Arabidopsis Book*, *13*(13), e0183. <https://doi.org/10.1199/tab.0183>
- Chinchilla, D., Bauer, Z., Regenass, M., Boller, T., & Felix, G. (2006). The *Arabidopsis* Receptor Kinase FLS2 Binds flg22 and Determines the Specificity of Flagellin Perception. *The Plant Cell*, *18*(2), 465–476. <https://doi.org/10.1105/TPC.105.036574>
- Chinchilla, D., Zipfel, C., Robatzek, S., Kemmerling, B., Nürnberger, T., Jones, J. D. G., Felix, G., & Boller, T. (2007). A flagellin-induced complex of the receptor FLS2 and BAK1 initiates plant defence. *Nature*. <https://doi.org/10.1038/nature05999>
- Chini, A., Fonseca, S., Fernández, G., Adie, B., Chico, J. M., Lorenzo, O., García-Casado, G., López-Vidriero, I., Lozano, F. M., Ponce, M. R., Micol, J. L., & Solano, R. (2007). The JAZ family of repressors is the missing link in jasmonate signalling. *Nature*, *448*(7154), 666–671. <https://doi.org/10.1038/nature06006>
- Chung, H. S., Cooke, T. F., DePew, C. L., Patel, L. C., Ogawa, N., Kobayashi, Y., & Howe, G. A. (2010). Alternative splicing expands the repertoire of dominant JAZ repressors of jasmonate signaling. *The Plant Journal : For Cell and Molecular Biology*, *63*(4), 613. <https://doi.org/10.1111/J.1365-313X.2010.04265.X>
- Chung, H. S., Koo, A. J. K., Gao, X., Jayanty, S., Thines, B., Jones, A. D., & Howe, G.

- A. (2008). Regulation and Function of Arabidopsis JASMONATE ZIM-Domain Genes in Response to Wounding and Herbivory. *Plant Physiology*, 146(3), 952–964. <https://doi.org/10.1104/PP.107.115691>
- Chung, M.-C., Chou, S.-J., Kuang, L.-Y., Charng, Y., & Yang, S. F. (2002). Subcellular Localization of 1-Aminocyclopropane-1-Carboxylic Acid Oxidase in Apple Fruit. *Plant and Cell Physiology*, 43(5), 549–554. <https://doi.org/10.1093/PCP/PCF067>
- Clarysg, D. O., & Rothmanj, J. E. (1990). Purification of Three Related Peripheral Membrane Proteins Needed for Vesicular Transport*. *THE JOURNAL OF BIOLOGICAL CHEMISTRY* (Cc), 265(17), 10109–10117. [https://doi.org/10.1016/S0021-9258\(19\)38786-1](https://doi.org/10.1016/S0021-9258(19)38786-1)
- Colcombet, J., & Hirt, H. (2008). Arabidopsis MAPKs: A complex signalling network involved in multiple biological processes. In *Biochemical Journal* (Vol. 413, Issue 2, pp. 217–226). Portland Press Ltd. <https://doi.org/10.1042/BJ20080625>
- Cole, B. J., & Tringe, S. G. (2021). Different threats, same response. *Nature Plants*, 7(5), 544–545. <https://doi.org/10.1038/s41477-021-00915-z>
- Collier, S. M., & Moffett, P. (2009). NB-LRRs work a “bait and switch” on pathogens. *Trends in Plant Science*, 14(10), 521–529. <https://doi.org/10.1016/j.tplants.2009.08.001>
- Collins, N. C., Thordal-Christensen, H., Lipka, V., Bau, S., Kombrink, E., Qiu, J.-L., Hüchelhoven, R., Stein, M., Freialdenhoven, A., Somerville, S. C., & Schulze-Lefert, P. (2003). SNARE-protein-mediated disease resistance at the plant cell wall. *Nature* 2003 425:6961, 425(6961), 973–977. <https://doi.org/10.1038/nature02076>
- Conrath, U. (2006). Systemic Acquired Resistance. *Plant Signaling & Behavior*, 1(4), 179. <https://doi.org/10.4161/PSB.1.4.3221>
- Contento, A. L., & Bassham, D. C. (2012). Structure and function of endosomes in plant cells. *Development and Cell Biology Publications Genetics, Development and Cell Biology*, 125, 3511–3518. <https://doi.org/10.1242/jcs.093559>
- Couto, D., & Zipfel, C. (2016). Regulation of pattern recognition receptor signalling in plants. *Nature Reviews Immunology* 2016 16:9, 16(9), 537–552. <https://doi.org/10.1038/nri.2016.77>
- Cui, F., Sun, W., & Kong, X. (2018). RLCKs Bridge Plant Immune Receptors and MAPK Cascades. *Trends in Plant Science*, 23(12), 1039–1041. <https://doi.org/10.1016/J.TPLANTS.2018.10.002>
- Cui, H., Gobbato, E., Kracher, B., Qiu, J., Bautor, J., & Parker, J. E. (2017). A core function of EDS1 with PAD4 is to protect the salicylic acid defense sector in Arabidopsis immunity. *New Phytologist*, 213(4), 1802–1817. <https://doi.org/10.1111/nph.14302>
- Cui, H., Qiu, J., Zhou, Y., Bhandari, D. D., Zhao, C., Bautor, J., & Parker, J. E. (2018). Antagonism of Transcription Factor MYC2 by EDS1/PAD4 Complexes Bolsters Salicylic Acid Defense in Arabidopsis Effector-Triggered Immunity. *Molecular Plant*, 11(8), 1053–1066. <https://doi.org/10.1016/J.MOLP.2018.05.007>
- Cui, H., Wang, Y., Xue, L., Chu, J., Yan, C., Fu, J., Chen, M., Innes, R. W., & Zhou, J. M. (2010). Pseudomonas syringae Effector Protein AvrB Perturbs Arabidopsis Hormone Signaling by Activating MAP Kinase 4. *Cell Host and Microbe*, 7(2), 164–175. <https://doi.org/10.1016/j.chom.2010.01.009>
- Dalio, R. J. D., Paschoal, D., Arena, G. D., Magalhães, D. M., Oliveira, T. S., Merfa, M. v., Maximo, H. J., & Machado, M. A. (2021). Hypersensitive response: From NLR pathogen recognition to cell death response. *Annals of Applied Biology*, 178(2), 268–280. <https://doi.org/10.1111/AAB.12657>
- Dard, N., & Peter, M. (2006). Scaffold proteins in MAP kinase signaling: More than

- simple passive activating platforms. *BioEssays*, 28(2), 146–156.
<https://doi.org/10.1002/bies.20351>
- Daudi, A., & O'Brien, J. A. (2012). Detection of Hydrogen Peroxide by DAB Staining in Arabidopsis Leaves. *Bio-Protocol*, 2(18). /pmc/articles/PMC4932902/
- Dean, J. v., & Delaney, S. P. (2008). Metabolism of salicylic acid in wild-type, ugt74f1 and ugt74f2 glucosyltransferase mutants of Arabidopsis thaliana. *Physiologia Plantarum*, 132(4), 417–425. <https://doi.org/10.1111/j.1399-3054.2007.01041.x>
- Delaney, T. P., Uknes, S., Vernooij, B., Friedrich, L., Weymann, K., Negrotto, D., Gaffney, T., Gut-Rella, M., Kessmann, H., Ward, E., & Ryals, J. (1994a). A central role of salicylic acid in plant disease resistance. *Science*, 266(5188), 1247–1250. <https://doi.org/10.1126/science.266.5188.1247>
- Dempsey, D. A., Vlot, A. C., Wildermuth, M. C., & Klessig, D. F. (2011). Salicylic Acid Biosynthesis and Metabolism. *The Arabidopsis Book*, 9, e0156. <https://doi.org/10.1199/tab.0156>
- Denancé, N., Sánchez-Vallet, A., Goffner, D., & Molina, A. (2013). Disease resistance or growth: the role of plant hormones in balancing immune responses and fitness costs. *Frontiers in Plant Science*, 4(MAY). <https://doi.org/10.3389/FPLS.2013.00155>
- Denoux, C., Galletti, R., Mammarella, N., Gopalan, S., Werck, D., de Lorenzo, G., Ferrari, S., Ausubel, F. M., & Dewdney, J. (2008). Activation of defense response pathways by OGs and Flg22 elicitors in Arabidopsis seedlings. *Molecular Plant*, 1(3), 423–445. <https://doi.org/10.1093/mp/ssn019>
- Després, C., DeLong, C., Glaze, S., Liu, E., & Fobert, P. R. (2000). The Arabidopsis NPR1/NIM1 protein enhances the DNA binding activity of a subgroup of the TGA family of bZIP transcription factors. *Plant Cell*, 12(2), 279–290. <https://doi.org/10.1105/tpc.12.2.279>
- Ding, P., & Ding, Y. (2020). Stories of Salicylic Acid: A Plant Defense Hormone. In *Trends in Plant Science* (Vol. 25, Issue 6, pp. 549–565). Elsevier Ltd. <https://doi.org/10.1016/j.tplants.2020.01.004>
- Ding, P., Rekhter, D., Ding, Y., Feussner, K., Busta, L., Haroth, S., Xu, S., Li, X., Jetter, R., Feussner, I., & Zhang, Y. (2016). Characterization of a pipercolic acid biosynthesis pathway required for systemic acquired resistance. *Plant Cell*, 28(10), 2603–2615. <https://doi.org/10.1105/tpc.16.00486>
- Ding, Y., Sun, T., Ao, K., Peng, Y., Zhang, Y., Li, X., & Zhang, Y. (2018). Opposite Roles of Salicylic Acid Receptors NPR1 and NPR3/NPR4 in Transcriptional Regulation of Plant Immunity. *Cell*, 173(6), 1454–1467.e10. <https://doi.org/10.1016/j.cell.2018.03.044>
- Djamei, A., Pitzschke, A., Nakagami, H., Rajh, I., & Hirt, H. (2007). Trojan horse strategy in Agrobacterium transformation: Abusing MAPK defense signaling. *Science*, 318(5849), 453–456. <https://doi.org/10.1126/science.1148110>
- Dóczi, R., Hatzimasoura, E., Farahi Biloei, S., Ahmad, Z., Ditengou, F. A., López-Juez, E., Palme, K., & Bögre, L. (2019). The MKK7-MPK6 MAP Kinase Module Is a Regulator of Meristem Quiescence or Active Growth in Arabidopsis. *Frontiers in Plant Science*, 0, 202. <https://doi.org/10.3389/FPLS.2019.00202>
- Does, D. van der, Leon-Reyes, A., Koornneef, A., Verk, M. C. van, Rodenburg, N., Pauwels, L., Goossens, A., Körbes, A. P., Memelink, J., Ritsema, T., Wees, S. C. M. van, & Pieterse, C. M. J. (2013). Salicylic Acid Suppresses Jasmonic Acid Signaling Downstream of SCFCO11-JAZ by Targeting GCC Promoter Motifs via Transcription Factor ORA59. *The Plant Cell*, 25(2), 744. <https://doi.org/10.1105/TPC.112.108548>

- Dombrecht, B., Gang, P. X., Sprague, S. J., Kirkegaard, J. A., Ross, J. J., Reid, J. B., Fitt, G. P., Sewelam, N., Schenk, P. M., Manners, J. M., & Kazana, K. (2007). MYC2 differentially modulates diverse jasmonate-dependent functions in Arabidopsis. *Plant Cell*, *19*(7), 2225–2245. <https://doi.org/10.1105/tpc.106.048017>
- Dong, O. X., Tong, M., Bonardi, V., Kasmi, F. el, Woloshen, V., Wunsch, L. K., Dangl, J. L., & Li, X. (2016). TNL-mediated immunity in Arabidopsis requires complex regulation of the redundant ADR1 gene family. *New Phytologist*, *210*(3), 960–973. <https://doi.org/10.1111/NPH.13821>
- Dongus, J. A., & Parker, J. E. (2021). EDS1 signalling: At the nexus of intracellular and surface receptor immunity. *Current Opinion in Plant Biology*, *62*, 102039. <https://doi.org/10.1016/J.PBI.2021.102039>
- Drakakaki, G., & Dandekar, A. (2013). Protein secretion: How many secretory routes does a plant cell have? *Plant Science*, *203–204*, 74–78. <https://doi.org/10.1016/J.PLANTSCI.2012.12.017>
- Dubiella, U., Seybold, H., Durian, G., Komander, E., Lassig, R., Witte, C.-P., Schulze, W. X., & Romeis, T. (2013). Calcium-dependent protein kinase/NADPH oxidase activation circuit is required for rapid defense signal propagation. *Proceedings of the National Academy of Sciences of the United States of America*, *110*(21), 8744. <https://doi.org/10.1073/PNAS.1221294110>
- Dubois, M., Van den Broeck, L., & Inzé, D. (2018). The Pivotal Role of Ethylene in Plant Growth. *Trends in Plant Science*, *23*(4), 311–323. <https://doi.org/10.1016/j.tplants.2018.01.003>
- Edwards, K., Johnstone, C., & Thompson, C. (1991). A simple and rapid method for the preparation of plant genomic DNA for PCR analysis. *Nucleic Acids Research*, *19*(6), 1349–1349. <https://doi.org/10.1093/NAR/19.6.1349>
- Elmore, J. M., Liu, J., Smith, B., Phinney, B., & Coaker, G. (2012). Quantitative Proteomics Reveals Dynamic Changes in the Plasma Membrane During Arabidopsis Immune Signaling. *Molecular & Cellular Proteomics : MCP*, *11*(4). <https://doi.org/10.1074/MCP.M111.014555>
- Eschen-Lippold, L., Landgraf, R., Smolka, U., Schulze, S., Heilmann, M., Heilmann, I., Hause, G., & Rosahl, S. (2012). Activation of defense against Phytophthora infestans in potato by down-regulation of syntaxin gene expression. *New Phytologist*, *193*(4), 985–996. <https://doi.org/10.1111/J.1469-8137.2011.04024.X>
- Fan, L., Li, R., Pan, J., Ding, Z., & Lin, J. (2015). Endocytosis and its regulation in plants. *Trends in Plant Science*, *20*(6), 388–397. <https://doi.org/10.1016/J.TPLANTS.2015.03.014>
- Fan, W., & Dong, X. (2002). In Vivo interaction between NPR1 and transcription factor TGA2 leads to salicylic acid-mediated gene activation in Arabidopsis. *Plant Cell*, *14*(6), 1377–1389. <https://doi.org/10.1105/tpc.001628>
- Fasshauer, D., Sutton, R. B., Brunger, A. T., & Jahn, R. (1998). Conserved structural features of the synaptic fusion complex: SNARE proteins reclassified as Q- and R-SNAREs. *Proceedings of the National Academy of Sciences of the United States of America*, *95*(26), 15781. <https://doi.org/10.1073/PNAS.95.26.15781>
- Feys, B. J. F., Benedetti, C. E., Penfold, C. N., & Turner, J. G. (1994). Arabidopsis mutants selected for resistance to the phytotoxin coronatine are male sterile, insensitive to methyl jasmonate, and resistant to a bacterial pathogen. *Plant Cell*, *6*(5), 751–759. <https://doi.org/10.1105/tpc.6.5.751>
- Flor, H. H. (2003). Current Status of the Gene-For-Gene Concept. <http://Dx.Doi.Org/10.1146/Annurev.Py.09.090171.001423>, *9*(1), 275–296. <https://doi.org/10.1146/ANNUREV.PY.09.090171.001423>

- Floyd, B. E., & Pioneer, D. (2015). *Autophagy and Endocytosis Springer Textbook Chapter for Cell Biology*. August.
- Frei dit Frey, N., Garcia, A. V., Bigeard, J., Zaag, R., Bueso, E., Garmier, M., Pateyron, S., de Tauzia-Moreau, M. L., Brunaud, V., Balzergue, S., Colcombet, J., Aubourg, S., Martin-Magniette, M. L., & Hirt, H. (2014). Functional analysis of Arabidopsis immune-related MAPKs uncovers a role for MPK3 as negative regulator of inducible defences. *Genome Biology*, *15*(6), 1–22. <https://doi.org/10.1186/gb-2014-15-6-r87>
- Fuchs, R., Kopischke, M., Klapprodt, C., Hause, G., Meyer, A. J., Schwarzländer, M., Fricker, M. D., & Lipka, V. (2016). Immobilized Subpopulations of Leaf Epidermal Mitochondria Mediate PENETRATION2-Dependent Pathogen Entry Control in Arabidopsis. *The Plant Cell*, *28*(1), 130. <https://doi.org/10.1105/TPC.15.00887>
- Furuya, T., Matsuoka, D., & Nanmori, T. (2013). Phosphorylation of Arabidopsis thaliana MEKK1 via Ca²⁺ signaling as a part of the cold stress response. *Journal of Plant Research* *2013 126:6*, *126*(6), 833–840. <https://doi.org/10.1007/S10265-013-0576-0>
- Gaffney, T., Friedrich, L., Vernooij, B., Negrotto, D., Gaffney, T., Friedrich, L., Vernooij, B., Negrotto, D., Nye, G., Uknes, S., Ward, E., Kessmann, H., & Ryals, J. (1993). *Requirement of Salicylic Acid for the Induction of Systemic Acquired Resistance Published by : American Association for the Advancement of Science Stable URL : https://www.jstor.org/stable/2882244 digitize , preserve and extend access to Science Requireme. 261*(5122), 754–756.
- Galán, J. E., Lara-Tejero, M., Marlovits, T. C., & Wagner, S. (2014). Bacterial type III secretion systems: Specialized nanomachines for protein delivery into target cells. *Annual Review of Microbiology*, *68*(June), 415–438. <https://doi.org/10.1146/annurev-micro-092412-155725>
- Gao, M., Liu, J., Bi, D., Zhang, Z., Cheng, F., Chen, S., & Zhang, Y. (2008). MEKK1, MKK1/MKK2 and MPK4 function together in a mitogen-activated protein kinase cascade to regulate innate immunity in plants. *Cell Research*, *18*(12), 1190–1198. <https://doi.org/10.1038/cr.2008.300>
- Gao, Q. M., Zhu, S., Kachroo, P., & Kachroo, A. (2015). Signal regulators of systemic acquired resistance. *Frontiers in Plant Science*, *6*(APR), 228. <https://doi.org/10.3389/fpls.2015.00228>
- Gao, Q.-M., Venugopal, S., Navarre, D., & Kachroo, A. (2011). Low Oleic Acid-Derived Repression of Jasmonic Acid-Inducible Defense Responses Requires the WRKY50 and WRKY51 Proteins. *Plant Physiology*, *155*(1), 464. <https://doi.org/10.1104/PP.110.166876>
- Gao, X., Chen, X., Lin, W., Chen, S., Lu, D., Niu, Y., Li, L., Cheng, C., McCormack, M., Sheen, J., Shan, L., & He, P. (2013). Bifurcation of Arabidopsis NLR Immune Signaling via Ca²⁺-Dependent Protein Kinases. *PLoS Pathogens*, *9*(1), 1003127. <https://doi.org/10.1371/journal.ppat.1003127>
- Garcion, C., Lohmann, A., Lamodièrè, E., Catinot, J., Buchala, A., Doermann, P., & Métraux, J. P. (2008). Characterization and biological function of the Isochorismate Synthase2 gene of Arabidopsis. *Plant Physiology*, *147*(3), 1279–1287. <https://doi.org/10.1104/pp.108.119420>
- Genot, B., Lang, J., Berriri, S., Garmier, M., Gilard, F., Pateyron, S., Haustreaete, K., van der Streaten, D., Hirt, H., & Colcombet, J. (2017). Constitutively active arabidopsis MAP kinase 3 triggers defense responses involving salicylic acid and SUMM2 resistance protein. *Plant Physiology*, *174*(2), 1238–1249. <https://doi.org/10.1104/pp.17.00378>

- Gergerich, R. C., & Dolja, V. v. (2006). Introduction to Plant Viruses, the Invisible Foe. *The Plant Health Instructor*. <https://doi.org/10.1094/PHI-I-2006-0414-01>
- Giraldo, M. C., & Valent, B. (2013). Filamentous plant pathogen effectors in action. In *Nature Reviews Microbiology* (Vol. 11, Issue 11, pp. 800–814). Nature Publishing Group. <https://doi.org/10.1038/nrmicro3119>
- Glazebrook, J. (2005). Contrasting mechanisms of defense against biotrophic and necrotrophic pathogens. In *Annual Review of Phytopathology* (Vol. 43, pp. 205–227). Annual Reviews . <https://doi.org/10.1146/annurev.phyto.43.040204.135923>
- Glazebrook, J., Chen, W., Estes, B., Chang, H.-S., Nawrath, C., Métraux, J.-P., Zhu, T., & Katagiri, F. (2003). Topology of the network integrating salicylate and jasmonate signal transduction derived from global expression phenotyping. *The Plant Journal*, *34*(2), 217–228. <https://doi.org/10.1046/J.1365-313X.2003.01717.X>
- Gonzalo, S., Greentree, W. K., & Linder, M. E. (1999). SNAP-25 Is Targeted to the Plasma Membrane through a Novel Membrane-binding Domain *. *Journal of Biological Chemistry*, *274*(30), 21313–21318. <https://doi.org/10.1074/JBC.274.30.21313>
- Gravino, M., Savatin, D. V., Macone, A., & Lorenzo, G. de. (2015). Ethylene production in *Botrytis cinerea*- and oligogalacturonide-induced immunity requires calcium-dependent protein kinases. *The Plant Journal*, *84*(6), 1073–1086. <https://doi.org/10.1111/TPJ.13057>
- Grefen, C., Städele, K., Růžička, K., Obrdlik, P., Harter, K., & Horák, J. (2008). Subcellular Localization and In Vivo Interactions of the Arabidopsis thaliana Ethylene Receptor Family Members. *Molecular Plant*, *1*(2), 308–320. <https://doi.org/10.1093/MP/SSM015>
- Gu, Y., Zavaliev, R., & Dong, X. (2017). Membrane Trafficking in Plant Immunity. In *Molecular Plant* (Vol. 10, Issue 8, pp. 1026–1034). Cell Press. <https://doi.org/10.1016/j.molp.2017.07.001>
- Guan, L., Denkert, N., Eisa, A., Lehmann, M., Sjuts, I., Weiberg, A., Soll, J., Meinecke, M., & Schwenkert, S. (2019). JASSY, a chloroplast outer membrane protein required for jasmonate biosynthesis. *Proceedings of the National Academy of Sciences of the United States of America*, *116*(21), 10568–10575. <https://doi.org/10.1073/pnas.1900482116>
- Guan, R., Su, J., Meng, X., Li, S., Liu, Y., Xu, J., & Zhang, S. (2015a). Focus on Ethylene: Multilayered Regulation of Ethylene Induction Plays a Positive Role in Arabidopsis Resistance against *Pseudomonas syringae*. *Plant Physiology*, *169*(1), 299. <https://doi.org/10.1104/PP.15.00659>
- Guan, R., Su, J., Meng, X., Li, S., Liu, Y., Xu, J., & Zhang, S. (2015b). Multilayered regulation of ethylene induction plays a positive role in arabidopsis resistance against *Pseudomonas syringae*. *Plant Physiology*, *169*(1), 299–312. <https://doi.org/10.1104/pp.15.00659>
- Guan, Y., Lu, J., Xu, J., McClure, B., & Zhang, S. (2014). Two mitogen-activated protein kinases, MPK3 and MPK6, are required for funicular guidance of pollen tubes in arabidopsis. *Plant Physiology*, *165*(2), 528–533. <https://doi.org/10.1104/pp.113.231274>
- Guerra, T., Schilling, S., Hake, K., Gorzolka, K., Sylvester, F. P., Conrads, B., Westermann, B., & Romeis, T. (2020). Calcium-dependent protein kinase 5 links calcium signaling with N-hydroxy-l-pipecolic acid- and SARD1-dependent immune memory in systemic acquired resistance. *New Phytologist*, *225*(1), 310–325. <https://doi.org/10.1111/nph.16147>
- Guo, H., & Ecker, J. R. (2003). Plant Responses to Ethylene Gas Are Mediated by

- SCFEBF1/EBF2-Dependent Proteolysis of EIN3 Transcription Factor. *Cell*, 115(6), 667–677. [https://doi.org/10.1016/S0092-8674\(03\)00969-3](https://doi.org/10.1016/S0092-8674(03)00969-3)
- Gupta, A., Bhardwaj, M., & Tran, L. S. P. (2020). Jasmonic acid at the crossroads of plant immunity and pseudomonas syringae virulence. In *International Journal of Molecular Sciences* (Vol. 21, Issue 20, pp. 1–19). MDPI AG. <https://doi.org/10.3390/ijms21207482>
- Han, G.-Z. (2019). Origin and evolution of the plant immune system. *New Phytologist*, 222(1), 70–83. <https://doi.org/10.1111/NPH.15596>
- Han, L., Li, G.-J., Yang, K.-Y., Mao, G., Wang, R., Liu, Y., & Zhang, S. (2010). Mitogen-activated protein kinase 3 and 6 regulate Botrytis cinerea-induced ethylene production in Arabidopsis. *The Plant Journal*, 64(1), 114–127. <https://doi.org/10.1111/J.1365-313X.2010.04318.X>
- Hatsugai, N., Iwasaki, S., Tamura, K., Kondo, M., Fuji, K., Ogasawara, K., Nishimura, M., & Hara-Nishimura, I. (2009). A novel membrane fusion-mediated plant immunity against bacterial pathogens. *Genes & Development*, 23(21), 2496. <https://doi.org/10.1101/GAD.1825209>
- Hatsugai, N., Kuroyanagi, M., Nishimura, M., & Hara-Nishimura, I. (2006). A cellular suicide strategy of plants: vacuole-mediated cell death. *Apoptosis* 2006 11:6, 11(6), 905–911. <https://doi.org/10.1007/S10495-006-6601-1>
- Heck, S., Grau, T., Buchala, A., Métraux, J.-P., & Nawrath, C. (2003). Genetic evidence that expression of NahG modifies defence pathways independent of salicylic acid biosynthesis in the Arabidopsis–Pseudomonas syringae pv. tomato interaction. *The Plant Journal*, 36(3), 342–352. <https://doi.org/10.1046/J.1365-313X.2003.01881.X>
- Heese, M., Gansel, X., Sticher, L., Wick, P., Grebe, M., Granier, F., & Jürgens, G. (2001). Functional characterization of the KNOLLE-interacting t-SNARE AtSNAP33 and its role in plant cytokinesis. *Journal of Cell Biology*, 155(2), 239–249. <https://doi.org/10.1083/jcb.200107126>
- Heidrich, K., Tsuda, K., Blanvillain-Baufumé, S., Wirthmueller, L., Bautor, J., & Parker, J. E. (2013). Arabidopsis TNL-WRKY domain receptor RRS1 contributes to temperature-conditioned RPS4 auto-immunity. *Frontiers in Plant Science*, 4(OCT). <https://doi.org/10.3389/FPLS.2013.00403>
- Heitz, T., Widemann, E., Lugan, R., Miesch, L., Ullmann, P., Désaubry, L., Holder, E., Grausem, B., Kandel, S., Miesch, M., Werck-Reichhart, D., & Pinot, F. (2012). Cytochromes P450 CYP94C1 and CYP94B3 catalyze two successive oxidation steps of plant hormone jasmonoyl-isoleucine for catabolic turnover. *Journal of Biological Chemistry*, 287(9), 6296–6306. <https://doi.org/10.1074/JBC.M111.316364>
- Herrera-Vásquez, A., Salinas, P., & Holuigue, L. (2015). Salicylic acid and reactive oxygen species interplay in the transcriptional control of defense genes expression. *Frontiers in Plant Science*, 0(MAR), 171. <https://doi.org/10.3389/FPLS.2015.00171>
- Hogenhout, S. A., Hoorn, R. A. L. van der, Terauchi, R., & Kamoun, S. (2009). Emerging Concepts in Effector Biology of Plant-Associated Organisms. <http://Dx.Doi.Org/10.1094/MPMI-22-2-0115>, 22(2), 115–122. <https://doi.org/10.1094/MPMI-22-2-0115>
- Hoppen, C., & Groth, G. (2020). Novel insights into the transfer routes of the essential copper cofactor to the ethylene plant hormone receptor family. *Plant Signaling & Behavior*, 15(2). <https://doi.org/10.1080/15592324.2020.1716512>
- Hoppen, C., Müller, L., Hänsch, S., Uzun, B., Milić, D., Meyer, A. J., Weidtkamp-Peters, S., & Groth, G. (2019). Soluble and membrane-bound protein carrier mediate direct copper transport to the ethylene receptor family. *Scientific Reports*,

- 9(1). <https://doi.org/10.1038/S41598-019-47185-6>
- Horsefield, S., Burdett, H., Zhang, X., Manik, M. K., Shi, Y., Chen, J., Qi, T., Gilley, J., Lai, J.-S., Rank, M. X., Casey, L. W., Gu, W., Ericsson, D. J., Foley, G., Hughes, R. O., Bosanac, T., Itzstein, M. von, Rathjen, J. P., Nanson, J. D., ... Kobe, B. (2019). NAD⁺ cleavage activity by animal and plant TIR domains in cell death pathways. *Science*, *365*(6455), 793–799. <https://doi.org/10.1126/SCIENCE.AAX1911>
- Hou, S., Liu, Z., Shen, H., & Wu, D. (2019). Damage-associated molecular pattern-triggered immunity in plants. In *Frontiers in Plant Science* (Vol. 10, p. 646). Frontiers Media S.A. <https://doi.org/10.3389/fpls.2019.00646>
- Hu, S., Li, Y., & Shen, J. (2020). A Diverse Membrane Interaction Network for Plant Multivesicular Bodies: Roles in Proteins Vacuolar Delivery and Unconventional Secretion. *Frontiers in Plant Science*, *0*, 425. <https://doi.org/10.3389/FPLS.2020.00425>
- Huang, C., Yan, Y., Zhao, H., Ye, Y., & Cao, Y. (2020). Arabidopsis CPK5 Phosphorylates the Chitin Receptor LYK5 to Regulate Plant Innate Immunity. *Frontiers in Plant Science*. <https://doi.org/10.3389/fpls.2020.00702>
- Huang, J. (2003). Ultrastructure of Bacterial Penetration in Plants. <Http://Dx.Doi.Org/10.1146/Annurev.Py.24.090186.001041>, *24*(1), 141–157. <https://doi.org/10.1146/ANNUREV.PY.24.090186.001041>
- Huang, J., Gu, M., Lai, Z., Fan, B., Shi, K., Zhou, Y. H., Yu, J. Q., & Chen, Z. (2010). Functional analysis of the Arabidopsis PAL gene family in plant growth, development, and response to environmental stress. *Plant Physiology*, *153*(4), 1526–1538. <https://doi.org/10.1104/pp.110.157370>
- Huang, W., Wang, Y., Li, X., & Zhang, Y. (2019). Biosynthesis and Regulation of Salicylic Acid and N-Hydroxypipicolinic Acid in Plant Immunity. In *Molecular Plant* (Vol. 13, Issue 1, pp. 31–41). Cell Press. <https://doi.org/10.1016/j.molp.2019.12.008>
- Huang, Y., Li, H., Hutchison, C. E., Laskey, J., & Kieber, J. J. (2003). Biochemical and functional analysis of CTR1, a protein kinase that negatively regulates ethylene signaling in Arabidopsis. *The Plant Journal*, *33*(2), 221–233. <https://doi.org/10.1046/J.1365-313X.2003.01620.X>
- Huffaker, A., Pearce, G., & Ryan, C. A. (2006). An endogenous peptide signal in Arabidopsis activates components of the innate immune response. *Proceedings of the National Academy of Sciences of the United States of America*, *103*(26), 10098. <https://doi.org/10.1073/PNAS.0603727103>
- Huot, B., Castroverde, C. D. M., Velásquez, A. C., Hubbard, E., Pulman, J. A., Yao, J., Childs, K. L., Tsuda, K., Montgomery, B. L., & He, S. Y. (2017). Dual impact of elevated temperature on plant defence and bacterial virulence in Arabidopsis. *Nature Communications* *2017 8:1*, *8*(1), 1–12. <https://doi.org/10.1038/s41467-017-01674-2>
- Ichimura, K., Mizoguchi, T., Irie, K., Morris, P., Giraudat, J., Matsumoto, K., & Shinozaki, K. (1998). Isolation of ATMEKK1 (a MAP kinase kinase kinase): Interacting proteins and analysis of a MAP kinase cascade in Arabidopsis. *Biochemical and Biophysical Research Communications*, *253*(2), 532–543. <https://doi.org/10.1006/bbrc.1998.9796>
- Ichimura, K., Shinozaki, K., Tena, G., Sheen, J., Henry, Y., Champion, A., Kreis, M., Zhang, S., Hirt, H., Wilson, C., Heberle-Bors, E., Ellis, B. E., Morris, P. C., Innes, R. W., Ecker, J. R., Scheel, D., Klessig, D. F., Machida, Y., Mundy, J., ... Walker, J. C. (2002). Mitogen-activated protein kinase cascades in plants: A new nomenclature. In *Trends in Plant Science*. [https://doi.org/10.1016/S1360-1385\(02\)02302-6](https://doi.org/10.1016/S1360-1385(02)02302-6)

- Inada, N., & Ueda, T. (2014). Membrane trafficking pathways and their roles in plant-microbe interactions. *Plant and Cell Physiology*, 55(4), 672–686.
<https://doi.org/10.1093/pcp/pcu046>
- Irani, N. G., & Russinova, E. (2009). Receptor endocytosis and signaling in plants. *Current Opinion in Plant Biology*, 12(6), 653–659.
<https://doi.org/10.1016/J.PBI.2009.09.011>
- Isono, E., Katsiarimpa, A., Müller, I. K., Anzenberger, F., Stierhof, Y.-D., Geldner, N., Chory, J., & Schwechheimer, C. (2010). The Deubiquitinating Enzyme AMSH3 Is Required for Intracellular Trafficking and Vacuole Biogenesis in *Arabidopsis thaliana*. *The Plant Cell*, 22(6), 1826–1837.
<https://doi.org/10.1105/TPC.110.075952>
- Jacinto, T., McGurl, B., Franceschi, V., Delano-Freier, J., & Ryan, C. A. (1997). Tomato prosystemin promoter confers wound-inducible, vascular bundle-specific expression of the β -glucuronidase gene in transgenic tomato plants. *Planta* 197 203:4, 203(4), 406–412. <https://doi.org/10.1007/S004250050207>
- Jacob, P., Kim, N. H., Wu, F., El-Kasmi, F., Chi, Y., Walton, W. G., Furzer, O. J., Lietzan, A. D., Sunil, S., Kempthorn, K., Redinbo, M. R., Pei, Z. M., Wan, L., & Dangl, J. L. (2021). Plant “helper” immune receptors are Ca^{2+} -permeable nonselective cation channels. *Science*, 373(6553), 420–425.
<https://doi.org/10.1126/SCIENCE.ABG7917>
- Jahn, R., Lang, T., & Südhof, T. C. (2003). Membrane Fusion. *Cell*, 112(4), 519–533.
[https://doi.org/10.1016/S0092-8674\(03\)00112-0](https://doi.org/10.1016/S0092-8674(03)00112-0)
- Janků, M., Luhová, L., & Petřivalský, M. (2019). On the Origin and Fate of Reactive Oxygen Species in Plant Cell Compartments. *Antioxidants*, 8(4).
<https://doi.org/10.3390/ANTIOX8040105>
- Jeworutzki, E., Roelfsema, M. R. G., Anshütz, U., Krol, E., Elzenga, J. T. M., Felix, G., Boller, T., Hedrich, R., & Becker, D. (2010). Early signaling through the *Arabidopsis* pattern recognition receptors FLS2 and EFR involves Ca^{2+} -associated opening of plasma membrane anion channels. *The Plant Journal*, 62(3), 367–378.
<https://doi.org/10.1111/J.1365-313X.2010.04155.X>
- Jin, S. L., Kyung, W. H., Bhargava, A., & Ellis, B. E. (2008). Comprehensive analysis of protein-protein interactions between *Arabidopsis* MAPKs and MAPK kinases helps define potential MAPK signalling modules. *Plant Signaling and Behavior*, 3(12), 1037–1041. <https://doi.org/10.4161/psb.3.12.6848>
- Jing, B., Xu, S., Xu, M., Li, Y., Li, S., Ding, J., & Zhang, Y. (2011). Brush and spray: A high-throughput systemic acquired resistance assay suitable for large-scale genetic screening. *Plant Physiology*, 157(3), 973–980.
<https://doi.org/10.1104/pp.111.182089>
- Johnson, L. N., & Lewis, R. J. (2001). Structural basis for control by phosphorylation. In *Chemical Reviews* (Vol. 101, Issue 8, pp. 2209–2242). Chem Rev.
<https://doi.org/10.1021/cr000225s>
- Jonak, C., Ökrész, L., Bögre, L., & Hirt, H. (2002). Complexity, Cross Talk and Integration of Plant MAP Kinase Signalling. *Current Opinion in Plant Biology*, 5(5), 415–424. [https://doi.org/10.1016/S1369-5266\(02\)00285-6](https://doi.org/10.1016/S1369-5266(02)00285-6)
- Jones, J. D. G., & Dangl, J. L. (2006a). The plant immune system. In *Nature* (Vol. 444, Issue 7117, pp. 323–329). <https://doi.org/10.1038/nature05286>
- Jones, J. D. G., & Dangl, J. L. (2006b). The plant immune system. In *Nature* (Vol. 444, Issue 7117, pp. 323–329). <https://doi.org/10.1038/nature05286>
- Ju, C., Yoon, G. M., Shemansky, J. M., Lin, D. Y., Ying, Z. I., Chang, J., Garrett, W. M., Kessenbrock, M., Groth, G., Tucker, M. L., Cooper, B., Kieber, J. J., & Chang, C.

- (2012). CTR1 phosphorylates the central regulator EIN2 to control ethylene hormone signaling from the ER membrane to the nucleus in Arabidopsis. *Proceedings of the National Academy of Sciences*, 109(47), 19486–19491. <https://doi.org/10.1073/PNAS.1214848109>
- Jubic, L. M., Saile, S., Furzer, O. J., el Kasmi, F., & Dangl, J. L. (2019). Help wanted: helper NLRs and plant immune responses. *Current Opinion in Plant Biology*, 50(Id), 82–94. <https://doi.org/10.1016/j.pbi.2019.03.013>
- Jürgens, G. (2004). Membrane trafficking in plants. *Annual Review of Cell and Developmental Biology*, 20, 481–504. <https://doi.org/10.1146/annurev.cellbio.20.082503.103057>
- Kachroo, P., Shanklin, J., Shah, J., Whittle, E. J., & Klessig, D. F. (2001). A fatty acid desaturase modulates the activation of defense signaling pathways in plants. *Proceedings of the National Academy of Sciences*, 98(16), 9448–9453. <https://doi.org/10.1073/PNAS.151258398>
- Kadota, Y., Sklenar, J., Derbyshire, P., Stransfeld, L., Asai, S., Ntoukakis, V., Jones, J. D., Shirasu, K., Menke, F., Jones, A., & Zipfel, C. (2014). Direct Regulation of the NADPH Oxidase RBOHD by the PRR-Associated Kinase BIK1 during Plant Immunity. *Molecular Cell*, 54(1), 43–55. <https://doi.org/10.1016/J.MOLCEL.2014.02.021>
- Kapos, P., Devendrakumar, K. T., & Li, X. (2019). Plant NLRs: From discovery to application. *Plant Science*, 279, 3–18. <https://doi.org/10.1016/j.plantsci.2018.03.010>
- Kasmi, F. el, Krause, C., Hiller, U., Stierhof, Y.-D., Mayer, U., Conner, L., Kong, L., Reichardt, I., Sanderfoot, A. A., & Jürgens, G. (2013). SNARE complexes of different composition jointly mediate membrane fusion in Arabidopsis cytokinesis. *Molecular Biology of the Cell*, 24(10), 1593. <https://doi.org/10.1091/MBC.E13-02-0074>
- Kaul, S., Koo, H. L., Jenkins, J., Rizzo, M., Rooney, T., Tallon, L. J., Feldblyum, T., Nierman, W., Benito, M. I., Lin, X., Town, C. D., Venter, J. C., Fraser, C. M., Tabata, S., Nakamura, Y., Kaneko, T., Sato, S., Asamizu, E., Kato, T., ... Somerville, C. (2000). Analysis of the genome sequence of the flowering plant Arabidopsis thaliana. *Nature* 2000 408:6814, 408(6814), 796–815. <https://doi.org/10.1038/35048692>
- Kerk, D., Bulgrien, J., Smith, D. W., Barsam, B., Veretnik, S., & Gribskov, M. (2002). The Complement of Protein Phosphatase Catalytic Subunits Encoded in the Genome of Arabidopsis. *Plant Physiology*, 129(2), 908–925. <https://doi.org/10.1104/PP.004002>
- Khurana, G. K., Vishwakarma, P., Puri, N., & Lynn, A. M. (2018). Phylogenetic Analysis of the vesicular fusion SNARE machinery revealing its functional divergence across Eukaryotes. *Bioinformatics*, 14(7), 361. <https://doi.org/10.6026/97320630014361>
- Kieber, J. J., Rothenberg, M., Roman, G., Feldmann, K. A., & Ecker, J. R. (1993a). CTR1, a negative regulator of the ethylene response pathway in arabidopsis, encodes a member of the Raf family of protein kinases. *Cell*, 72(3), 427–441. [https://doi.org/10.1016/0092-8674\(93\)90119-B](https://doi.org/10.1016/0092-8674(93)90119-B)
- Kieber, J. J., Rothenberg, M., Roman, G., Feldmann, K. A., & Ecker, J. R. (1993b). CTR1, a negative regulator of the ethylene response pathway in arabidopsis, encodes a member of the Raf family of protein kinases. *Cell*, 72(3), 427–441. [https://doi.org/10.1016/0092-8674\(93\)90119-B](https://doi.org/10.1016/0092-8674(93)90119-B)
- Kim, H., O’Connell, R., Maekawa-Yoshikawa, M., Uemura, T., Neumann, U., & Schulze-Lefert, P. (2014). The powdery mildew resistance protein RPW8.2 is

- carried on VAMP721/722 vesicles to the extrahaustorial membrane of haustorial complexes. *The Plant Journal*, 79(5), 835–847. <https://doi.org/10.1111/TPJ.12591>
- Kim, S. H., Kwon, S. Il, Saha, D., Anyanwu, N. C., & Gassmann, W. (2009). Resistance to the *Pseudomonas syringae* effector hopA1 is governed by the TIR-NBS-LRR Protein rps6 and is enhanced by mutations in srfr1. *Plant Physiology*, 150(4), 1723–1732. <https://doi.org/10.1104/pp.109.139238>
- Kim, S.-J., & Brandizzi, F. (2016). The plant secretory pathway for the trafficking of cell wall polysaccharides and glycoproteins. *Glycobiology*, 26(9), 940–949. <https://doi.org/10.1093/GLYCOB/CWW044>
- Kim, Y., Tsuda, K., Igarashi, D., Hillmer, R. A., Sakakibara, H., Myers, C. L., & Katagiri, F. (2014). Signaling mechanisms underlying the robustness and tunability of the plant immune network. *Cell Host & Microbe*, 15(1), 84. <https://doi.org/10.1016/J.CHOM.2013.12.002>
- Kleffmann, T., Russenberger, D., Zychlinski, A. von, Christopher, W., Sjölander, K., Gruissem, W., & Baginsky, S. (2004). The *Arabidopsis thaliana* Chloroplast Proteome Reveals Pathway Abundance and Novel Protein Functions. *Current Biology*, 14(5), 354–362. <https://doi.org/10.1016/J.CUB.2004.02.039>
- Kloek, A. P., Verbsky, M. L., Sharma, S. B., Schoelz, J. E., Vogel, J., Klessig, D. F., & Kunkel, B. N. (2001). Resistance to *Pseudomonas syringae* conferred by an *Arabidopsis thaliana* coronatine-insensitive (*coi1*) mutation occurs through two distinct mechanisms. *The Plant Journal*, 26(5), 509–522. <https://doi.org/10.1046/J.1365-313X.2001.01050.X>
- Kong, Q., Qu, N., Gao, M., Zhang, Z., Ding, X., Yang, F., Li, Y., Dong, O. X., Chen, S., Li, X., & Zhang, Y. (2012). The MEKK1-MKK1/MKK2-MPK4 kinase cascade negatively regulates immunity mediated by a mitogen-activated protein kinase kinase kinase in *Arabidopsis*. *Plant Cell*, 24(5), 2225–2236. <https://doi.org/10.1105/tpc.112.097253>
- Kong, Q., Sun, T., Qu, N., Ma, J., Li, M., Cheng, Y. T., Zhang, Q., Wu, D., Zhang, Z., & Zhang, Y. (2016). Two redundant receptor-like cytoplasmic kinases function downstream of pattern recognition receptors to regulate activation of SA biosynthesis. *Plant Physiology*, 171(2), 1344–1354. <https://doi.org/10.1104/pp.15.01954>
- Koo, A. J., Thireault, C., Zemelis, S., Poudel, A. N., Zhang, T., Kitaoka, N., Brandizzi, F., Matsuura, H., & Howe, G. A. (2014). Endoplasmic Reticulum-associated Inactivation of the Hormone Jasmonoyl-l-Isoleucine by Multiple Members of the Cytochrome P450 94 Family in *Arabidopsis*. *The Journal of Biological Chemistry*, 289(43), 29728. <https://doi.org/10.1074/JBC.M114.603084>
- Kosetsu, K., Matsunaga, S., Nakagami, H., Colcombet, J., Sasabe, M., Soyano, T., Takahashi, Y., Hirt, H., & Machida, Y. (2010). The MAP kinase MPK4 Is required for cytokinesis in *Arabidopsis thaliana*. *Plant Cell*, 22(11), 3778–3790. <https://doi.org/10.1105/tpc.110.077164>
- Krol, E., Mentzel, T., Chinchilla, D., Boller, T., Felix, G., Kemmerling, B., Postel, S., Arents, M., Jeworutzki, E., Al-Rasheid, K. A. S., Becker, D., & Hedrich, R. (2010). Perception of the *Arabidopsis* Danger Signal Peptide 1 Involves the Pattern Recognition Receptor AtPEPR1 and Its Close Homologue AtPEPR2. *The Journal of Biological Chemistry*, 285(18), 13471. <https://doi.org/10.1074/JBC.M109.097394>
- Kumar, D., & Klessig, D. F. (2003). High-affinity salicylic acid-binding protein 2 is required for plant innate immunity and has salicylic acid-stimulated lipase activity. *Proceedings of the National Academy of Sciences of the United States of America*, 100(26), 16101–16106. <https://doi.org/10.1073/pnas.0307162100>

- Kwon, C., Bednarek, P., & Schulze-Lefert, P. (2008). Secretory Pathways in Plant Immune Responses. *Plant Physiology*, *147*(4), 1575–1583.
<https://doi.org/10.1104/pp.108.121566>
- Kwon, C., Lee, J.-H., & Yun, H. S. (2020). SNAREs in Plant Biotic and Abiotic Stress Responses. *Molecules and Cells*, *43*(6), 501.
<https://doi.org/10.14348/MOLCELLS.2020.0007>
- Kwon, C., Neu, C., Pajonk, S., Yun, H. S., Lipka, U., Humphry, M., Bau, S., Straus, M., Kwaaitaal, M., Rampelt, H., Kasmi, F. el, Jürgens, G., Parker, J., Panstruga, R., Lipka, V., & Schulze-Lefert, P. (2008). Co-option of a default secretory pathway for plant immune responses. *Nature*, *451*(7180), 835–840.
<https://doi.org/10.1038/nature06545>
- Lagow, R. D., Bao, H., Cohen, E. N., Daniels, R. W., Zuzek, A., Williams, W. H., Macleod, G. T., Sutton, R. B., & Zhang, B. (2007). Modification of a Hydrophobic Layer by a Point Mutation in Syntaxin 1A Regulates the Rate of Synaptic Vesicle Fusion. *PLOS Biology*, *5*(4), e72.
<https://doi.org/10.1371/JOURNAL.PBIO.0050072>
- Lai, Y., & Eulgem, T. (2018). Transcript-level expression control of plant NLR genes. *Molecular Plant Pathology*, *19*(5), 1267–1281. <https://doi.org/10.1111/MPP.12607>
- Land use in agriculture by the numbers | Sustainable Food and Agriculture | Food and Agriculture Organization of the United Nations*. (2020). Food and Agriculture Organisation of the United Nations.
<http://www.fao.org/sustainability/news/detail/en/c/1274219/>
- Landoni, M., Francesco, A. de, Bellatti, S., Delledonne, M., Ferrarini, A., Venturini, L., Pilu, R., Bononi, M., & Tonelli, C. (2013). A mutation in the FZL gene of Arabidopsis causing alteration in chloroplast morphology results in a lesion mimic phenotype. *Journal of Experimental Botany*, *64*(14), 4313.
<https://doi.org/10.1093/JXB/ERT237>
- Lang, J., Genot, B., Bigeard, J., & Colcombet, J. (2021). Both transient and sustained MPK3/6 activities positively control expression of NLR genes in PTI and ETI. *BioRxiv*, 2021.04.01.437866. <https://doi.org/10.1101/2021.04.01.437866>
- Lapin, D., Kovacova, V., Sun, X., Dongus, J. A., Bhandari, D., Von Born, P., Bautor, J., Guarneri, N., Rzemieniewski, J., Stuttmann, J., Beyer, A., & Parker, J. E. (2019). A coevolved EDS1-SAG101-NRG1 module mediates cell death signaling by TIR-domain immune receptors. *Plant Cell*, *31*(10), 2430–2455.
<https://doi.org/10.1105/tpc.19.00118>
- Lassowskat, I., Böttcher, C., Eschen-Lippold, L., Scheel, D., & Lee, J. (2014). Sustained mitogen-activated protein kinase activation reprograms defense metabolism and phosphoprotein profile in Arabidopsis thaliana. *Frontiers in Plant Science*, *5*(OCT).
<https://doi.org/10.3389/fpls.2014.00554>
- Lauber, M. H., Waizenegger, I., Steinmann, T., Schwarz, H., Mayer, U., Hwang, I., Lukowitz, W., & Jürgens, G. (1997). The Arabidopsis KNOLLE Protein Is a Cytokinesis-specific Syntaxin. *The Journal of Cell Biology*, *139*(6), 1485.
<https://doi.org/10.1083/JCB.139.6.1485>
- Laurie-Berry, N., Joardar, V., Street, I. H., & Kunkel, B. N. (2007). The Arabidopsis thaliana JASMONATE INSENSITIVE 1 Gene Is Required for Suppression of Salicylic Acid-Dependent Defenses During Infection by Pseudomonas syringae. <http://Dx.Doi.Org/10.1094/MPMI-19-0789>, *19*(7), 789–800.
<https://doi.org/10.1094/MPMI-19-0789>
- L-C Wang, K., Li, H., & Ecker, J. R. (2002). *Ethylene Biosynthesis and Signaling Networks*. <https://doi.org/10.1105/tpc.001768>

- Leborgne-Castel, N., Adam, T., & Bouhidel, K. (2010). Endocytosis in plant–microbe interactions. *Protoplasma* 247:3, 247(3), 177–193.
<https://doi.org/10.1007/S00709-010-0195-8>
- Lecture, N., & Fi S C H, D. H. (1992). *PROTEIN PHOSPHORYLATION AND CELLULAR REGULATION, II*.
- Lee, J., Eschen-Lippold, L., Lassowskat, I., Böttcher, C., & Scheel, D. (2015). Cellular reprogramming through mitogen-activated protein kinases. *Frontiers in Plant Science*, 6(OCTOBER), 1–11. <https://doi.org/10.3389/fpls.2015.00940>
- Lee, J. S., & Ellis, B. E. (2007). Arabidopsis MAPK Phosphatase 2 (MKP2) Positively Regulates Oxidative Stress Tolerance and Inactivates the MPK3 and MPK6 MAPKs *. *Journal of Biological Chemistry*, 282(34), 25020–25029.
<https://doi.org/10.1074/JBC.M701888200>
- Lefoulon, C., Waghmare, S., Karnik, R., & Blatt, M. R. (2018). Gating control and K⁺ uptake by the KAT1 K⁺ channel leveraged through membrane anchoring of the trafficking protein SYP121. *Plant, Cell & Environment*, 41(11), 2668.
<https://doi.org/10.1111/PCE.13392>
- Le Roux, C., Huet, G., Jauneau, A., Camborde, L., Trémousaygue, D., Kraut, A., Zhou, B., Levailant, M., Adachi, H., Yoshioka, H., Raffaele, S., Berthomé, R., Couté, Y., Parker, J. E., & Deslandes, L. (2015). A Receptor Pair with an Integrated Decoy Converts Pathogen Disabling of Transcription Factors to Immunity. *Cell*, 161(5), 1074–1088. <https://doi.org/10.1016/J.CELL.2015.04.025>
- Levine, A., Tenhaken, R., Dixon, R., & Lamb, C. (1994). H₂O₂ from the oxidative burst orchestrates the plant hypersensitive disease resistance response. *Cell*.
[https://doi.org/10.1016/0092-8674\(94\)90544-4](https://doi.org/10.1016/0092-8674(94)90544-4)
- Li, G., Meng, X., Wang, R., Mao, G., Han, L., Liu, Y., & Zhang, S. (2012). Dual-Level Regulation of ACC Synthase Activity by MPK3/MPK6 Cascade and Its Downstream WRKY Transcription Factor during Ethylene Induction in Arabidopsis. *PLOS Genetics*, 8(6), e1002767.
<https://doi.org/10.1371/JOURNAL.PGEN.1002767>
- Li, J., Brader, G., Kariola, T., & Palva, E. T. (2006). WRKY70 modulates the selection of signaling pathways in plant defense. *The Plant Journal*, 46(3), 477–491.
<https://doi.org/10.1111/J.1365-313X.2006.02712.X>
- Li, J., Brader, G., & Palva, E. T. (2004). The WRKY70 Transcription Factor: A Node of Convergence for Jasmonate-Mediated and Salicylate-Mediated Signals in Plant Defense. *The Plant Cell*, 16(2), 319–331. <https://doi.org/10.1105/TPC.016980>
- Li, L., Li, M., Yu, L., Zhou, Z., Liang, X., Liu, Z., Cai, G., Gao, L., Zhang, X., Wang, Y., Chen, S., & Zhou, J.-M. (2014). The FLS2-Associated Kinase BIK1 Directly Phosphorylates the NADPH Oxidase RbohD to Control Plant Immunity. *Cell Host & Microbe*, 15(3), 329–338. <https://doi.org/10.1016/J.CHOM.2014.02.009>
- Li, N., Han, X., Feng, D., Yuan, D., & Huang, L.-J. (2019). Signaling Crosstalk between Salicylic Acid and Ethylene/Jasmonate in Plant Defense: Do We Understand What They Are Whispering? *International Journal of Molecular Sciences* 2019, Vol. 20, Page 671, 20(3), 671. <https://doi.org/10.3390/IJMS20030671>
- Li, W., Ma, M., Feng, Y., Li, H., Wang, Y., Ma, Y., Li, M., An, F., & Guo, H. (2015). EIN2-Directed Translational Regulation of Ethylene Signaling in Arabidopsis. *Cell*, 163(3), 670–683. <https://doi.org/10.1016/J.CELL.2015.09.037>
- Li, X., Bao, H., Wang, Z., Wang, M., Fan, B., Zhu, C., & Chen, Z. (2018). Biogenesis and Function of Multivesicular Bodies in Plant Immunity. *Frontiers in Plant Science*, 9. <https://doi.org/10.3389/FPLS.2018.00979>
- Li, X., Kapos, P., & Zhang, Y. (2015). NLRs in plants. *Current Opinion in Immunology*,

- 32, 114–121. <https://doi.org/10.1016/j.coi.2015.01.014>
- Li, Y., Tessaro, M. J., Li, X., & Zhang, Y. (2010). Regulation of the Expression of Plant Resistance Gene SNC1 by a Protein with a Conserved BAT2 Domain. *Plant Physiology*, *153*(3), 1425–1434. <https://doi.org/10.1104/PP.110.156240>
- Lim, G. H., Shine, M. B., de Lorenzo, L., Yu, K., Cui, W., Navarre, D., Hunt, A. G., Lee, J. Y., Kachroo, A., & Kachroo, P. (2016). Plasmodesmata Localizing Proteins Regulate Transport and Signaling during Systemic Acquired Immunity in Plants. *Cell Host and Microbe*, *19*(4), 541–549. <https://doi.org/10.1016/j.chom.2016.03.006>
- Lipka, V., Dittgen, J., Bednarek, P., Bhat, R., Wiermer, M., Stein, M., Landtag, J., Brandt, W., Rosahl, S., Scheel, D., Llorente, F., Molina, A., Parker, J., Somerville, S., & Schulze-Lefert, P. (2005). Pre- and Postinvasion Defenses Both Contribute to Nonhost Resistance in Arabidopsis. *Science*, *310*(5751), 1180–1183. <https://doi.org/10.1126/SCIENCE.1119409>
- Lipka, V., Kwon, C., & Panstruga, R. (2007). SNARE-Ware: The Role of SNARE-Domain Proteins in Plant Biology. <Http://Dx.Doi.Org/10.1146/Annurev.Cellbio.23.090506.123529>, *23*, 147–174. <https://doi.org/10.1146/ANNUREV.CELLBIO.23.090506.123529>
- Liu, L., Sonbol, F.-M., Huot, B., Gu, Y., Withers, J., Mwimba, M., Yao, J., He, S. Y., & Dong, X. (2016). Salicylic acid receptors activate jasmonic acid signalling through a non-canonical pathway to promote effector-triggered immunity. *Nature Communications* *2016 7:1*, *7*(1), 1–10. <https://doi.org/10.1038/ncomms13099>
- Liu, N., Hake, K., Wang, W., Zhao, T., Romeis, T., & Tang, D. (2017). CALCIUM-DEPENDENT PROTEIN KINASE5 Associates with the Truncated NLR Protein TIR-NBS2 to Contribute to exo70B1-Mediated Immunity. *The Plant Cell*, *29*(4), 746. <https://doi.org/10.1105/TPC.16.00822>
- Liu, P. P., von Dahl, C. C., & Klessig, D. F. (2011). The extent to which methyl salicylate is required for signaling systemic acquired resistance is dependent on exposure to light after infection. *Plant Physiology*, *157*(4), 2216–2226. <https://doi.org/10.1104/pp.111.187773>
- Liu, T., Liu, Z., Song, C., Hu, Y., Han, Z., She, J., Fan, F., Wang, J., Jin, C., Chang, J., Zhou, J.-M., & Chai, J. (2012). Chitin-Induced Dimerization Activates a Plant Immune Receptor. *Science*, *336*(6085), 1160–1164. <https://doi.org/10.1126/SCIENCE.1218867>
- Liu, X., Afrin, T., & Pajerowska-Mukhtar, K. M. (2019). Arabidopsis GCN2 kinase contributes to ABA homeostasis and stomatal immunity. *Communications Biology*, *2*(1). <https://doi.org/10.1038/S42003-019-0544-X>
- Liu, Y., & He, C. (2016). Regulation of plant reactive oxygen species (ROS) in stress responses: learning from AtRBOHD. *Plant Cell Reports*, *35*(5), 995–1007. <https://doi.org/10.1007/s00299-016-1950-x>
- Liu, Y., & Zhang, S. (2004). Phosphorylation of 1-aminocyclopropane-1-carboxylic acid synthase by MPK6, a stress-responsive mitogen-activated protein kinase, induces ethylene biosynthesis in arabidopsis. *Plant Cell*. <https://doi.org/10.1105/tpc.104.026609>
- Lorenzo, O., Chico, J. M., Sánchez-Serrano, J. J., & Solano, R. (2004). JASMONATE-INSENSITIVE1 encodes a MYC transcription factor essential to discriminate between different jasmonate-regulated defense responses in arabidopsis. *Plant Cell*, *16*(7), 1938–1950. <https://doi.org/10.1105/tpc.022319>
- Lorenzo, O., Piqueras, R., Sánchez-Serrano, J. J., & Solano, R. (2003). ETHYLENE RESPONSE FACTOR1 integrates signals from ethylene and jasmonate pathways in

- plant defense. *Plant Cell*, *15*(1), 165–178. <https://doi.org/10.1105/tpc.007468>
- Loreti, E., & Perata, P. (2020). The Many Facets of Hypoxia in Plants. *Plants*, *9*(6), 745. <https://doi.org/10.3390/PLANTS9060745>
- Lu, D., Wu, S., Gao, X., Zhang, Y., Shan, L., & He, P. (2010). A receptor-like cytoplasmic kinase, BIK1, associates with a flagellin receptor complex to initiate plant innate immunity. *Proceedings of the National Academy of Sciences*, *107*(1), 496–501. <https://doi.org/10.1073/PNAS.0909705107>
- Luan, S. (2003). Protein Phosphatases in Plants. *Annual Review of Plant Biology*, *54*, 63–92. <https://doi.org/10.1146/annurev.arplant.54.031902.134743>
- Lukowitz, W., Mayer, U., & Jürgens, G. (1996). Cytokinesis in the Arabidopsis Embryo Involves the Syntaxin-Related KNOLLE Gene Product. *Cell*, *84*(1), 61–71. [https://doi.org/10.1016/S0092-8674\(00\)80993-9](https://doi.org/10.1016/S0092-8674(00)80993-9)
- Macho, A. P., & Zipfel, C. (2014). *Molecular Cell Review Plant PRRs and the Activation of Innate Immune Signaling*. <https://doi.org/10.1016/j.molcel.2014.03.028>
- Mackey, D., Belkhadir, Y., Alonso, J. M., Ecker, J. R., & Dangl, J. L. (2003). Arabidopsis RIN4 Is a Target of the Type III Virulence Effector AvrRpt2 and Modulates RPS2-Mediated Resistance. *Cell*, *112*(3), 379–389. [https://doi.org/10.1016/S0092-8674\(03\)00040-0](https://doi.org/10.1016/S0092-8674(03)00040-0)
- Mackey, D., Holt, B. F., Wiig, A., & Dangl, J. L. (2002). RIN4 Interacts with *Pseudomonas syringae* Type III Effector Molecules and Is Required for RPM1-Mediated Resistance in Arabidopsis. *Cell*, *108*(6), 743–754. [https://doi.org/10.1016/S0092-8674\(02\)00661-X](https://doi.org/10.1016/S0092-8674(02)00661-X)
- Mair, A., Xu, S. L., Branon, T. C., Ting, A. Y., & Bergmann, D. C. (2019). Proximity labeling of protein complexes and cell type specific organellar proteomes in Arabidopsis enabled by TurboID. *ELife*, *8*. <https://doi.org/10.7554/ELIFE.47864>
- Manna, M., Achary, V. M. M., & Reddy, M. K. (2019). ROS Signaling and Its Role in Plants. *Sensory Biology of Plants*, 361–388. https://doi.org/10.1007/978-981-13-8922-1_14
- Mao, G., Meng, X., Liu, Y., Zheng, Z., Chen, Z., & Zhang, S. (2011). Phosphorylation of a WRKY transcription factor by two pathogen-responsive MAPKs drives phytoalexin biosynthesis in Arabidopsis. *Plant Cell*. <https://doi.org/10.1105/tpc.111.084996>
- Marathe, R., & Dinesh-Kumar, S. P. (2003). Plant defense: One post, multiple guards?! *Molecular Cell*, *11*(2), 284–286. [https://doi.org/10.1016/S1097-2765\(03\)00072-8](https://doi.org/10.1016/S1097-2765(03)00072-8)
- Marion, J., Bach, L., Bellec, Y., Meyer, C., Gissot, L., & Faure, J. D. (2008). Systematic analysis of protein subcellular localization and interaction using high-throughput transient transformation of Arabidopsis seedlings. *Plant Journal*, *56*(1), 169–179. <https://doi.org/10.1111/j.1365-313X.2008.03596.x>
- Martin, R. M. (2008). Deforestation, land-use change and REDD. *Food and Agriculture Organisation of the United Nations*. [http://www.fao.org/docrep/011/i0440e/i0440e02.htm\[9/26/20122:30:34PM\]](http://www.fao.org/docrep/011/i0440e/i0440e02.htm[9/26/20122:30:34PM])
- Matsushima, R., Hayashi, Y., Kondo, M., Shimada, T., Nishimura, M., & Hara-Nishimura, I. (2002). An Endoplasmic Reticulum-Derived Structure That Is Induced under Stress Conditions in Arabidopsis. *Plant Physiology*, *130*(4), 1807. <https://doi.org/10.1104/PP.009464>
- Matsushima, R., Kondo, M., Nishimura, M., & Hara-Nishimura, I. (2003). A novel ER-derived compartment, the ER body, selectively accumulates a β -glucosidase with an ER-retention signal in Arabidopsis. *The Plant Journal*, *33*(3), 493–502. <https://doi.org/10.1046/J.1365-313X.2003.01636.X>
- Mbengue, M., Bourdais, G., Gervasi, F., Beck, M., Zhou, J., Spallek, T., Bartels, S.,

- Boller, T., Ueda, T., Kuhn, H., & Robatzek, S. (2016). Clathrin-dependent endocytosis is required for immunity mediated by pattern recognition receptor kinases. *Proceedings of the National Academy of Sciences*, *113*(39), 11034–11039. <https://doi.org/10.1073/PNAS.1606004113>
- Melkamu G. Woldemariam, Nawaporn Onkokesung†, I. T. B. and I. G. (2012). Jasmonoyl-L-isoleucine hydrolase 1 (JIH1) regulates jasmonoyl-L-isoleucine levels and attenuates plant defenses against herbivores. *The Plant Journal : For Cell and Molecular Biology*, *72*(5), 758–767. <https://doi.org/10.1111/J.1365-313X.2012.05117.X>
- Meng, X., Xu, J., He, Y., Yang, K. Y., Mordorski, B., Liu, Y., & Zhang, S. (2013). Phosphorylation of an ERF transcription factor by Arabidopsis MPK3/MPK6 regulates plant defense gene induction and fungal resistance. *Plant Cell*, *25*(3), 1126–1142. <https://doi.org/10.1105/tpc.112.109074>
- Meng, X., & Zhang, S. (2013). MAPK Cascades in Plant Disease Resistance Signaling. <Http://Dx.Doi.Org/10.1146/Annurev-Phyto-082712-102314>, *51*, 245–266. <https://doi.org/10.1146/ANNUREV-PHYTO-082712-102314>
- Merchante, C., Brumos, J., Yun, J., Hu, Q., Spencer, K. R., Enríquez, P., Binder, B. M., Heber, S., Stepanova, A. N., & Alonso, J. M. (2015). Gene-Specific Translation Regulation Mediated by the Hormone-Signaling Molecule EIN2. *Cell*, *163*(3), 684–697. <https://doi.org/10.1016/J.CELL.2015.09.036>
- Mishina, T. E., & Zeier, J. (2006). The Arabidopsis flavin-dependent monooxygenase FMO1 is an essential component of biologically induced systemic acquired resistance. *Plant Physiology*, *141*(4), 1666–1675. <https://doi.org/10.1104/pp.106.081257>
- Mishina, T. E., & Zeier, J. (2007). Pathogen-associated molecular pattern recognition rather than development of tissue necrosis contributes to bacterial induction of systemic acquired resistance in Arabidopsis. *The Plant Journal*, *50*(3), 500–513. <https://doi.org/10.1111/J.1365-313X.2007.03067.X>
- Misura, K. M. S., Scheller, R. H., & Weis, W. I. (2001). Self-association of the H3 Region of Syntaxin 1A: IMPLICATIONS FOR INTERMEDIATES IN SNARE COMPLEX ASSEMBLY *. *Journal of Biological Chemistry*, *276*(16), 13273–13282. <https://doi.org/10.1074/JBC.M009636200>
- Mohr, T. J., Mammarella, N. D., Hoff, T., Woffenden, B. J., Jelesko, J. G., & McDowell, J. M. (2010). *The Arabidopsis Downy Mildew Resistance Gene RPP8 Is Induced by Pathogens and Salicylic Acid and Is Regulated by W Box cis Elements*. *23*(10), 1303–1315. <https://doi.org/10.1094/MPMI>
- More, K., Klinger, C. M., Barlow, L. D., & Dacks, J. B. (2020). Evolution and Natural History of Membrane Trafficking in Eukaryotes. *Current Biology*, *30*(10), R553–R564. <https://doi.org/10.1016/J.CUB.2020.03.068>
- Moreno, J. E., Shyu, C., Campos, M. L., Patel, L. C., Chung, H. S., Yao, J., He, S. Y., & Howe, G. A. (2013). Negative Feedback Control of Jasmonate Signaling by an Alternative Splice Variant of JAZ10. *Plant Physiology*, *162*(2), 1006. <https://doi.org/10.1104/PP.113.218164>
- Mou, Z., Fan, W., & Dong, X. (2003). Inducers of plant systemic acquired resistance Regulate NPR1 function through redox changes. *Cell*, *113*(7), 935–944. [https://doi.org/10.1016/S0092-8674\(03\)00429-X](https://doi.org/10.1016/S0092-8674(03)00429-X)
- Munson, M., Chen, X., Cocina, A. E., Schultz, S. M., & Hughson, F. M. (2000). Interactions within the yeast t-SNARE Sso1p that control SNARE complex assembly. *Nature Structural Biology* *2000 7:10*, *7*(10), 894–902.

<https://doi.org/10.1038/79659>

- Nakano, R. T., Yamada, K., Bednarek, P., Nishimura, M., & Hara-Nishimura, I. (2014). ER bodies in plants of the Brassicales order: biogenesis and association with innate immunity. *Frontiers in Plant Science*, 5(MAR).
<https://doi.org/10.3389/FPLS.2014.00073>
- Navarro, L., Zipfel, C., Rowland, O., Keller, I., Robatzek, S., Boller, T., & Jones, J. D. G. (2004). The transcriptional innate immune response to flg22. Interplay and overlap with Avr gene-dependent defense responses and bacterial pathogenesis. *Plant Physiology*. <https://doi.org/10.1104/pp.103.036749>
- Nawrath, C., Heck, S., Parinthewong, N., & Métraux, J. P. (2002). EDS5, an essential component of salicylic acid-dependent signaling for disease resistance in arabidopsis, is a member of the MATE transporter family. *Plant Cell*, 14(1), 275–286. <https://doi.org/10.1105/tpc.010376>
- Nawrath, C., & Métraux, J.-P. (1999). Salicylic Acid Induction-Deficient Mutants of Arabidopsis Express PR-2 and PR-5 and Accumulate High Levels of Camalexin after Pathogen Inoculation. In *The Plant Cell* (Vol. 11). www.plantcell.org
- Ngou, B. P. M., Ahn, H. K., Ding, P., & Jones, J. D. G. (2021). Mutual potentiation of plant immunity by cell-surface and intracellular receptors. *Nature*, 592(7852), 110–115. <https://doi.org/10.1038/s41586-021-03315-7>
- Nguyen, Q. M., Iswanto, A. B. B., Son, G. H., & Kim, S. H. (2021). Recent Advances in Effector-Triggered Immunity in Plants: New Pieces in the Puzzle Create a Different Paradigm. *International Journal of Molecular Sciences*, 22(9).
<https://doi.org/10.3390/ijms22094709>
- Nickel, W., & Rabouille, C. (2009). Mechanisms of regulated unconventional protein secretion. *Nature Reviews Molecular Cell Biology*, 10(2), 148–155.
<https://doi.org/10.1038/NRM2617>
- Nitta, Y., Qiu, Y., Yaghmaiean, H., Zhang, Q., Huang, J., Adams, K., & Zhang, Y. (2020). MEKK2 inhibits activation of MAP kinases in Arabidopsis. *Plant Journal*, 103(2), 705–714. <https://doi.org/10.1111/tpj.14763>
- Noctor, G., Reichheld, J. P., & Foyer, C. H. (2018). ROS-related redox regulation and signaling in plants. *Seminars in Cell and Developmental Biology*, 80, 3–12.
<https://doi.org/10.1016/j.semcdb.2017.07.013>
- Noirot, E., Der, C., Lherminier, J., Robert, F., Moricova, P., Kiêu, K., Leborgne-Castel, N., Simon-Plas, F., & Bouhidel, K. (2014). Dynamic changes in the subcellular distribution of the tobacco ROS-producing enzyme RBOHD in response to the oomycete elicitor cryptogein. *Journal of Experimental Botany*, 65(17), 5011.
<https://doi.org/10.1093/JXB/ERU265>
- Nomura, H., Komori, T., Uemura, S., Kanda, Y., Shimotani, K., Nakai, K., Furuichi, T., Takebayashi, K., Sugimoto, T., Sano, S., Suwastika, I. N., Fukusaki, E., Yoshioka, H., Nakahira, Y., & Shiina, T. (2012). Chloroplast-mediated activation of plant immune signalling in Arabidopsis. *Nature Communications*.
<https://doi.org/10.1038/ncomms1926>
- Nühse, T. S., Bottrill, A. R., Jones, A. M. E., & Peck, S. C. (2007). Quantitative phosphoproteomic analysis of plasma membrane proteins reveals regulatory mechanisms of plant innate immune responses. *Plant Journal*, 51(5), 931–940.
<https://doi.org/10.1111/j.1365-313X.2007.03192.x>
- Nühse, T. S., Peck, S. C., Hirt, H., & Boller, T. (2000). Microbial Elicitors Induce Activation and Dual Phosphorylation of the Arabidopsis thaliana MAPK 6 *. *Journal of Biological Chemistry*, 275(11), 7521–7526.
<https://doi.org/10.1074/JBC.275.11.7521>

- O'Brien, J. A., Daudi, A., Butt, V. S., & Paul Bolwell, G. (2012). Reactive oxygen species and their role in plant defence and cell wall metabolism. *Planta* 236:3, 236(3), 765–779. <https://doi.org/10.1007/S00425-012-1696-9>
- Ogasawara, Y., Kaya, H., Hiraoka, G., Yumoto, F., Kimura, S., Kadota, Y., Hishinuma, H., Senzaki, E., Yamagoe, S., Nagata, K., Nara, M., Suzuki, K., Tanokura, M., & Kuchitsu, K. (2008). Synergistic activation of the arabidopsis NADPH oxidase AtrbohD by Ca²⁺ and phosphorylation. *Journal of Biological Chemistry*. <https://doi.org/10.1074/jbc.M708106200>
- Olsen, J. v., & Mann, M. (2013). Status of Large-scale Analysis of Post-translational Modifications by Mass Spectrometry. *Molecular & Cellular Proteomics : MCP*, 12(12), 3444. <https://doi.org/10.1074/MCP.O113.034181>
- Ossig, R., Schmitt, H. D., Groot, B. de, Riedel, D., Keränen, S., Ronne, H., Grubmüller, H., & Jahn, R. (2000). Exocytosis requires asymmetry in the central layer of the SNARE complex. *The EMBO Journal*, 19(22), 6000–6010. <https://doi.org/10.1093/EMBOJ/19.22.6000>
- Palma, K., Zhang, Y., & Li, X. (2005). An importin α homolog, MOS6, plays an important role in plant innate immunity. *Current Biology*, 15(12), 1129–1135. <https://doi.org/10.1016/j.cub.2005.05.022>
- Park, J.-H., Halitschke, R., Kim, H. B., Baldwin, I. T., Feldmann, K. A., & Feyereisen, R. Â. (n.d.). A knock-out mutation in allene oxide synthase results in male sterility and defective wound signal transduction in Arabidopsis due to a block in jasmonic acid biosynthesis.
- Park, S. W., Kaimoyo, E., Kumar, D., Mosher, S., & Klessig, D. F. (2007). Methyl salicylate is a critical mobile signal for plant systemic acquired resistance. *Science*, 318(5847), 113–116. <https://doi.org/10.1126/science.1147113>
- Pauwels, L., Barbero, G. F., Geerinck, J., Tilleman, S., Grunewald, W., Pérez, A. C., Chico, J. M., Bossche, R. vanden, Sewell, J., Gil, E., García-Casado, G., Witters, E., Inzé, D., Long, J. A., Jaeger, G. de, Solano, R., & Goossens, A. (2010). NINJA connects the co-repressor TOPLESS to jasmonate signalling. *Nature*, 464(7289), 788. <https://doi.org/10.1038/NATURE08854>
- Pečenková, T., Hála, M., Kulich, I., Kocourková, D., Drdová, E., Fendrych, M., Toupalová, H., & Žárský, V. (2011). The role for the exocyst complex subunits Exo70B2 and Exo70H1 in the plant–pathogen interaction. *Journal of Experimental Botany*, 62(6), 2107–2116. <https://doi.org/10.1093/JXB/ERQ402>
- Pečenková, T., Pleskot, R., & Žárský, V. (2017). Subcellular Localization of Arabidopsis Pathogenesis-Related 1 (PR1) Protein. *International Journal of Molecular Sciences*, 18(4). <https://doi.org/10.3390/IJMS18040825>
- Peltier, J.-B., Ytterberg, A. J., Sun, Q., & Wijk, K. J. van. (2004). New Functions of the Thylakoid Membrane Proteome of Arabidopsis thaliana Revealed by a Simple, Fast, and Versatile Fractionation Strategy *. *Journal of Biological Chemistry*, 279(47), 49367–49383. <https://doi.org/10.1074/JBC.M406763200>
- Pena-Cortés, H., Albrecht, T., Prat, S., Weiler, E. W., & Willmitzer, L. (1993). Aspirin prevents wound-induced gene expression in tomato leaves by blocking jasmonic acid biosynthesis. *Planta* 193:1, 191(1), 123–128. <https://doi.org/10.1007/BF00240903>
- Peng, Y., van Wersch, R., & Zhang, Y. (2018). Convergent and divergent signaling in PAMP-triggered immunity and effector-triggered immunity. In *Molecular Plant-Microbe Interactions* (Vol. 31, Issue 4, pp. 403–409). American Phytopathological Society. <https://doi.org/10.1094/MPMI-06-17-0145-CR>
- Penninckx, I. A. M. A., Thomma, B. P. H. J., Buchala, A., Métraux, J.-P., & Broekaert,

- W. F. (1998). Concomitant Activation of Jasmonate and Ethylene Response Pathways Is Required for Induction of a Plant Defensin Gene in Arabidopsis. *The Plant Cell*, *10*, 2103–2113. www.plantcell.org
- Petersen, M., Brodersen, P., Naested, H., Andreasson, E., Lindhart, U., Johansen, B., Nielsen, H. B., Lacy, M., Austin, M. J., Parker, J. E., Sharma, S. B., Klessig, D. F., Martienssen, R., Mattsson, O., Jensen, A. B., & Mundy, J. (2000). Arabidopsis MAP kinase 4 negatively regulates systemic acquired resistance. *Cell*, *103*(7), 1111–1120. [https://doi.org/10.1016/S0092-8674\(00\)00213-0](https://doi.org/10.1016/S0092-8674(00)00213-0)
- Piasecka, A., Jedrzejczak-Rey, N., & Bednarek, P. (2015). Secondary metabolites in plant innate immunity: conserved function of divergent chemicals. *New Phytologist*, *206*(3), 948–964. <https://doi.org/10.1111/nph.13325>
- Pieterse, C. M. J., van der Does, D., Zamioudis, C., Leon-Reyes, A., & van Wees, S. C. M. (2012). Hormonal modulation of plant immunity. *Annual Review of Cell and Developmental Biology*, *28*, 489–521. <https://doi.org/10.1146/ANNUREV-CELLBIO-092910-154055>
- Piper, R. C., Dikic, I., & Lukacs, G. L. (2014). Ubiquitin-Dependent Sorting in Endocytosis. *Cold Spring Harbor Perspectives in Biology*, *6*(1). <https://doi.org/10.1101/CSHPERSPECT.A016808>
- Qiao, H., Chang, K. N., Yazaki, J., & Ecker, J. R. (2009). Interplay between ethylene, ETP1/ETP2 F-box proteins, and degradation of EIN2 triggers ethylene responses in Arabidopsis. *Genes & Development*, *23*(4), 512. <https://doi.org/10.1101/GAD.1765709>
- Qiu, J.-L., Fiil, B. K., Petersen, K., Nielsen, H. B., Botanga, C. J., Thorgrimsen, S., Palma, K., Suarez-Rodriguez, M. C., Sandbech-Clausen, S., Lichota, J., Brodersen, P., Grasser, K. D., Mattsson, O., Glazebrook, J., Mundy, J., & Petersen, M. (2008). Arabidopsis MAP kinase 4 regulates gene expression through transcription factor release in the nucleus. *The EMBO Journal*, *27*(16), 2214–2221. <https://doi.org/10.1038/emboj.2008.147>
- Queval, G., Issakidis-Bourguet, E., Hoeberichts, F. A., Vandenborgh, M., Gakière, B., Vanacker, H., Miginiac-Maslow, M., Breusegem, F. van, & Noctor, G. (2007). Conditional oxidative stress responses in the Arabidopsis photorespiratory mutant *cat2* demonstrate that redox state is a key modulator of daylength-dependent gene expression, and define photoperiod as a crucial factor in the regulation of H₂O₂-induced cell death. *The Plant Journal*, *52*(4), 640–657. <https://doi.org/10.1111/J.1365-313X.2007.03263.X>
- Radojčić, A., Li, X., & Zhang, Y. (2018). Salicylic Acid: A Double-Edged Sword for Programed Cell Death in Plants. *Frontiers in Plant Science*, *0*, 1133. <https://doi.org/10.3389/FPLS.2018.01133>
- Rao, S., Zhou, Z., Miao, P., Bi, G., Hu, M., Wu, Y., Feng, F., Zhang, X., & Zhou, J.-M. (2018). Roles of Receptor-Like Cytoplasmic Kinase VII Members in Pattern-Triggered Immune Signaling. *Plant Physiology*, *177*(4), 1679. <https://doi.org/10.1104/PP.18.00486>
- Rayapuram, N., Bigeard, J., Alhoraibi, H., Bonhomme, L., Hesse, A. M., Vinh, J., Hirt, H., & Pflieger, D. (2018). Quantitative phosphoproteomic analysis reveals shared and specific targets of Arabidopsis mitogen-activated protein kinases (MAPKs) MPK3, MPK4, and MPK6. *Molecular and Cellular Proteomics*, *17*(1), 61–80. <https://doi.org/10.1074/mcp.RA117.000135>
- Rayapuram, N., Jarad, M., Alhoraibi, H. M., Bigeard, J., Abulfaraj, A. A., Völz, R., Mariappan, K. G., Almeida-Trapp, M., Schlöffel, M., Lastrucci, E., Bonhomme, L., Gust, A. A., Mithöfer, A., Arold, S. T., Pflieger, D., & Hirt, H. (2021). Chromatin

- phosphoproteomics unravels a function for AT-hook motif nuclear localized protein AHL13 in PAMP-triggered immunity. *Proceedings of the National Academy of Sciences*, 118(3), 2004670118. <https://doi.org/10.1073/PNAS.2004670118>
- Reinhardt, D., Kende, H., & Boiler, T. (1994). Subcellular localization of 1-aminocyclopropane-1-carboxylate oxidase in tomato cells. *Planta* 195:1, 195(1), 142–146. <https://doi.org/10.1007/BF00206302>
- Rekhter, D., Mohnike, L., Feussner, K., Zienkiewicz, K., Zhang, Y., & Feussner, I. (2019). The plastidial exporter Enhanced Disease Susceptibility 5 is required for the biosynthesis of N-hydroxy pipelicolic acid. *BioRxiv*, 630723. <https://doi.org/10.1101/630723>
- Ren, D., Liu, Y., Yang, K. Y., Han, L., Mao, G., Glazebrook, J., & Zhang, S. (2008). A fungal-responsive MAPK cascade regulates phytoalexin biosynthesis in Arabidopsis. *Proceedings of the National Academy of Sciences of the United States of America*, 105(14), 5638–5643. <https://doi.org/10.1073/pnas.0711301105>
- Ren, D., Yang, H., & Zhang, S. (2002). Cell death mediated by MAPK is associated with hydrogen peroxide production in Arabidopsis. *Journal of Biological Chemistry*, 277(1), 559–565. <https://doi.org/10.1074/jbc.M109495200>
- Reyes, F. C., Buono, R., & Otegui, M. S. (2011). Plant endosomal trafficking pathways. *Current Opinion in Plant Biology*, 14(6), 666–673. <https://doi.org/10.1016/J.PBI.2011.07.009>
- Rigaille, G., Balzergue, S., Brunaud, V., Blondet, E., Rau, A., Rogier, O., Caius, J., Maugis-Rabusseau, C., Soubigou-Taconnat, L., Aubourg, S., Lurin, C., Martin-Magniette, M.-L., & Delannoy, E. (2018). Synthetic data sets for the identification of key ingredients for RNA-seq differential analysis. *Briefings in Bioinformatics*, 19(1), 65–76. <https://doi.org/10.1093/BIB/BBW092>
- Robatzek, S., Chinchilla, D., & Boller, T. (2006). Ligand-induced endocytosis of the pattern recognition receptor FLS2 in Arabidopsis. *Genes & Development*, 20(5), 537. <https://doi.org/10.1101/GAD.366506>
- Robinson, M. D., McCarthy, D. J., & Smyth, G. K. (2010). edgeR: a Bioconductor package for differential expression analysis of digital gene expression data. *Bioinformatics*, 26(1), 139. <https://doi.org/10.1093/BIOINFORMATICS/BTP616>
- Rochon, A., Boyle, P., Wignes, T., Fobert, P. R., & Després, C. (2006). The coactivator function of Arabidopsis NPR1 requires the core of its BTB/POZ domain and the oxidation of C-terminal cysteines. *Plant Cell*, 18(12), 3670–3685. <https://doi.org/10.1105/tpc.106.046953>
- Rodriguez-Moreno, L., Ebert, M. K., Bolton, M. D., & Thomma, B. P. H. J. (2018). Tools of the crook- infection strategies of fungal plant pathogens. *The Plant Journal*, 93(4), 664–674. <https://doi.org/10.1111/TPJ.13810>
- Rothman, J. E. (2013). *James E. Rothman - Nobel Lecture: The Principle of Membrane Fusion in the Cell*.
- Roux, C. le, Prete, S. del, Boutet-Mercey, S., Perreau, F., Balagué, C., Roby, D., Fagard, M., & Gaudin, V. (2014). The hnRNP-Q Protein LIF2 Participates in the Plant Immune Response. *PLOS ONE*, 9(6), e99343. <https://doi.org/10.1371/JOURNAL.PONE.0099343>
- Roux, M. E., Rasmussen, M. W., Palma, K., Lolle, S., Regué, À. M., Bethke, G., Glazebrook, J., Zhang, W., Sieburth, L., Larsen, M. R., Mundy, J., & Petersen, M. (2015). The mRNA decay factor PAT 1 functions in a pathway including MAP kinase 4 and immune receptor SUMM 2. *The EMBO Journal*, 34(5), 593–608. <https://doi.org/10.15252/embj.201488645>
- Ruano, G., & Scheuring, D. (2020). Plant Cells under Attack: Unconventional

- Endomembrane Trafficking during Plant Defense. *Plants*, 9(3).
<https://doi.org/10.3390/PLANTS9030389>
- Ryder, L. S., & Talbot, N. J. (2015). Regulation of appressorium development in pathogenic fungi. *Current Opinion in Plant Biology*, 26, 8.
<https://doi.org/10.1016/J.PBI.2015.05.013>
- Saile Id, S. C., Id, P. J., Castel, B., 4th, I. D., Jubic, L. M., Salas-González, I., Bă Cker Id, M., Jones Id, J. D. G., Dangl Id, J. L., El, F., & Id, K. (2020). *Two unequally redundant “helper” immune receptor families mediate Arabidopsis thaliana intracellular “sensor” immune receptor functions.*
<https://doi.org/10.1371/journal.pbio.3000783>
- Šamaj, J., Read, N. D., Volkmann, D., Menzel, D., & Baluška, F. (2005). The endocytic network in plants. *Trends in Cell Biology*, 15(8), 425–433.
<https://doi.org/10.1016/J.TCB.2005.06.006>
- Sanderfoot, A. A., Assaad, F. F., & Raikhel, N. v. (2000). The Arabidopsis Genome. An Abundance of Soluble N-Ethylmaleimide-Sensitive Factor Adaptor Protein Receptors. *Plant Physiology*, 124(4), 1558–1569.
<https://doi.org/10.1104/PP.124.4.1558>
- Sasaki-Sekimoto, Y., Jikumaru, Y., Obayashi, T., Saito, H., Masuda, S., Kamiya, Y., Ohta, H., & Shirasu, K. (2013). Basic Helix-Loop-Helix Transcription Factors JASMONATE-ASSOCIATED MYC2-LIKE1 (JAM1), JAM2, and JAM3 Are Negative Regulators of Jasmonate Responses in Arabidopsis. *Plant Physiology*, 163(1), 291. <https://doi.org/10.1104/PP.113.220129>
- Sato, T., & Theologis, A. (1989). Cloning the mRNA encoding 1-aminocyclopropane-1-carboxylate synthase, the key enzyme for ethylene biosynthesis in plants. *Proceedings of the National Academy of Sciences of the United States of America*, 86(17), 6621. <https://doi.org/10.1073/PNAS.86.17.6621>
- Savary, S., Ficke, A., Aubertot, J. N., & Hollier, C. (2012). Crop losses due to diseases and their implications for global food production losses and food security. In *Food Security* (Vol. 4, Issue 4, pp. 519–537). Springer. <https://doi.org/10.1007/s12571-012-0200-5>
- Scales, S. J., Yoo, B. Y., & Scheller, R. H. (2001). The ionic layer is required for efficient dissociation of the SNARE complex by α -SNAP and NSF. *Proceedings of the National Academy of Sciences*, 98(25), 14262–14267.
<https://doi.org/10.1073/PNAS.251547598>
- Schaller, G. E., & Kieber, J. J. (2002). Ethylene. *The Arabidopsis Book / American Society of Plant Biologists*, 1(1), 1–17. <https://doi.org/10.1199/TAB.0071>
- Schweighofer, A., Kazanaviciute, V., Scheikl, E., Teige, M., Doczi, R., Hirt, H., Schwanninger, M., Kant, M., Schuurink, R., Mauch, F., Buchala, A., Cardinale, F., & Meskiene, I. (2007). The PP2C-Type Phosphatase AP2C1, Which Negatively Regulates MPK4 and MPK6, Modulates Innate Immunity, Jasmonic Acid, and Ethylene Levels in Arabidopsis. *The Plant Cell*, 19(7), 2213–2224.
<https://doi.org/10.1105/TPC.106.049585>
- Seo, H. S., Song, J. T., Cheong, J. J., Lee, Y. H., Lee, Y. W., Hwang, I., Lee, J. S., & Choi, Y. do. (2001). Jasmonic acid carboxyl methyltransferase: A key enzyme for jasmonate-regulated plant responses. *Proceedings of the National Academy of Sciences of the United States of America*, 98(8), 4788–4793.
<https://doi.org/10.1073/pnas.081557298>
- Shao, F., Golstein, C., Ade, J., Stoutemyer, M., Dixon, J. E., & Innes, R. W. (2003). Cleavage of Arabidopsis PBS1 by a bacterial type III effector. *Science*, 301(5637), 1230–1233. <https://doi.org/10.1126/science.1085671>

- Shao, Z.-Q., Xue, J.-Y., Wu, P., Zhang, Y.-M., Wu, Y., Hang, Y.-Y., Wang, B., & Chen, J.-Q. (2016). Large-Scale Analyses of Angiosperm Nucleotide-Binding Site-Leucine-Rich Repeat Genes Reveal Three Anciently Diverged Classes with Distinct Evolutionary Patterns. *Plant Physiology*, *170*(4), 2095.
<https://doi.org/10.1104/PP.15.01487>
- Shen, Q. H., Saijo, Y., Mauch, S., Biskup, C., Bieri, S., Keller, B., Seki, H., Ülker, B., Somssich, I. E., & Schulze-Lefert, P. (2007). Nuclear activity of MLA immune receptors links isolate-specific and basal disease-resistance responses. *Science*.
<https://doi.org/10.1126/science.1136372>
- Shine, M. B., Xiao, X., Kachroo, P., & Kachroo, A. (2019). Signaling mechanisms underlying systemic acquired resistance to microbial pathogens. In *Plant Science* (Vol. 279, pp. 81–86). Elsevier Ireland Ltd.
<https://doi.org/10.1016/j.plantsci.2018.01.001>
- Shirano, Y., Kachroo, P., Shah, J., & Klessig, D. F. (2002). A Gain-of-Function Mutation in an Arabidopsis Toll Interleukin1 Receptor–Nucleotide Binding Site–Leucine-Rich Repeat Type R Gene Triggers Defense Responses and Results in Enhanced Disease Resistance. *The Plant Cell*, *14*(12), 3149–3162.
<https://doi.org/10.1105/TPC.005348>
- Shulaev, V., Leon, J., & Raskin, I. (1995). Is salicylic acid a translocated signal of systemic acquired resistance in tobacco? *Plant Cell*, *7*(10), 1691–1701.
<https://doi.org/10.1105/tpc.7.10.1691>
- Shulaev, V., Silverman, P., & Raskin, I. (1997). Airborne signalling by methyl salicylate in plant pathogen resistance. *Nature*, *385*(6618), 718–721.
<https://doi.org/10.1038/385718a0>
- Shyu, C., Figueroa, P., DePew, C. L., Cooke, T. F., Sheard, L. B., Moreno, J. E., Katsir, L., Zheng, N., Browse, J., & Howe, G. A. (2012). JAZ8 Lacks a Canonical Degron and Has an EAR Motif That Mediates Transcriptional Repression of Jasmonate Responses in Arabidopsis. *The Plant Cell*, *24*(2), 536–550.
<https://doi.org/10.1105/TPC.111.093005>
- Smith, J. M., Leslie, M. E., Robinson, S. J., Korasick, D. A., Zhang, T., Backues, S. K., Cornish, P. v., Koo, A. J., Bednarek, S. Y., & Heese, A. (2014). Loss of Arabidopsis thaliana Dynamin-Related Protein 2B Reveals Separation of Innate Immune Signaling Pathways. *PLOS Pathogens*, *10*(12), e1004578.
<https://doi.org/10.1371/JOURNAL.PPAT.1004578>
- Smith, T., Heger, A., & Sudbery, I. (2017). UMI-tools: modeling sequencing errors in Unique Molecular Identifiers to improve quantification accuracy. *Genome Research*, *27*(3), 491. <https://doi.org/10.1101/GR.209601.116>
- Sohn, K. H., Segonzac, C., Rallapalli, G., Sarris, P. F., Woo, J. Y., Williams, S. J., Newman, T. E., Paek, K. H., Kobe, B., & Jones, J. D. G. (2014). The Nuclear Immune Receptor RPS4 Is Required for RRS1SLH1-Dependent Constitutive Defense Activation in Arabidopsis thaliana. *PLOS Genetics*, *10*(10), e1004655.
<https://doi.org/10.1371/JOURNAL.PGEN.1004655>
- Söllner, T., Bennett, M. K., Whiteheart, S. W., Scheller, R. H., & Rothman, J. E. (1993). A protein assembly-disassembly pathway in vitro that may correspond to sequential steps of synaptic vesicle docking, activation, and fusion. *Cell*, *75*(3), 409–418.
[https://doi.org/10.1016/0092-8674\(93\)90376-2](https://doi.org/10.1016/0092-8674(93)90376-2)
- Song, J. T. (2006). Induction of a salicylic acid glucosyltransferase, AtSGT1, is an early disease response in Arabidopsis thaliana. *Molecules and Cells*, *22*(2), 233–238.
- Song, J. T., Koo, Y. J., Seo, H. S., Kim, M. C., Choi, Y. do, & Kim, J. H. (2008). Overexpression of AtSGT1, an Arabidopsis salicylic acid glucosyltransferase, leads

- to increased susceptibility to *Pseudomonas syringae*. *Phytochemistry*, *69*(5), 1128–1134. <https://doi.org/10.1016/j.phytochem.2007.12.010>
- Song, J. T., Lu, H., & Greenberg, J. T. (2004). Divergent Roles in *Arabidopsis thaliana* Development and Defense of Two Homologous Genes, Aberrant Growth and Death2 And AGD2-Like Defense Response Protein 1, Encoding Novel Aminotransferases. *Plant Cell*, *16*(2), 353–366. <https://doi.org/10.1105/tpc.019372>
- Song, S., Huang, H., Gao, H., Wang, J., Wu, D., Liu, X., Yang, S., Zhai, Q., Li, C., Qi, T., & Xie, D. (2014). Interaction between MYC2 and ETHYLENE INSENSITIVE3 Modulates Antagonism between Jasmonate and Ethylene Signaling in *Arabidopsis*. *The Plant Cell*, *26*(1), 263. <https://doi.org/10.1105/TPC.113.120394>
- Spallek, T., Beck, M., Khaled, S. ben, Salomon, S., Bourdais, G., Schellmann, S., & Robatzek, S. (2013). ESCRT-I Mediates FLS2 Endosomal Sorting and Plant Immunity. *PLOS Genetics*, *9*(12), e1004035. <https://doi.org/10.1371/JOURNAL.PGEN.1004035>
- Sparkes, I. A., Runions, J., Kearns, A., & Hawes, C. (2006). Rapid, transient expression of fluorescent fusion proteins in tobacco plants and generation of stably transformed plants. *Nature Protocols* *2006 1:4*, *1*(4), 2019–2025. <https://doi.org/10.1038/nprot.2006.286>
- Spoel, S. H., & Dong, X. (2008). Making Sense of Hormone Crosstalk during Plant Immune Responses. *Cell Host & Microbe*, *3*(6), 348–351. <https://doi.org/10.1016/J.CHOM.2008.05.009>
- Spoel, S. H., Johnson, J. S., & Dong, X. (2007). Regulation of tradeoffs between plant defenses against pathogens with different lifestyles. *Proceedings of the National Academy of Sciences of the United States of America*, *104*(47), 18842. <https://doi.org/10.1073/PNAS.0708139104>
- Spoel, S. H., Koornneef, A., Claessens, S. M. C., Korzelius, J. P., Pelt, J. A. van, Mueller, M. J., Buchala, A. J., Métraux, J.-P., Brown, R., Kazan, K., Loon, L. C. van, Dong, X., & Pieterse, C. M. J. (2003). NPR1 Modulates Cross-Talk between Salicylate- and Jasmonate-Dependent Defense Pathways through a Novel Function in the Cytosol. *The Plant Cell*, *15*(3), 760. <https://doi.org/10.1105/TPC.009159>
- Staswick, P. E., & Tiryaki, I. (2004a). The oxylipin signal jasmonic acid is activated by an enzyme that conjugate it to isoleucine in *Arabidopsis* W inside box sign. *Plant Cell*, *16*(8), 2117–2127. <https://doi.org/10.1105/tpc.104.023549>
- Staswick, P. E., & Tiryaki, I. (2004b). The oxylipin signal jasmonic acid is activated by an enzyme that conjugate it to isoleucine in *Arabidopsis* W inside box sign. *Plant Cell*, *16*(8), 2117–2127. <https://doi.org/10.1105/tpc.104.023549>
- Stegmann, M., Anderson, R. G., Ichimura, K., Pecenkova, T., Reuter, P., Žárský, V., McDowell, J. M., Shirasu, K., & Trujillo, M. (2012). The Ubiquitin Ligase PUB22 Targets a Subunit of the Exocyst Complex Required for PAMP-Triggered Responses in *Arabidopsis*. *The Plant Cell*, *24*(11), 4703. <https://doi.org/10.1105/TPC.112.104463>
- Stegmann, M., Anderson, R. G., Westphal, L., Rosahl, S., McDowell, J. M., & Trujillo, M. (2013). The exocyst subunit Exo70B1 is involved in the immune response of *Arabidopsis thaliana* to different pathogens and cell death. *Plant Signaling & Behavior*, *8*(12). <https://doi.org/10.4161/PSB.27421>
- Stein, M., Dittgen, J., Sánchez-Rodríguez, C., Hou, B.-H., Molina, A., Schulze-Lefert, P., Lipka, V., & Somerville, S. (2006). *Arabidopsis* PEN3/PDR8, an ATP Binding Cassette Transporter, Contributes to Nonhost Resistance to Inappropriate Pathogens That Enter by Direct Penetration. *The Plant Cell*, *18*(3), 731. <https://doi.org/10.1105/TPC.105.038372>

- Stenmark, H. (2009). Rab GTPases as coordinators of vesicle traffic. *Nature Reviews Molecular Cell Biology* 2009 10:8, 10(8), 513–525.
<https://doi.org/10.1038/nrm2728>
- Su, J., Xu, J., & Zhang, S. (2015). RACK1, scaffolding a heterotrimeric G protein and a MAPK cascade. *Trends in Plant Science*, 20(7), 405–407.
<https://doi.org/10.1016/j.tplants.2015.05.002>
- Su, J., Yang, L., Zhu, Q., Wu, H., He, Y., Liu, Y., Xu, J., Jiang, D., & Zhang, S. (2018). Active photosynthetic inhibition mediated by MPK3/MPK6 is critical to effector-triggered immunity. *PLoS Biology*, 16(5).
<https://doi.org/10.1371/JOURNAL.PBIO.2004122>
- Su, J., Zhang, M., Zhang, L., Sun, T., Liu, Y., Lukowitz, W., Xu, J., & Zhang, S. (2017). Regulation of stomatal immunity by interdependent functions of a pathogen-responsive MPK3/MPK6 cascade and abscisic acid. *Plant Cell*, 29(3), 526–542.
<https://doi.org/10.1105/tpc.16.00577>
- Su, S.-H., Suarez-Rodriguez, M. C., & Krysan, P. (2007). Genetic interaction and phenotypic analysis of the Arabidopsis MAP kinase pathway mutations mekk1 and mpk4 suggests signaling pathway complexity. *FEBS Letters*, 581(17), 3171–3177.
<https://doi.org/10.1016/J.FEBSLET.2007.05.083>
- Sun, T., Busta, L., Zhang, Q., Ding, P., Jetter, R., & Zhang, Y. (2018). TGACG-BINDING FACTOR 1 (TGA1) and TGA4 regulate salicylic acid and pipelicolic acid biosynthesis by modulating the expression of SYSTEMIC ACQUIRED RESISTANCE DEFICIENT 1 (SARD1) and CALMODULIN-BINDING PROTEIN 60g (CBP60g). *New Phytologist*, 217(1), 344–354.
<https://doi.org/10.1111/nph.14780>
- Sun, T., Nitta, Y., Zhang, Q., Wu, D., Tian, H., Lee, J. S., & Zhang, Y. (2018). Antagonistic interactions between two MAP kinase cascades in plant development and immune signaling. *EMBO Reports*, 19(7), e45324.
<https://doi.org/10.15252/embr.201745324>
- Sun, X., Lapin, D., Feehan, J. M., Stolze, S. C., Kramer, K., Dongus, J. A., Rzemieniewski, J., Blanvillain-Baufumé, S., Harzen, A., Bautor, J., Derbyshire, P., Menke, F. L. H., Finkemeier, I., Nakagami, H., Jones, J. D. G., & Parker, J. E. (2020). Pathogen effector recognition-dependent association of NRG1 with EDS1 and SAG101 in TNL receptor immunity. *BioRxiv*, 1–15.
<https://doi.org/10.1101/2020.12.21.423810>
- Suzuki, N., Miller, G., Morales, J., Shulaev, V., Torres, M. A., & Mittler, R. (2011). Respiratory burst oxidases: the engines of ROS signaling. *Current Opinion in Plant Biology*, 14(6), 691–699. <https://doi.org/10.1016/J.PBI.2011.07.014>
- Taj, G., Agarwal, P., Grant, M., & Kumar, A. (2010). MAPK machinery in plants: Recognition and response to different stresses through multiple signal transduction pathways. *Plant Signaling & Behavior*, 5(11), 1370.
<https://doi.org/10.4161/PSB.5.11.13020>
- Takagi, M., Hamano, K., Takagi, H., Morimoto, T., Akimitsu, K., Terauchi, R., Shirasu, K., & Ichimura, K. (2019). Disruption of the MAMP-Induced MEKK1-MKK1/MKK2-MPK4 Pathway Activates the TNL Immune Receptor SMN1/RPS6. *Plant and Cell Physiology*, 60(4), 778–787. <https://doi.org/10.1093/pcp/pcy243>
- Takken, F. L. W., & Govere, A. (2012). How to build a pathogen detector: Structural basis of NB-LRR function. *Current Opinion in Plant Biology*, 15(4), 375–384.
<https://doi.org/10.1016/j.pbi.2012.05.001>
- Tanoue, T., Adachi, M., Moriguchi, T., & Nishida, E. (2000). A conserved docking motif in MAP kinases common to substrates, activators and regulators. *Nature Cell*

- Biology*, 2(2), 110–116. <https://doi.org/10.1038/35000065>
- Teige, M., Scheikl, E., Eulgem, T., Dóczi, R., Ichimura, K., Shinozaki, K., Dangl, J. L., & Hirt, H. (2004). The MKK2 pathway mediates cold and salt stress signaling in Arabidopsis. *Molecular Cell*, 15(1), 141–152. <https://doi.org/10.1016/j.molcel.2004.06.023>
- Tena, G., Boudsocq, M., & Sheen, J. (2011). Protein kinase signaling networks in plant innate immunity. *Current Opinion in Plant Biology*, 14(5), 519–529. <https://doi.org/10.1016/j.pbi.2011.05.006>
- Thain, S. C., Vandenbussche, F., Laarhoven, L. J. J., Dowson-Day, M. J., Wang, Z.-Y., Tobin, E. M., Harren, F. J. M., Millar, A. J., & van der Straeten, D. (2004). Circadian Rhythms of Ethylene Emission in Arabidopsis. *Plant Physiology*, 136(3), 3751–3761. <https://doi.org/10.1104/PP.104.042523>
- Theodoulou, F. L., Job, K., Slocombe, S. P., Footitt, S., Holdsworth, M., Baker, A., Larson, T. R., & Graham, I. A. (2005). Jasmonic acid levels are reduced in COMATOSE ATP-binding cassette transporter mutants. Implications for transport of jasmonate precursors into peroxisomes. *Plant Physiology*, 137(3), 835–840. <https://doi.org/10.1104/pp.105.059352>
- Thines, B., Katsir, L., Melotto, M., Niu, Y., Mandaokar, A., Liu, G., Nomura, K., He, S. Y., Howe, G. A., & Browse, J. (2007). JAZ repressor proteins are targets of the SCFCO11 complex during jasmonate signalling. *Nature*, 448(7154), 661–665. <https://doi.org/10.1038/nature05960>
- Thomma, B. P. H. J., Penninckx, I. A. M. A., Broekaert, W. F., & Cammue, B. P. A. (2001). The complexity of disease signaling in Arabidopsis. *Current Opinion in Immunology*, 13(1), 63–68. [https://doi.org/10.1016/S0952-7915\(00\)00183-7](https://doi.org/10.1016/S0952-7915(00)00183-7)
- Thor, K., Jiang, S., Michard, E., George, J., Scherzer, S., Huang, S., Dindas, J., Derbyshire, P., Leitão, N., DeFalco, T. A., Köster, P., Hunter, K., Kimura, S., Gronnier, J., Stransfeld, L., Kadota, Y., Bücherl, C. A., Charpentier, M., Wrzaczek, M., ... Zipfel, C. (2020). The calcium-permeable channel OSCA1.3 regulates plant stomatal immunity. *Nature* 2020 585:7826, 585(7826), 569–573. <https://doi.org/10.1038/s41586-020-2702-1>
- Tian, H., Chen, S., Wu, Z., Ao, K., Yaghmaiean, H., Sun, T., Huang, W., Xu, F., Zhang, Y., Wang, S., Li, X., & Zhang, Y. (2020). Activation of TIR signaling is required for pattern-triggered immunity. In *bioRxiv* (p. 2020.12.27.424494). Cold Spring Harbor Laboratory. <https://doi.org/10.1101/2020.12.27.424494>
- Tian, H., & Zhang, Y. (2019). The emergence of a mobile signal for systemic acquired resistance. In *Plant Cell* (Vol. 31, Issue 7, pp. 1414–1415). American Society of Plant Biologists. <https://doi.org/10.1105/tpc.19.00350>
- Tian, W., Hou, C., Ren, Z., Wang, C., Zhao, F., Dahlbeck, D., Hu, S., Zhang, L., Niu, Q., Li, L., Staskawicz, B. J., & Luan, S. (2019). A calmodulin-gated calcium channel links pathogen patterns to plant immunity. *Nature* 2019 572:7767, 572(7767), 131–135. <https://doi.org/10.1038/s41586-019-1413-y>
- Tintor, N., Ross, A., Kanehara, K., Yamada, K., Fan, L., Kemmerling, B., Nürnberger, T., Tsuda, K., & Saijo, Y. (2013). Layered pattern receptor signaling via ethylene and endogenous elicitor peptides during Arabidopsis immunity to bacterial infection. *Proceedings of the National Academy of Sciences of the United States of America*. <https://doi.org/10.1073/pnas.1216780110>
- Torrens-Spence, M. P., Bobokalonova, A., Carballo, V., Glinkerman, C. M., Pluskal, T., Shen, A., & Weng, J. K. (2019). PBS3 and EPS1 Complete Salicylic Acid Biosynthesis from Isochorismate in Arabidopsis. *Molecular Plant*, 12(12), 1577–1586. <https://doi.org/10.1016/J.MOLP.2019.11.005>

- Torsten Schultz-Larsen, A., Lenk, A., Kalinowska, K., Kraesing Vestergaard, L., Pedersen, C., Isono, E., Thordal-Christensen, H., & Schultz-Larsen, T. (2018). The AMSH3 ESCRT-III-Associated Deubiquitinase Is Essential for Plant Immunity. *Cell Reports*, 25. <https://doi.org/10.1016/j.celrep.2018.11.011>
- Toruño, T. Y., Stergiopoulos, I., & Coaker, G. (2016). Plant-Pathogen Effectors: Cellular Probes Interfering with Plant Defenses in Spatial and Temporal Manners. *Annual Review of Phytopathology*, 54, 419. <https://doi.org/10.1146/ANNUREV-PHYTO-080615-100204>
- Tse, Y. C., Mo, B., Hillmer, S., Zhao, M., Lo, S. W., Robinson, D. G., & Jiang, L. (2004). Identification of Multivesicular Bodies as Prevacuolar Compartments in *Nicotiana tabacum* BY-2 Cells. *The Plant Cell*, 16(3), 672. <https://doi.org/10.1105/TPC.019703>
- Tsuda, K., & Katagiri, F. (2010). Comparing signaling mechanisms engaged in pattern-triggered and effector-triggered immunity. *Current Opinion in Plant Biology*, 13(4), 459–465. <https://doi.org/10.1016/J.PBI.2010.04.006>
- Tsuda, K., Mine, A., Bethke, G., Igarashi, D., Botanga, C. J., Tsuda, Y., Glazebrook, J., Sato, M., & Katagiri, F. (2013). Dual Regulation of Gene Expression Mediated by Extended MAPK Activation and Salicylic Acid Contributes to Robust Innate Immunity in *Arabidopsis thaliana*. *PLoS Genetics*, 9(12). <https://doi.org/10.1371/journal.pgen.1004015>
- Tsuda, K., Sato, M., Stoddard, T., Glazebrook, J., & Katagiri, F. (2009). Network properties of robust immunity in plants. *PLoS Genetics*. <https://doi.org/10.1371/journal.pgen.1000772>
- Turner, J. G., Ellis, C., & Devoto, A. (2002). The jasmonate signal pathway. *Plant Cell*, 14(SUPPL.), s153. <https://doi.org/10.1105/tpc.000679>
- Uemura, T., Ueda, T., Ohniwa, R. L., Nakano, A., Takeyasu, K., & Sato, M. H. (2004). Systematic Analysis of SNARE Molecules in *Arabidopsis*: Dissection of the post-Golgi Network in Plant Cells. *Cell Structure and Function*, 29(2), 49–65. <https://doi.org/10.1247/CSF.29.49>
- Ulm, R., Ichimura, K., Mizoguchi, T., Peck, S. C., Zhu, T., Wang, X., Shinozaki, K., & Paszkowski, J. (2002). Distinct regulation of salinity and genotoxic stress responses by *Arabidopsis* MAP kinase phosphatase 1. *The EMBO Journal*, 21(23), 6483–6493. <https://doi.org/10.1093/EMBOJ/CDF646>
- Umezawa, T., Sugiyama, N., Takahashi, F., Anderson, J. C., Ishihama, Y., Peck, S. C., & Shinozaki, K. (2013). Genetics and phosphoproteomics reveal a protein phosphorylation network in the abscisic acid signaling pathway in *Arabidopsis thaliana*. *Science Signaling*, 6(270). <https://doi.org/10.1126/SCISIGNAL.2003509>
- Vaca, E., Behrens, C., Theccanat, T., Choe, J. Y., & Dean, J. v. (2017). Mechanistic differences in the uptake of salicylic acid glucose conjugates by vacuolar membrane-enriched vesicles isolated from *Arabidopsis thaliana*. *Physiologia Plantarum*, 161(3), 322–338. <https://doi.org/10.1111/ppl.12602>
- Valencia, J. P., Goodman, K., & Otegui, M. S. (2016). Endocytosis and Endosomal Trafficking in Plants. <http://Dx.Doi.Org/10.1146/Annurev-Arplant-043015-112242>, 67, 309–335. <https://doi.org/10.1146/ANNUREV-ARPLANT-043015-112242>
- Van de Weyer, A. L., Monteiro, F., Furzer, O. J., Nishimura, M. T., Cevik, V., Witek, K., Jones, J. D. G., Dangl, J. L., Weigel, D., & Bemm, F. (2019). A Species-Wide Inventory of NLR Genes and Alleles in *Arabidopsis thaliana*. *Cell*, 178(5), 1260–1272.e14. <https://doi.org/10.1016/j.cell.2019.07.038>
- van der Hoorn, R. A. L., & Kamoun, S. (2008). From Guard to Decoy: A New Model for Perception of Plant Pathogen Effectors. *The Plant Cell*, 20(8), 2009 LP – 2017.

- <https://doi.org/10.1105/tpc.108.060194>
- van Verk, M. C., Bol, J. F., & Linthorst, H. J. M. (2011). WRKY Transcription Factors Involved in Activation of SA Biosynthesis Genes. *BMC Plant Biology*, *11*, 89. <https://doi.org/10.1186/1471-2229-11-89>
- Vernooij, B., Friedrich, L., Morse, A., Reist, R., Kolditz-Jawhar, R., Ward, E., Uknes, S., Kessmann, H., & Ryals, J. (1994). Salicylic acid is not the translocated signal responsible for inducing systemic acquired resistance but is required in signal transduction. *Plant Cell*, *6*(7), 959–965. <https://doi.org/10.1105/tpc.6.7.959>
- Viotti, C., Bubeck, J., Stierhof, Y.-D., Krebs, M., Langhans, M., van den Berg, W., van Dongen, W., Richter, S., Geldner, N., Takano, J., Jürgens, G., de Vries, S. C., Robinson, D. G., & Schumacher, K. (2012). Endocytic and Secretory Traffic in Arabidopsis Merge in the Trans-Golgi Network/Early Endosome, an Independent and Highly Dynamic Organelle. *The Plant Cell*, *22*(4), 1344–1357. <https://doi.org/10.1105/TPC.109.072637>
- Vitale, A., & Denecke, J. (1999). The endoplasmic reticulum-gateway of the secretory pathway. *The Plant Cell*, *11*(4), 615. <https://doi.org/10.1105/TPC.11.4.615>
- Vlot, A. C., Liu, P. P., Cameron, R. K., Park, S. W., Yang, Y., Kumar, D., Zhou, F., Padukkavidana, T., Gustafsson, C., Pichersky, E., & Klessig, D. F. (2008). Identification of likely orthologs of tobacco salicylic acid-binding protein 2 and their role in systemic acquired resistance in Arabidopsis thaliana. *Plant Journal*, *56*(3), 445–456. <https://doi.org/10.1111/j.1365-313X.2008.03618.x>
- Vos, I. A., Verhage, A., Schuurink, R. C., Watt, L. G., Pieterse, C. M. J., & van Wees, S. C. M. (2013). Onset of herbivore-induced resistance in systemic tissue primed for jasmonate-dependent defenses is activated by abscisic acid. *Frontiers in Plant Science*, *4*(DEC). <https://doi.org/10.3389/fpls.2013.00539>
- Waghmare, S., Lefoulon, C., Zhang, B., Liliekyte, E., Donald, N., & Blatt, M. R. (2019). K⁺ Channel-SEC11 Binding Exchange Regulates SNARE Assembly for Secretory Traffic. *Plant Physiology*, *181*(3), 1096–1113. <https://doi.org/10.1104/PP.19.00919>
- Waghmare, S., Lileikyte, E., Karnik, R., Goodman, J. K., Blatt, M. R., & Jones, A. M. E. (2018). SNAREs SYP121 and SYP122 Mediate the Secretion of Distinct Cargo Subsets. *Plant Physiology*, *178*(4), 1679. <https://doi.org/10.1104/PP.18.00832>
- Wan, L., Essuman, K., Anderson, R. G., Sasaki, Y., Monteiro, F., Chung, E.-H., Nishimura, E. O., DiAntonio, A., Milbrandt, J., Dangl, J. L., & Nishimura, M. T. (2019). TIR domains of plant immune receptors are NAD⁺-cleaving enzymes that promote cell death. *Science*, *365*(6455), 799–803. <https://doi.org/10.1126/SCIENCE.AAX1771>
- Wan, W. L., Fröhlich, K., Pruitt, R. N., Nürnberger, T., & Zhang, L. (2019). Plant cell surface immune receptor complex signaling. *Current Opinion in Plant Biology*, *50*(Figure 1), 18–28. <https://doi.org/10.1016/j.pbi.2019.02.001>
- Wang, C., El-Shetehy, M., Shine, M. B., Yu, K., Navarre, D., Wendehenne, D., Kachroo, A., & Kachroo, P. (2014). Free Radicals Mediate Systemic Acquired Resistance. *Cell Reports*, *7*(2), 348–355. <https://doi.org/10.1016/j.celrep.2014.03.032>
- Wang, D., & Dong, X. (2011). A Highway for War and Peace: The Secretory Pathway in Plant–Microbe Interactions. *Molecular Plant*, *4*(4), 581–587. <https://doi.org/10.1093/MP/SSR053>
- Wang, F., Shang, Y., Fan, B., Yu, J.-Q., & Chen, Z. (2014). Arabidopsis LIP5, a Positive Regulator of Multivesicular Body Biogenesis, Is a Critical Target of Pathogen-Responsive MAPK Cascade in Plant Basal Defense. *PLOS Pathogens*, *10*(7), e1004243. <https://doi.org/10.1371/JOURNAL.PPAT.1004243>
- Wang, G., Roux, B., Feng, F., Guy, E., Li, L., Li, N., Zhang, X., Lautier, M., Jardinaud,

- M. F., Chabannes, M., Arlat, M., Chen, S., He, C., Noël, L. D., & Zhou, J. M. (2015). The Decoy Substrate of a Pathogen Effector and a Pseudokinase Specify Pathogen-Induced Modified-Self Recognition and Immunity in Plants. *Cell Host & Microbe*, 18(3), 285–295. <https://doi.org/10.1016/J.CHOM.2015.08.004>
- Wang, J., Ding, Y., Wang, J., Hillmer, S., Miao, Y., Lo, S. W., Wang, X., Robinson, D. G., & Jiang, L. (2010). EXPO, an Exocyst-Positive Organelle Distinct from Multivesicular Endosomes and Autophagosomes, Mediates Cytosol to Cell Wall Exocytosis in Arabidopsis and Tobacco Cells. *The Plant Cell*, 22(12), 4009. <https://doi.org/10.1105/TPC.110.080697>
- Wang, J., Hu, M., Wang, J., Qi, J., Han, Z., Wang, G., Qi, Y., Wang, H.-W., Zhou, J.-M., & Chai, J. (2019). Reconstitution and structure of a plant NLR resistosome conferring immunity. *Science*, 364(6435). <https://doi.org/10.1126/SCIENCE.AAV5870>
- Wang, J., Wang, J., Hu, M., Wu, S., Qi, J., Wang, G., Han, Z., Qi, Y., Gao, N., Wang, H.-W., Zhou, J.-M., & Chai, J. (2019). Ligand-triggered allosteric ADP release primes a plant NLR complex. *Science*, 364(6435). <https://doi.org/10.1126/SCIENCE.AAV5868>
- Wang, L., Tsuda, K., Sato, M., Cohen, J. D., Katagiri, F., & Glazebrook, J. (2009). Arabidopsis CaM binding protein CBP60g contributes to MAMP-induced SA accumulation and is involved in disease resistance against *Pseudomonas syringae*. *PLoS Pathogens*, 5(2), 1000301. <https://doi.org/10.1371/journal.ppat.1000301>
- Wang, L., Tsuda, K., Truman, W., Sato, M., Nguyen, L. v., Katagiri, F., & Glazebrook, J. (2011). CBP60g and SARD1 play partially redundant critical roles in salicylic acid signaling. *Plant Journal*, 67(6), 1029–1041. <https://doi.org/10.1111/j.1365-313X.2011.04655.x>
- Wang, L., Wang, S., & Li, W. (2012). RSeQC: quality control of RNA-seq experiments. *Bioinformatics*, 28(16), 2184–2185. <https://doi.org/10.1093/BIOINFORMATICS/BTS356>
- Wang, P., Hsu, C.-C., Du, Y., Zhu, P., Zhao, C., Fu, X., Zhang, C., Paez, J. S., Macho, A. P., Tao, W. A., & Zhu, J.-K. (2020). Mapping proteome-wide targets of protein kinases in plant stress responses. *Proceedings of the National Academy of Sciences*, 117(6), 3270–3280. <https://doi.org/10.1073/PNAS.1919901117>
- Wang, P., Sun, Y., Pei, Y., Li, X., Zhang, X., Li, F., & Hou, Y. (2018). GhSNAP33, a t-SNARE Protein From *Gossypium hirsutum*, Mediates Resistance to *Verticillium dahliae* Infection and Tolerance to Drought Stress. *Frontiers in Plant Science*, 9. <https://doi.org/10.3389/FPLS.2018.00896>
- Wang, P., Zhang, X., Ma, X., Sun, Y., Liu, N., Li, F., & Hou, Y. (2017). Identification of CkSNAP33, a gene encoding synaptosomal-associated protein from *Cynanchum komarovii*, that enhances Arabidopsis resistance to *Verticillium dahliae*. *PLoS ONE*, 12(6). <https://doi.org/10.1371/JOURNAL.PONE.0178101>
- Wang, W., Esch, J. J., Shiu, S.-H., Agula, H., Binder, B. M., Chang, C., Patterson, S. E., & Bleecker, A. B. (2006). Identification of Important Regions for Ethylene Binding and Signaling in the Transmembrane Domain of the ETR1 Ethylene Receptor of Arabidopsis. *The Plant Cell*, 18(12), 3429. <https://doi.org/10.1105/TPC.106.044537>
- Wang, W., Liu, N., Gao, C., Cai, H., Romeis, T., & Tang, D. (2020). The Arabidopsis exocyst subunits EXO70B1 and EXO70B2 regulate FLS2 homeostasis at the plasma membrane. *New Phytologist*, 227(2), 529–544. <https://doi.org/10.1111/NPH.16515>
- Wang, W., Liu, N., Gao, C., Rui, L., & Tang, D. (2019). The *Pseudomonas Syringae* Effector AvrPtoB Associates With and Ubiquitinates Arabidopsis Exocyst Subunit

- EXO70B1. *Frontiers in Plant Science*, 10.
<https://doi.org/10.3389/FPLS.2019.01027>
- Wang, X., Xu, M., Gao, C., Zeng, Y., Cui, Y., Shen, W., & Jiang, L. (2020). The roles of endomembrane trafficking in plant abiotic stress responses. *Journal of Integrative Plant Biology*, 62(1), 55–69. <https://doi.org/10.1111/JIPB.12895>
- Warren, R. F., Holub, E., & Innes, R. W. (1999). Identification of three putative signal transduction genes involved in R gene-specified disease resistance in Arabidopsis. *Genetics*, 152(1), 401–412. <https://doi.org/10.1093/genetics/152.1.401>
- Wasternack, C., & Strnad, M. (2018). Jasmonates: News on Occurrence, Biosynthesis, Metabolism and Action of an Ancient Group of Signaling Compounds. *International Journal of Molecular Sciences*, 19(9).
<https://doi.org/10.3390/IJMS19092539>
- Watanabe, S., Shimada, T. L., Hiruma, K., & Takano, Y. (2013). Pathogen Infection Trial Increases the Secretion of Proteins Localized in the Endoplasmic Reticulum Body of Arabidopsis. *Plant Physiology*, 163(2), 659.
<https://doi.org/10.1104/PP.113.217364>
- Waters, M. G., & Hughson, F. M. (2000). Membrane Tethering and Fusion in the Secretory and Endocytic Pathways. *Traffic*, 1(8), 588–597.
<https://doi.org/10.1034/J.1600-0854.2000.010802.X>
- Wees, S. van. (2008). Phenotypic Analysis of Arabidopsis Mutants: Trypan Blue Stain for Fungi, Oomycetes, and Dead Plant Cells. *Cold Spring Harbor Protocols*, 2008(8), pdb.prot4982. <https://doi.org/10.1101/PDB.PROT4982>
- Weimbs, T., Low, S. H., Chapin, S. J., Mostov, K. E., Bucher, P., & Hofmann, K. (1997). A conserved domain is present in different families of vesicular fusion proteins: A new superfamily. *Proceedings of the National Academy of Sciences of the United States of America*, 94(7), 3046. <https://doi.org/10.1073/PNAS.94.7.3046>
- Wen, X., Zhang, C., Ji, Y., Zhao, Q., He, W., An, F., Jiang, L., & Guo, H. (2012). Activation of ethylene signaling is mediated by nuclear translocation of the cleaved EIN2 carboxyl terminus. *Cell Research*, 22(11), 1613.
<https://doi.org/10.1038/CR.2012.145>
- Whyte, J. R. C., & Munro, S. (2002). Vesicle tethering complexes in membrane traffic. *Journal of Cell Science*, 115(13), 2627–2637.
<https://doi.org/10.1242/JCS.115.13.2627>
- Wick, P., Gansel, X., Oulevey, C., Page, V., Studer, I., Dürst, M., & Sticher, L. (2003). The expression of the t-SNARE AtSNAP33 is induced by pathogens and mechanical stimulation. *Plant Physiology*, 132(1), 343–351.
<https://doi.org/10.1104/pp.102.012633>
- WIDMANN, C., GIBSON, S., JARPE, M. B., & JOHNSON, G. L. (1999). Mitogen-Activated Protein Kinase: Conservation of a Three-Kinase Module From Yeast to Human. <https://doi.org/10.1152/Physrev.1999.79.1.143>, 79(1), 143–180.
<https://doi.org/10.1152/PHYSREV.1999.79.1.143>
- Wildermuth, M. C., Dewdney, J., Wu, G., & Ausubel, F. M. (2001). Isochorismate synthase is required to synthesize salicylic acid for plant defence. *Nature*, 414(6863), 562–565. <https://doi.org/10.1038/35107108>
- Williams, S. J., Sohn, K. H., Wan, L., Bernoux, M., Sarris, P. F., Segonzac, C., Ve, T., Ma, Y., Saucet, S. B., Ericsson, D. J., Casey, L. W., Lonhienne, T., Winzor, D. J., Zhang, X., Coerd, A., Parker, J. E., Dodds, P. N., Kobe, B., & Jones, J. D. G. (2014). Structural Basis for Assembly and Function of a Heterodimeric Plant Immune Receptor. *Science*, 344(6181), 299–303.
<https://doi.org/10.1126/SCIENCE.1247357>

- Wilson, D. B. (2008). Three Microbial Strategies for Plant Cell Wall Degradation. *Annals of the New York Academy of Sciences*, 1125(1), 289–297. <https://doi.org/10.1196/ANNALS.1419.026>
- Wirthmueller, L., Zhang, Y., Jones, J. D. G., & Parker, J. E. (2007). Nuclear Accumulation of the Arabidopsis Immune Receptor RPS4 Is Necessary for Triggering EDS1-Dependent Defense. *Current Biology*. <https://doi.org/10.1016/j.cub.2007.10.042>
- Won, K.-H., & Kim, H. (2020). Functions of the Plant Qbc SNARE SNAP25 in Cytokinesis and Biotic and Abiotic Stress Responses. *Molecules and Cells*, 43(4), 313. <https://doi.org/10.14348/MOLCELLS.2020.2245>
- Wu, L., Chen, H., Curtis, C., & Fu, Z. Q. (2014). Go in for the kill: How plants deploy effector-triggered immunity to combat pathogens. *Virulence*, 5(7), 710. <https://doi.org/10.4161/VIRU.29755>
- Wu, Y., Gao, Y., Zhan, Y., Kui, H., Liu, H., Yan, L., Kemmerling, B., Zhou, J.-M., He, K., & Li, J. (2020). Loss of the common immune coreceptor BAK1 leads to NLR-dependent cell death. *Proceedings of the National Academy of Sciences*, 117(43), 27044–27053. <https://doi.org/10.1073/PNAS.1915339117>
- Xie, D. X., Feys, B. F., James, S., Nieto-Rostro, M., & Turner, J. G. (1998). COI1: An Arabidopsis gene required for jasmonate-regulated defense and fertility. *Science*, 280(5366), 1091–1094. <https://doi.org/10.1126/science.280.5366.1091>
- Xin, X., Chen, W., Wang, B., Zhu, F., Li, Y., Yang, H., Li, J., & Ren, D. (2018). Arabidopsis MKK10-MPK6 mediates red-light-regulated opening of seedling cotyledons through phosphorylation of PIF3. *Journal of Experimental Botany*, 69(3), 423–439. <https://doi.org/10.1093/JXB/ERX418>
- Xu, J., Li, Y., Wang, Y., Liu, H., Lei, L., Yang, H., Liu, G., & Ren, D. (2008). Activation of MAPK Kinase 9 Induces Ethylene and Camalexin Biosynthesis and Enhances Sensitivity to Salt Stress in Arabidopsis * □ S. *Journal of Biological Chemistry*, 283, 26996–27006. <https://doi.org/10.1074/jbc.M801392200>
- Xu, J., Meng, J., Meng, X., Zhao, Y., Liu, J., Sun, T., Liu, Y., Wang, Q., & Zhang, S. (2016). Pathogen-responsive MPK3 and MPK6 reprogram the biosynthesis of indole glucosinolates and their derivatives in arabidopsis immunity. *Plant Cell*, 28(5), 1144–1162. <https://doi.org/10.1105/tpc.15.00871>
- Xu, J., Xie, J., Yan, C., Zou, X., Ren, D., & Zhang, S. (2014). A chemical genetic approach demonstrates that MPK3/MPK6 activation and NADPH oxidase-mediated oxidative burst are two independent signaling events in plant immunity. *The Plant Journal*, 77(2), 222–234. <https://doi.org/10.1111/TPJ.12382>
- Yan, J., Zhang, C., Gu, M., Bai, Z., Zhang, W., Qi, T., Cheng, Z., Peng, W., Luo, H., Nan, F., Wang, Z., & Xie, D. (2009). The arabidopsis CORONATINE INSENSITIVE1 protein is a jasmonate receptor. *Plant Cell*, 21(8), 2220–2236. <https://doi.org/10.1105/tpc.109.065730>
- Yang, T., Ali, G. S., Yang, L., Du, L., Reddy, A., & Poovaiah, B. (2010). Calcium/calmodulin-regulated receptor-like kinase CRLK1 interacts with MEKK1 in plants. *Plant Signaling & Behavior*, 5(8), 991. <https://doi.org/10.4161/PSB.5.8.12225>
- Yang Y.X., Ahammed G.J., Wu C., Fan S.Y., Zhou Y.H. (2015). Crosstalk among Jasmonate, Salicylate and Ethylene Signaling Pathways in Plant Disease and Immune Responses. *Current Protein & Peptide Science*, 16(5), 450–461. <https://doi.org/10.2174/1389203716666150330141638>
- Yip Delormel, T., & Boudsocq, M. (2019). Properties and functions of calcium-dependent protein kinases and their relatives in Arabidopsis thaliana. *New*

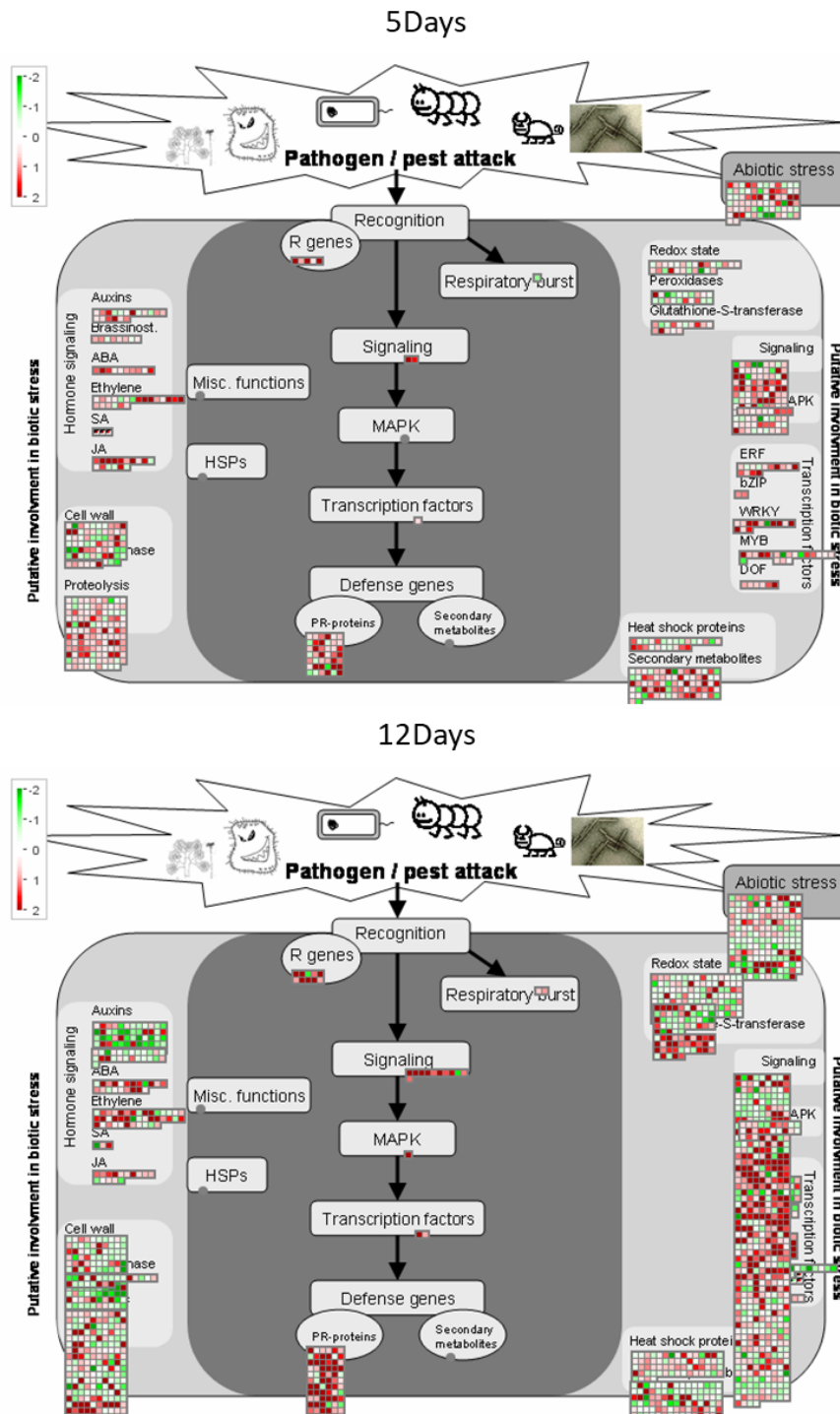
- Phytologist*, 224(2), 585–604. <https://doi.org/10.1111/nph.16088>
- Yoshioka, K. (2004). Scaffold Proteins in Mammalian MAP Kinase Cascades. *JB Minireview-Functions of MAP Kinase Cascades J. Biochem*, 135, 657–661. <https://doi.org/10.1093/j>
- Yu, C., Lin, Y., & Li, H. (2020). Increased ratio of galactolipid MGDG : DGDG induces jasmonic acid overproduction and changes chloroplast shape. *The New Phytologist*, 228(4), 1327. <https://doi.org/10.1111/NPH.16766>
- Yu, K., Soares, J. M., Mandal, M. K., Wang, C., Chanda, B., Gifford, A. N., Fowler, J. S., Navarre, D., Kachroo, A., & Kachroo, P. (2013). A Feedback Regulatory Loop between G3P and Lipid Transfer Proteins DIR1 and AZI1 Mediates Azelaic-Acid-Induced Systemic Immunity. *Cell Reports*, 3(4), 1266–1278. <https://doi.org/10.1016/j.celrep.2013.03.030>
- Yu, X., Feng, B., He, P., & Shan, L. (2017). From Chaos to Harmony: Responses and Signaling upon Microbial Pattern Recognition. *Annual Review of Phytopathology*, 55(1), 109–137. <https://doi.org/10.1146/annurev-phyto-080516-035649>
- Yuan, M., Jiang, Z., Bi, G., Nomura, K., Liu, M., Wang, Y., Cai, B., Zhou, J. M., He, S. Y., & Xin, X. F. (2021). Pattern-recognition receptors are required for NLR-mediated plant immunity. *Nature*, 592(7852), 105–109. <https://doi.org/10.1038/s41586-021-03316-6>
- Yuan, M., Ngou, B. P. M., Ding, P., & Xin, X. F. (2021). PTI-ETI crosstalk: an integrative view of plant immunity. *Current Opinion in Plant Biology*, 62, 102030. <https://doi.org/10.1016/j.pbi.2021.102030>
- Yuan, P., Jauregui, E., Du, L., Tanaka, K., & Poovaiah, B. W. (2017). Calcium signatures and signaling events orchestrate plant–microbe interactions. *Current Opinion in Plant Biology*, 38, 173–183. <https://doi.org/10.1016/J.PBI.2017.06.003>
- Yun, H. S., Kwaaitaal, M., Kato, N., Yi, C., Park, S., Sato, M. H., Schulze-Lefert, P., & Kwon, C. (2013). Requirement of vesicle-associated membrane protein 721 and 722 for sustained growth during immune responses in Arabidopsis. *Molecules and Cells* 2013 35:6, 35(6), 481–488. <https://doi.org/10.1007/S10059-013-2130-2>
- Zander, M., Camera, S. la, Lamotte, O., Métraux, J.-P., & Gatz, C. (2010). Arabidopsis thaliana class-II TGA transcription factors are essential activators of jasmonic acid/ethylene-induced defense responses. *The Plant Journal*, 61(2), 200–210. <https://doi.org/10.1111/J.1365-313X.2009.04044.X>
- Zander, M., Thurow, C., & Gatz, C. (2014). TGA Transcription Factors Activate the Salicylic Acid-Suppressible Branch of the Ethylene-Induced Defense Program by Regulating ORA59 Expression. *Plant Physiology*, 165(4), 1671–1683. <https://doi.org/10.1104/PP.114.243360>
- Zarei, A., Körbes, A. P., Younessi, P., Montiel, G., Champion, A., & Memelink, J. (2011). Two GCC boxes and AP2/ERF-domain transcription factor ORA59 in jasmonate/ethylene-mediated activation of the PDF1.2 promoter in Arabidopsis. *Plant Molecular Biology*, 75(4), 321. <https://doi.org/10.1007/S11103-010-9728-Y>
- Žárský, V., Kulich, I., Fendrych, M., & Pečenková, T. (2013). Exocyst complexes multiple functions in plant cells secretory pathways. *Current Opinion in Plant Biology*, 16(6), 726–733. <https://doi.org/10.1016/J.PBI.2013.10.013>
- Zhang, C., Guo, X., Xie, H., Li, J., Liu, X., Zhu, B., Liu, S., Li, H., Li, M., He, M., & Chen, P. (2019). Quantitative phosphoproteomics of lectin receptor-like kinase VI.4 dependent abscisic acid response in Arabidopsis thaliana. *Physiologia Plantarum*, 165(4), 728–745. <https://doi.org/10.1111/PPL.12763>
- Zhang, F., Qi, B., Wang, L., Zhao, B., Rode, S., Riggan, N. D., Ecker, J. R., & Qiao, H. (2016). EIN2-dependent regulation of acetylation of histone H3K14 and non-

- canonical histone H3K23 in ethylene signalling. *Nature Communications*, 7. <https://doi.org/10.1038/NCOMMS13018>
- Zhang, F., Wang, L., Qi, B., Zhao, B., Ko, E. E., Riggan, N. D., Chin, K., & Qiao, H. (2017). EIN2 mediates direct regulation of histone acetylation in the ethylene response. *Proceedings of the National Academy of Sciences*, 114(38), 10274–10279. <https://doi.org/10.1073/PNAS.1707937114>
- Zhang, J., Shao, F., Li, Y., Cui, H., Chen, L., Li, H., Zou, Y., Long, C., Lan, L., Chai, J., Chen, S., Tang, X., & Zhou, J. M. (2007). A *Pseudomonas syringae* Effector Inactivates MAPKs to Suppress PAMP-Induced Immunity in Plants. *Cell Host and Microbe*, 1(3), 175–185. <https://doi.org/10.1016/j.chom.2007.03.006>
- Zhang, J., & Zhou, J. M. (2010). Plant Immunity Triggered by Microbial Molecular Signatures. *Molecular Plant*, 3(5), 783–793. <https://doi.org/10.1093/MP/SSQ035>
- Zhang, L., Ma, J., Liu, H., Yi, Q., Wang, Y., Xing, J., Zhang, P., Ji, S., Li, M., Li, J., Shen, J., & Lin, J. (2021). SNARE proteins VAMP721 and VAMP722 mediate the post-Golgi trafficking required for auxin-mediated development in Arabidopsis. *The Plant Journal*, tpj.15450. <https://doi.org/10.1111/TPJ.15450>
- Zhang, T., Chen, S., & Harmon, A. C. (2016). Protein-protein interactions in plant mitogen-activated protein kinase cascades. In *Journal of Experimental Botany* (Vol. 67, Issue 3, pp. 607–618). Oxford University Press. <https://doi.org/10.1093/jxb/erv508>
- Zhang, X. C., & Gassmann, W. (2007). Alternative splicing and mRNA levels of the disease resistance gene RPS4 are induced during defense responses. *Plant Physiology*. <https://doi.org/10.1104/pp.107.108720>
- Zhang, X., Zhu, Z., An, F., Hao, D., Li, P., Song, J., Yi, C., & Guo, H. (2014). Jasmonate-Activated MYC2 Represses ETHYLENE INSENSITIVE3 Activity to Antagonize Ethylene-Promoted Apical Hook Formation in Arabidopsis. *The Plant Cell*, 26(3), 1105. <https://doi.org/10.1105/TPC.113.122002>
- Zhang, Y., & Li, X. (2005). A putative nucleoporin 96 is required for both basal defense and constitutive resistance responses mediated by suppressor of npr1-1, constitutive 1. *Plant Cell*. <https://doi.org/10.1105/tpc.104.029926>
- Zhang, Y., & Li, X. (2019). Salicylic acid: biosynthesis, perception, and contributions to plant immunity. *Current Opinion in Plant Biology*, 50, 29–36. <https://doi.org/10.1016/j.pbi.2019.02.004>
- Zhang, Y., Song, G., Lal, N. K., Nagalakshmi, U., Li, Y., Zheng, W., Huang, P., Branon, T. C., Ting, A. Y., Walley, J. W., & Dinesh-Kumar, S. P. (2019). TurboID-based proximity labeling reveals that UBR7 is a regulator of N NLR immune receptor-mediated immunity. *Nature Communications* 2019 10:1, 10(1), 1–17. <https://doi.org/10.1038/s41467-019-11202-z>
- Zhang, Y., & Turner, J. G. (2008). Wound-Induced Endogenous Jasmonates Stunt Plant Growth by Inhibiting Mitosis. *PLoS ONE*, 3(11), 3699. <https://doi.org/10.1371/JOURNAL.PONE.0003699>
- Zhang, Y., Xu, S., Ding, P., Wang, D., Cheng, Y. T., He, J., Gao, M., Xu, F., Li, Y., Zhu, Z., Li, X., & Zhang, Y. (2010). Control of salicylic acid synthesis and systemic acquired resistance by two members of a plant-specific family of transcription factors. *Proceedings of the National Academy of Sciences of the United States of America*, 107(42), 18220–18225. <https://doi.org/10.1073/pnas.1005225107>
- Zhang, Z., Lenk, A., Andersson, M. X., Gjetting, T., Pedersen, C., Nielsen, M. E., Newman, M. A., Hou, B. H., Somerville, S. C., & Thordal-Christensen, H. (2008). A Lesion-Mimic Syntaxin Double Mutant in Arabidopsis Reveals Novel Complexity of Pathogen Defense Signaling. *Molecular Plant*, 1(3), 510–527.

- <https://doi.org/10.1093/MP/SSN011>
- Zhang, Z., Liu, Y., Huang, H., Gao, M., Wu, D., Kong, Q., & Zhang, Y. (2017). The NLR protein SUMM 2 senses the disruption of an immune signaling MAP kinase cascade via CRCK 3. *EMBO Reports*, *18*(2), 292–302.
<https://doi.org/10.15252/embr.201642704>
- Zhang, Z., Wu, Y., Gao, M., Zhang, J., Kong, Q., Liu, Y., Ba, H., Zhou, J., & Zhang, Y. (2012). Disruption of PAMP-induced MAP kinase cascade by a pseudomonas syringae effector activates plant immunity mediated by the NB-LRR protein SUMM2. *Cell Host and Microbe*, *11*(3), 253–263.
<https://doi.org/10.1016/j.chom.2012.01.015>
- Zhao, T., Rui, L., Li, J., Nishimura, M. T., Vogel, J. P., Liu, N., Liu, S., Zhao, Y., Dangl, J. L., & Tang, D. (2015). A Truncated NLR Protein, TIR-NBS2, Is Required for Activated Defense Responses in the exo70B1 Mutant. *PLoS Genetics*, *11*(1).
<https://doi.org/10.1371/JOURNAL.PGEN.1004945>
- Zheng, X., Spivey, N. W., Zeng, W., Liu, P.-P., Fu, Z. Q., Klessig, D. F., He, S. Y., & Dong, X. (2012). Coronatine promotes Pseudomonas syringae virulence in plants by activating a signaling cascade that inhibits salicylic acid accumulation. *Cell Host & Microbe*, *11*(6), 587. <https://doi.org/10.1016/J.CHOM.2012.04.014>
- Zheng, Z., Qualley, A., Fan, B., Dudareva, N., & Chen, Z. (2009). An important role of a BAHD acyl transferase-like protein in plant innate immunity. *Plant Journal*, *57*(6), 1040–1053. <https://doi.org/10.1111/j.1365-313X.2008.03747.x>
- Zhou, J., Wang, X., He, Y., Sang, T., Wang, P., Dai, S., Zhang, S., & Meng, X. (2020). Differential phosphorylation of the transcription factor WRKY33 by the protein kinases CPK5/CPK6 and MPK3/MPK6 cooperatively regulates camalexin biosynthesis in arabidopsis. *Plant Cell*, *32*(8), 2621–2638.
<https://doi.org/10.1105/tpc.19.00971>
- Zhu, Z., An, F., Feng, Y., Li, P., Xue, L., A, M., Jiang, Z., Kim, J.-M., To, T. K., Li, W., Zhang, X., Yu, Q., Dong, Z., Chen, W.-Q., Seki, M., Zhou, J.-M., & Guo, H. (2011). Derepression of ethylene-stabilized transcription factors (EIN3/EIL1) mediates jasmonate and ethylene signaling synergy in Arabidopsis. *Proceedings of the National Academy of Sciences*, *108*(30), 12539–12544.
<https://doi.org/10.1073/PNAS.1103959108>
- Zhu, Z., Xu, F., Zhang, Y., Cheng, Y. T., Wiermer, M., Li, X., & Zhang, Y. (2010). Arabidopsis resistance protein SNC1 activates immune responses through association with a transcriptional corepressor. *Proceedings of the National Academy of Sciences of the United States of America*.
<https://doi.org/10.1073/pnas.1002828107>
- Zipfel, C. (2008). Pattern-recognition receptors in plant innate immunity. In *Current Opinion in Immunology*. <https://doi.org/10.1016/j.coi.2007.11.003>
- Zipfel, C., Kunze, G., Chinchilla, D., Caniard, A., Jones, J. D. G., Boller, T., & Felix, G. (2006). Perception of the Bacterial PAMP EF-Tu by the Receptor EFR Restricts Agrobacterium-Mediated Transformation. *Cell*, *125*(4), 749–760.
<https://doi.org/10.1016/J.CELL.2006.03.037>
- Zipfel, C., Robatzek, S., Navarro, L., Oakeley, E. J., Jones, J. D. G., Felix, G., & Boller, T. (2004). Bacterial disease resistance in Arabidopsis through flagellin perception. *Nature*. <https://doi.org/10.1038/nature02485>
- Ziv, C., Zhao, Z., Gao, Y. G., & Xia, Y. (2018). Multifunctional Roles of Plant Cuticle During Plant-Pathogen Interactions. *Frontiers in Plant Science*, *0*, 1088.
<https://doi.org/10.3389/FPLS.2018.01088>
- Zwilling, D., Cypionka, A., Pohl, W. H., Fasshauer, D., Walla, P. J., Wahl, M. C., &

Jahn, R. (2007). Early endosomal SNAREs form a structurally conserved SNARE complex and fuse liposomes with multiple topologies. *The EMBO Journal*, 26(1), 9. <https://doi.org/10.1038/SJ.EMBOJ.7601467>

SUPPLEMENTARY DATA



Supplementary figure 1. MapMan analyses of the DEGs between *snap33-1* and WT-1 at 5 and 12 days. MapMan analyses of the DEGs in *snap33-1* at 5 and 12 days showing an overview of the altered biotic-stress dependent pathways in the *snap33-1* mutant: All DEGs at 5 and 12 days with p -values ≤ 0.05 were used to perform a MapMan analysis. Red boxes indicate up-regulated genes, and green boxes represent down-regulated genes found in *snap33-1* compared to WT-1. Each square represents a gene.



Supplementary figure 2. Representative picture of the root phenotype of *snap33-1* and WT-1 plants. Seedlings of the indicated genotypes were grown on sucrose-free $\frac{1}{2}$ MS medium with 0.5% agar for 14 days. Scale bar represents 1cm.

Supplementary Table 1. GO enrichment analyses of molecular functions (MF) in *snap33-1* at 12 days obtained by g: Profiler (<https://biit.cs.ut.ee/gprofiler/gost>) analyses on the 2015 genes up-regulated 2-fold or more ($\text{Log}_2\text{FC} \geq 1$) in *snap33-1*. P-values are adjusted (Padj) for multiple testing using the Benjamini-Hochberg method. Greater- $\text{Log}_{10}(\text{p-value})$ scores correlate with increased statistical significance.

GO:MF	stats		
Term name	Term ID	Padj	$-\log_{10}(\text{Padj})$
protein serine kinase activity	GO:0106310	1.134×10^{-19}	16.94
protein threonine kinase activity	GO:0106311	1.134×10^{-19}	16.94
protein serine/threonine kinase activity	GO:0004674	5.124×10^{-18}	17.29
protein kinase activity	GO:0004672	3.209×10^{-14}	13.72
ion binding	GO:0043167	7.796×10^{-14}	13.61
ADP binding	GO:0043531	1.887×10^{-13}	13.53
carbohydrate binding	GO:0030246	3.998×10^{-13}	13.42
NAD+ nucleosidase activity	GO:0003953	2.260×10^{-12}	12.65
NAD(P)+ nucleosidase activity	GO:0050135	2.260×10^{-12}	12.65
NAD+ nucleotidase, cyclic ADP-ribose generating	GO:0061809	2.260×10^{-12}	12.65
glutathione transferase activity	GO:0004364	4.782×10^{-12}	12.55
anion binding	GO:0043168	2.394×10^{-11}	11.82
phosphotransferase activity, alcohol group as acceptor	GO:0016773	7.338×10^{-11}	11.73
hydrolase activity, hydrolyzing N-glycosyl compounds	GO:0016799	4.067×10^{-10}	10.91
kinase activity	GO:0016301	2.064×10^{-9}	9.29
adenyl ribonucleotide binding	GO:0032559	3.673×10^{-9}	8.53
adenyl nucleotide binding	GO:0030554	5.890×10^{-9}	8.23
catalytic activity	GO:0003824	1.489×10^{-8}	7.83
hydrolase activity, acting on glycosyl bonds	GO:0016798	7.991×10^{-8}	7.10
transmembrane signaling receptor activity	GO:0004888	1.002×10^{-7}	6.90
carbohydrate derivative binding	GO:0097367	1.545×10^{-7}	6.81
small molecule binding	GO:0036094	2.186×10^{-7}	6.65
transmembrane receptor protein kinase activity	GO:0019199	2.959×10^{-7}	6.53
calmodulin binding	GO:0005516	3.951×10^{-7}	6.41
nucleotide binding	GO:0000166	6.201×10^{-7}	6.21
nucleoside phosphate binding	GO:1901265	6.201×10^{-7}	6.21
calcium ion binding	GO:0005509	6.217×10^{-7}	6.20
purine ribonucleotide binding	GO:0032555	1.460×10^{-6}	5.83
ribonucleotide binding	GO:0032553	1.699×10^{-6}	5.77
purine nucleotide binding	GO:0017076	2.225×10^{-6}	5.64
transferase activity	GO:0016740	2.806×10^{-6}	5.55
transmembrane receptor protein serine/threonine kinase ac...	GO:0004675	4.899×10^{-5}	4.31
ATP binding	GO:0005524	6.712×10^{-5}	4.17
transferase activity, transferring phosphorus-containing gro...	GO:0016772	1.281×10^{-4}	3.87
catalytic activity, acting on a protein	GO:0140096	4.064×10^{-4}	3.39
heme binding	GO:0020037	7.486×10^{-4}	3.12
glutathione binding	GO:0043295	1.081×10^{-3}	2.96
oligopeptide binding	GO:1900750	1.081×10^{-3}	2.96
signaling receptor activity	GO:0038023	3.226×10^{-3}	2.49
transferase activity, transferring alkyl or aryl (other than met...	GO:0016765	3.845×10^{-3}	2.41
purine ribonucleoside triphosphate binding	GO:0035639	5.526×10^{-3}	2.25
peroxidase activity	GO:0004601	7.513×10^{-3}	2.12
tetrapyrrole binding	GO:0046906	1.013×10^{-2}	1.98
antioxidant activity	GO:0016209	1.209×10^{-2}	1.91
oxidoreductase activity, acting on peroxide as acceptor	GO:0016684	1.551×10^{-2}	1.81
chitin binding	GO:0008061	1.591×10^{-2}	1.79
quercetin 3-O-glucosyltransferase activity	GO:0080043	1.812×10^{-2}	1.74
modified amino acid binding	GO:0072341	4.393×10^{-2}	1.56
molecular transducer activity	GO:0060089	4.972×10^{-2}	1.50

Supplementary Table 2. List of genes found in the GO categories “protein serine kinase activity”, “protein threonine kinase activity”, “protein serine/threonine kinase activity”, and “protein kinase activity” up-regulated 2-fold or more ($\text{Log}_2\text{FC} \geq 1$) in the *snap33-1* mutant at 12 days.

Locus Identifier	Gene Description	Primary Gene Symbol
AT5G46080	Protein kinase superfamily protein;(source:Araport11)	
AT4G39270	Leucine-rich repeat protein kinase family protein;(source:Araport11)	
AT1G66920	Protein kinase superfamily protein;(source:Araport11)	
AT5G41730	Protein kinase family protein;(source:Araport11)	
AT5G38250	Protein kinase family protein;(source:Araport11)	
AT1G67520	lectin protein kinase family protein;(source:Araport11)	
AT4G00955	wall-associated receptor kinase-like protein;(source:Araport11)	
AT1G35710	kinase family with leucine-rich repeat domain-containing protein;(source:Araport11)	
AT2G23200	Protein kinase superfamily protein;(source:Araport11)	
AT4G13000	AGC (cAMP-dependent, cGMP-dependent and protein kinase C) kinase family protein;(source:Araport11)	
AT1G66830	Leucine-rich repeat protein kinase family protein;(source:Araport11)	
AT1G61370	S-locus lectin protein kinase family protein;(source:Araport11)	
AT1G51790	Leucine-rich repeat protein kinase family protein;(source:Araport11)	
AT4G36945	PLC-like phosphodiesterases superfamily protein;(source:Araport11)	
AT5G59670	Leucine-rich repeat protein kinase family protein;(source:Araport11)	
AT1G56120	Leucine-rich repeat transmembrane protein kinase;(source:Araport11)	
AT1G51890	Leucine-rich repeat protein kinase family protein;(source:Araport11)	
AT1G61420	S-locus lectin protein kinase family protein;(source:Araport11)	
AT4G35500	Protein kinase superfamily protein;(source:Araport11)	
AT1G66880	Protein kinase superfamily protein;(source:Araport11)	
AT5G55560	Protein kinase superfamily protein;(source:Araport11)	
AT1G67000	Protein kinase superfamily protein;(source:Araport11)	
AT2G19130	S-locus lectin protein kinase family protein;(source:Araport11)	
AT1G51620	Protein kinase superfamily protein;(source:Araport11)	
AT3G09010	Protein kinase superfamily protein;(source:Araport11)	
AT1G61360	S-locus lectin protein kinase family protein;(source:Araport11)	
AT1G51860	Leucine-rich repeat protein kinase family protein;(source:Araport11)	
AT5G24430	Calcium-dependent protein kinase (CDPK) family protein;(source:Araport11)	
AT1G69730	Wall-associated kinase family protein;(source:Araport11)	
AT1G61610	S-locus lectin protein kinase family protein;(source:Araport11)	
AT1G34420	leucine-rich repeat transmembrane protein kinase family protein;(source:Araport11)	
AT5G42440	Protein kinase superfamily protein;(source:Araport11)	
AT5G66790	Protein kinase superfamily protein;(source:Araport11)	
AT4G27300	S-locus lectin protein kinase family protein;(source:Araport11)	
AT3G47090	Leucine-rich repeat protein kinase family protein;(source:Araport11)	
AT1G48210	Protein kinase superfamily protein;(source:Araport11)	
AT4G25390	Protein kinase superfamily protein;(source:Araport11)	
AT5G58540	Protein kinase superfamily protein;(source:Araport11)	
AT5G57035	U-box domain-containing protein kinase family protein;(source:Araport11)	
AT5G59680	Leucine-rich repeat protein kinase family protein;(source:Araport11)	
AT5G25930	kinase family with leucine-rich repeat domain-containing protein;(source:Araport11)	
AT4G18250	receptor Serine/Threonine kinase-like protein;(source:Araport11)	
AT4G11900	S-locus lectin protein kinase family protein;(source:Araport11)	
AT3G08760	Encodes an osmotic stress-inducible kinase that functions as a negative regulator of osmotic stress signaling in plants.	(ATSIK)
AT4G21390	S-locus lectin protein kinase family protein;(source:Araport11)	(B120)
AT5G02290	Encodes a candidate protein kinase NAK that is similar to the oncogenes met and abl.	(NAK)
AT1G76360	Protein kinase superfamily protein;(source:Araport11)	(PBL31)
AT5G61560	Plant U-box type E3 ubiquitin ligase (PUB).	(PUB51)
AT3G57700	Protein kinase superfamily protein;(source:Araport11)	(ZRK10)
AT1G67470	Protein kinase superfamily protein;(source:Araport11)	(ZRK12)
AT1G65250	Protein kinase superfamily protein;(source:Araport11)	(ZRK14)
AT3G57640	Protein kinase superfamily protein;(source:Araport11)	(ZRK15)
AT4G11890	Encodes a receptor-like cytosolic kinase ARCK1. Negatively controls abscisic acid and osmotic stress signal transduction.	ABA- AND OSMOTIC-STRESS-INDUCIBLE RECEPTOR-LIKE CYTOSOLIC KINASE 1 (ARCK1)
AT3G25250	Arabidopsis protein kinase The mRNA is cell-to-cell mobile.	AGC2 KINASE 1 (AGC2-1)
AT3G04690	Receptor-like kinase required for maintenance of pollen tube growth. Display polar localization at the plasma membrane of the pollen tube tip.	ANXUR1 (ANX1)
AT5G48380	Encodes a BAK1-interacting receptor-like kinase named BIR1. Negatively regulates multiple plant resistance signaling pathways, one of which is the SOBIR1(AT2G31880)-dependent pathway.	BAK1-INTERACTING RECEPTOR-LIKE KINASE 1 (BIR1)
AT1G55610	mutant has Altered vascular cell differentiation; LRR Receptor Kinase	BR11 LIKE (BRL1)
AT3G13380	Similar to BRL, brassinosteroid receptor protein.	BR11-LIKE 3 (BRL3)
AT2G17290	Encodes calcium dependent protein kinase 6 (CPK6), a member of the Arabidopsis CDPK gene family. CDPKs contain an intrinsic Ca ²⁺ -activation domain with four EF hand Ca ²⁺ -binding sites. CDPKs protein kinases have been proposed to function in multiple plant signal transduction pathways downstream of [Ca ²⁺] _{cyt} elevations, thus transducing various physiological responses. CPK6 is expressed in both guard cells and mesophyll cells. Functions in guard cell ion channel regulation.	CALCIUM DEPENDENT PROTEIN KINASE 6 (CPK6)

AT1G18890	encodes a calcium-dependent protein kinase whose gene expression is induced by dehydration and high salt. Kinase activity could not be detected in vitro.	CALCIUM-DEPENDENT PROTEIN KINASE 1 (CDPK1)
AT4G04710	member of Calcium Dependent Protein Kinase	CALCIUM-DEPENDENT PROTEIN KINASE 22 (CPK22)
AT1G76040	member of Calcium Dependent Protein Kinase	CALCIUM-DEPENDENT PROTEIN KINASE 29 (CPK29)
AT4G04695	member of Calcium Dependent Protein Kinase. Involved in response to salicylic acid, regulated by <i>Bacillus amyloliquefaciens</i> under high calcium stress.	CALCIUM-DEPENDENT PROTEIN KINASE 31 (CPK31)
AT3G16030	lectin protein kinase family protein;(source:Araport11)	CALLUS EXPRESSION OF RBCS 101 (CES101)
AT5G58940	<i>Arabidopsis thaliana</i> calmodulin-binding receptor-like kinase mRNA The mRNA is cell-to-cell mobile.	CALMODULIN-BINDING RECEPTOR-LIKE CYTOPLASMIC KINASE 1 (CRCK1)
AT5G12480	calmodulin-domain protein kinase CDPK isoform 7 (CPK7)	CALMODULIN-DOMAIN PROTEIN KINASE 7 (CPK7)
AT3G20410	calmodulin-domain protein kinase CDPK isoform 9 (CPK9)	CALMODULIN-DOMAIN PROTEIN KINASE 9 (CPK9)
AT4G35600	Encodes a receptor-like cytoplasmic kinase that acts as a spatial inhibitor of cell separation. Analysis of the cDNA previously described in Meiners et al., 1991 revealed mistakes in the predicted open reading frame. The mRNA is cell-to-cell mobile.	CAST AWAY (CST)
AT1G48260	Encodes a member of the SNF1-related kinase (SnRK) gene family (SnRK3.21), which has also been reported as a member of the CBL-interacting protein kinases (CIPK17).	CBL-INTERACTING PROTEIN KINASE 17 (CIPK17)
AT1G30270	<i>Arabidopsis thaliana</i> CBL-interacting protein kinase 23. CIPK23 serves as a positive regulator of the potassium transporter AKT1 by directly phosphorylating AKT1. CIPK23 is activated by the binding of two calcineurin B-like proteins, CBL1 and CBL9. The mRNA is cell-to-cell mobile.	CBL-INTERACTING PROTEIN KINASE 23 (CIPK23)
AT1G21250	Encodes a cell wall-associated kinase that interacts with AtGRP3 and may function as a signaling receptor of extracellular matrix component such as oligogalacturonides. The mRNA is cell-to-cell mobile.	CELL WALL-ASSOCIATED KINASE 1 (WAK1)
AT3G21630	LysM receptor-like kinase, based on protein sequence alignment analysis, it has a typical RD signaling domain in its catalytic loop and possesses autophosphorylation activity. Involved in the perception and transduction of the chitin oligosaccharide elicitor. Located in the plasma membrane. CERK1 phosphorylates LK1, a LLR-RLK that is involved in innate immunity.	CHITIN ELICITOR RECEPTOR KINASE 1 (CERK1)
AT1G16670	Encodes a cold-activated plasma membrane protein cold-responsive protein kinase that phosphorylates 14-3-3 proteins. The phosphorylated 14-3-3 proteins shuttle from the cytosol to the nucleus, where they interact with and destabilize the key cold-responsive C-repeat-binding factor (CBF) proteins, modulate CBF stability and the response to	COLD-RESPONSIVE PROTEIN KINASE 1 (CRPK1)
AT3G55950	CRINKLY4 related 3;(source:Araport11)	CRINKLY4 RELATED 3 (CCR3)
AT5G47850	CRINKLY4 related 4;(source:Araport11)	CRINKLY4 RELATED 4 (CCR4)
AT4G23190	Encodes putative receptor-like protein kinase that is induced by the soil-borne vascular bacteria, <i>Ralstonia solanacearum</i> . Naming convention from Chen et al 2003 (PMID 14756307)	CYSTEINE-RICH RLK (RECEPTOR-LIKE PROTEIN KINASE) 11 (CRK11)
AT4G23200	Encodes a cysteine-rich receptor-like protein kinase.	CYSTEINE-RICH RLK (RECEPTOR-LIKE PROTEIN KINASE) 12 (CRK12)
AT4G23210	Encodes a Cysteine-rich receptor-like kinase (CRK13). Overexpression of CRK13 leads to hypersensitive response cell death, and induces defense against pathogens by causing increased accumulation of salicylic acid.	CYSTEINE-RICH RLK (RECEPTOR-LIKE PROTEIN KINASE) 13 (CRK13)
AT4G23220	Encodes a cysteine-rich receptor-like protein kinase.	CYSTEINE-RICH RLK (RECEPTOR-LIKE PROTEIN KINASE) 14 (CRK14)
AT4G23240	Encodes a cysteine-rich receptor-like protein kinase.	CYSTEINE-RICH RLK (RECEPTOR-LIKE PROTEIN KINASE) 16 (CRK16)
AT4G23270	Encodes a cysteine-rich receptor-like protein kinase. The mRNA is cell-to-cell mobile.	CYSTEINE-RICH RLK (RECEPTOR-LIKE PROTEIN KINASE) 19 (CRK19)
AT4G23310	Encodes a cysteine-rich receptor-like protein kinase.	CYSTEINE-RICH RLK (RECEPTOR-LIKE PROTEIN KINASE) 23 (CRK23)
AT4G23320	Encodes a cysteine-rich receptor-like protein kinase.	CYSTEINE-RICH RLK (RECEPTOR-LIKE PROTEIN KINASE) 24 (CRK24)
AT4G38830	Encodes a cysteine-rich receptor-like protein kinase.	CYSTEINE-RICH RLK (RECEPTOR-LIKE PROTEIN KINASE) 26 (CRK26)
AT4G21400	Encodes a cysteine-rich receptor-like protein kinase.	CYSTEINE-RICH RLK (RECEPTOR-LIKE PROTEIN KINASE) 28 (CRK28)
AT1G70530	Encodes a cysteine-rich receptor-like protein kinase.	CYSTEINE-RICH RLK (RECEPTOR-LIKE PROTEIN KINASE) 3 (CRK3)
AT4G11470	Encodes a cysteine-rich receptor-like protein kinase.	CYSTEINE-RICH RLK (RECEPTOR-LIKE PROTEIN KINASE) 31 (CRK31)
AT4G04490	Encodes a cysteine-rich receptor-like protein kinase.	CYSTEINE-RICH RLK (RECEPTOR-LIKE PROTEIN KINASE) 36 (CRK36)
AT4G04500	Encodes a cysteine-rich receptor-like protein kinase.	CYSTEINE-RICH RLK (RECEPTOR-LIKE PROTEIN KINASE) 37 (CRK37)
AT4G04510	Encodes a cysteine-rich receptor-like protein kinase.	CYSTEINE-RICH RLK (RECEPTOR-LIKE PROTEIN KINASE) 38 (CRK38)
AT4G04540	Encodes a cysteine-rich receptor-like protein kinase.	CYSTEINE-RICH RLK (RECEPTOR-LIKE PROTEIN KINASE) 39 (CRK39)
AT3G45860	Encodes a cysteine-rich receptor-like protein kinase. Involved in programmed cell death and defense response to pathogen.	CYSTEINE-RICH RLK (RECEPTOR-LIKE PROTEIN KINASE) 4 (CRK4)
AT4G23130	Encodes a receptor-like protein kinase. Naming convention from Chen et al 2003 (PMID 14756307)	CYSTEINE-RICH RLK (RECEPTOR-LIKE PROTEIN KINASE) 5 (CRK5)
AT4G23140	<i>Arabidopsis thaliana</i> receptor-like protein kinase. Naming convention from Chen et al 2003 (PMID 14756307)	CYSTEINE-RICH RLK (RECEPTOR-LIKE PROTEIN KINASE) 6 (CRK6)
AT4G23150	Encodes a cysteine-rich receptor-like protein kinase.	CYSTEINE-RICH RLK (RECEPTOR-LIKE PROTEIN KINASE) 7 (CRK7)
AT4G23160	Encodes a cysteine-rich receptor-like protein kinase.	CYSTEINE-RICH RLK (RECEPTOR-LIKE PROTEIN KINASE) 8 (CRK8)
AT1G70520	Encodes a cysteine-rich receptor-like protein kinase located to the plasma membrane. Involved in regulating microbe-associated molecular pattern-triggered ROS production and stress induced callose deposition at the plasmodesmata in roots. Required for MAMP-triggered responses and resistance to <i>Pseudomonas syringae</i> pv. tomato 118 DC3000 .	CYSTEINE-RICH RLK2 (CRK2)

AT5G20480	Encodes a predicted leucine-rich repeat receptor kinase (LRR-RLK). Functions as the receptor for bacterial PAMP (pathogen associated molecular patterns) EF-Tu.	EF-TU RECEPTOR (EFR)
AT1G11300	The annotation for At1g11300 in TAIR10 is incorrect. This locus has been split into two At1g11300 (symbol: EGM1) and At1g11305 (symbol: EGM2) (Olivier Loudet, personal communication, 2013-04-03). See Comment field for revised	ENHANCED SHOOT GROWTH UNDER MANNITOL STRESS 1 (EGM1)
AT2G19190	Encodes a receptor-like protein kinase that is involved in early defense signaling. Expression of this gene is strongly induced during leaf senescence. It is a target of the transcription factor AtWRKY6.	FLG22-INDUCED RECEPTOR-LIKE KINASE 1 (FRK1)
AT3G17420	Serine/threonine protein kinase-like protein expressed in etiolated cotyledons and found in glyoxysomes.	GLYOXYSOMAL PROTEIN KINASE 1 (GPK1)
AT4G28490	Member of Receptor kinase-like protein family. Controls the separation step of floral organ abscission. The mRNA is cell-to-cell mobile.	HAESA (HAE)
AT1G51800	The gene encodes a putative member of the LRR-RLK protein family. Expressin and mutant analysis revealed that it contributes to the interaction between Arabidopsis and Hyaloperonospora arabidopsidis. and The mRNA is cell-to-cell	IMPAIRED OOMYCETE SUSCEPTIBILITY 1 (IOS1)
AT2G17220	Encodes a putative serine/threonine-specific protein kinase kin3. Protein is N-myristoylated.	KINASE 3 (KIN3)
AT2G29250	Concanavalin A-like lectin protein kinase family protein;(source:Araport11)	L-TYPE LECTIN RECEPTOR KINASE III.2 (LECRK-III.2)
AT2G37710	Induced in response to Salicylic acid. The mRNA is cell-to-cell mobile.	L-TYPE LECTIN RECEPTOR KINASE IV.1 (LECRK-IV.1)
AT3G53810	Concanavalin A-like lectin protein kinase family protein;(source:Araport11)	L-TYPE LECTIN RECEPTOR KINASE IV.2 (LECRK-IV.2)
AT5G65600	L-type lectin receptor kinase which modulates metabolites and abiotic stress responses. Phosphorylates AvrPtB which in turn reduces its virulence.	L-TYPE LECTIN RECEPTOR KINASE IX.2 (LECRK-IX.2)
AT2G32800	protein kinase family protein;(source:Araport11)	L-TYPE LECTIN RECEPTOR KINASE S.2 (LECRK-S.2)
AT5G06740	Concanavalin A-like lectin protein kinase family protein;(source:Araport11)	L-TYPE LECTIN RECEPTOR KINASE S.5 (LECRK-S.5)
AT1G70130	Concanavalin A-like lectin protein kinase family protein;(source:Araport11)	L-TYPE LECTIN RECEPTOR KINASE V.2 (LECRK-V.2)
AT3G59700	Member of Receptor kinase-like protein family. Represses stomatal immunity induced by Pseudomonas syringae pv. tomato DC3000.	L-TYPE LECTIN RECEPTOR KINASE V.5 (LECRK-V.5)
AT4G29050	Concanavalin A-like lectin protein kinase family protein;(source:Araport11)	L-TYPE LECTIN RECEPTOR KINASE V.9 (LECRK-V.9)
AT3G08870	Concanavalin A-like lectin protein kinase family protein;(source:Araport11)	L-TYPE LECTIN RECEPTOR KINASE VI.1 (LECRK-VI.1)
AT5G01550	Encodes LecRKA4.2, a member of the lectin receptor kinase subfamily A4 (LecRKA4.1 At5g01540; LecRKA4.2 At5g01550; LecRKA4.3 At5g01560). Together with other members of the subfamily, functions redundantly in the negative regulation of ABA response in seed germination.	L-TYPE LECTIN RECEPTOR KINASE VI.3 (LECRK-VI.3)
AT4G04960	Concanavalin A-like lectin protein kinase family protein;(source:Araport11)	L-TYPE LECTIN RECEPTOR KINASE VII.1 (LECRK-VII.1)
AT4G28350	Concanavalin A-like lectin protein kinase family protein;(source:Araport11)	L-TYPE LECTIN RECEPTOR KINASE VII.2 (LECRK-VII.2)
AT5G01540	Encodes LecRKA4.1, a member of the lectin receptor kinase subfamily A4 (LecRKA4.1 At5g01540; LecRKA4.2 At5g01550; LecRKA4.3 At5g01560). Together with other members of the subfamily, functions redundantly in the negative regulation of ABA response in seed germination. Positively regulates pattern-triggered immunity.	L-TYPE LECTIN RECEPTOR KINASE-VI.2 (LECRK-VI.2)
AT1G18390	Serine/Threonine kinase family catalytic domain protein;(source:Araport11)	LEAF RUST 10 DISEASE-RESISTANCE LOCUS RECEPTOR- LIKE PROTEIN KINASE- LIKE 1.2 (LRK10L1.2)
AT5G38210	Protein kinase family protein;(source:Araport11)	LEAF RUST 10 DISEASE-RESISTANCE LOCUS RECEPTOR- LIKE PROTEIN KINASE-
AT5G01560	Encodes LecRKA4.3, a member of the lectin receptor kinase subfamily A4 (LecRKA4.1 At5g01540; LecRKA4.2 At5g01550; LecRKA4.3 At5g01560). Together with other members of the subfamily, functions redundantly in the negative regulation of ABA response in seed germination.	LECTIN RECEPTOR KINASE A4.3 (LECRKA4.3)
AT3G14840	Encodes LRR-RLK protein that is localized to the plasma membrane and is involved in regulation of plant innate immunity to microbes. LIK1 is phosphorylated by CERK1, a kinase involved in chitin perception. The mRNA is cell-to-	LYSM RLK1-INTERACTING KINASE 1 (LIK1)
AT2G33580	Encodes a putative LysM-containing receptor-like kinase. LYK5 is a major chitin receptor and forms a chitin-induced complex with related kinase CERK1. Based on protein sequence alignment analysis, it was determined as a pseudo kinase due to a lack of the ATP-binding P-loop in the kinase domain.	LYSM-CONTAINING RECEPTOR-LIKE KINASE 5 (LYK5)
AT5G45840	Encodes a leucine-rich-repeat RLK that is localized to the plasma membrane of pollen tubes and functions with MIK1/2 as the male receptor of the pollen tube chemo-attractant LURE1.MDIS1 forms a complex with MIK1/2 and binds	MALE DISCOVERER1 (MDIS1)
AT1G01560	Member of MAP Kinase family. Flg22-induced activation is blocked by AvrRpt2.	MAP KINASE 11 (MPK11)
AT4G01370	Encodes a nuclear and cytoplasmically localized MAP kinase involved in mediating responses to pathogens. Its substrates include MKS1 and probably MAP65-1.The MAP65-1 interaction is involved in mediating cortical microtubule organization. Required for male-specific meiotic cytokinesis. The mRNA is cell-to-cell mobile.	MAP KINASE 4 (MPK4)
AT1G73500	member of MAP Kinase Kinase family. Autophosphorylates and also phosphorylates MPK3 and MPK6. Independently involved in ethylene and calmalexin biosynthesis. Induces transcription of ACS2, ACS6, ERF1, ERF2, ERF5, ERF6, CYP79B2, CYP79B3, CYP71A13 and PAD3.	MAP KINASE KINASE 9 (MKK9)
AT4G26070	Member of MAP Kinase Kinase. Likely functions in a stress-activated MAPK pathway. Can phosphorylate the MAPK AtMPK4, in response to stress. Gets phosphorylated by MEKK1 in response to wounding.	MAP KINASE/ ERK KINASE 1 (MEK1)
AT4G08470	Encodes a member of the A1 subgroup of the MEKK (MAPK/ERK kinase kinase) family. MEKK is another name for Mitogen-Activated Protein Kinase Kinase (MAPKK or MAP3K). This subgroup has four members: At4g08500 (MEKK1, also known as ARAKIN, MAP3Kb1, MAPKKK8), At4g08480 (MEKK2, also known as MAP3Kb4, MAPKKK9), At4g08470 (MEKK3, also known as MAP3Kb3, MAPKKK10) and At4g12020 (MEKK4, also known as MAP3Kb5, MAPKKK11, WRKY19). Nomenclatures for mitogen-activated protein kinases are described in Trends in	MAPK/ERK KINASE KINASE 3 (MEKK3)
AT5G39020	Involved in growth adaptation upon exposure to metal ions. Contributes together with the other MDS genes to the complex network of CrRLK1Ls that positively and negatively affect growth.	MEDOS 3 (MDS3)
AT5G39030	Involved in growth adaptation upon exposure to metal ions. Contributes together with the other MDS genes to the complex network of CrRLK1Ls that positively and negatively affect growth.	MEDOS 4 (MDS4)
AT3G45640	Encodes a mitogen-activated kinase whose mRNA levels increase in response to touch, cold, salinity stress and chitin oligomers.Also functions in ovule development. Heterozygous MPK3 mutants in a homozygous MPK6 background are female sterile due to defects in integument development. MPK3 can be dephosphorylated by MKP2 in vitro. The mRNA is cell-to-cell mobile.	MITOGEN-ACTIVATED PROTEIN KINASE 3 (MPK3)
AT1G51660	Encodes a mitogen-activated map kinase kinase (there are nine in Arabidopsis) involved in innate immunity. This protein activates MPK3/MPK6 and early-defense genes redundantly with MKK5. In plants with both MKK5 and MKK4 levels reduced by RNAi plants, floral organs do not abscise suggestion a role for both proteins in mediating floral organ abscission. The mRNA is cell-to-cell mobile.	MITOGEN-ACTIVATED PROTEIN KINASE KINASE 4 (MKK4)
AT1G05100	member of MEKK subfamily. Negatively regulated by RGLG1 and RGLG2; involved in drought stress tolerance.	MITOGEN-ACTIVATED PROTEIN KINASE KINASE KINASE 18 (MAPKKK18)

AT5G67080	member of MEKK subfamily	MITOGEN-ACTIVATED PROTEIN KINASE KINASE 19 (MAPKKK19)
AT4G36950	member of MEKK subfamily	MITOGEN-ACTIVATED PROTEIN KINASE KINASE 21 (MAPKKK21)
AT4G08480	Encodes a member of the A1 subgroup of the MEKK (MAPK/ERK kinase) family. MEKK is another name for Mitogen-Activated Protein Kinase Kinase Kinase (MAPKKK or MAP3K). This subgroup has four members: At4g08500 (MEKK1, also known as ARAKIN, MAP3Kb1, MAPKKK8), At4g08480 (MEKK2, also known as MAP3Kb4, MAPKKK9), At4g08470 (MEKK3, also known as MAP3Kb3, MAPKKK10) and At4g12020 (MEKK4, also known as MAP3Kb5, MAPKKK11, WRKY19). Nomenclatures for mitogen-activated protein kinases are described in Trends in Plant Science 2002, 7(7):301.	MITOGEN-ACTIVATED PROTEIN KINASE KINASE 9 (MAPKKK9)
AT1G74360	NILR1 encodes a serine/threonine kinase involved in defense response to nematodes.	NEMATODE-INDUCED LRR-RLK 1 (NILR1)
AT3G20860	Encodes a member of the NIMA-related serine/threonine kinases (Neks) that have been linked to cell-cycle regulation in fungi and mammals. Plant Neks might be involved in plant development processes.	NIMA-RELATED KINASE 5 (NEK5)
AT3G09830	Encodes a member of subfamily VIIa of the receptor-like cytoplasmic kinases (RLCKs). It contributes to pattern-triggered immunity in response to <i>P. syringae</i> .	PATTERN-TRIGGERED IMMUNITY (PTI) COMPROMISED RECEPTOR-LIKE CYTOPLASMIC KINASE 1 (PCRK1)
AT5G03320	Protein kinase superfamily protein;(source:Araport11)	PATTERN-TRIGGERED IMMUNITY COMPROMISED RECEPTOR-LIKE CYTOPLASMIC KINASE 2 (PCRK2)
AT2G07180	Protein kinase superfamily protein;(source:Araport11)	PBS1-LIKE 17 (PBL17)
AT1G69790	Protein kinase superfamily protein;(source:Araport11)	PBS1-LIKE 18 (PBL18)
AT5G47070	Encodes a member of the RLCK VII-4 subfamily of receptor-like cytoplasmic kinases that has been shown to phosphorylate MAPKKK5 Ser-599 and MEKK1 Ser-603, both players in PRR-mediated resistance to bacterial and	PBS1-LIKE 19 (PBL19)
AT4G17660	Protein kinase superfamily protein;(source:Araport11)	PBS1-LIKE 20 (PBL20)
AT1G72540	Protein kinase superfamily protein;(source:Araport11)	PBS1-LIKE 33 (PBL33)
AT3G26500	Encodes PIRL2, a member of the Plant Intracellular Ras-group-related LRRs (Leucine rich repeat proteins). PIRLs are a distinct, plant-specific class of intracellular LRRs that likely mediate protein interactions, possibly in the context of	PLANT INTRACELLULAR RAS GROUP-RELATED LRR 2 (PIRL2)
AT1G68690	Encodes a member of the proline-rich extensin-like receptor kinase (PERK) family. This family consists of 15 predicted receptor kinases (PMID: 15653807).	PROLINE-RICH EXTENSIN-LIKE RECEPTOR KINASE 9 (PERK9)
AT1G14370	Encodes protein kinase APK2a. Protein is N-myristoylated.	PROTEIN KINASE 2A (APK2A)
AT3G46930	Encodes a Raf-Like Mitogen-Activated Protein Kinase Kinase Kinase Raf43. Required for tolerance to multiple abiotic stresses.	RAF-LIKE MITOGEN-ACTIVATED PROTEIN KINASE KINASE KINASE 43 (RAF43)
AT1G65790	An alternatively spliced gene that encodes a functional transmembrane receptor serine/threonine kinase, alternate form may not have transmembrane domain.	RECEPTOR KINASE 1 (RK1)
AT1G65800	Encodes a putative receptor-like serine/threonine protein kinases that is similar to brassica self-incompatibility (S) locus. expressed in specifically in cotyledons, leaves, and sepals, in correlation with the maturation of these structures. Together with AtPUB9, it is required for auxin-mediated lateral root development under phosphate-starved conditions. The mRNA is cell-to-cell mobile.	RECEPTOR KINASE 2 (RK2)
AT4G21380	encodes a putative receptor-like serine/threonine protein kinases that is similar to Brassica self-incompatibility (S) locus. Expressed in root. Shoot expression limited to limited to the root-hypocotyl transition zone and at the base of lateral roots as well as in axillary buds and pedicels.	RECEPTOR KINASE 3 (RK3)
AT1G11330	S-locus lectin protein kinase family protein;(source:Araport11)	RESISTANT TO DFPM INHIBITION OF ABA SIGNALING 2 (RDA2)
AT2G05940	Encodes a receptor-like cytoplasmic kinase that phosphorylates the host target RIN4, leading to the activation of a plant innate immune receptor RPM1.	RPM1-INDUCED PROTEIN KINASE (RIPK)
AT3G08720	Encodes a ribosomal-protein S6 kinase. Gene expression is induced by cold and salt (NaCl). Activation of ATS6k is regulated by 1-naphthylacetic acid and kinetin, at least in part, via a lipid kinase-dependent pathway. Phosphorylates specifically mammalian and plant S6 at 25 degrees C but not at 37 degrees C. Involved in translational up-regulation of ribosomal proteins.	SERINE/THREONINE PROTEIN KINASE 2 (S6K2)
AT2G13790	somatic embryogenesis receptor-like kinase 4;(source:Araport11)	SOMATIC EMBRYOGENESIS RECEPTOR-LIKE KINASE 4 (SERK4)
AT2G31880	Encodes a putative leucine rich repeat transmembrane protein that is expressed in response to <i>Pseudomonas syringae</i> . Expression of SRRLK may be required for silencing via siRNAs. Regulates cell death and innate immunity.	SUPPRESSOR OF BIR1 1 (SOBIR1)
AT5G25440	Receptor like kinase involved in HopZ1a effector triggered immunity. Interacts with ZAR1. Localization to membrane is dependent on N-terminal myristoylation domain.	SUPPRESSOR OF ZED1-D1 (SZE1)
AT1G79680	Encodes a twin-domain, kinase-GC signaling molecule that may function in biotic stress responses that is critically dependent on the second messenger cGMP.	WALL ASSOCIATED KINASE (WAK)-LIKE 10 (WAKL10)
AT1G21240	encodes a wall-associated kinase The mRNA is cell-to-cell mobile.	WALL ASSOCIATED KINASE 3 (WAK3)
AT1G16110	Encodes a WAK-like receptor-like kinase with a cytoplasmic Ser/Thr protein kinase domain and an extracellular domain with EGF-like repeats. It has been shown to be localized to the cell wall.	WALL ASSOCIATED KINASE-LIKE 6 (WAKL6)
AT1G21270	cytoplasmic serine/threonine protein kinase induced by salicylic acid. mutant plants exhibit a loss of cell expansion and dependence on sugars and salts for seedling growth, affecting the expression and activity of vacuolar invertase.	WALL-ASSOCIATED KINASE 2 (WAK2)

Supplementary Table 3. List of genes found in the GO categories "ADP-binding", "NAD+ nucleotidase, cyclic ADP-ribose generating", "NAD+ nucleosidase activity" and "NAD(P)+ nucleosidase activity" up-regulated 2-fold or more ($\text{Log}_2\text{FC} \geq 1$) in the *snap33-1* mutant at 12 days.

Locus Identifier	Gene Description	Primary Gene Symbol
AT1G51270	vesicle-associated protein 1-4;(source:Araport11)	
AT1G31540	Disease resistance protein (TIR-NBS-LRR class) family;(source:Araport11)	
AT2G20142	Toll-Interleukin-Resistance (TIR) domain family protein;(source:Araport11)	
AT3G04220	Target of miR825/825. Mutants have decreased resistance to fungal pathogens.	
AT3G25510	disease resistance protein (TIR-NBS-LRR class) family protein;(source:Araport11)	
AT4G16920	Disease resistance protein (TIR-NBS-LRR class) family;(source:Araport11)	
AT5G51630	Disease resistance protein (TIR-NBS-LRR class) family;(source:Araport11)	
AT5G46260	disease resistance protein (TIR-NBS-LRR class) family;(source:Araport11)	
AT5G41750	Disease resistance protein (TIR-NBS-LRR class) family;(source:Araport11)	
AT5G41740	Disease resistance protein (TIR-NBS-LRR class) family;(source:Araport11)	
AT3G14470	NB-ARC domain-containing disease resistance protein;(source:Araport11)	
AT1G15890	Disease resistance protein (CC-NBS-LRR class) family;(source:Araport11)	
AT1G57650	ATP binding protein;(source:Araport11)	
AT4G36150	Disease resistance protein (TIR-NBS-LRR class) family;(source:Araport11)	
AT4G19520	disease resistance protein (TIR-NBS-LRR class) family;(source:Araport11)	
AT5G18350	Disease resistance protein (TIR-NBS-LRR class) family;(source:Araport11)	
AT1G56540	Disease resistance protein (TIR-NBS-LRR class) family;(source:Araport11)	
AT5G45510	Leucine-rich repeat (LRR) family protein;(source:Araport11)	
AT1G63740	Disease resistance protein (TIR-NBS-LRR class) family;(source:Araport11)	
AT5G45240	Disease resistance protein (TIR-NBS-LRR class);(source:Araport11)	
AT1G57630	Toll-Interleukin-Resistance (TIR) domain family protein;(source:Araport11)	
AT3G44400	Disease resistance protein (TIR-NBS-LRR class) family;(source:Araport11)	
AT2G16870	Disease resistance protein (TIR-NBS-LRR class) family;(source:Araport11)	
AT1G63350	Disease resistance protein (CC-NBS-LRR class) family;(source:Araport11)	
AT4G14370	Disease resistance protein (TIR-NBS-LRR class) family;(source:Araport11)	
AT1G59620	Encodes CW9.	(CW9)
AT1G12290	NLR protein localized to plasma membrane. Overexpression triggers cell death. Has myristolation site at Gly2 which is required for membrane localization.	(L5)
AT1G17600	SOC3 is a TIR-NB-leucine-rich repeat (TNL) protein.Mutants suppress loss of chs2 phenotype of auto-activation of immunity. When the TIR domain of SOC3 interacts with CHS2 the binding results in temperature activation of cell death, the suppressors inhibit this interaction.	(SOC3)
AT3G04210	TN13 is a TIR-NBS protein involved in immune response. It co localizes with the ER and perinuclear membranes and interacts with MOS6. It also associates with the CC-NBS-LRR resistance protein RPS5 and contributes to RPS5-triggered immunity.	(TN13)
AT1G33560	Encodes a NBS-LRR disease resistance protein that possesses N-terminal kinase subdomains. Activation tagged mutant of ADR1 showed elevated levels of SA and reactive oxygen species in addition to number of defense gene transcripts. Exhibits resistance to number of microbial pathogens.	ACTIVATED DISEASE RESISTANCE 1 (ADR1)
AT4G33300	Encodes a member of the ADR1 family nucleotide-binding leucine-rich repeat (NB-LRR) immune receptors.	ADR1-LIKE 1 (ADR1-L1)
AT5G26920	Encodes a calmodulin-binding protein CBP60g (calmodulin binding protein 60-like.g). The calmodulin-binding domain is located near the N-terminus; calmodulin binding is dependent on Ca(2+). Inducible by both bacterial pathogen and MAMP (microbe-associated molecular pattern) treatments. Bacterial growth is enhanced in cbp60g mutants. cbp60g mutants also show defects in salicylic acid (SA) accumulation and SA signaling.	CAM-BINDING PROTEIN 60-LIKE G (CBP60G)
AT1G17610	TN-type protein that controls temperature-dependent growth and defense responses .Mutant accumulates steryl-esters at low temperatures and shows temperature dependent activation of defense responses..	CHILLING SENSITIVE 1 (CHS1)
AT5G66630	DA1-related protein 5;(source:Araport11)	DA1-RELATED PROTEIN 5 (DAR5)

AT4G12010	Leucine-rich repeat domain (NLR) receptor. Dominant negative alleles suppress catma3 autoimmunity. Co-regulates with WRKY19 basal levels of immunity to root-knot nematodes.	DOMINANT SUPPRESSOR OF CAMTA3 NUMBER 1 (DSC1)
AT1G47370	RBA1 variant in Ag0 background is a TIR-only receptor protein that binds to the bacterial type III effector protein HopBA. The Col-0 variant, which is not expressed, is likely a pseudogene and more highly methylated than the Ag0 variant which is expressed.	RESPONSE TO THE BACTERIAL TYPE III EFFECTOR PROTEIN HOPBA1 (RBA1)
AT3G50950	Encodes a canonical CC-type NLR protein that is required for the recognition of the T3SE HopZ1a as well as several other Hop effectors from the pathogenic bacteria <i>P. syringae</i> .	HOPZ-ACTIVATED RESISTANCE 1 (ZAR1)
AT3G14460	Leucine rich repeat protein that also contains an adenylate cyclase catalytic core motif. Capable of converting ATP to cAMP in vitro. Mutants show increased susceptibility to fungal pathogens.	LEUCINE-RICH REPEAT (LRR) PROTEIN 1 (LRRAC1)
AT5G66910	RPW8 -CNL gene is required for signal transduction of TNLs; functionally redundant to NRG1.1.	N REQUIREMENT GENE 1.2 (NRG1.2)
AT3G09830	Encodes a member of subfamily VIIa of the receptor-like cytoplasmic kinases (RLCKs). It contributes to pattern-triggered immunity in response to <i>P. syringae</i> .	PATTERN-TRIGGERED IMMUNITY (PTI) COMPROMISED RECEPTOR-LIKE CYTOPLASMIC KINASE 1 (PCRK1)
AT5G03320	Protein kinase superfamily protein;(source:Araport11)	PATTERN-TRIGGERED IMMUNITY COMPROMISED RECEPTOR-LIKE CYTOPLASMIC KINASE 2 (PCRK2)
AT4G16860	Confers resistance to <i>Peronospora parasitica</i> . RPP4 is coordinately regulated by transcriptional activation and RNA silencing.	RECOGNITION OF PERONOSPORA PARASITICA 4 (RPP4)
AT4G11170	Encodes RMG1 (Resistance Methylated Gene 1), a NB-LRR disease resistance protein with a Toll/interleukin-1 receptor (TIR) domain at its N terminus. RMG1 is expressed at high levels in response to flg22 and in naive met1/nrpd2 relative to wild-type plants. Expression of this gene is controlled by DNA methylation in its promoter region. The RMG1 promoter region is constitutively demethylated by active DNA demethylation mediated by the DNA glycosylase ROS1.	RESISTANCE METHYLATED GENE 1 (RMG1)
AT4G26090	Encodes a plasma membrane protein with leucine-rich repeat, leucine zipper, and P loop domains that confers resistance to <i>Pseudomonas syringae</i> infection by interacting with the avirulence gene avrRpt2. RPS2 protein interacts directly with plasma membrane associated protein RIN4 and this interaction is disrupted by avrRpt2. The mRNA is cell-to-cell mobile.	RESISTANT TO <i>P. SYRINGAE</i> 2 (RPS2)
AT1G12210	RFL1 has high sequence similarity to the adjacent disease resistance (R) gene RPS5.	RPS5-LIKE 1 (RFL1)
AT4G16960	Redundant function together with SIKIC1 and 2 in SNC1-mediated autoimmunity. Protein levels controlled by MUSE1 and MUSE2.	SIDEKICK SNC1 3 (SIKIC3)
AT1G72940	Nucleotide-binding, leucine-rich repeat (NLR) gene regulated by nonsense-mediated mRNA decay (NMD) genes UPF1 and UPF3.	TIR-NBS11 (TN11)
AT1G72950	Disease resistance protein (TIR-NBS class);(source:Araport11)	TIR-NBS12 (TN12)
AT1G17615	TN2 is an atypical TIR-NBS protein that lacks the LRR domain common in typical NLR receptors. It interacts with EXO70B1, a subunit of the exocyst complex. Loss of function mutants in TN2 can suppress EXO70B1 mutants suggesting that EXO70B1 acts through TN2.	TIR-NBS2 (TN2)
AT1G66090	Disease resistance protein (TIR-NBS class);(source:Araport11)	TIR-NBS3 (TN3)
AT1G72890	NBS TIR protein.	TIR-NBS6 (TN6)
AT1G72900	Toll-Interleukin-Resistance (TIR) domain-containing protein;(source:Araport11)	TIR-NBS7 (TN7)
AT1G72910	Nucleotide-binding, leucine-rich repeat (NLR) gene regulated by nonsense-mediated mRNA decay (NMD) genes UPF1 and UPF3.	TIR-NBS8 (TN8)
AT1G72930	Toll/interleukin-1 receptor-like protein (TIR) protein. It is induced in response to bacterial pathogens and overexpression results in cell death in leaves.	TOLL/INTERLEUKIN-1 RECEPTOR-LIKE (TIR)
AT5G46520	VICTR (VARIATION IN COMPOUND TRIGGERED ROOT growth response) encodes a TIR-NB-LRR (for Toll-Interleukin1 Receptor-nucleotide binding-Leucine-rich repeat) protein. VICTR is necessary for DFPM-induced root growth arrest and inhibition of abscisic acid-induced stomatal closing (DFPM is [5-(3,4-dichlorophenyl)furan-2-yl]-piperidine-1-ylmethanethione)(PMID:21620700). DFPM-mediated root growth arrest is accession-specific and depends on EDS1 and PAD4; Col-0 has a functional copy of VICTR. Induction of the VICTR gene by DFPM treatment requires functional VICTR (Col). A close homolog to VICTR, named VICTL (At5g46510) lies in tandem with VICTR. The mRNA is cell-to-cell mobile.	VARIATION IN COMPOUND TRIGGERED ROOT GROWTH RESPONSE (VICTR)

Supplementary Table 4.

GO enrichment analyses of KEGG pathways in *snap33-1* at 12 days obtained by g: Profiler (<https://biit.cs.ut.ee/gprofiler/gost>) analyses on the 2015 genes up-regulated 2-fold or more ($\text{Log}_2\text{FC} \geq 1$) in *snap33-1*. P-values are adjusted (P_{adj}) for multiple testing using the Benjamini-Hochberg method. Greater $-\text{Log}_{10}(\text{p-value})$ scores correlate with increased statistical significance.

KEGG		stats	
Term name	Term ID	P_{adj}	$-\log_{10}(P_{\text{adj}})$
Plant-pathogen interaction	KEGG:04626	6.202×10^{-15}	15.20
Phenylpropanoid biosynthesis	KEGG:00940	5.729×10^{-7}	6.84
MAPK signaling pathway - plant	KEGG:04016	1.199×10^{-6}	6.22
Glutathione metabolism	KEGG:00480	2.149×10^{-6}	6.17
Cyanoamino acid metabolism	KEGG:00460	2.134×10^{-3}	2.67
Metabolic pathways	KEGG:01100	1.265×10^{-2}	1.89
Biosynthesis of secondary metabolites	KEGG:01110	1.458×10^{-2}	1.85

Supplementary Table 5. List of the molecular functions enriched in the set of genes found in common between *snap33-1* 12 days transcriptome ($\text{Log}_2\text{FC} \geq 1$) and *P35S::RPS4-HS* transcriptome and obtained by the g:Profiler tool. P-values are adjusted (P_{adj}) for multiple testing using the Benjamini-Hochberg method. Greater $-\text{Log}_{10}(\text{p-value})$ scores correlate with increased statistical significance.

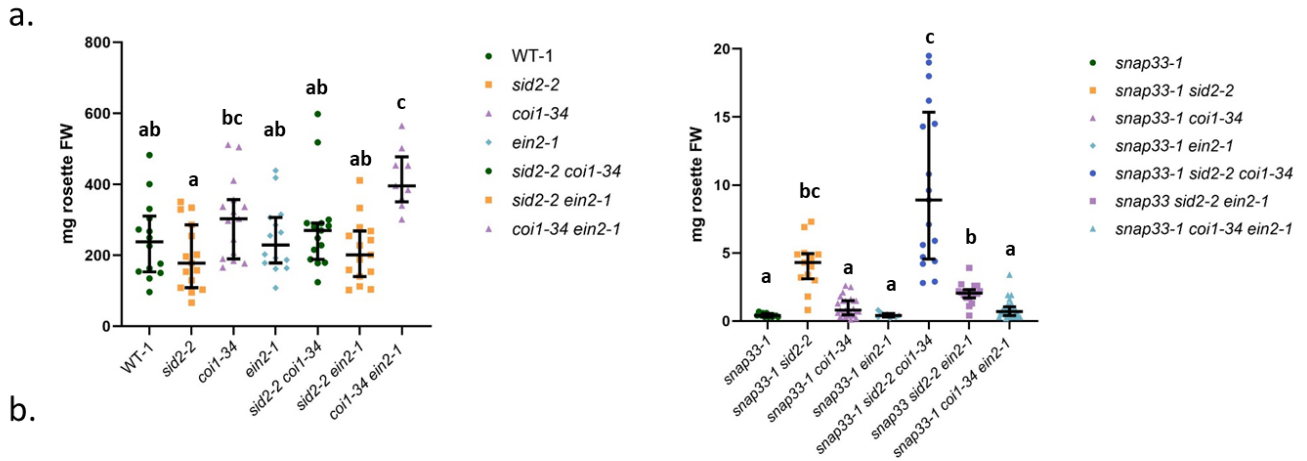
GO:MF	stats			
Term name	Term ID	P _{adj}	$-\log_{10}(\text{P}_{\text{adj}})$	≤ 16
protein serine kinase activity	GO:0106310	7.079×10^{-27}		
protein threonine kinase activity	GO:0106311	7.079×10^{-27}		
protein serine/threonine kinase activity	GO:0004674	1.817×10^{-26}		
ion binding	GO:0043167	2.680×10^{-24}		
anion binding	GO:0043168	5.224×10^{-23}		
protein kinase activity	GO:0004672	7.688×10^{-23}		
adenyl ribonucleotide binding	GO:0032559	1.499×10^{-21}		
adenyl nucleotide binding	GO:0030554	2.597×10^{-21}		
phosphotransferase activity, alcohol group as acceptor	GO:0016773	2.349×10^{-20}		
carbohydrate derivative binding	GO:0097367	2.785×10^{-20}		
purine ribonucleotide binding	GO:0032555	9.486×10^{-19}		
ribonucleotide binding	GO:0032553	1.450×10^{-18}		
purine nucleotide binding	GO:0017076	1.610×10^{-18}		
nucleotide binding	GO:0000166	2.378×10^{-18}		
nucleoside phosphate binding	GO:1901265	2.378×10^{-18}		
small molecule binding	GO:0036094	2.445×10^{-18}		
kinase activity	GO:0016301	1.759×10^{-17}		
catalytic activity, acting on a protein	GO:0140096	3.358×10^{-16}		
ATP binding	GO:0005524	1.137×10^{-15}		
ADP binding	GO:0043531	5.834×10^{-14}		
catalytic activity	GO:0003824	1.760×10^{-13}		
purine ribonucleoside triphosphate binding	GO:0035639	2.530×10^{-13}		
transferase activity, transferring phosphorus-containing gro...	GO:0016772	3.413×10^{-12}		
calcium ion binding	GO:0005509	5.467×10^{-10}		
transferase activity	GO:0016740	1.908×10^{-9}		
transmembrane signaling receptor activity	GO:0004888	2.620×10^{-9}		
transmembrane receptor protein kinase activity	GO:0019199	3.737×10^{-9}		
NAD ⁺ nucleotidase, cyclic ADP-ribose generating	GO:0061809	7.623×10^{-9}		
NAD(P) ⁺ nucleosidase activity	GO:0050135	7.623×10^{-9}		
NAD ⁺ nucleosidase activity	GO:0003953	7.623×10^{-9}		
calmodulin binding	GO:0005516	9.326×10^{-9}		
glutathione transferase activity	GO:0004364	4.025×10^{-8}		
hydrolase activity, hydrolyzing N-glycosyl compounds	GO:0016799	8.448×10^{-7}		
carbohydrate binding	GO:0030246	9.820×10^{-6}		
transmembrane receptor protein serine/threonine kinase ac...	GO:0004675	5.485×10^{-5}		
signaling receptor activity	GO:0038023	8.853×10^{-5}		
binding	GO:0005488	1.086×10^{-4}		
molecular transducer activity	GO:0060089	1.206×10^{-3}		
chitin binding	GO:0008061	2.717×10^{-3}		
ATPase-coupled intramembrane lipid transporter activity	GO:0140326	3.654×10^{-3}		
intramembrane lipid transporter activity	GO:0140303	6.167×10^{-3}		
hydrolase activity, acting on glycosyl bonds	GO:0016798	7.733×10^{-3}		
chitinase activity	GO:0004568	2.112×10^{-2}		
transmembrane receptor protein tyrosine kinase activity	GO:0004714	3.262×10^{-2}		

Supplementary Table 6. List of genes found in the GO categories, "ADP-binding", "NAD+ nucleotidase, cyclic ADP-ribose generating", "NAD+ nucleosidase activity" and "NAD(P)+ nucleosidase activity" of genes found in common between *snap33-1* 12 days transcriptome (Log2FC≥1) and *P35S::RPS4-HS* transcriptome ((Heidrich et al., 2013) GSE50019).

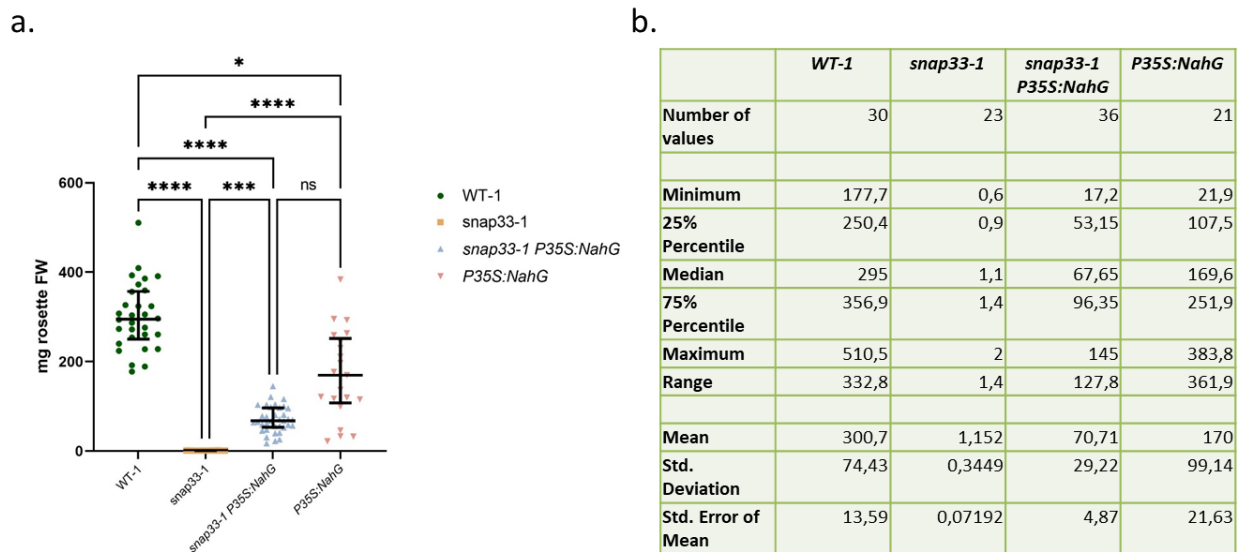
Locus Identifier	Gene Description	Primary Gene Symbol
AT1G51270	vesicle-associated protein 1-4;(source:Araport11)	
AT1G31540	Disease resistance protein (TIR-NBS-LRR class) family;(source:Araport11)	
AT2G20142	Toll-Interleukin-Resistance (TIR) domain family protein;(source:Araport11)	
AT3G04220	Target of miR825/825. Mutants have decreased resistance to fungal pathogens.	
AT4G16920	Disease resistance protein (TIR-NBS-LRR class) family;(source:Araport11)	
AT5G51630	Disease resistance protein (TIR-NBS-LRR class) family;(source:Araport11)	
AT5G41740	Disease resistance protein (TIR-NBS-LRR class) family;(source:Araport11)	
AT3G14470	NB-ARC domain-containing disease resistance protein;(source:Araport11)	
AT1G15890	Disease resistance protein (CC-NBS-LRR class) family;(source:Araport11)	
AT1G57650	ATP binding protein;(source:Araport11)	
AT4G36150	Disease resistance protein (TIR-NBS-LRR class) family;(source:Araport11)	
AT5G45510	Leucine-rich repeat (LRR) family protein;(source:Araport11)	
AT1G57630	Toll-Interleukin-Resistance (TIR) domain family protein;(source:Araport11)	
AT3G44400	Disease resistance protein (TIR-NBS-LRR class) family;(source:Araport11)	
AT2G16870	Disease resistance protein (TIR-NBS-LRR class) family;(source:Araport11)	
AT1G63350	Disease resistance protein (CC-NBS-LRR class) family;(source:Araport11)	
AT1G59620	Encodes CW9.	(CW9)
AT1G12290	NLR protein localized to plasma membrane. Overexpression triggers cell death. Has myristolation site at Gly2 which is required for membrane localization.	(L5)
AT1G17600	SOC3 is a TIR-NB-leucine-rich repeat (TNL) protein.Mutants suppress loss of chs2 phenotype of auto-activation of immunity. When the TIR domain of SOC3 interacts with CHS2 the binding results in temperature activation of cell death, the suppressors inhibit this interaction.	(SOC3)
AT3G04210	TN13 is a TIR-NBS protein involved in immune response. It co localizes with the ER and perinuclear membranes and interacts with MOS6. It also associates with the CC-NBS-LRR resistance protein RPS5 and contributes to RPS5-triggered immunity.	(TN13)
AT1G33560	Encodes a NBS-LRR disease resistance protein that possesses N-terminal kinase subdomains. Activation tagged mutant of ADR1 showed elevated levels of SA and reactive oxygen species in addition to number of defense gene transcripts. Exhibits resistance to number of microbial pathogens.	ACTIVATED DISEASE RESISTANCE 1 (ADR1)
AT4G33300	Encodes a member of the ADR1 family nucleotide-binding leucine-rich repeat (NB-LRR) immune receptors.	ADR1-LIKE 1 (ADR1-L1)
AT5G26920	Encodes a calmodulin-binding protein CBP60g (calmodulin binding protein 60-like.g). The calmodulin-binding domain is located near the N-terminus; calmodulin binding is dependent on Ca(2+). Inducible by both bacterial pathogen and MAMP (microbe-associated molecular pattern) treatments. Bacterial growth is enhanced in cbp60g mutants. cbp60g mutants also show defects in salicylic acid (SA) accumulation and SA signaling.	CAM-BINDING PROTEIN 60-LIKE G (CBP60G)
AT1G17610	TN-type protein that controls temperature-dependent growth and defense responses .Mutant accumulates steryl-esters at low temperatures and shows temperature dependent activation of defense responses..	CHILLING SENSITIVE 1 (CHS1)
AT5G66630	DA1-related protein 5;(source:Araport11)	DA1-RELATED PROTEIN 5 (DAR5)
AT4G12010	Leucine-rich repeat domain (NLR) receptor. Dominant negative alleles suppress catma3 autoimmunity. Co-regulates with WRKY19 basal levels of immunity to root-knot nematodes.	DOMINANT SUPPRESSOR OF CAMTA3 NUMBER 1 (DSC1)
AT3G50950	Encodes a canonical CC-type NLR protein that is required for the recognition of the T3SE HopZ1a as well as several other Hop effectors from the pathogenic bacteria <i>P. syringae</i> .	HOPZ-ACTIVATED RESISTANCE 1 (ZAR1)

AT5G66910	RPW8 -CNL gene is required for signal transduction of TNLs; functionally redundant to NRG1.1.	N REQUIREMENT GENE 1.2 (NRG1.2)
AT3G09830	Encodes a member of subfamily VIIa of the receptor-like cytoplasmic kinases (RLCKs). It contributes to pattern-triggered immunity in response to <i>P. syringae</i> .	PATTERN-TRIGGERED IMMUNITY (PTI) COMPROMISED RECEPTOR-LIKE CYTOPLASMIC KINASE 1 (PCRK1)
AT5G03320	Protein kinase superfamily protein;(source:Araport11)	PATTERN-TRIGGERED IMMUNITY COMPROMISED RECEPTOR-LIKE CYTOPLASMIC KINASE 2 (PCRK2)
AT4G16860	Confers resistance to <i>Peronospora parasitica</i> . RPP4 is coordinately regulated by transcriptional activation and RNA silencing.	RECOGNITION OF PERONOSPORA PARASITICA 4 (RPP4)
AT4G11170	Encodes RMG1 (Resistance Methylated Gene 1), a NB-LRR disease resistance protein with a Toll/interleukin-1 receptor (TIR) domain at its N terminus. RMG1 is expressed at high levels in response to flg22 and in naive met1/nrpd2 relative to wild-type plants. Expression of this gene is controlled by DNA methylation in its promoter region. The RMG1 promoter region is constitutively demethylated by active DNA demethylation mediated by the DNA glycosylase ROS1.	RESISTANCE METHYLATED GENE 1 (RMG1)
AT4G26090	Encodes a plasma membrane protein with leucine-rich repeat, leucine zipper, and P loop domains that confers resistance to <i>Pseudomonas syringae</i> infection by interacting with the avirulence gene <i>avrRpt2</i> . RPS2 protein interacts directly with plasma membrane associated protein RIN4 and this interaction is disrupted by <i>avrRpt2</i> . The mRNA is cell-to-cell mobile.	RESISTANT TO <i>P. SYRINGAE</i> 2 (RPS2)
AT1G12210	RFL1 has high sequence similarity to the adjacent disease resistance (R) gene RPS5.	RPS5-LIKE 1 (RFL1)
AT1G72940	Nucleotide-binding, leucine-rich repeat (NLR) gene regulated by nonsense-mediated mRNA decay (NMD) genes UPF1 and UPF3.	TIR-NBS11 (TN11)
AT1G72950	Disease resistance protein (TIR-NBS class);(source:Araport11)	TIR-NBS12 (TN12)
AT1G17615	TN2 is an atypical TIR-NBS protein that lacks the LRR domain common in typical NLR receptors. It interacts with EXO70B1, a subunit of the exocyst complex. Loss of function mutants in TN2 can suppress EXO70B1 mutants suggesting that EXO70B1 acts through TN2.	TIR-NBS2 (TN2)
AT1G66090	Disease resistance protein (TIR-NBS class);(source:Araport11)	TIR-NBS3 (TN3)
AT1G72890	NBS TIR protein.	TIR-NBS6 (TN6)
AT1G72900	Toll-Interleukin-Resistance (TIR) domain-containing protein;(source:Araport11)	TIR-NBS7 (TN7)
AT5G46520	VICTR (VARIATION IN COMPOUND TRIGGERED ROOT growth response) encodes a TIR-NB-LRR (for Toll-Interleukin1 Receptor-nucleotide binding-Leucine-rich repeat) protein. VICTR is necessary for DFPM-induced root growth arrest and inhibition of abscisic acid-induced stomatal closing (DFPM is [5-(3,4-dichlorophenyl)furan-2-yl]-piperidine-1-ylmethanethione)(PMID:21620700). DFPM-mediated root growth arrest is accession-specific and depends on EDS1 and PAD4; Col-0 has a functional copy of VICTR. Induction of the VICTR gene by DFPM treatment requires functional VICTR (Col). A close homolog to VICTR, named VICTL (At5g46510) lies in tandem with VICTR. The mRNA is cell-to-cell mobile.	VARIATION IN COMPOUND TRIGGERED ROOT GROWTH RESPONSE (VICTR)

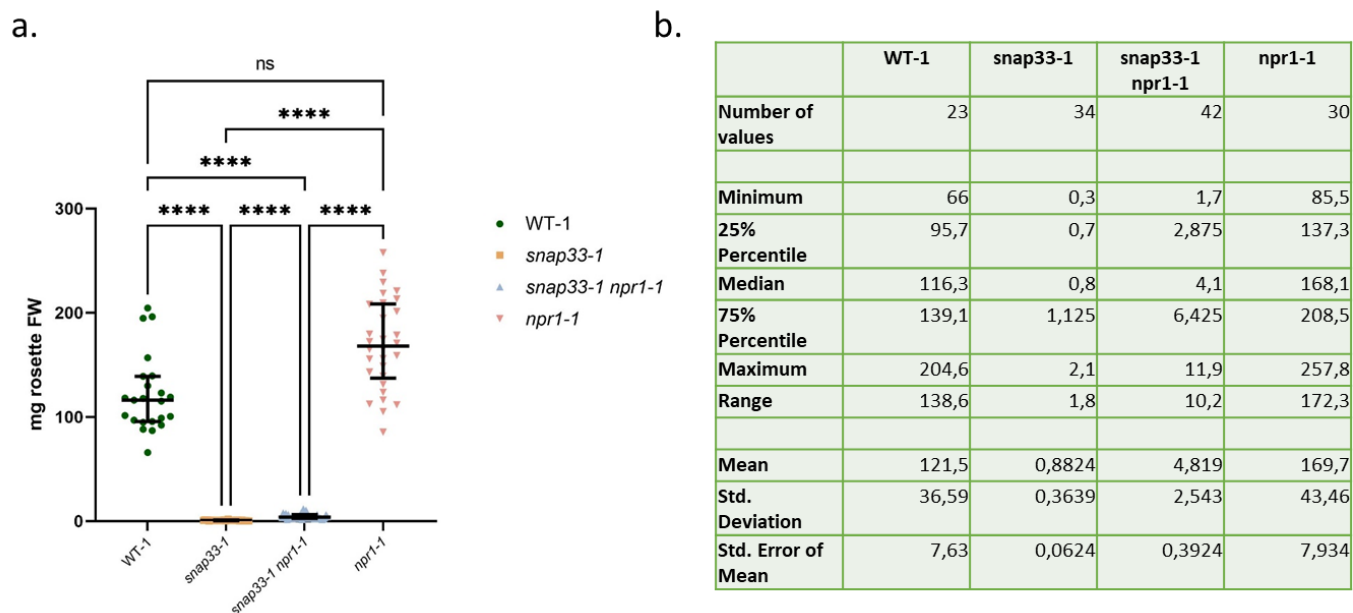
Supplementary data 1. a. Bar graphs of FW linear values of WT-1, *snap33-1*, *snap33-1 sid2-2*, *snap33-1 coi1-34*, *snap33-1 ein2-1*, *sid2-2*, *coi1-34*, *ein2-1*, *snap33-1 sid2-2 coi1-34*, *snap33-1 sid2-2 ein2-1*, *snap33-1 coi1-34 ein2-1*, *sid2-2 coi1-34*, *sid2-2 ein2-1* and *coi1-34 ein2-1*. **b.** Descriptive statistics of each dataset.



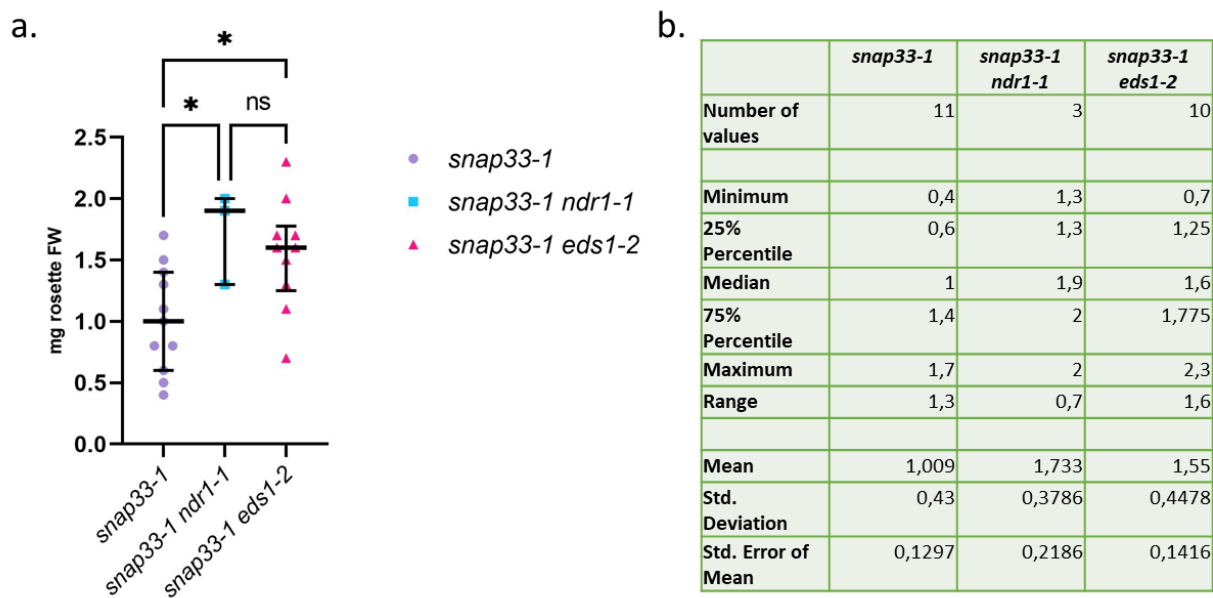
Supplementary data 2. a. Bar graphs of FW linear values of WT-1, *snap33-1*, *snap33-1 P35S::NahG*, and *P35S::NahG*. **b.** Descriptive statistics of each dataset.



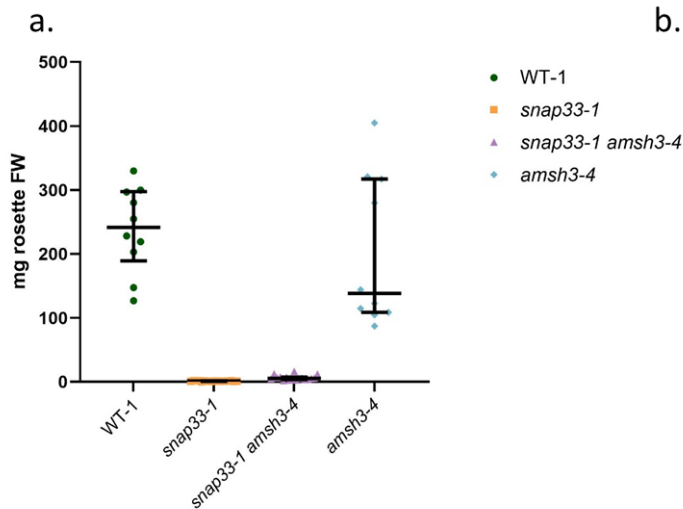
Supplementary data 3. a. Bar graphs of FW linear values of WT-1, *snap33-1*, *snap33-1 npr1-1*, and *npr1-1*. **b.** Descriptive statistics of each dataset.



Supplementary data 4. a. Bar graphs of FW linear values of *snap33-1*, *snap33-1 ndr1-1*, and *snap33-1 eds1-2*. **b.** Descriptive statistics of each dataset.



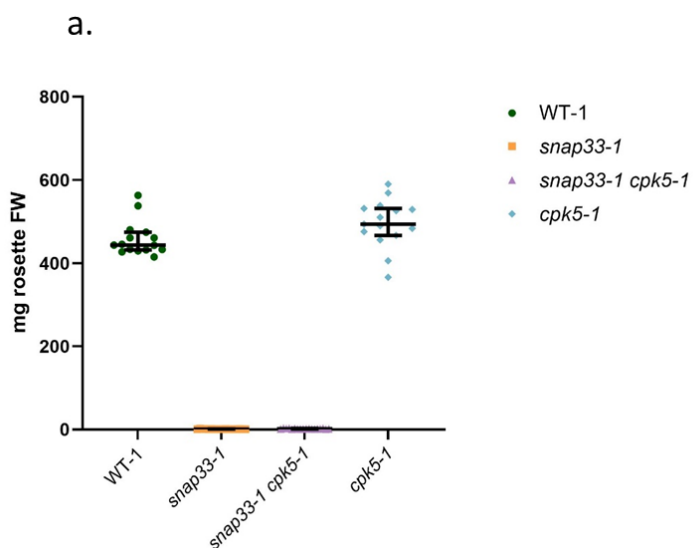
Supplementary data 5. a. Bar graphs of FW linear values of WT-1, *snap33-1*, *snap33-1 amsh3-4*, and *amsh3-4*. **b.** Descriptive statistics of each dataset.



b.

	WT-1	<i>snap33-1</i>	<i>snap33-1 amsh3-4</i>	<i>amsh3-4</i>
Number of values	10	18	17	11
Minimum	126,9	0,2	2,1	87,3
25% Percentile	189,2	0,775	3,6	108,6
Median	241,6	1,25	5,3	138,4
75% Percentile	297,6	1,625	7,55	317
Maximum	330	2,1	16,6	405
Range	203,1	1,9	14,5	317,7
Mean	238,7	1,183	6,506	194,8
Std. Deviation	66,71	0,5762	3,893	112,6
Std. Error of Mean	21,09	0,1358	0,9441	33,94

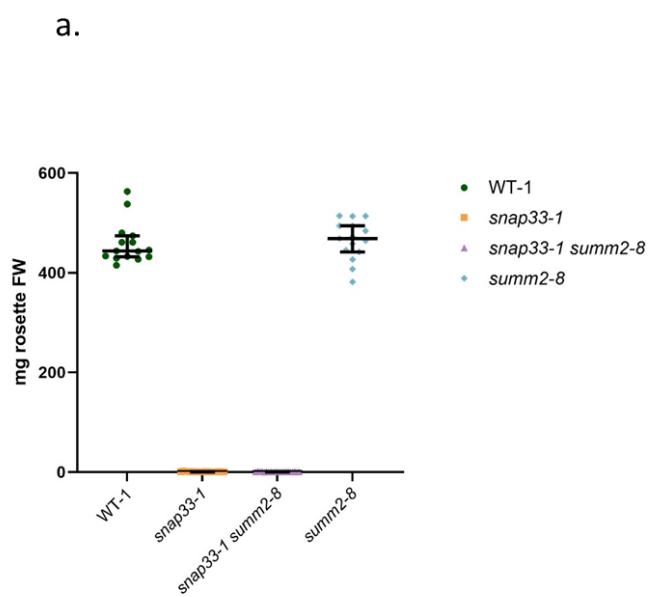
Supplementary data 6. a. Bar graphs of FW linear values of WT-1, *snap33-1*, *snap33-1 cpk5-1*, and *cpk5-1*. **b.** Descriptive statistics of each dataset.



b.

	WT-1	<i>snap33-1</i>	<i>snap33-1 cpk5-1</i>	<i>cpk5-1</i>
Number of values	15	18	18	15
Minimum	414,9	0,5	0,8	366,2
25% Percentile	432,1	0,6	1,25	466,8
Median	443,6	0,85	1,55	493,8
75% Percentile	474,3	1,125	2,45	531,7
Maximum	563	2,3	3,3	590,3
Range	148,1	1,8	2,5	224,1
Mean	458,6	0,9333	1,794	495,7
Std. Deviation	41,67	0,4311	0,7981	58,28
Std. Error of Mean	10,76	0,1016	0,1881	15,05

Supplementary data 7. a. Bar graphs of FW linear values of WT-1, *snap33-1*, *snap33-1 summ2-8*, and *summ2-8*. **b.** Descriptive statistics of each dataset.



b.

	WT-1	<i>snap33-1</i>	<i>snap33-1 summ2-8</i>	<i>summ2-8</i>
Number of values	15	18	21	15
Minimum	414,9	0,5	0,3	381,7
25% Percentile	432,1	0,6	0,65	441,8
Median	443,6	0,85	0,8	468,8
75% Percentile	474,3	1,125	1,25	494,1
Maximum	563	2,3	1,6	514,2
Range	148,1	1,8	1,3	132,5
Mean	458,6	0,9333	0,9095	465,4
Std. Deviation	41,67	0,4311	0,3714	39,61
Std. Error of Mean	10,76	0,1016	0,08104	10,23

Supplementary Table 7. List of genes found in the GO categories "NAD+ nucleotidase, cyclic ADP-ribose generating", "NAD+ nucleosidase activity" and "NAD(P)+ nucleosidase activity." Of genes found in common between *snap33-1* up-regulated at 12 days (Log2FC \geq 1) and SA-treated plants from the study of (Liu et al., 2019) GSE34047)

Locus Identifier	Representative Gene Model Name	Gene Description	Gene Model Type	Primary Gene Symbol	All Gene Symbols
AT2G20142	AT2G20142.1	Toll-Interleukin-Resistance (TIR) domain family protein;(source:Araport11)	protein_coding		
AT3G44400	AT3G44400.1	Disease resistance protein (TIR-NBS-LRR class) family;(source:Araport11)	protein_coding		
AT1G57630	AT1G57630.1	Toll-Interleukin-Resistance (TIR) domain family protein;(source:Araport11)	protein_coding		
AT5G45510	AT5G45510.1	Leucine-rich repeat (LRR) family protein;(source:Araport11)	protein_coding		
AT4G36150	AT4G36150.1	Disease resistance protein (TIR-NBS-LRR class) family;(source:Araport11)	protein_coding		
AT5G41740	AT5G41740.2	Disease resistance protein (TIR-NBS-LRR class) family;(source:Araport11)	protein_coding		
AT3G04210	AT3G04210.1	TN13 is a TIR-NBS protein involved in immune response. It co localizes with the ER and perinuclear membranes and interacts with MOS6. It also associates with the CC-NBS-LRR resistance protein RPS5 and contributes to RPS5-triggered immunity.	protein_coding	(TN13)	(TN13)
AT1G17610	AT1G17610.1	TN-type protein that controls temperature-dependent growth and defense responses .Mutant accumulates steryl-esters at low temperatures and shows temperature dependent activation of defense responses..	protein_coding	CHILLING SENSITIVE 1 (CHS1)	CHILLING SENSITIVE 1 (CHS1)
AT4G12010	AT4G12010.1	Leucine-rich repeat domain (NLR) receptor. Dominant negative alleles suppress catma3 autoimmunity. Co-regulates with WRKY19 basal levels of immunity to root-knot nematodes.	protein_coding	DOMINANT SUPPRESSOR OF CAMTA3 NUMBER 1 (DSC1)	DOMINANT SUPPRESSOR OF CAMTA3 NUMBER 1 (DSC1)
AT4G16860	AT4G16860.1	Confers resistance to Peronospora parasitica. RPP4 is coordinately regulated by transcriptional activation and RNA silencing.	protein_coding	RECOGNITION OF PERONOSPORA PARASITICA 4 (RPP4)	RECOGNITION OF PERONOSPORA PARASITICA 4 (RPP4) (CHS2) CHILLING SENSITIVE 2 (CHS2)
AT1G72900	AT1G72900.1	Toll-Interleukin-Resistance (TIR) domain-containing protein;(source:Araport11)	protein_coding	TIR-NBS7 (TN7)	TIR-NBS7 (TN7)
AT1G72930	AT1G72930.1	Toll/interleukin-1 receptor-like protein (TIR) protein. It is induced in response to bacterial pathogens and overexpression results in cell death in leaves.	protein_coding	TOLL/INTERLEUKIN-1 RECEPTOR-LIKE (TIR)	TOLL/INTERLEUKIN-1 RECEPTOR-LIKE (TIR) (ATTN10) TIR-NUCLEOTIDE BINDING SITE FAMILY 10 (TN10)

Supplementary Table 8. List of genes found in the GO categories “cellular response to hypoxia”, up-regulated in *snap33-1* (Log2FC \geq 1) compared to WT-1 at 12 days.

Representative Gene Model Name	Gene Description	Primary Gene Symbol
AT1G66880.1	Protein kinase superfamily protein;(source:Araport11)	
AT3G03670.1	Peroxidase superfamily protein;(source:Araport11)	
AT1G53620.1	transmembrane protein;(source:Araport11)	
AT3G04640.1	glycine-rich protein;(source:Araport11)	
AT5G63130.1	Octicosapeptide/Phox/Bem1p family protein;(source:Araport11)	
AT4G29780.1	Expression of the gene is affected by multiple stresses. Knockout and overexpression lines show no obvious phenotypes.	
AT1G68620.1	alpha/beta-Hydrolases superfamily protein;(source:Araport11)	
AT3G56880.1	VQ motif-containing protein;(source:Araport11)	
AT5G45630.1	senescence regulator (Protein of unknown function, DUF584);(source:Araport11)	
AT1G10140.1	Uncharacterized conserved protein UCP031279;(source:Araport11)	
AT4G19520.1	disease resistance protein (TIR-NBS-LRR class) family;(source:Araport11)	
AT3G55790.1	transmembrane protein;(source:Araport11)	
AT1G02360.1	Chitinase family protein;(source:Araport11)	
AT1G23710.1	hypothetical protein (DUF1645);(source:Araport11)	
AT1G14550.1	Peroxidase superfamily protein;(source:Araport11)	
AT5G35735.1	Auxin-responsive family protein;(source:Araport11)	
AT1G50740.1	Transmembrane proteins 14C;(source:Araport11)	
AT4G34150.1	Calcium-dependent lipid-binding (CaLB domain) family protein;(source:Araport11)	
AT1G76600.1	PADRE protein up-regulated after infection by <i>S. sclerotiorum</i> .	
AT1G21550.1	Calcium-binding EF-hand family protein;(source:Araport11)	
AT5G19240.1	Glycoprotein membrane precursor GPI-anchored;(source:Araport11)	
AT2G25735.1	hypothetical protein;(source:Araport11)	
AT3G46080.1	C2H2-type zinc finger family protein;(source:Araport11)	
AT1G57630.1	Toll-Interleukin-Resistance (TIR) domain family protein;(source:Araport11)	
AT1G15010.1	mediator of RNA polymerase II transcription subunit;(source:Araport11)	
AT1G07135.1	glycine-rich protein;(source:Araport11)	
AT5G57510.1	cotton fiber protein;(source:Araport11)	
AT2G14247.1	Expressed protein;(source:Araport11)	
AT2G36220.1	hypothetical protein;(source:Araport11)	
AT1G30720.1	FAD-binding Berberine family protein;(source:Araport11)	(ATBBE10)
AT1G26410.1	FAD-binding Berberine family protein;(source:Araport11)	(ATBBE6)
AT2G40140.1	zinc finger (CCCH-type) family protein;(source:Araport11)	(CZF1)
AT1G69890.1	Encodes a member of a conserved DUF domain family that is induced by NO. Based on mutant phenotype may be involved in NO stress response.	(DUF569)
AT2G26190.1	IQM4 is a plastid localized, Ca ²⁺ independent calmodulin binding protein that is involved in promoting seed dormancy.	(IQM4)
AT4G12720.4	Encodes a protein with ADP-ribose hydrolase activity. Negatively regulates EDS1-conditioned plant defense and programmed cell death.	(NUDT7)
AT3G46090.1	C2H2 and C2HC zinc fingers superfamily protein;(source:Araport11)	(ZAT7)
AT4G24230.6	acyl-CoA-binding protein ACBP3. Localized extracellularly in transiently expressed tobacco BY-2 cells and onion epidermal cells. Binds arachidonyl-CoA with high affinity. Microarray data shows up-regulation of many biotic- and abiotic-stress-related genes in an ACBP3 OE-1 in comparison to wild type.	ACYL-COA-BINDING DOMAIN 3 (ACBP3)
AT3G25250.1	Arabidopsis protein kinase The mRNA is cell-to-cell mobile.	AGC2 KINASE 1 (AGC2-1)
AT2G18670.1	RING/U-box superfamily protein;(source:Araport11)	ARABIDOPSIS T??XICOS EN LEVADURA 56 (ATL56)
AT1G05880.2	Encodes ARI12 (ARIADNE 12). ARI12 belongs to a family of 'RING between RING fingers' (RBR) domain proteins with E3 ligase activity. Expression of ARI12 is induced by UV-B exposure.	ARIADNE 12 (ARI12)
AT5G42050.1	Stress responsive asparagine-rich protein. Binds to PevD (<i>Verticillium dahliae</i>) fungal effector protein. NRP interacts with CRY2, leading to increased cytoplasmic accumulation of CRY2 in a blue light-independent manner (PMID:28633330).NRP also binds FyPP3 and recruits it to endosomes and thus targets it for degradation.	ASPARAGINE-RICH PROTEIN (NRP)

AT5G13320.1	Encodes an enzyme capable of conjugating amino acids to 4-substituted benzoates. 4-HBA (4-hydroxybenzoic acid) and pABA (4-aminobenzoate) may be targets of the enzyme in Arabidopsis, leading to the production of pABA-Glu, 4HBA-Glu, or other related compounds. This enzyme is involved in disease-resistance signaling. It is required for the accumulation of salicylic acid, activation of defense responses, and resistance to <i>Pseudomonas syringae</i> . Salicylic acid can decrease this enzyme's activity in vitro and may act as a competitive inhibitor. Expression of PBS3/GH3.12 can be detected in cotyledons, true leaves, hypocotyls, and occasionally in some parts of roots from 10-day-old seedlings. No expression has been detected in root, stem, rosette or cauline leaves of mature 4- to 5-week-old plants.	AVRPPHB SUSCEPTIBLE 3 (PBS3)
AT5G20230.1	Encodes a Al-stress-induced gene. Along with TCF, it promotes lignin biosynthesis in response to cold stress. The mRNA is cell-to-cell mobile.	BLUE-COPPER-BINDING PROTEIN (BCB)
AT4G01360.1	Encodes a protein related to BYPASS1 (BPS1). Regulates production of mobile compound: bps signal.	BYPASS 3 (BPS3)
AT4G27280.1	EF-hand Ca ²⁺ -binding protein, which is a Ca ²⁺ -dependent transducer of auxin-regulated gene expression and interacts with ICR1.	CA ²⁺ -DEPENDENT MODULATOR OF ICR1 (CMI1)
AT2G41090.1	Encodes a cytoplasmic, calcium binding calmodulin variant. CML10 interacts with phosphomannomutase (PMM) in vivo and increases its activity thereby affecting ascorbic acid biosynthesis. Its expression is induced by oxidative and other stress. The mRNA is cell-to-cell mobile.	CALMODULIN LIKE 10 (CML10)
AT5G42380.1	calmodulin like 37;(source:Araport11)	CALMODULIN LIKE 37 (CML37)
AT1G76640.1	Calcium-binding EF-hand family protein;(source:Araport11)	CALMODULIN LIKE 39 (CML39)
AT1G76650.1	calmodulin-like 38;(source:Araport11)	CALMODULIN-LIKE 38 (CML38)
AT5G26920.1	Encodes a calmodulin-binding protein CBP60g (calmodulin binding protein 60-like.g). The calmodulin-binding domain is located near the N-terminus; calmodulin binding is dependent on Ca ²⁺ . Inducible by both bacterial pathogen and MAMP (microbe-associated molecular pattern) treatments. Bacterial growth is enhanced in cbp60g mutants. cbp60g mutants also show defects in salicylic acid (SA) accumulation and SA signaling.	CAM-BINDING PROTEIN 60-LIKE G (CBP60G)
AT5G27420.1	Encodes CNI1 (Carbon/Nitrogen Insensitive1) (also named as ATL31), a RING type ubiquitin ligase that functions in the Carbon/Nitrogen response for growth phase transition in Arabidopsis seedlings. The mRNA is cell-to-cell mobile.	CARBON/NITROGEN INSENSITIVE 1 (CNI1)
AT4G27460.1	Cystathionine beta-synthase (CBS) family protein;(source:Araport11)	CBS DOMAIN CONTAINING PROTEIN 5 (CBSX5)
AT5G66650.1	Chloroplast localized mitochondrial calcium uniporter.	CHLOROPLAST-LOCALIZED MITOCHONDRIAL CALCIUM UNIPORTER (CMCU)
AT2G32200.1	cysteine-rich/transmembrane domain A-like protein;(source:Araport11)	CYSTEINE-RICH TRANSMEMBRANE MODULE 5 (ATHCYSTM5)
AT2G32210.1	cysteine-rich/transmembrane domain A-like protein;(source:Araport11)	CYSTEINE-RICH TRANSMEMBRANE MODULE 6 (ATHCYSTM6)
AT5G57220.1	member of CYP81F, involved in glucosinolate metabolism. Mutants had impaired resistance to fungi. The mRNA is cell-to-cell mobile.	CYTOCHROME P450, FAMILY 81, SUBFAMILY F, POLYPEPTIDE 2 (CYP81F2)
AT4G31970.1	Functions in the biosynthesis of 4-hydroxy indole-3-carbonyl nitrile (4-OH-ICN), a cyanogenic phytoalexin in Arabidopsis. CYP82C2 acts as a hydroxylase on indole-3-carbonyl nitrile to generate 4-OH-ICN.	CYTOCHROME P450, FAMILY 82, SUBFAMILY C, POLYPEPTIDE 2 (CYP82C2)
AT5G24530.1	Encodes a putative 2OG-Fe(II) oxygenase that is defense-associated but required for susceptibility to downy mildew. The mRNA is cell-to-cell mobile.	DOWNY MILDEW RESISTANT 6 (DMR6)
AT5G64905.1	elicitor peptide 3 precursor;(source:Araport11)	ELICITOR PEPTIDE 3 PRECURSOR (PROPEP3)
AT2G47520.1	encodes a member of the ERF (ethylene response factor) subfamily B-2 of ERF/AP2 transcription factor family. The protein contains one AP2 domain. There are 5 members in this subfamily including RAP2.2 AND RAP2.12. It plays a role in hypoxia-induced root slanting.	ETHYLENE RESPONSE FACTOR 71 (ERF71)
AT1G61340.2	Encodes a F-box protein induced by various biotic or abiotic stress.	F-BOX STRESS INDUCED 1 (FBS1)
AT1G26380.1	Functions in the biosynthesis of 4-hydroxy indole-3-carbonyl nitrile (4-OH-ICN), a cyanogenic phytoalexin in Arabidopsis. FOX1 acts as a dehydrogenase on indole cyanohydrin to form indole carbonyl nitrile.	FAD-LINKED OXIDOREDUCTASE 1 (FOX1)

AT1G19250.1	FMO1 is required for full expression of TIR-NB-LRR conditioned resistance to avirulent pathogens and for basal resistance to invasive virulent pathogens. Functions in an EDS1-regulated but SA-independent mechanism that promotes resistance and cell death at pathogen infection sites. FMO1 functions as a piperolate N-hydroxylase and catalyzes the biochemical conversion of piperolic acid to N-hydroxypiperolic acid (NHP). NHP systemically accumulates in the plant foliage and induces systemic acquired resistance to pathogen infection.	FLAVIN-DEPENDENT MONOOXYGENASE 1 (FMO1)
AT5G25250.1	Encodes a protein that is involved in a membrane microdomain-dependent, but clathrin-independent, endocytic pathway required for optimal seedling development. The mRNA is cell-to-cell mobile.	FLOTILLIN 1 (FLOT1)
AT1G30040.1	Encodes a gibberellin 2-oxidase that acts on C-19 gibberellins. AtGA2OX2 expression is responsive to cytokinin and KNOX activities.	GIBBERELLIN 2-OXIDASE (GA2OX2)
AT5G13190.1	Encodes a plasma membrane localized LITAF domain protein that interacts with LSD1 and acts as a negative regulation of hypersensitive cell death.	GSH-INDUCED LITAF DOMAIN PROTEIN (GILP)
AT3G46230.1	Member of the class I small heat-shock protein (sHSP) family, which accounts for the majority of sHSPs in maturing seeds. Induced by heat, cold, salt, drought and high-light.	HEAT SHOCK PROTEIN 17.4 (HSP17.4)
AT4G16660.1	heat shock protein 70 (Hsp 70) family protein;(source:Araport11)	HEAT SHOCK PROTEIN 70 (HSP70)
AT1G25550.1	Member of HHO/HRS GARP type transcriptional repressor family. Involved in Pi uptake and Pi starvation signaling. Transcriptional repressors that functions with other NIGT genes as an important hub in the nutrient signaling network associated with the acquisition and use of nitrogen and phosphorus.	HRS1 HOMOLOG3 (HHO3)
AT4G27450.1	aluminum induced protein with YGL and LRDR motifs;(source:Araport11)	HYPOXIA RESPONSE UNKNOWN PROTEIN 54 (HUP54)
AT3G10020.1	plant/protein;(source:Araport11)	HYPOXIA RESPONSE UNKNOWN PROTEIN 26 (HUP26)
AT1G67360.2	Encodes a small rubber particle protein homolog. Plays dual roles as positive factors for tissue growth and development and in drought stress responses.	LD-ASSOCIATED PROTEIN 1 (LDAP1)
AT1G73500.1	member of MAP Kinase Kinase family. Autophosphorylates and also phosphorylates MPK3 and MPK6. Independently involved in ethylene and calmaxin biosynthesis. Induces transcription of ACS2, ACS6, ERF1, ERF2, ERF5, ERF6, CYP79B2, CYP79B3, CYP71A13 and PAD3.	MAP KINASE KINASE 9 (MKK9)
AT2G15890.1	Encodes CBP1, a regulator of transcription initiation in central cell-mediated pollen tube guidance.	MATERNAL EFFECT EMBRYO ARREST 14 (MEE14)
AT1G26800.1	MPSR1 is cytoplasmic E3 ligase that senses misfolded proteins independently of chaperones and targets those proteins for degradation via the 26S proteasome. Involved in the regulation of the homeostasis of sensor NLR immune receptors.	MISFOLDED PROTEIN SENSING RING E3 LIGASE 1 (MPSR1)
AT5G63790.1	Encodes a member of the NAC family of transcription factors. ANAC102 appears to have a role in mediating response to low oxygen stress (hypoxia) in germinating seedlings. Its expression can be induced by beta-cyclocitral, an oxidized by-product of beta-carotene generated in the chloroplasts, mediates a protective retrograde response that lowers the levels of toxic peroxides and carbonyls, limiting damage to intracellular components.	NAC DOMAIN CONTAINING PROTEIN 102 (NAC102)
AT5G06320.1	encodes a protein whose sequence is similar to tobacco hairpin-induced gene (HIN1) and Arabidopsis non-race specific disease resistance gene (NDR1). Expression of this gene is induced by cucumber mosaic virus, spermine and Pseudomonas syringae pv. tomato DC3000. The gene product is localized to the plasma membrane.	NDR1/HIN1-LIKE 3 (NHL3)
AT1G18300.1	nudix hydrolase homolog 4;(source:Araport11)	NUDIX HYDROLASE HOMOLOG 4 (NUDT4)
AT2G40000.1	ortholog of sugar beet HS1 PRO-1 2;(source:Araport11)	ORTHOLOG OF SUGAR BEET HS1 PRO-1 2 (HSPRO2)
AT1G14540.1	Class III peroxidase cell wall-targeted protein localized to the micropylar endosperm facing the radicle. Involved in seed germination.	PEROXIDASE 4 (PER4)
AT1G73010.1	Encodes PPsPase1, a pyrophosphate-specific phosphatase catalyzing the specific cleavage of pyrophosphate (Km 38.8 uM) with an alkaline catalytic pH optimum. Expression is upregulated in the shoot of cax1/cax3 mutant.	PHOSPHATE STARVATION-INDUCED GENE 2 (PS2)
AT2G01180.1	Encodes phosphatidate phosphatase. Up-regulated by genotoxic stress (gamma ray or UV-B) and elicitor treatments with mastoparan and harpin. Expressed in roots and leaves.	PHOSPHATIDIC ACID PHOSPHATASE 1 (PAP1)
AT4G26270.1	phosphofructokinase 3;(source:Araport11)	PHOSPHOFRUCTOKINASE 3 (PFK3)
AT2G26560.1	Encodes a lipid acyl hydrolase with wide substrate specificity that accumulates upon infection by fungal and bacterial pathogens. Protein is localized in the cytoplasm in healthy leaves, and in membranes in infected cells. Plays a role in cell death and differentially affects the accumulation of oxylipins. Contributes to resistance to virus.	PHOSPHOLIPASE A 2A (PLA2A)

AT5G54490.1	Encodes a PINOID (PID)-binding protein containing putative EF-hand calcium-binding motifs. The interaction is dependent on the presence of calcium. mRNA expression is up-regulated by auxin. Not a phosphorylation target of PID, likely acts upstream of PID to regulate the activity of this protein in response to changes in calcium levels.	PINOID-BINDING PROTEIN 1 (PBP1)
AT2G23270.1	Encoding a precursor protein of a secreted peptide that is responsive to flg22 stimulus. Finetuning role in modulation of immunity through the regulation of SA and JA biosynthesis and signalling pathways.	PRECURSOR OF PAMP-INDUCED PEPTIDE 3 (PREPIP3)
AT1G68690.1	Encodes a member of the proline-rich extensin-like receptor kinase (PERK) family. This family consists of 15 predicted receptor kinases (PMID: 15653807).	PROLINE-RICH EXTENSIN-LIKE RECEPTOR KINASE 9 (PERK9)
AT5G47910.1	NADPH/respiratory burst oxidase protein D (RbohD). Interacts with AtrbohF gene to fine tune the spatial control of ROI production and hypersensitive response to cell in and around infection site. The mRNA is cell-to-cell mobile.	RESPIRATORY BURST OXIDASE HOMOLOGUE D (RBOHD)
AT5G59820.1	Encodes a zinc finger protein involved in high light and cold acclimation. Overexpression of this putative transcription factor increases the expression level of 9 cold-responsive genes and represses the expression level of 15 cold-responsive genes, including CBF genes. Also, lines overexpressing this gene exhibits a small but reproducible increase in freeze tolerance. Because of the repression of the CBF genes by the overexpression of this gene, the authors speculate that this gene may be involved in	RESPONSIVE TO HIGH LIGHT 41 (RHL41)
AT1G19530.1	Direct target of RGA, plays an essential role in GA-mediated tapetum and pollen development.	RGA TARGET 1 (RGAT1)
AT4G13395.1	ROTUNDIFOLIA like 12;(source:Araport11)	ROTUNDIFOLIA LIKE 12 (RTFL12)
AT1G27730.1	Related to Cys2/His2-type zinc-finger proteins found in higher plants. Compensated for a subset of calcineurin deficiency in yeast. Salt tolerance produced by ZAT10 appeared to be partially dependent on ENA1/PMR2, a P-type ATPase required for Li+ and Na+ efflux in yeast. The protein is localized to the nucleus, acts as a transcriptional repressor and is responsive to chitin oligomers. Also involved in response to photooxidative stress.	SALT TOLERANCE ZINC FINGER (STZ)
AT3G08720.1	Encodes a ribosomal-protein S6 kinase. Gene expression is induced by cold and salt (NaCl). Activation of AtS6k is regulated by 1-naphthylacetic acid and kinetin, at least in part, via a lipid kinase-dependent pathway. Phosphorylates specifically mammalian and plant S6 at 25 degrees C but not at 37 degrees C. Involved in translational up-regulation of ribosomal proteins.	SERINE/THREONINE PROTEIN KINASE 2 (S6K2)
AT1G19020.1	Modulates defense against bacterial pathogens and tolerance to oxidative stress.	SMALL DEFENSE-ASSOCIATED PROTEIN 1 (SDA1)
AT2G13790.1	somatic embryogenesis receptor-like kinase 4;(source:Araport11)	SOMATIC EMBRYOGENESIS RECEPTOR-LIKE KINASE 4 (SERK4)
AT1G09070.1	SRC2 specifically binds the peptide PIEPPPHH, and moves from ER to a vacuole fraction where it gets internalized. Involved in Protein Storage Vacuole targeting. The mRNA is cell-to-cell mobile.	SOYBEAN GENE REGULATED BY COLD-2 (SRC2)
AT5G24590.2	Member of NAc protein family. Interacts with turnip crinkle virus (TCV) capsid protein. Transcription factor involved in regulating the defense response of Arabidopsis to TCV.	TCV-INTERACTING PROTEIN (TIP)
AT1G72940.1	Nucleotide-binding, leucine-rich repeat (NLR) gene regulated by nonsense-mediated mRNA decay (NMD) genes UPF1 and UPF3.	TIR-NBS11 (TN11)
AT1G66090.1	Disease resistance protein (TIR-NBS class);(source:Araport11)	TIR-NBS3 (TN3)
AT1G72900.1	Toll-Interleukin-Resistance (TIR) domain-containing protein;(source:Araport11)	TIR-NBS7 (TN7)
AT1G72910.1	Nucleotide-binding, leucine-rich repeat (NLR) gene regulated by nonsense-mediated mRNA decay (NMD) genes UPF1 and UPF3.	TIR-NBS8 (TN8)
AT1G72920.1	Toll-Interleukin-Resistance (TIR) domain family protein;(source:Araport11)	TIR-NBS9 (TN9)
AT2G41100.1	encodes a calmodulin-like protein, with six potential calcium binding domains. Calcium binding shown by Ca(2+)-specific shift in electrophoretic mobility. Expression induced by touch and darkness. Expression may also be developmentally controlled. Expression in growing regions of roots, vascular tissue, root/shoot junctions, trichomes, branch points of the shoot, and regions of siliques and flowers. The mRNA is cell-to-cell mobile.	TOUCH 3 (TCH3)
AT2G22500.1	Encodes one of the mitochondrial dicarboxylate carriers (DIC): DIC1 (AT2G22500), DIC2 (AT4G24570), DIC3 (AT5G09470).	UNCOUPLING PROTEIN 5 (UCP5)
AT4G37710.1	VQ motif-containing protein;(source:Araport11)	VQ MOTIF-CONTAINING PROTEIN 29 (VQ29)
AT2G46400.1	Encodes a WRKY transcription factor that contributes to the feedforward inhibition of osmotic/salt stress-dependent LR inhibition via regulation of ABA signaling and auxin homeostasis.	WRKY DNA-BINDING PROTEIN 46 (WRKY46)
AT3G56400.1	Member of WRKY Transcription Factor; Group III. Function as activator of SA-dependent defense genes and a repressor of JA-regulated genes. WRKY70-controlled suppression of JA-signaling is partly executed by NPR1.	WRKY DNA-BINDING PROTEIN 70 (WRKY70)

Description et caractérisation fonctionnelle du t-SNARE SNAP33 chez *Arabidopsis thaliana*

Introduction

Les protéines SNAREs (soluble N-ethylmaleimide-sensitive factor attachment protein receptors) sont impliquées dans le trafic vésiculaire au cours de plusieurs processus chez les plantes et contribuent à l'homéostasie, l'immunité, la croissance et le développement (Lipka et al., 2007).

Parmi cette famille de gènes, *SNAP33* code pour une protéine t-SNARE (target-SNARE) impliquée dans la fusion des vésicules à la membrane plasmique au cours de la cytokinèse et de l'immunité (Heese et al., 2001; Wick et al., 2003). L'un des traits les plus intrigants du mutant perte de fonction *snap33* est le développement précoce de lésions spontanées dans des conditions de croissance normales ainsi qu'une morphologie très naine (Heese et al., 2001). Les objectifs du doctorat étaient d'abord de mieux caractériser le phénotype de *snap33* aux niveaux macroscopique et moléculaire et de déterminer les voies génétiques impliquées dans ce phénotype. Ensuite, le deuxième objectif était d'évaluer un lien potentiel, suggéré par la littérature, entre SNAP33 et des protéines MAPK (mitogen-activated protein kinase) connues pour être également impliquées dans l'immunité des plantes (Bigeard et al., 2015).

Résultats

1. Caractérisation du mutant *snap33*

1.1. Isolation des mutants *snap33*

Un grand nombre de mutants nains et développant des lésions nécrotiques de manière spontanée, rapportés dans la littérature, sont liés à une activation constitutive des réponses immunitaires (Bruggeman et al., 2015). Nous avons examiné si cela était aussi le cas pour le mutant *snap33*. Pour cela, nous avons identifié trois lignées d'insertions à partir de la collection d'ADN-T du Centre de ressources biologiques d'*Arabidopsis* (ABRC) et qui présentent des insertions ADN-T à différents endroits dans le locus du gène *SNAP33* dans l'écotype Col-0

d'Arabidopsis. Ces lignées ont été désignées *snap33-1*, *snap33-2* et *snap33-3*. L'isolation des mutants homozygotes de chaque lignée montre que les trois mutants ont le même phénotype nain et nécrotique rapporté précédemment par Heese et al., pour le mutant *snap33* dans l'écotype Wassilewskija (Ws) (Heese et al., 2001).

La caractérisation des mutants *snap33* identifiés a été faite par des colorations au DAB (3,3'-Diaminobenzidine) et au bleu de Trypan qui permettent de mettre en évidence l'accumulation d'espèces réactives de l'oxygène de type H₂O₂ et la mort cellulaire, respectivement.

Ces colorations ont permis de voir que chez les plantes *snap33* issues des trois lignées T-DNA il y a une suraccumulation de H₂O₂ et la présence de cellules mortes qui se manifestent de manière spontanée dans des conditions de culture normales.

Plusieurs mutants auto-immuns rapportés dans la littérature montrent une suppression partielle ou totale de leur phénotype nain par les températures élevées (Huot et al., 2017). Pour étudier si cela est aussi le cas pour le mutant *snap33*, nous avons cultivé le mutant *snap33* à 30°C en parallèle avec des plantes sauvages ainsi que des plantes cultivées à 22°C dans les mêmes conditions de culture. Après 21 jours de croissance, les plantes *snap33* montrent en effet une suppression partielle de leur phénotype par les fortes températures avec une taille de rosette plus large comparé aux plantes *snap33* cultivées à 22°C. Ces résultats suggèrent que le phénotype de *snap33* pourrait en effet être lié à de l'auto-immunité.

Pour étudier davantage l'auto-immunité dans le mutant *snap33*, nous avons analysé l'activation de MAPK impliquées dans l'immunité, à savoir MPK3, MPK4 et MPK6. Cette analyse a été faite suite à une application de stress avec flg22, un peptide conservé dans le flagelle des bactéries et qui induit les réponses immunitaires chez les plantes (Chinchilla et al., 2006). Chez les plantes sauvages, le stress avec flg22 active les MAPKs MPK3, MPK4 et MPK6 très rapidement, avec un maximum d'activation à 15 minutes (Nühse et al., 2000; Zipfel et al., 2006). Les MAPK activées vont contribuer à la génération de la réponse immunitaire en phosphorylant divers substrats (enzymes, facteurs de transcription, etc.). L'analyse de l'activation des

MAPKs par traitement avec flg22 se fait par un anticorps anti-pTpY qui reconnaît la forme doublement phosphorylée et donc activée de la MAPK. L'analyse de l'activation des MAPKs chez *snap33* suite à un stress flg22 a montré que MPK3, MPK4 et MPK6 s'activent d'une manière plus intense par rapport au sauvage. De plus, l'analyse de l'accumulation des trois MAPKs chez *snap33* a montré que les MAPKs sont suraccumulées chez les trois mutants *snap33* par rapport au sauvage. Ce résultat reflète un état d'amorçage de l'immunité chez le mutant *snap33*.

1.2. Etude transcriptomique du mutant *snap33*

Pour mieux caractériser le mutant *snap33* et identifier les voies moléculaires à l'origine de son phénotype, nous avons réalisé des analyses transcriptomiques par séquençage d'ARN (RNA-seq) sur de jeunes plantes *snap33-1* âgées de 5 et 12 jours, respectivement avant et après l'apparition des lésions, comparé à des plantes sauvages du même âge. Les plantes sauvages et *snap33-1* ont été cultivées dans les mêmes conditions, et trois réplicas biologiques ont été réalisés pour chaque génotype et chaque temps.

Les données transcriptomiques ont montré que 2591 gènes sont exprimés de manière différentielle entre le mutant *snap33* et les plantes sauvages à 5 jours, et 7998 gènes sont exprimés de manière différentielle à 12 jours. L'analyse d'annotation Gene Ontology (GO) des gènes surexprimés dans le mutant *snap33* a révélé un enrichissement des processus biologiques impliqués dans la réponse aux stress, aux agents pathogènes, à l'hypoxie ainsi que la réponse à l'acide salicylique (SA) et l'acide jasmonique (JA), et la réponse d'hypersensibilité. De plus, nous avons trouvé une régulation positive de l'expression d'environ 50 gènes de résistance (R) dans le mutant *snap33* à 12 jours par rapport aux plantes sauvages. Ces résultats confirment l'auto-immunité observée chez le mutant *snap33* et suggèrent que SNAP33 joue un rôle critique dans la modulation des réponses immunitaires chez *Arabidopsis*.

Pour valider les résultats de l'analyse transcriptomique, nous avons quantifié l'expression de certains gènes impliqués dans les voies hormonales de l'immunité par Reverse Transcription et PCR quantitative (RT-qPCR). Les expériences RT-qPCR de

validation ont été faites sur des plantes *snap33* issues de la lignée T-DNA *snap33-3* cultivée en même temps et dans les mêmes conditions que les plantes *snap33-1* utilisées pour l'analyse transcriptomique. Les résultats des RT-qPCR ont permis de valider la surexpression de certains gènes impliqués dans les voies hormonales de l'immunité, c'est-à-dire JA, SA et éthylène (ET), ainsi que la validation d'autres gènes impliqués dans l'immunité et précédemment décrits chez *Arabidopsis*.

1.3. Etude génétique du mutant *snap33*

Suite à la validation de la surexpression des gènes impliqués dans les voies hormonales de l'immunité chez les mutants *snap33*, les hormones SA, JA et ET ont été quantifiées chez ce mutant. Les résultats montrent qu'il y a une suraccumulation de des hormones SA, JA et ET chez le mutant *snap33* par rapport aux plantes sauvages. A l'issue de ces résultats, le rôle des voies hormonales dans le développement du phénotype de *snap33* a été étudié par des croisements génétiques entre le mutant *snap33* et des mutants des trois voies hormonales (mutant de biosynthèse d'hormones et/ou mutants insensibles aux hormones). Les doubles mutants générés ont montré que le phénotype de *snap33* n'est pas supprimé par des mutants altérés dans les voies de signalisations JA ou ET, mais est partiellement supprimé par le mutant *sid2/ics1*, qui est largement altéré dans la biosynthèse de SA (Wildermuth et al., 2001). En effet, le double mutant *snap33 sid2* montre un poids de rosette significativement plus élevé comparé au simple mutant *snap33*, et les symptômes de mort cellulaire, suraccumulation de ROS et suraccumulation des MAPKs sont partiellement supprimés chez le double mutant *snap33 sid2*. De plus, l'abolition complète de l'accumulation de SA par l'expression ectopique de l'enzyme bactérienne NahG, qui convertit le SA en catéchol (Delaney et al., 1994), a presque complètement supprimé le phénotype morphologique de *snap33*. Ces résultats montrent que le phénotype de *snap33* est majoritairement lié à la suraccumulation de SA.

Pendant l'immunité chez *Arabidopsis*, la reconnaissance de l'effet des protéines de virulence des pathogènes sur leurs cibles chez les plantes se fait par les protéines de

résistance de type nucleotide-binding (NB) leucine-rich receptors (LRR) (NB-LRR) (Jones & Dangl, 2006). Ces protéines de résistance activent l'immunité par EDS1 et NDR1, deux protéines nécessaires à la signalisation en aval des protéines de résistance R du type TIR (toll-Interleukin)-NB-LRR et CC (coiled-coil)-NB-LRR, respectivement (Aarts et al., 1998). EDS1 et NDR1 activent l'immunité par la voie de l'acide salicylique. Le triple mutant *snap33 eds1 ndr1* montre qu'il y a une suppression partielle par la mutation de *EDS1 et NDR1* et montre ainsi l'implication des protéines de résistance dans le phénotype de *snap33*, suggérant ainsi que la protéine SNAP33 pourrait être une cible des agents pathogènes et que SNAP33 elle-même, ou sa fonction, est gardée par une ou plusieurs protéines R. Dans l'ensemble, nos résultats permettent une meilleure compréhension du phénotype du mutant *snap33* et révèlent l'importance du secteur de défense lié au SA en aval de *snap33*.

2. Etude du lien entre SNAP33 et les MAPKs impliquées dans l'immunité

Un module MAPK est constitué de trois protéines qui agissent successivement : une MAP Kinase Kinase Kinase, une MAP Kinase Kinase et une MAP Kinase. Le module MAPK formé des protéines MEKK1-MKK1/MKK2-MPK4 est rapidement activé en réponse à une infection pathogène et contribue à l'établissement de réponses immunitaires en phosphorylant divers substrats (Bigeard et al., 2015). Les mutants *mpk4* et *mekk1*, ainsi que le double mutant *mkk1 mkk2*, présentent également un phénotype auto-immun similaire à celui de *snap33*. SNAP33, MEKK1, MKK2 et MPK4 ont des profils d'expression similaires, selon l'analyse de co-expression génique (Genevestigator). De plus, les protéines MPK4 et SNAP33 sont toutes deux impliquées dans la cytokinèse (Kasmi et al., 2013; Kosetsu et al., 2010). Par ailleurs, SNAP33 est connue pour être phosphorylée *in vivo* sur des sites dont les motifs kinases sont compatibles avec la signature MAPK. Prises ensemble, ces données nous ont incités à examiner la possibilité d'une relation entre SNAP33 et le module MEKK1-MKK1/MKK2-MPK4. Nous avons émis les hypothèses que le module MAPK pourrait être impliqué dans la régulation de l'activité SNAP33 lors de l'immunité et/ou que SNAP33 pourrait réguler le module MAPK.

En utilisant des tests de complémentation de fluorescence bimoléculaire (BiFC), nous avons observé que SNAP33 interagit *in vivo* avec MEKK1, MKK2 et MPK4. Cependant, ces résultats n'ont pas pu être confirmés par des approches complémentaires de co-immunoprécipitation, pull-down et double hybride en levures (Y2H), suggérant que, si elles sont physiologiquement vraies, ces interactions sont susceptibles d'être transitoires.

Nous avons également exploré si SNAP33 pouvait être un substrat *in vitro* de MPK4 et de deux autres MAPKs, MPK3 et MPK6, impliquées dans l'immunité. Ces trois protéines ne phosphorylent pas SNAP33 *in vitro* par un test kinase radioactif, ce qui suggère fortement que SNAP33 n'est un substrat d'aucune de ces MAPKs. Nous avons finalement examiné une possible connexion génétique entre SNAP33 et le module MEKK1-MKK1/MKK2-MPK4 en croisant *snap33* avec plusieurs suppresseurs connus des phénotypes de *mekk1*, *mkk1 mkk2* et *mpk4*. Aucun d'entre eux n'a supprimé le phénotype de *snap33*, suggérant que SNAP33 et le module MAPK ne font pas partie de la même voie génétique.

Ainsi l'ensemble de nos données suggèreraient que SNAP33 et le module MAPK fonctionneraient indépendamment, bien que les deux soient impliqués dans la réponse immunitaire.

Conclusion et perspectives

L'ensemble des résultats obtenus à l'issue de ces travaux suggèrent que SNAP33 joue un rôle important dans le système immunitaire de la plante, et pourrait être une cible des agents pathogènes étant donné son implication dans la sécrétion de substances antimicrobiennes en réponse aux infections par des agents pathogènes (Kwon et al., 2008). La perturbation de SNAP33 par des protéines de virulence d'agents pathogènes conduirait ainsi à l'induction des réponses immunitaires activées par les protéines de résistance qui gardent SNAP33. Ainsi, dans le mutant *snap33* il y a une activation constitutive des réponses immunitaire due à l'absence de SNAP33 qui mime sa perturbation. Pour valider ces résultats, un crible de mutations qui

supprimer le phénotype de *snap33* pourrait être réalisé. Ces expériences pourraient en effet révéler la protéine de résistance qui garde SNAP33 et qui active l'immunité de manière spontanée et constitutive en l'absence de SNAP33.

Il serait également intéressant d'étudier le rôle des phosphorylations de SNAP33 notamment sur l'activité de la protéine, sa localisation, son abondance, et d'identifier les protéines qui phosphorylent SNAP33 et réguleraient ainsi son activité. En effet, les régulations post-traductionnelles des protéines SNAREs sont encore peu étudiées chez les plantes.

- Aarts, N., Metz, M., Holub, E., Staskawicz, B. J., Daniels, M. J., & Parker, J. E. (1998). Different requirements for EDS1 and NDR1 by disease resistance genes define at least two R gene-mediated signaling pathways in Arabidopsis. *Proceedings of the National Academy of Sciences of the United States of America*, *95*(17), 10306–10311. <https://doi.org/10.1073/pnas.95.17.10306>
- Bigeard, J., Colcombet, J., & Hirt, H. (2015). Signaling mechanisms in pattern-triggered immunity (PTI). In *Molecular Plant* (Vol. 8, Issue 4, pp. 521–539). Cell Press. <https://doi.org/10.1016/j.molp.2014.12.022>
- Bruggeman, Q., Raynaud, C., Benhamed, M., & Delarue, M. (2015). To die or not to die? Lessons from lesion mimic mutants. *Frontiers in Plant Science*, *6*(JAN), 1–22. <https://doi.org/10.3389/FPLS.2015.00024>
- Chinchilla, D., Bauer, Z., Regenass, M., Boller, T., & Felix, G. (2006). The Arabidopsis Receptor Kinase FLS2 Binds flg22 and Determines the Specificity of Flagellin Perception. *The Plant Cell*, *18*(2), 465–476. <https://doi.org/10.1105/TPC.105.036574>
- Delaney, T. P., Uknes, S., Vernooij, B., Friedrich, L., Weymann, K., Negrotto, D., Gaffney, T., Gut-Rella, M., Kessmann, H., Ward, E., & Ryals, J. (1994). A central role of salicylic acid in plant disease resistance. *Science*, *266*(5188), 1247–1250. <https://doi.org/10.1126/science.266.5188.1247>
- Heese, M., Gansel, X., Sticher, L., Wick, P., Grebe, M., Granier, F., & Jürgens, G. (2001). Functional characterization of the KNOLLE-interacting t-SNARE AtSNAP33 and its role in plant cytokinesis. *Journal of Cell Biology*, *155*(2), 239–249. <https://doi.org/10.1083/jcb.200107126>
- Huot, B., Castroverde, C. D. M., Velásquez, A. C., Hubbard, E., Pulman, J. A., Yao, J., Childs, K. L., Tsuda, K., Montgomery, B. L., & He, S. Y. (2017). Dual impact of elevated temperature on plant defence and bacterial virulence in Arabidopsis. *Nature Communications*, *8*(1), 1–12. <https://doi.org/10.1038/s41467-017-01674-2>
- Jones, J. D. G., & Dangl, J. L. (2006). The plant immune system. In *Nature* (Vol. 444, Issue 7117, pp. 323–329). <https://doi.org/10.1038/nature05286>
- Kasmi, F. el, Krause, C., Hiller, U., Stierhof, Y.-D., Mayer, U., Conner, L., Kong, L., Reichardt, I., Sanderfoot, A. A., & Jürgens, G. (2013). SNARE complexes of different composition jointly mediate membrane fusion in Arabidopsis cytokinesis. *Molecular Biology of the Cell*, *24*(10), 1593. <https://doi.org/10.1091/MBC.E13-02-0074>
- Kosetsu, K., Matsunaga, S., Nakagami, H., Colcombet, J., Sasabe, M., Soyano, T., Takahashi, Y., Hirt, H., & Machida, Y. (2010). The MAP kinase MPK4 Is required for cytokinesis in Arabidopsis thaliana. *Plant Cell*, *22*(11), 3778–3790. <https://doi.org/10.1105/tpc.110.077164>
- Kwon, C., Neu, C., Pajonk, S., Yun, H. S., Lipka, U., Humphry, M., Bau, S., Straus, M., Kwaaitaal, M., Rampelt, H., Kasmi, F. el, Jürgens, G., Parker, J., Panstruga, R., Lipka, V., & Schulze-Lefert, P. (2008). Co-option of a default secretory pathway for plant immune responses. *Nature*, *451*(7180), 835–840. <https://doi.org/10.1038/nature06545>
- Lipka, V., Kwon, C., & Panstruga, R. (2007). SNARE-Ware: The Role of SNARE-Domain Proteins in Plant Biology. <http://Dx.Doi.Org/10.1146/Annurev.Cellbio.23.090506.123529>, *23*, 147–174. <https://doi.org/10.1146/ANNUREV.CELLBIO.23.090506.123529>
- Nühse, T. S., Peck, S. C., Hirt, H., & Boller, T. (2000). Microbial Elicitors Induce Activation and Dual Phosphorylation of the Arabidopsis thaliana MAPK 6 *. *Journal of Biological Chemistry*, *275*(11), 7521–7526. <https://doi.org/10.1074/JBC.275.11.7521>
- Wick, P., Gansel, X., Oulevey, C., Page, V., Studer, I., Dürst, M., & Sticher, L. (2003). The expression of the t-SNARE AtSNAP33 is induced by pathogens and mechanical stimulation. *Plant Physiology*, *132*(1), 343–351. <https://doi.org/10.1104/pp.102.012633>

- Wildermuth, M. C., Dewdney, J., Wu, G., & Ausubel, F. M. (2001). Isochorismate synthase is required to synthesize salicylic acid for plant defence. *Nature*, *414*(6863), 562–565.
<https://doi.org/10.1038/35107108>
- Zipfel, C., Kunze, G., Chinchilla, D., Caniard, A., Jones, J. D. G., Boller, T., & Felix, G. (2006). Perception of the Bacterial PAMP EF-Tu by the Receptor EFR Restricts Agrobacterium-Mediated Transformation. *Cell*, *125*(4), 749–760.
<https://doi.org/10.1016/J.CELL.2006.03.037>

Titre : Description et caractérisation fonctionnelle du t-SNARE SNAP33 chez *Arabidopsis thaliana*

Mots clés : SNAP33, MAPK, stress, phytohormones, Arabidopsis, immunité

Résumé Les SNAREs (soluble N-ethylmaleimide-sensitive factor attachment protein receptors) sont impliqués dans le trafic vésiculaire au cours de plusieurs processus chez les plantes et contribuent à l'homéostasie, l'immunité, la croissance et le développement. Parmi cette famille de gènes, *SNAP33* code pour une protéine t-SNARE (target-SNARE) impliquée dans la fusion des vésicules à la membrane plasmique au cours de la cytokinèse et de l'immunité. L'un des traits les plus intrigants du mutant perte de fonction *snap33* est le développement précoce de lésions spontanées et une morphologie naine dans des conditions de croissance normales. Les objectifs de mes travaux de thèse étaient d'abord de mieux caractériser le phénotype de *snap33* aux niveaux macroscopique et moléculaire et de déterminer les voies biologiques responsables de ce phénotype. Ensuite, le deuxième objectif était d'évaluer un lien potentiel entre SNAP33 et des protéines MAPKs (Mitogen-activated protein kinases) également connues pour être impliquées dans l'immunité des plantes. La caractérisation phénotypique de trois mutants alléliques *snap33* a révélé que le mutant *snap33* présente plusieurs caractéristiques de mutants auto-immuns, notamment de la mort cellulaire spontanée, l'expression constitutive de gènes marqueurs de stress biotique, la suraccumulation des trois principales phytohormones de défense, l'acide salicylique (SA), l'acide jasmonique (JA), et l'éthylène (ET), et la suraccumulation d'espèces réactives de l'oxygène (ROS). Des analyses transcriptomiques de type séquençage d'ARN (RNA-seq) sur des plantes *snap33* âgées de 5 et 12 jours, avant et après l'apparition des lésions, respectivement ont montré que de nombreux gènes impliqués dans les réponses immunitaires sont surxprimés dans le mutant *snap33* dès le stade 5 jours. De plus, le mutant *snap33* montre une surepression de nombreux gènes de résistance (R) à 12 jours par rapport aux plantes sauvages (WT). Nos analyses génétiques ont montré que le phénotype de *snap33* dépend principalement de la voie SA et ont indiqué l'implication de la signalisation par les protéines R. Ces résultats suggèrent fortement que SNAP33, ou sa fonction, est gardée par une ou plusieurs protéines R. Le module MAPK MEKK1-MKK1/MKK2-MPK4 est rapidement activé en réponse à une infection pathogène et contribue à l'établissement de réponses immunitaires en phosphorylant divers substrats. Les mutants simples *mpk4* et *mekk1*, ainsi que le double mutant *mkk1 mkk2*, présentent un phénotype similaire à celui du mutant *snap33*. Par ailleurs, SNAP33 est connue pour être phosphorylé *in vivo* sur des sites dont les motifs kinases sont compatibles avec la signature MAPK kinase. Ces données nous ont incités à examiner la possibilité d'une relation entre SNAP33 et MEKK1-MKK1/MKK2-MPK4. Nous avons émis l'hypothèse que le module MAPK pourrait être impliqué dans la régulation de l'activité SNAP33 pendant l'immunité ou que SNAP33 pourrait réguler le module MAPK. En utilisant des tests de complémentation de fluorescence bimoléculaire (BiFC), nous avons constaté que SNAP33 interagit *in vivo* avec MEKK1, MKK2 et MPK4. Cependant, ces résultats n'ont pas pu être confirmés par des approches complémentaires, suggérant que, si elles sont physiologiquement vraies, ces interactions sont susceptibles d'être transitoires. Nous avons également exploré si SNAP33 est phosphorylée *in vitro* par MPK4 et deux autres MAPK impliquées dans l'immunité, à savoir MPK3 et MPK6. MPK3, MPK4 et MPK6 n'ont pas phosphorylé SNAP33, ce qui suggère fortement que SNAP33 n'est un substrat d'aucune de ces MAPK. Nous avons finalement examiné une éventuelle connexion génétique entre SNAP33 et le module MEKK1-MKK1/MKK2-MPK4. Cependant, aucun des suppresseurs connus des phénotypes de *mekk1*, *mkk1 mkk2* et *mpk4* n'a supprimé le phénotype *snap33*. Dans l'ensemble, nos données suggèrent que SNAP33 et le module de MAPK fonctionnent indépendamment, bien que tous deux soient impliqués dans les réponses immunitaires.

Title: Description and functional characterization of the t-SNARE SNAP33 in *Arabidopsis thaliana*

Key word: SNAP33, MAPK, stress, phytohormones, Arabidopsis, immunity

Abstract SNAREs (soluble N-ethylmaleimide-sensitive factor attachment protein receptors) mediate vesicle fusion during several processes in plants and contribute to homeostasis, immunity, growth, and development. Among this gene family, *SNAP33* codes for a t-SNARE (target-SNARE) protein involved in vesicle fusion to the plasma membrane during cytokinesis and immunity. One of the most intriguing traits of the *snap33* knock-out mutant is the early development of spontaneous lesions and a severely dwarf morphology under normal growth conditions. My Ph.D.'s objectives were first to better characterize the phenotype of *snap33* at both macroscopic and molecular levels and to determine the pathways responsible for this phenotype. Then, my second Ph.D. objective was to assess a potential connection, suggested by literature data, between SNAP33 and mitogen-activated protein kinases (MAPKs) also known to be involved in plant immunity. Phenotypic characterization of three allelic *snap33* mutants revealed that *snap33* exhibits features of a lesion-mimic phenotype, including spontaneous cell death, constitutive expression of biotic stress marker genes, over-accumulation of the three main defense phytohormones salicylic acid (SA), jasmonic acid (JA), and ethylene (ET), and over-accumulation of reactive oxygen species (ROS). RNA-seq analyses of 5- and 12-day-old *snap33* seedlings, respectively before and after the onset of lesions, showed that numerous genes involved in defense-responses are up-regulated as early as in the 5-day-old *snap33* mutant. Additionally, we found an up-regulation of numerous Resistance (R) genes in *snap33* at 12 days compared to WT. Genetic analyses showed that *snap33*'s phenotype mainly depends on the SA pathway, and indicated the involvement of R protein signaling. These results strongly suggest that SNAP33, or its function, is guarded by one or several R proteins. The MEKK1-MKK1/MKK2-MPK4 MAPK module is rapidly activated in response to pathogen infection and contributes to the establishment of immune responses by phosphorylating various substrates. The *mpk4* and *mekk1* single mutants, as well as the *mkk1 mkk2* double mutant, display a lesion-mimic phenotype similar to that of the *snap33* mutant. Besides, SNAP33 is known to be phosphorylated *in vivo* on sites whose kinase motifs are compatible with the MAPK kinase signature. These data prompted us to examine the possibility of a relationship between SNAP33 and MEKK1-MKK1/MKK2-MPK4. We hypothesized that the MAPK module might be involved in regulating SNAP33 activity during immunity or that SNAP33 might regulate the MAPK module. Using bimolecular fluorescence complementation (BiFC) assays, we found that SNAP33 interacts *in vivo* with MEKK1, MKK2 and MPK4. However, these results could not be confirmed by complementary approaches, suggesting that, if physiologically true, these interactions are likely to be transient. We also explored whether SNAP33 is an *in vitro* substrate of MPK4 and of two other MAPKs involved in immunity, namely MPK3 and MPK6. MPK3, MPK4 and MPK6 did not phosphorylate SNAP33, strongly suggesting that SNAP33 is not a substrate of any of these MAPKs. We finally examined a possible genetic connection between SNAP33 and the MEKK1-MKK1/MKK2-MPK4 MAPK module. However, none of known suppressors of *mekk1*, *mkk1 mkk2* and *mpk4* phenotype reverted *snap33* phenotype. Overall, our data suggest that SNAP33 and the MAPK module function independently, albeit both are involved in immune responses.